Elucidating the Formation and Chemistry of Chromophores during Kraft Pulping

Volume 2

A Dissertation Submitted by

Thomas J. Dyer

B.S. 1999, University of Wisconsin-Stevens Point

This Thesis is in Partial Fulfillment of the Requirements from the
Institute of Paper Science and Technology
for the Degree of Doctor of Philosophy
Atlanta, Georgia

Publication rights reserved by the
Institute of Paper Science and Technology
August 2004

LIST OF APPENDICES

15. APPENDIX 1. SUPPORTING DATA FOR CHAPTER #1

15.1 Summary of Experimental Conditions

Table A-1-1. Constant kappa number (approximately 30) conditions for pulps produced from unextracted softwood chips.

Condition	Alias	EA % as Na_2O	Sulfidity % as Na_2O	Maximum Temperature	H-Factor
1	31	16.0	30.0	165.0	1294
2	32	20.0	30.0	165.0	790
3	33	16.0	50.0	165.0	929
4	34	20.0	50.0	165.0	570
5	35	16.0	30.0	175.0	1294
6	36	20.0	30.0	175.0	790
7	37	16.0	50.0	175.0	929
8	38	20.0	50.0	175.0	522
9	39	14.6	40.0	170.0	1352
10	40	21.4	40.0	170.0	565
11	41	18.0	23.2	170.0	1217
12	42	18.0	56.8	170.0	646
13	43	18.0	40.0	161.6	806
14	44	18.0	40.0	178.4	806
15	45	18.0	40.0	170.0	806
16	46	18.0	40.0	170.0	806
17	47	18.0	40.0	170.0	806
18	48	18.0	40.0	170.0	806
19	49	18.0	40.0	170.0	806
20	50	18.0	40.0	170.0	806

Table A-1-2. Constant kappa number conditions (approximately 30) for pulps produced from extracted softwood chips.

Condition	Alias	EA % as Na_2O	Sulfidity % as Na_2O	Maximum Temperature	H-Factor
1	51	16.0	30.0	165.0	1335
2	52	20.0	30.0	165.0	803
3	53	16.0	50.0	165.0	929
4	54	20.0	50.0	165.0	516
5	55	16.0	30.0	175.0	1335
6	56	20.0	30.0	175.0	803
7	57	16.0	50.0	175.0	929
8	58	20.0	50.0	175.0	550
9	59	14.6	40.0	170.0	1352
10	60	21.4	40.0	170.0	590
11	61	18.0	23.2	170.0	1217
12	62	18.0	56.8	170.0	620
13	63	18.0	40.0	161.6	806
14	64	18.0	40.0	178.4	806
15	65	18.0	40.0	170.0	806
16	66	18.0	40.0	170.0	806
17	67	18.0	40.0	170.0	806
18	68	18.0	40.0	170.0	806
19	69	18.0	40.0	170.0	806
20	70	18.0	40.0	170.0	806

Table A-1-3. Incremental cook conditions for softwood kraft pulps produced under Condition A and Condition B pulping conditions. Condition A had a high effective alkali and low sulfidity while Condition B had a low effective alkali and high sulfidity.

Condition	Alias	EA % as Na_2O	Sulfidity % as Na_2O	Maximum Temperature	H-factor
A-1	71-1	21.4	23.2	170.0	120
A-2	71-2	21.4	23.2	170.0	240
A-3	71-3	21.4	23.2	170.0	360
A-4	71-4	21.4	23.2	170.0	480
A-5	71-5	21.4	23.2	170.0	600
A-6	71-6	21.4	23.2	170.0	720
A-7	71-7	21.4	23.2	170.0	840
A-8	71-8	21.4	23.2	170.0	863
B-1	72-1	14.6	56.8	170.0	120
B-2	72-2	14.6	56.8	170.0	240
B-3	72-3	14.6	56.8	170.0	360
B-4	72-4	14.6	56.8	170.0	480
B-5	72-5	14.6	56.8	170.0	600
B-6	72-6	14.6	56.8	170.0	720
B-7	72-7	14.6	56.8	170.0	840
B-8	72-8	14.6	56.8	170.0	960
B-9	72-9	14.6	56.8	170.0	1080
B-10	72-10	14.6	56.8	170.0	1151

15.2 Scattering Coefficient Spectra from Transmitting Sheet Method

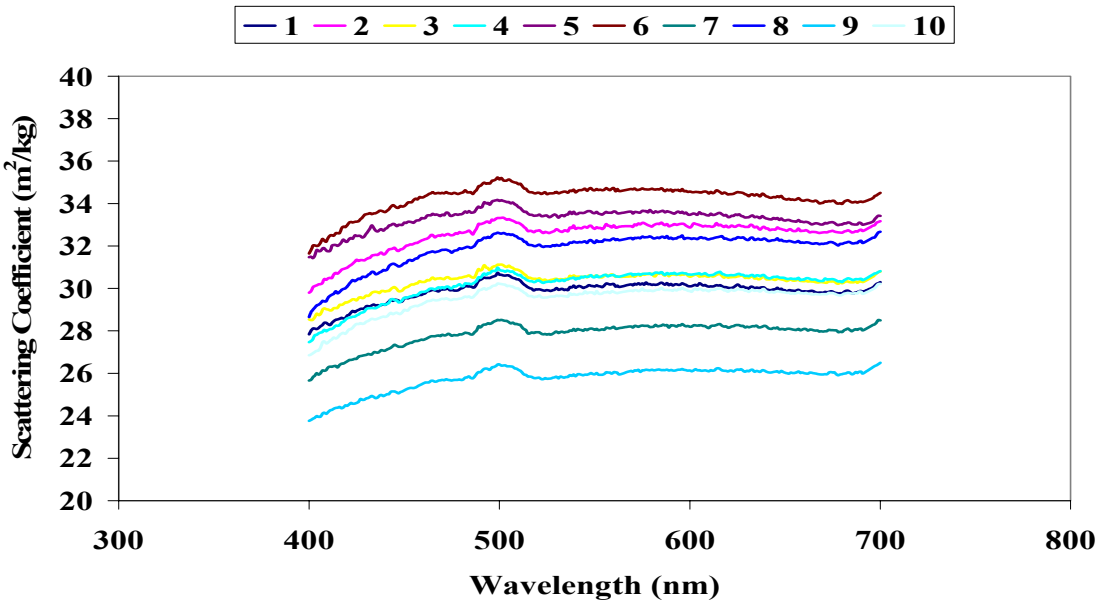

Figure A-1-1. Scattering coefficients of constant kappa number (approximately 30) series made from unextracted wood chips using transmitting sheet method. The pulping conditions are summarized in Table A-1-1.

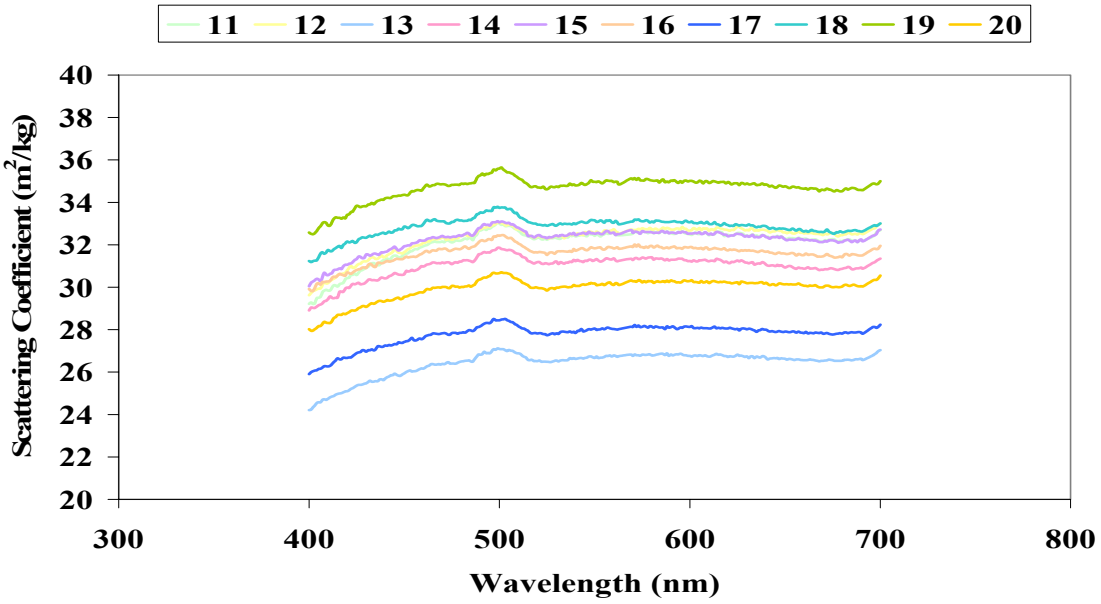

Figure A-1-2. Scattering coefficients of constant kappa number (approximately 30) series made from unextracted wood chips using transmitting sheet method. The pulping conditions are summarized in Table A-1-1.

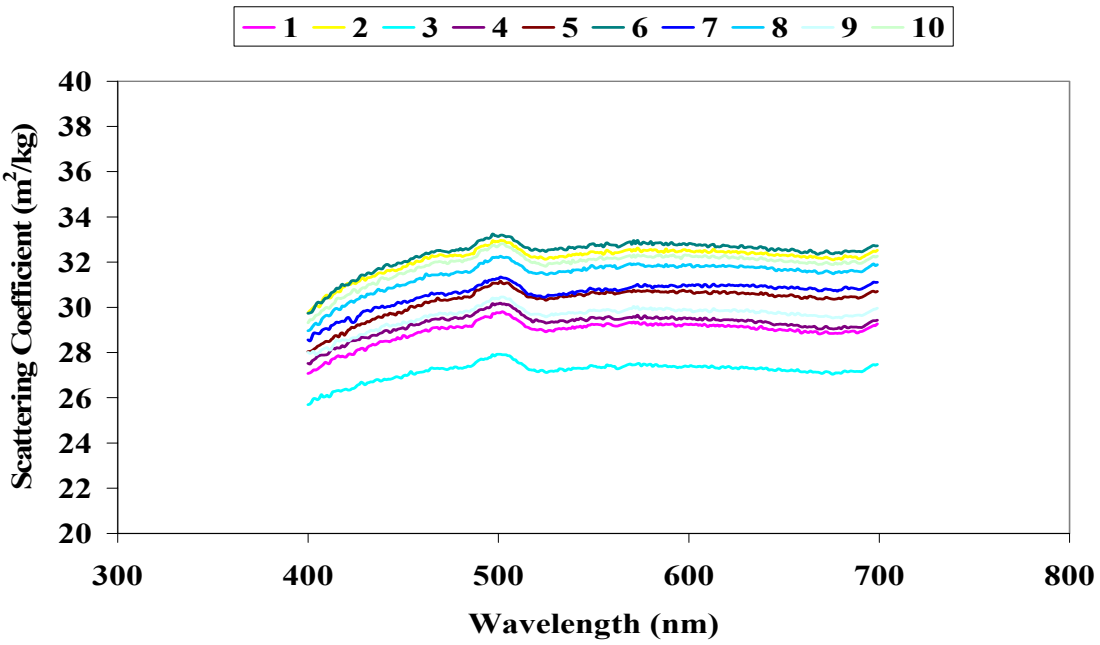

Figure A-1-3. Scattering coefficients of constant kappa number (approximately 30) series made from extracted wood chips using transmitting sheet method. The pulping conditions are summarized in Table A-1-2.

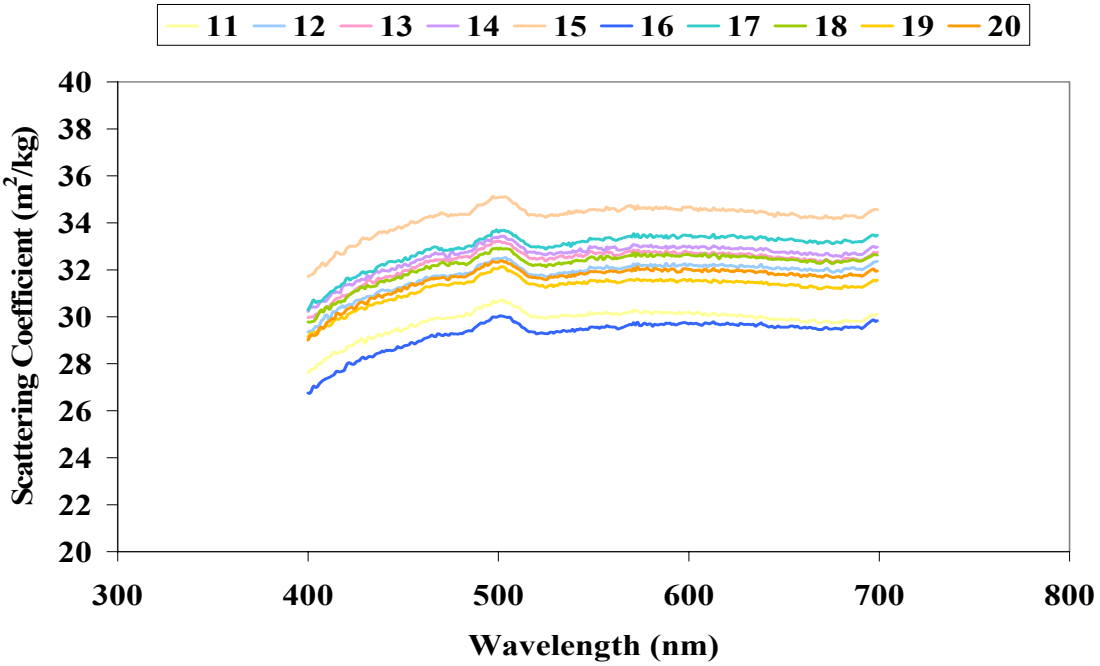

Figure A-1-4. Scattering coefficients of constant kappa number (approximately 30) series made from extracted wood chips using transmitting sheet method. The pulping conditions are summarized in Table A-1-2.

15.3 Absorption Coefficient Spectra from Transmitting Sheet Method

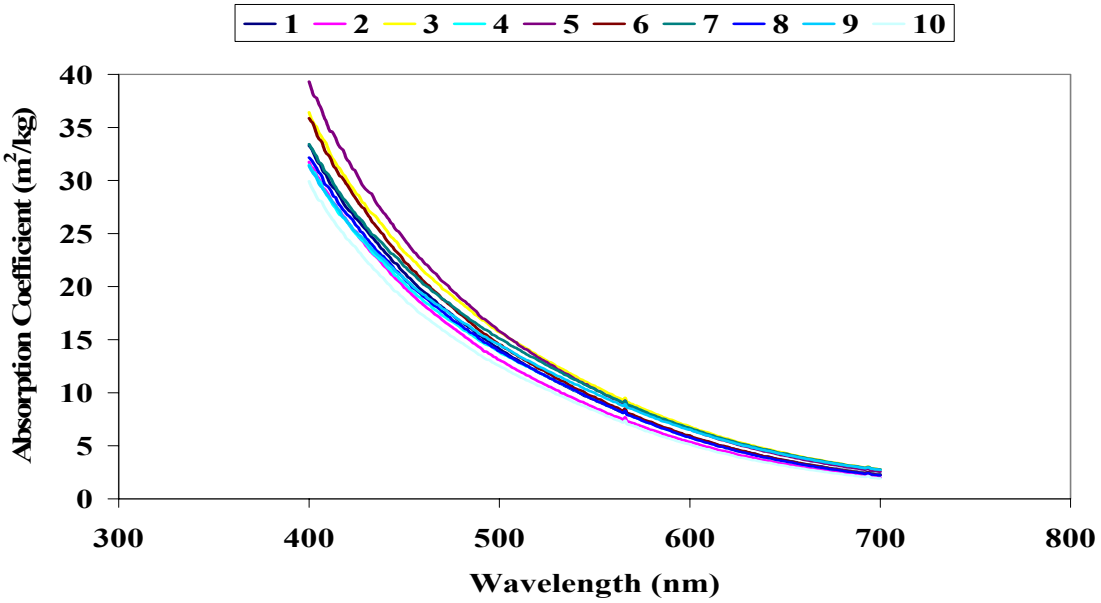

Figure A-1-5. Absorption coefficients of constant kappa number (approximately 30) series made from unextracted wood chips using transmitting sheet method. The pulping conditions are summarized in Table A-1-1.

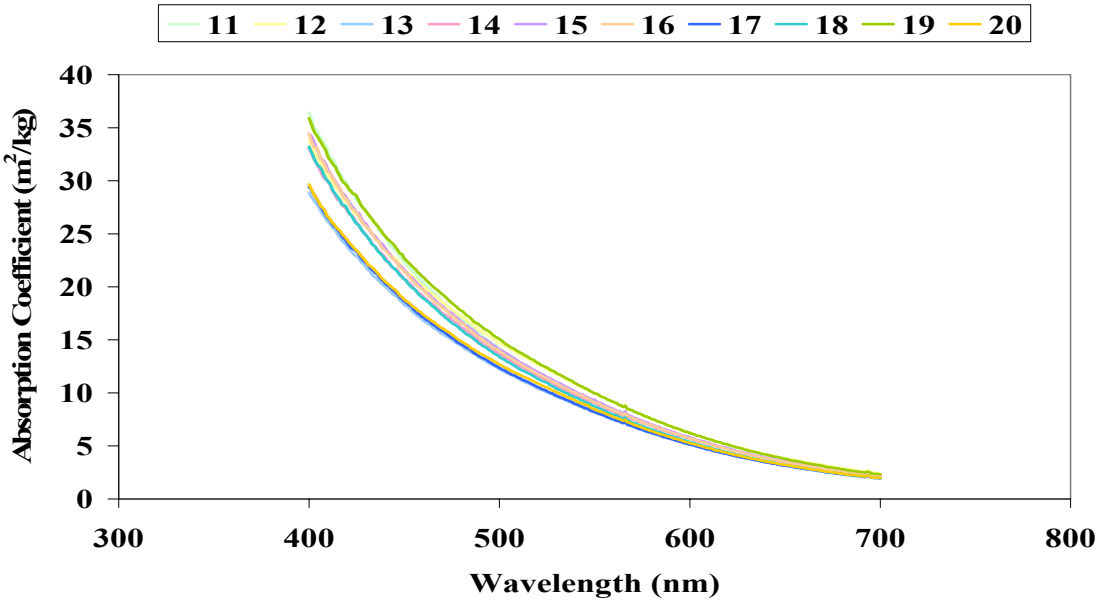

Figure A-1-6. Absorption coefficients of constant kappa number (approximately 30) series made from unextracted wood chips using transmitting sheet method. The pulping conditions are summarized in Table A-1-1.

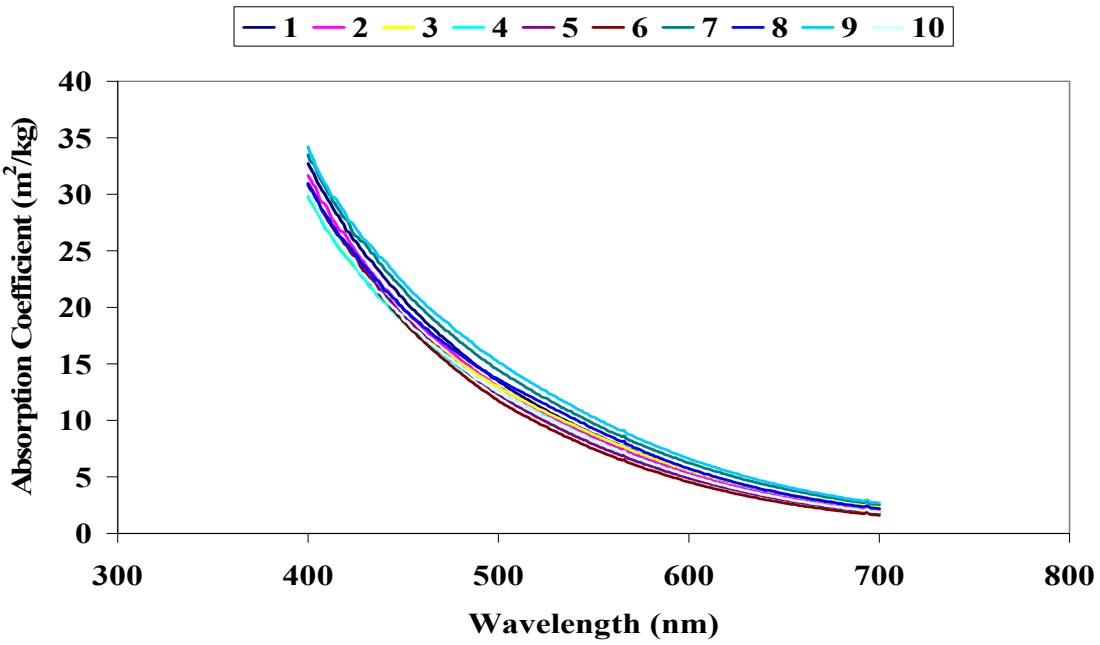

Figure A-1-7. Absorption coefficients of constant kappa number (approximately 30) series made from extracted wood chips using transmitting sheet method. The pulping conditions are summarized in Table A-1-2.

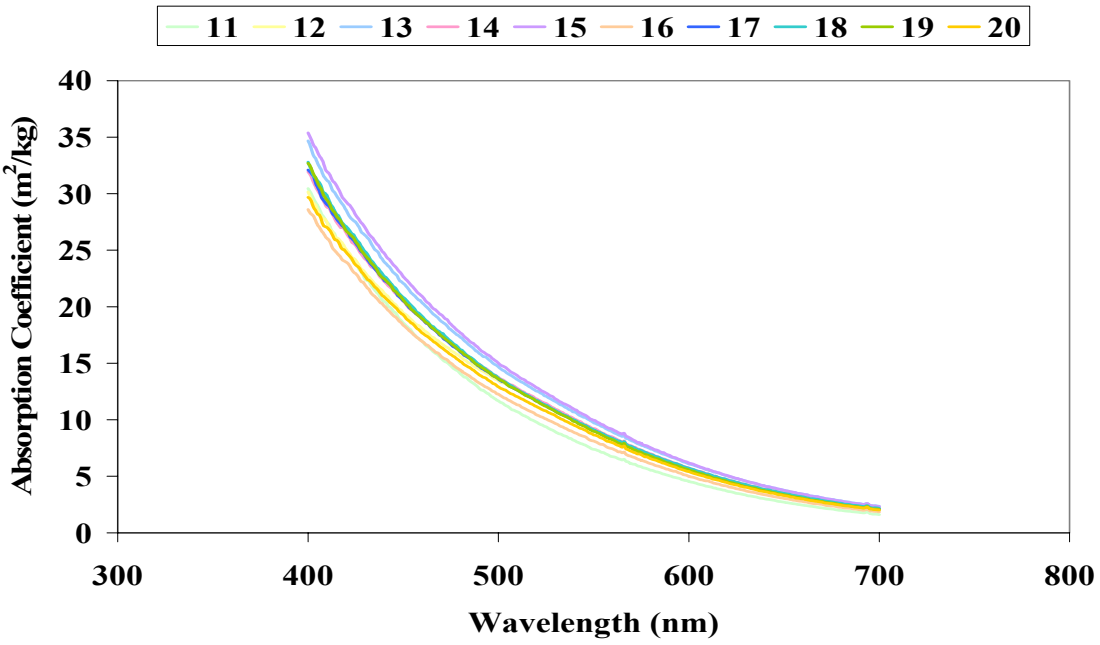

Figure A-1-8. Absorption coefficients of constant kappa number (approximately 30) series made from extracted wood chips using transmitting sheet method. The pulping conditions are summarized in Table A-1-2.

15.4 Apparent Scattering and Absorption Coefficients from Dilution Pulp Method

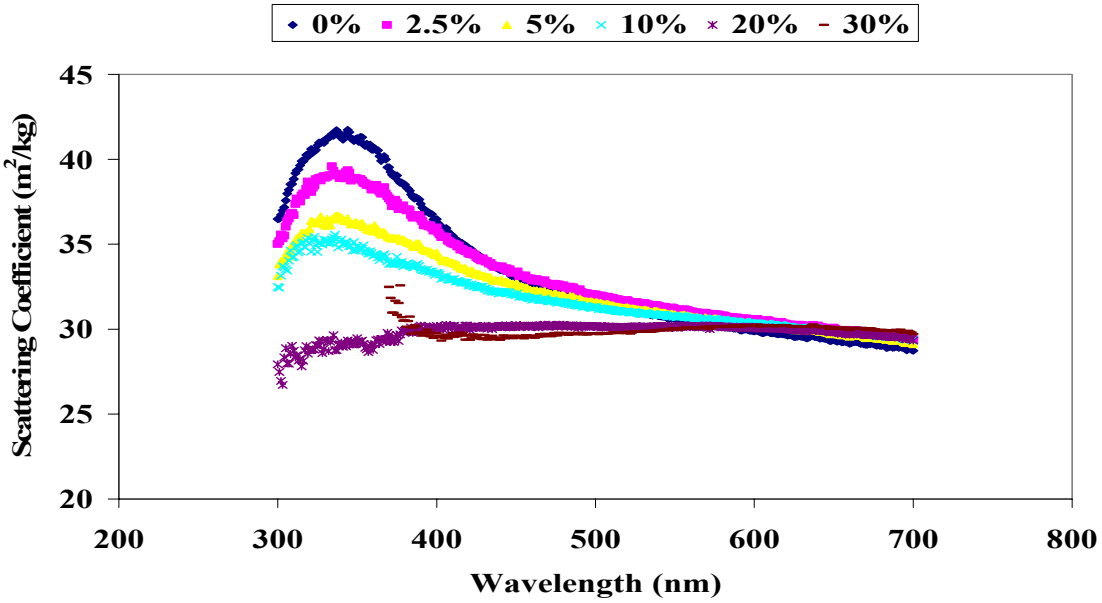

Figure A-1-9. Scattering coefficients of A-1 mixed sheet containing increasing amounts of unbleached pulp and decreasing amounts of fully bleached pulp using dilution pulp method. The conditions for A-1 are summarized in Table A-1-3.

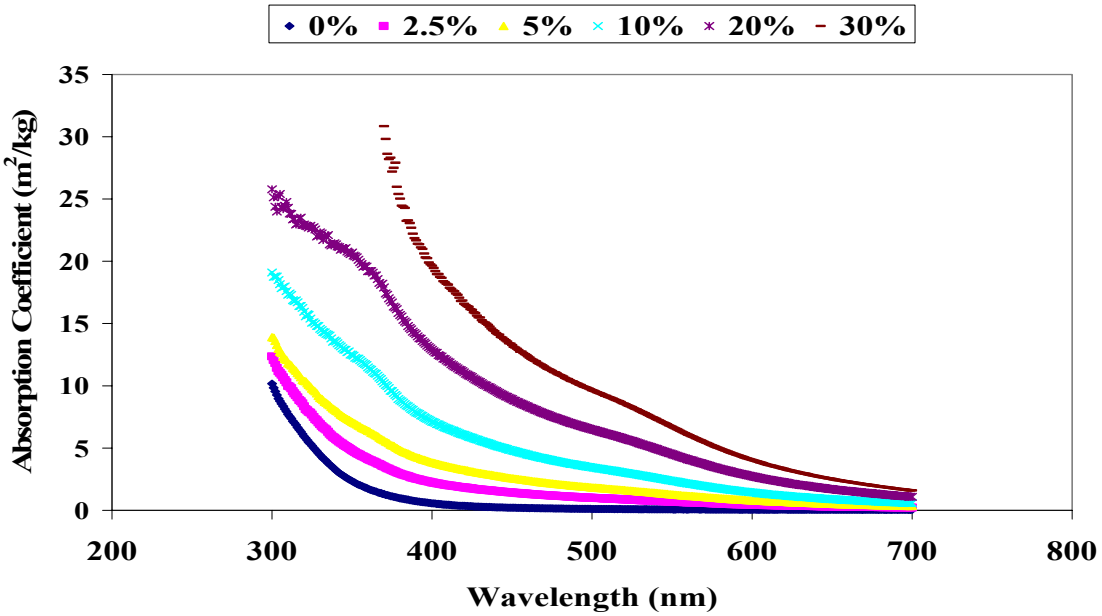

Figure A-1-10. Absorption coefficients of A-1 mixed sheet containing increasing amounts of unbleached pulp and decreasing amounts of fully bleached pulp using dilution pulp method. The conditions for A-1 are summarized in Table A-1-3.

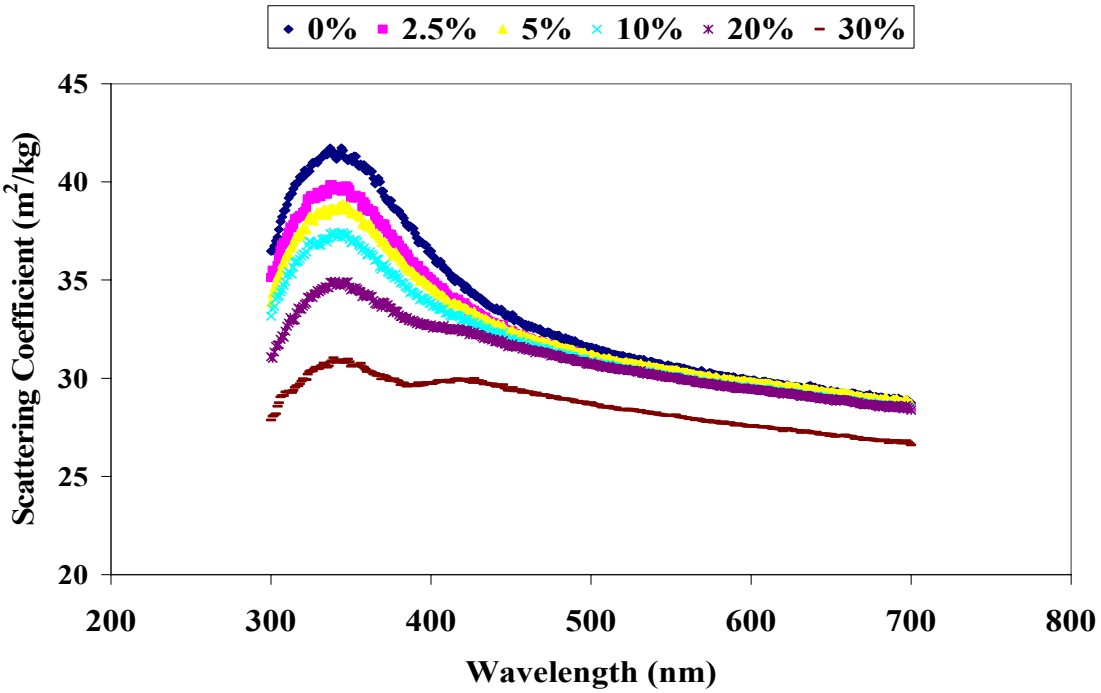

Figure A-1-11. Scattering coefficients of wood meal mixed sheet containing increasing amounts of wood meal using the dilution pulp method.

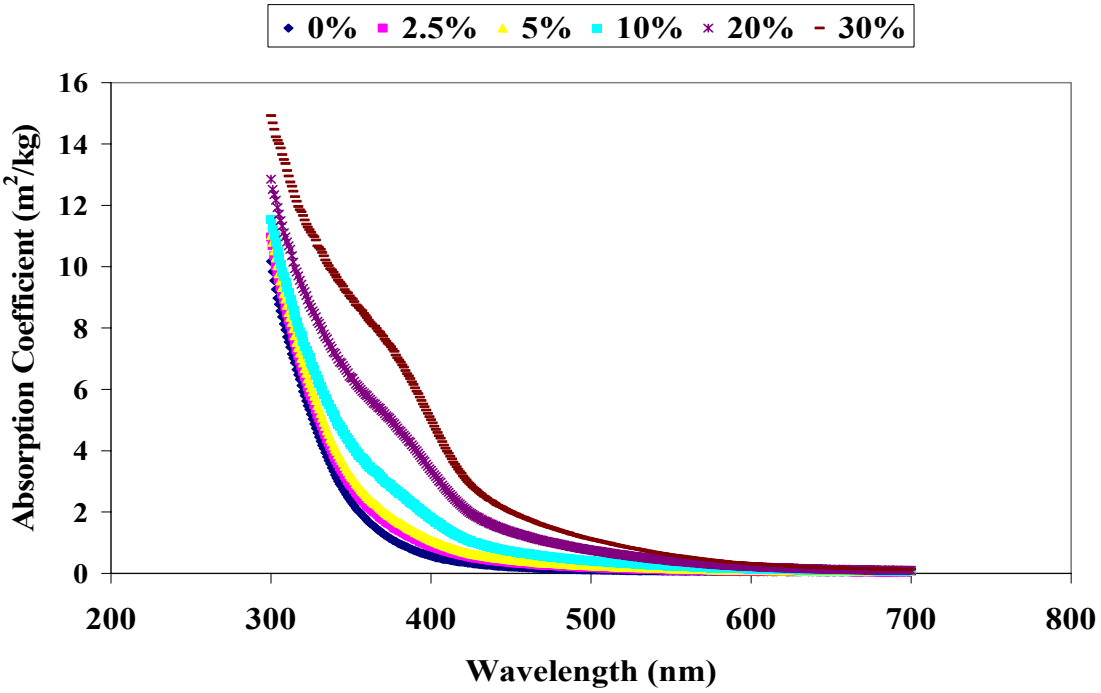

Figure A-1-12. Absorption coefficients of wood meal mixed sheet containing increasing amounts of wood meal using dilution pulp method.

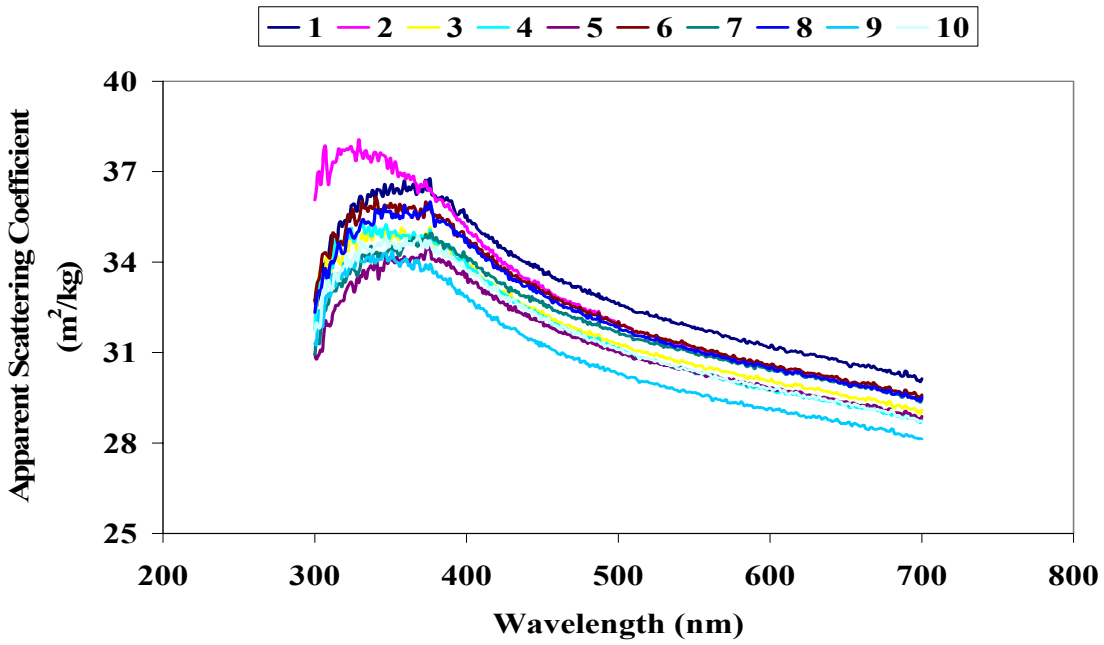

Figure A-1-13. Apparent scattering coefficient from mixed sheets of the constant kappa number (approximately 30) series made at 90:10 dilution to sample ratio. The pulping conditions are summarized in Table A-1-1.

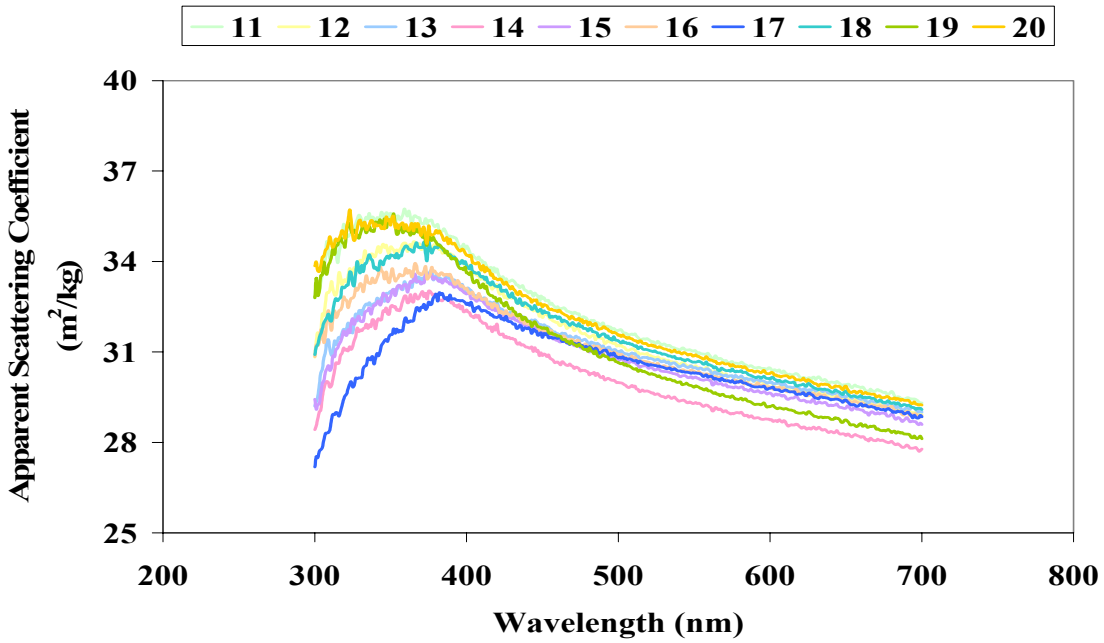

Figure A-1-14. Apparent scattering coefficient from mixed sheets of the constant kappa number (approximately 30) series made at 90:10 dilution to sample ratio. The pulping conditions are summarized in Table A-1-1.

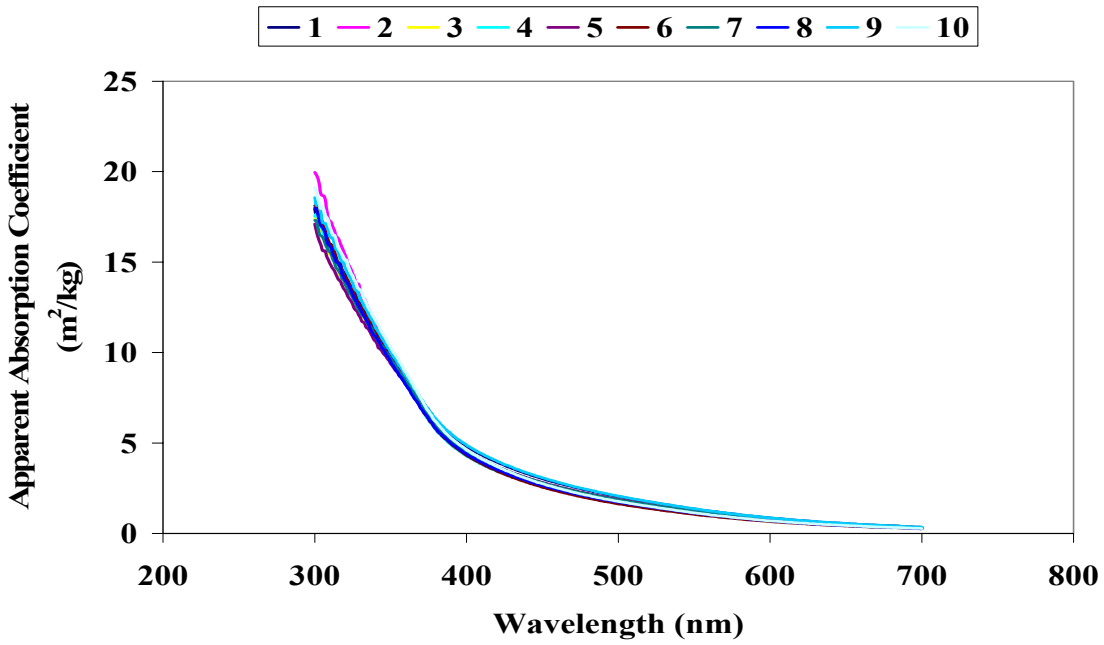

Figure A-1-15. Apparent absorption coefficient from mixed sheets of the constant kappa number (approximately 30) series made at 90:10 dilution to sample ratio. The pulping conditions are summarized in Table A-1-1.

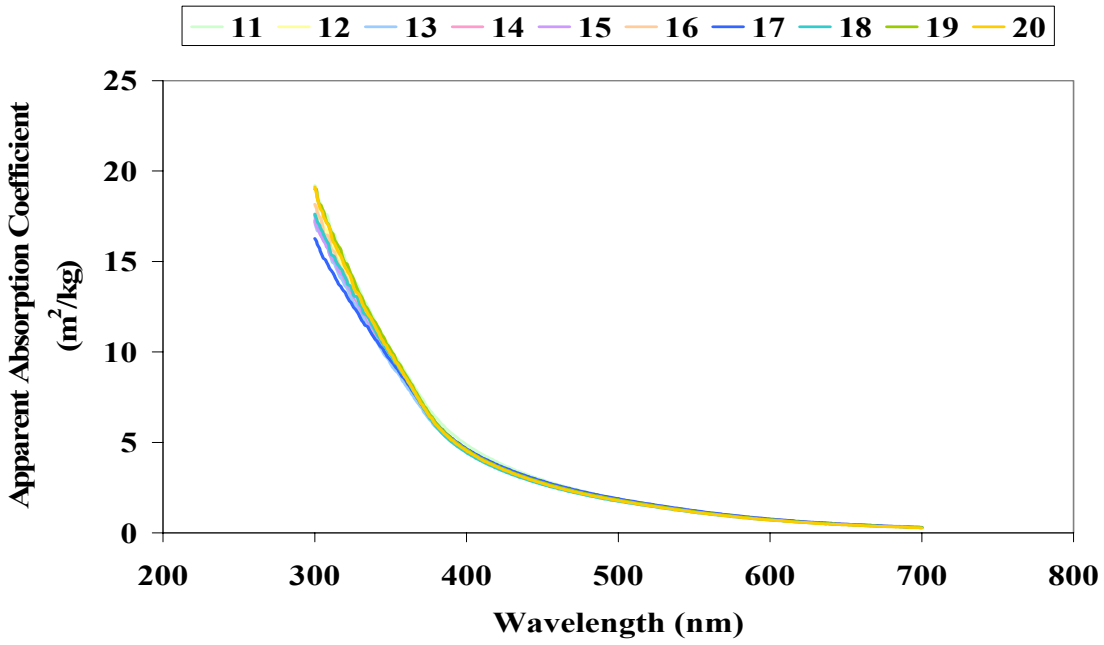

Figure A-1-16. Apparent absorption coefficient from mixed sheets of the constant kappa number (approximately 30) series made at 90:10 dilution to sample ratio. The pulping conditions are summarized in Table A-1-1.

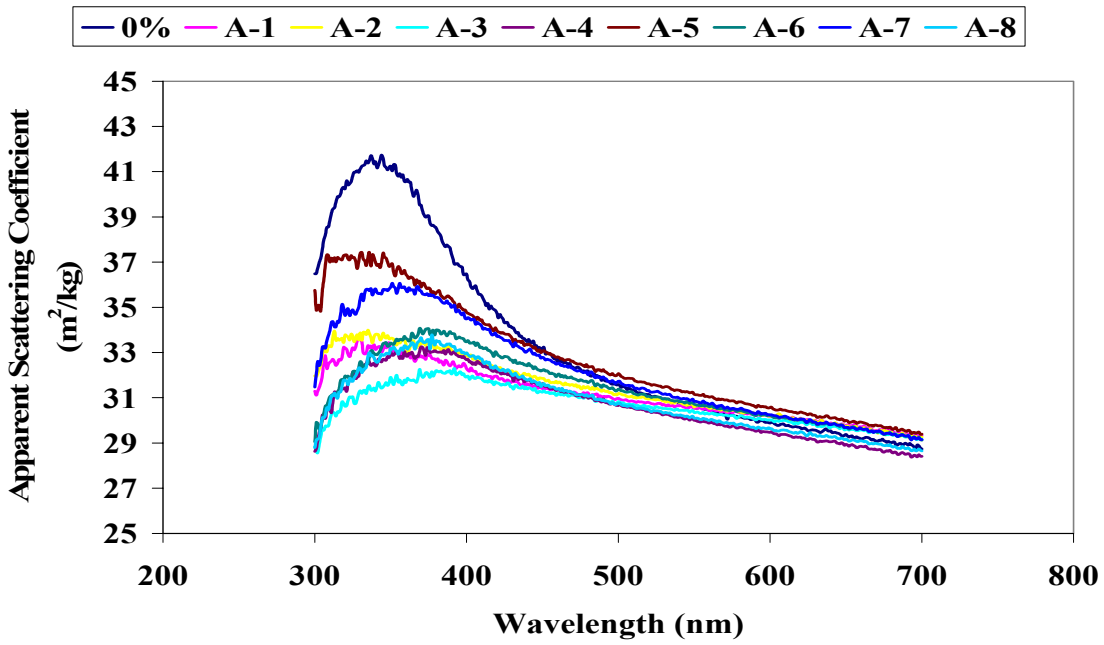

Figure A-1-17. Apparent scattering coefficient from mixed sheets of the incremental cook series made at 90:10 dilution to sample ratio. The pulping conditions are summarized in Table A-1-3.

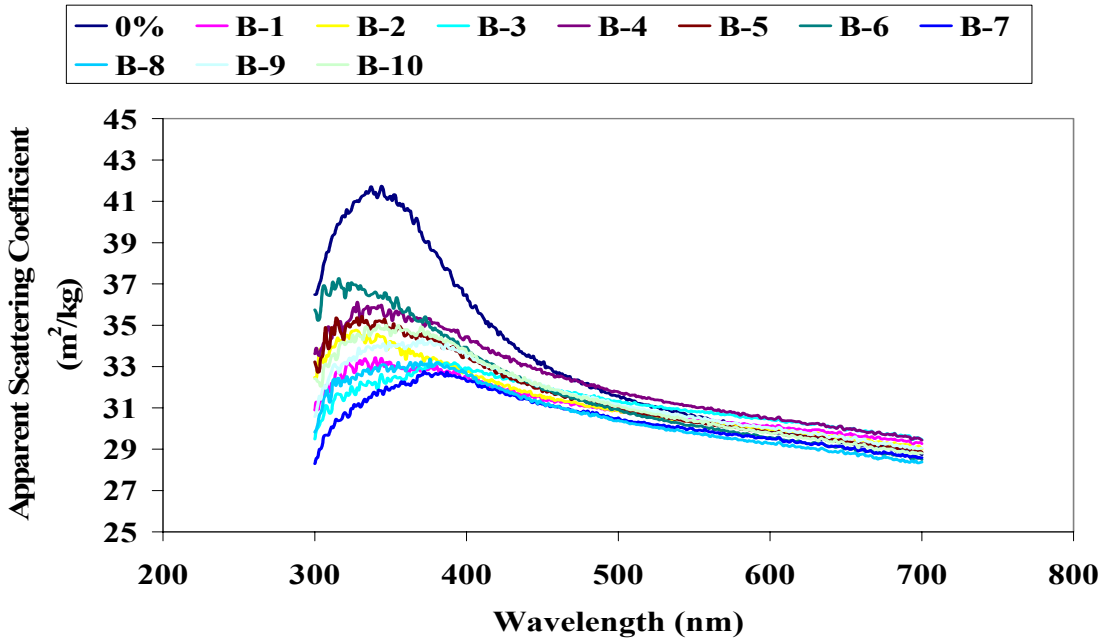

Figure A-1-18. Apparent scattering coefficient from mixed sheets of the incremental cook series made at 90:10 dilution to sample ratio. The pulping conditions are summarized in Table A-1-3.

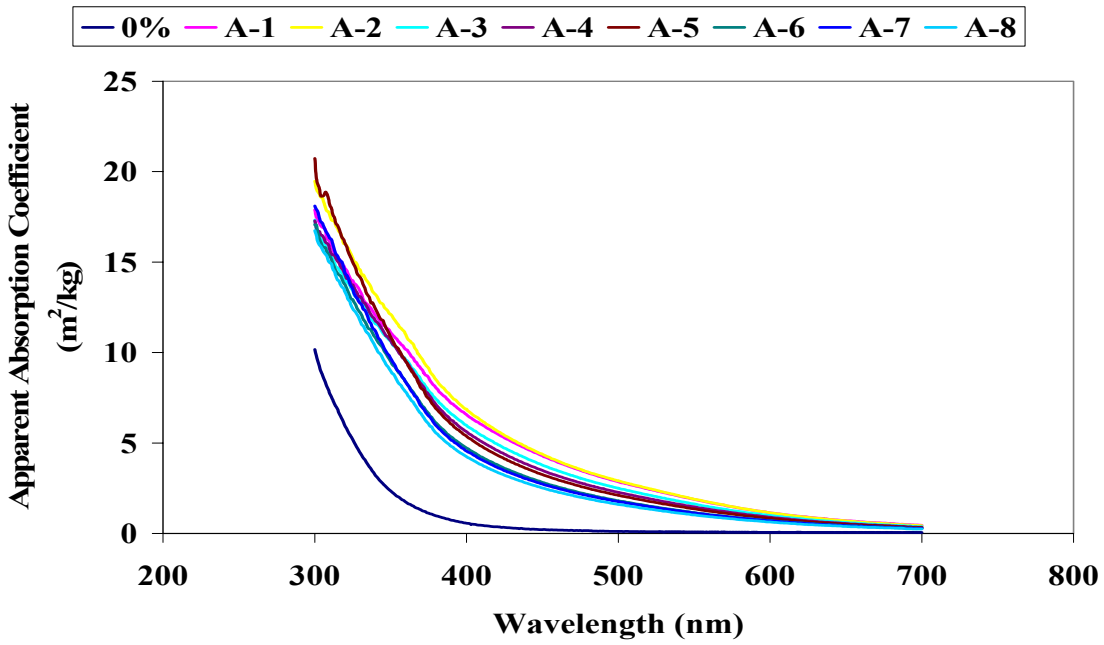

Figure A-1-19. Apparent absorption coefficient from mixed sheets of the incremental cook series made at 90:10 dilution to sample ratio. The pulping conditions are summarized in Table A-1-3.

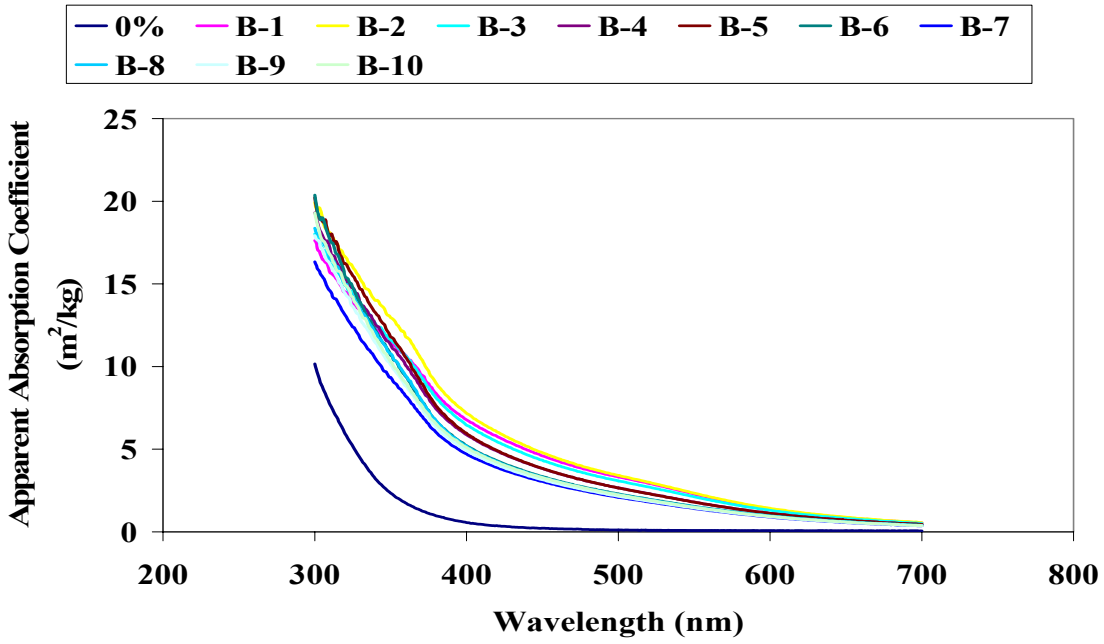

Figure A-1-20. Apparent absorption coefficient from mixed sheets of the incremental cook series made at 90:10 dilution to sample ratio. The pulping conditions are summarized in Table A-1-3.

15.5 Actual Absorption Coefficients from Dilution Pulp Method

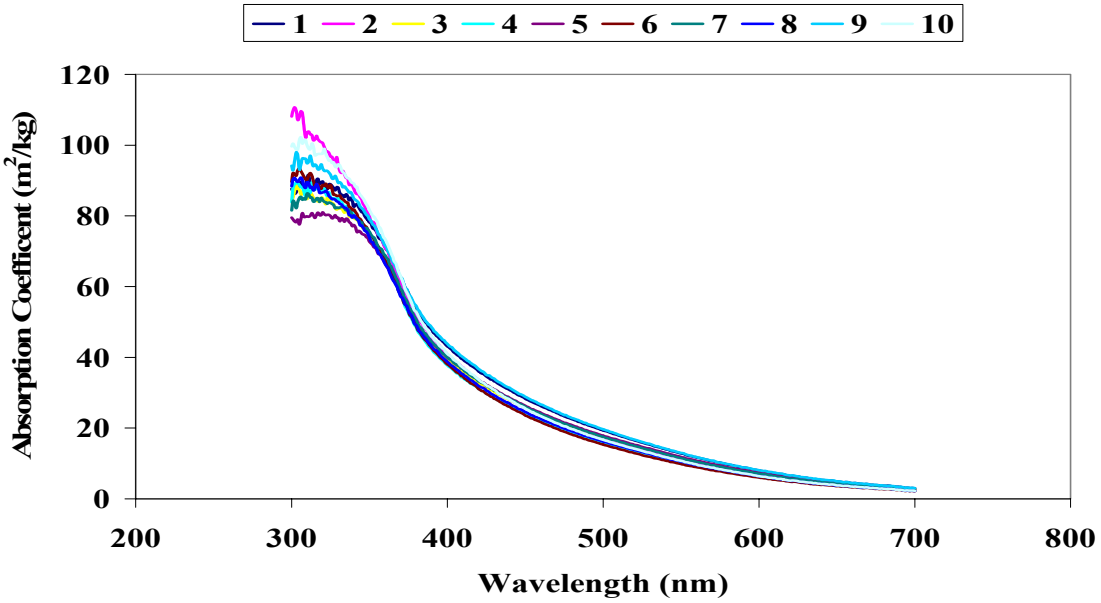

Figure A-1-21. Actual absorption coefficient from mixed sheets of the constant kappa number series made at 90:10 dilution to sample ratio. The pulping conditions are summarized in Table A-1-1.

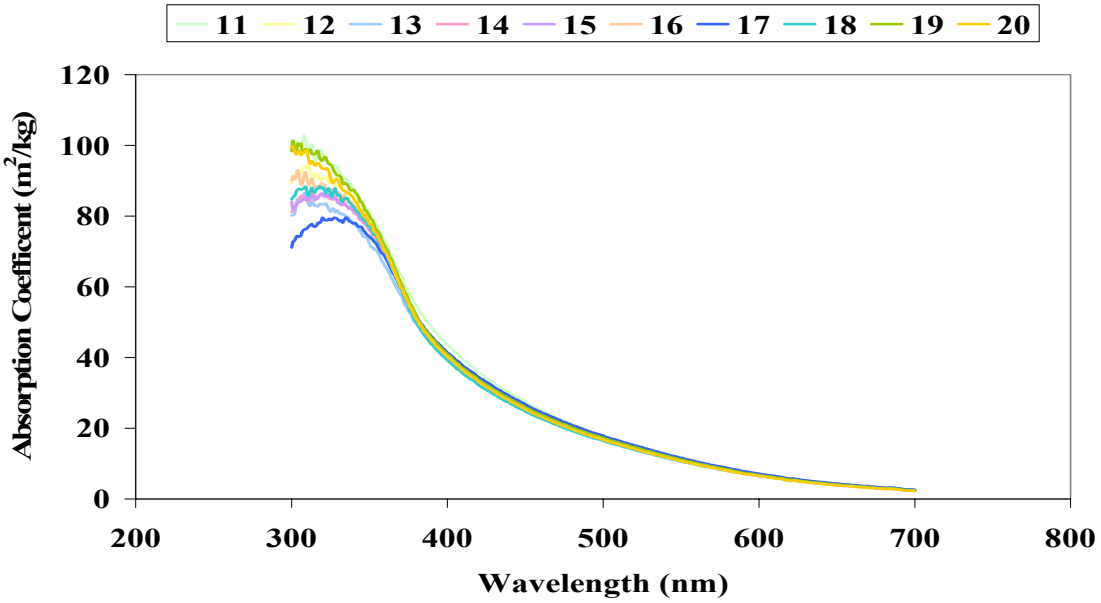

Figure A-1-22. Actual absorption coefficient from mixed sheets of the constant kappa number series made at 90:10 dilution to sample ratio. The pulping conditions are summarized in Table A-1-1.

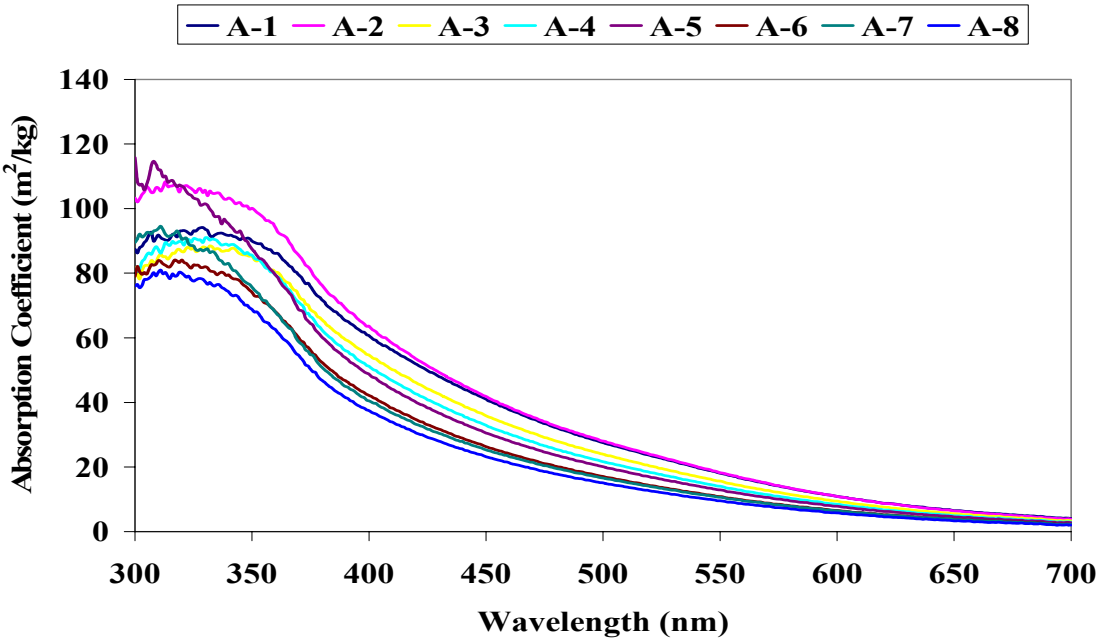

Figure A-1-23. Actual absorption coefficient from mixed sheets of the incremental cook series made at 90:10 dilution to sample ratio. The pulping conditions are summarized in Table A-1-3.

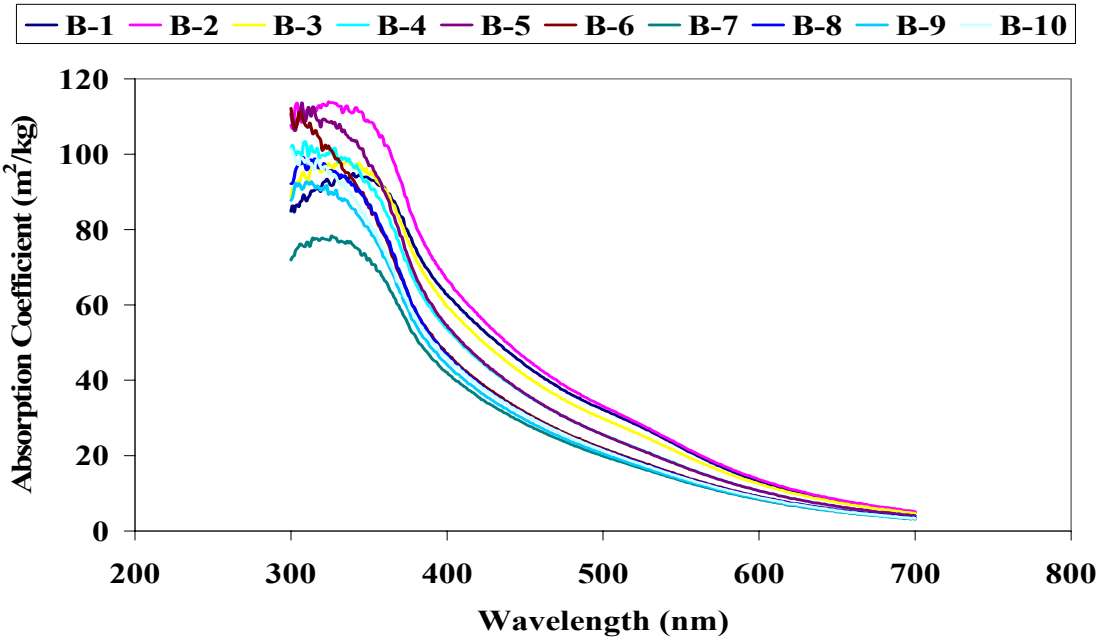

Figure A-1-24. Actual absorption coefficient from mixed sheets of the incremental cook series made at 90:10 dilution to sample ratio. The pulping conditions are summarized in Table A-1-3.

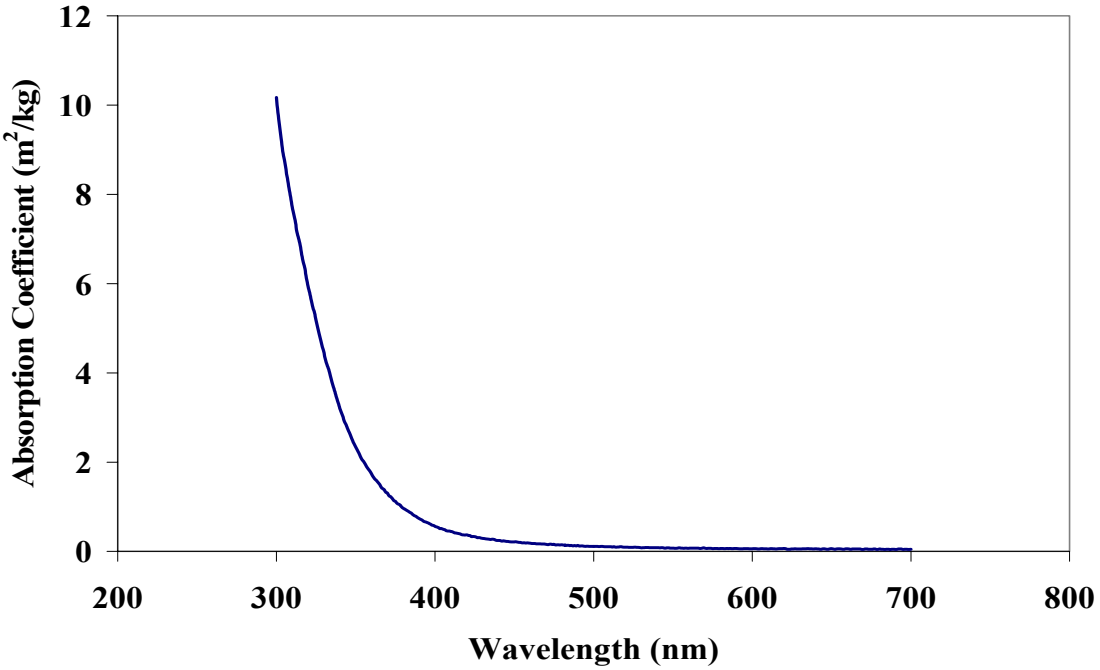

Figure A-1-25. Actual absorption coefficient of a softwood fully bleached kraft pulp.

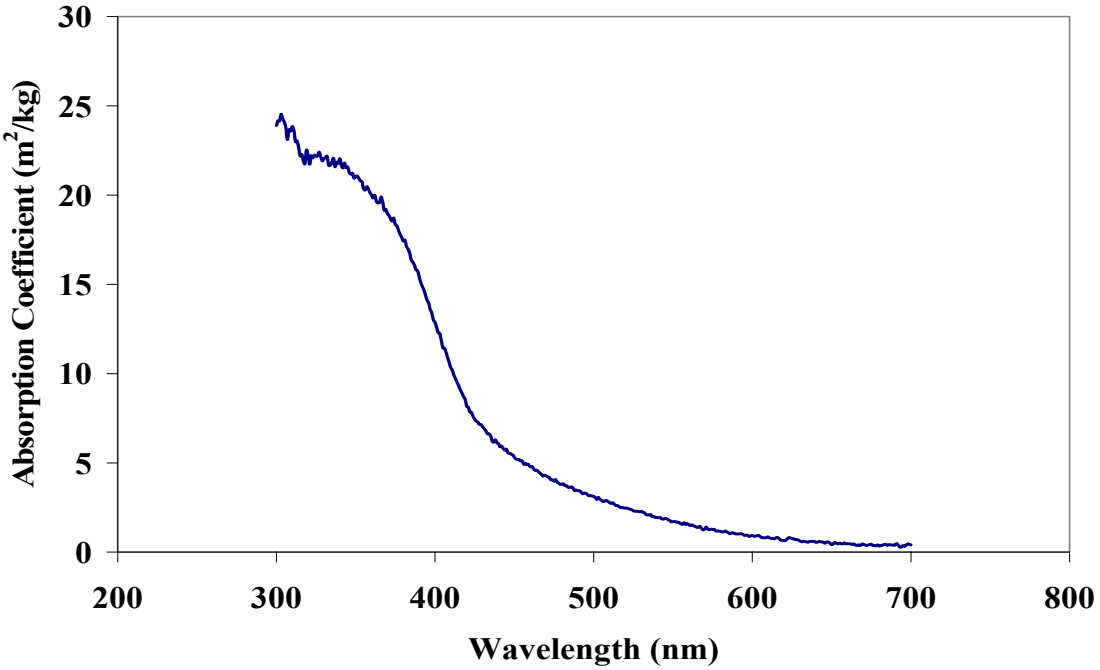

Figure A-1-26. Actual absorption coefficient of *Pinus taeda* wood meal made at 90:10 dilution to sample ratio.

15.6 Kubelka-Munk Remission Function as a function of Wavelength

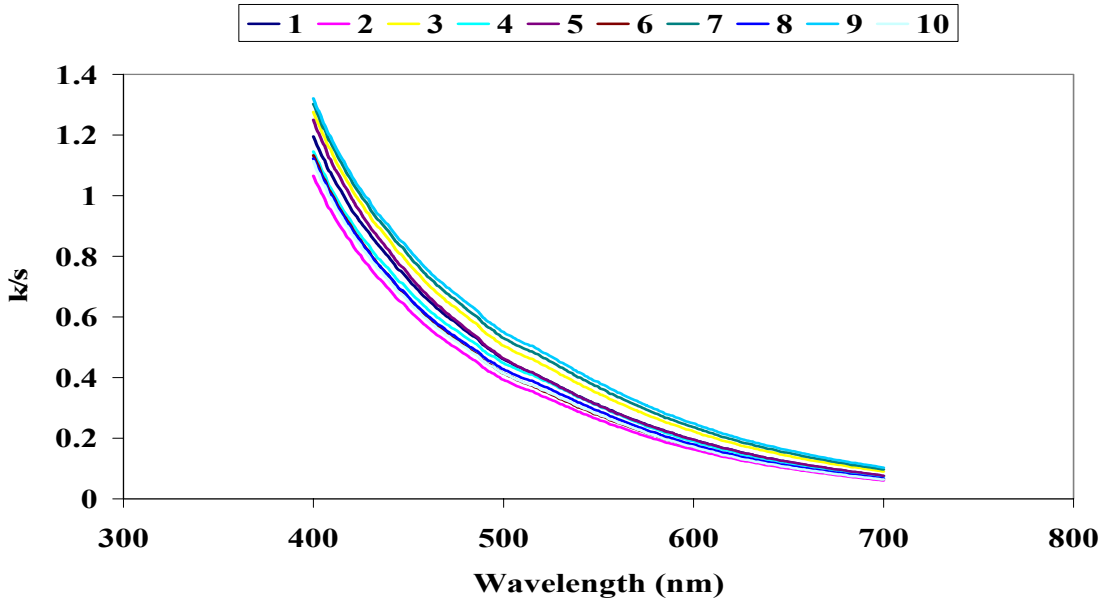

Figure A-1-27. Kubelka-Munk remission function from optically thick sheets of the constant kappa number series made from unextracted wood chips. The pulping conditions are summarized in Table A-1-1.

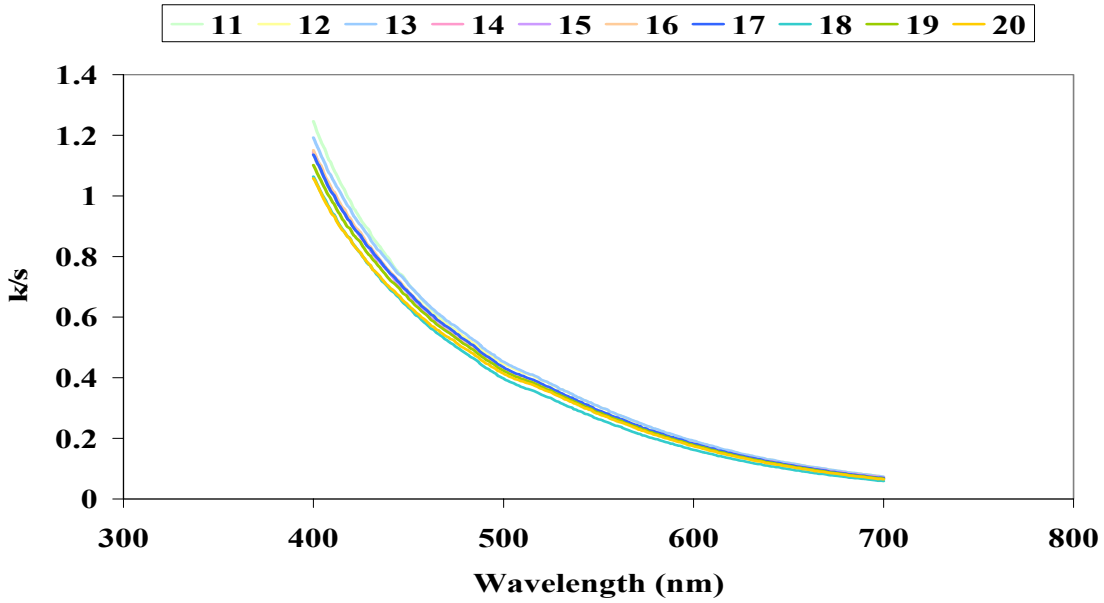

Figure A-1-28. Kubelka-Munk remission function from optically thick sheets of the constant kappa number series made from unextracted wood chips. The pulping conditions are summarized in Table A-1-1.

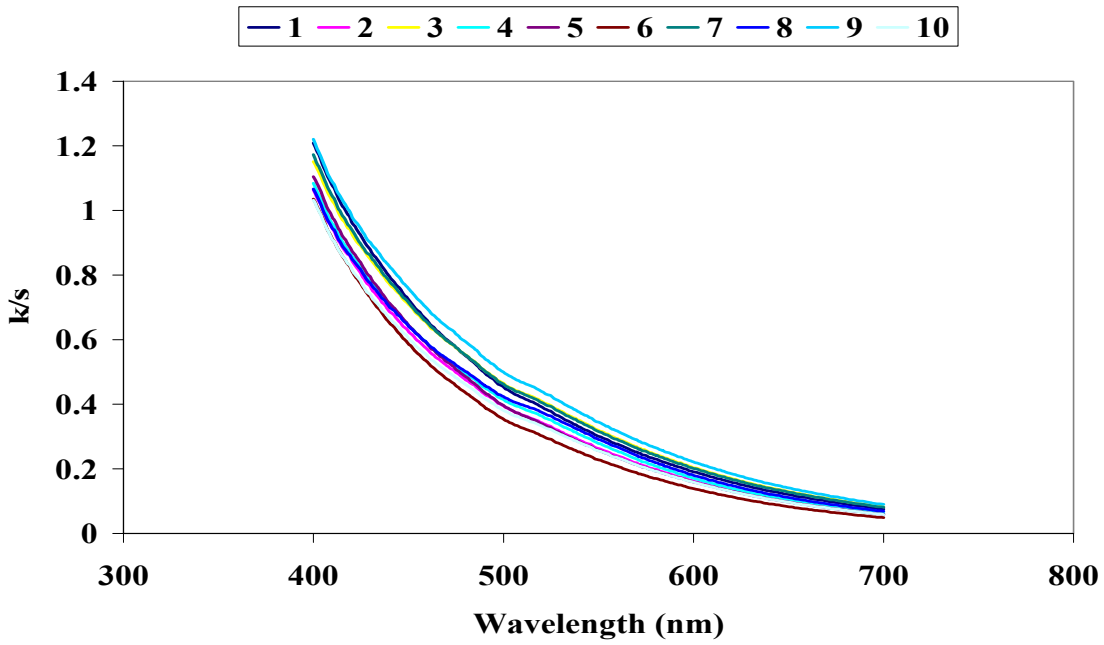

Figure A-1-29. Kubelka-Munk remission function from optically thick sheets of the constant kappa number (approximately 30) series made from extracted wood chips. The pulping conditions are summarized in Table A-1-2.

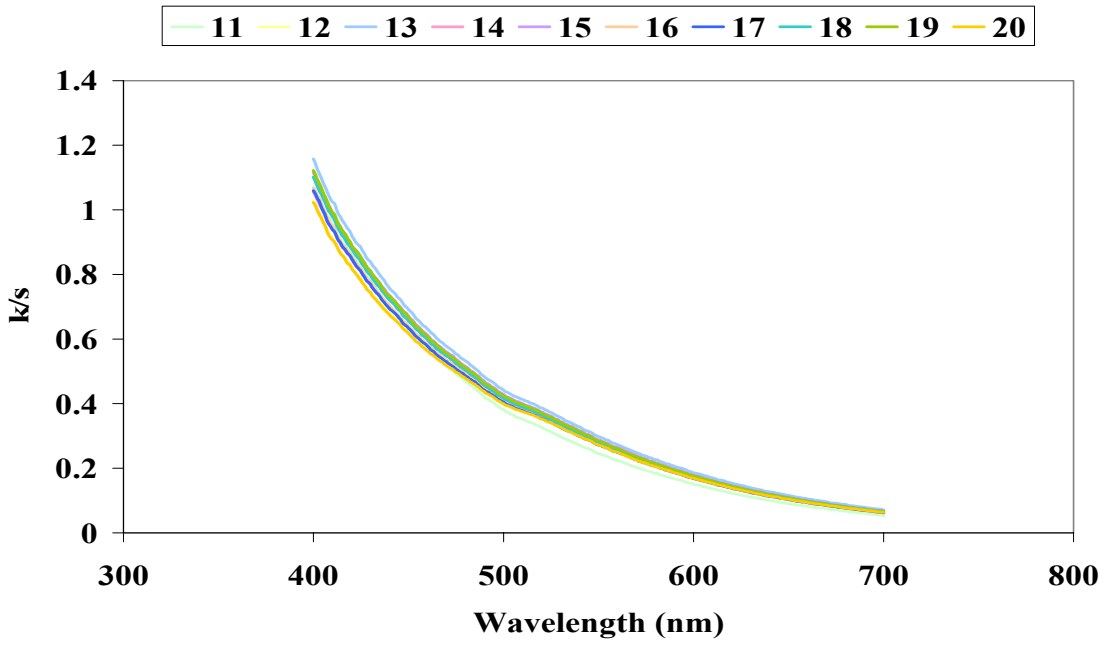

Figure A-1-30. Kubelka-Munk remission function from optically thick sheets of the constant kappa number (approximately 30) series made from extracted wood chips. The pulping conditions are summarized in Table A-1-2.

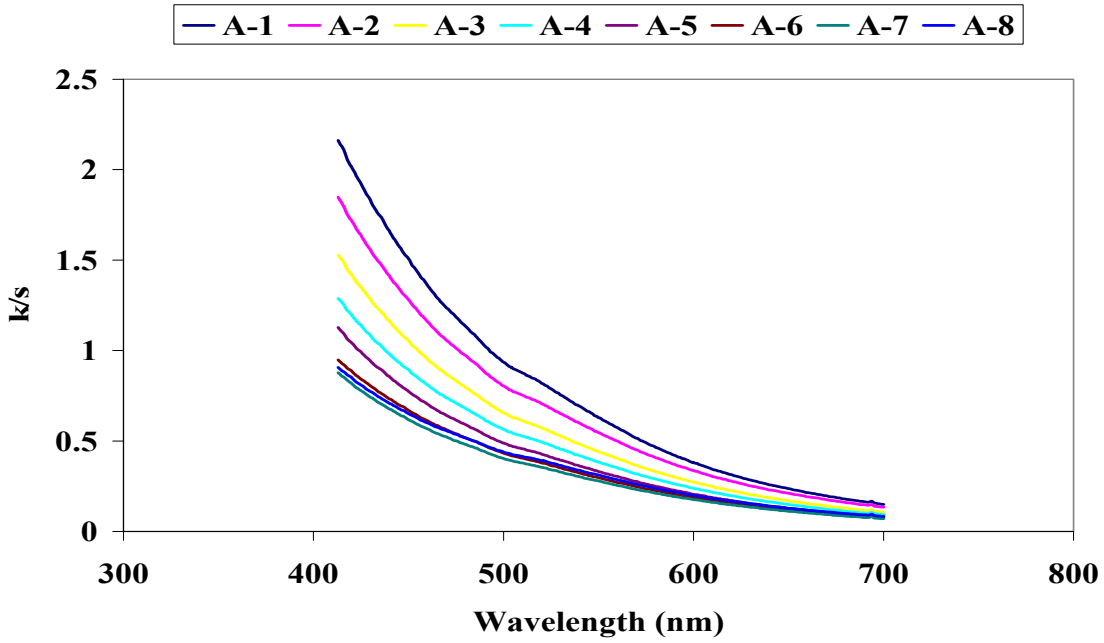

Figure A-1-31. Kubelka-Munk remission function from optically thick sheets of the incremental cook series made from extracted wood chips. The pulping conditions are summarized in Table A-1-3.

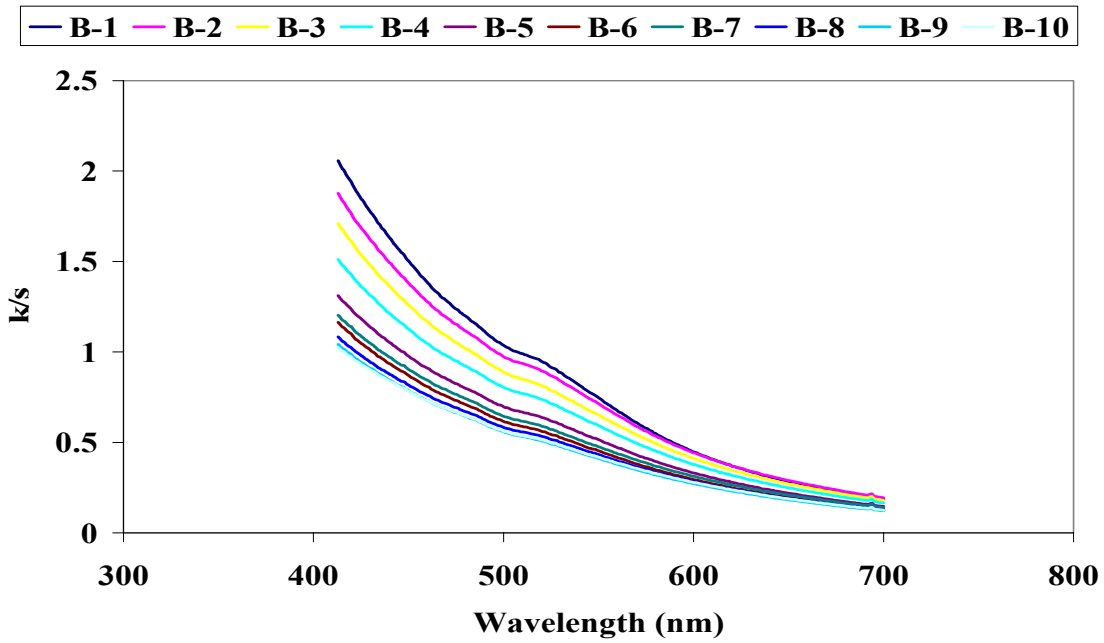

Figure A-1-32. Kubelka-Munk remission function from optically thick sheets of the incremental cook series made from extracted wood chips. The pulping conditions are summarized in Table A-1-3.

15.7 Total Visible Absorption Data

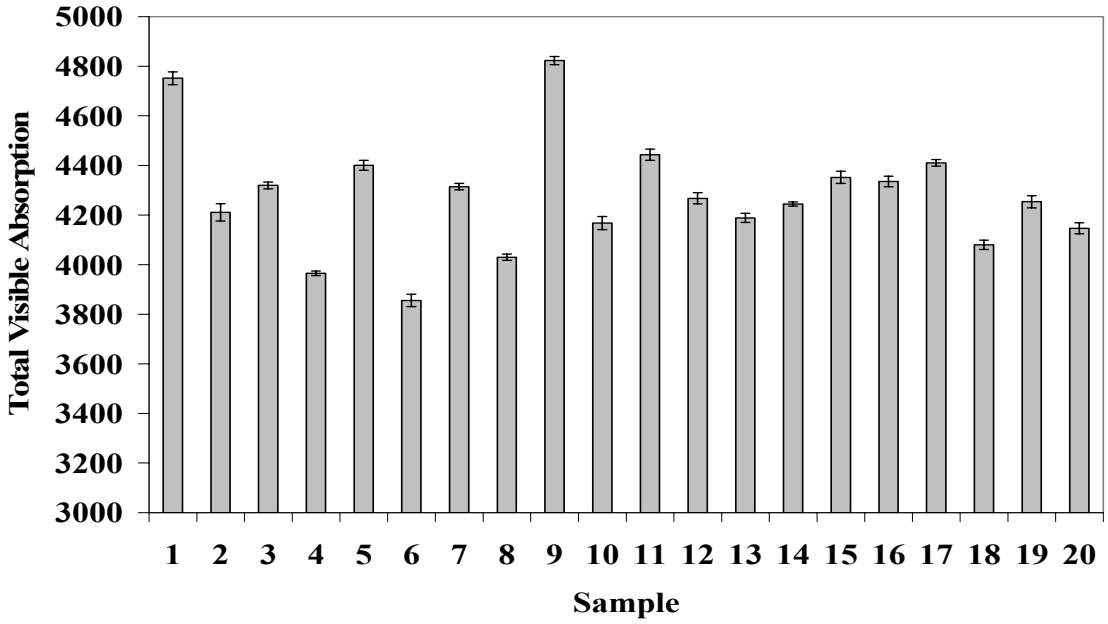

Figure A-1-33. Total visible absorption of the constant kappa number (approximately 30) series made from unextracted wood chips. The pulping conditions are summarized in Table A-1-1.

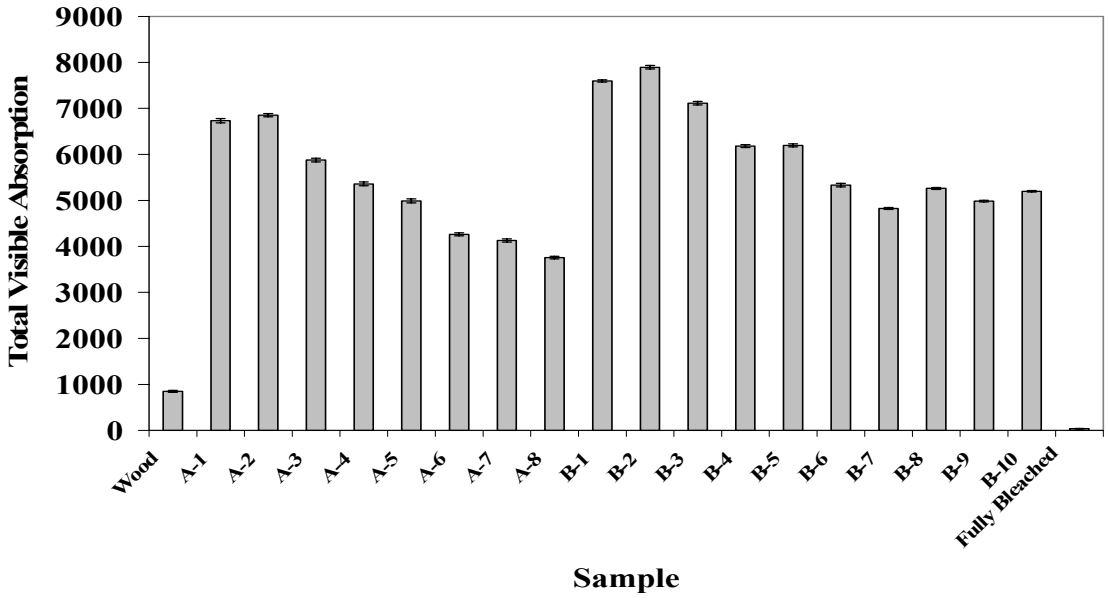

Figure A-1-34. Total visible absorption of the incremental cook series, wood, and fully bleached kraft pulps. The pulping conditions are summarized in Table A-1-3.

15.8 Chromophore Index Data

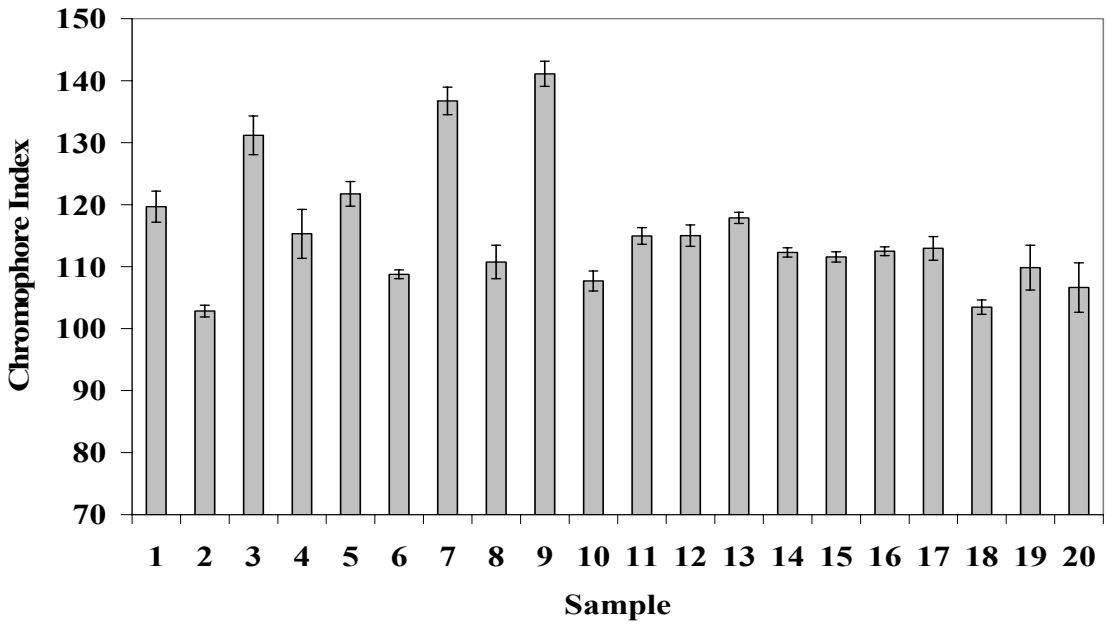

Figure A-1-35. Chromophore index of the constant kappa number (approximately 30) series made from unextracted wood chips. The pulping conditions are summarized in Table A-1-1.

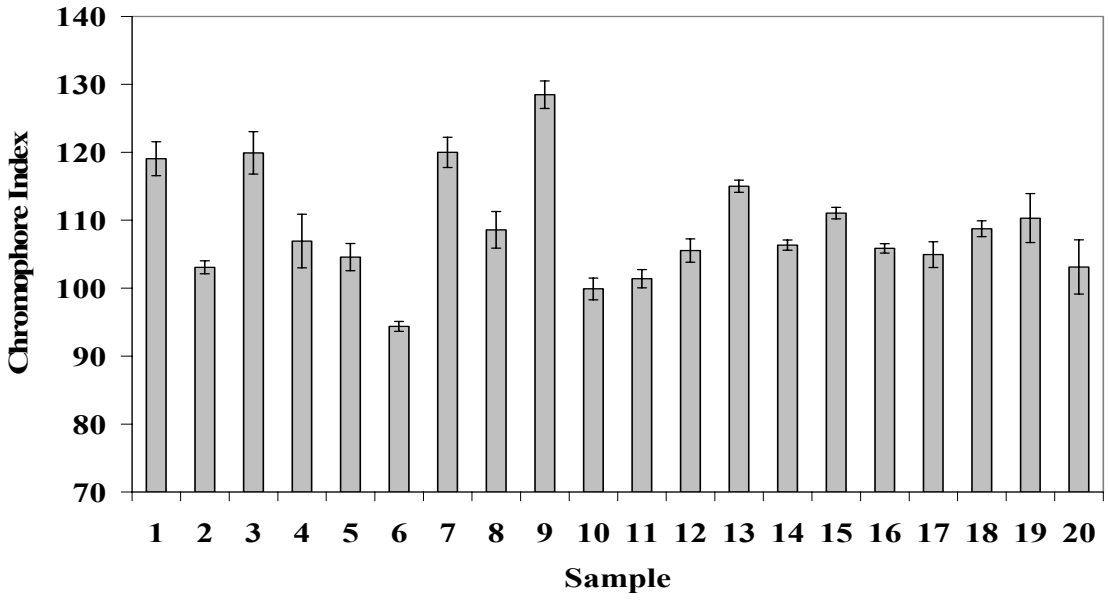

Figure A-1-36. Chromophore index of the constant kappa number series made from extracted wood chips. The pulping conditions are summarized in Table A-1-2.

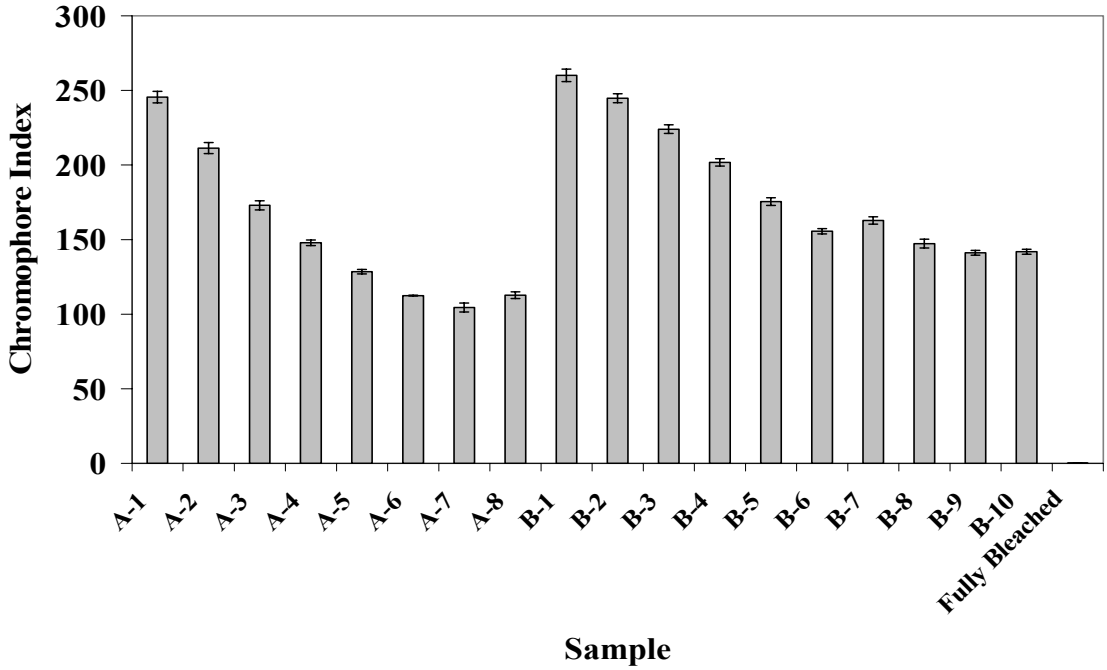

Figure A-1-37. Chromophore index of the incremental cook series and fully bleached kraft pulp. The pulping conditions are summarized in Table A-1-3.

16. APPENDIX 2. SUPPORTING DATA FOR CHAPTER #2

16.1 Experimental Data for Regression Model

Table A-2-1. Conditions and kappa numbers used for regression model.

Condition	EA % as Na_2O	Sulfidity % as Na_2O	Maximum Temperature	H-Factor	Kappa Number
1-1	13.0	15.2	165.0	1200	92.2
1-2	13.0	15.2	165.0	1400	77.5
1-3	13.0	15.2	165.0	1600	71.8
1-4	13.0	15.2	165.0	1800	68.6
1-5	13.0	15.2	165.0	2000	67.1
1-6	13.0	15.2	165.0	2200	55.7
2-1	19.0	15.2	165.0	400	111.6
2-2	19.0	15.2	165.0	600	72.4
2-3	19.0	15.2	165.0	800	54.6
2-4	19.0	15.2	165.0	1000	41.5
2-5	19.0	15.2	165.0	1200	35.5
2-6	19.0	15.2	165.0	1400	28.0
3-1	13.0	44.8	165.0	400	101.0
3-2	13.0	44.8	165.0	600	73.8
3-3	13.0	44.8	165.0	800	61.9
3-4	13.0	44.8	165.0	1000	52.0
3-5	13.0	44.8	165.0	1200	46.9
3-6	13.0	44.8	165.0	1400	38.7
4-1	19.0	44.8	165.0	400	48.4
4-2	19.0	44.8	165.0	600	29.7
4-3	19.0	44.8	165.0	800	24.6
4-4	19.0	44.8	165.0	1000	20.1
4-5	19.0	44.8	165.0	1200	17.8
4-6	19.0	44.8	165.0	1400	14.8

Table A-2-2. Conditions and kappa numbers used for regression model.

Condition	EA % as Na_2O	Sulfidity % as Na_2O	Maximum Temperature	H-Factor	Kappa Number
5-1	13.0	15.2	175.0	1200	85.7
5-2	13.0	15.2	175.0	1400	77.7
5-3	13.0	15.2	175.0	1600	69.9
5-4	13.0	15.2	175.0	1800	66.0
5-5	13.0	15.2	175.0	2000	59.1
5-6	13.0	15.2	175.0	2200	51.9
6-1	19.0	15.2	175.0	400	115.9
6-2	19.0	15.2	175.0	600	77.6
6-3	19.0	15.2	175.0	800	59.2
6-4	19.0	15.2	175.0	1000	46.6
6-5	19.0	15.2	175.0	1200	36.9
6-6	19.0	15.2	175.0	1400	29.7
7-1	13.0	44.8	175.0	400	105.7
7-2	13.0	44.8	175.0	600	76.8
7-3	13.0	44.8	175.0	800	63.1
7-4	13.0	44.8	175.0	1000	52.7
7-5	13.0	44.8	175.0	1200	45.5
7-6	13.0	44.8	175.0	1400	37.9
8-1	19.0	44.8	175.0	400	48.9
8-2	19.0	44.8	175.0	600	31.2
8-3	19.0	44.8	175.0	800	23.8
8-4	19.0	44.8	175.0	1000	21.2
8-5	19.0	44.8	175.0	1200	17.8
8-6	19.0	44.8	175.0	1400	15.8

Table A-2-3. Conditions and kappa numbers used for regression model.

Condition	EA % as Na_2O	Sulfidity % as Na_2O	Maximum Temperature	H-Factor	Kappa Number
9-1	11.0	30.0	170.0	1000	103.5
9-2	11.0	30.0	170.0	1200	99.2
9-3	11.0	30.0	170.0	1400	88.4
9-4	11.0	30.0	170.0	1600	84.3
9-5	11.0	30.0	170.0	1800	79.0
9-6	11.0	30.0	170.0	2000	71.3
10-1	21.1	30.0	170.0	400	55.3
10-2	21.1	30.0	170.0	600	32.3
10-3	21.1	30.0	170.0	800	26.9
10-4	21.1	30.0	170.0	1000	20.8
10-5	21.1	30.0	170.0	1200	17.9
10-6	21.1	30.0	170.0	1400	14.9
11-1	16.0	5.1	170.0	1200	103.3
11-2	16.0	5.1	170.0	1400	84.3
11-3	16.0	5.1	170.0	1600	79.3
11-4	16.0	5.1	170.0	1800	73.0
11-5	16.0	5.1	170.0	2000	66.2
11-6	16.0	5.1	170.0	2200	53.7
12-1	16.0	54.9	170.0	400	65.0
12-2	16.0	54.9	170.0	600	44.1
12-3	16.0	54.9	170.0	800	31.0
12-4	16.0	54.9	170.0	1000	25.5
12-5	16.0	54.9	170.0	1200	23.0
12-6	16.0	54.9	170.0	1400	18.6

Table A-2-4. Conditions and kappa numbers used for regression model.

Condition	EA % as Na_2O	Sulfidity % as Na_2O	Maximum Temperature	H-Factor	Kappa Number
13-1	16.0	30.0	161.6	400	101.5
13-2	16.0	30.0	161.6	600	65.5
13-3	16.0	30.0	161.6	800	47.9
13-4	16.0	30.0	161.6	1000	41.3
13-5	16.0	30.0	161.6	1200	34.4
13-6	16.0	30.0	161.6	1400	27.6
14-1	16.0	30.0	178.4	400	100.8
14-2	16.0	30.0	178.4	600	69.0
14-3	16.0	30.0	178.4	800	52.3
14-4	16.0	30.0	178.4	1000	47.6
14-5	16.0	30.0	178.4	1200	36.3
14-6	16.0	30.0	178.4	1400	29.2
15-1	16.0	30.0	170.0	400	99.6
15-2	16.0	30.0	170.0	600	70.0
15-3	16.0	30.0	170.0	800	52.5
15-4	16.0	30.0	170.0	1000	43.4
15-5	16.0	30.0	170.0	1200	34.3
15-6	16.0	30.0	170.0	1400	28.0
16-1	15.0	15.2	165.0	1200	49.3
16-2	15.0	15.2	165.0	1350	51.6
16-3	15.0	15.2	165.0	1500	38.8
16-4	15.0	15.2	165.0	1650	39.9
16-5	15.0	15.2	165.0	1800	35.8
16-6	15.0	15.2	165.0	1950	32.7

Table A-2-5. Conditions and kappa numbers used for regression model.

Condition	EA % as Na_2O	Sulfidity % as Na_2O	Maximum Temperature	H-Factor	Kappa Number
17-1	21.0	15.2	165.0	1200	22.6
17-2	21.0	15.2	165.0	1350	21.9
17-3	21.0	15.2	165.0	1500	21.8
17-4	21.0	15.2	165.0	1650	19.6
17-5	21.0	15.2	165.0	1800	13.8
17-6	21.0	15.2	165.0	1950	17.4
18-1	15.0	44.8	165.0	1200	24.2
18-2	15.0	44.8	165.0	1350	24.0
18-3	15.0	44.8	165.0	1500	23.4
18-4	15.0	44.8	165.0	1650	20.7
18-5	15.0	44.8	165.0	1800	14.3
18-6	15.0	44.8	165.0	1950	18.3
19-1	21.0	44.8	165.0	960	20.3
19-2	21.0	44.8	165.0	1200	15.1
19-3	21.0	44.8	165.0	1350	14.8
19-4	21.0	44.8	165.0	1650	13.5
19-5	21.0	44.8	165.0	1800	12.7
20-1	15.0	15.2	175.0	1200	54.0
20-2	15.0	15.2	175.0	1350	49.8
20-3	15.0	15.2	175.0	1500	39.8
20-4	15.0	15.2	175.0	1650	43.3
20-5	15.0	15.2	175.0	1800	38.7

Table A-2-6. Conditions and kappa numbers used for regression model.

Condition	EA % as Na_2O	Sulfidity % as Na_2O	Maximum Temperature	H-Factor	Kappa Number
21-1	13.0	15.2	165.0	1400	78.7
21-2	13.0	15.2	165.0	1800	63.0
21-3	13.0	15.2	165.0	2200	54.8
22-1	19.0	15.2	165.0	600	71.6
22-2	19.0	15.2	165.0	1000	47.2
22-3	19.0	15.2	165.0	1400	28.7
23-1	13.0	44.8	165.0	600	77.0
23-2	13.0	44.8	165.0	1000	51.1
23-3	13.0	44.8	165.0	1400	36.1
24-1	19.0	44.8	165.0	400	47.9
24-2	19.0	44.8	165.0	800	24.2
24-3	19.0	44.8	165.0	1200	16.5

Table A-2-7. Conditions and kappa numbers used for model validation and cooked in the M-K Digesters.

Condition	EA % as Na_2O	Sulfidity % as Na_2O	Maximum Temperature	H-Factor	Kappa Number
1	13.6	30.0	170.0	1294	39.6
2	20.4	30.0	170.0	1293	14.8
3	18.7	30.0	170.0	1807	13.8
4	17.0	30.0	170.0	1285	25.8
5	15.3	30.0	170.0	1781	20.3
6	17.0	30.0	170.0	1784	16.4
7	18.7	30.0	170.0	1287	15.8
8	15.3	30.0	170.0	1323	26.2
9	20.4	30.0	170.0	1795	11.8
10	11.9	30.0	170.0	1046	81.5
11	11.9	30.0	170.0	1298	75.3
12	11.9	30.0	170.0	1532	62.6
13	11.1	30.0	170.0	1037	88
14	11.9	30.0	170.0	831	86.5
15	13.6	30.0	170.0	1050	52.9
16	15.7	30.0	170.0	1435	31.7
17	15.7	30.0	170.0	1443	30.7

16.2 Summary of Experimental Conditions

Table A-2-8. Constant kappa number (approximately 30) conditions for pulps produced from unextracted wood chips.

Condition	Alias	EA % as Na_2O	Sulfidity % as Na_2O	Maximum Temperature	H-Factor
1	31	16.0	30.0	165.0	1294
2	32	20.0	30.0	165.0	790
3	33	16.0	50.0	165.0	929
4	34	20.0	50.0	165.0	570
5	35	16.0	30.0	175.0	1294
6	36	20.0	30.0	175.0	790
7	37	16.0	50.0	175.0	929
8	38	20.0	50.0	175.0	522
9	39	14.6	40.0	170.0	1352
10	40	21.4	40.0	170.0	565
11	41	18.0	23.2	170.0	1217
12	42	18.0	56.8	170.0	646
13	43	18.0	40.0	161.6	806
14	44	18.0	40.0	178.4	806
15	45	18.0	40.0	170.0	806
16	46	18.0	40.0	170.0	806
17	47	18.0	40.0	170.0	806
18	48	18.0	40.0	170.0	806
19	49	18.0	40.0	170.0	806
20	50	18.0	40.0	170.0	806

Table A-2-9. Constant kappa number (approximately 30) conditions for pulps produced from extracted wood chips.

Condition	Alias	EA % as Na_2O	Sulfidity % as Na_2O	Maximum Temperature	H-Factor
1	51	16.0	30.0	165.0	1335
2	52	20.0	30.0	165.0	803
3	53	16.0	50.0	165.0	929
4	54	20.0	50.0	165.0	516
5	55	16.0	30.0	175.0	1335
6	56	20.0	30.0	175.0	803
7	57	16.0	50.0	175.0	929
8	58	20.0	50.0	175.0	550
9	59	14.6	40.0	170.0	1352
10	60	21.4	40.0	170.0	590
11	61	18.0	23.2	170.0	1217
12	62	18.0	56.8	170.0	620
13	63	18.0	40.0	161.6	806
14	64	18.0	40.0	178.4	806
15	65	18.0	40.0	170.0	806
16	66	18.0	40.0	170.0	806
17	67	18.0	40.0	170.0	806
18	68	18.0	40.0	170.0	806
19	69	18.0	40.0	170.0	806
20	70	18.0	40.0	170.0	806

16.3 Wood Chip Properties

Table A-2-10. Extractives content of the wood chips employed in these studies

Condition	Extractives (%)
Extracted, washed	0.049
Extracted, unwashed	0.060
Unextracted, unwashed	1.81

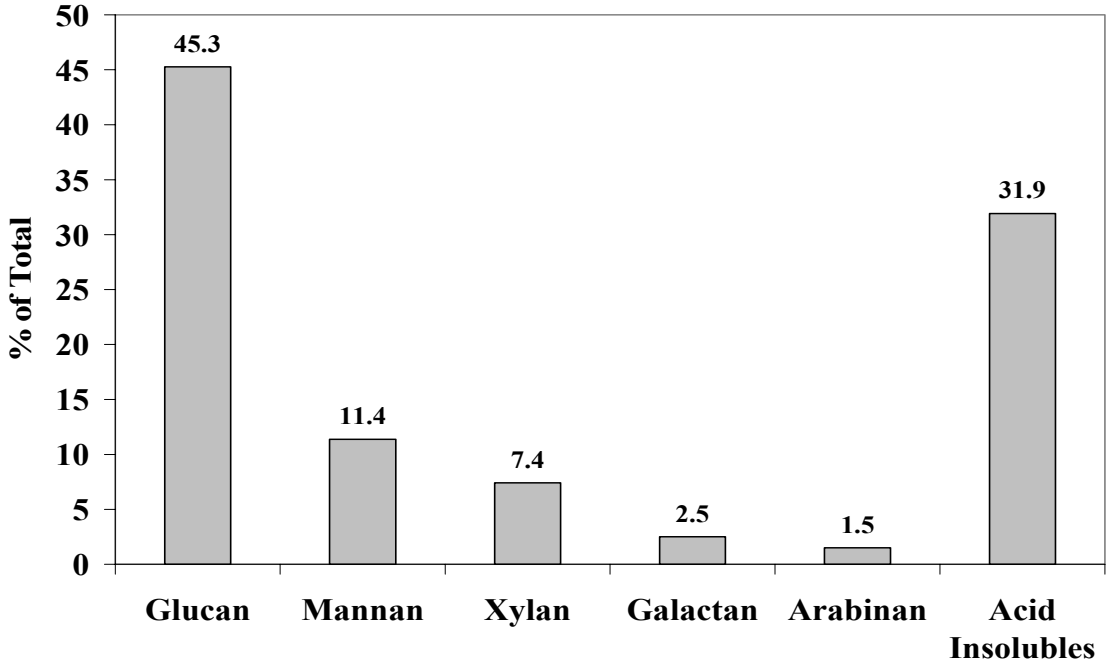

Figure A-2-1. Carbohydrate analysis of *Pinus taeda* wood chips employed in this study.

Table A-2-11. Metals contents of wood chips employed in this study. Metals contents are in units of mg/kg.

Metals	Extracted and Washed	Extracted and Unwashed	Unextracted and Unwashed
Cr	0.1	0.1	0.1
Mn	112.7	89.4	88.0
Fe	5.8	5.0	7.1
Co	0.1	0.1	0.1
Ni	0.2	0.2	0.2
Cu	0.8	0.9	0.9
Zn	9.4	7.8	6.8
Al	6.9	7.2	8.9
B	2.3	1.9	2.2
Si	7.6	8.0	9.7
P	32.2	43.8	40.8
S	62.6	80.3	81.9
Se	2.0	2.0	2.0
As	1.6	1.6	1.5
Mo	0.3	0.3	0.3
Sn	0.8	0.8	0.8
Sb	0.9	0.9	0.9
Pb	1.0	1.0	0.9
Tl	2.1	2.1	2.0
Sr	3.0	2.6	2.6
Ba	7.6	4.2	4.9
Na	6.0	4.3	4.0
Mg	163.5	169.6	151.4
K	519.9	619.6	487.9
Ca	638.6	627.9	572.4

16.4 Extractives Properties in Kraft Pulps

Table A-2-12. Extractives present in the constant kappa number (approximately 30) pulps and their relative abundance.

Extractive	Trial #1 (%)	Trial #2 (%)	Trial #3 (%)	Average (%)
Glycerol	2.1	0.0	0.0	0.7
Vanillin	13.7	10.9	13.5	12.7
Vanillyl Alcohol	0.0	0.0	0.0	0.6
Vanillic acid	5.3	8.4	1.7	8.5
3-[4-Hydroxy-3-methoxyphenyl]-propanol	2.6	4.5	11.7	3.4
Tetradecanoic acid	0.0	2.9	3.1	1.9
Unidentified Compound	7.4	11.9	3.0	9.2
Unidentified Compound	7.9	11.8	8.2	6.6
Hexadecanoic acid	9.3	20.9	0.0	15.4
Octadecenoic acid	4.8	13.1	16.1	10.1
Octadecanoic acid	3.6	8.7	12.3	7.2
Unidentified compound	17.4	0.0	9.3	11.8
Stearin	2.7	6.8	3.0	4.2

Table A-2-13. Extractives content of the constant kappa number (approximately 30) pulps produced from unextracted wood chips.

Condition	Alias	Extractives (%)
1	31	0.025
2	32	0.037
3	33	0.041
4	34	0.029
5	35	0.045
6	36	0.027
7	37	0.052
8	38	0.078
9	39	0.041
10	40	0.051
11	41	0.044
12	42	0.045
13	43	0.050
14	44	0.041
15	45	0.058
16	46	0.021
17	47	0.045
18	48	0.023
19	49	0.055
20	50	0.016

Table A-2-14. Extractives content of the constant kappa number pulps produced from extracted wood chips.

Condition	Alias	Extractives (%)
1	51	0.026
2	52	0.028
3	53	0.022
4	54	0.032
5	55	0.034
6	56	0.029
7	57	0.021
8	58	0.025
9	59	0.022
10	60	0.025
11	61	0.033
12	62	0.030
13	63	0.025
14	64	0.034
15	65	0.032
16	66	0.012
17	67	0.036
18	68	0.025
19	69	0.028
20	70	0.033

16.5 Summary of Pulp Properties

Table A-2-15. Elemental analysis of selected pulps from the constant kappa number (approximately 30) series of pulps produced from unextracted and extracted wood chips.

Condition	Alias	Extracted Wood Chips (y/n)	C (%)	H (%)	N (%)	S (%)
4	31	n	43.40	5.96	0.00	0.09
11	42	n	43.41	6.41	0.00	0.08
12	43	n	43.42	6.43	0.00	0.08
15	45	n	43.65	6.24	0.00	0.07
16	46	n	43.60	6.40	0.00	0.07
4	54	y	43.16	6.06	0.00	0.09
11	61	y	43.19	6.35	0.00	0.07
12	62	y	43.28	6.00	0.00	0.07
15	65	y	43.46	6.40	0.00	0.07
16	66	y	43.19	5.99	0.00	0.06

Table A-2-16. Carbohydrate analysis of the constant kappa (approximately 30) number series of pulps produced from unextracted wood chips. The pulping conditions are summarized in Table A-2-8.

Condition	Arabinan (%)	Xylan (%)	Mannan (%)	Galactan (%)	Glucan (%)	Acid Insoluble (%)
1	0.8	9.3	6.0	0.4	79.0	4.4
2	0.6	7.6	6.3	0.5	80.8	4.1
3	0.8	9.0	6.2	0.5	79.4	4.1
4	0.7	7.4	6.7	0.4	80.3	4.5
5	0.7	8.6	6.1	0.5	79.9	4.2
6	0.6	7.1	6.5	0.4	80.9	4.4
7	0.8	8.8	5.7	0.4	79.9	4.3
8	0.7	7.0	6.5	0.5	80.4	4.8
9	0.8	9.2	5.7	0.5	79.3	4.5
10	0.6	6.8	6.5	0.5	80.5	5.0
11	0.6	8.1	6.4	0.4	80.2	4.2
12	0.7	8.0	6.0	0.4	80.6	4.2
13	0.8	8.1	6.3	0.4	80.1	4.2
14	0.6	7.7	5.9	0.5	80.8	4.4
15	0.9	8.1	6.0	0.4	80.4	4.1
16	0.7	7.5	6.2	0.4	80.6	4.6
17	0.8	7.8	6.5	0.4	80.1	4.4
18	0.8	7.9	6.2	0.5	80.4	4.3

Table A-2-17. Hexenuronic and carboxylic acid group analysis of the constant kappa number (approximately 30) series of pulps produced from unextracted wood chips. The pulping conditions are summarized in Tables A-2-8 and A-2-9.

Condition	HexA (μmol/g pulp)	Carboxylic Acid (μmol/g pulp)
1	35.9	70.2
2	25.2	55.6
3	47.0	74.8
4	33.9	57.5
5	34.9	66.6
6	23.1	53.9
7	42.1	78.4
8	33.3	61.0
9	46.5	87.5
10	28.0	60.4
11	24.3	56.8
12	40.6	62.1
13	37.9	71.5
14	32.7	66.1
15	33.3	64.1
16	34.0	65.4
17	34.6	71.0
18	33.2	64.5
19	35.5	70.1
20	35.1	68.7

Table A-2-18. Hexenuronic and carboxylic acid group analysis of the constant kappa number (approximately 30) series of pulps produced from extracted wood chips. The pulping conditions are summarized in Table A-2-8.

Condition	HexA (μmol/g pulp)	Carboxylic Acid (μmol/g pulp)
1	36.2	70.3
2	24.0	57.1
3	44.6	76.9
4	34.7	58.4
5	33.5	70.0
6	21.2	51.9
7	43.3	73.8
8	31.5	65.2
9	44.8	77.4
10	24.1	54.3
11	22.7	59.3
12	36.7	70.3
13	34.9	68.4
14	31.5	63.6
15	33.6	68.2
16	33.8	68.4
17	34.5	67.4
18	31.3	58.5
19	33.0	56.3
20	34.6	70.6

Table A-2-19. Kappa number, brightness, and chromophore index of the constant kappa number (approximately 30) series of pulps produced from unextracted wood chips. The pulping conditions are summarized in Table A-2-8.

Condition	Kappa Number	Brightness (%)	Chromophore Index
1	28.8	29.2 ± 0.19	119.7 ± 2.5
2	28.4	32.1 ± 0.19	102.8 ± 0.9
3	27.6	28.2 ± 0.43	131.2 ± 3.1
4	30.6	30.3 ± 0.32	115.3 ± 3.9
5	28.9	29.2 ± 0.51	121.7 ± 2.0
6	29.9	30.8 ± 0.32	108.8 ± 0.7
7	29.6	27.7 ± 0.55	136.7 ± 2.2
8	30.9	31.2 ± 0.41	110.7 ± 2.7
9	28.2	27.5 ± 0.15	141.1 ± 2.0
10	29.7	31.6 ± 0.19	107.7 ± 1.6
11	27.8	30.2 ± 0.28	115.0 ± 1.3
12	28.25	30.6 ± 0.23	115.0 ± 1.7
13	30.3	29.9 ± 0.34	117.9 ± 0.9
14	27.8	30.6 ± 0.17	112.3 ± 0.8
15	29.1	30.5 ± 0.43	111.6 ± 0.8
16	29.7	30.1 ± 0.43	112.5 ± 0.7
17	30.9	29.9 ± 0.43	112.9 ± 1.9
18	28.1	31.1 ± 0.43	103.5 ± 1.2
19	30.3	30.0 ± 0.43	109.8 ± 3.6
20	28.6	30.6 ± 0.43	106.6 ± 4.0

Table A-2-20. Kappa number, brightness, and chromophore index of the constant kappa number (approximately 30) series of pulps produced from extracted wood chips. The pulping conditions are summarized in Table A-2-9.

Condition	Kappa Number	Brightness (%)	Chromophore Index
1	27.9	28.7 ± 0.66	119.0 ± 2.5
2	27.8	31.3 ± 0.43	103.1 ± 0.9
3	28.2	28.9 ± 0.34	119.9 ± 3.1
4	29.7	31.0 ± 0.21	106.9 ± 3.9
5	28.0	30.2 ± 0.58	104.6 ± 2.0
6	26.9	32.2 ± 0.70	94.4 ± 0.7
7	28.3	28.4 ± 0.55	120.0 ± 2.2
8	30.5	30.5 ± 0.23	108.6 ± 2.7
9	27.7	27.8 ± 0.53	128.5 ± 2.0
10	27.8	31.7 ± 0.32	99.9 ± 1.6
11	27.3	31.1 ± 0.30	101.4 ± 1.3
12	28.8	30.7 ± 0.26	105.5 ± 1.7
13	28.5	29.6 ± 0.43	115.0 ± 0.9
14	26.9	30.5 ± 0.60	106.4 ± 0.8
15	28.1	29.8 ± 0.35	111.1 ± 0.8
16	28.7	30.4 ± 0.35	105.8 ± 0.7
17	30.4	30.3 ± 0.35	104.9 ± 1.9
18	27.9	30.4 ± 0.35	108.7 ± 1.2
19	29.3	29.9 ± 0.35	110.3 ± 3.6
20	27.6	30.7 ± 0.35	103.1 ± 4.0

Table A-2-21. Contribution of each color component to the chromophore index for pulps from the constant kappa number (approximately 30) series. Table A-2-8 summarizes the pulping conditions for this series.

Condition	% Violet	% Blue	% Cyan	% Green	% Yellow	% Orange	% Red
1	28.9	34.3	7.0	12.5	5.0	5.3	7.1
2	29.6	34.4	6.9	12.3	4.8	5.1	6.7
3	28.2	33.9	7.0	12.8	5.1	5.5	7.5
4	28.6	34.1	7.1	12.8	5.0	5.3	7.0
5	29.4	34.4	6.9	12.3	4.9	5.2	7.0
6	29.8	344	6.9	12.3	4.8	5.1	6.7
7	27.7	33.7	7.1	13.0	5.2	5.6	7.7
8	29.1	34.2	7.0	12.7	5.0	5.2	6.9
9	27.3	33.6	7.1	13.1	5.3	5.7	7.9
10	29.5	34.3	7.0	12.5	4.9	5.1	6.7
11	30.7	34.6	6.7	11.9	4.7	4.9	6.4
12	28.5	34.0	7.1	12.8	5.1	5.4	7.1
13	29.1	343.2	7.0	12.5	5.	5.3	7.0
14	29.2	34.2	6.9	12.4	4.9	5.3	7.0
15	29.5	34.3	6.9	12.4	4.9	5.2	6.8
16	29.4	34.4	6.9	12.4	4.9	5.2	6.8
17	29.0	34.3	7.0	12.6	5.0	5.3	6.9
18	29.6	34.6	7.0	12.4	4.8	5.1	6.6
19	29.0	34.3	7.0	12.6	5.0	5.3	6.9
20	28.7	34.2	7.1	12.8	5.0	5.3	6.9

Table A-2-22. Unscreened and screened yields for the constant kappa number (approximately 30) pulps produced from unextracted wood chips. The pulping conditions are summarized in Table A-2-8.

Condition	Unscreened Yield (%)	Screened Yield (%)
1	43.7	43.7
2	43.4	43.4
3	44.3	44.3
4	44.5	44.5
5	43.5	43.5
6	42.5	42.5
7	446	44.5
8	43.8	43.8
9	44.7	44.7
10	43.1	43.1
11	43.1	43.1
12	42.9	42.9
13	43.4	43.4
14	43.6	43.6
15	44.0	44.0
16	43.4	43.1
17	43.9	43.9
18	43.1	43.1
19	43.1	43.1
20	43.0	43.0

Table A-2-23. Unscreened and screened yields for the constant kappa number (approximately 30) pulps produced from extracted wood chips. The pulping conditions are summarized in Table A-2-9.

Condition	Unscreened Yield (%)	Screened Yield (%)
1	44.8	44.7
2	45.2	45.2
3	44.6	44.6
4	45.2	45.1
5	45.2	45.2
6	44.2	44.2
7	45.7	45.7
8	44.4	44.4
9	45.4	45.4
10	43.8	43.8
11	44.6	44.6
12	45.5	45.5
13	45.5	45.5
14	44.7	44.7
15	45.2	45.2
16	44.9	44.9
17	44.9	44.9
18	44.3	44.3
19	45.0	45.0
20	44.5	44.5

Table A-2-24. Viscosity for the constant kappa number (approximately 30) pulps produced from unextracted softwood chips. The pulping conditions are summarized in Table A-2-8.

Condition	Viscosity (cP)
1	29.5
2	29.4
3	39.2
4	39.9
5	33.0
6	25.8
7	35.7
8	33.7
9	37.1
10	30.0
11	24.8
12	34.6
13	33.2
14	28.1
15	34.7
16	38.5
17	40.7
18	32.4
19	33.8
20	29.7

16.6 Summary of Residual Alkali from Kraft Cooks

Table A-2-25. Residual alkali for constant kappa number (approximately 30) pulps produced from unextracted wood chips. The pulping conditions are summarized in Table A-2-8.

Condition	Residual NaOH (g Na_2O/L)	Residual Na_2S (g Na_2O/L)	Residual AA (g Na_2O/L)	Residual EA (g Na_2O/L)
1	10.6	9.5	20.1	15.3
2	17.5	11.9	29.4	23.5
3	5.4	19.6	25.0	15.2
4	12.4	23.9	36.3	24.3
5	10.1	8.9	19.0	14.5
6	16.9	12.4	29.3	23.1
7	5.4	18.9	24.3	14.8
8	12.7	26.4	39.1	25.9
9	5.6	12.3	18.0	11.8
10	16.8	20.4	37.2	27.0
11	12.8	9.0	21.8	17.3
12	7.0	26.5	33.4	20.2
13	12.2	16.1	28.3	20.3
14	12.1	15.7	27.8	19.9
15	12.4	15.4	27.9	20.1
16	12.6	15.7	28.4	20.5
17	12.1	16.1	28.2	20.2
18	12.0	16.1	28.0	20.0
19	12.9	15.4	28.3	20.6
20	12.5	16.2	28.6	20.5

16.7 T-Tests on Pulps Produced from Unextracted and Extracted Wood Chips

Table A-2-26. T-test to compare means of extractives contents of pulps produced from unextracted and extracted wood chips. The pulping conditions are summarized in Tables A-2-8 and A-2-9.

	Unextracted Wood Chips	**Extracted Wood Chips**
Average	0.04	0.03
Standard Deviation	0.01	0.01
# of Samples	20	20
Pooled S.D.	0.01	
H_0:	$\mu_1 = \mu_2$	
H_1:	$\mu_1 > \mu_2$ or $\mu_1 < \mu_2$	
α=	0.05	
Critical region:	$t > 2.0252$ with $\nu = 38$	
t value (calculated)	3.83	
Conclusion:	Reject H_0 Means are statistically different at 95% C.I.	

Table A-2-27. T-test to compare means of kappa numbers of pulps produced from unextracted and extracted wood chips using center points from central composite design. The kappa numbers are summarized in Tables A-2-19 and A-2-20.

	Unextracted Wood Chips	**Extracted Wood Chips**
Average	29.4	28.7
Standard Deviation	1.06	1.05
# of Samples	6	6
Pooled S.D.	1.06	
H_0:	$\mu_1 = \mu_2$	
H_1:	$\mu_1 > \mu_2$ or $\mu_1 < \mu_2$	
α=	0.05	
Critical region:	$t > 2.228$ with $\nu = 10$	
t value (calculated)	1.24	
Conclusion:	Accept H_0 Means are statistically equivalent at 95% C.I.	

Table A-2-28. T-test to compare means of hexenuronic acid content of pulps produced from unextracted and extracted wood chips using center points from central composite design. The hexenuronic acid contents are summarized in Table A-2- 17 and A-2-18.

	Unextracted Wood Chips	**Extracted Wood Chips**
Average	34.3	33.5
Standard Deviation	0.96	1.22
# of Samples	6	6
Pooled S.D.	1.09	
H_0:	$\mu_1 = \mu_2$	
H_1:	$\mu_1 > \mu_2$ or $\mu_1 < \mu_2$	
α=	0.05	
Critical region:	$t > 2.228$ with $\nu = 10$	
t value (calculated)	1.26	
Conclusion:	Accept H_0 Means are statistically equivalent at 95% C.I.	

Table A-2-29. T-test to compare means of carboxylic acid content of pulps produced from unextracted and extracted wood chips using center points from central composite design. The carboxylic acid contents are summarized in Tables A-2- 17 and A-2-18.

	Unextracted Wood Chips	**Extracted Wood Chips**
Average	67.3	64.9
Standard Deviation	3.01	5.96
# of Samples	6	6
Pooled S.D.	4.73	
H_0:	$\mu_1 = \mu_2$	
H_1:	$\mu_1 > \mu_2$ or $\mu_1 < \mu_2$	
α=	0.05	
Critical region:	$t > 2.228$ with $\nu = 10$	
t value (calculated)	0.88	
Conclusion:	Accept H_0 Means are statistically equivalent at 95% C.I.	

Table A-2-30. T-test to compare means of screened and unscreened yields of pulps produced from unextracted and extracted wood chips. The unscreened and screened yields are summarized in Tables A-2-21 and A-2-22.

	Unextracted Wood Chips	Extracted Wood Chips
Average	43.6	44.9
Standard Deviation	0.60	0.49
# of Samples	40	40
Pooled S.D.	0.55	
H_0:	$\mu_1 = \mu_2$	
H_1:	$\mu_1 > \mu_2$ or $\mu_1 < \mu_2$	
α=	0.05	
Critical region:	$t > 1.994$ with $\nu = 78$	
t value (calculated)	10.63	
Conclusion:	Reject H_0 Means are statistically different at 95% C.I.	

Table A-2-31. T-test to compare means of brightness of pulps produced from unextracted and extracted wood chips. The brightness values are summarized in Tables A-2-19 and A-2-20.

	Unextracted Wood Chips	**Extracted Wood Chips**
Average	30.1	30.2
Standard Deviation	1.21	1.10
# of Samples	20	20
Pooled S.D.	1.16	
H_0:	$\mu_1 = \mu_2$	
H_1:	$\mu_1 > \mu_2$ or $\mu_1 < \mu_2$	
α=	0.05	
Critical region:	$t > 2.0252$ with $\nu = 38$	
t value (calculated)	0.42	
Conclusion:	Accept H_0 Means are statistically equivalent at 95% C.I.	

Table A-2-32. T-test to compare means of chromophore index of pulps produced from unextracted and extracted wood chips. The chromophore index values are summarized in Tables A-2-19 and A-2-20.

	Unextracted Wood Chips	**Extracted Wood Chips**
Average	115.6	108.9
Standard Deviation	10.3	8.1
# of Samples	20	20
Pooled S.D.	9.3	
H_0:	$\mu_1 = \mu_2$	
H_1:	$\mu_1 > \mu_2$ or $\mu_1 < \mu_2$	
α=	0.05	
Critical region:	$t > 2.0252$ with $\nu = 38$	
t value (calculated)	2.32	
Conclusion:	Reject H_0 Means are statistically different at 95% C.I.	

17. APPENDIX 3. SUPPORTING DATA FOR CHAPTER #3

17.1 Summary of Experimental Conditions

Table A-3-1. Incremental cook conditions. Condition A pulps were produced under high effective alkali, low sulfidity while Condition B pulps were produced under low effective alkali, high sulfidity conditions.

Condition	Alias	EA, %	Sulfidity, %	Temperature (ºC)	H-factor
A-1	71-1	21.4	23.2	170.0	120
A-2	71-2	21.4	23.2	170.0	240
A-3	71-3	21.4	23.2	170.0	360
A-4	71-4	21.4	23.2	170.0	480
A-5	71-5	21.4	23.2	170.0	600
A-6	71-6	21.4	23.2	170.0	720
A-7	71-7	21.4	23.2	170.0	840
A-8	71-8	21.4	23.2	170.0	863
B-1	72-1	14.6	56.8	170.0	120
B-2	72-2	14.6	56.8	170.0	240
B-3	72-3	14.6	56.8	170.0	360
B-4	72-4	14.6	56.8	170.0	480
B-5	72-5	14.6	56.8	170.0	600
B-6	72-6	14.6	56.8	170.0	720
B-7	72-7	14.6	56.8	170.0	840
B-8	72-8	14.6	56.8	170.0	960
B-9	72-9	14.6	56.8	170.0	1080
B-10	72-10	14.6	56.8	170.0	1151

17.2 Summary of Pulp Properties

Table A-3-2. Incremental cook kappa number and klason lignin content. The pulping conditions are summarized in Table A-3-1.

Condition	Kappa Number	Klason Lignin (%)
Wood	-	29.1
A-1	162.8	21.8
A-2	129.7	16.5
A-3	88.5	11.4
A-4	69.2	9.1
A-5	52.2	6.5
A-6	37.9	4.7
A-7	30.5	4.2
A-8	28.8	3.9
B-1	152.0	20.3
B-2	118.4	15.3
B-3	93.1	11.6
B-4	69.5	8.6
B-5	56.1	5.8
B-6	44.1	5.3
B-7	36.5	5.2
B-8	32.5	4.3
B-9	30.3	3.8
B-10	27.7	3.5

Table A-3-3. Incremental cook unscreened and screened pulp yields. The pulping conditions are summarized in Table A-3-1.

Condition	Unscreened Yield (%)	Screened Yield (%)
A-1	60.1	59.9
A-2	54.4	54.4
A-3	50.2	50.2
A-4	46.7	46.7
A-5	44.6	44.6
A-6	43.0	43.0
A-7	42.0	42.0
A-8	41.8	41.8
B-1	61.0	60.7
B-2	55.2	55.1
B-3	52.2	52.2
B-4	47.7	47.7
B-5	46.6	46.5
B-6	45.2	45.2
B-7	46.2	46.2
B-8	45.2	45.2
B-9	44.2	44.2
B-10	43.7	43.7

Table A-3-4. Incremental cook hexenuronic and carboxylic acid group content. The pulping conditions are summarized in Table A-3-1.

Condition	HexA (μmol/g pulp)	Carboxylic Acid (μmol/g pulp)
A-1	47.4	184.0
A-2	45.6	161.9
A-3	39.1	131.6
A-4	34.1	112.2
A-5	28.5	83.9
A-6	22.9	66.4
A-7	19.7	58.8
A-8	18.9	61.2
B-1	33.9	205.5
B-2	44.6	183.8
B-3	50.5	170.5
B-4	53.2	146.2
B-5	56.8	134.2
B-6	56.7	127.7
B-7	54.9	118.0
B-8	53.9	104.6
B-9	53.7	103.5
B-10	51.9	96.3

Table A-3-5. Incremental cook brightness and chromophore index responses. The pulping conditions are summarized in Table A-3-1.

Condition	Brightness (%)	Chromophore Index
A-1	17.4 ± 0.4	245.5 ± 3.9
A-2	19.6 ± 0.1	211.3 ± 3.7
A-3	22.2 ± 0.2	173.0 ± 3.1
A-4	24.9 ± 0.4	147.9 ± 1.9
A-5	27.1 ± 0.7	128.5 ± 1.5
A-6	29.4 ± 0.3	112.4 ± 0.3
A-7	30.8 ± 0.3	104.5 ± 3.0
A-8	29.8 ± 0.4	112.7 ± 2.3
B-1	17.0 ± 0.1	260.1 ± 4.1
B-2	18.0 ± 0.2	244.8 ± 3.0
B-3	19.1 ± 0.2	224.0 ± 3.0
B-4	20.7 ± 0.1	201.8 ± 2.5
B-5	22.5 ± 0.1	175.5 ± 2.6
B-6	24.0 ± 0.4	155.6 ± 1.8
B-7	23.2 ± 0.2	162.8 ± 2.5
B-8	24.8 ± 0.3	147.3 ± 2.9
B-9	25.3 ± 0.3	141.2 ± 1.6
B-10	25.2 ± 0.3	141.9 ± 1.6

Table A-3-6. Carbohydrate analysis of the incremental cook series of pulps. The pulping conditions are summarized in Table A-3-1.

Condition	Arabinan (%)	Xylan (%)	Mannan (%)	Galactan (%)	Glucan (%)	Acid Insoluble (%)
A-1	1.1	7.7	5.9	1.3	60.2	23.8
A-3	0.8	6.6	6.8	0.7	72.8	12.2
A-5	0.6	6.6	7.3	0.6	77.9	6.9
A-7	0.5	7.3	6.7	0.6	80.7	4.3
B-1	1.4	9.3	5.4	1.1	60.7	22.0
B-3	1.0	9.0	5.5	0.9	70.8	12.7
B-5	1.0	9.5	6.0	0.7	75.6	7.1
B-10	0.8	9.8	5.9	0.5	79.4	3.5

Table A-3-7. Contribution of each color component to the chromophore index. The pulping conditions are summarized in Table A-3-1.

Condition	% Violet	% Blue	% Cyan	% Green	% Yellow	% Orange	% Red
A-1	28.1	32.8	6.6	11.8	4.6	4.8	11.3
A-2	27.8	32.5	6.6	11.9	4.6	4.9	11.6
A-3	28.1	32.6	6.5	11.7	4.6	4.9	11.5
A-4	27.7	32.4	6.6	11.9	4.7	5.0	11.7
A-5	27.9	32.4	6.6	11.8	4.7	5.0	11.7
A-6	26.8	32.2	6.6	12.0	4.8	5.2	12.3
A-7	26.7	32.1	6.6	12.1	4.9	5.2	12.4
A-8	25.6	31.5	6.7	12.5	5.1	5.5	13.2
B-1	25.2	31.6	7.0	13.1	5.1	5.3	12.7
B-2	24.4	31.0	7.0	13.2	5.2	5.6	13.6
B-3	24.2	30.9	6.9	13.1	5.3	5.7	13.8
B-4	23.8	30.8	7.0	13.2	5.3	5.8	14.1
B-5	23.7	30.7	6.9	13.2	5.3	5.8	14.3
B-6	23.7	30.8	6.9	13.1	5.3	5.8	14.4
B-7	23.4	30.6	6.9	13.1	5.4	5.9	14.6
B-8	23.3	30.6	6.9	13.1	5.4	6.0	14.7
B-9	23.4	30.7	6.9	13.1	5.4	6.0	14.7
B-10	22.9	30.5	6.9	13.2	5.5	6.1	15.0

17.3 Summary of Residual Alkali from Kraft Cooks

Table A-3-8. Residual alkali for incremental cook series of pulps. The pulping conditions are summarized in Table A-3-1.

Condition	Residual NaOH (g Na_2O/L)	Residual Na_2S (g Na_2O/L)	Residual AA (g Na_2O/L)	Residual EA (g Na_2O/L)
A-1	26.5	9.1	35.6	31.0
A-2	24.9	8.3	33.2	29.1
A-3	24.5	8.2	32.7	28.6
A-4	23.5	8.2	31.7	27.6
A-5	23.1	7.9	31.0	27.1
A-6	22.0	7.8	29.8	25.9
A-7	21.9	7.5	39.4	25.7
A-8	21.5	7.9	29.5	25.5
B-1	4.9	23.1	28.1	16.5
B-2	4.4	22.4	26.7	15.6
B-3	3.7	21.9	25.5	14.6
B-4	3.5	21.2	24.7	14.1
B-5	3.4	20.9	24.3	13.9
B-6	3.0	20.5	23.5	13.2
B-7	3.0	20.3	23.2	13.1
B-8	2.4	20.6	23.0	12.7
B-9	2.2	20.2	22.2	12.2
B-10	2.1	19.7	21.8	11.9

18. APPENDIX 4. SUPPORTING DATA FOR CHAPTER #4

18.1 Summary of Experimental Conditions

Table A-4-1. Constant kappa number (approximately 30) conditions for pulps produced from unextracted wood chips.

Condition	Alias	EA % as Na_2O	Sulfidity % as Na_2O	Maximum Temperature	H-Factor
1	31	16.0	30.0	165.0	1294
2	32	20.0	30.0	165.0	790
3	33	16.0	50.0	165.0	929
4	34	20.0	50.0	165.0	570
5	35	16.0	30.0	175.0	1294
6	36	20.0	30.0	175.0	790
7	37	16.0	50.0	175.0	929
8	38	20.0	50.0	175.0	522
9	39	14.6	40.0	170.0	1352
10	40	21.4	40.0	170.0	565
11	41	18.0	23.2	170.0	1217
12	42	18.0	56.8	170.0	646
13	43	18.0	40.0	161.6	806
14	44	18.0	40.0	178.4	806
15	45	18.0	40.0	170.0	806
16	46	18.0	40.0	170.0	806
17	47	18.0	40.0	170.0	806
18	48	18.0	40.0	170.0	806
19	49	18.0	40.0	170.0	806
20	50	18.0	40.0	170.0	806

Table A-4-2. Incremental cook conditions. Condition A pulps were produced under high effective alkali, low sulfidity while Condition B pulps were produced under low effective alkali, high sulfidity conditions.

Condition	Alias	EA % as Na_2O	Sulfidity % as Na_2O	Maximum Temperature	H-factor
A-1	71-1	21.4	23.2	170.0	120
A-2	71-2	21.4	23.2	170.0	240
A-3	71-3	21.4	23.2	170.0	360
A-4	71-4	21.4	23.2	170.0	480
A-5	71-5	21.4	23.2	170.0	600
A-6	71-6	21.4	23.2	170.0	720
A-7	71-7	21.4	23.2	170.0	840
A-8	71-8	21.4	23.2	170.0	863
B-1	72-1	14.6	56.8	170.0	120
B-2	72-2	14.6	56.8	170.0	240
B-3	72-3	14.6	56.8	170.0	360
B-4	72-4	14.6	56.8	170.0	480
B-5	72-5	14.6	56.8	170.0	600
B-6	72-6	14.6	56.8	170.0	720
B-7	72-7	14.6	56.8	170.0	840
B-8	72-8	14.6	56.8	170.0	960
B-9	72-9	14.6	56.8	170.0	1080
B-10	72-10	14.6	56.8	170.0	1151

18.2 ESCA Spectra

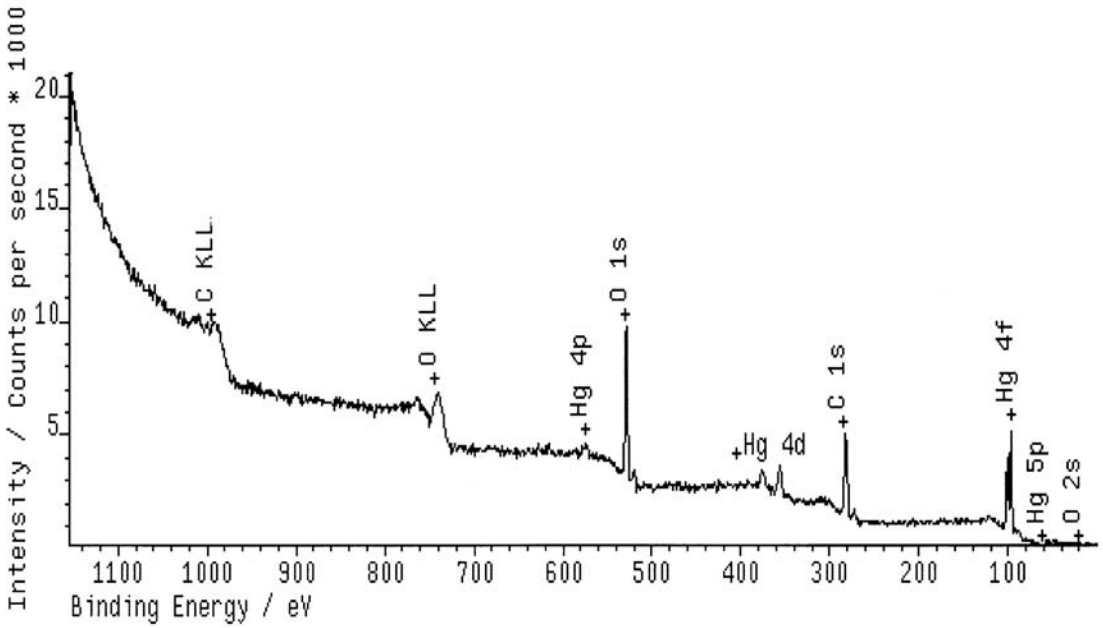

Figure A-4-1. Wide ESCA spectrum of Condition A-1 from the incremental cook series of pulps. Table A-4-2 summarizes the pulping conditions for this pulp.

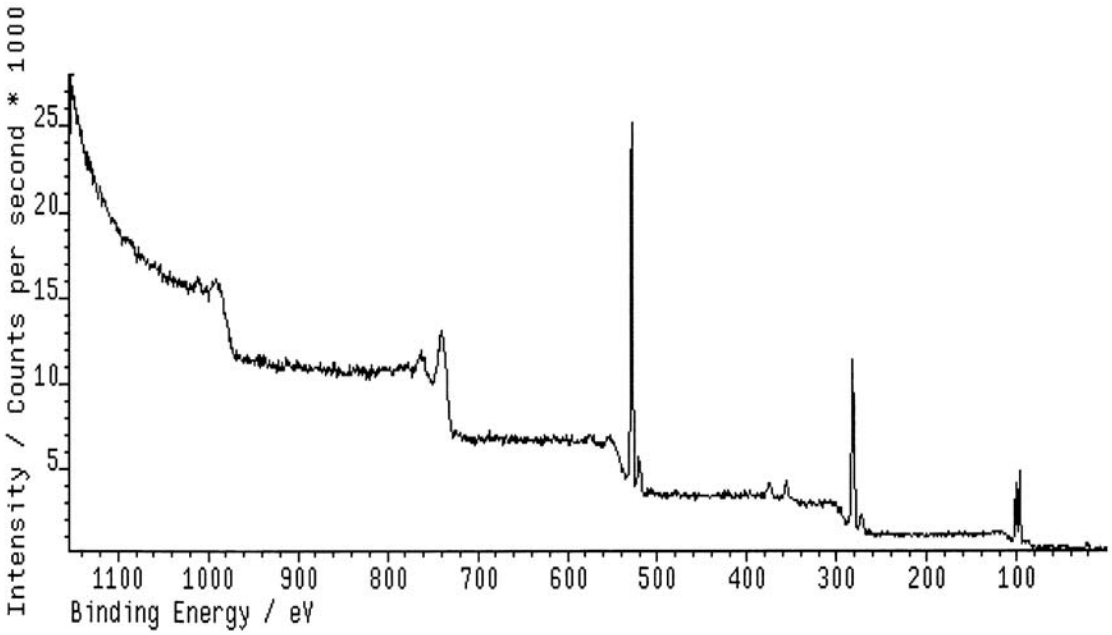

Figure A-4-2. Wide ESCA spectrum of Condition A-4 from the incremental cook series of pulps. Table A-4-2 summarizes the pulping conditions for this pulp.

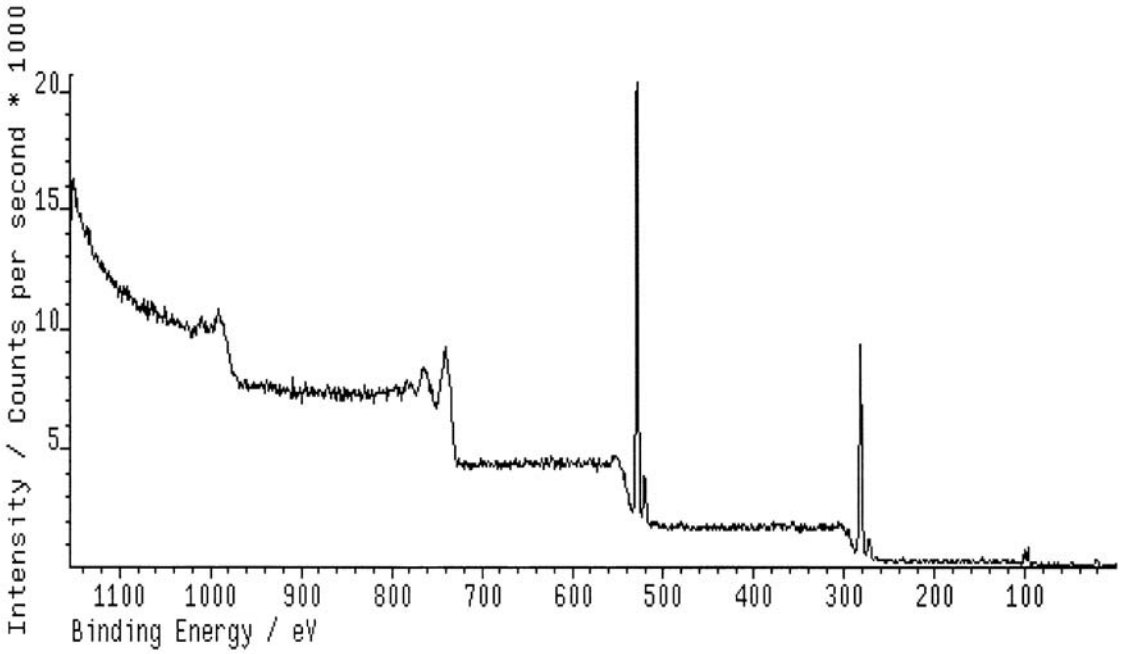

Figure A-4-3. Wide ESCA spectrum of Condition A-7 from the incremental cook series of pulps. Table A-4-2 summarizes the pulping conditions for this pulp.

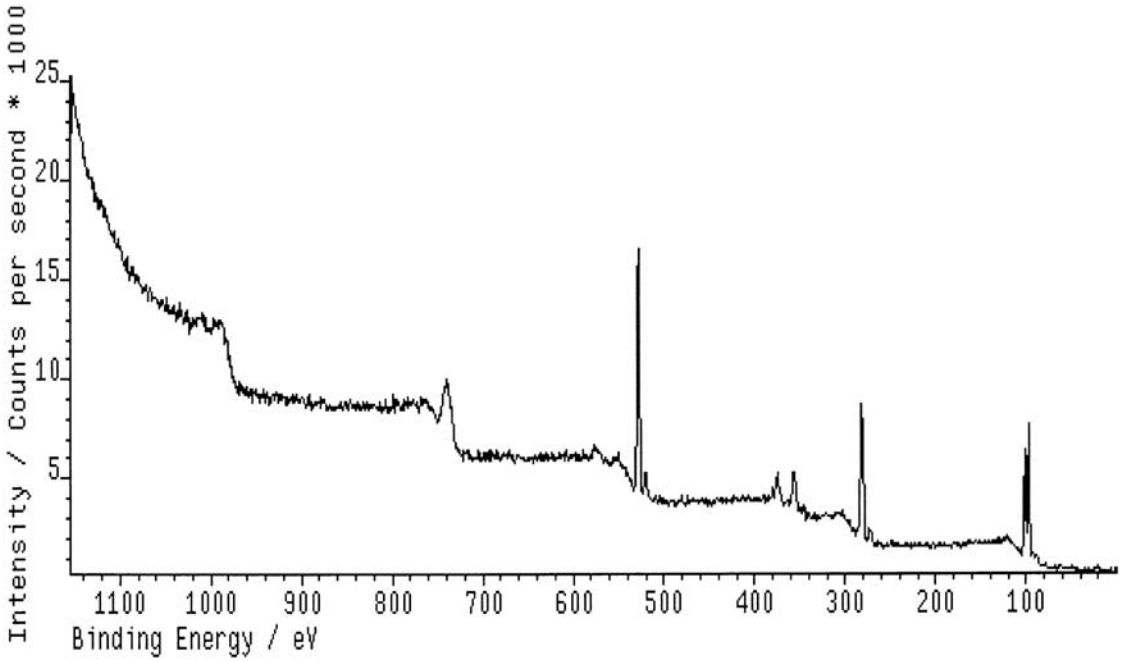

Figure A-4-4. Wide ESCA spectrum of Condition B-1 from the incremental cook series of pulps. Table A-4-2 summarizes the pulping conditions for this pulp.

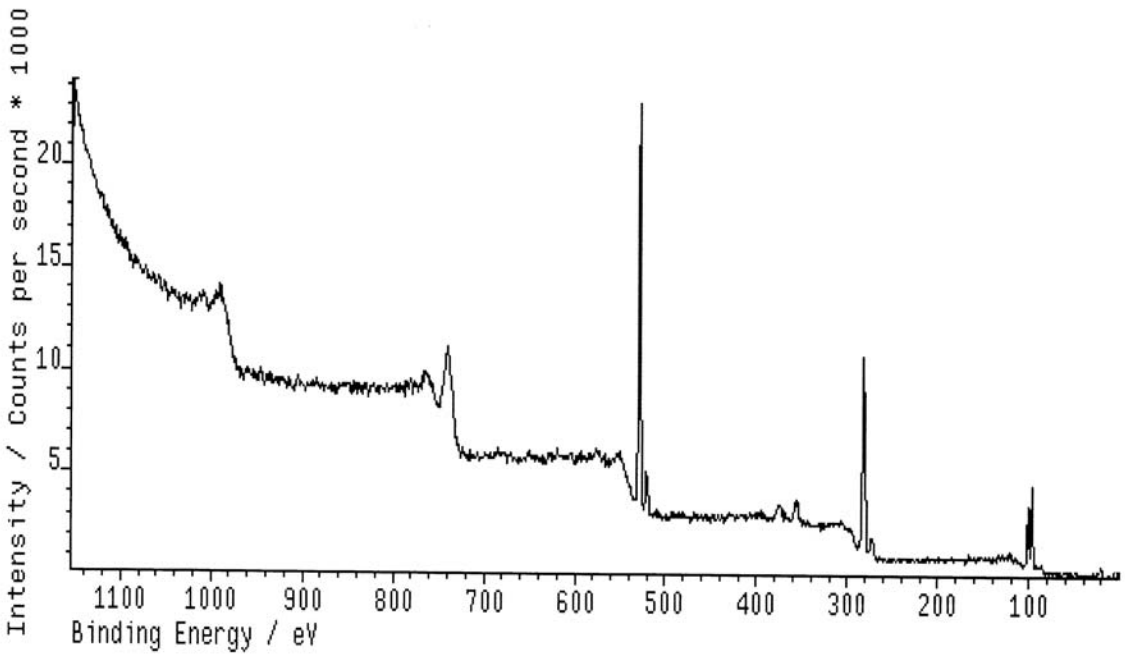

Figure A-4-5. Wide ESCA spectrum of Condition B-4 from the incremental cook series of pulps. Table A-4-2 summarizes the pulping conditions for this pulp.

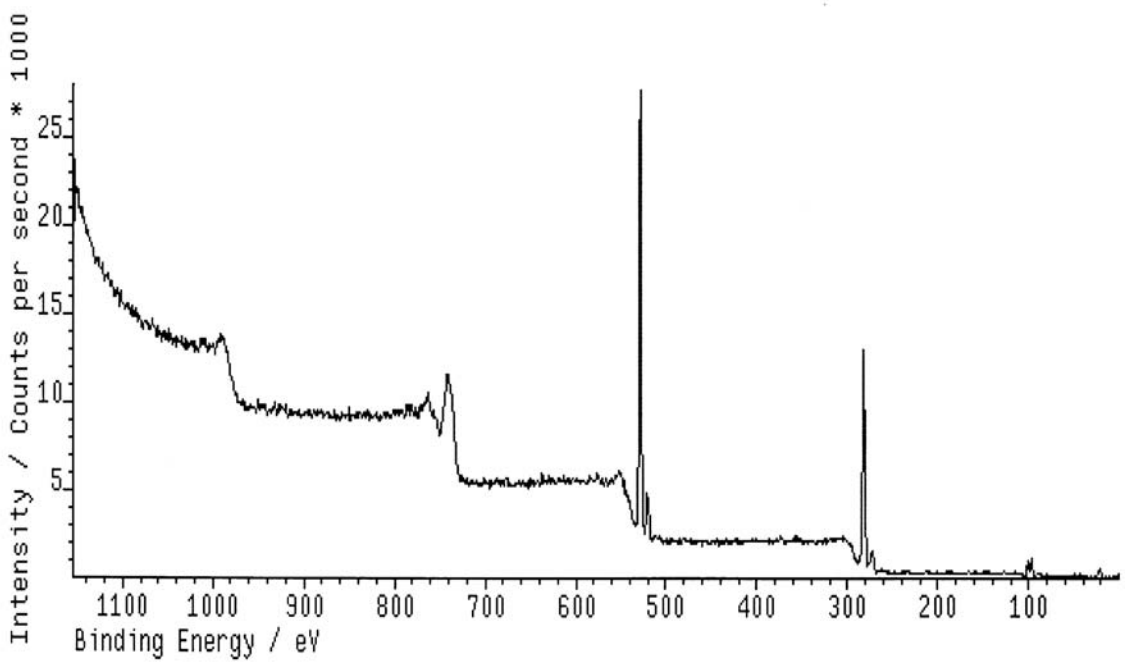

Figure A-4-6. Wide ESCA spectrum of Condition B-9 from the incremental cook series of pulps. Table A-4-2 summarizes the pulping conditions for this pulp.

18.3 Summary of ESCA Data

Table A-4-3. ESCA results from select incremental cook kraft pulps. Table A-4-2 summarizes the pulping conditions for these pulps.

Condition	% C	% O	% Hg	O/C	C1	C2	C3	C4
A-1	61.24	34.21	4.55	0.559	28.69	46.60	18.73	5.98
	62.97	33.56	3.47	0.533	28.51	47.62	19.36	4.52
A-4	58.40	39.72	1.88	0.680	20.18	61.47	15.53	2.82
	59.49	38.72	1.79	0.651	24.00	59.22	14.41	2.37
A-7	55.76	43.84	0.41	0.786	11.28	67.53	19.26	1.93
	56.15	43.02	0.50	0.766	12.26	63.39	21.48	2.88
B-1	61.86	34.72	3.42	0.561	33.38	51.98	11.37	3.26
	61.69	34.17	3.81	0.554	32.00	51.46	13.38	3.15
B-4	59.73	38.39	1.88	0.643	24.11	58.46	14.95	2.48
	59.62	38.87	1.50	0.652	21.21	60.23	16.27	2.29
B-9	57.12	42.31	0.57	0.741	13.44	67.38	17.98	1.19
	56.35	43.23	0.42	0.767	12.59	66.44	18.95	2.01

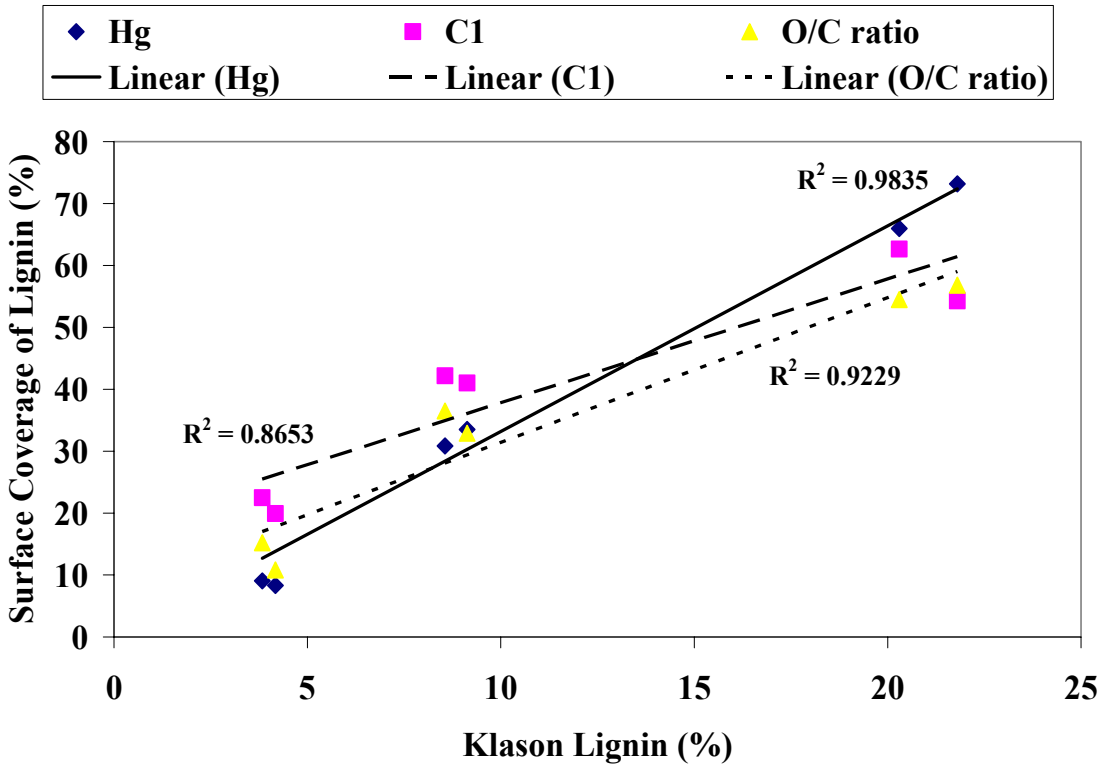

Figure A-4-7. Surface lignin as a function of klason lignin for the mercurization (Hg), C1S, and O/C ratio methods of determining surface lignin with ESCA. The pulps used for this analysis were obtained from Table A-4-2.

18.4 Summary of Residual Lignin Yields

Table A-4-4. Residual lignin yields from acid hydrolysis of constant kappa number (approximately 30) pulps. Table A-4-1 summarizes the pulping conditions for these pulps.

Condition	Kappa Number	Pulp Wt. (g)	"Lignin" Wt. (g)	Ash (%)	"Real" Lignin Weight (g)	Theoretical Lignin Weight (g)	%Yield
1	28.8	38.974	0.9399	2.43	0.9170	1.65	55.7
2	28.4	38.867	0.9336	2.73	0.9081	1.62	56.1
3	27.6	40.662	0.8587	1.78	0.8434	1.65	51.1
4	30.6	40.017	0.9573	1.10	0.9468	1.80	52.6
5	28.9	40.348	0.9932	1.99	0.9735	1.71	56.8
6	29.9	39.311	0.9315	2.00	0.9129	1.73	52.8
7	29.6	40.756	0.9831	1.62	0.9671	1.8	54.5
8	30.9	40.609	0.9815	1.88	0.9631	1.84	52.3
9	28.2	40.761	0.9432	2.30	0.9215	1.69	54.6
10	29.7	40.447	0.9829	2.02	0.9630	1.77	54.5
11	27.8	39.256	0.8669	2.29	0.8470	1.60	52.8
12	28.3	39.489	0.8681	2.98	0.8423	1.60	51.4
13	30.3	40.173	0.9571	2.49	0.9333	1.79	52.1
14	27.8	39.995	0.9469	1.78	0.9300	1.63	56.9
15	29.1	39.954	0.9413	2.66	0.9162	1.71	53.7
16	29.7	39.989	0.9760	2.03	0.9562	1.74	54.8
17	30.9	40.700	1.0947	1.96	1.0732	1.85	58.1
18	28.1	39.585	1.0292	1.88	1.0098	1.63	61.9
19	30.3	39.592	0.9753	0.93	0.9663	1.76	54.8
20	28.6	40.054	0.8820	0.71	0.8758	1.68	52.1

Table A-4-5. Residual lignin yields from acid hydrolysis of incremental cook pulps. Table A-4-2 summarizes the pulping conditions for these pulps.

Condition	Kappa Number	Pulp Wt. (g)	"Lignin" Wt. (g)	Ash (%)	"Real" Lignin Weight (g)	Theoretical Lignin Weight (g)	%Yield
A-1	162.8	30.0	2.3221	2.43	2.2656	7.18	31.6
A-2	129.7	30.0	2.4402	2.73	2.3735	5.72	41.5
A-3	88.5	30.0	2.3378	1.78	2.2962	3.90	58.9
A-4	69.2	30.0	1.7264	1.10	1.7074	3.05	56.0
A-5	52.2	30.0	1.1517	1.99	1.1288	2.30	49.0
A-6	37.9	30.0	0.9186	2.00	0.9003	1.67	53.8
A-7	30.5	30.0	0.7636	1.62	0.7511	1.35	55.8
A-8	28.8	30.0	0.7835	1.88	0.7688	1.27	60.6
B-1	152.0	30.0	1.8846	2.30	1.8413	6.70	27.5
B-2	118.4	30.0	1.8893	2.02	1.8511	5.22	35.5
B-3	93.1	30.0	1.6521	2.29	1.6142	4.11	39.3
B-4	69.5	30.0	1.3733	2.98	1.3324	3.07	43.5
B-5	56.1	30.0	1.1280	2.49	1.1000	2.47	44.5
B-6	44.1	30.0	0.9658	1.78	0.9486	1.95	48.8
B-7	36.5	30.0	0.7642	2.66	0.7438	1.61	46.2
B-8	32.5	30.0	0.7016	2.03	0.6874	1.43	47.9
B-9	30.3	30.0	0.6499	1.96	0.6371	1.34	47.6
B-10	27.7	30.0	0.6643	1.88	0.6518	1.22	53.3

18.5 Summary of Residual Lignin Elemental Analysis

Table A-4-6. Residual lignin elemental analysis and lignin molecular formulas from acid hydrolysis of constant kappa number pulps. Table A-4-1 summarizes the pulping conditions used to produce the pulps for the respective residual lignins.

Condition	% C	%H	%O	%S	%OMe	Molecular Formula
1	61.90	5.25	28.06	1.39	12.8	$C_9H_{7.6}O_{2.5}S_{0.08}(OCH_3)_{0.78}$
2	62.41	5.47	27.66	1.48	12.9	$C_9H_{7.9}O_{2.5}S_{0.09}(OCH_3)_{0.78}$
3	62.38	5.31	28.11	1.54	12.5	$C_9H_{7.7}O_{2.5}S_{0.09}(OCH_3)_{0.76}$
4	62.65	5.50	28.22	1.54	13.2	$C_9H_{7.9}O_{2.5}S_{0.09}(OCH_3)_{0.80}$
5	62.45	5.27	28.32	1.65	13.0	$C_9H_{7.6}O_{2.5}S_{0.10}(OCH_3)_{0.79}$
6	62.44	5.33	28.07	1.56	13.2	$C_9H_{7.6}O_{2.5}S_{0.09}(OCH_3)_{0.80}$
7	63.01	5.37	28.51	1.42	13.0	$C_9H_{7.7}O_{2.5}S_{0.08}(OCH_3)_{0.78}$
8	62.57	5.51	28.56	1.60	13.3	$C_9H_{7.9}O_{2.6}S_{0.09}(OCH_3)_{0.81}$
9	62.43	5.46	28.62	1.29	12.9	$C_9H_{7.5}O_{2.6}S_{0.08}(OCH_3)_{0.78}$
10	62.66	5.32	28.27	1.44	13.7	$C_9H_{7.3}O_{2.5}S_{0.08}(OCH_3)_{0.83}$
11	62.87	5.19	28.47	1.54	13.6	$C_9H_{7.5}O_{2.5}S_{0.09}(OCH_3)_{0.82}$
12	6..23	5.32	28.35	1.58	13.1	$C_9H_{7.6}O_{2.5}S_{0.09}(OCH_3)_{0.78}$
13	62.57	5.32	28.20	1.48	13.4	$C_9H_{7.6}O_{2.5}S_{0.09}(OCH_3)_{0.81}$
14	63.23	5.35	28.23	1.49	13.2	$C_9H_{7.6}O_{2.5}S_{0.09}(OCH_3)_{0.79}$
15	63.47	5.41	28.31	1.62	13.6	$C_9H_{7.7}O_{2.5}S_{0.09}(OCH_3)_{0.81}$
16	63.28	5.42	28.47	1.64	13.3	$C_9H_{7.6}O_{2.5}S_{0.10}(OCH_3)_{0.80}$
17	63.09	5.39	29.07	1.46	13.4	$C_9H_{7.6}O_{2.6}S_{0.08}(OCH_3)_{0.81}$
18	62.93	5.34	29.37	1.49	12.6	$C_9H_{7.7}O_{2.6}S_{0.09}(OCH_3)_{0.76}$
19	63.66	5.43	28.54	1.42	13.4	$C_9H_{7.6}O_{2.5}S_{0.08}(OCH_3)_{0.80}$
20	63.44	5.51	28.91	1.40	12.9	$C_9H_{7.9}O_{2.6}S_{0.08}(OCH_3)_{0.77}$

Table A-4-7. Residual lignin elemental analysis and lignin molecular formulas from acid hydrolysis of incremental cook pulps. Table A-4-2 summarizes the pulping conditions used to produce the pulps for the respective residual lignins.

Condition	% C	%H	%O	%S	%OMe	Molecular Formula
A-1	63.10	5.51	29.05	1.10	14.9	$C_9H_{7.7}O_{2.5}S_{0.06}(OCH_3)_{0.91}$
A-2	64.16	5.75	27.86	1.25	14.7	$C_9H_{8.0}O_{2.3}S_{0.07}(OCH_3)_{0.88}$
A-3	64.67	5.92	27.14	1.01	14.7	$C_9H_{8.2}O_{2.2}S_{0.06}(OCH_3)_{0.87}$
A-4	64.57	5.77	26.91	1.04	14.5	$C_9H_{8.0}O_{2.2}S_{0.06}(OCH_3)_{0.86}$
A-5	63.42	5.42	28.28	1.52	14.5	$C_9H_{7.5}O_{2.4}S_{0.09}(OCH_3)_{0.87}$
A-6	64.27	5.65	27.27	1.54	14.4	$C_9H_{7.8}O_{2.3}S_{0.09}(OCH_3)_{0.85}$
A-7	63.62	5.42	27.86	1.66	13.9	$C_9H_{7.6}O_{2.4}S_{0.10}(OCH_3)_{0.83}$
A-8	64.52	5.72	26.72	1.57	13.5	$C_9H_{8.0}O_{2.3}S_{0.09}(OCH_3)_{0.79}$
B-1	63.71	5.63	28.73	1.04	14.9	$C_9H_{7.8}O_{2.5}S_{0.06}(OCH_3)_{0.90}$
B-2	63.89	5.59	28.60	1.08	14.8	$C_9H_{7.7}O_{2.4}S_{0.06}(OCH_3)_{0.89}$
B-3	64.00	5.50	28.50	1.22	14.7	$C_9H_{7.6}O_{2.4}S_{0.07}(OCH_3)_{0.88}$
B-4	64.18	5.61	27.92	1.29	14.4	$C_9H_{7.8}O_{2.4}S_{0.07}(OCH_3)_{0.86}$
B-5	64.21	5.55	27.80	1.38	14.2	$C_9H_{7.7}O_{2.4}S_{0.08}(OCH_3)_{0.84}$
B-6	64.71	5.86	26.88	1.41	14.0	$C_9H_{8.2}O_{2.2}S_{0.08}(OCH_3)_{0.82}$
B-7	63.77	5.44	28.32	1.44	13.7	$C_9H_{7.6}O_{2.5}S_{0.08}(OCH_3)_{0.82}$
B-8	64.26	5.81	27.44	1.43	13.4	$C_9H_{8.3}O_{2.4}S_{0.08}(OCH_3)_{0.79}$
B-9	64.27	5.50	27.73	1.64	13.2	$C_9H_{7.7}O_{2.4}S_{0.09}(OCH_3)_{0.78}$
B-10	64.64	5.90	26.84	1.35	13.1	$C_9H_{8.4}O_{2.3}S_{0.08}(OCH_3)_{0.77}$

18.6 UV/vis Neutral Spectra of Residual Lignins

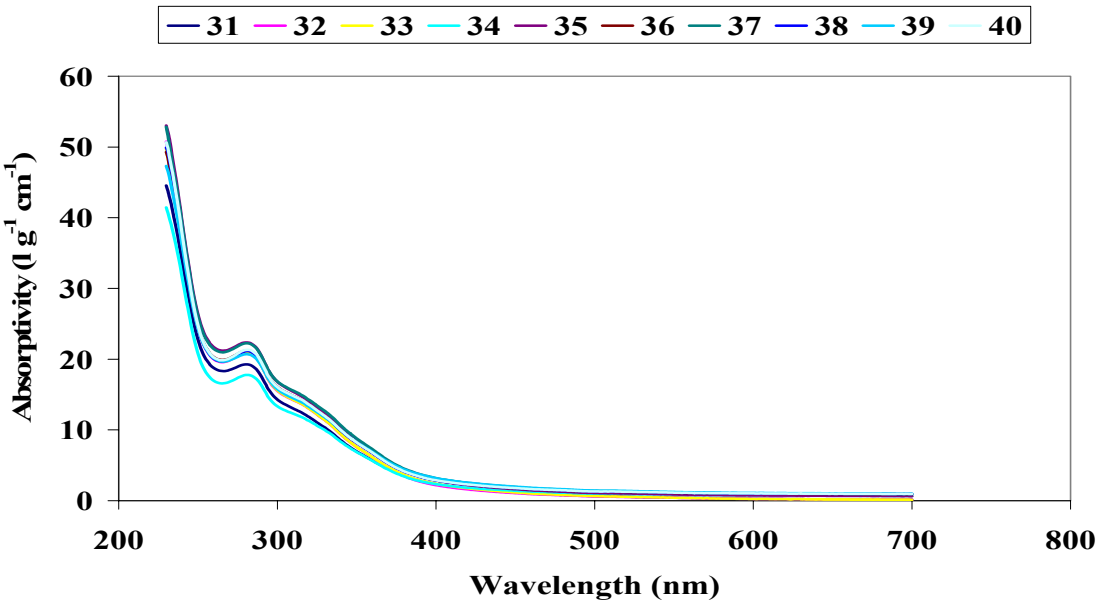

Figure A-4-8. Neutral UV/vis spectra of residual lignins from constant kappa number (approximately 30) series of pulps. Table A-4-1 summarizes the pulping conditions used to produce the pulps for the respective residual lignins.

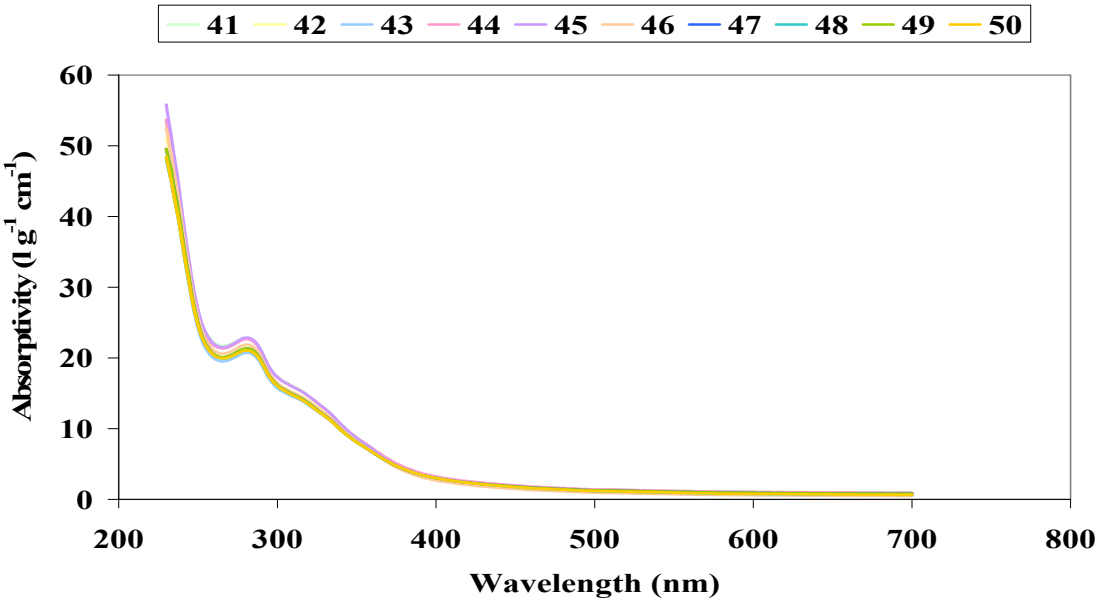

Figure A-4-9. Neutral UV/vis spectra of residual lignins from constant kappa number (approximately 30) series of pulps. Table A-4-1 summarizes the pulping conditions used to produce the pulps for the respective residual lignins.

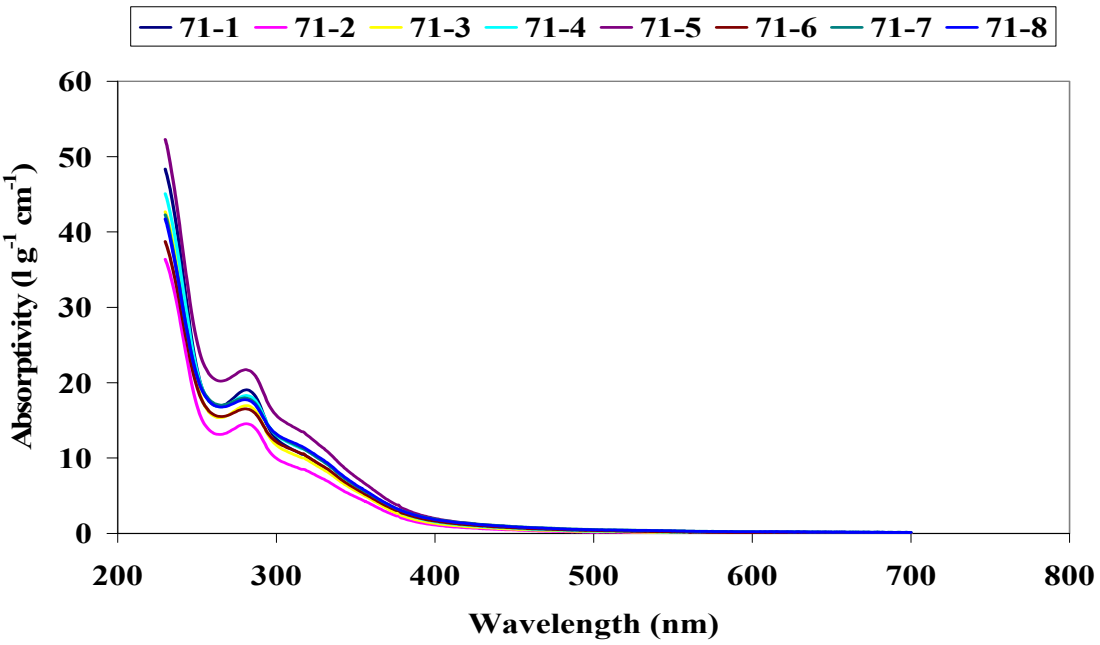

Figure A-4-10. Neutral UV/vis spectra of residual lignins from incremental cook series of pulps. Table A-4-2 summarizes the pulping conditions used to produce the pulps for the respective residual lignins.

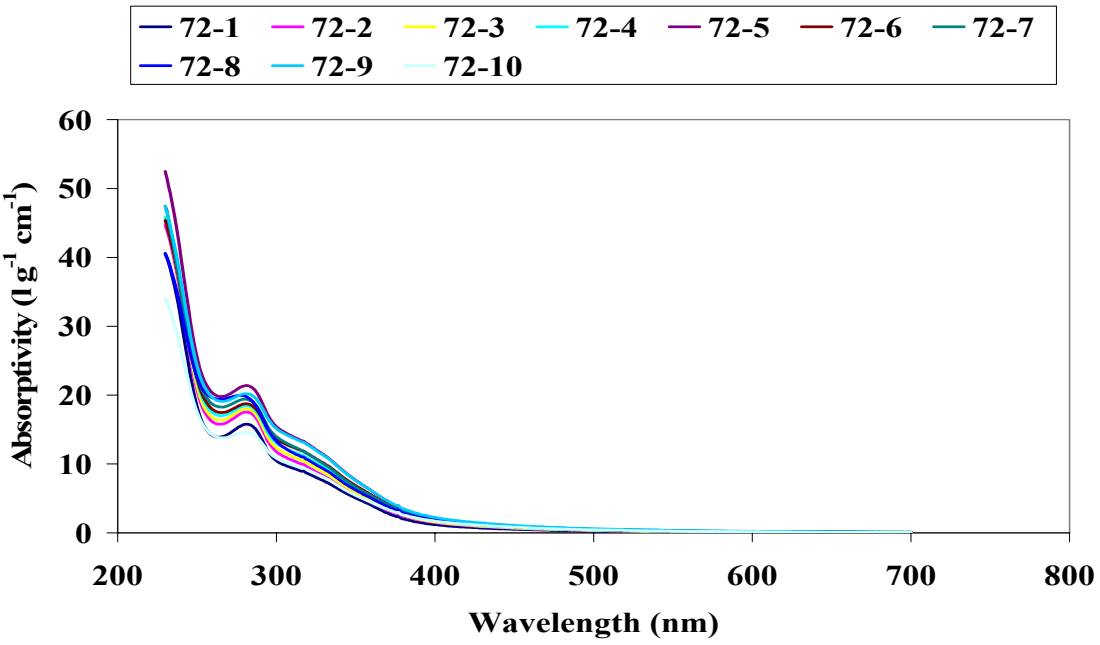

Figure A-4-11. Neutral UV/vis spectra of residual lignins from incremental cook series of pulps. Table A-4-2 summarizes the pulping conditions used to produce the pulps for the respective residual lignins.

18.7 UV/vis Ionization Spectra of Residual Lignins

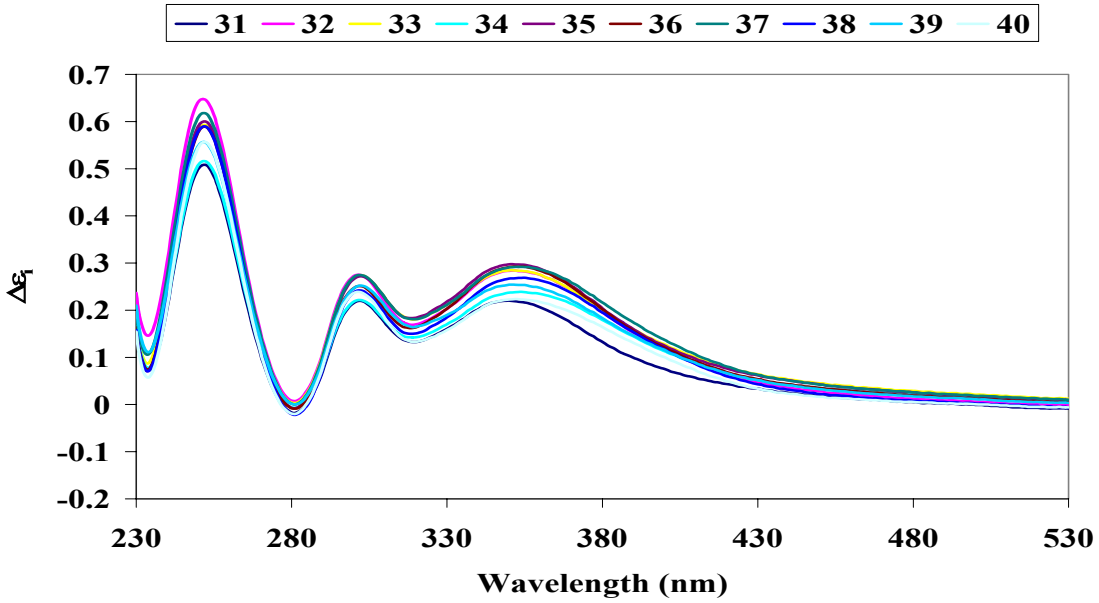

Figure A-4-12. UV ionization spectra of residual lignins from constant kappa number series of pulps. Table A-4-1 summarizes the pulping conditions used to produce the pulps for the respective residual lignins.

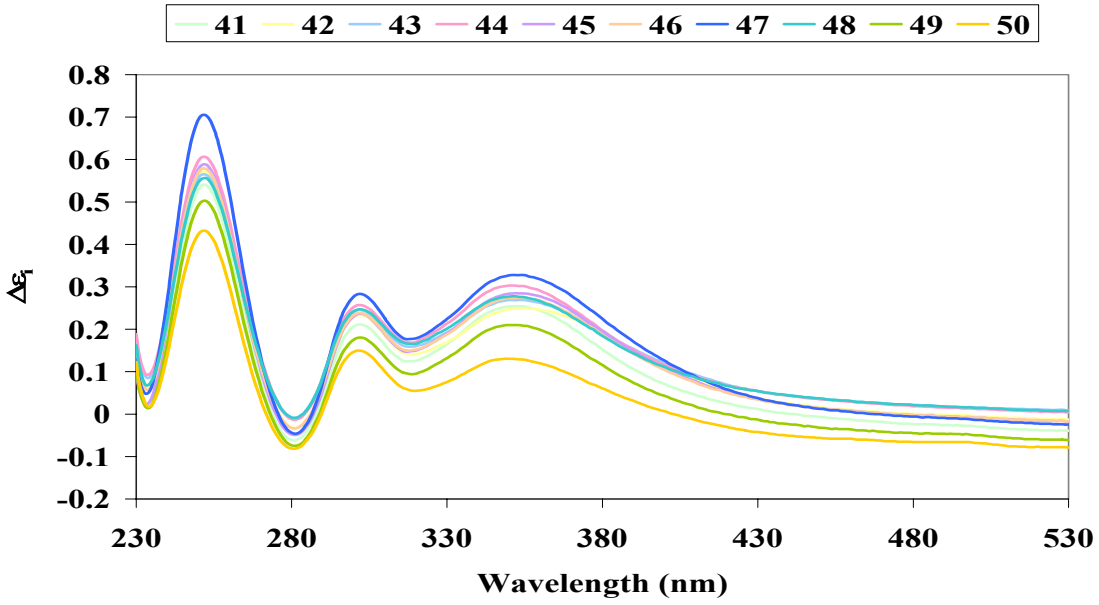

Figure A-4-13. UV ionization spectra of residual lignins from constant kappa number series of pulps. Table A-4-1 summarizes the pulping conditions used to produce the pulps for the respective residual lignins.

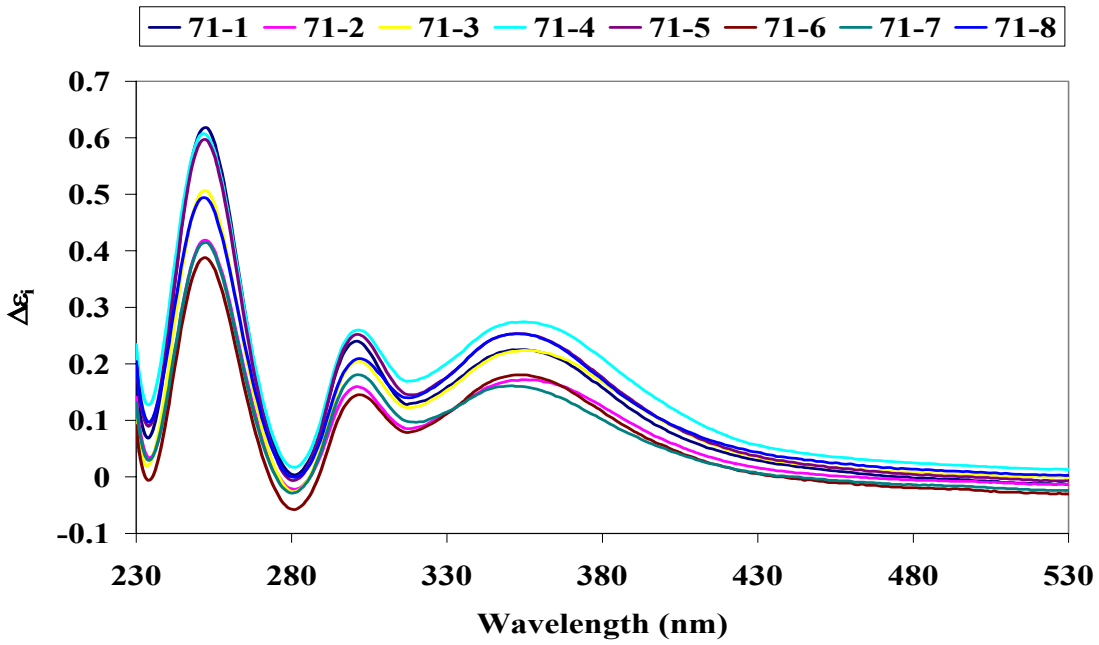

Figure A-4-14. UV ionization spectra of residual lignins from incremental cook series of pulps. Table A-4-2 summarizes the pulping conditions used to produce the pulps for the respective residual lignins.

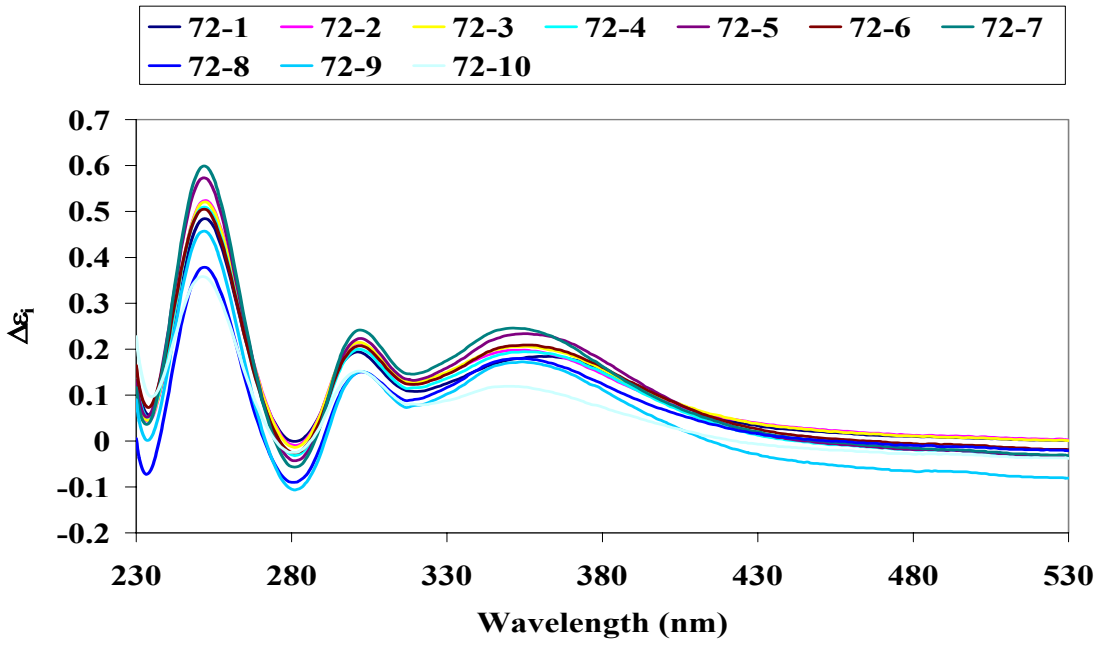

Figure A-4-15. UV ionization spectra of residual lignins from incremental cook series of pulps. Table A-4-2 summarizes the pulping conditions used to produce the pulps for the respective residual lignins.

18.8 FT-IR Spectra of Residual Lignins

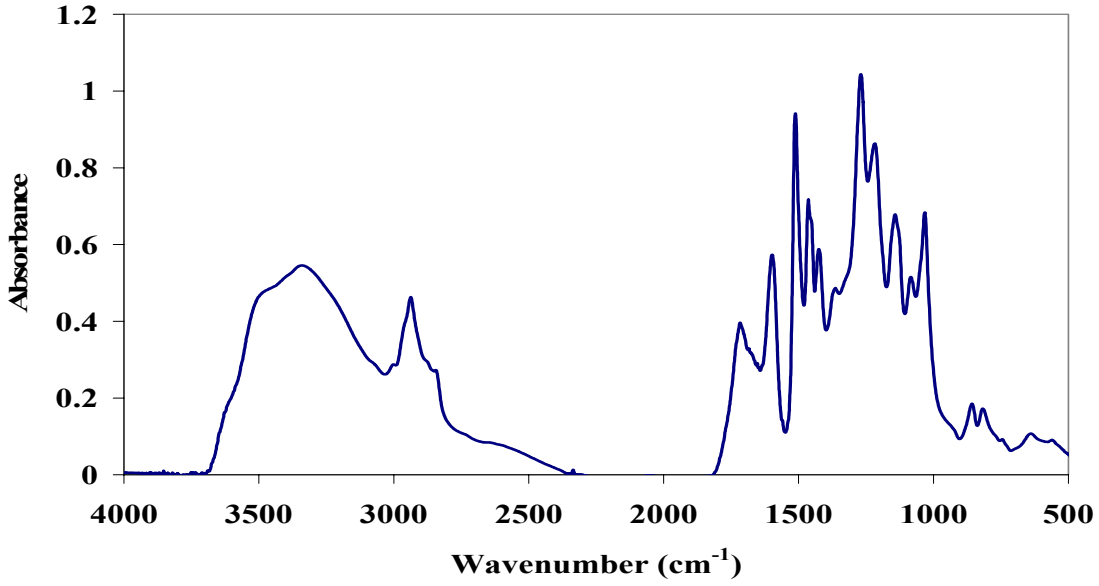

Figure A-4-16. FT-IR spectrum of Condition 1 residual lignin from constant kappa number (approximately 30) series of pulps. Table A-4-1 summarizes the pulping conditions used to produce the pulp for the respective residual lignin.

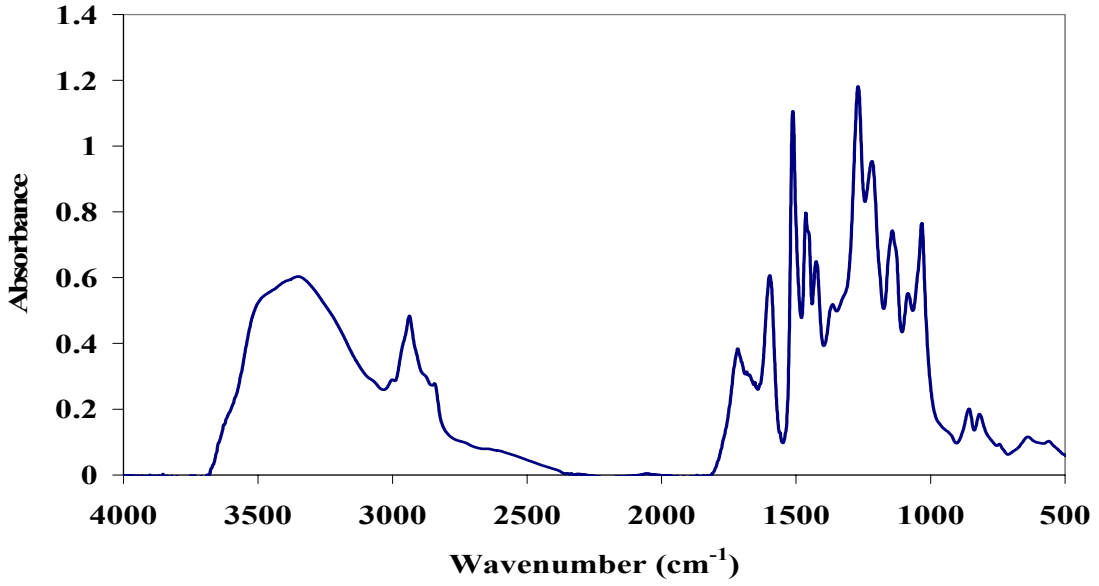

Figure A-4-17. FT-IR spectrum of Condition 2 residual lignin from constant kappa number (approximately 30) series of pulps. Table A-4-1 summarizes the pulping conditions used to produce the pulp for the respective residual lignin.

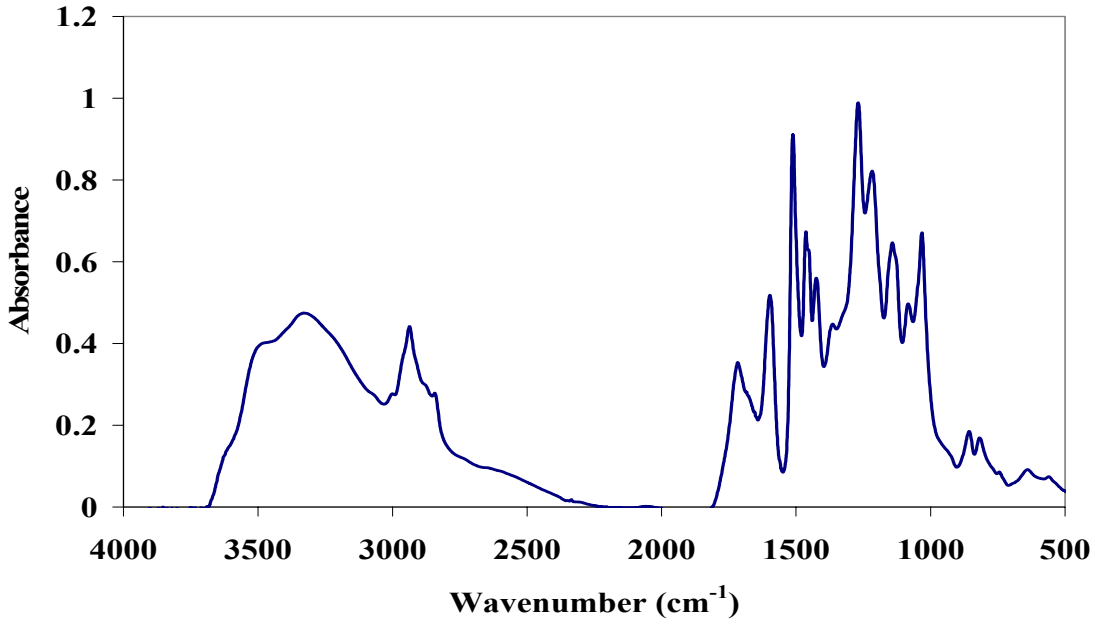

Figure A-4-18. FT-IR spectrum of Condition 3 residual lignin from constant kappa number (approximately 30) series of pulps. Table A-4-1 summarizes the pulping conditions used to produce the pulp for the respective residual lignin.

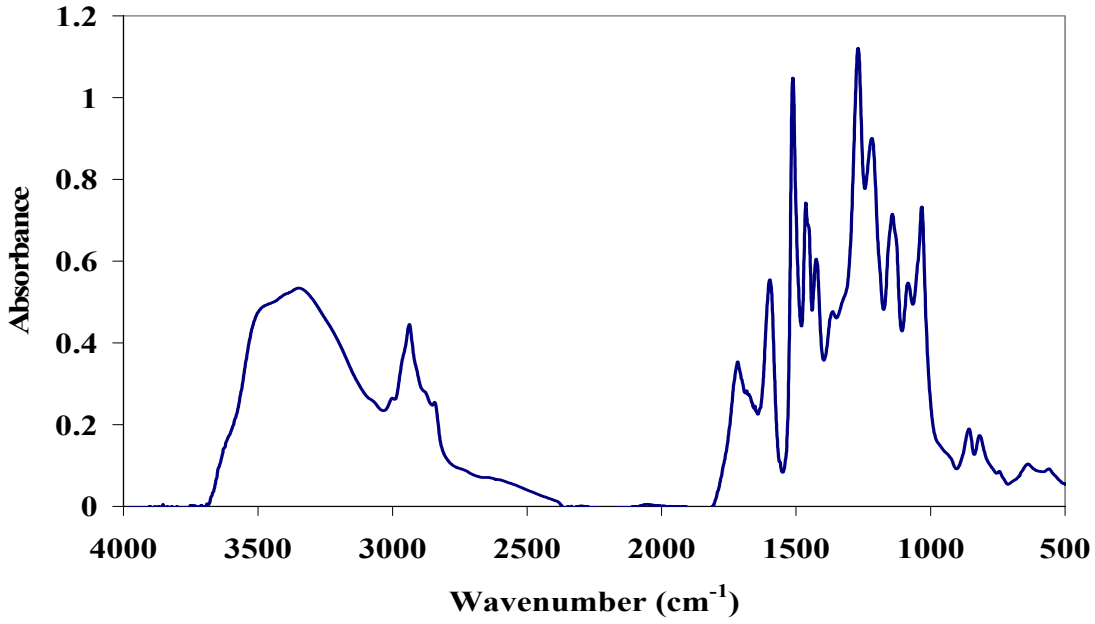

Figure A-4-19. FT-IR spectrum of Condition 4 residual lignin from constant kappa number (approximately 30) series of pulps. Table A-4-1 summarizes the pulping conditions used to produce the pulp for the respective residual lignin.

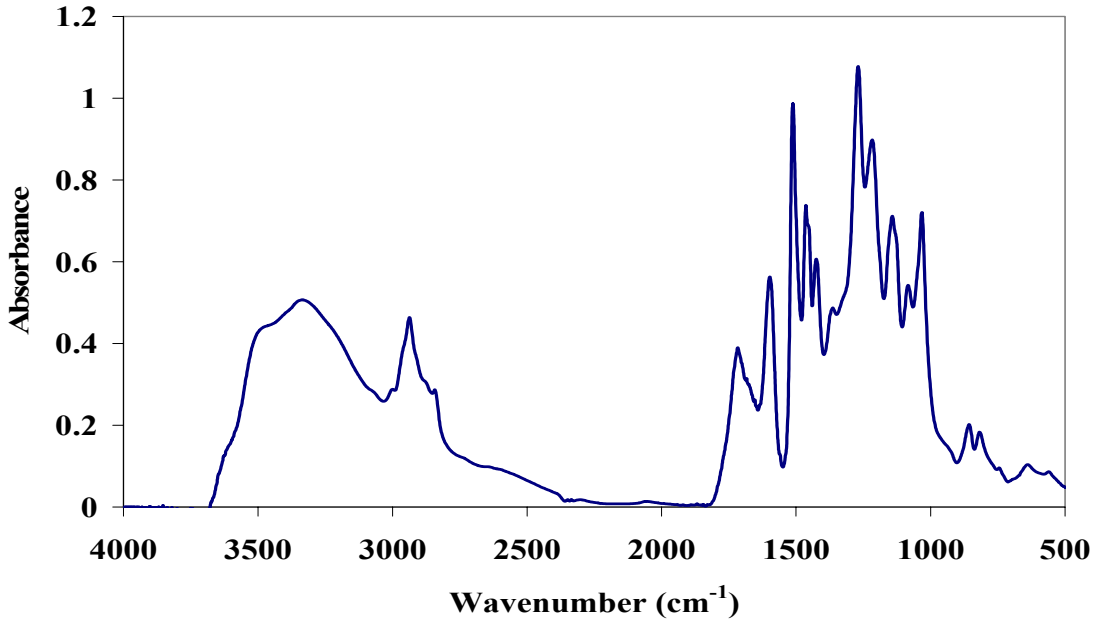

Figure A-4-20. FT-IR spectrum of Condition 5 residual lignin from constant kappa number (approximately 30) series of pulps. Table A-4-1 summarizes the pulping conditions used to produce the pulp for the respective residual lignin.

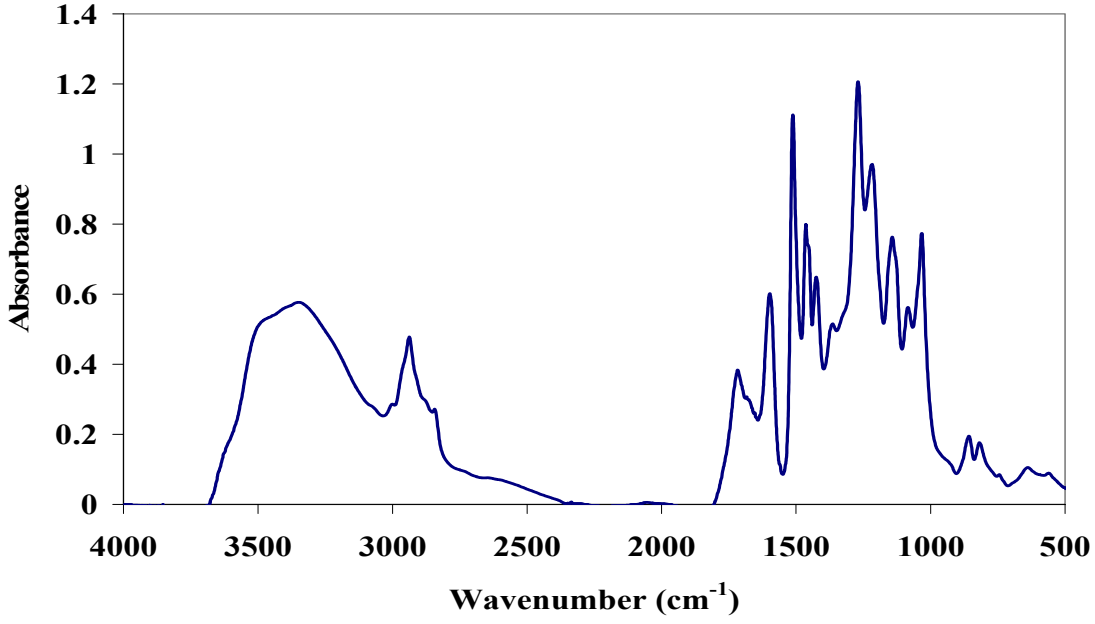

Figure A-4-21. FT-IR spectrum of Condition 6 residual lignin from constant kappa number (approximately 30) series of pulps. Table A-4-1 summarizes the pulping conditions used to produce the pulp for the respective residual lignin.

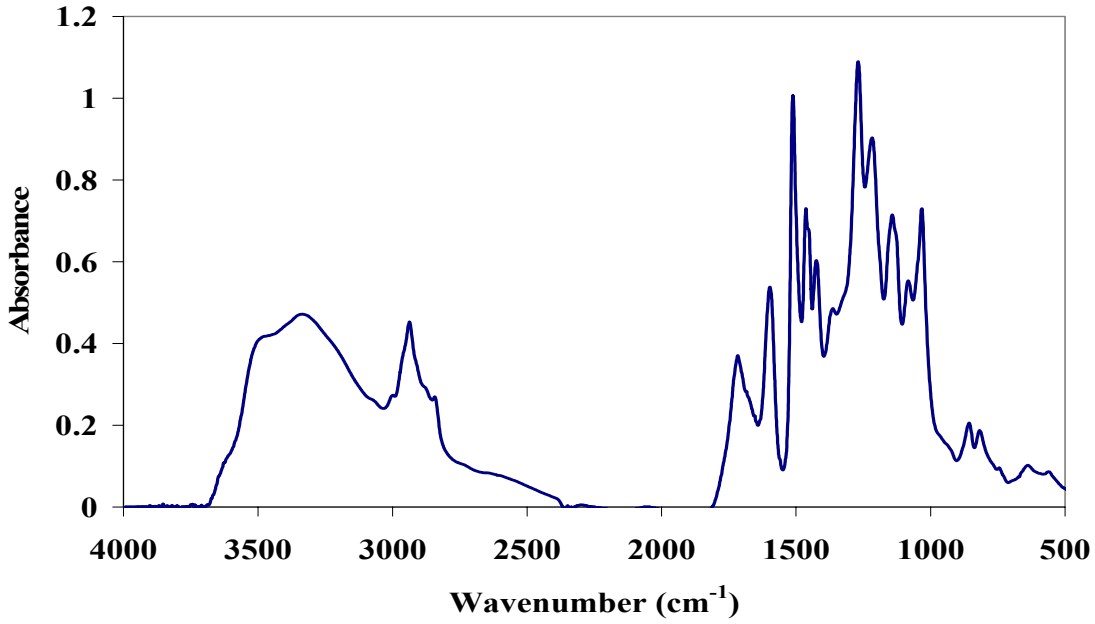

Figure A-4-22. FT-IR spectrum of Condition 7 residual lignin from constant kappa number (approximately 30) series of pulps. Table A-4-1 summarizes the pulping conditions used to produce the pulp for the respective residual lignin.

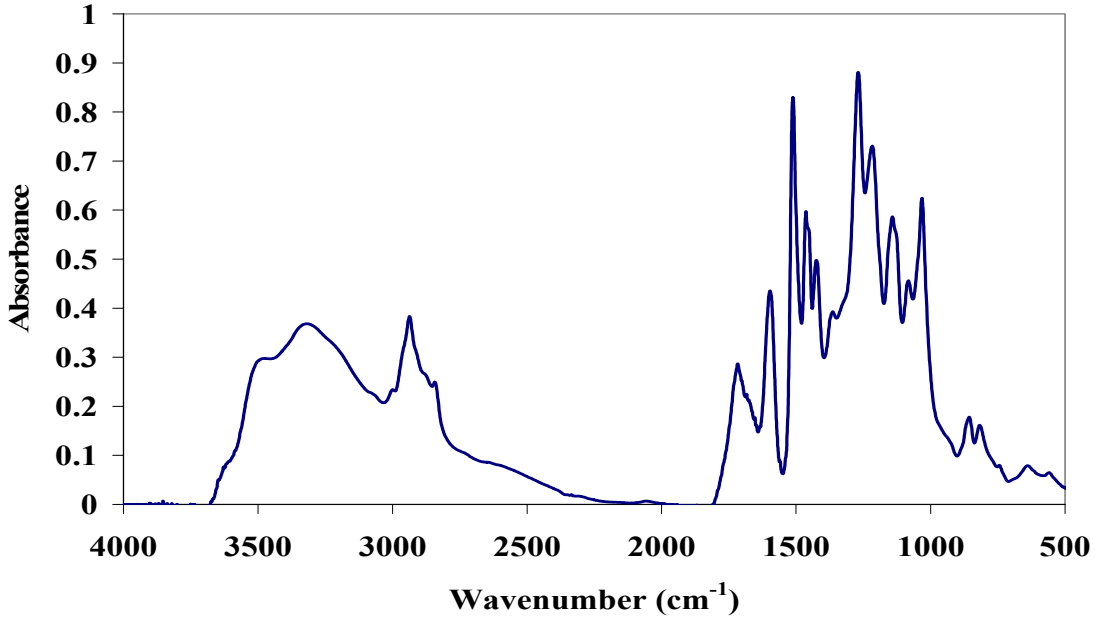

Figure A-4-23. FT-IR spectrum of Condition 8 residual lignin from constant kappa number (approximately 30) series of pulps. Table A-4-1 summarizes the pulping conditions used to produce the pulp for the respective residual lignin.

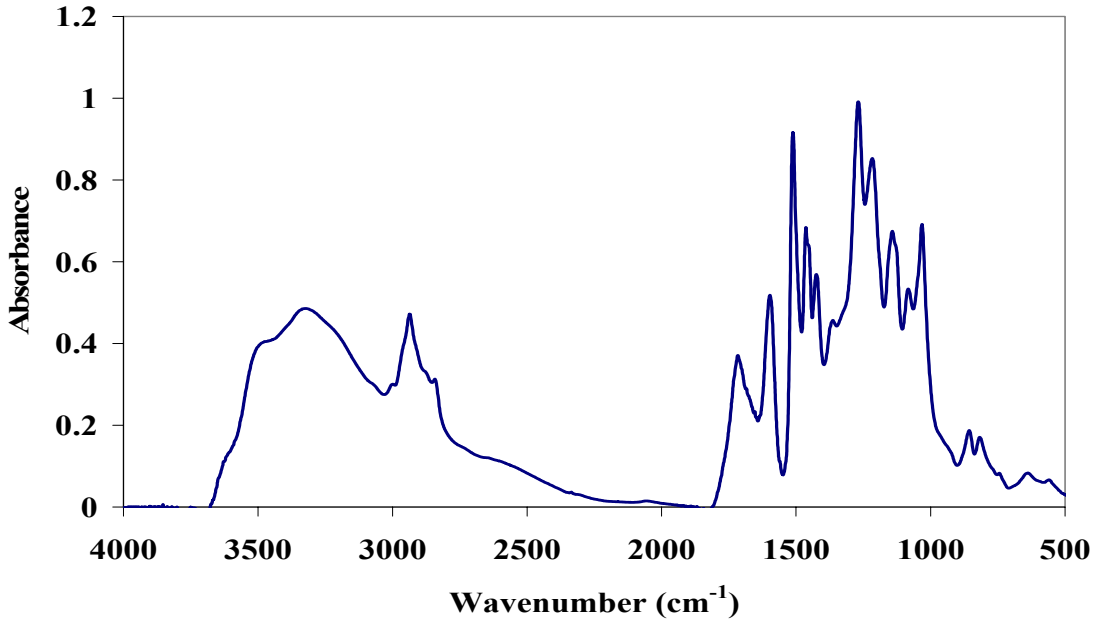

Figure A-4-24. FT-IR spectrum of Condition 9 residual lignin from constant kappa number (approximately 30) series of pulps. Table A-4-1 summarizes the pulping conditions used to produce the pulp for the respective residual lignin.

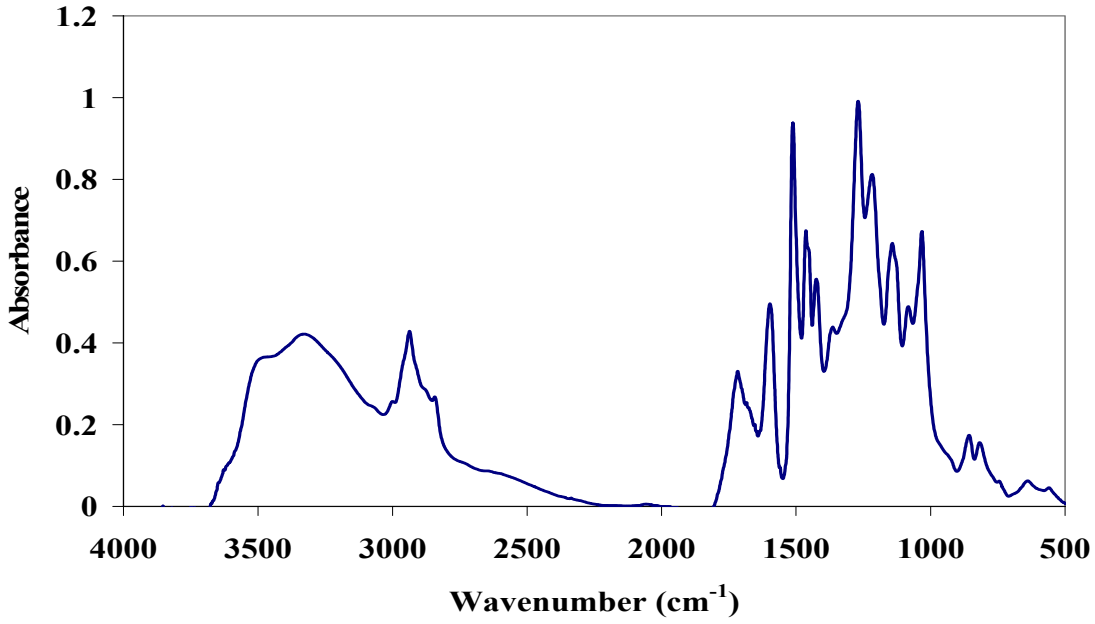

Figure A-4-25. FT-IR spectrum of Condition 10 residual lignin from constant kappa number (approximately 30) series of pulps. Table A-4-1 summarizes the pulping conditions used to produce the pulp for the respective residual lignin.

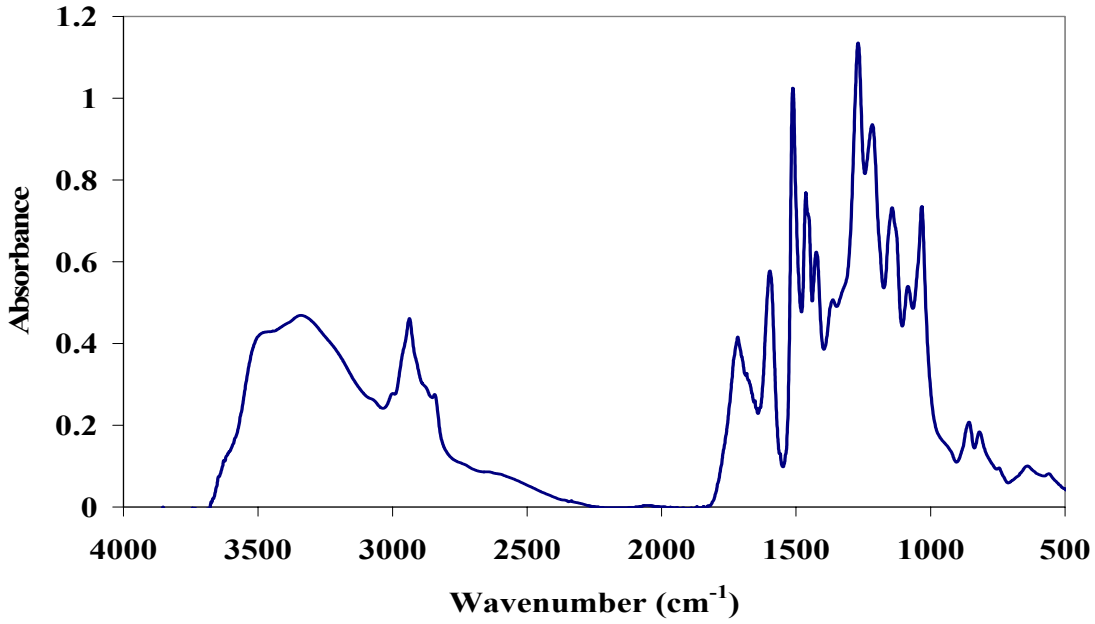

Figure A-4-26. FT-IR spectrum of Condition 11 residual lignin from constant kappa number (approximately 30) series of pulps. Table A-4-1 summarizes the pulping conditions used to produce the pulp for the respective residual lignin.

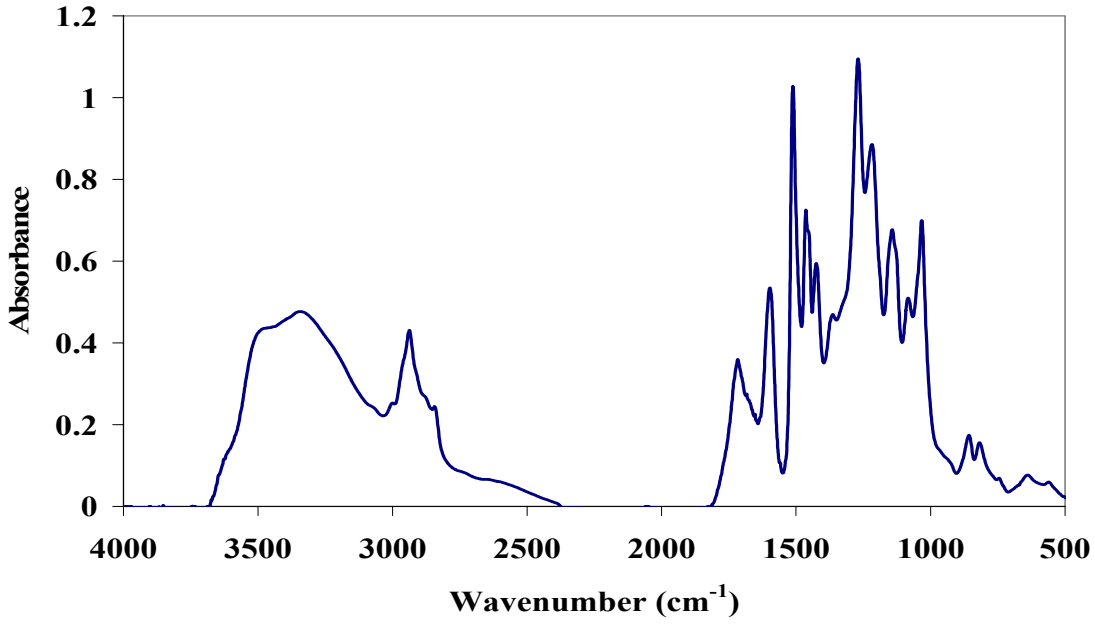

Figure A-4-27. FT-IR spectrum of Condition 12 residual lignin from constant kappa number (approximately 30) series of pulps. Table A-4-1 summarizes the pulping conditions used to produce the pulp for the respective residual lignin.

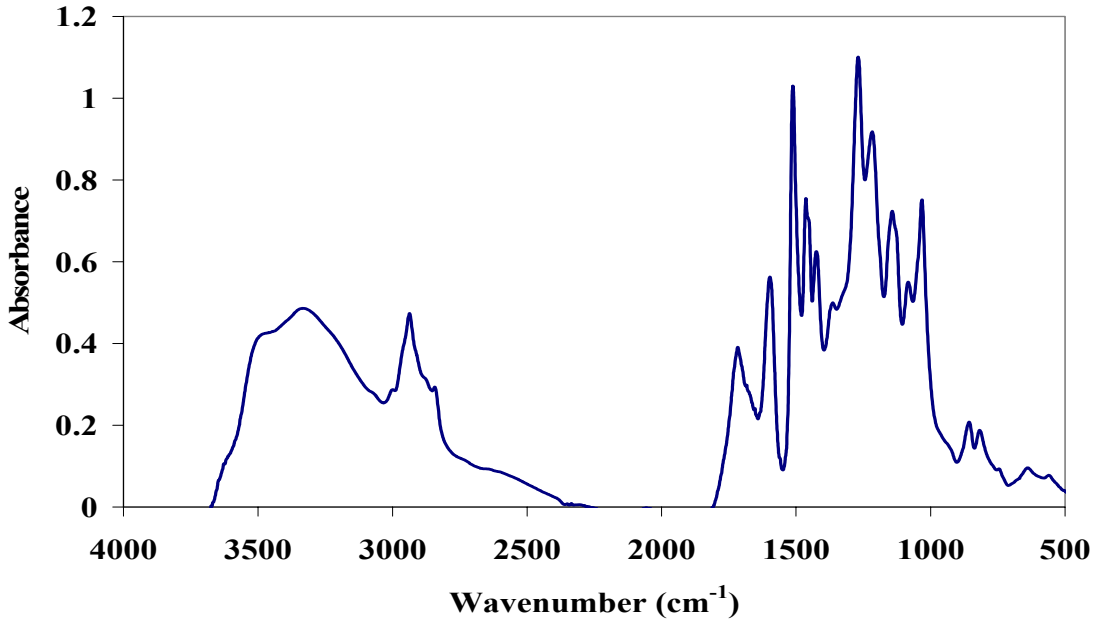

Figure A-4-28. FT-IR spectrum of Condition 13 residual lignin from constant kappa number (approximately 30) series of pulps. Table A-4-1 summarizes the pulping conditions used to produce the pulp for the respective residual lignin.

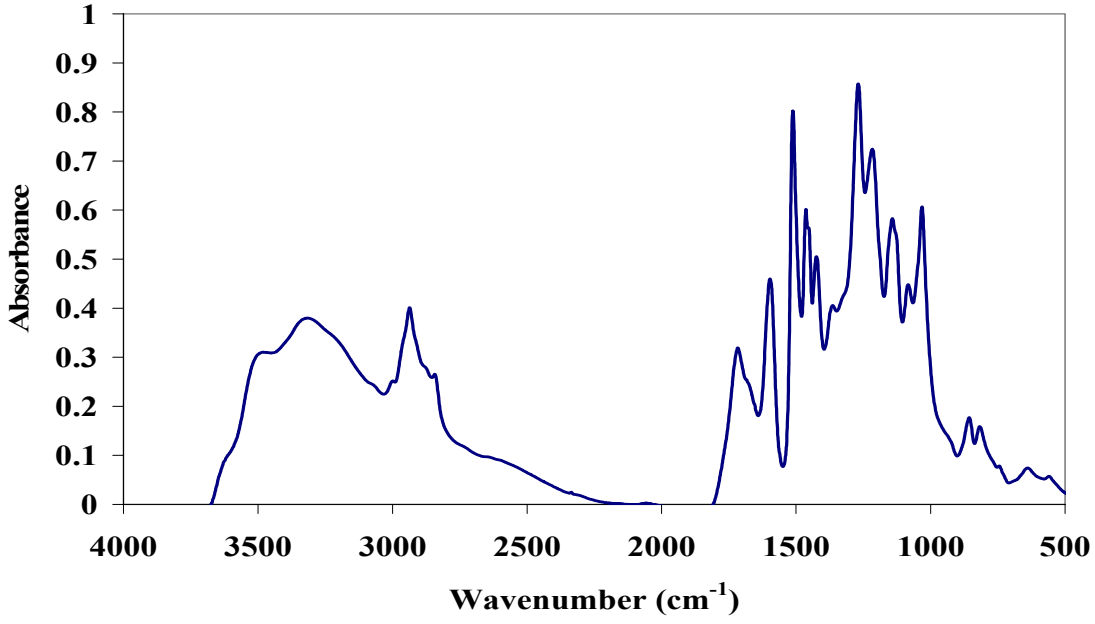

Figure A-4-29. FT-IR spectrum of Condition 14 residual lignin from constant kappa number (approximately 30) series of pulps. Table A-4-1 summarizes the pulping conditions used to produce the pulp for the respective residual lignin.

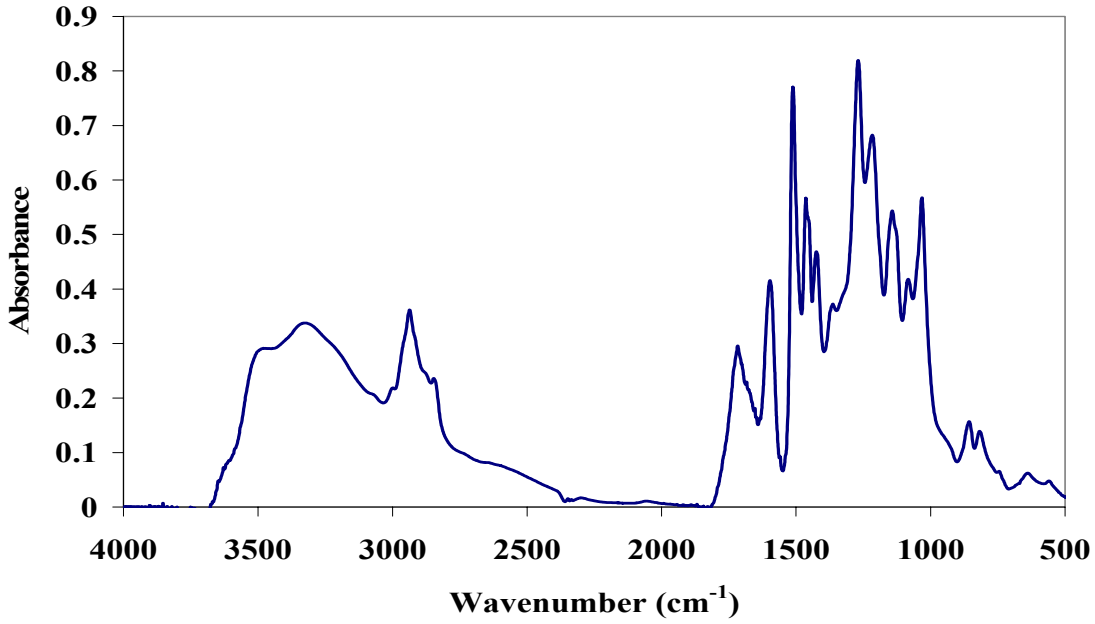

Figure A-4-30. FT-IR spectrum of Condition 15 residual lignin from constant kappa number (approximately 30) series of pulps. Table A-4-1 summarizes the pulping conditions used to produce the pulp for the respective residual lignin.

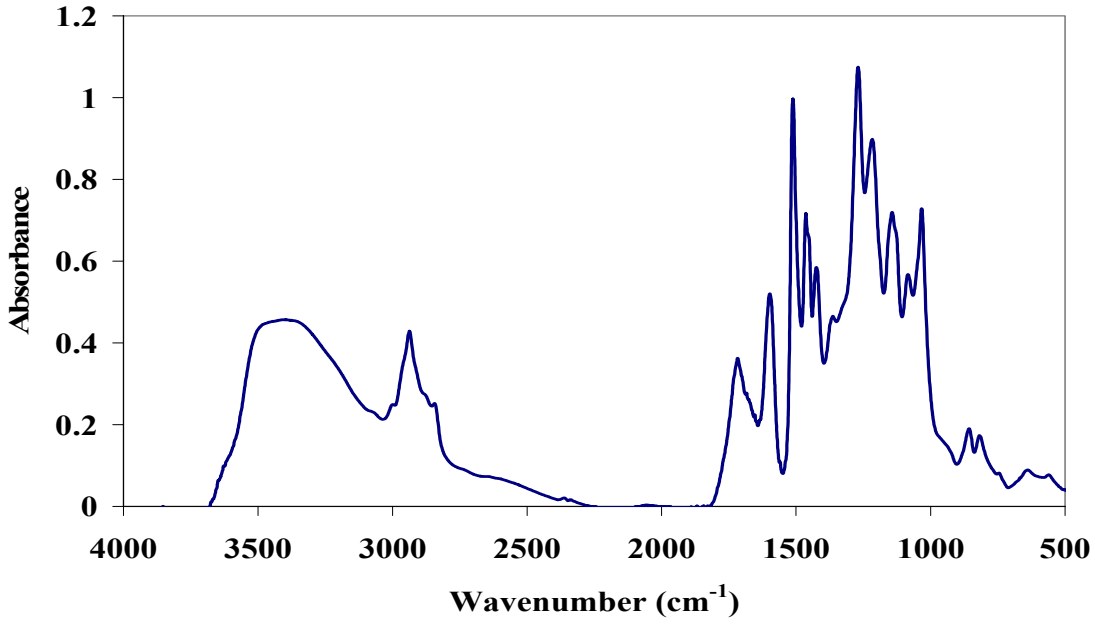

Figure A-4-31. FT-IR spectrum of Condition 16 residual lignin from constant kappa number (approximately 30) series of pulps. Table A-4-1 summarizes the pulping conditions used to produce the pulp for the respective residual lignin.

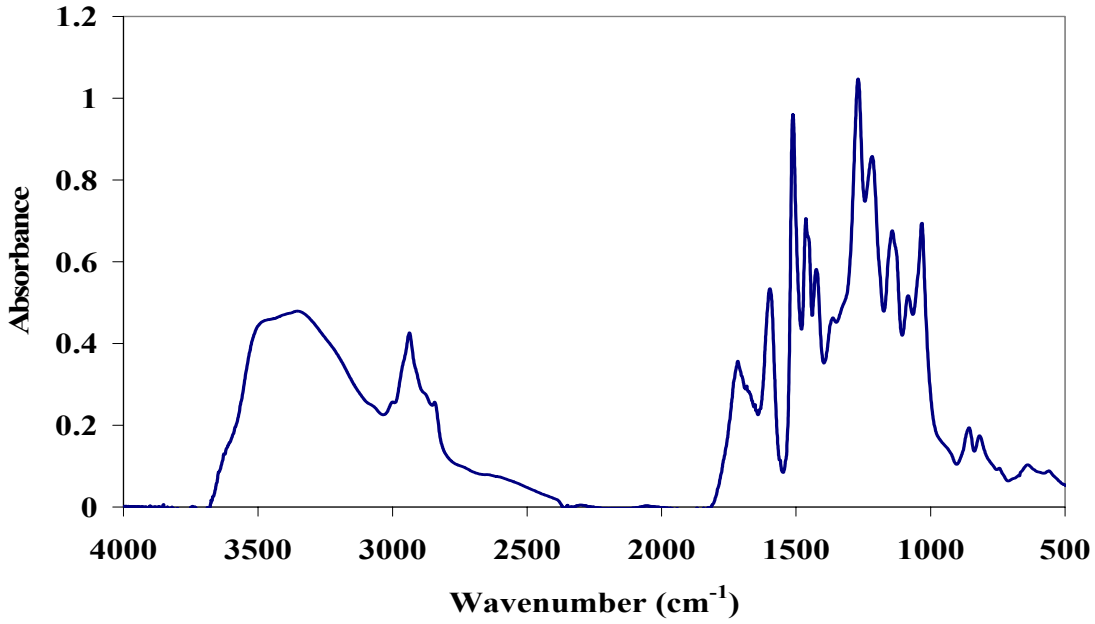

Figure A-4-32. FT-IR spectrum of Condition 17 residual lignin from constant kappa number (approximately 30) series of pulps. Table A-4-1 summarizes the pulping conditions used to produce the pulp for the respective residual lignin.

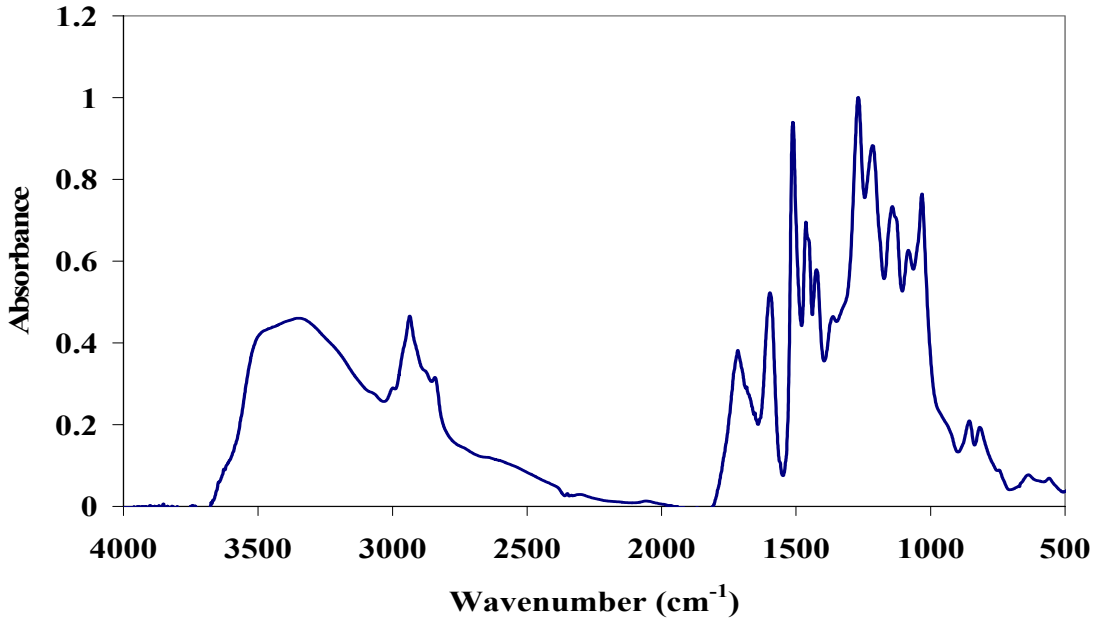

Figure A-4-33. FT-IR spectrum of Condition 18 residual lignin from constant kappa number (approximately 30) series of pulps. Table A-4-1 summarizes the pulping conditions used to produce the pulp for the respective residual lignin.

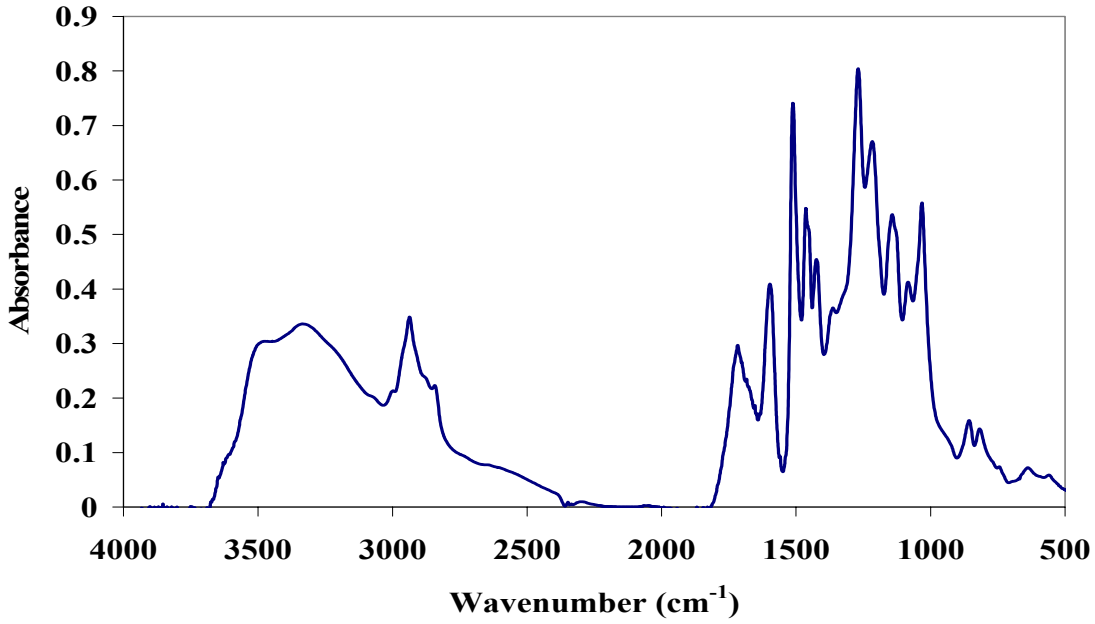

Figure A-4-34. FT-IR spectrum of Condition 19 residual lignin from constant kappa number (approximately 30) series of pulps. Table A-4-1 summarizes the pulping conditions used to produce the pulp for the respective residual lignin.

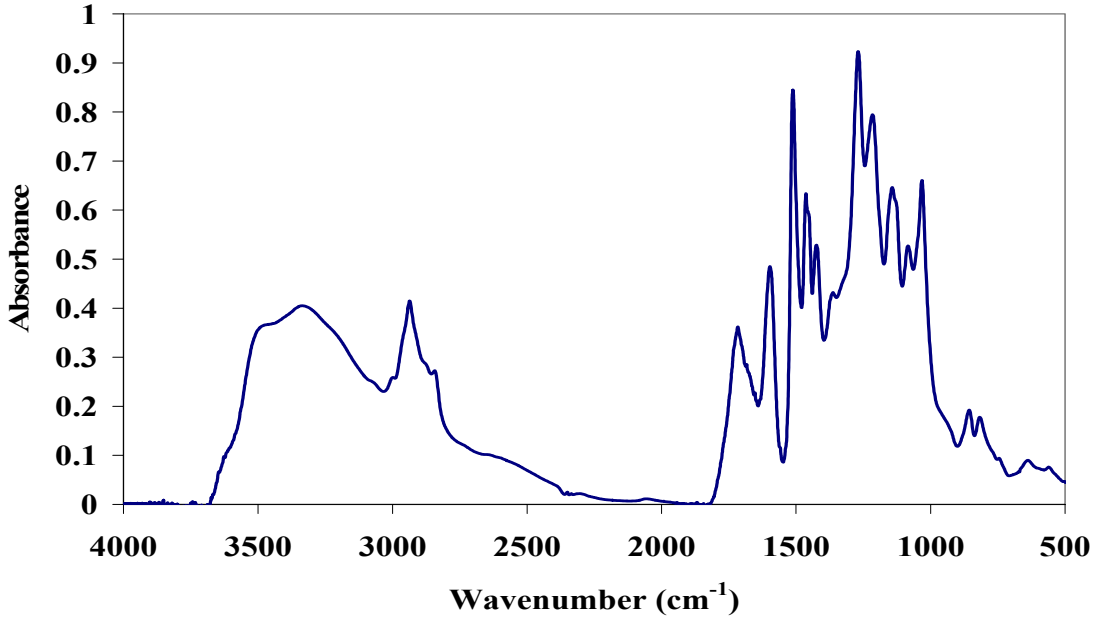

Figure A-4-35. FT-IR spectrum of Condition 20 residual lignin from constant kappa number (approximately 30) series of pulps. Table A-4-1 summarizes the pulping conditions used to produce the pulp for the respective residual lignin.

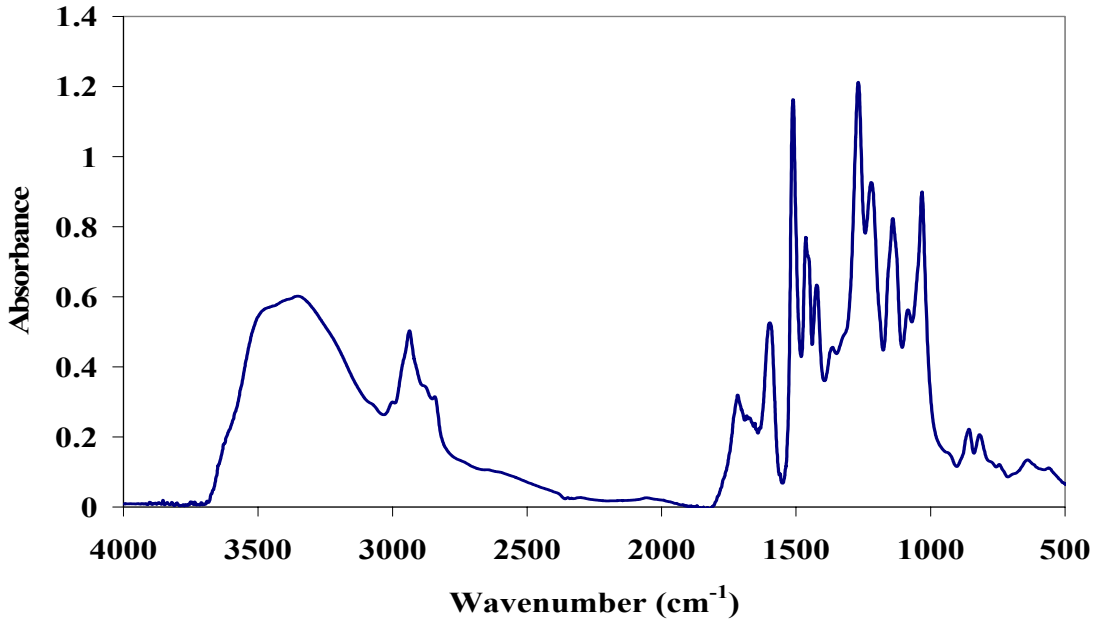

Figure A-4-36. FT-IR spectrum of Condition A-1 residual lignin from incremental cook series of pulps. Table A-4-2 summarizes the pulping conditions used to produce the pulp for the respective residual lignin.

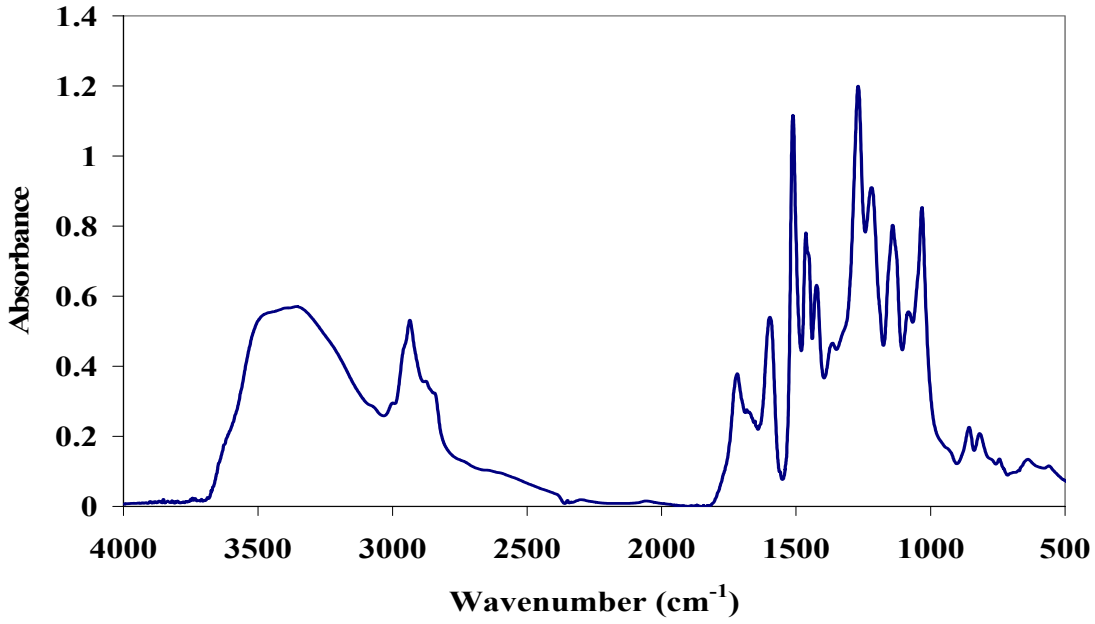

Figure A-4-37. FT-IR spectrum of Condition A-2 residual lignin from incremental cook series of pulps. Table A-4-2 summarizes the pulping conditions used to produce the pulp for the respective residual lignin.

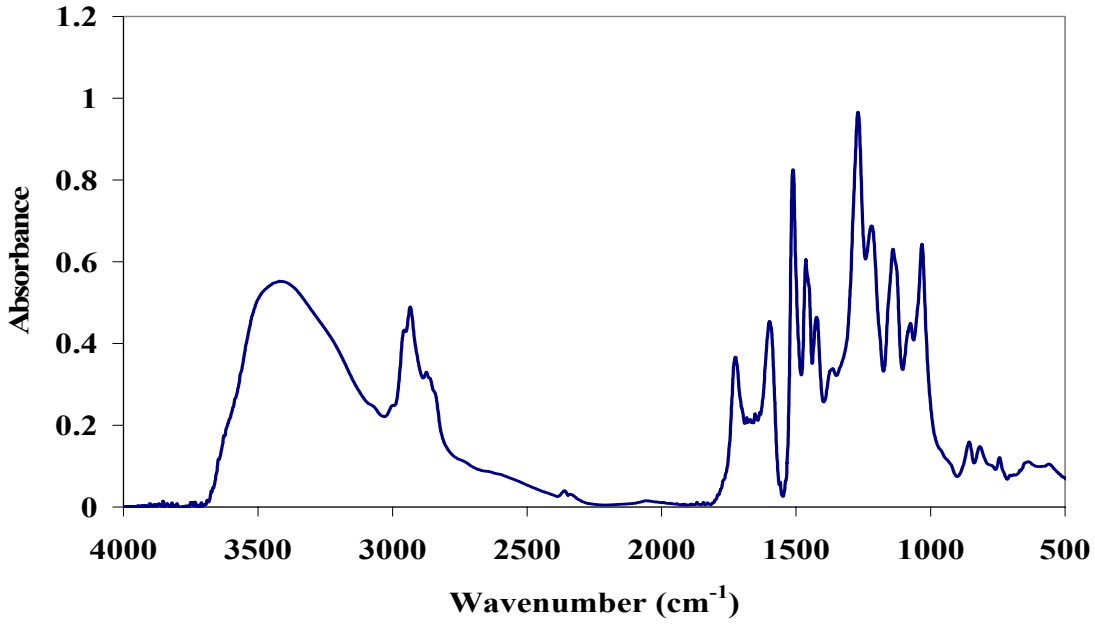

Figure A-4-38. FT-IR spectrum of Condition A-3 residual lignin from incremental cook series of pulps. Table A-4-2 summarizes the pulping conditions used to produce the pulp for the respective residual lignin.

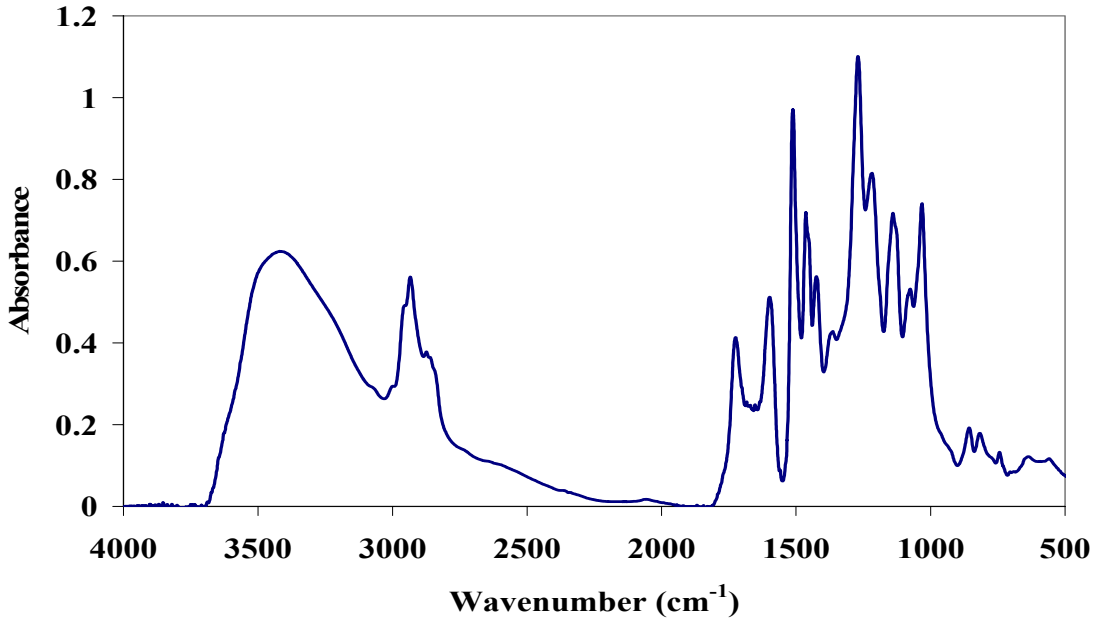

Figure A-4-39. FT-IR spectrum of Condition A-4 residual lignin from incremental cook series of pulps. Table A-4-2 summarizes the pulping conditions used to produce the pulp for the respective residual lignin.

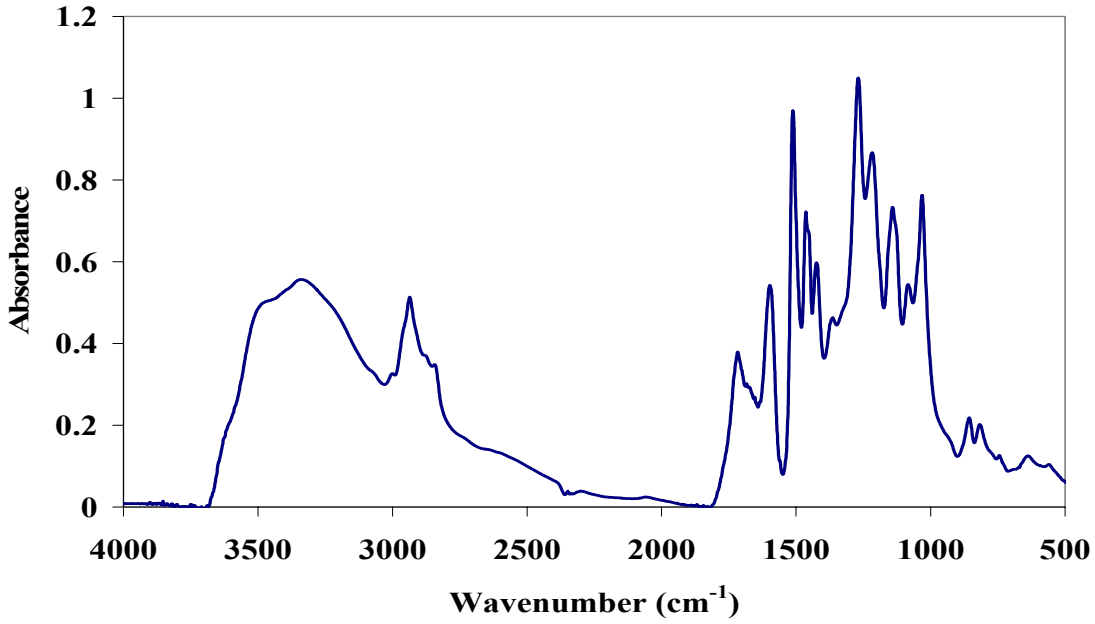

Figure A-4-40. FT-IR spectrum of Condition A-5 residual lignin from incremental cook series of pulps. Table A-4-2 summarizes the pulping conditions used to produce the pulp for the respective residual lignin.

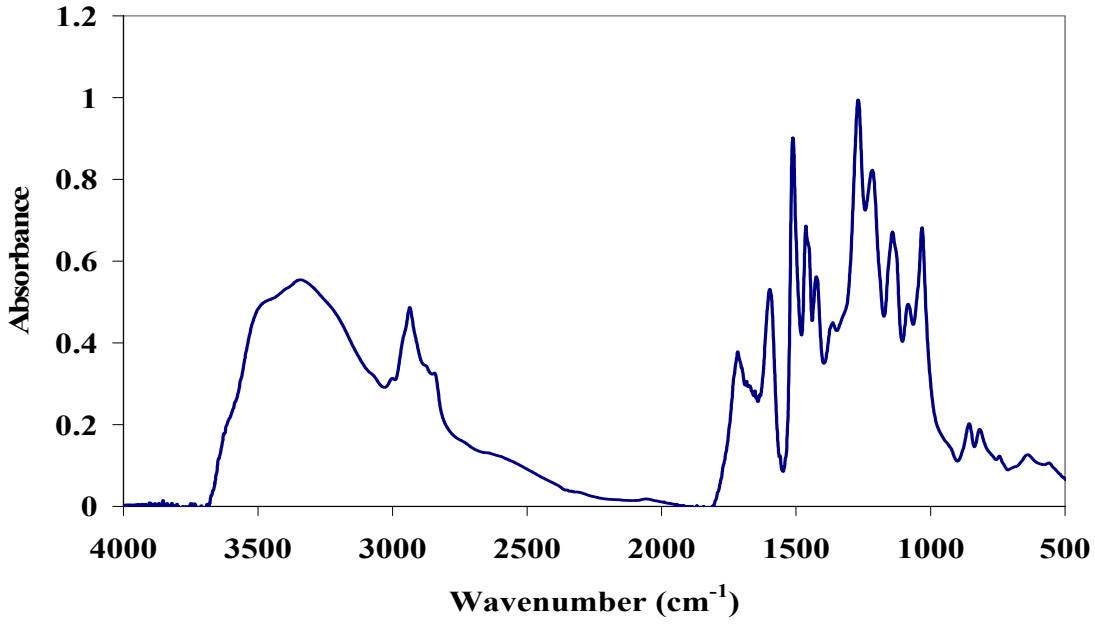

Figure A-4-41. FT-IR spectrum of Condition A-6 residual lignin from incremental cook series of pulps. Table A-4-2 summarizes the pulping conditions used to produce the pulp for the respective residual lignin.

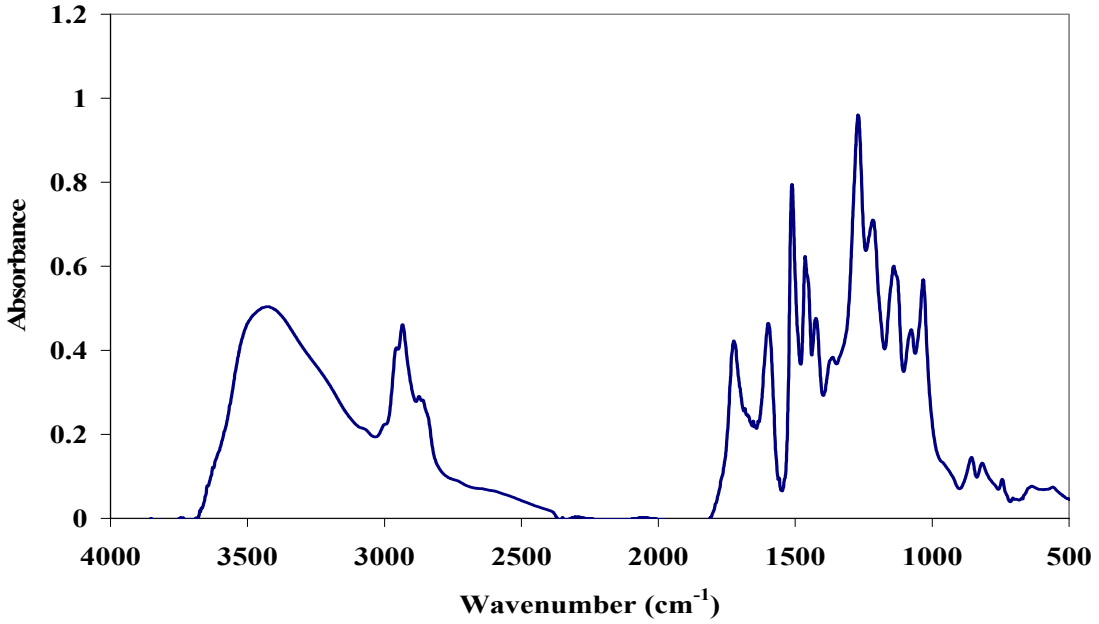

Figure A-4-42. FT-IR spectrum of Condition A-7 residual lignin from incremental cook series of pulps. Table A-4-2 summarizes the pulping conditions used to produce the pulp for the respective residual lignin.

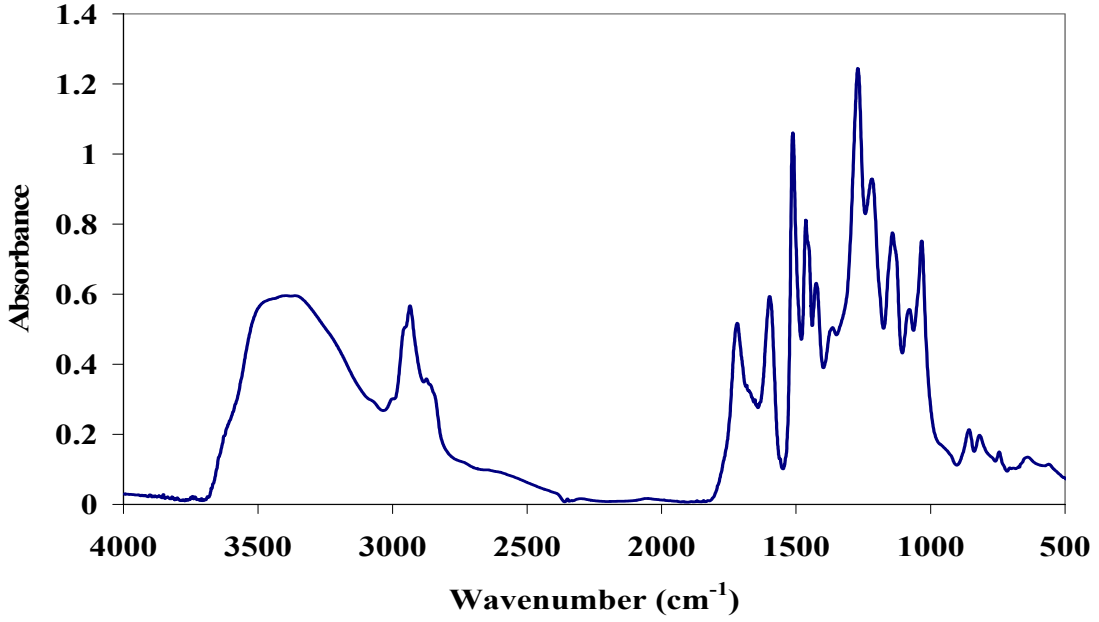

Figure A-4-43. FT-IR spectrum of Condition A-8 residual lignin from incremental cook series of pulps. Table A-4-2 summarizes the pulping conditions used to produce the pulp for the respective residual lignin.

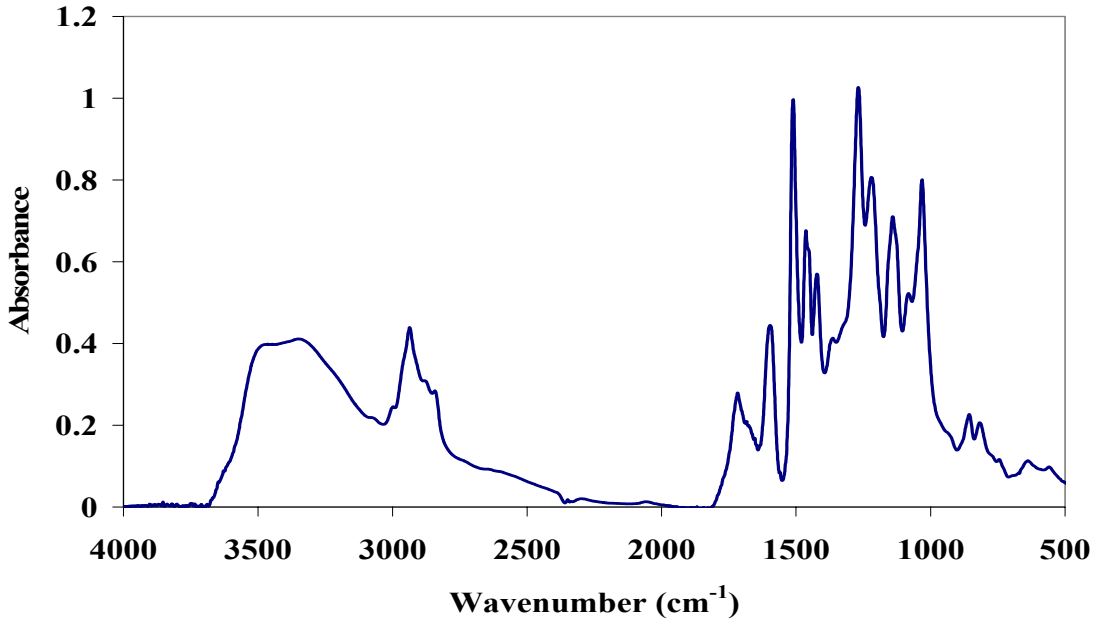

Figure A-4-44. FT-IR spectrum of Condition B-1 residual lignin from incremental cook series of pulps. Table A-4-2 summarizes the pulping conditions used to produce the pulp for the respective residual lignin.

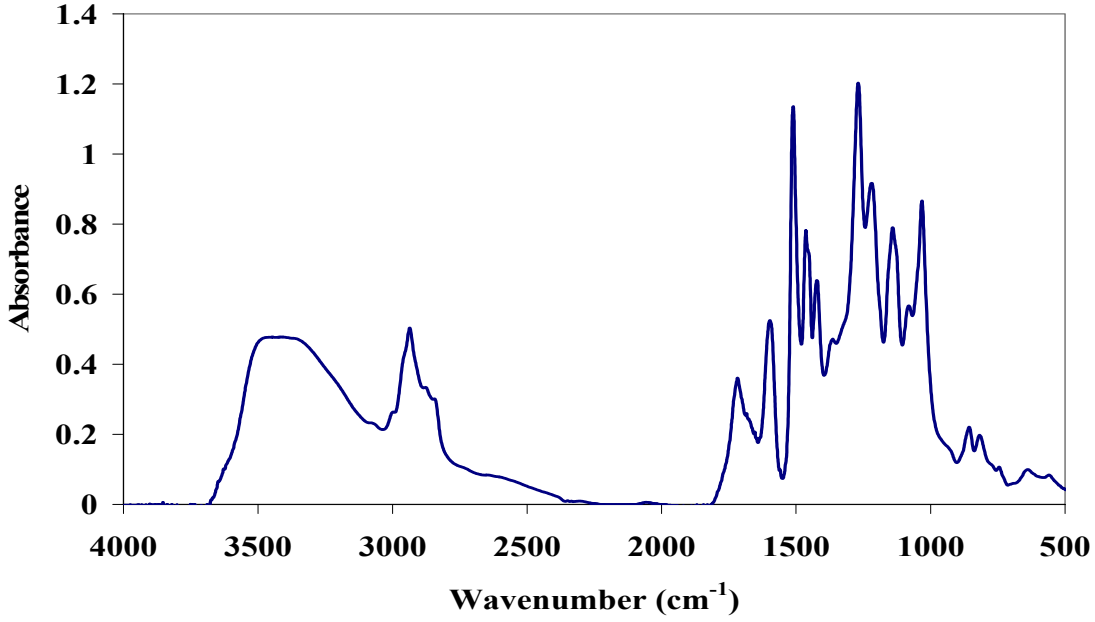

Figure A-4-45. FT-IR spectrum of Condition B-2 residual lignin from incremental cook series of pulps. Table A-4-2 summarizes the pulping conditions used to produce the pulp for the respective residual lignin.

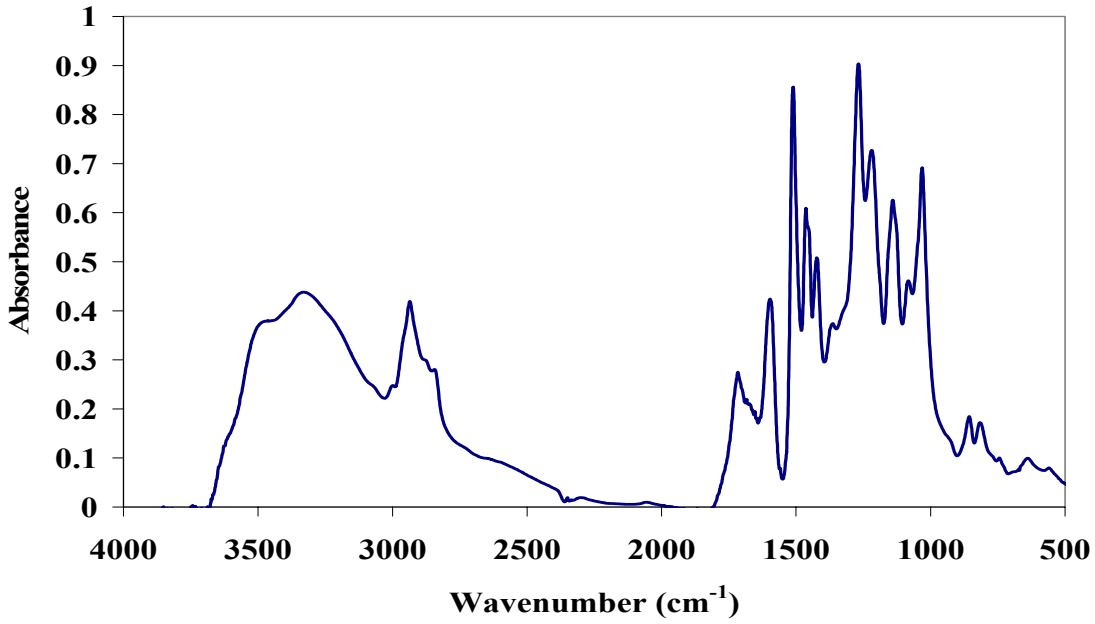

Figure A-4-46. FT-IR spectrum of Condition B-3 residual lignin from incremental cook series of pulps. Table A-4-2 summarizes the pulping conditions used to produce the pulp for the respective residual lignin.

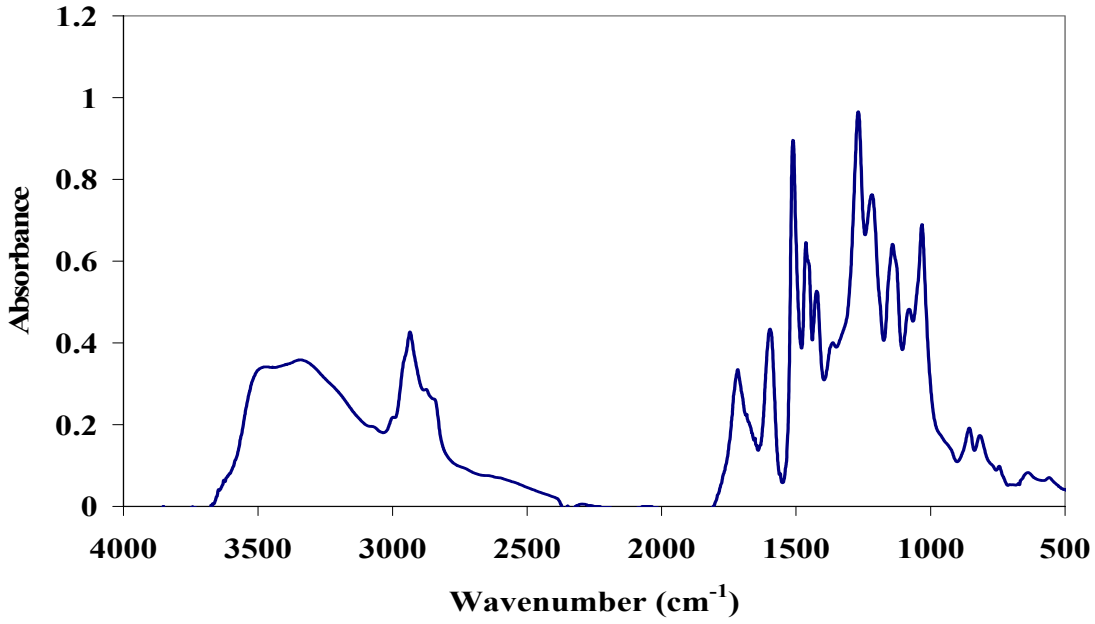

Figure A-4-47. FT-IR spectrum of Condition B-4 residual lignin from incremental cook series of pulps. Table A-4-2 summarizes the pulping conditions used to produce the pulp for the respective residual lignin.

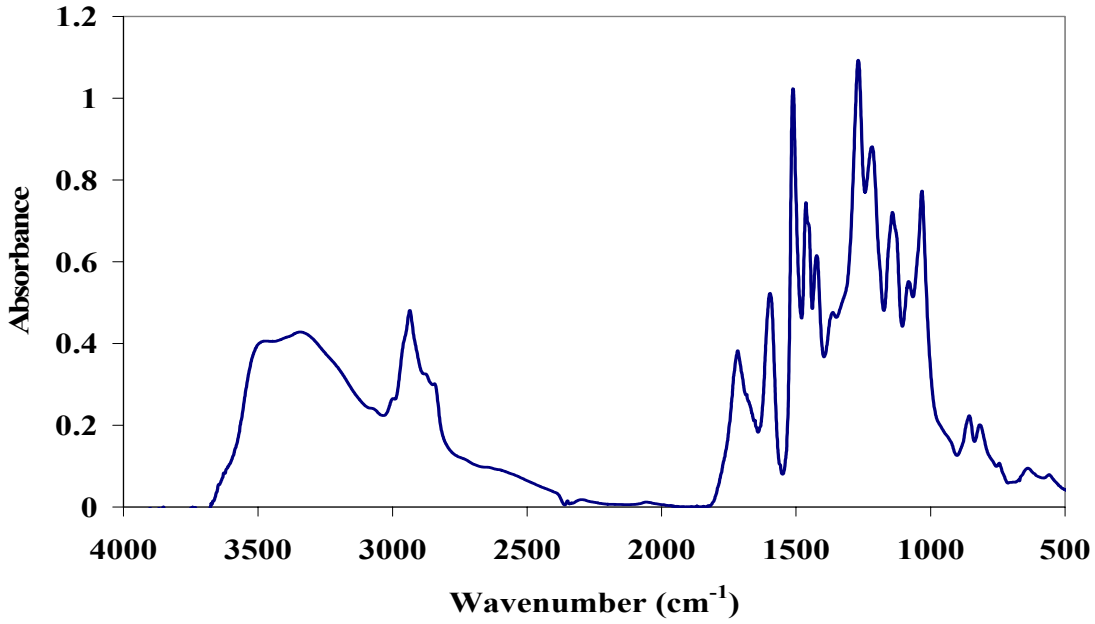

Figure A-4-48. FT-IR spectrum of Condition B-5 residual lignin from incremental cook series of pulps. Table A-4-2 summarizes the pulping conditions used to produce the pulp for the respective residual lignin.

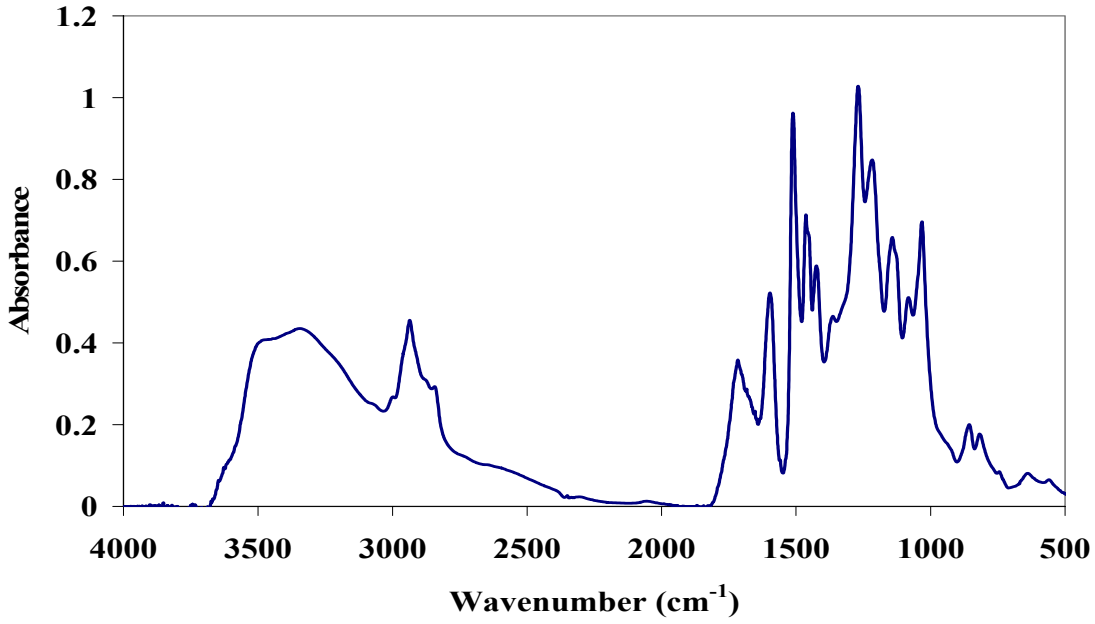

Figure A-4-49. FT-IR spectrum of Condition B-6 residual lignin from incremental cook series of pulps. Table A-4-2 summarizes the pulping conditions used to produce the pulp for the respective residual lignin.

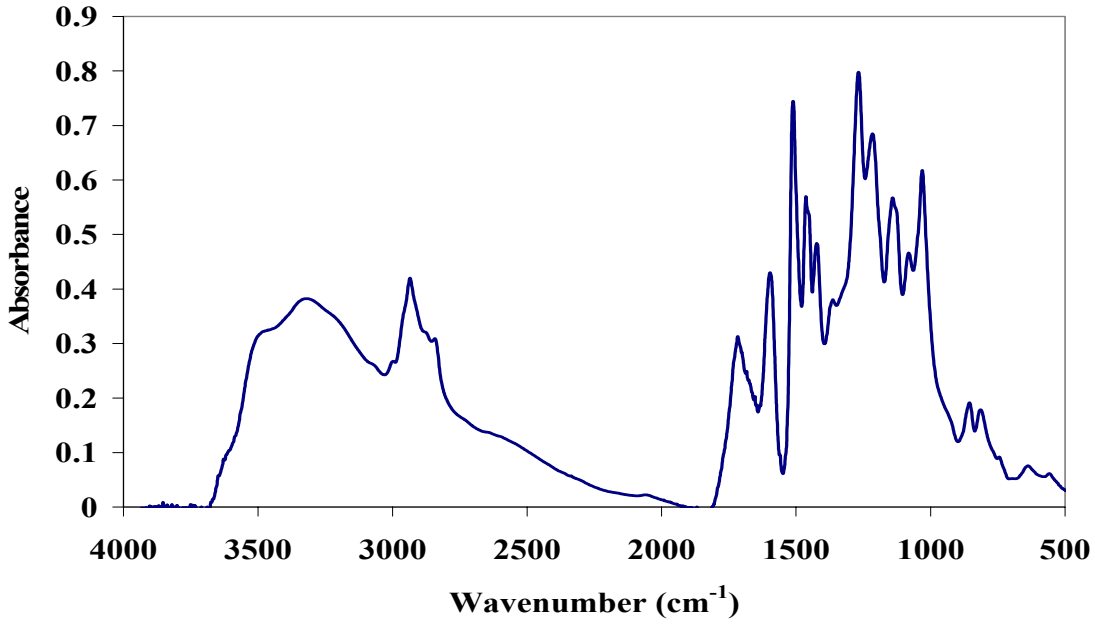

Figure A-4-50. FT-IR spectrum of Condition B-7 residual lignin from incremental cook series of pulps. Table A-4-2 summarizes the pulping conditions used to produce the pulp for the respective residual lignin.

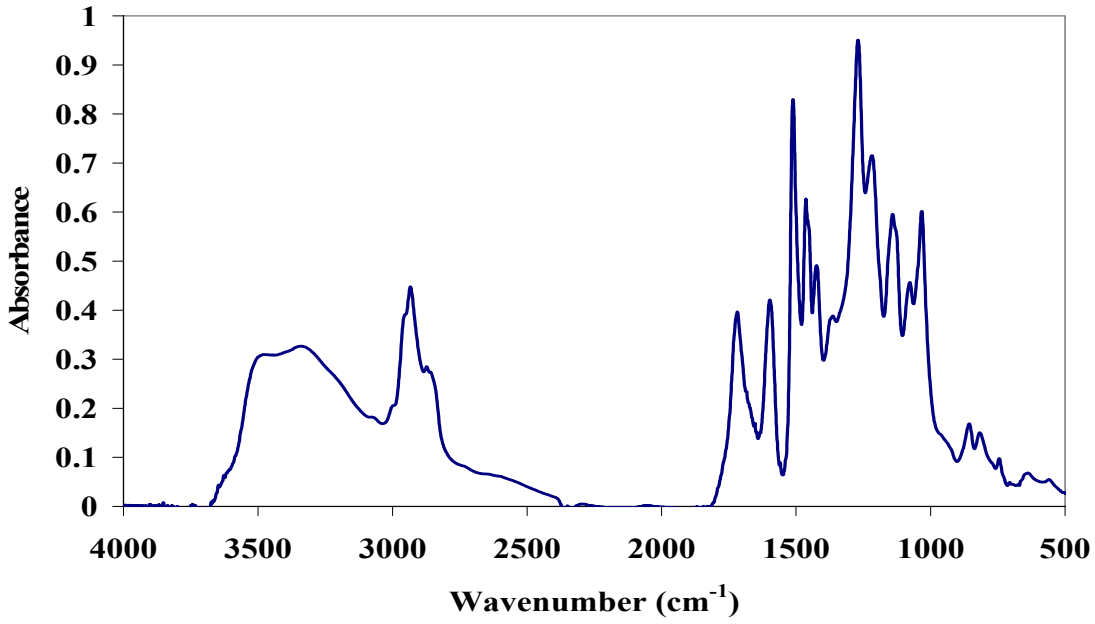

Figure A-4-51. FT-IR spectrum of Condition B-8 residual lignin from incremental cook series of pulps. Table A-4-2 summarizes the pulping conditions used to produce the pulp for the respective residual lignin.

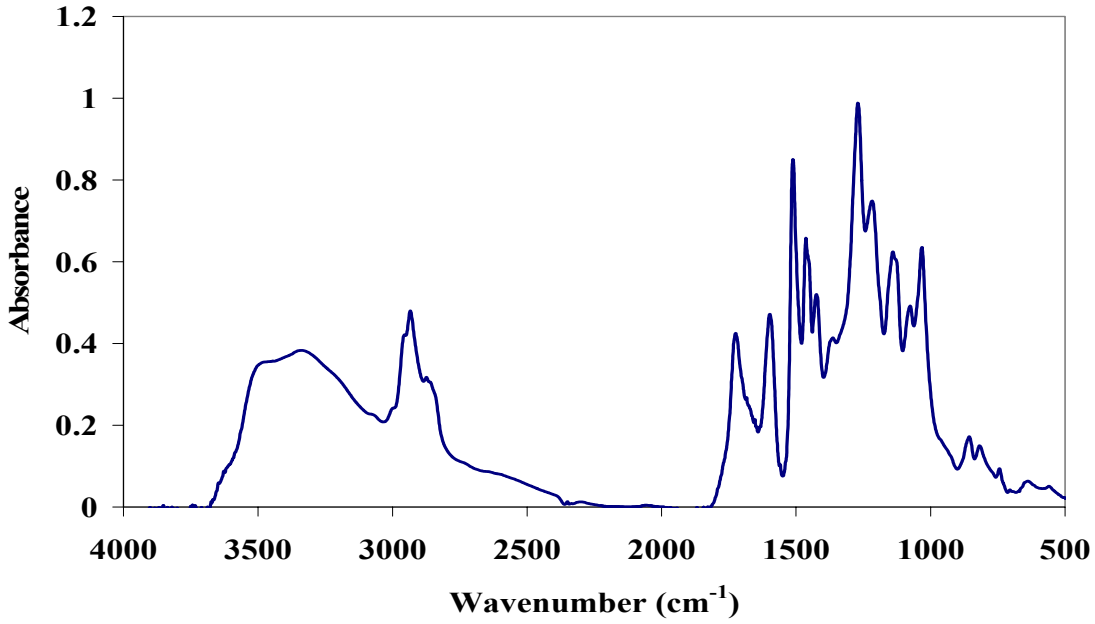

Figure A-4-52. FT-IR spectrum of Condition B-9 residual lignin from incremental cook series of pulps. Table A-4-2 summarizes the pulping conditions used to produce the pulp for the respective residual lignin.

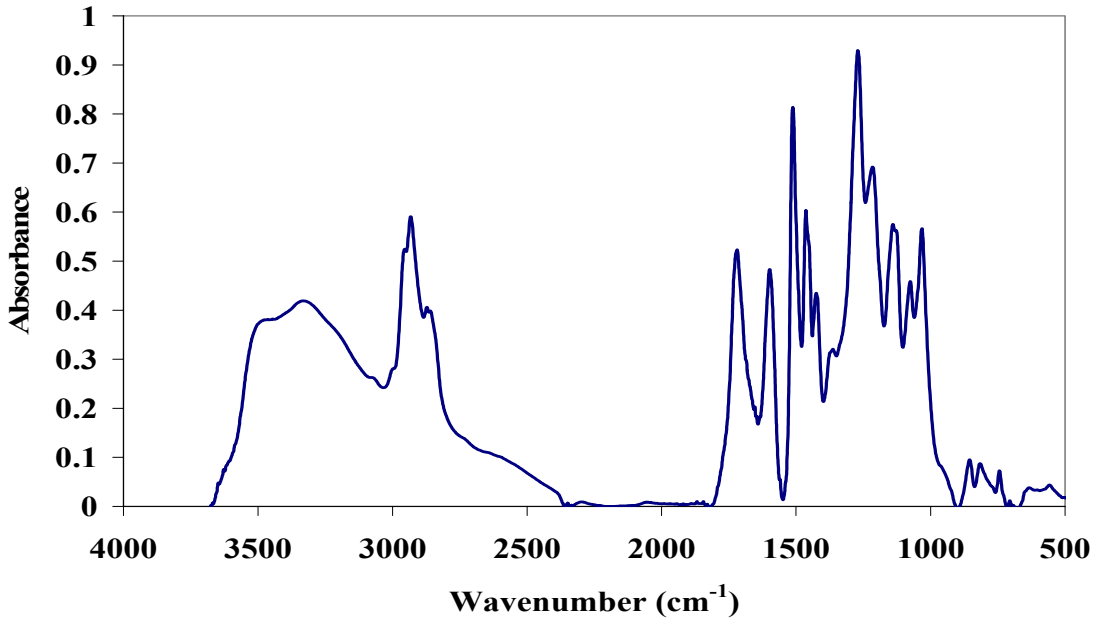

Figure A-4-53. FT-IR spectrum of Condition B-10 residual lignin from incremental cook series of pulps. Table A-4-2 summarizes the pulping conditions used to produce the pulp for the respective residual lignin.

18.9 Summary of FT-IR Data for Residual Lignins

Table A-4-8. FT-IR analysis of residual lignins obtained from constant kappa number pulps. Table A-4-1 summarizes the pulping conditions used to produce the pulps for the respective residual lignins.

Condition	Peak 1704-1739 cm^{-1}	Peak 1600 cm^{-1}	Area 1840-1550 cm^{-1}	% CO
1	0.40	0.57	72.07	4.70
2	0.38	0.61	70.22	4.15
3	0.35	0.52	62.07	4.36
4	0.35	0.55	63.20	4.14
5	0.39	0.56	69.26	4.57
6	0.38	0.60	67.90	4.06
7	0.37	0.54	62.92	4.22
8	0.29	0.44	49.12	3.98
9	0.37	0.52	62.80	4.43
10	0.33	0.50	55.92	3.99
11	0.42	0.58	71.73	4.57
12	0.36	0.54	61.87	4.13
13	0.39	0.56	66.32	4.31
14	0.32	0.46	55.67	4.44
15	0.30	0.42	50.07	4.35
16	0.36	0.52	62.28	4.38
17	0.36	0.53	64.51	4.47
18	0.38	0.52	63.92	4.53
19	0.30	0.41	51.01	4.60
20	0.36	0.48	62.39	4.87

Table A-4-9. FT-IR analysis of residual lignins obtained from incremental cook pulps. Table A-4-2 summarizes the pulping conditions used to produce the pulp for the respective residual lignin.

Condition	Peak 1704-1739 cm^{-1}	Peak 1600 cm^{-1}	Area 1840-1550 cm^{-1}	% CO
A-1	0.32	0.53	57.92	3.87
A-2	0.38	0.54	63.06	4.23
A-3	0.37	0.45	53.66	4.35
A-4	0.41	0.51	62.00	4.47
A-5	0.38	0.54	66.23	4.52
A-6	0.38	0.53	66.29	4.64
A-7	0.42	0.46	60.53	4.95
A-8	0.52	0.59	77.96	4.98
B-1	0.28	0.44	47.78	3.84
B-2	0.36	0.52	58.86	4.06
B-3	0.28	0.42	47.94	4.11
B-4	0.34	0.43	49.81	4.19
B-5	0.38	0.52	62.16	4.37
B-6	0.36	0.52	62.68	4.42
B-7	0.31	0.43	53.56	4.61
B-8	0.40	0.42	53.08	4.70
B-9	0.43	0.47	61.08	4.87
B-10	0.52	0.48	64.72	5.11

18.10 ^{31}P NMR for Hydroxyl Groups Spectra of Residual Lignins

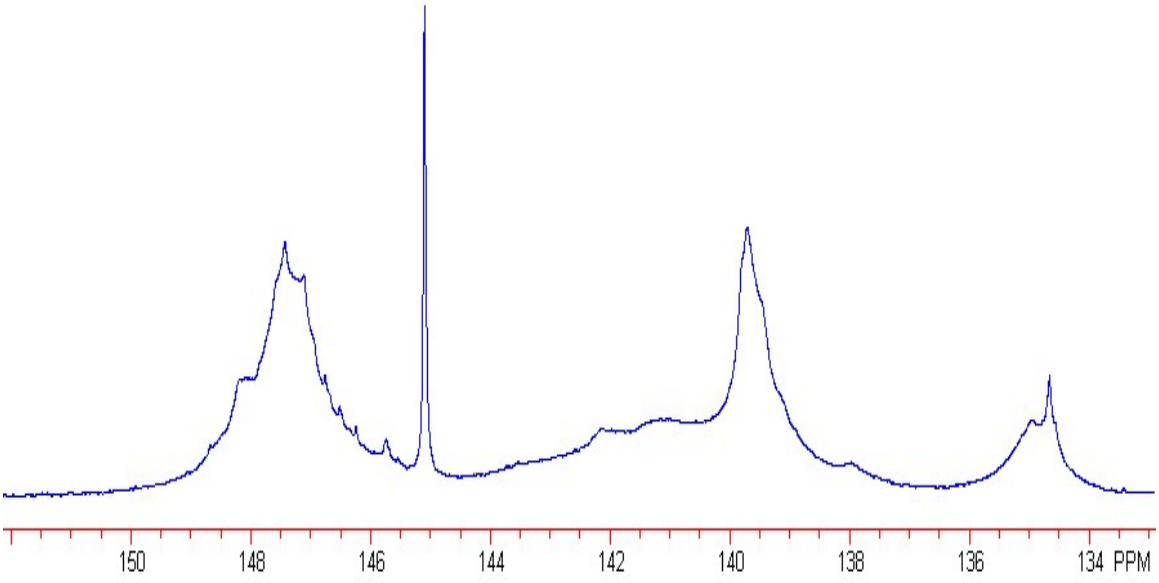

Figure A-4-54. ^{31}P NMR spectrum of residual lignin from Condition 1 of the constant kappa number (approximately 30) series of pulps. Table A-4-1 summarizes the pulping conditions used to produce the pulp for the respective residual lignin.

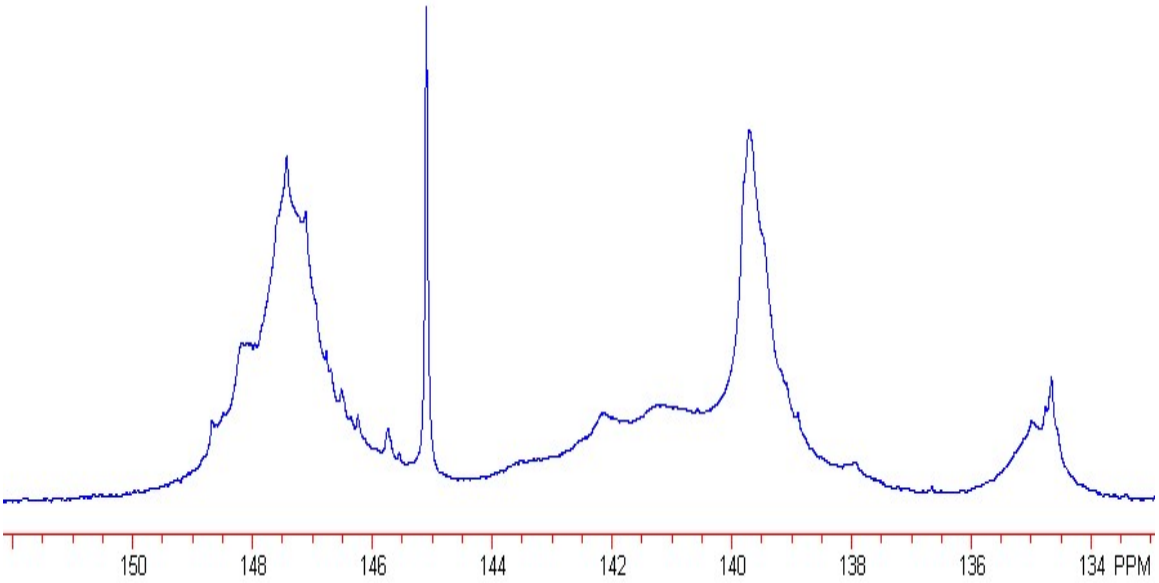

Figure A-4-55. ^{31}P NMR spectrum of residual lignin from Condition 2 of the constant kappa number (approximately 30) series of pulps. Table A-4-1 summarizes the pulping conditions used to produce the pulp for the respective residual lignin.

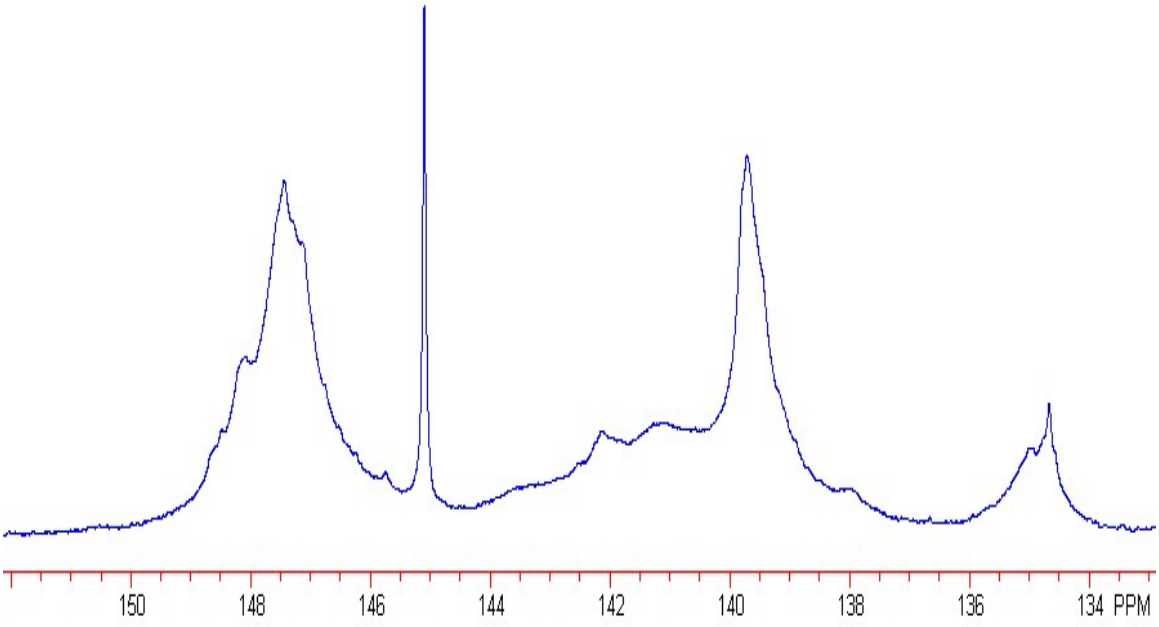

Figure A-4-56. ^{31}P NMR spectrum of residual lignin from Condition 3 of the constant kappa number (approximately 30) series of pulps. Table A-4-1 summarizes the pulping conditions used to produce the pulp for the respective residual lignin.

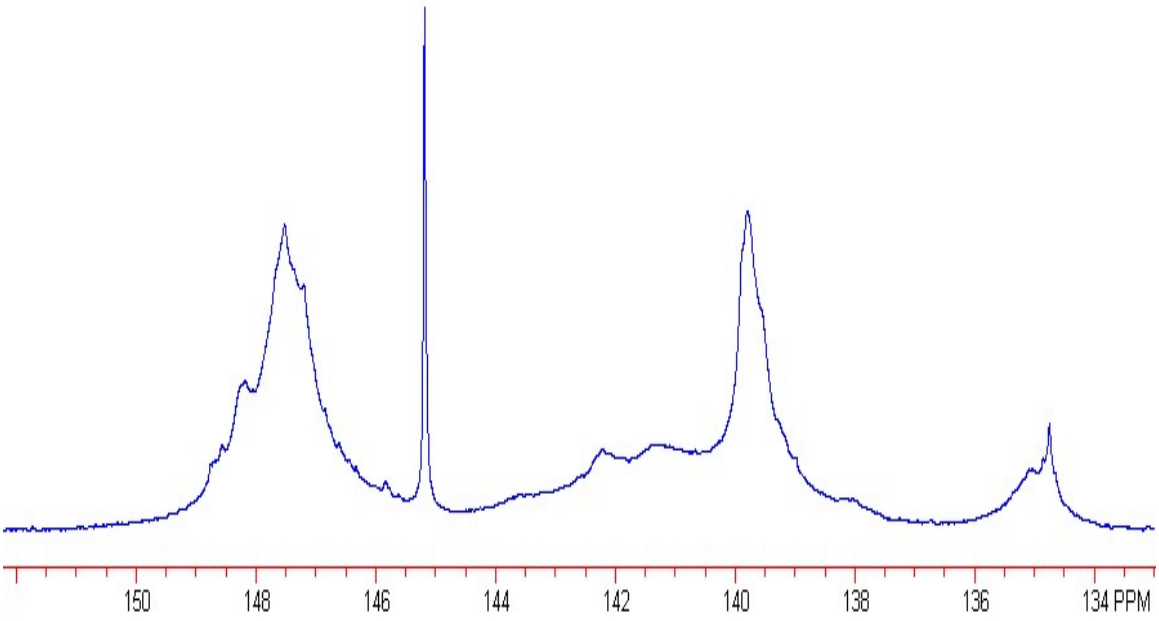

Figure A-4-57. ^{31}P NMR spectrum of residual lignin from Condition 4 of the constant kappa number (approximately 30) series of pulps. Table A-4-1 summarizes the pulping conditions used to produce the pulp for the respective residual lignin.

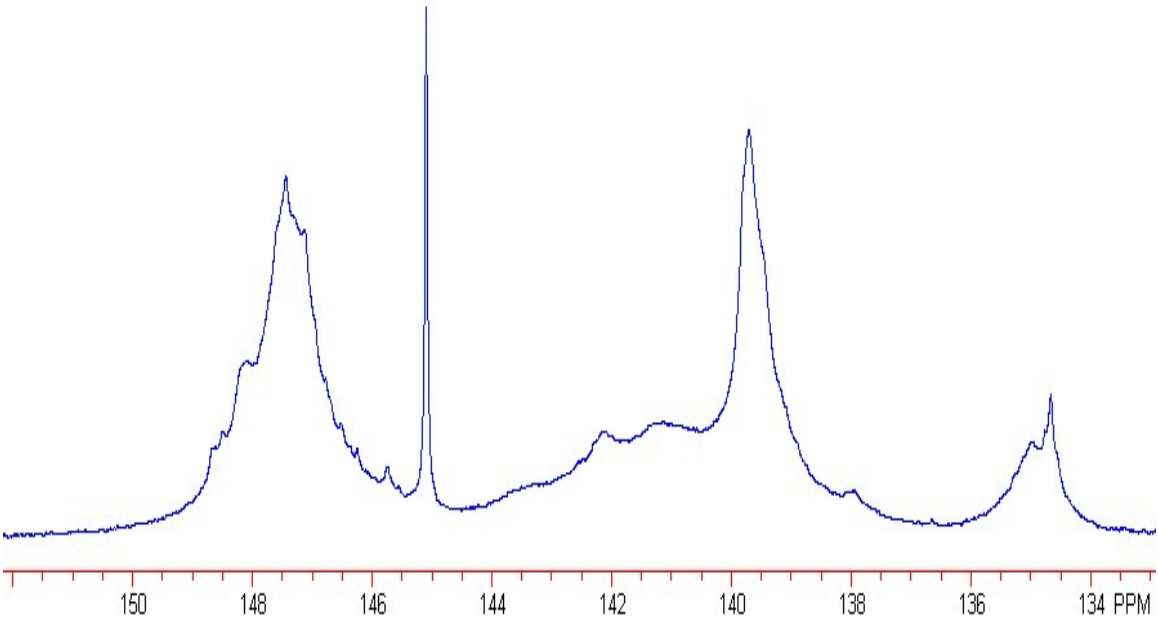

Figure A-4-58. ^{31}P NMR spectrum of residual lignin from Condition 5 of the constant kappa number (approximately 30) series of pulps. Table A-4-1 summarizes the pulping conditions used to produce the pulp for the respective residual lignin.

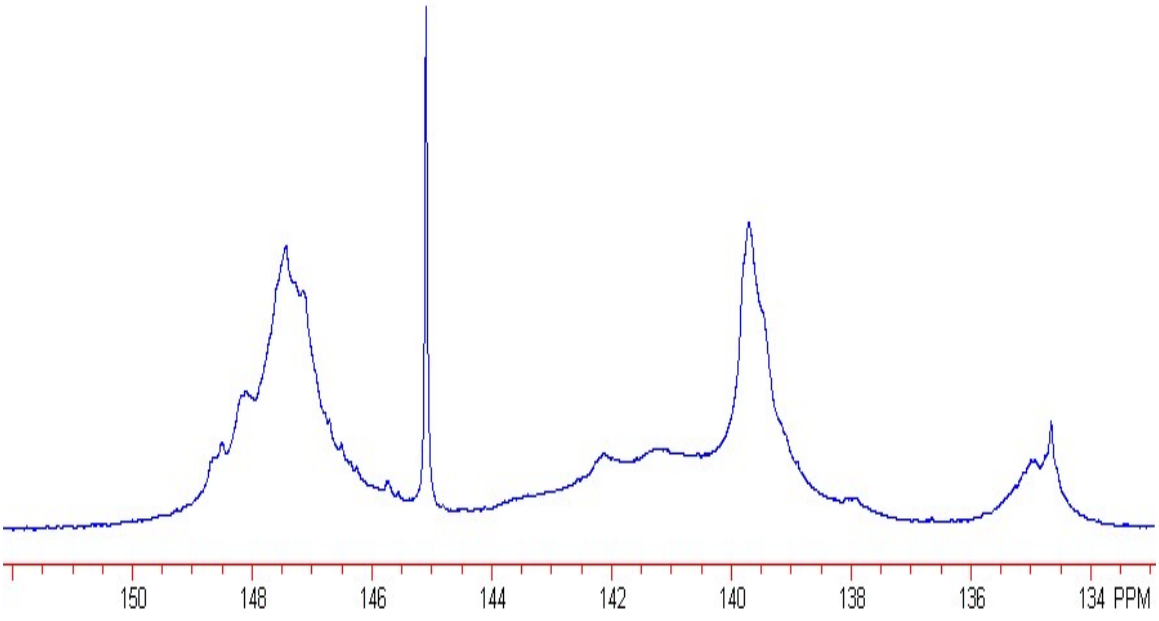

Figure A-4-59. ^{31}P NMR spectrum of residual lignin from Condition 6 of the constant kappa number (approximately 30) series of pulps. Table A-4-1 summarizes the pulping conditions used to produce the pulp for the respective residual lignin.

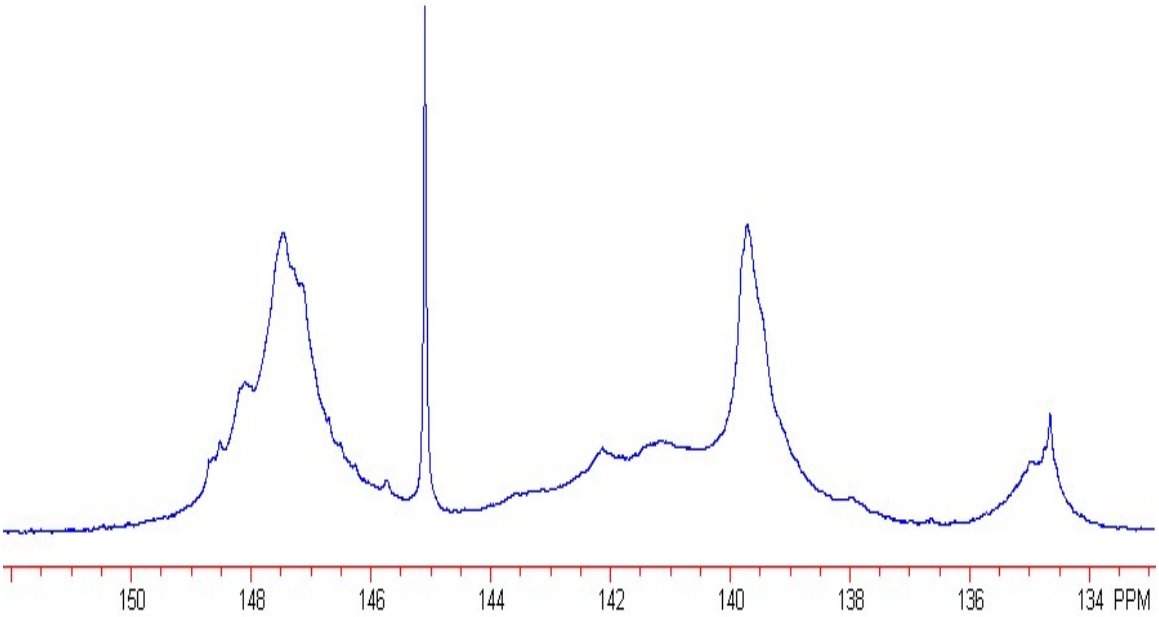

Figure A-4-60. ^{31}P NMR spectrum of residual lignin from Condition 7 of the constant kappa number (approximately 30) series of pulps. Table A-4-1 summarizes the pulping conditions used to produce the pulp for the respective residual lignin.

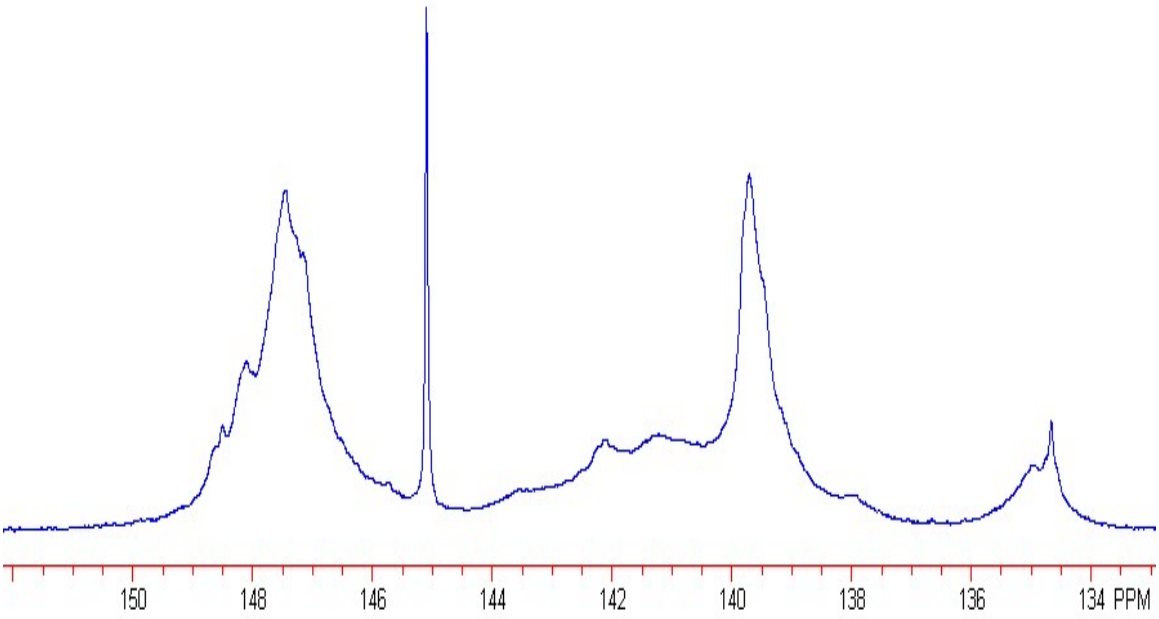

Figure A-4-61. ^{31}P NMR spectrum of residual lignin from Condition 8 of the constant kappa number (approximately 30) series of pulps. Table A-4-1 summarizes the pulping conditions used to produce the pulp for the respective residual lignin.

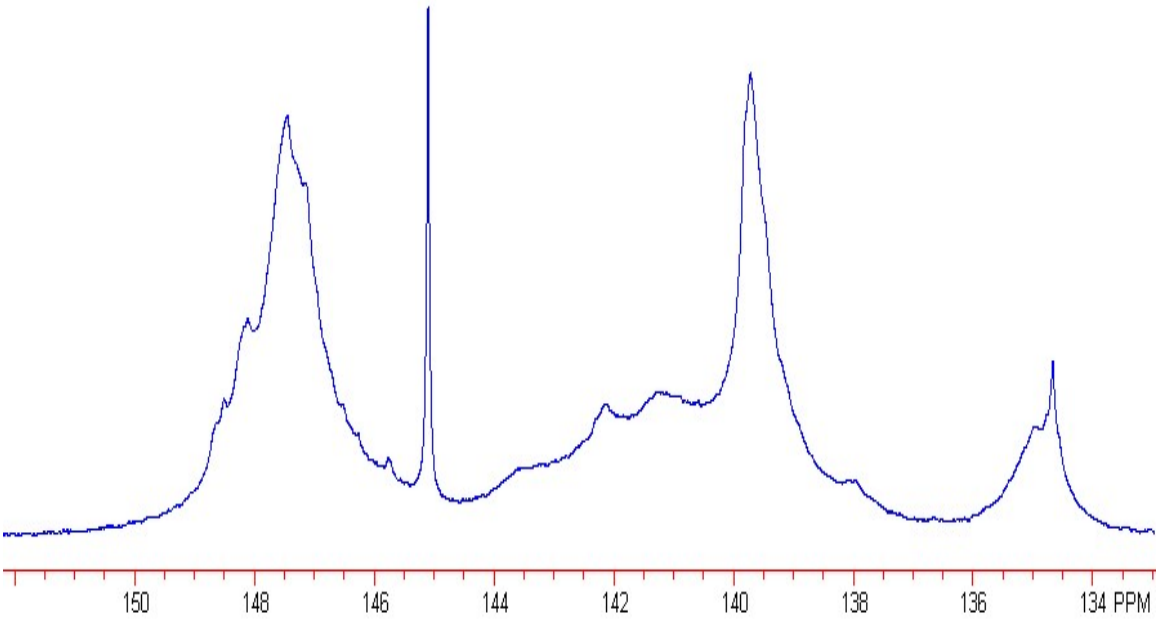

Figure A-4-62. ^{31}P NMR spectrum of residual lignin from Condition 9 of the constant kappa number (approximately 30) series of pulps. Table A-4-1 summarizes the pulping conditions used to produce the pulp for the respective residual lignin.

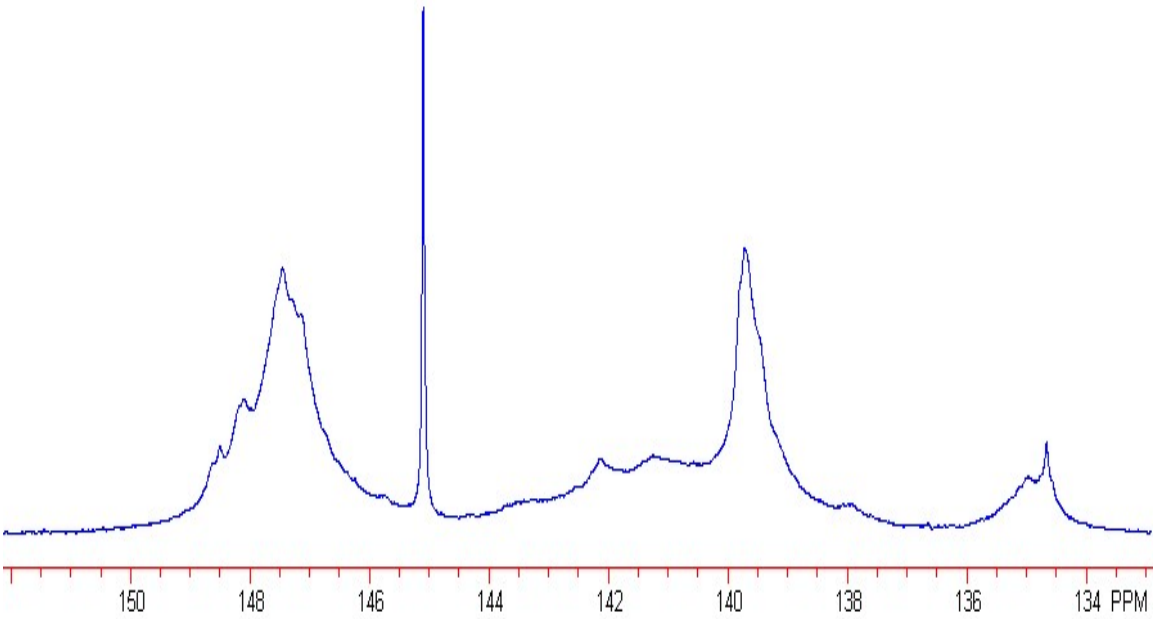

Figure A-4-63. ^{31}P NMR spectrum of residual lignin from Condition 10 of the constant kappa number (approximately 30) series of pulps. Table A-4-1 summarizes the pulping conditions used to produce the pulp for the respective residual lignin.

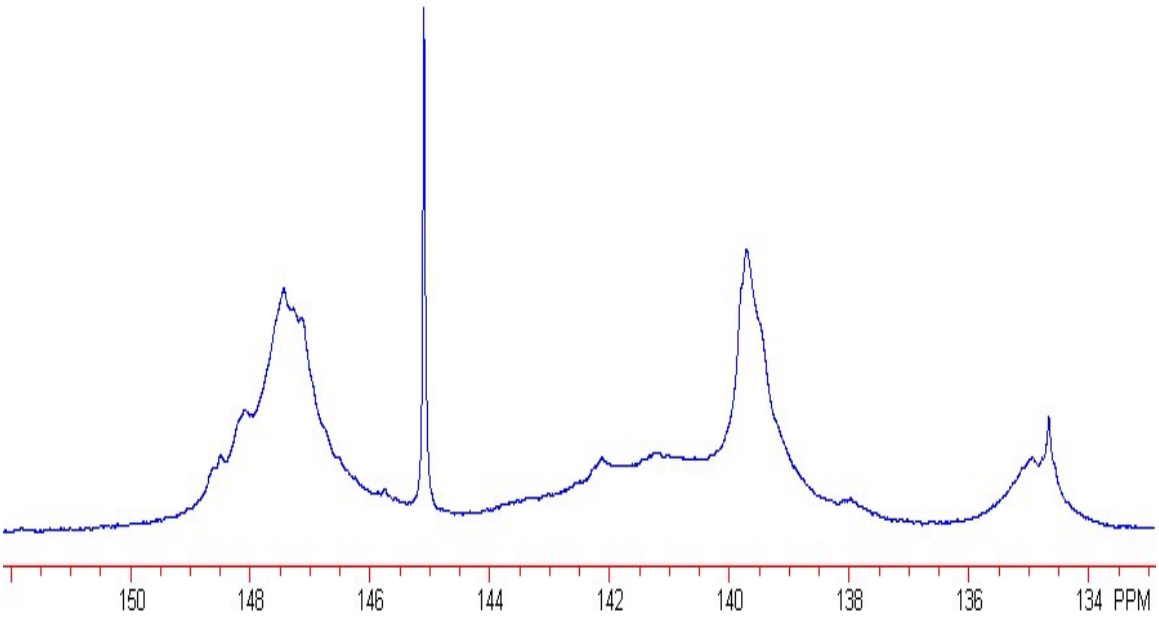

Figure A-4-64. ^{31}P NMR spectrum of residual lignin from Condition 11 of the constant kappa number (approximately 30) series of pulps. Table A-4-1 summarizes the pulping conditions used to produce the pulp for the respective residual lignin.

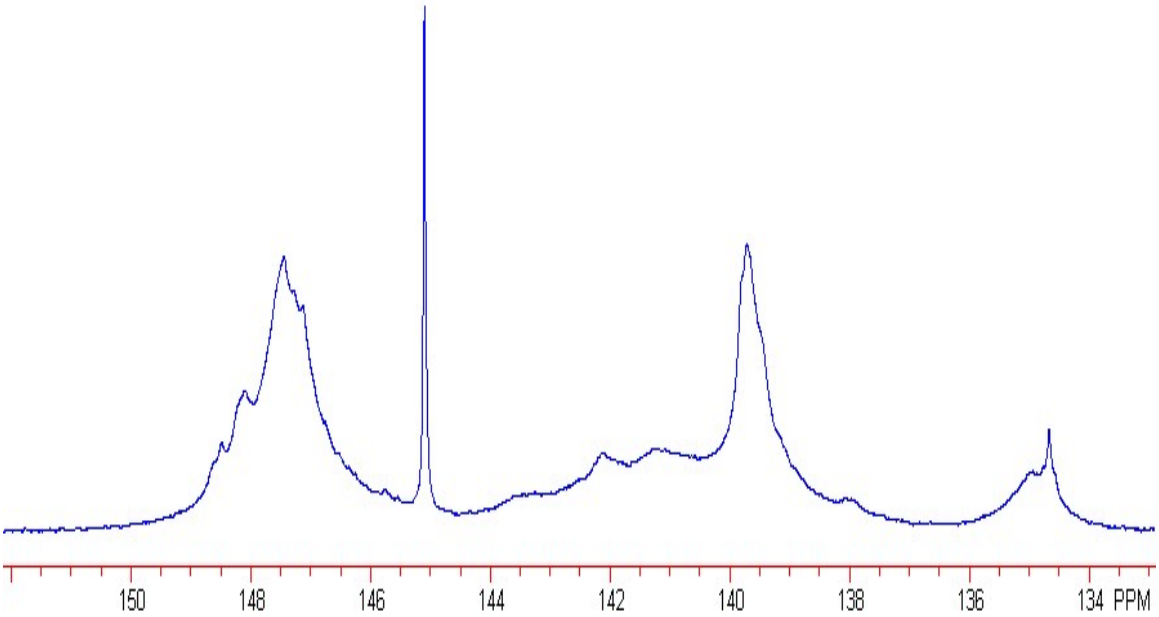

Figure A-4-65. ^{31}P NMR spectrum of residual lignin from Condition 12 of the constant kappa number (approximately 30) series of pulps. Table A-4-1 summarizes the pulping conditions used to produce the pulp for the respective residual lignin.

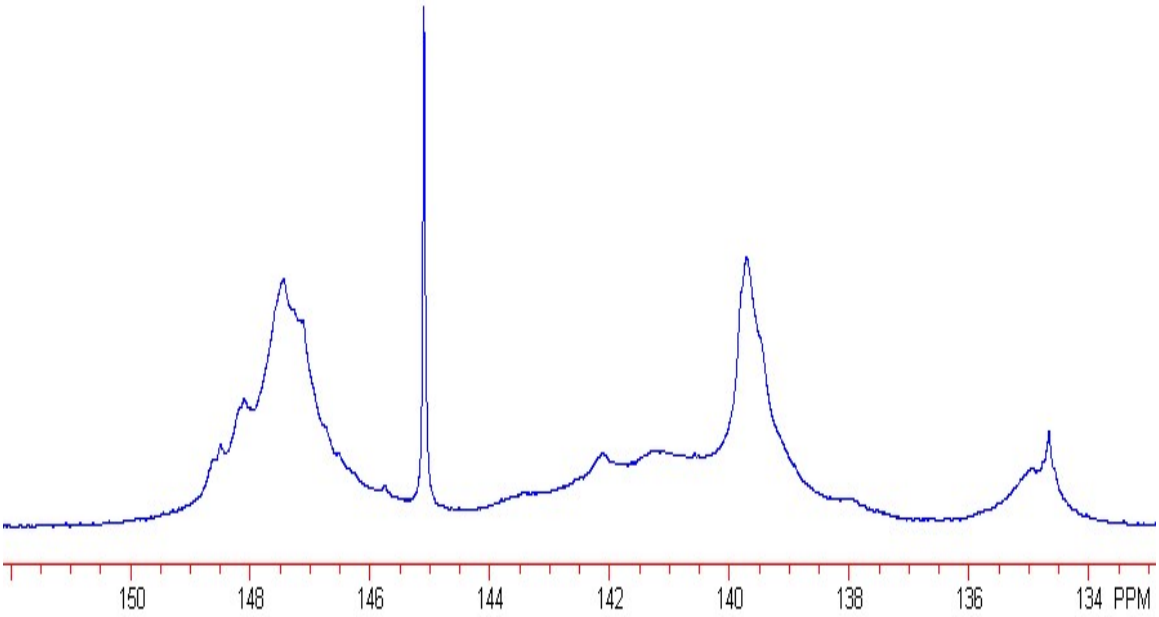

Figure A-4-66. ^{31}P NMR spectrum of residual lignin from Condition 13 of the constant kappa number (approximately 30) series of pulps. Table A-4-1 summarizes the pulping conditions used to produce the pulp for the respective residual lignin.

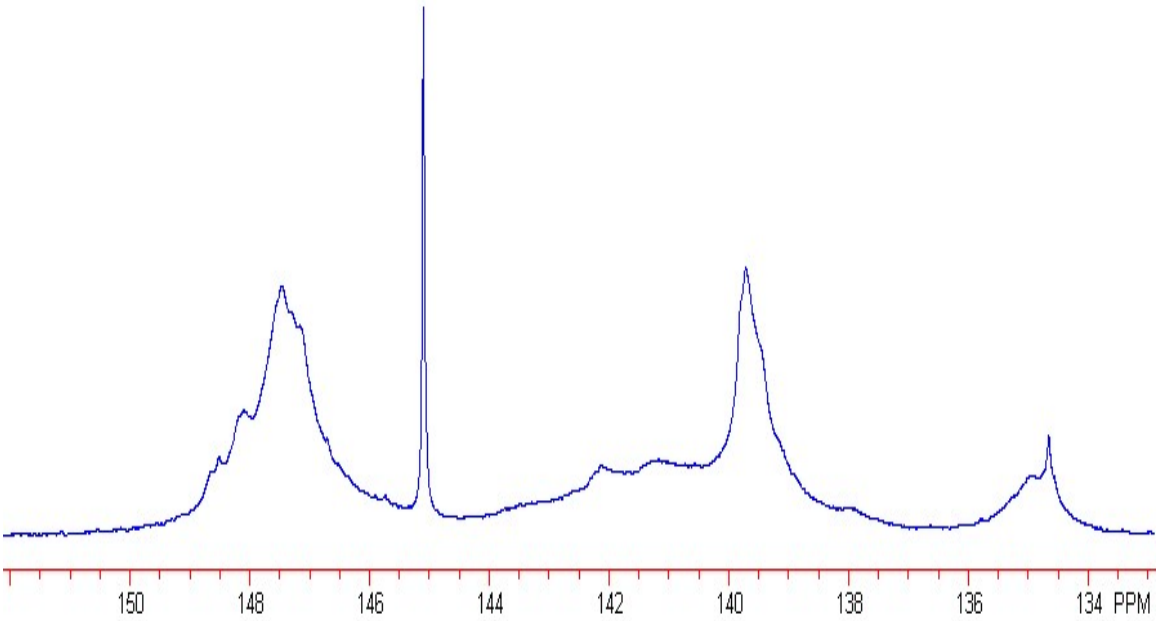

Figure A-4-67. ^{31}P NMR spectrum of residual lignin from Condition 14 of the constant kappa number (approximately 30) series of pulps. Table A-4-1 summarizes the pulping conditions used to produce the pulp for the respective residual lignin.

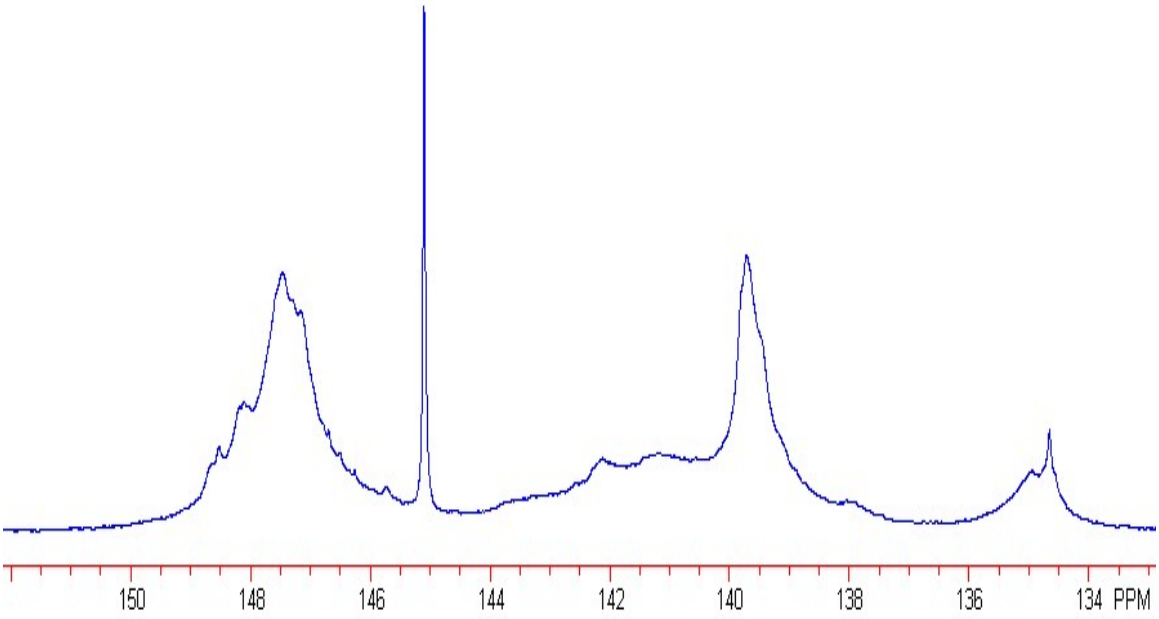

Figure A-4-68. ^{31}P NMR spectrum of residual lignin from Condition 15 of the constant kappa number (approximately 30) series of pulps. Table A-4-1 summarizes the pulping conditions used to produce the pulp for the respective residual lignin.

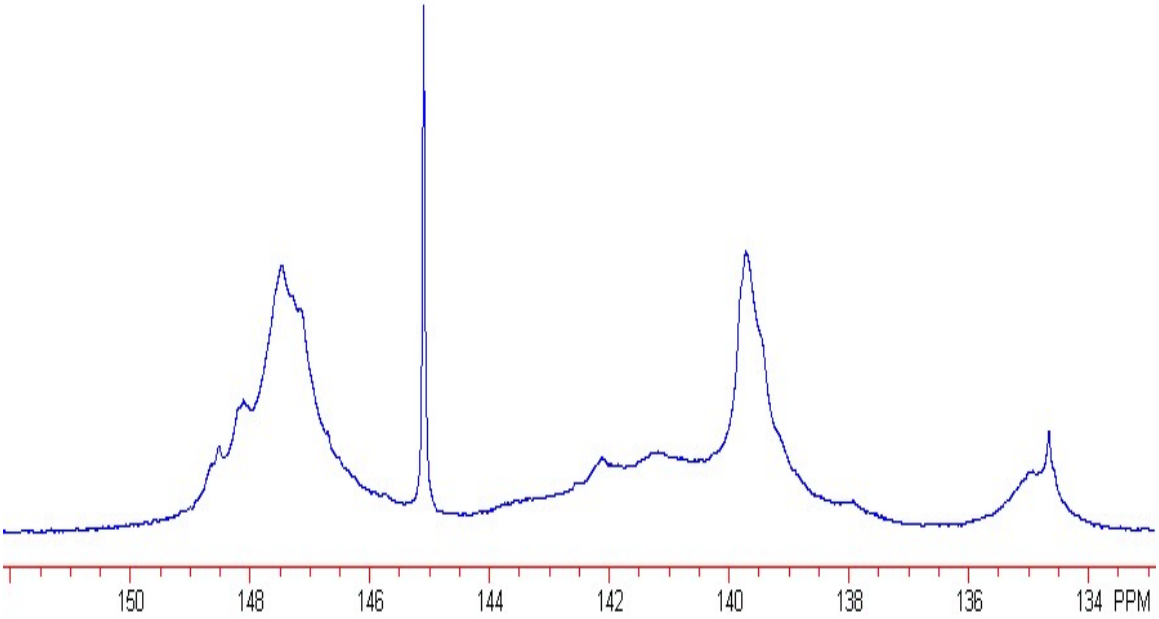

Figure A-4-69. ^{31}P NMR spectrum of residual lignin from Condition 16 of the constant kappa number (approximately 30) series of pulps. Table A-4-1 summarizes the pulping conditions used to produce the pulp for the respective residual lignin.

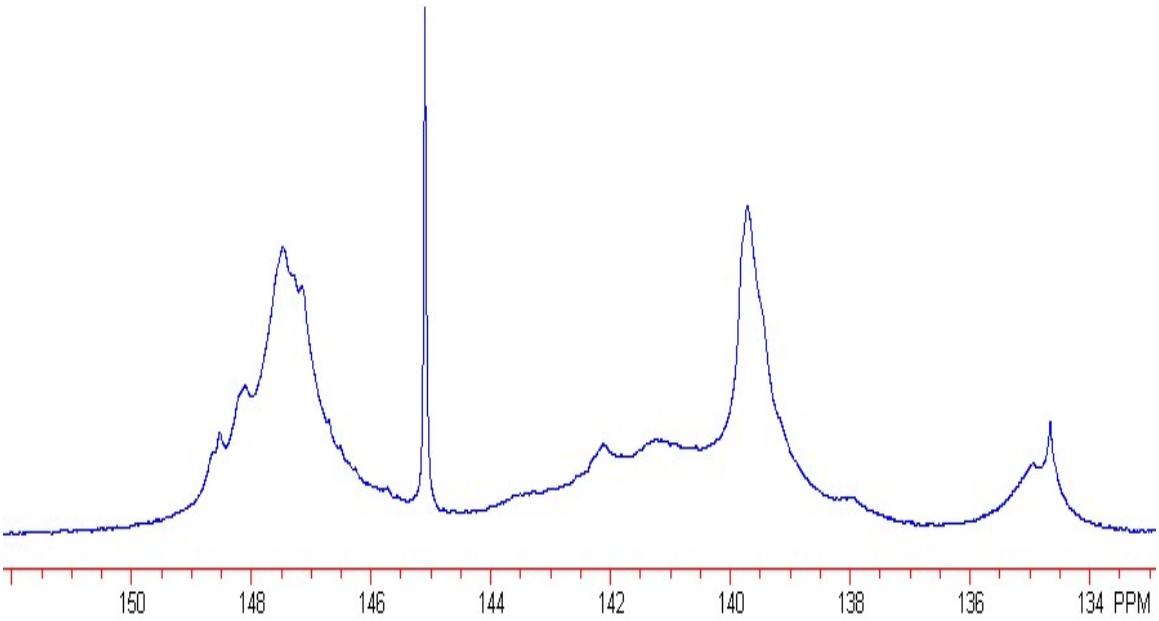

Figure A-4-70. ^{31}P NMR spectrum of residual lignin from Condition 17 of the constant kappa number (approximately 30) series of pulps. Table A-4-1 summarizes the pulping conditions used to produce the pulp for the respective residual lignin.

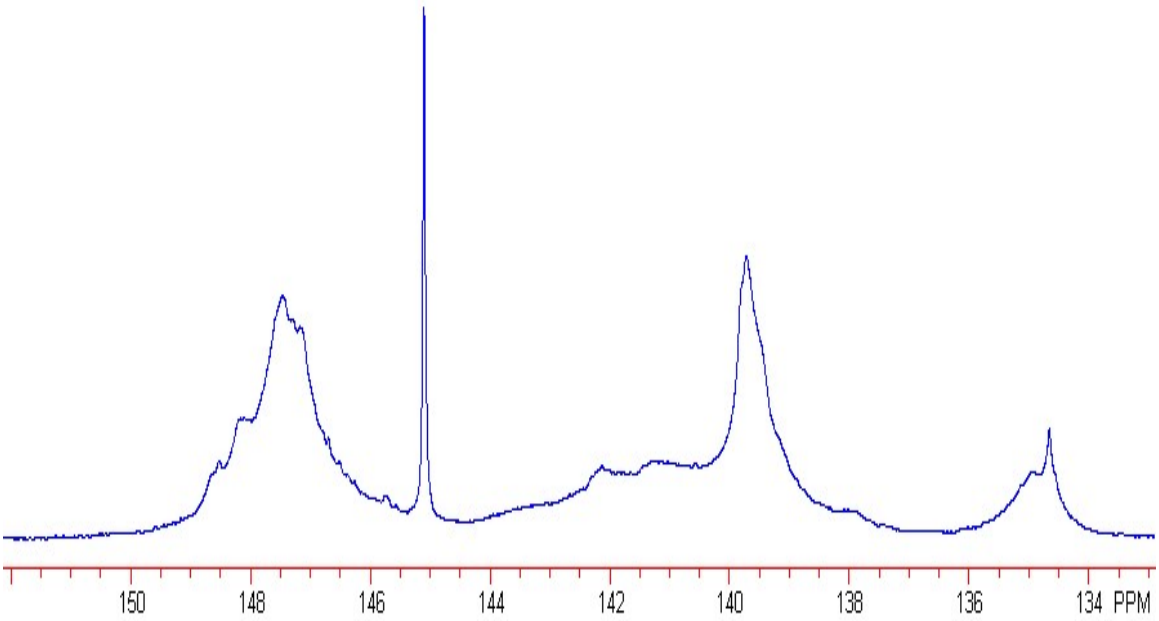

Figure A-4-71. ^{31}P NMR spectrum of residual lignin from Condition 18 of the constant kappa number (approximately 30) series of pulps. Table A-4-1 summarizes the pulping conditions used to produce the pulp for the respective residual lignin.

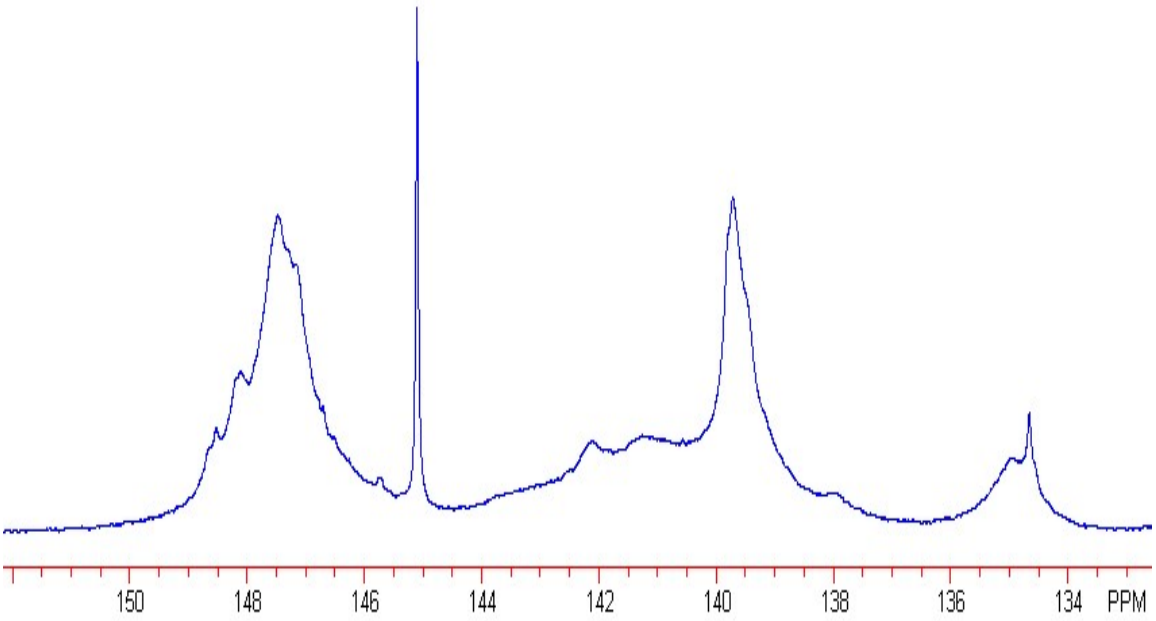

Figure A-4-72. ^{31}P NMR spectrum of residual lignin from Condition 19 of the constant kappa number (approximately 30) series of pulps. Table A-4-1 summarizes the pulping conditions used to produce the pulp for the respective residual lignin.

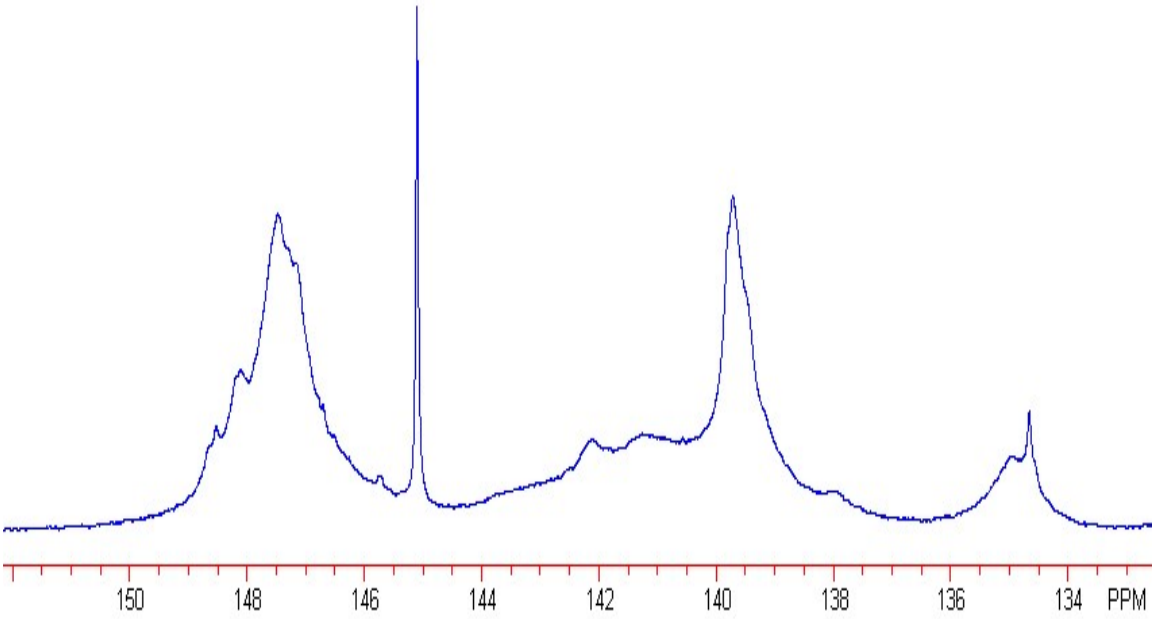

Figure A-4-73. ^{31}P NMR spectrum of residual lignin from Condition 20 of the constant kappa number (approximately 30) series of pulps. Table A-4-1 summarizes the pulping conditions used to produce the pulp for the respective residual lignin.

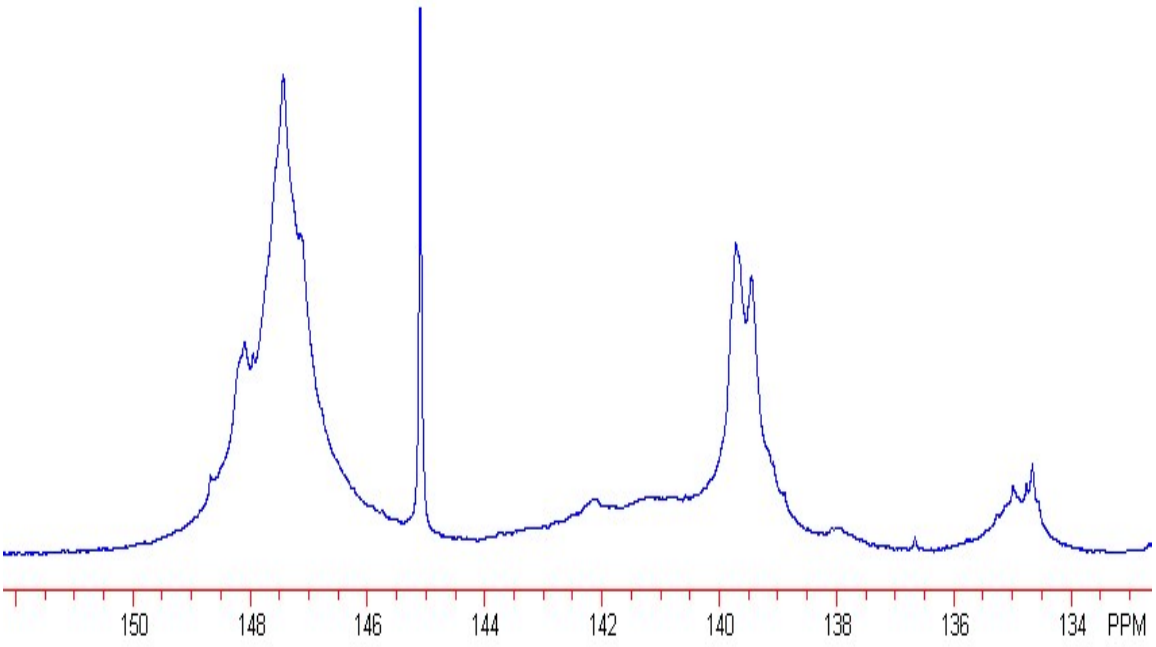

Figure A-4-74. ^{31}P NMR spectrum of residual lignin from Condition A-1 of the incremental cook series of pulps. Table A-4-2 summarizes the pulping conditions used to produce the pulp for the respective residual lignin.

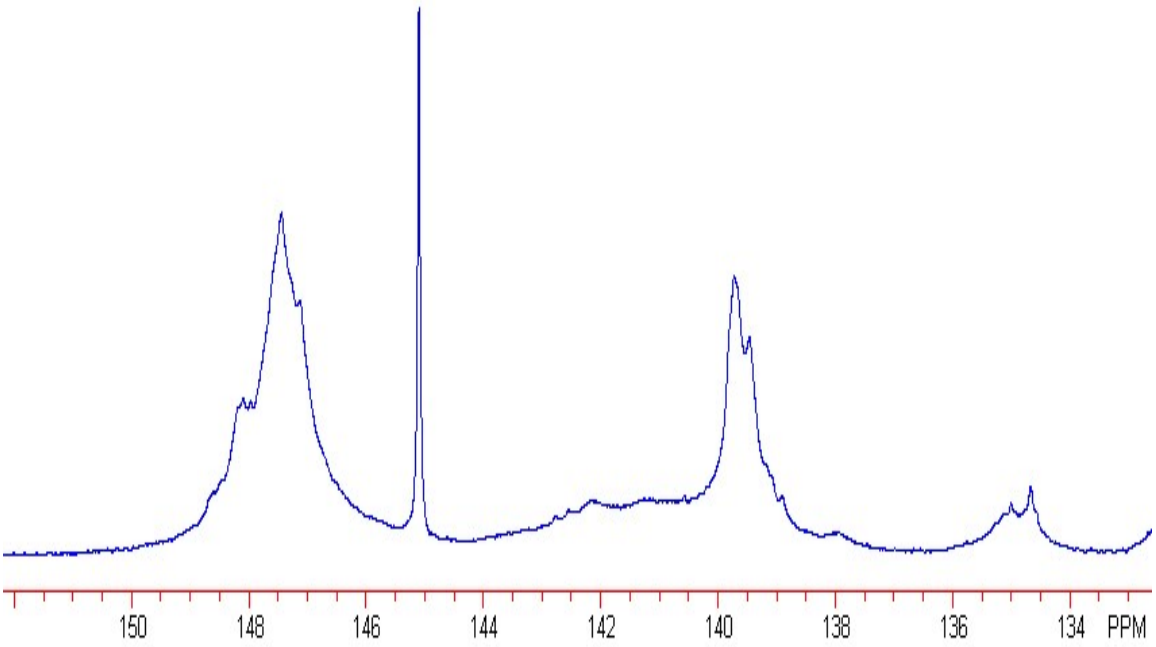

Figure A-4-75. ^{31}P NMR spectrum of residual lignin from Condition A-2 of the incremental cook series of pulps. Table A-4-2 summarizes the pulping conditions used to produce the pulp for the respective residual lignin.

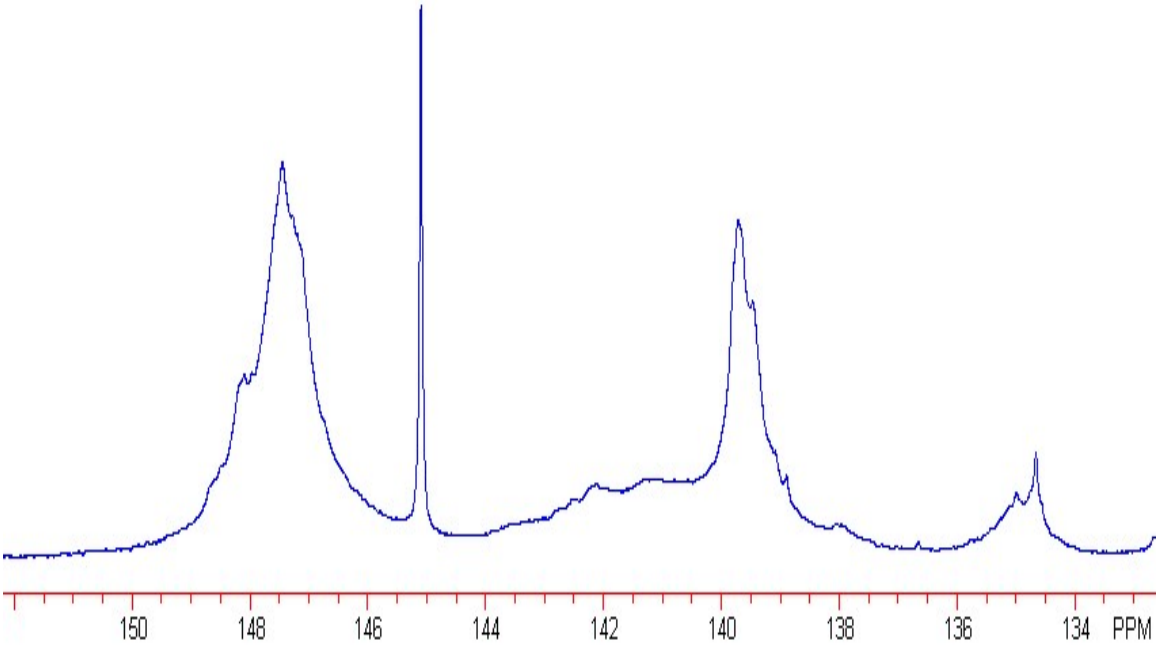

Figure A-4-76. ^{31}P NMR spectrum of residual lignin from Condition A-3 of the incremental cook series of pulps. Table A-4-2 summarizes the pulping conditions used to produce the pulp for the respective residual lignin.

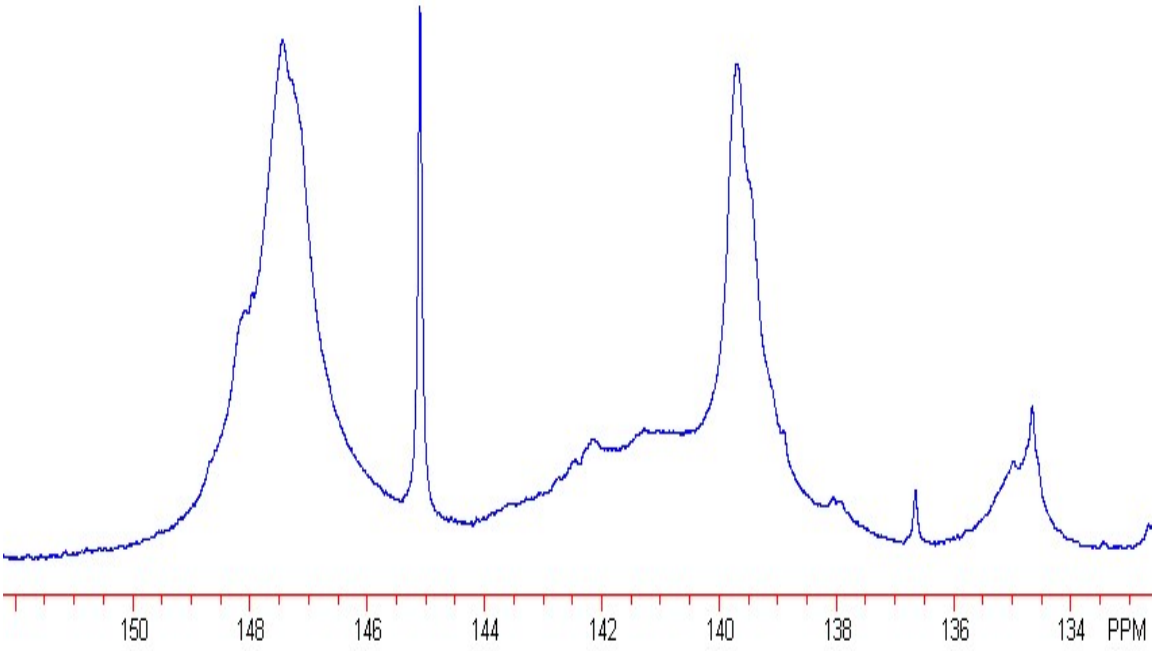

Figure A-4-77. ^{31}P NMR spectrum of residual lignin from Condition A-4 of the incremental cook series of pulps. Table A-4-2 summarizes the pulping conditions used to produce the pulp for the respective residual lignin.

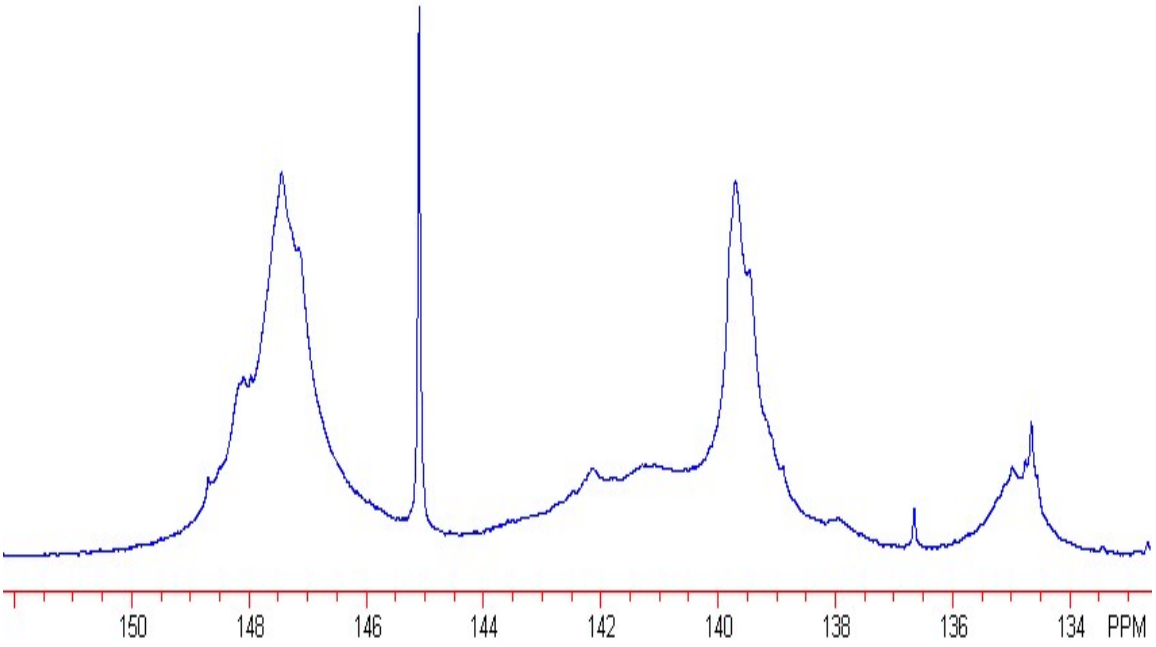

Figure A-4-78. ^{31}P NMR spectrum of residual lignin from Condition A-5 of the incremental cook series of pulps. Table A-4-2 summarizes the pulping conditions used to produce the pulp for the respective residual lignin.

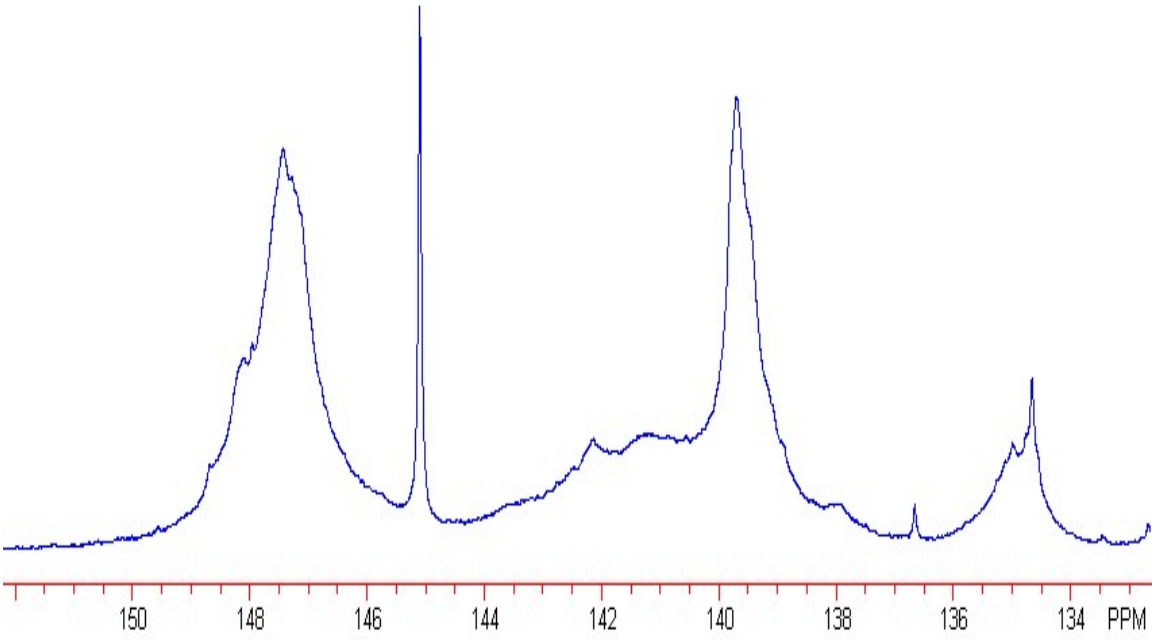

Figure A-4-79. ^{31}P NMR spectrum of residual lignin from Condition A-6 of the incremental cook series of pulps. Table A-4-2 summarizes the pulping conditions used to produce the pulp for the respective residual lignin.

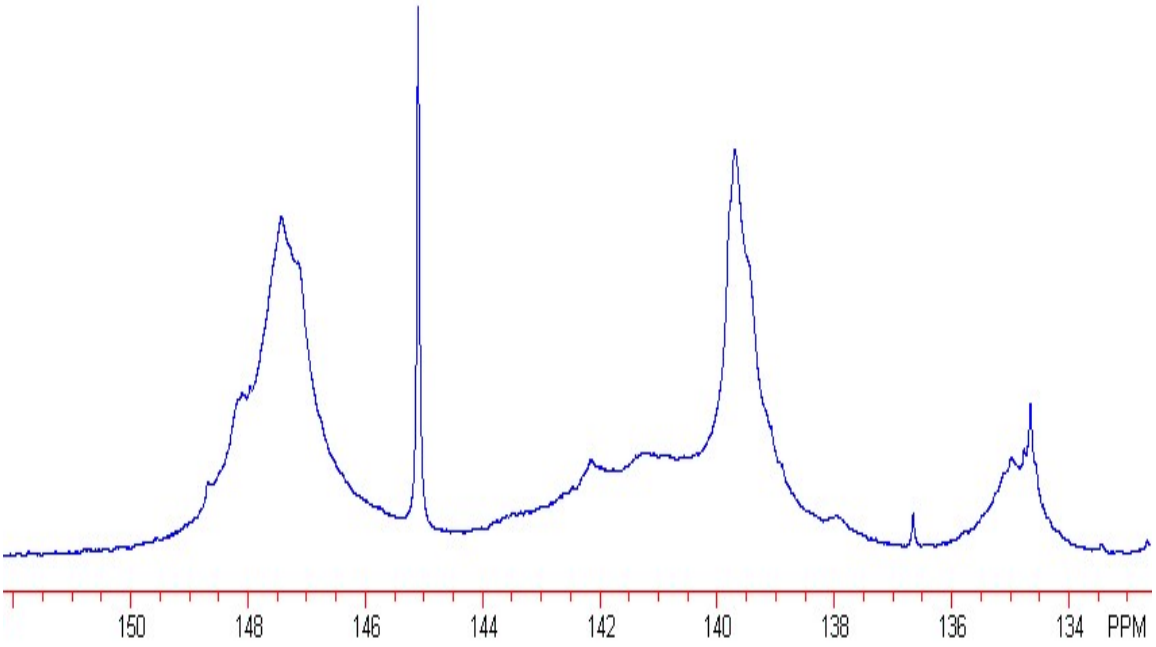

Figure A-4-80. ^{31}P NMR spectrum of residual lignin from Condition A-7 of the incremental cook series of pulps. Table A-4-2 summarizes the pulping conditions used to produce the pulp for the respective residual lignin.

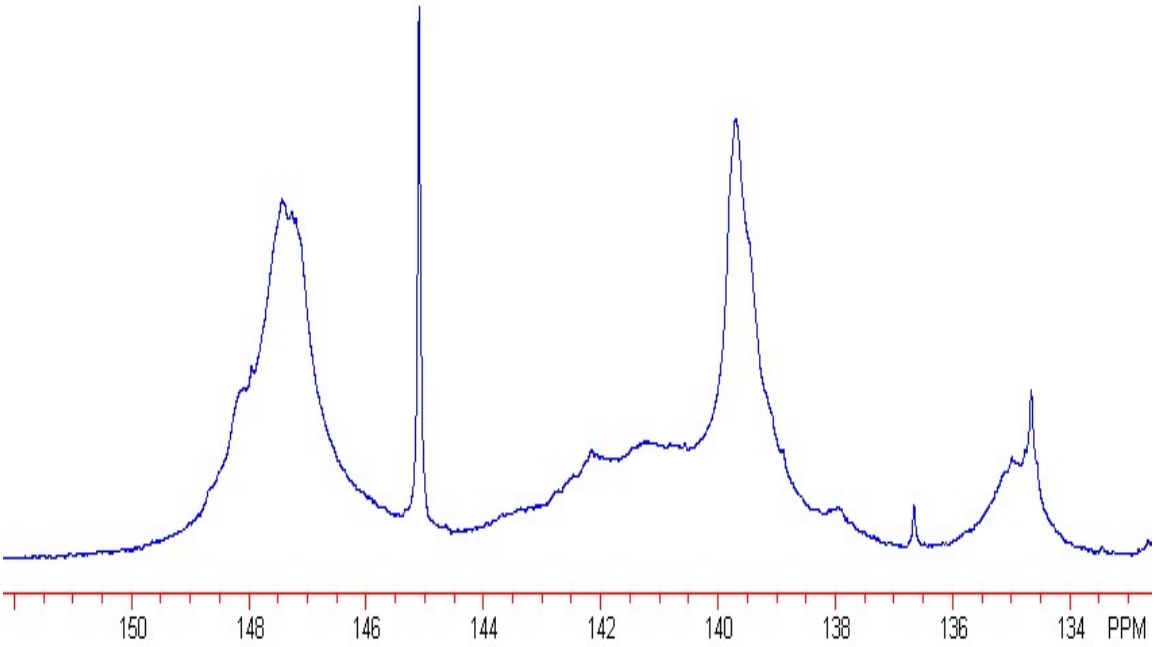

Figure A-4-81. ^{31}P NMR spectrum of residual lignin from Condition A-8 of the incremental cook series of pulps. Table A-4-2 summarizes the pulping conditions used to produce the pulp for the respective residual lignin.

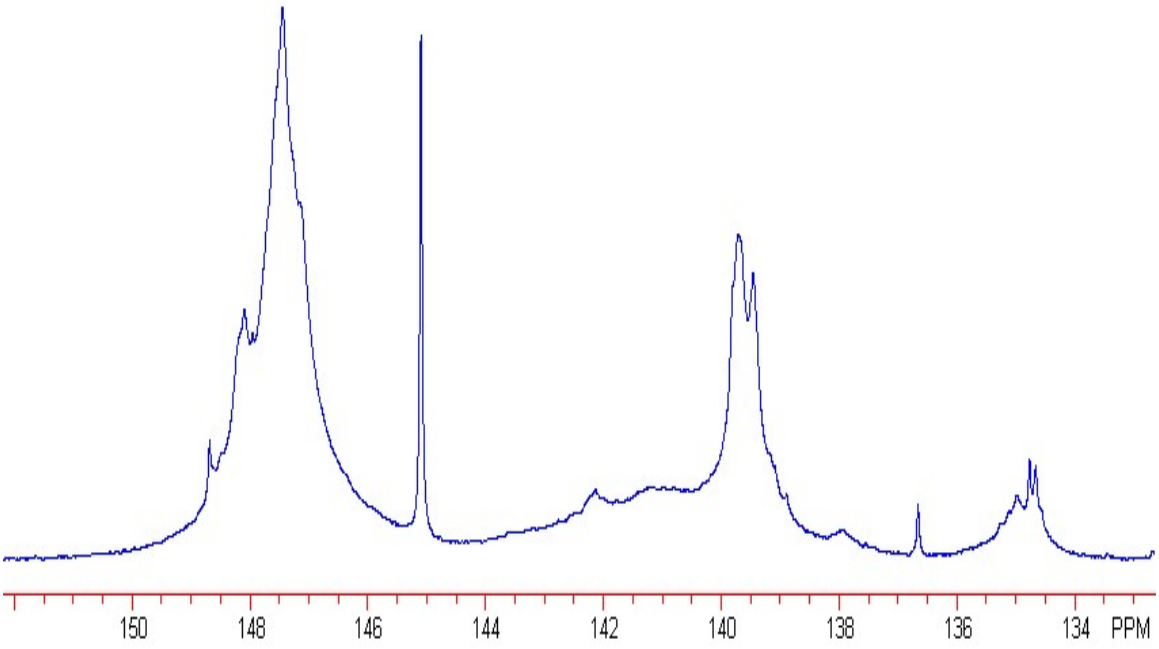

Figure A-4-82. ^{31}P NMR spectrum of residual lignin from Condition B-1 of the incremental cook series of pulps. Table A-4-2 summarizes the pulping conditions used to produce the pulp for the respective residual lignin.

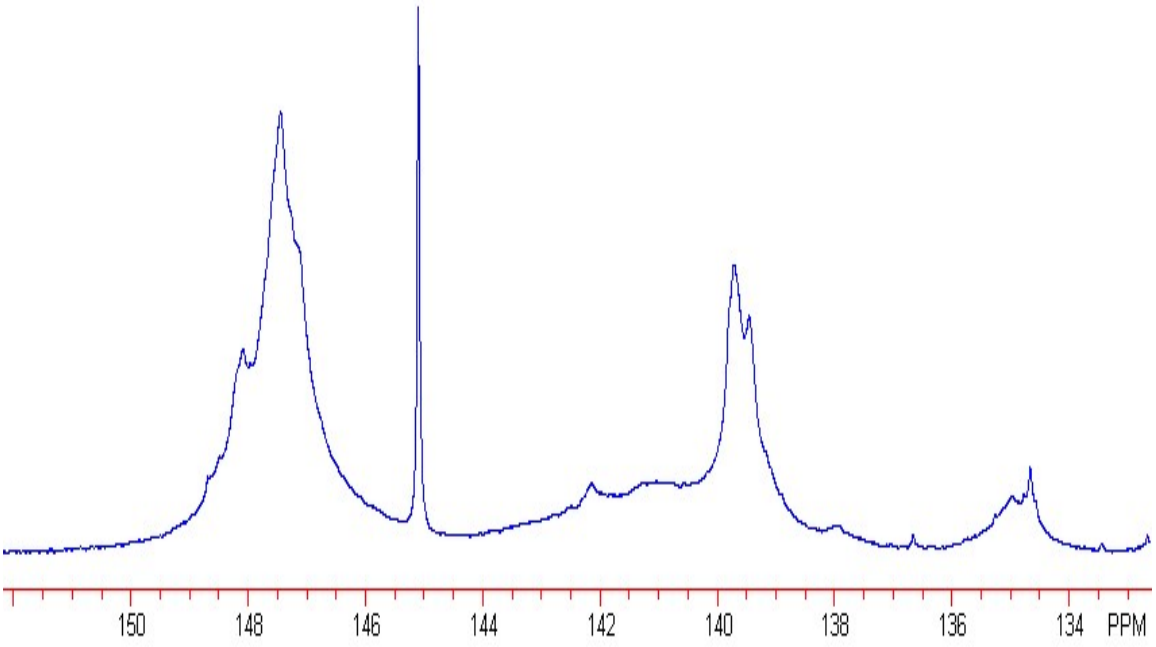

Figure A-4-83. ^{31}P NMR spectrum of residual lignin from Condition B-2 of the incremental cook series of pulps. Table A-4-2 summarizes the pulping conditions used to produce the pulp for the respective residual lignin.

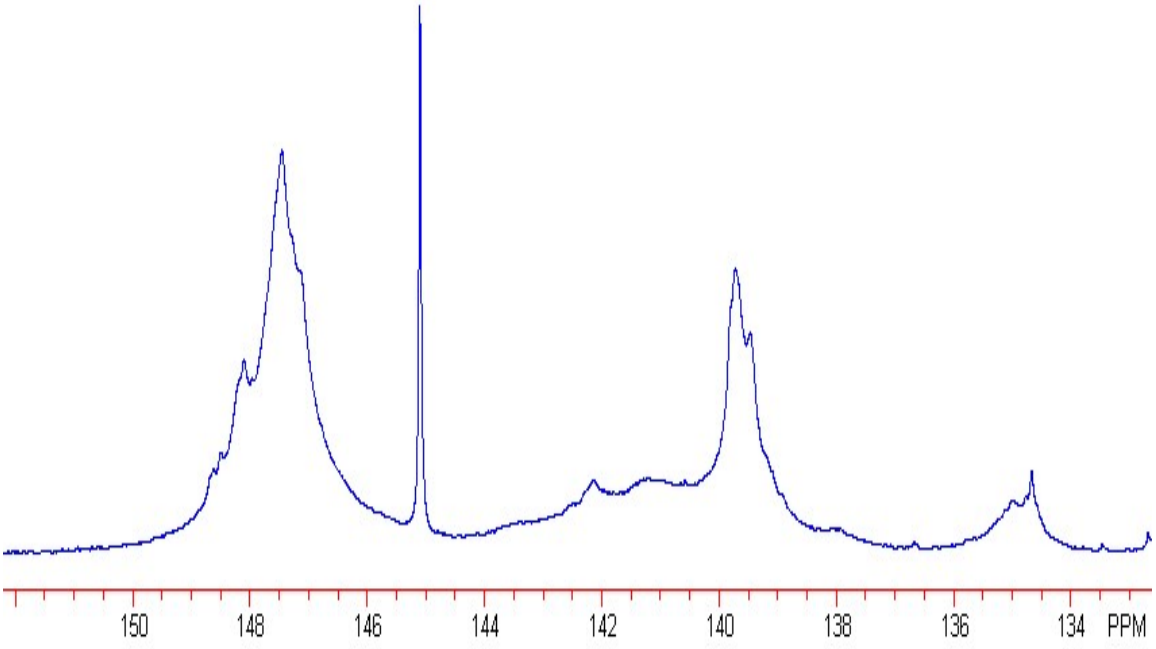

Figure A-4-84. ^{31}P NMR spectrum of residual lignin from Condition B-3 of the incremental cook series of pulps. Table A-4-2 summarizes the pulping conditions used to produce the pulp for the respective residual lignin.

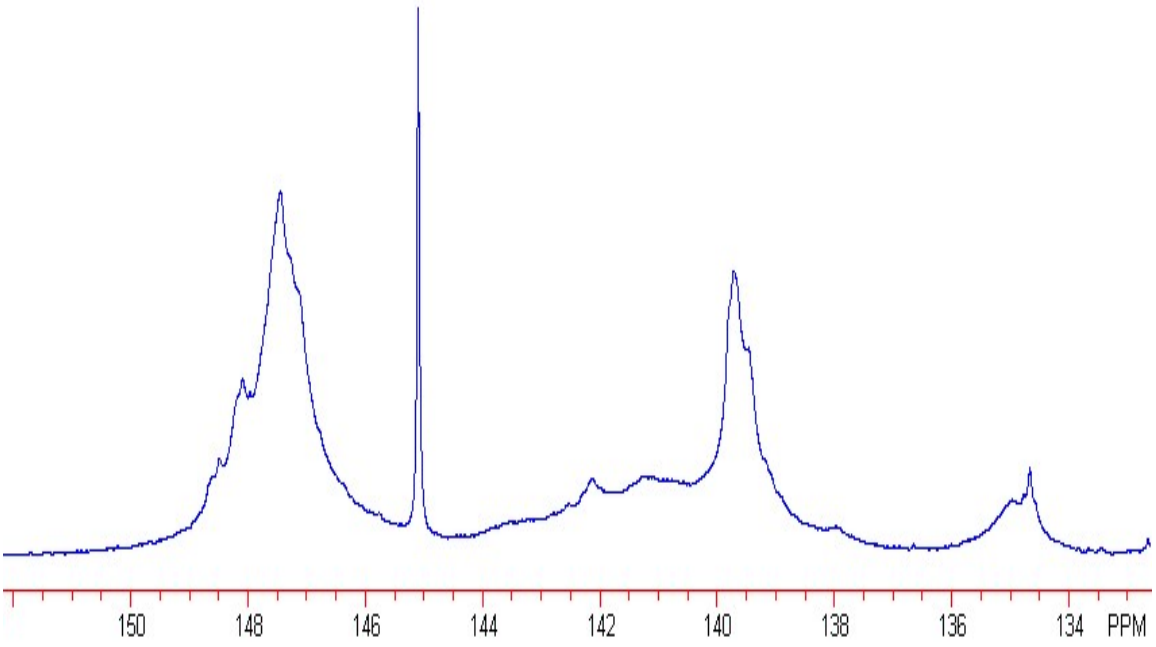

Figure A-4-85. ^{31}P NMR spectrum of residual lignin from Condition B-4 of the incremental cook series of pulps. Table A-4-2 summarizes the pulping conditions used to produce the pulp for the respective residual lignin.

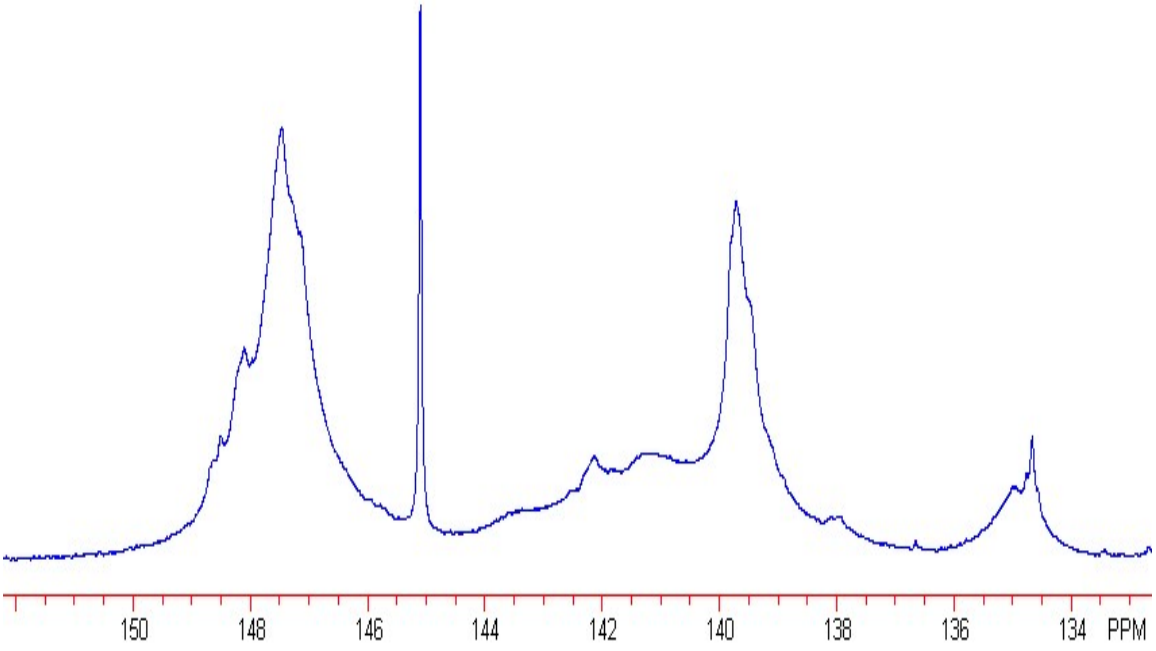

Figure A-4-86. ^{31}P NMR spectrum of residual lignin from Condition B-5 of the incremental cook series of pulps. Table A-4-2 summarizes the pulping conditions used to produce the pulp for the respective residual lignin.

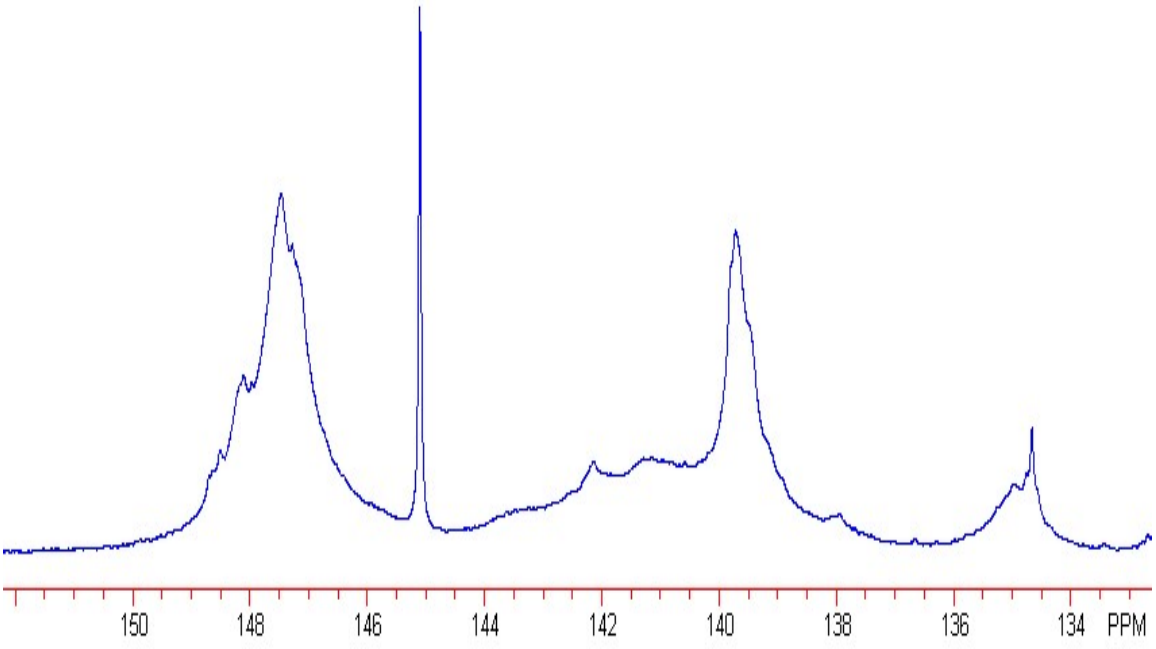

Figure A-4-87. ^{31}P NMR spectrum of residual lignin from Condition B-6 of the incremental cook series of pulps. Table A-4-2 summarizes the pulping conditions used to produce the pulp for the respective residual lignin.

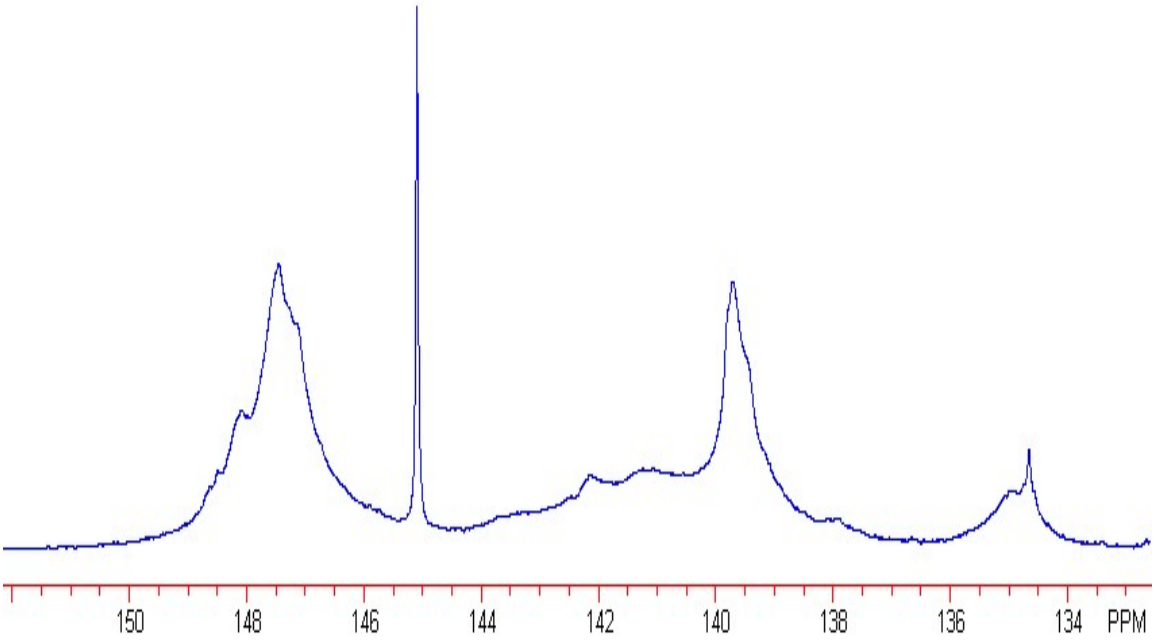

Figure A-4-88. ^{31}P NMR spectrum of residual lignin from Condition B-7 of the incremental cook series of pulps. Table A-4-2 summarizes the pulping conditions used to produce the pulp for the respective residual lignin.

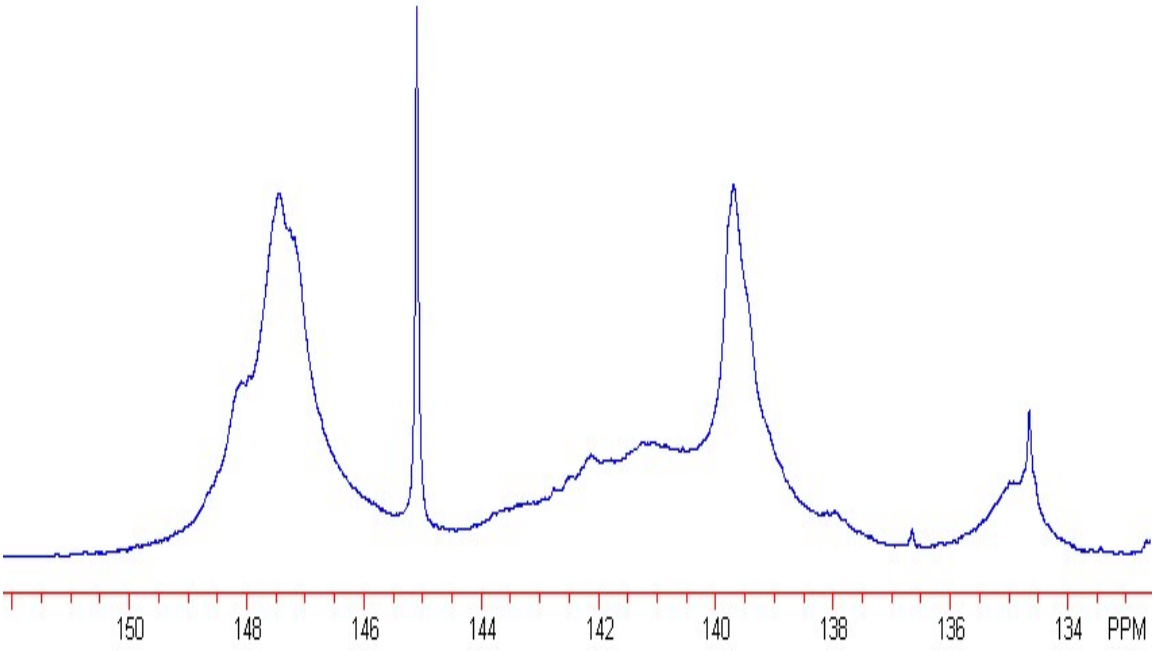

Figure A-4-89. ^{31}P NMR spectrum of residual lignin from Condition B-8 of the incremental cook series of pulps. Table A-4-2 summarizes the pulping conditions used to produce the pulp for the respective residual lignin.

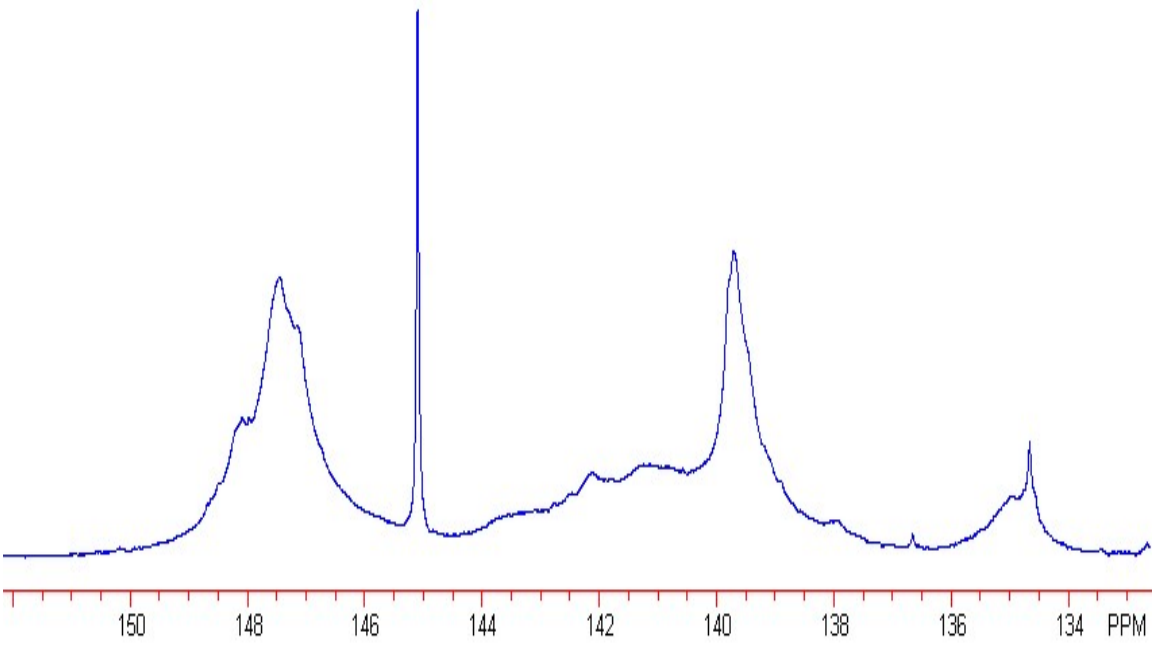

Figure A-4-90. ^{31}P NMR spectrum of residual lignin from Condition B-9 of the incremental cook series of pulps. Table A-4-2 summarizes the pulping conditions used to produce the pulp for the respective residual lignin.

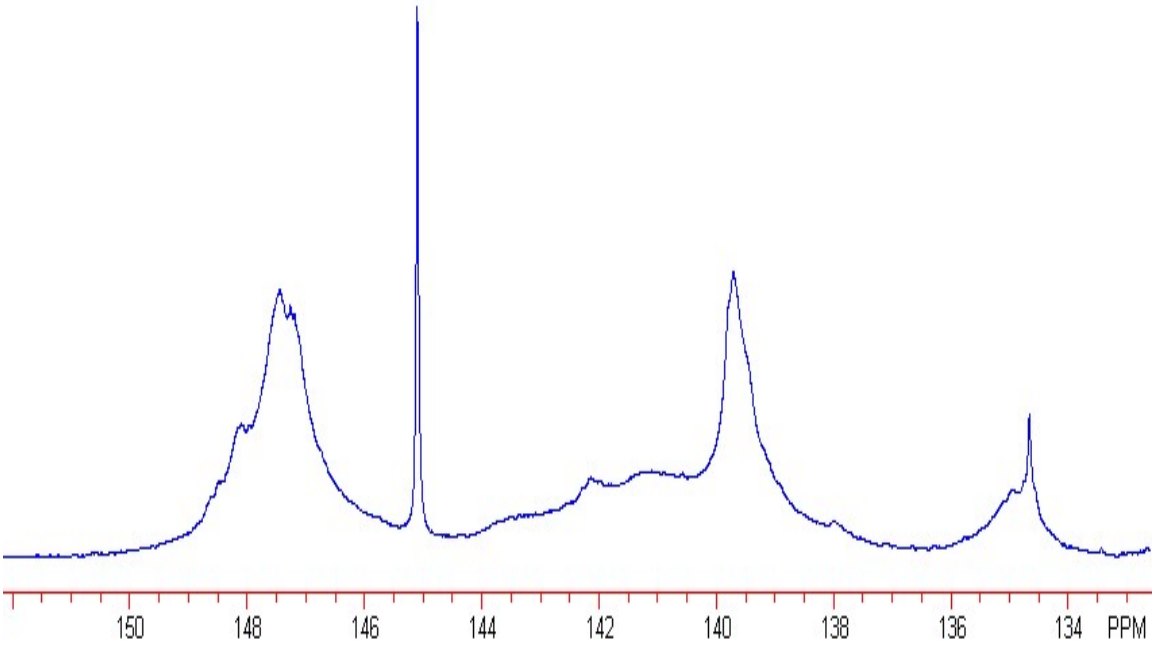

Figure A-4-91. ^{31}P NMR spectrum of residual lignin from Condition B-10 of the incremental cook series of pulps. Table A-4-2 summarizes the pulping conditions used to produce the pulp for the respective residual lignin.

18.11 Summary of ^{31}P NMR for Hydroxyl Group Data for Residual Lignins

Table A-4-10. ^{31}P NMR data for residual lignins from the constant kappa number (approximately 30) series of pulps. Table A-4-1 summarizes the pulping conditions used to produce the pulps for the respective residual lignins.

Functional group	Integration Region/ppm	1 (mmol/g)	2 (mmol/g)	3 (mmol/g)	4 (mmol/g)	5 (mmol/g)
Aliphatic OH	149.0-145.6	1.607	1.563	1.589	1.780	1.479
C5 condensed phenolic OH	144.4-140.4	0.922	0.851	0.947	1.012	0.891
5-5'-Biphenyl OH	141.7-140.4	0.494	0.456	0.499	0.530	0.469
C5 noncondensed phenolic OH	140.4-137.6	1.121	1.074	1.116	1.167	1.056
Catechol OH	139.0-138.2	0.164	0.147	0.166	0.152	0.147
p-hydroxyphenyl OH	138.2-137.3	0.101	0.083	0.102	0.092	0.088
Carboxyl OH	136.0-133.8	0.396	0.305	0.341	0.323	0.324

Table A-4-11. ^{31}P NMR data for residual lignins from the constant kappa number (approximately 30) series of pulps. Table A-4-1 summarizes the pulping conditions used to produce the pulps for the respective residual lignins.

Functional group	Integration Region/ppm	6 (mmol/g)	7 (mmol/g)	8 (mmol/g)	9 (mmol/g)	10 (mmol/g)
Aliphatic OH	149.0-145.6	1.635	1.809	1.675	1.313	1.804
C5 condensed phenolic OH	144.4-140.4	0.890	1.033	0.912	0.837	0.978
5-5'-Biphenyl OH	141.7-140.4	0.472	0.546	0.481	0.432	0.522
C5 noncondensed phenolic OH	140.4-137.6	1.103	1.213	1.107	0.919	1.197
Catechol OH	139.0-138.2	0.150	0.174	0.150	0.133	0.160
p-hydroxyphenyl OH	138.2-137.3	0.088	0.101	0.088	0.081	0.096
Carboxyl OH	136.0-133.8	0.330	0.367	0.283	0.284	0.322

Table A-4-12. ^{31}P NMR data for residual lignins from the constant kappa number (approximately 30) series of pulps. Table A-4-1 summarizes the pulping conditions used to produce the pulps for the respective residual lignins.

Functional group	Integration Region/ppm	11 (mmol/g)	12 (mmol/g)	13 (mmol/g)	14 (mmol/g)	15 (mmol/g)
Aliphatic OH	149.0-145.6	1.598	1.713	1.668	1.866	1.819
C5 condensed phenolic OH	144.4-140.4	0.944	0.983	0.981	1.046	1.016
5-5'-Biphenyl OH	141.7-140.4	0.503	0.515	0.513	0.560	0.538
C5 noncondensed phenolic OH	140.4-137.6	1.163	1.138	1.136	1.263	1.213
Catechol OH	139.0-138.2	0.163	0.160	0.162	0.176	0.170
p-hydroxyphenyl OH	138.2-137.3	0.098	0.098	0.100	0.103	0.103
Carboxyl OH	136.0-133.8	0.400	0.324	0.353	0.382	0.358

Table A-4-13. ^{31}P NMR data for residual lignins from the constant kappa number (approximately 30) series of pulps. Table A-4-1 summarizes the pulping conditions used to produce the pulps for the respective residual lignins.

Functional group	Integration Region/ppm	16 (mmol/g)	17 (mmol/g)	18 (mmol/g)	19 (mmol/g)	20 (mmol/g)
Aliphatic OH	149.0-145.6	1.856	1.582	1.645	1.621	1.557
C5 condensed phenolic OH	144.4-140.4	1.031	0.939	0.889	0.914	0.878
5-5'-Biphenyl OH	141.7-140.4	0.552	0.498	0.496	0.485	0.463
C5 noncondensed phenolic OH	140.4-137.6	1.248	1.104	1.147	0.914	1.035
Catechol OH	139.0-138.2	0.173	0.154	0.144	0.157	0.148
p-hydroxyphenyl OH	138.2-137.3	0.105	0.094	0.070	0.096	0.091
Carboxyl OH	136.0-133.8	0.365	0.316	0.322	0.346	0.300

Table A-4-14. ^{31}P NMR data for residual lignins from the incremental cook series of pulps. Table A-4-2 summarizes the pulping conditions used to produce the pulps for the respective residual lignins.

Functional group	Integration Region/ppm	A-1 (mmol/g)	A-2 (mmol/g)	A-3 (mmol/g)	A-4 (mmol/g)
Aliphatic OH	149.0-145.6	2.186	1.875	1.767	1.521
C5 condensed phenolic OH	144.4-140.4	0.637	0.705	0.749	0.746
5-5'-Biphenyl OH	141.7-140.4	0.342	0.369	0.393	0.393
C5 noncondensed phenolic OH	140.4-137.6	1.026	1.011	1.003	0.969
Catechol OH	139.0-138.2	0.114	0.117	0.128	0.135
p-hydroxyphenyl OH	138.2-137.3	0.070	0.065	0.750	0.081
Carboxyl OH	136.0-133.8	0.270	0.243	0.248	0.254

Table A-4-15. ^{31}P NMR data for residual lignins from the incremental cook series of pulps. Table A-4-2 summarizes the pulping conditions used to produce the pulps for the respective residual lignins.

Functional group	Integration Region/ppm	A-5 (mmol/g)	A-6 (mmol/g)	A-7 (mmol/g)	A-8 (mmol/g)
Aliphatic OH	149.0-145.6	1.634	1.486	1.547	1.262
C5 condensed phenolic OH	144.4-140.4	0.786	0.817	0.883	0.757
5-5'-Biphenyl OH	141.7-140.4	0.423	0.440	0.479	0.408
C5 noncondensed phenolic OH	140.4-137.6	1.066	1.062	1.153	0.973
Catechol OH	139.0-138.2	0.140	0.141	0.154	0.135
p-hydroxyphenyl OH	138.2-137.3	0.081	0.079	0.086	0.080
Carboxyl OH	136.0-133.8	0.317	0.321	0.363	0.290

Table A-4-16. ^{31}P NMR data for residual lignins from the incremental cook series of pulps. Table A-4-2 summarizes the pulping conditions used to produce the pulps for the respective residual lignins.

Functional group	Integration Region/ppm	B-1 (mmol/g)	B-2 (mmol/g)	B-3 (mmol/g)	B-4 (mmol/g)	B-5 (mmol/g)
Aliphatic OH	149.0-145.6	2.193	2.157	2.124	2.081	1.638
C5 condensed phenolic OH	144.4-140.4	0.682	0.771	0.853	0.943	0.829
5-5'-Biphenyl OH	141.7-140.4	0.373	0.418	0.457	0.500	0.433
C5 noncondensed phenolic OH	140.4-137.6	0.964	1.020	1.044	1.115	0.938
Catechol OH	139.0-138.2	0.107	0.122	0.126	0.144	0.130
p-hydroxyphenyl OH	138.2-137.3	0.067	0.073	0.072	0.083	0.082
Carboxyl OH	136.0-133.8	0.232	0.260	0.260	0.291	0.255

Table A-4-17. ^{31}P NMR data for residual lignins from the incremental cook series of pulps. Table A-4-2 summarizes the pulping conditions used to produce the pulps for the respective residual lignins.

Functional group	Integration Region/ppm	B-6 (mmol/g)	B-7 (mmol/g)	B-8 (mmol/g)	B-9 (mmol/g)	B-10 (mmol/g)
Aliphatic OH	149.0-145.6	1.687	1.755	1.480	1.627	1.467
C5 condensed phenolic OH	144.4-140.4	0.898	0.970	0.894	1.033	0.903
5-5'-Biphenyl OH	141.7-140.4	0.471	0.514	0.473	0.540	0.474
C5 noncondensed phenolic OH	140.4-137.6	1.021	1.120	1.020	1.163	1.03
Catechol OH	139.0-138.2	0.139	0.158	0.149	0.168	0.155
p-hydroxyphenyl OH	138.2-137.3	0.086	0.094	0.086	0.097	0.089
Carboxyl OH	136.0-133.8	0.288	0.322	0.279	0.308	0.322

18.12 ^{13}C NMR Spectra of Residual Lignins

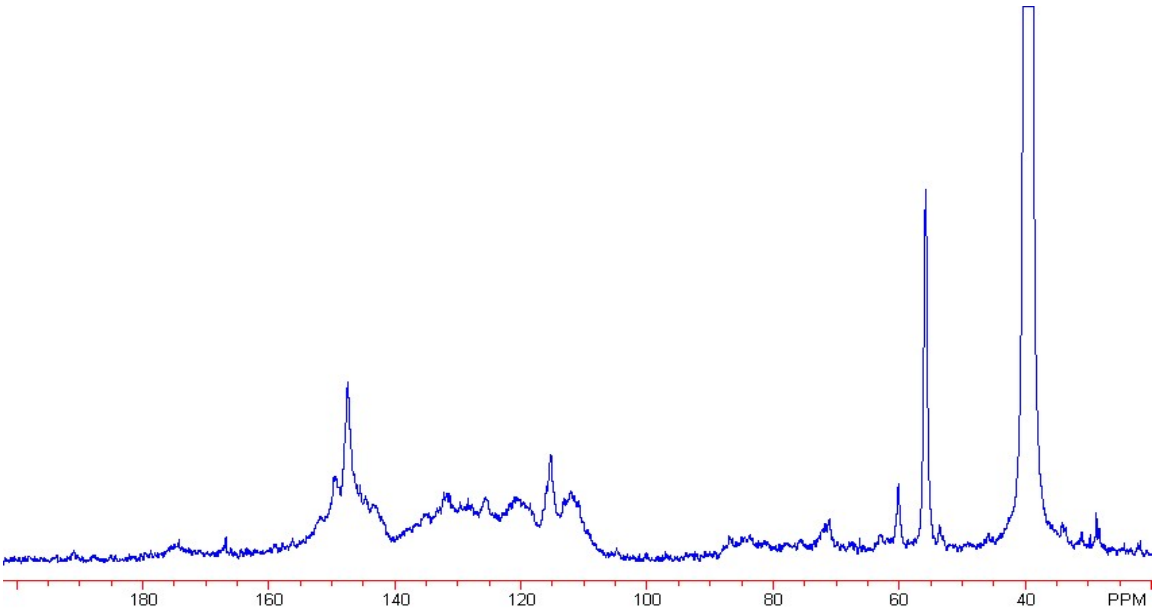

Figure A-4-92. ^{13}C NMR spectrum of residual lignin from Condition 1 of the constant kappa number (approximately 30) series of pulps. Table A-4-1 summarizes the pulping conditions used to produce the pulp for the respective residual lignin.

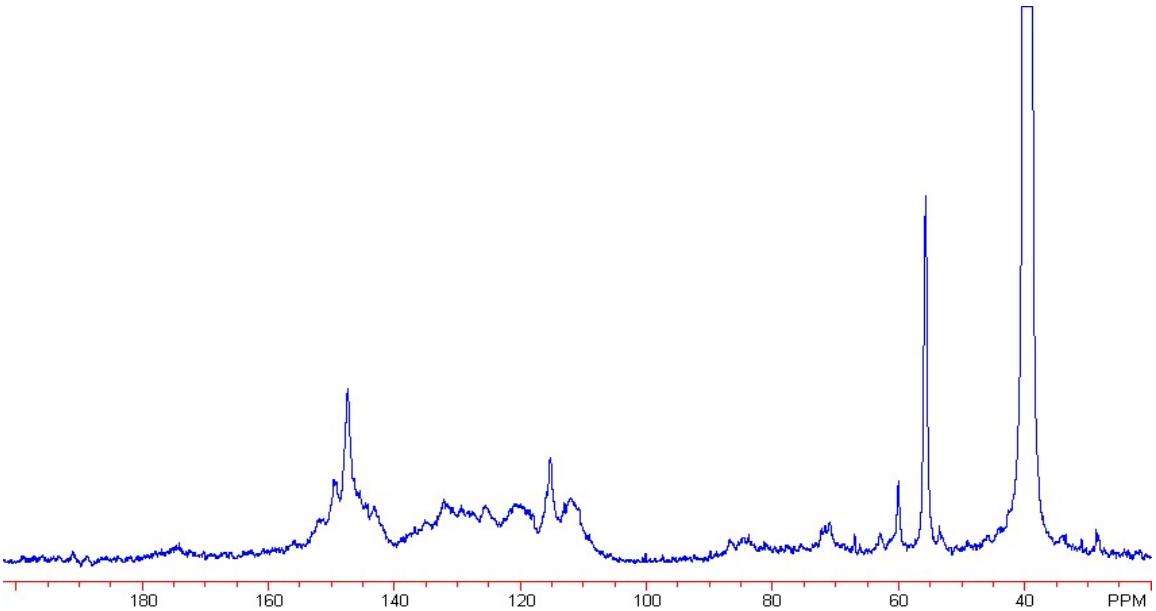

Figure A-4-93. ^{13}C NMR spectrum of residual lignin from Condition 2 of the constant kappa number (approximately 30) series of pulps. Table A-4-1 summarizes the pulping conditions used to produce the pulp for the respective residual lignin.

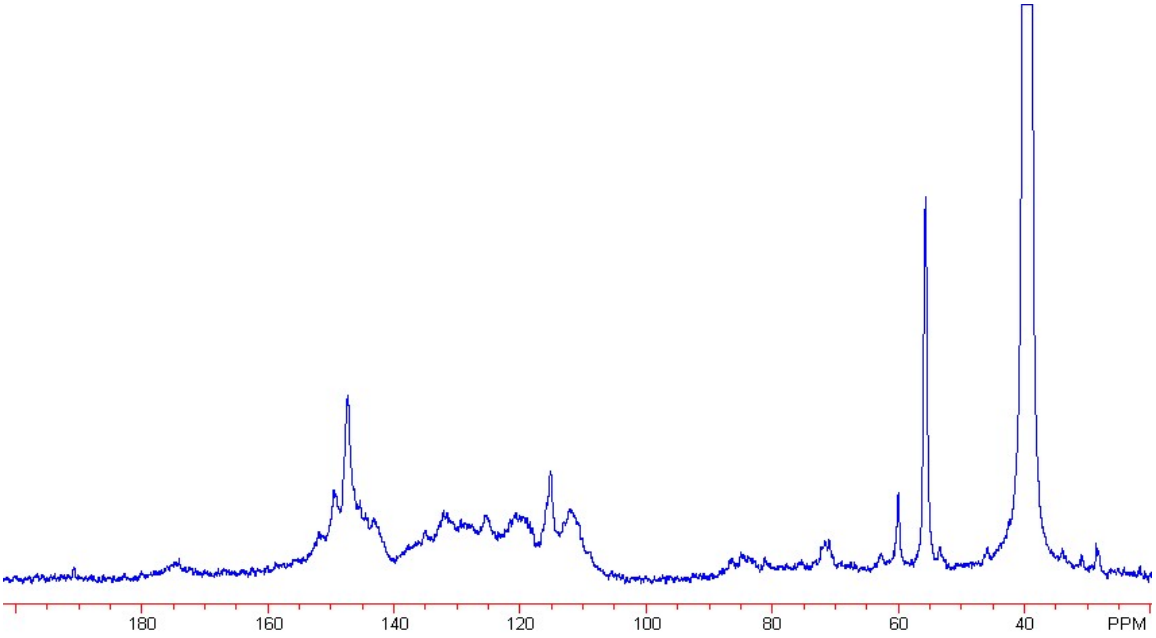

Figure A-4-94. ^{13}C NMR spectrum of residual lignin from Condition 3 of the constant kappa number (approximately 30) series of pulps. Table A-4-1 summarizes the pulping conditions used to produce the pulp for the respective residual lignin.

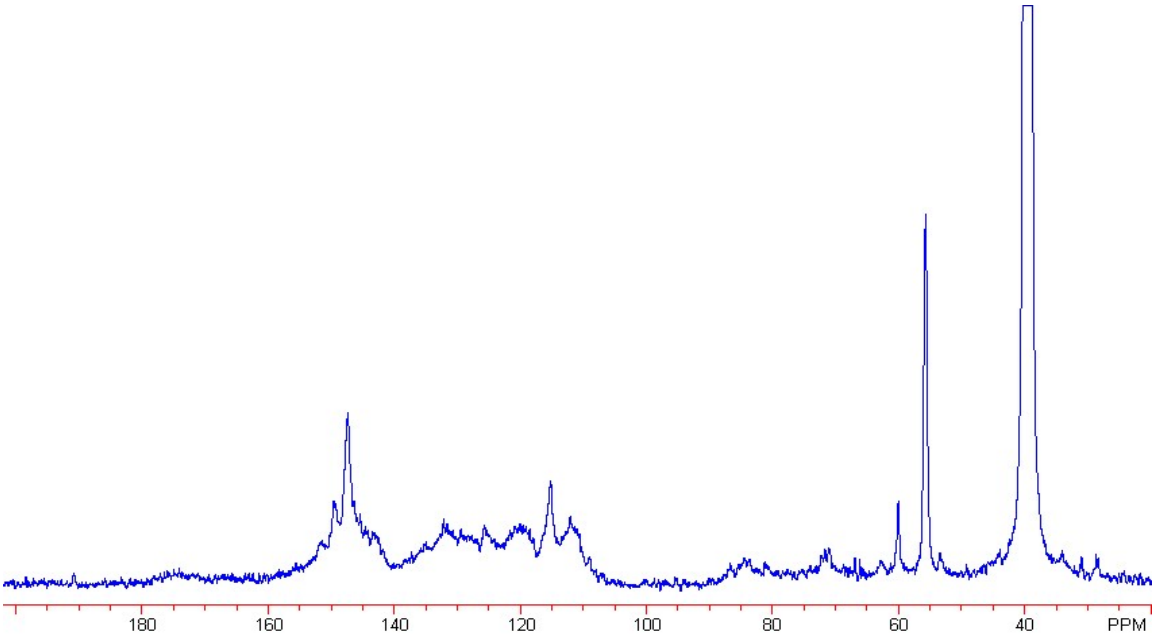

Figure A-4-95. ^{13}C NMR spectrum of residual lignin from Condition 4 of the constant kappa number (approximately 30) series of pulps. Table A-4-1 summarizes the pulping conditions used to produce the pulp for the respective residual lignin.

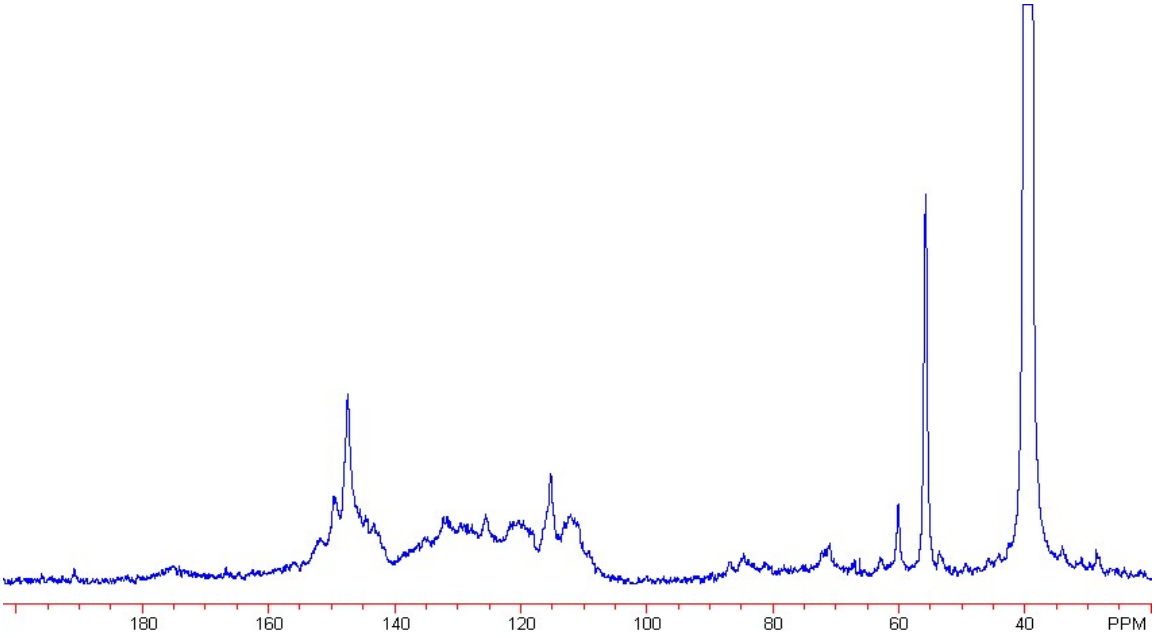

Figure A-4-96. ^{13}C NMR spectrum of residual lignin from Condition 5 of the constant kappa number (approximately 30) series of pulps. Table A-4-1 summarizes the pulping conditions used to produce the pulp for the respective residual lignin.

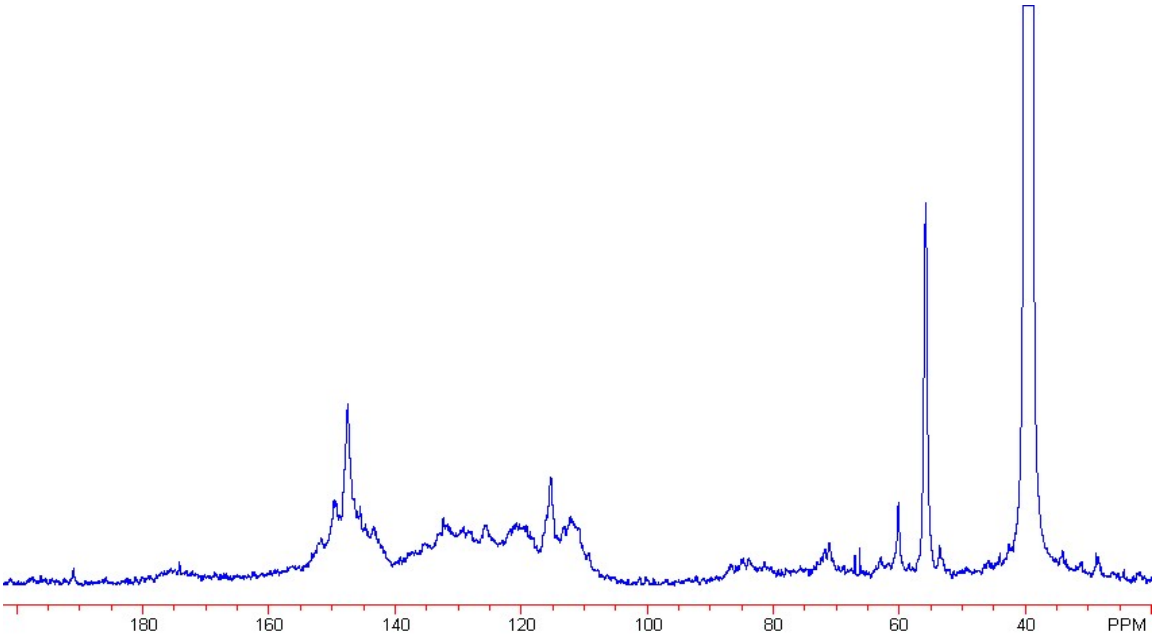

Figure A-4-97. ^{13}C NMR spectrum of residual lignin from Condition 6 of the constant kappa number (approximately 30) series of pulps. Table A-4-1 summarizes the pulping conditions used to produce the pulp for the respective residual lignin.

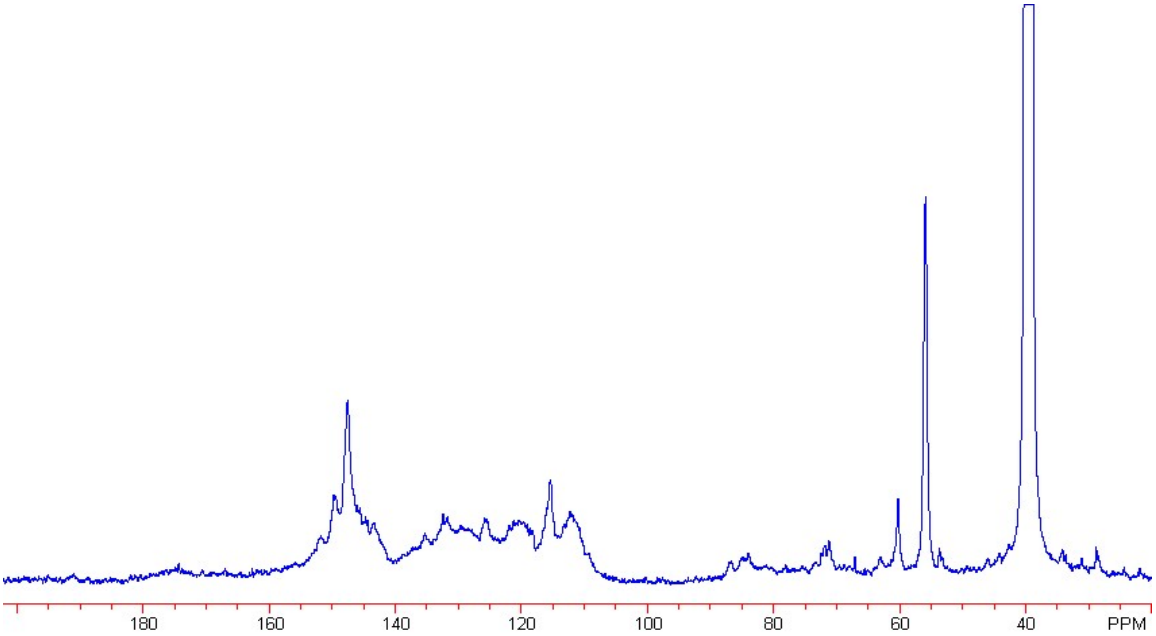

Figure A-4-98. ^{13}C NMR spectrum of residual lignin from Condition 7 of the constant kappa number (approximately 30) series of pulps. Table A-4-1 summarizes the pulping conditions used to produce the pulp for the respective residual lignin.

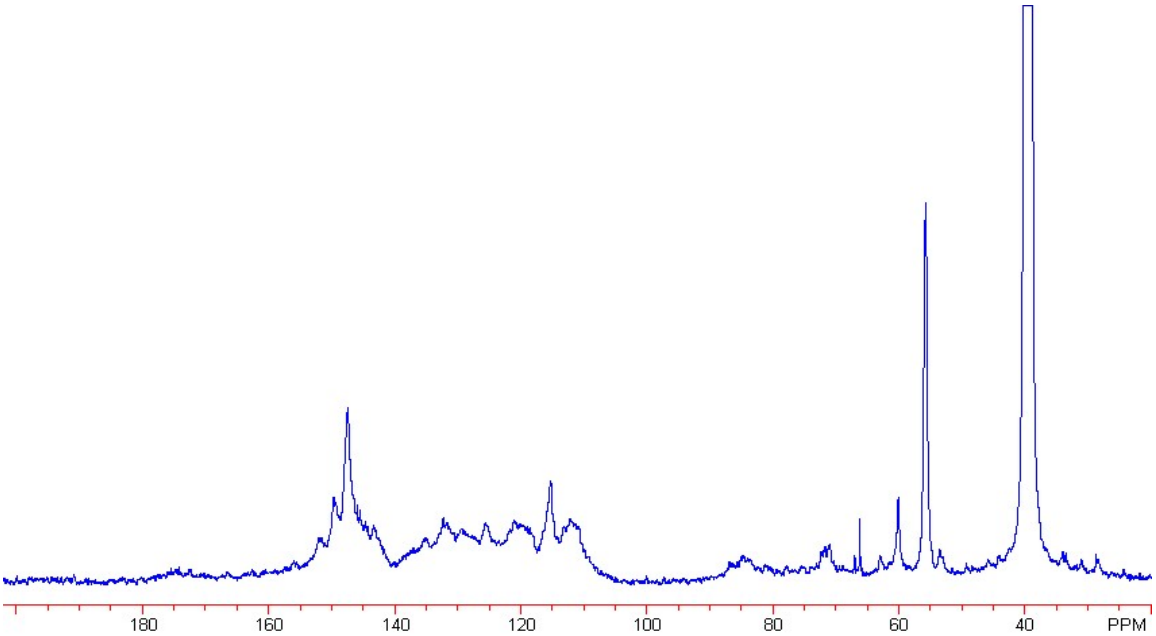

Figure A-4-99. ^{13}C NMR spectrum of residual lignin from Condition 8 of the constant kappa number (approximately 30) series of pulps. Table A-4-1 summarizes the pulping conditions used to produce the pulp for the respective residual lignin.

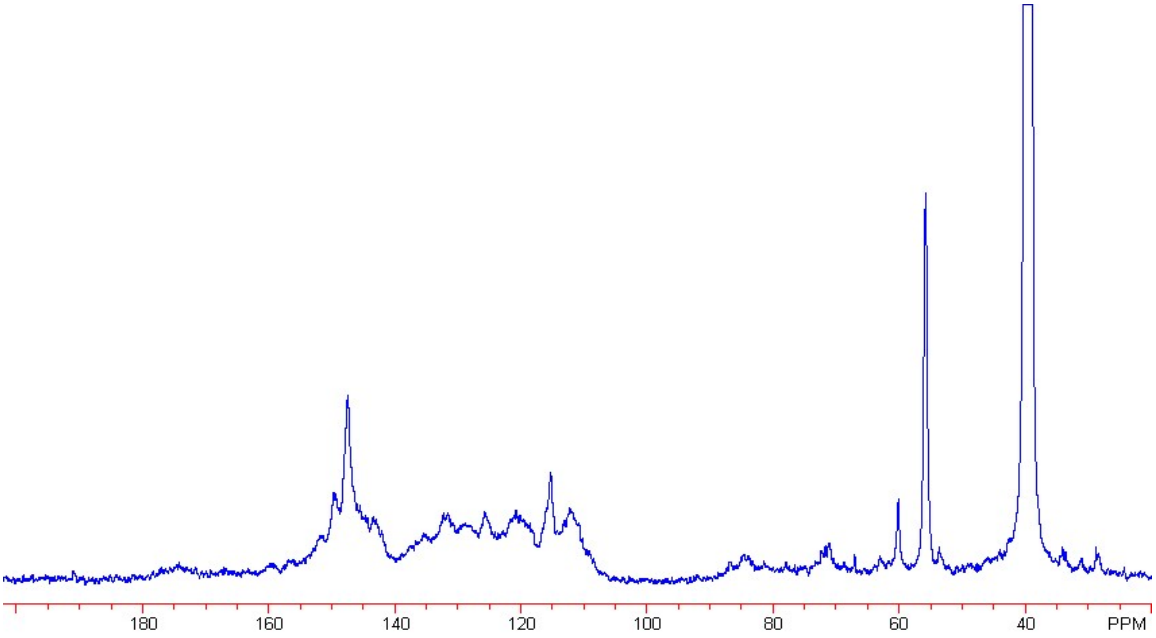

Figure A-4-100. ^{13}C NMR spectrum of residual lignin from Condition 9 of the constant kappa number (approximately 30) series of pulps. Table A-4-1 summarizes the pulping conditions used to produce the pulp for the respective residual lignin.

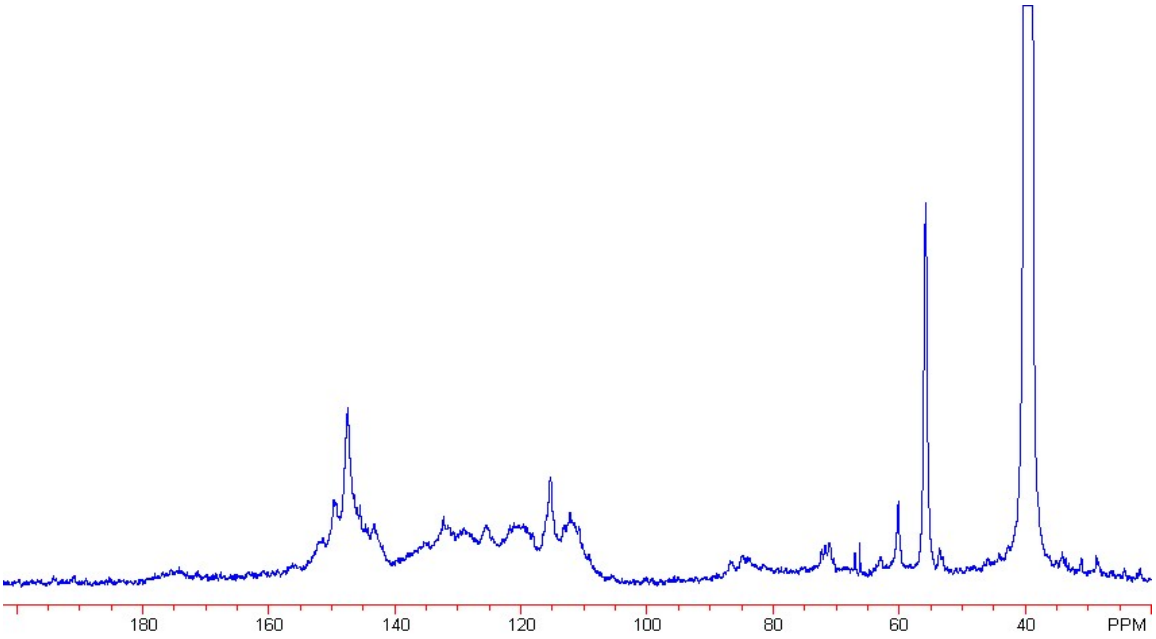

Figure A-4-101. ^{13}C NMR spectrum of residual lignin from Condition 10 of the constant kappa number (approximately 30) series of pulps. Table A-4-1 summarizes the pulping conditions used to produce the pulp for the respective residual lignin.

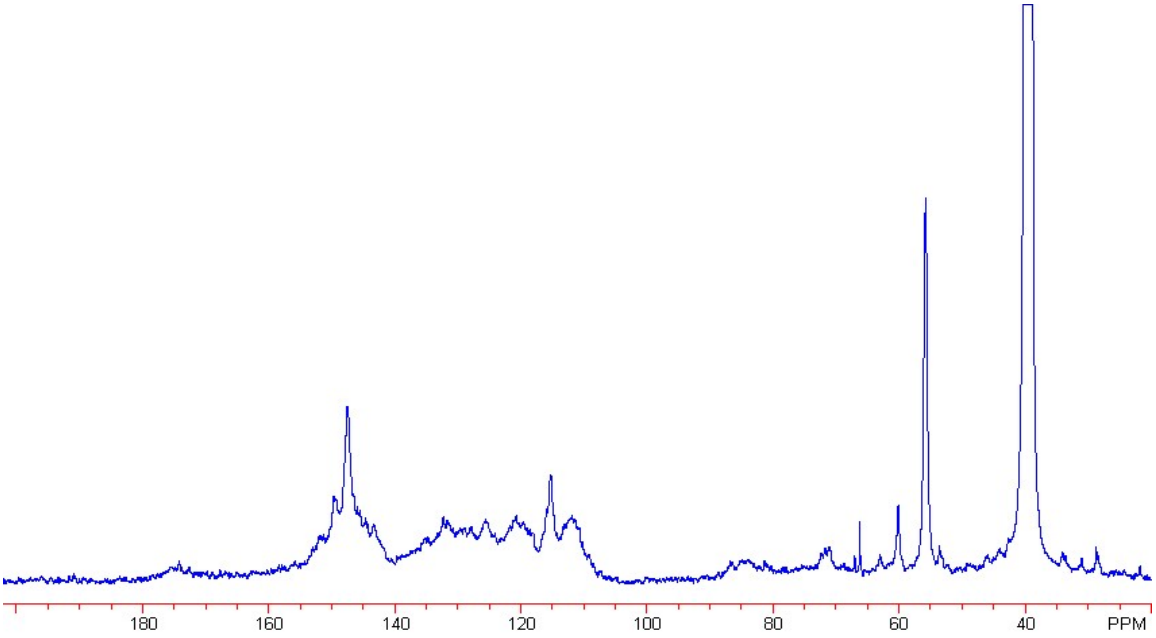

Figure A-4-102. ^{13}C NMR spectrum of residual lignin from Condition 11 of the constant kappa number (approximately 30) series of pulps. Table A-4-1 summarizes the pulping conditions used to produce the pulp for the respective residual lignin.

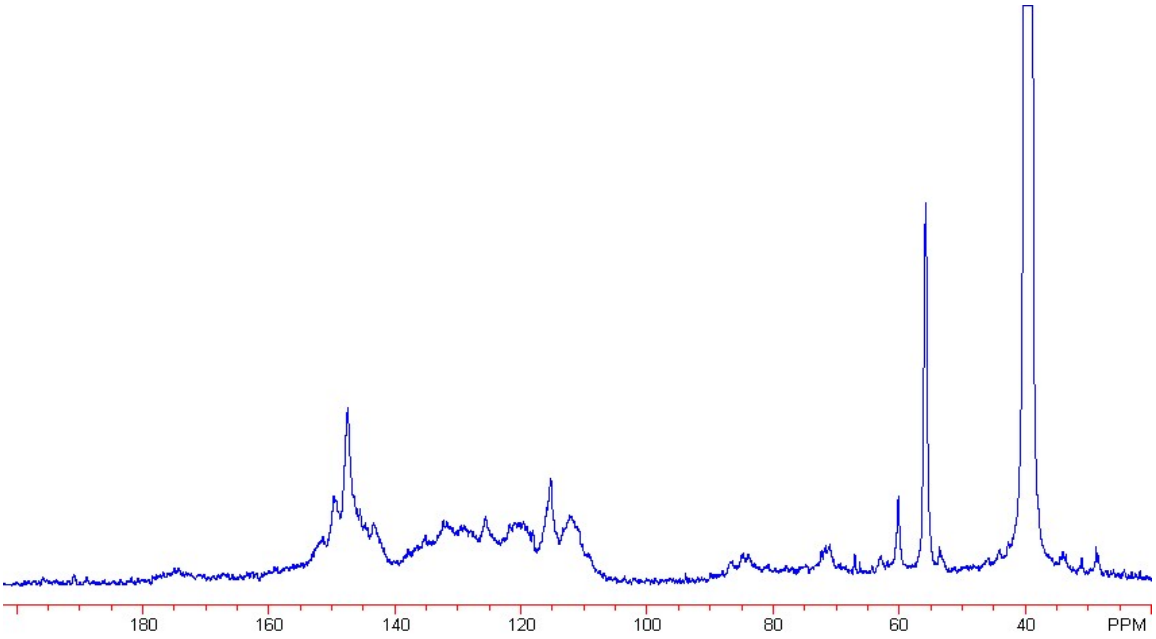

Figure A-4-103. ^{13}C NMR spectrum of residual lignin from Condition 12 of the constant kappa number (approximately 30) series of pulps. Table A-4-1 summarizes the pulping conditions used to produce the pulp for the respective residual lignin.

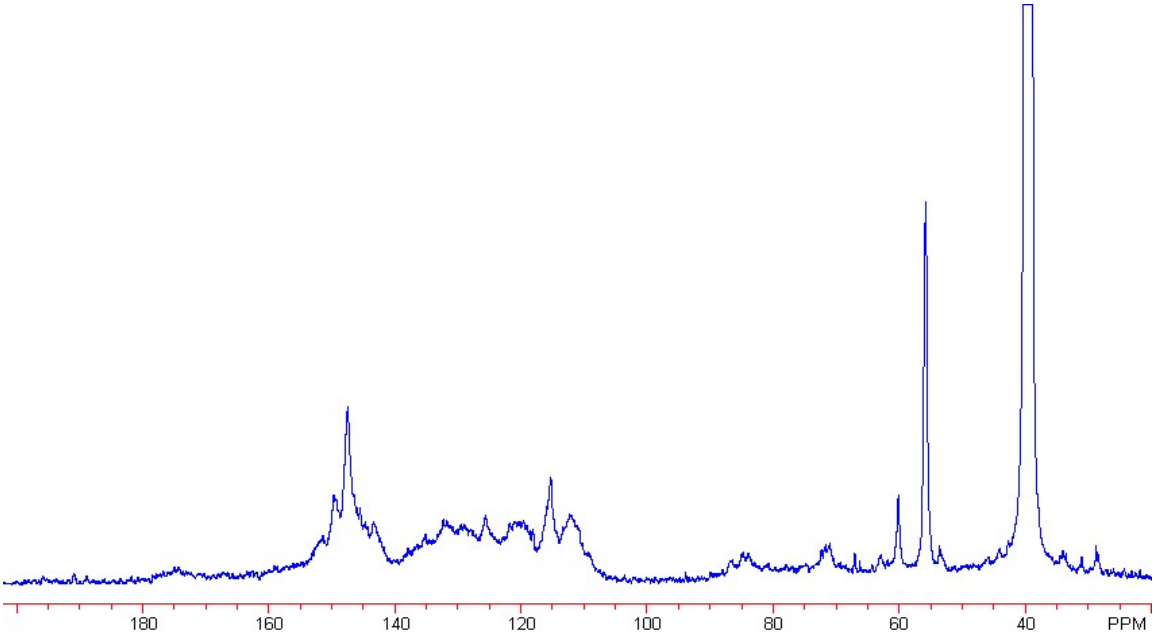

Figure A-4-104. ^{13}C NMR spectrum of residual lignin from Condition 13 of the constant kappa number (approximately 30) series of pulps. Table A-4-1 summarizes the pulping conditions used to produce the pulp for the respective residual lignin.

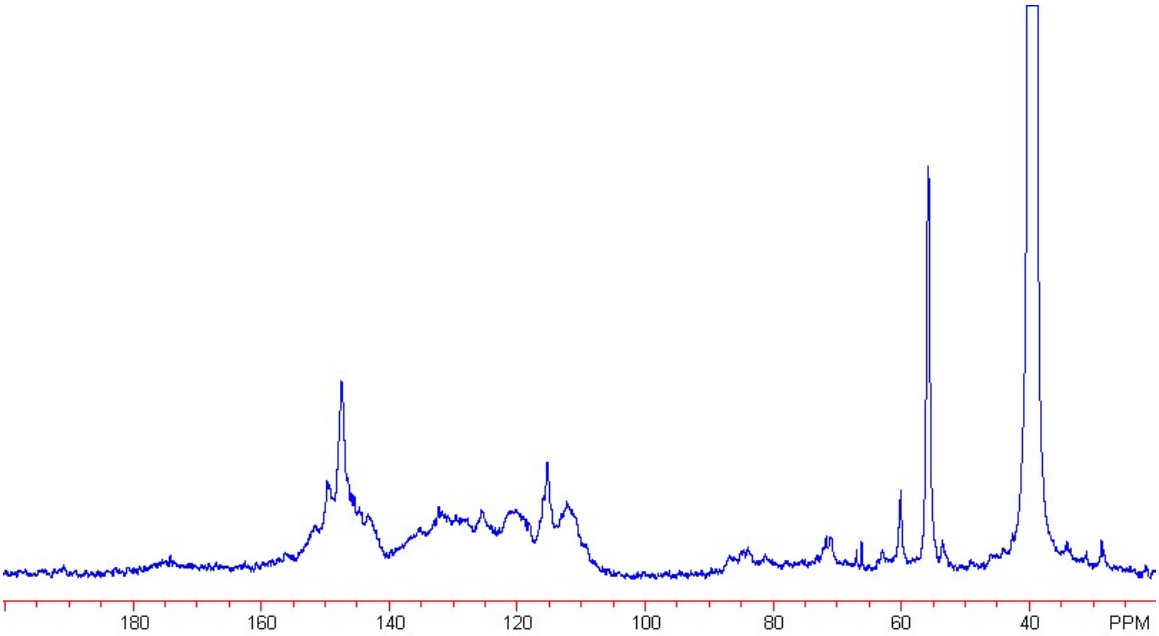

Figure A-4-105. ^{13}C NMR spectrum of residual lignin from Condition 14 of the constant kappa number (approximately 30) series of pulps. Table A-4-1 summarizes the pulping conditions used to produce the pulp for the respective residual lignin.

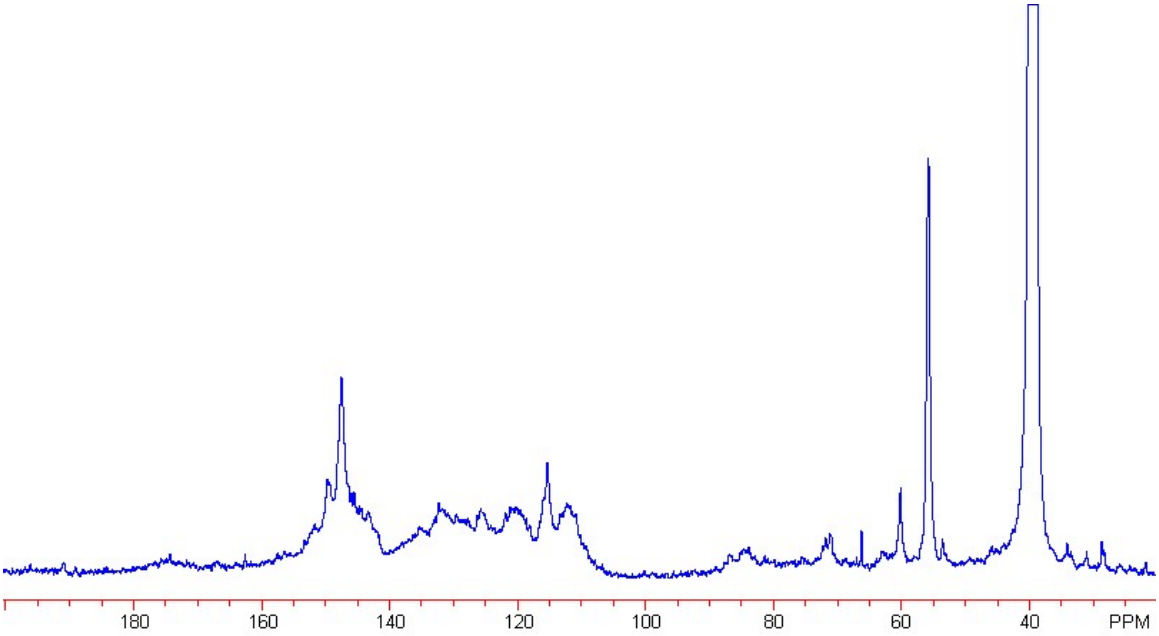

Figure A-4-106. ^{13}C NMR spectrum of residual lignin from Condition 15 of the constant kappa number (approximately 30) series of pulps. Table A-4-1 summarizes the pulping conditions used to produce the pulp for the respective residual lignin.

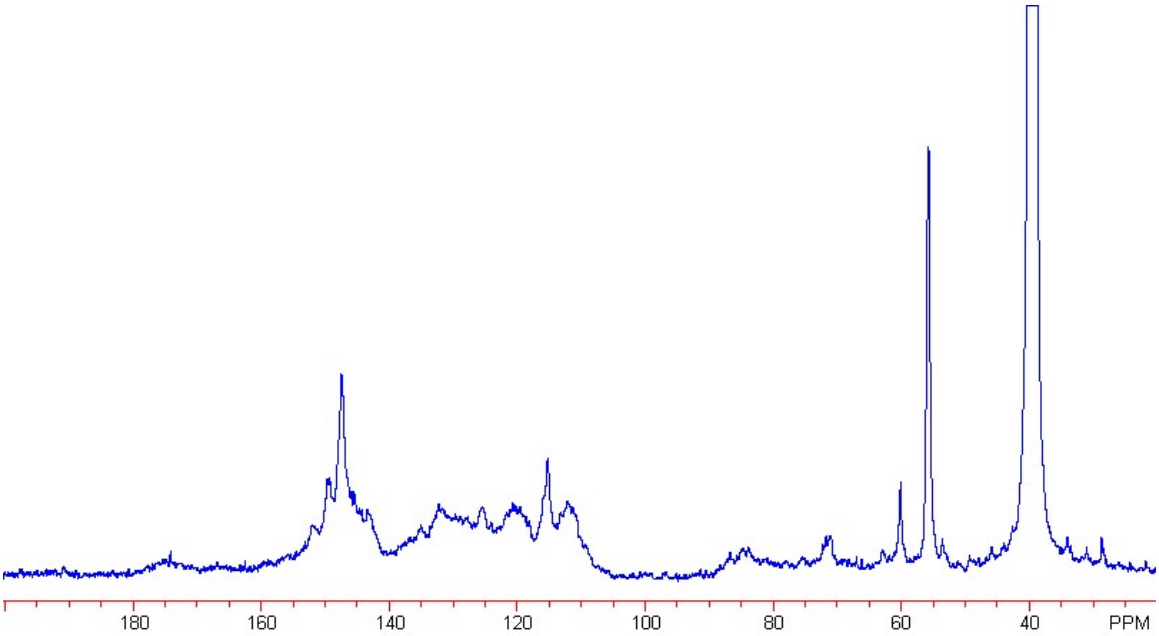

Figure A-4-107. ^{13}C NMR spectrum of residual lignin from Condition 16 of the constant kappa number (approximately 30) series of pulps. Table A-4-1 summarizes the pulping conditions used to produce the pulp for the respective residual lignin.

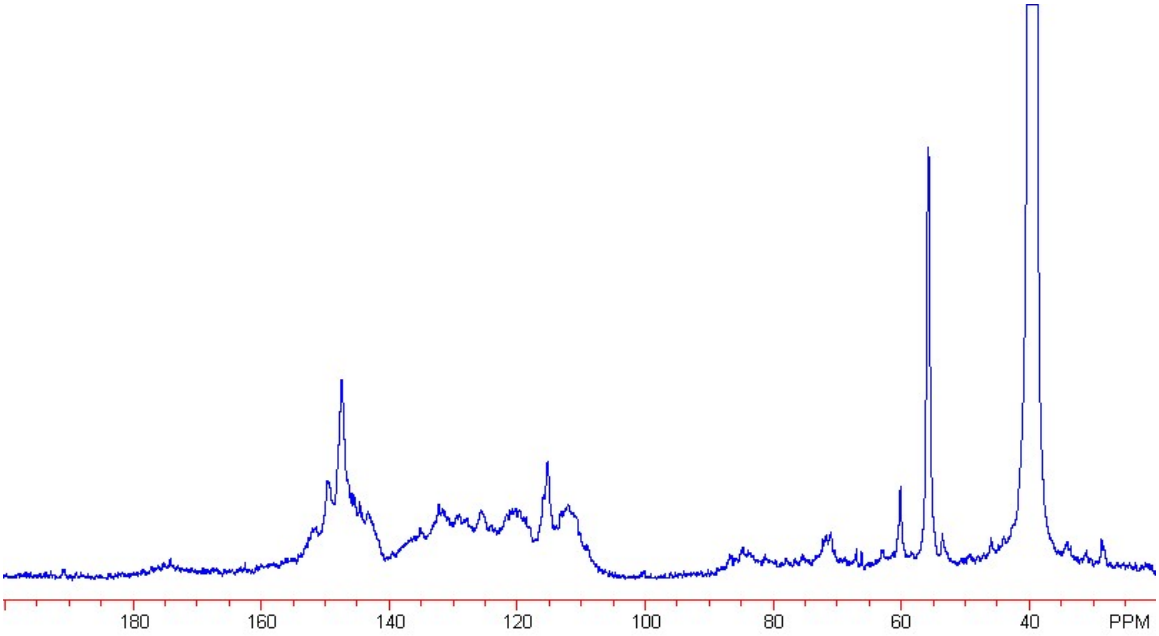

Figure A-4-108. ^{13}C NMR spectrum of residual lignin from Condition 17 of the constant kappa number (approximately 30) series of pulps. Table A-4-1 summarizes the pulping conditions used to produce the pulp for the respective residual lignin.

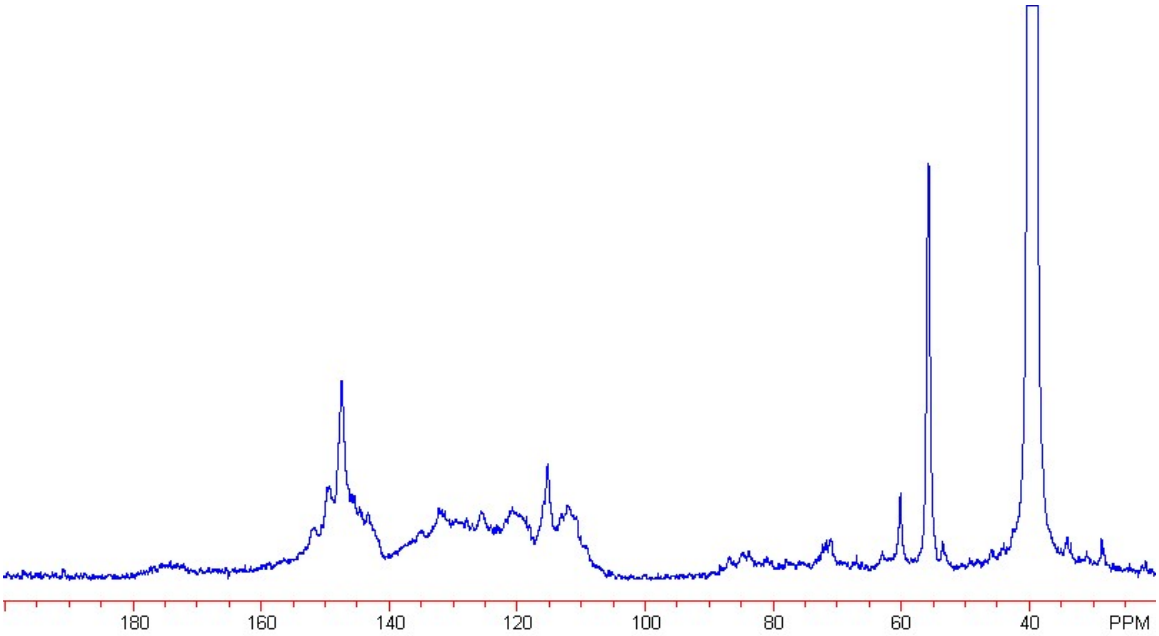

Figure A-4-109. ^{13}C NMR spectrum of residual lignin from Condition 18 of the constant kappa number (approximately 30) series of pulps. Table A-4-1 summarizes the pulping conditions used to produce the pulp for the respective residual lignin.

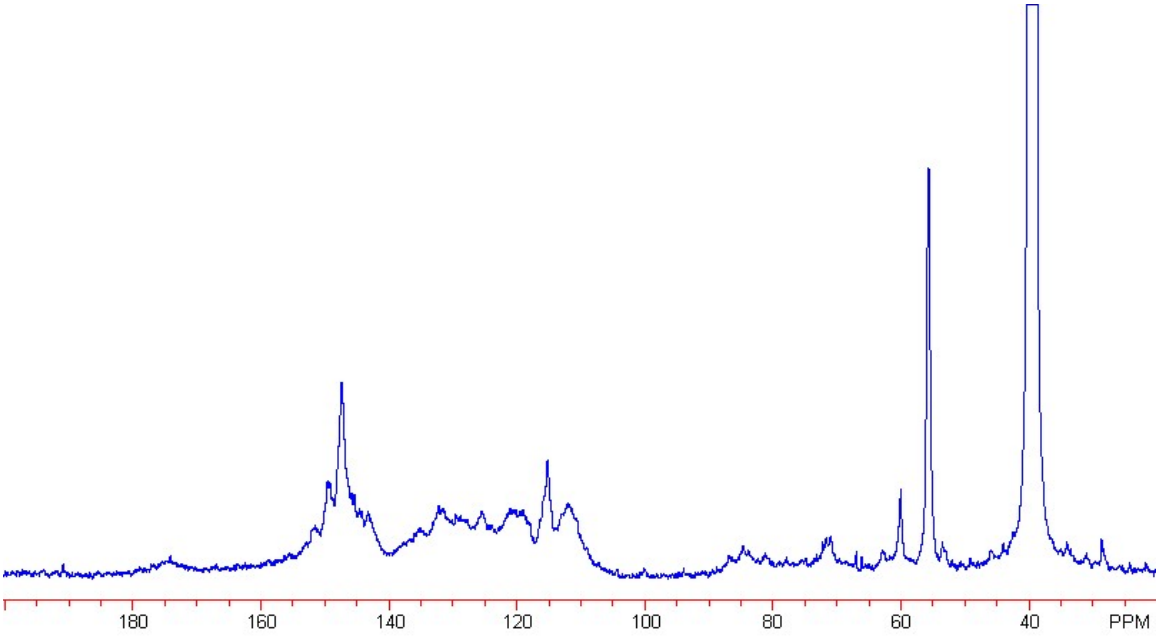

Figure A-4-110. ^{13}C NMR spectrum of residual lignin from Condition 19 of the constant kappa number (approximately 30) series of pulps. Table A-4-1 summarizes the pulping conditions used to produce the pulp for the respective residual lignin.

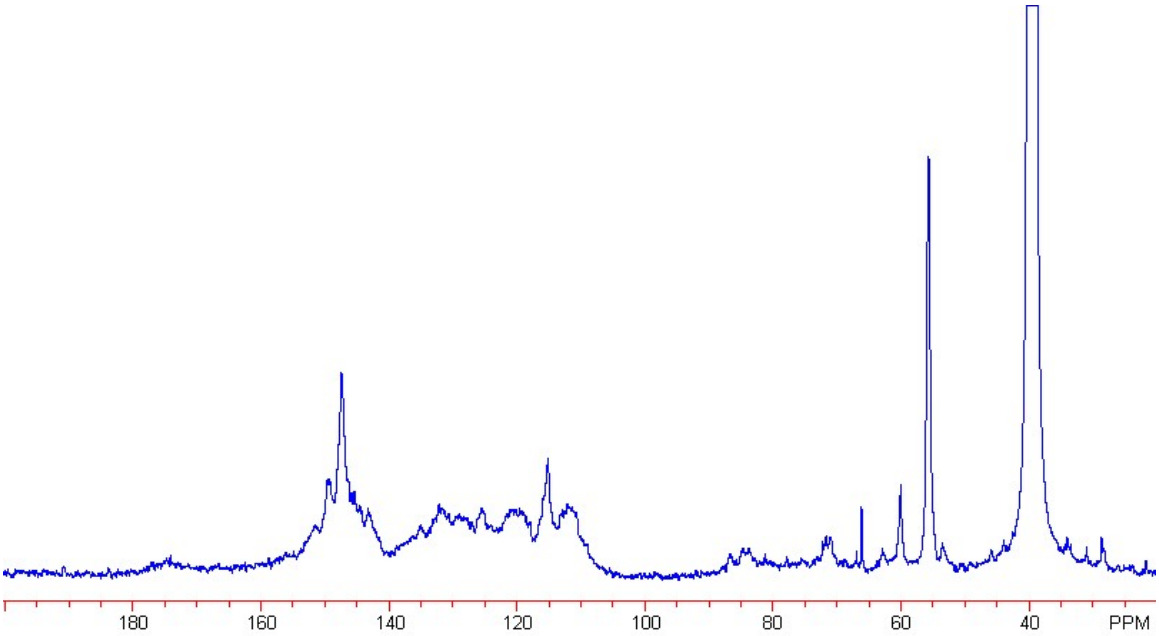

Figure A-4-111. ^{13}C NMR spectrum of residual lignin from Condition 20 of the constant kappa number (approximately 30) series of pulps. Table A-4-1 summarizes the pulping conditions used to produce the pulp for the respective residual lignin.

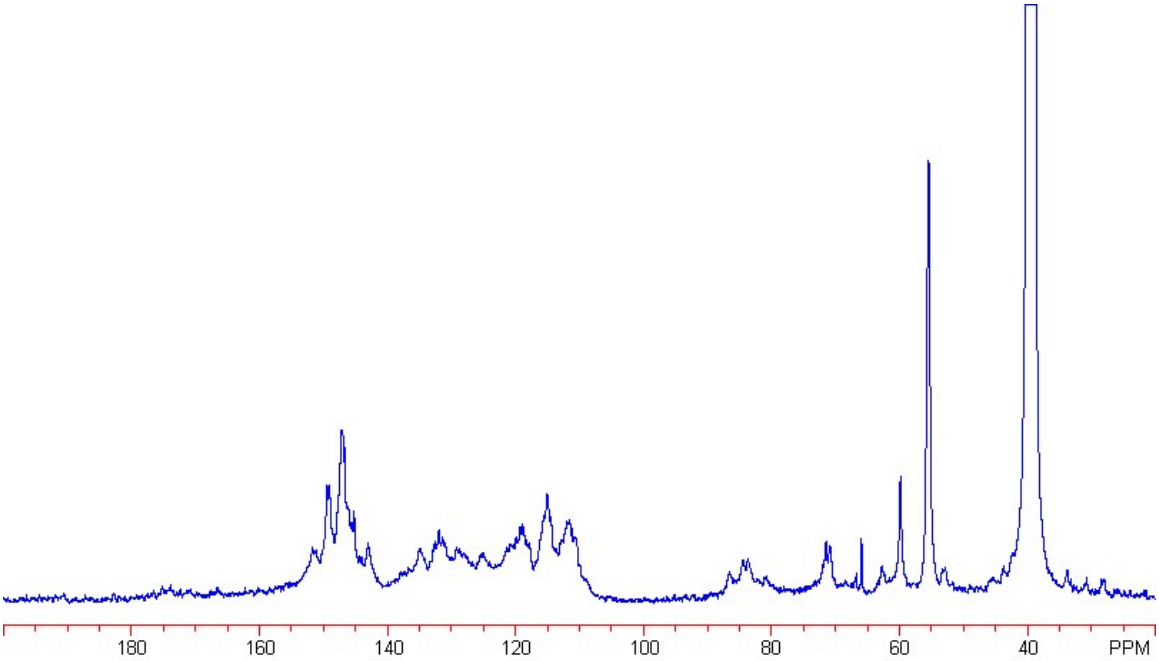

Figure A-4-112. ^{13}C NMR spectrum of residual lignin from Condition A-1 of the incremental cook series of pulps. Table A-4-2 summarizes the pulping conditions used to produce the pulp for the respective residual lignin.

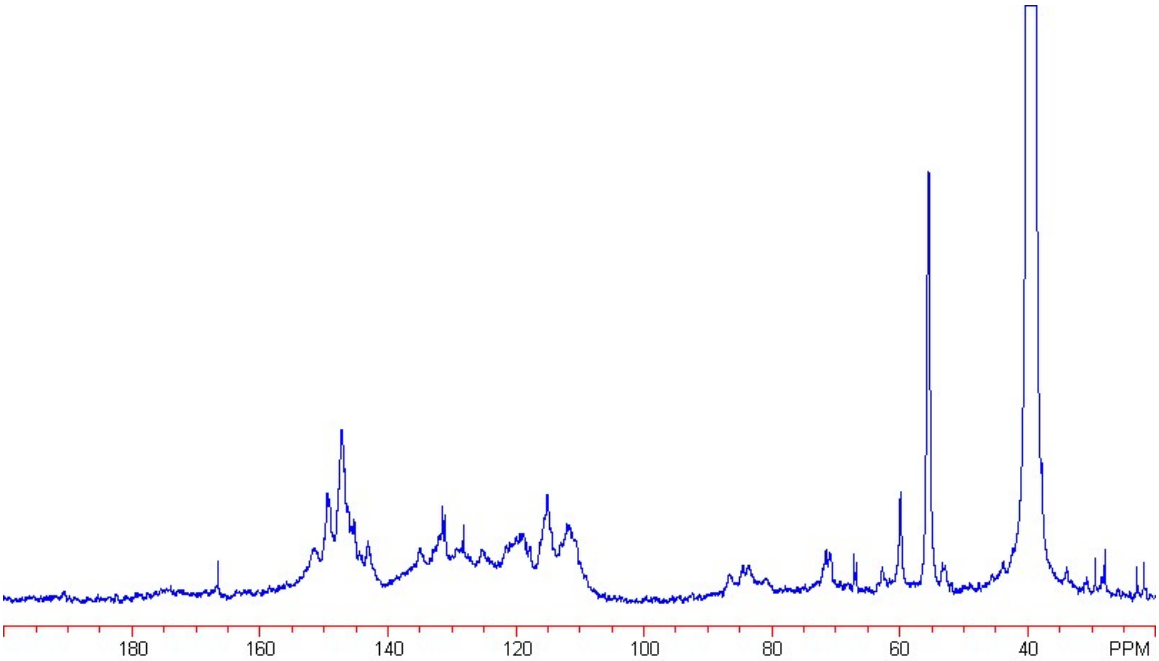

Figure A-4-113. ^{13}C NMR spectrum of residual lignin from Condition A-2 of the incremental cook series of pulps. Table A-4-2 summarizes the pulping conditions used to produce the pulp for the respective residual lignin.

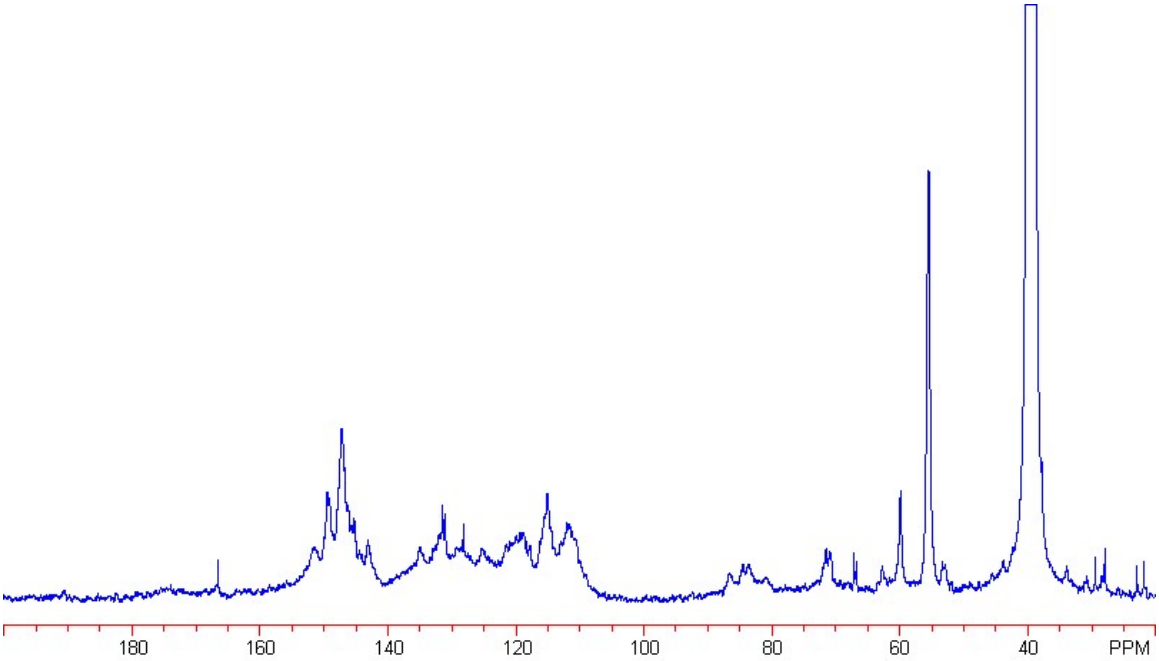

Figure A-4-114. ^{13}C NMR spectrum of residual lignin from Condition A-3 of the incremental cook series of pulps. Table A-4-2 summarizes the pulping conditions used to produce the pulp for the respective residual lignin.

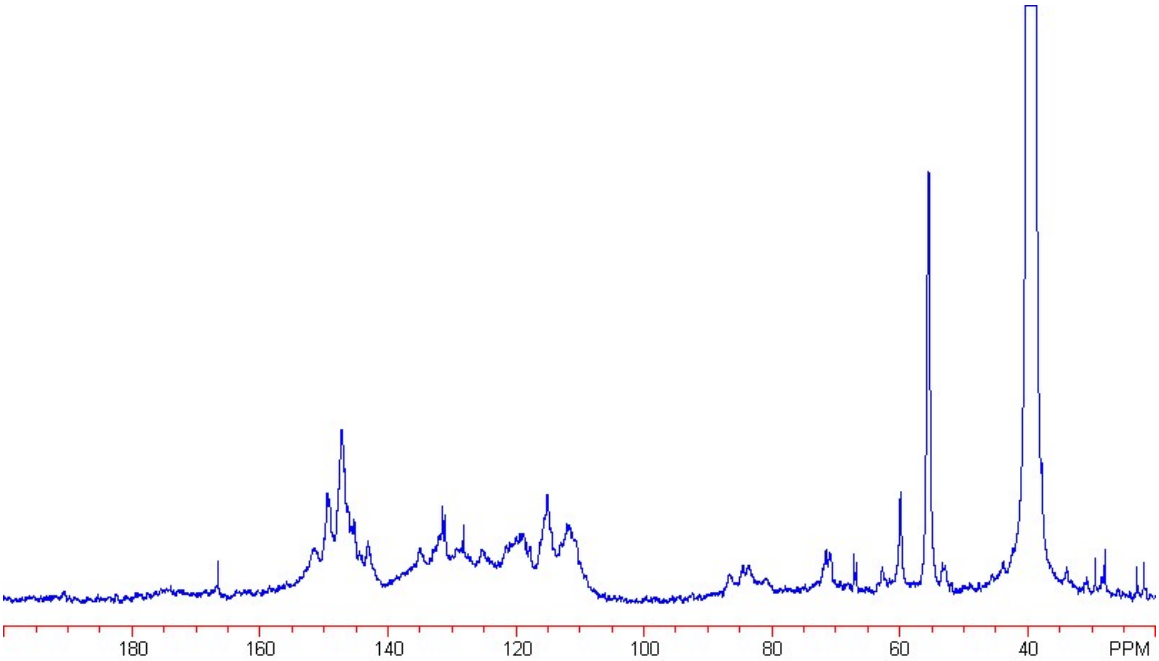

Figure A-4-115. ^{13}C NMR spectrum of residual lignin from Condition A-4 of the incremental cook series of pulps. Table A-4-2 summarizes the pulping conditions used to produce the pulp for the respective residual lignin.

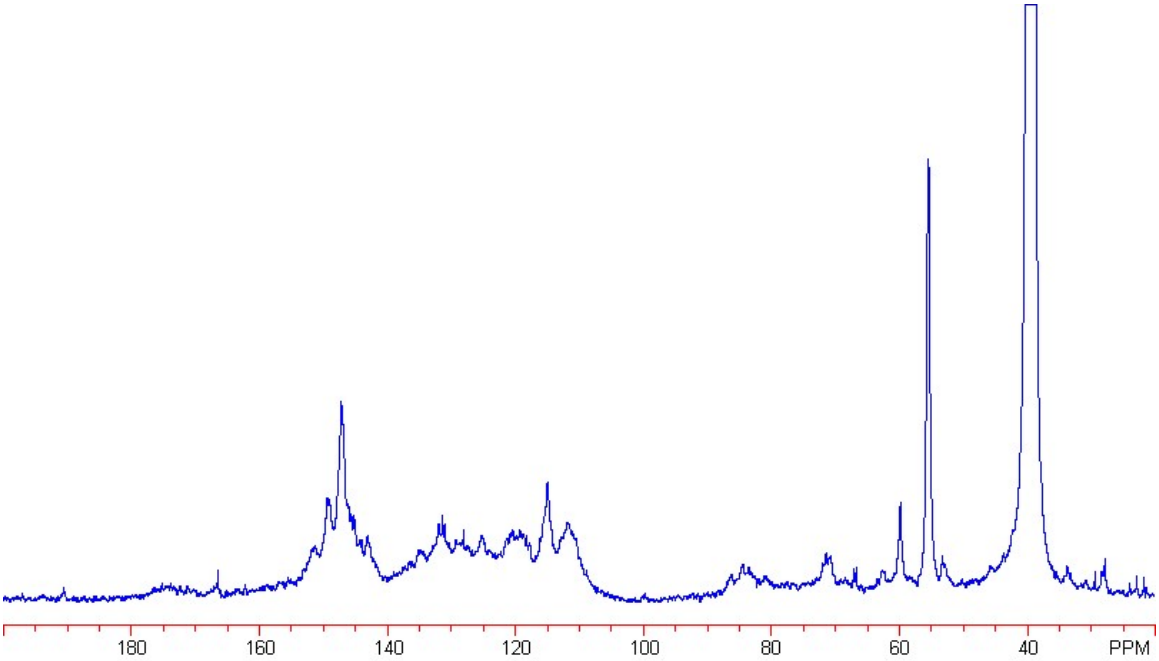

Figure A-4-116. ^{13}C NMR spectrum of residual lignin from Condition A-5 of the incremental cook series of pulps. Table A-4-2 summarizes the pulping conditions used to produce the pulp for the respective residual lignin.

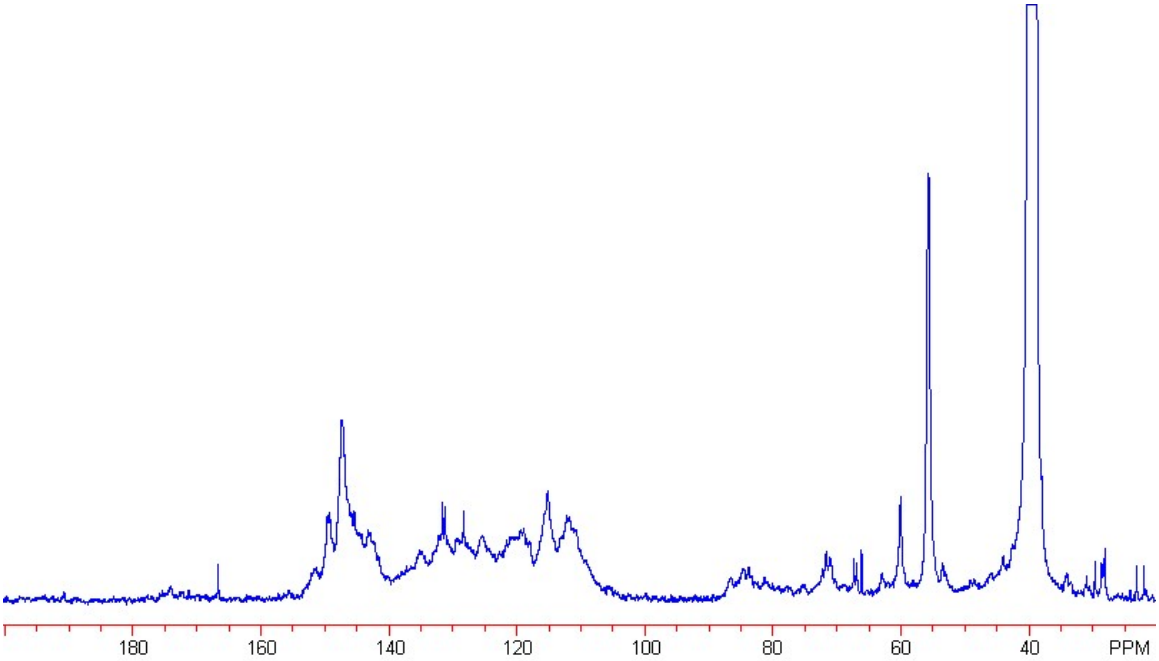

Figure A-4-117. ^{13}C NMR spectrum of residual lignin from Condition A-6 of the incremental cook series of pulps. Table A-4-2 summarizes the pulping conditions used to produce the pulp for the respective residual lignin.

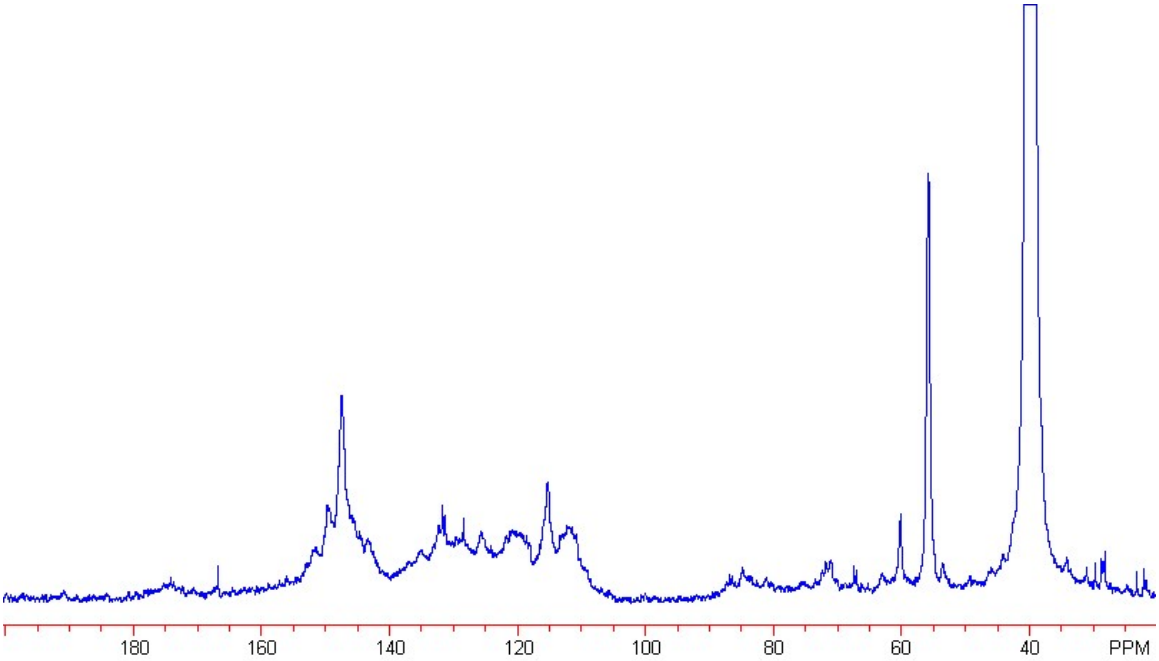

Figure A-4-118. ^{13}C NMR spectrum of residual lignin from Condition A-7 of the incremental cook series of pulps. Table A-4-2 summarizes the pulping conditions used to produce the pulp for the respective residual lignin.

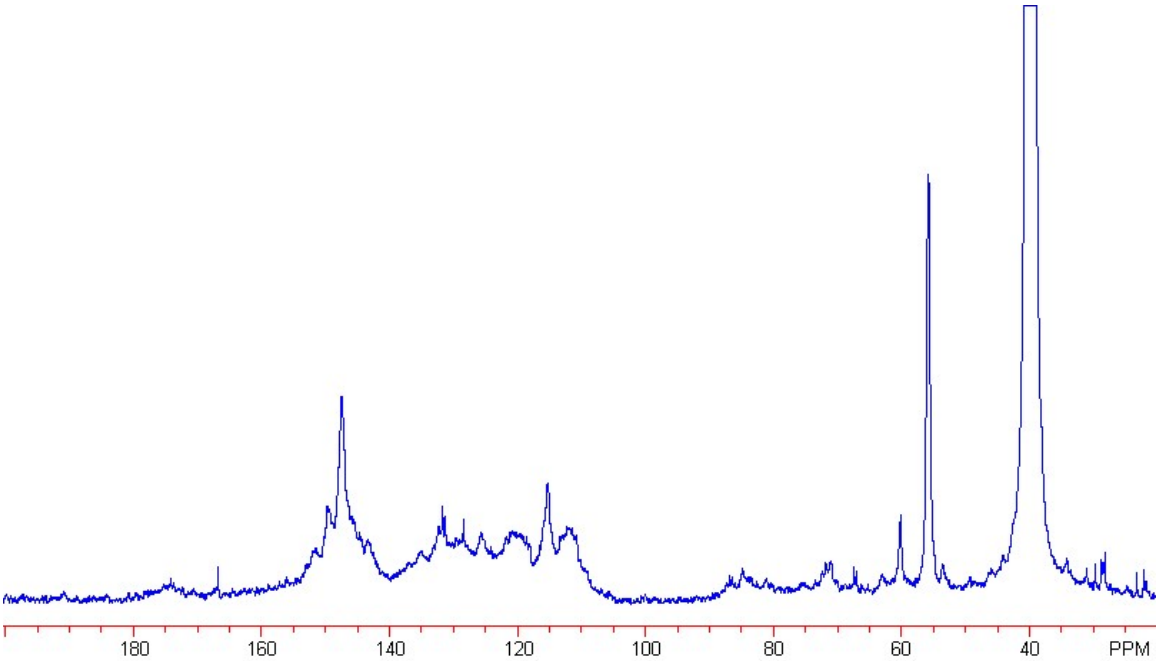

Figure A-4-119. ^{13}C NMR spectrum of residual lignin from Condition A-8 of the incremental cook series of pulps. Table A-4-2 summarizes the pulping conditions used to produce the pulp for the respective residual lignin.

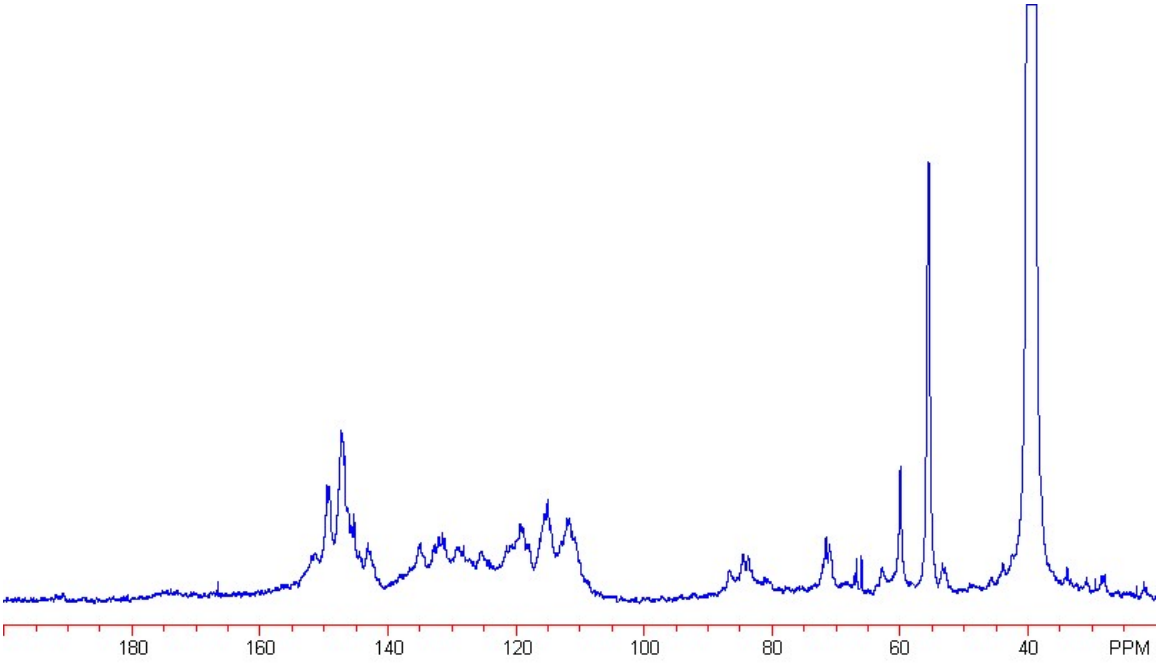

Figure A-4-120. ^{13}C NMR spectrum of residual lignin from Condition B-1 of the incremental cook series of pulps. Table A-4-2 summarizes the pulping conditions used to produce the pulp for the respective residual lignin.

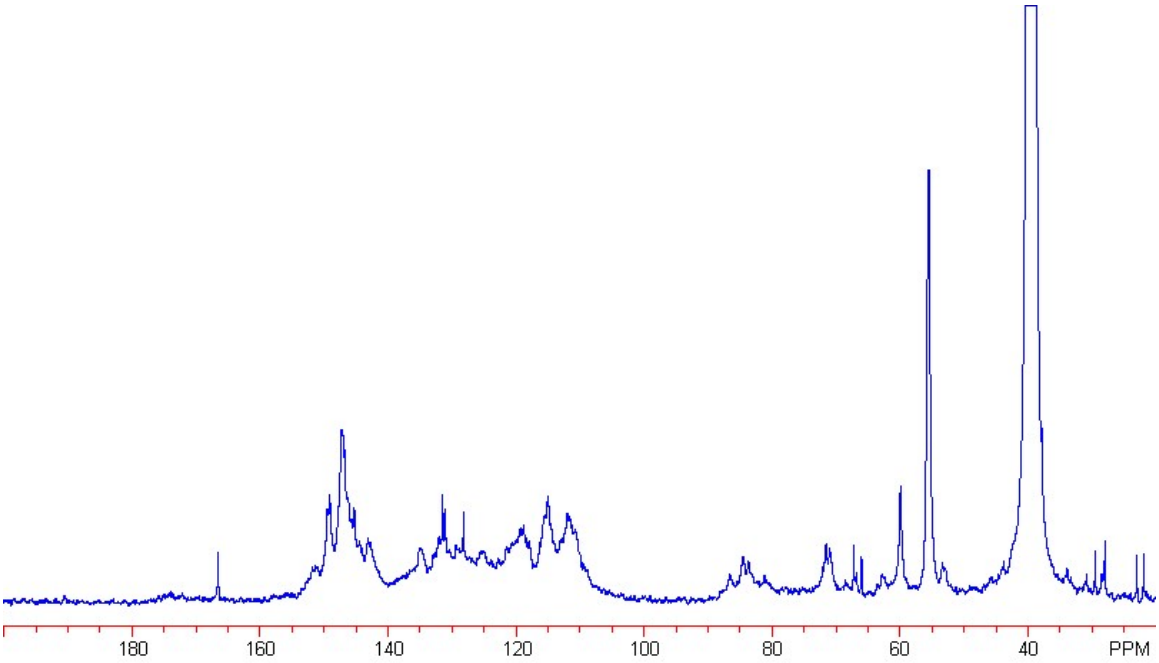

Figure A-4-121. ^{13}C NMR spectrum of residual lignin from Condition B-2 of the incremental cook series of pulps. Table A-4-2 summarizes the pulping conditions used to produce the pulp for the respective residual lignin.

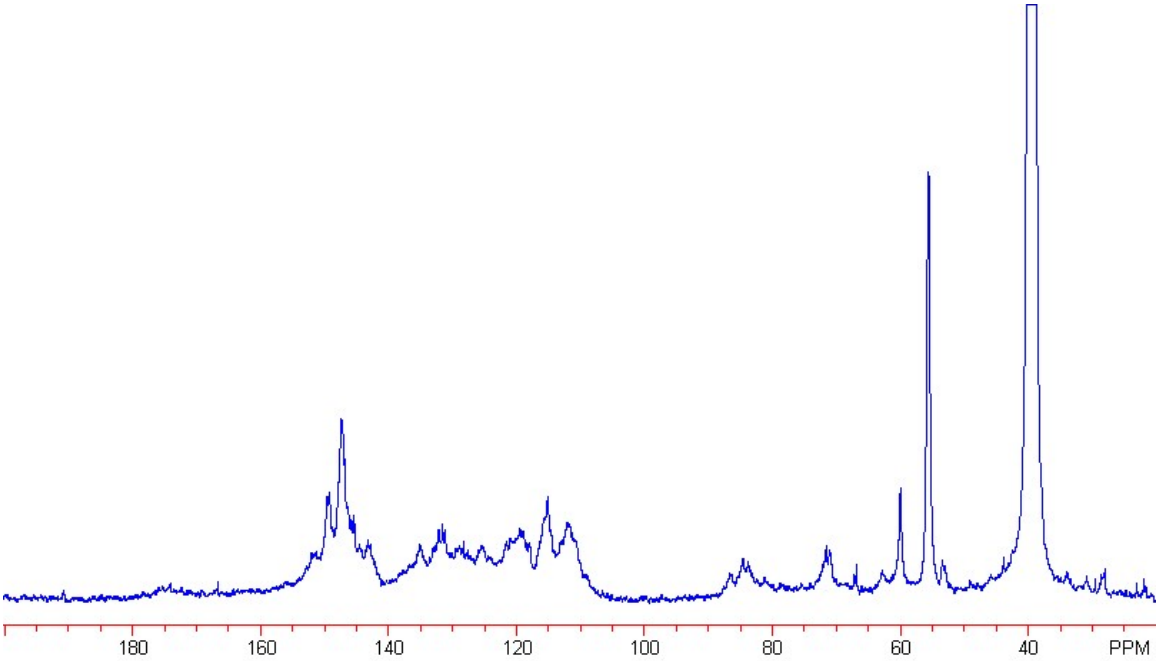

Figure A-4-122. ^{13}C NMR spectrum of residual lignin from Condition B-3 of the incremental cook series of pulps. Table A-4-2 summarizes the pulping conditions used to produce the pulp for the respective residual lignin.

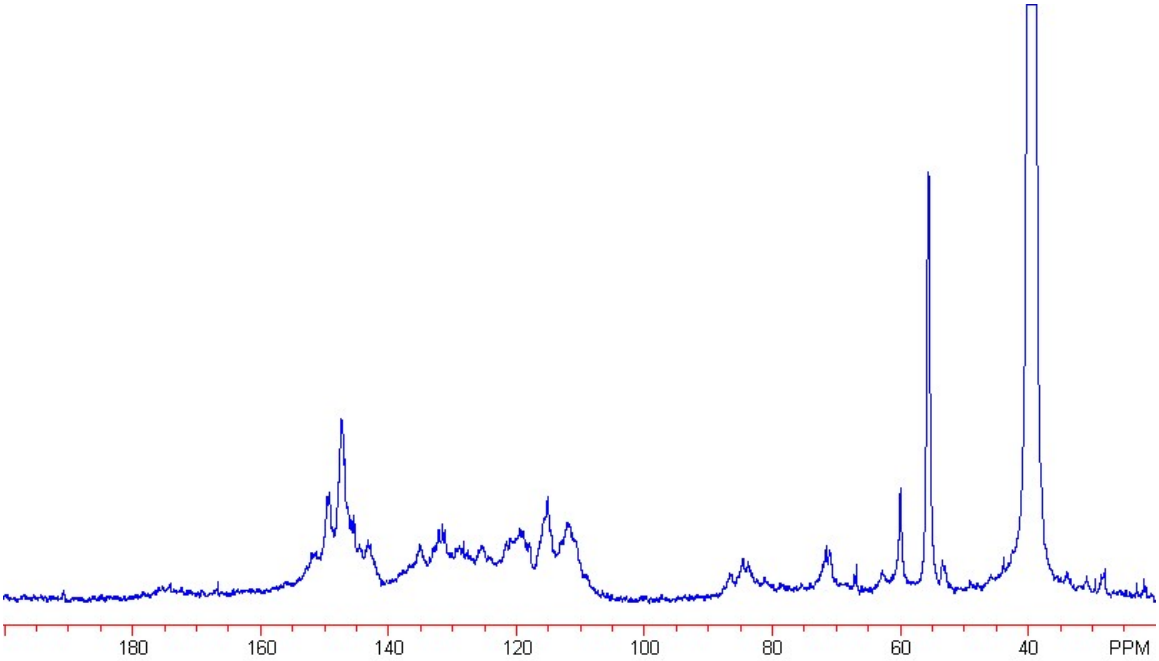

Figure A-4-123. ^{13}C NMR spectrum of residual lignin from Condition B-4 of the incremental cook series of pulps. Table A-4-2 summarizes the pulping conditions used to produce the pulp for the respective residual lignin.

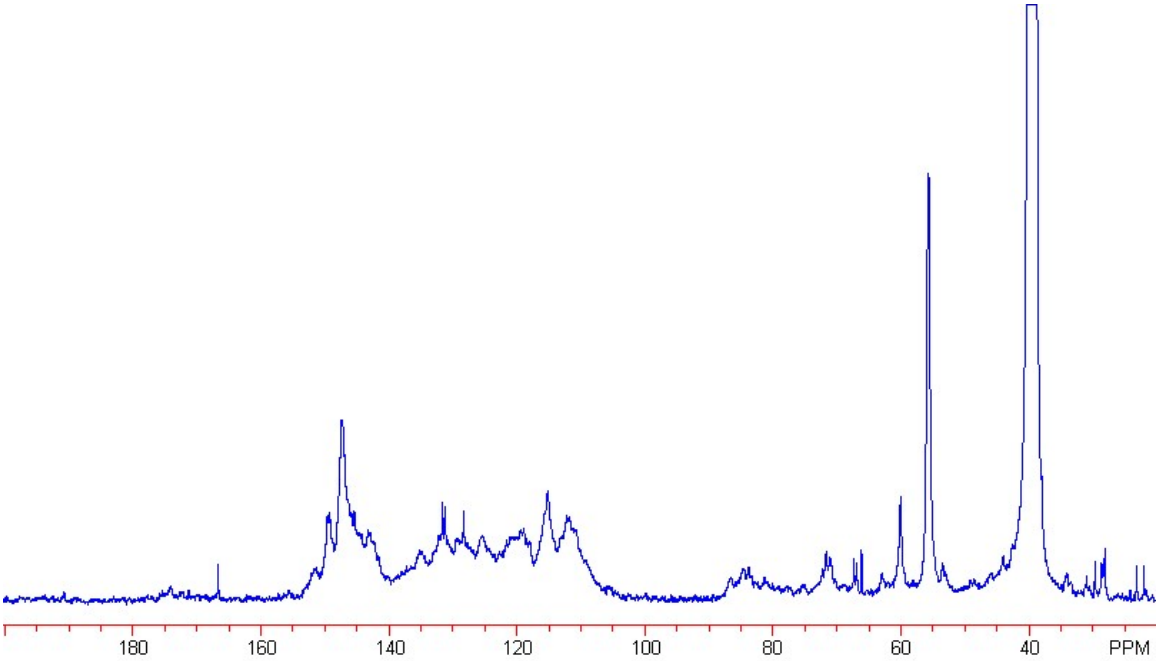

Figure A-4-124. ^{13}C NMR spectrum of residual lignin from Condition B-5 of the incremental cook series of pulps. Table A-4-2 summarizes the pulping conditions used to produce the pulp for the respective residual lignin.

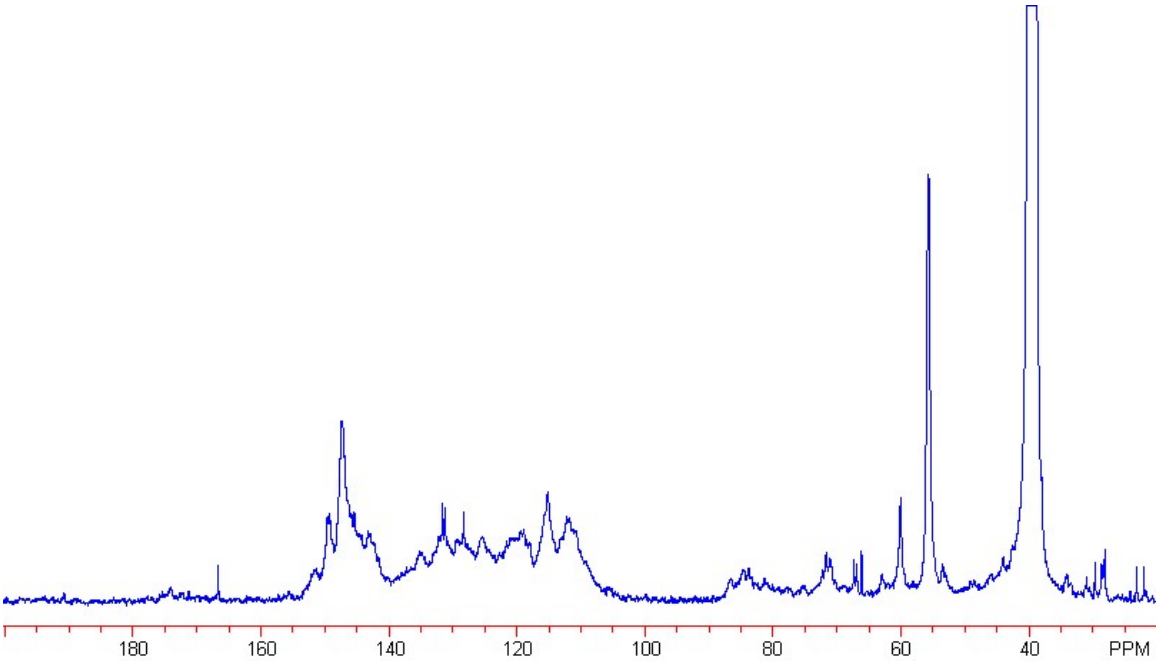

Figure A-4-125. ^{13}C NMR spectrum of residual lignin from Condition B-6 of the incremental cook series of pulps. Table A-4-2 summarizes the pulping conditions used to produce the pulp for the respective residual lignin.

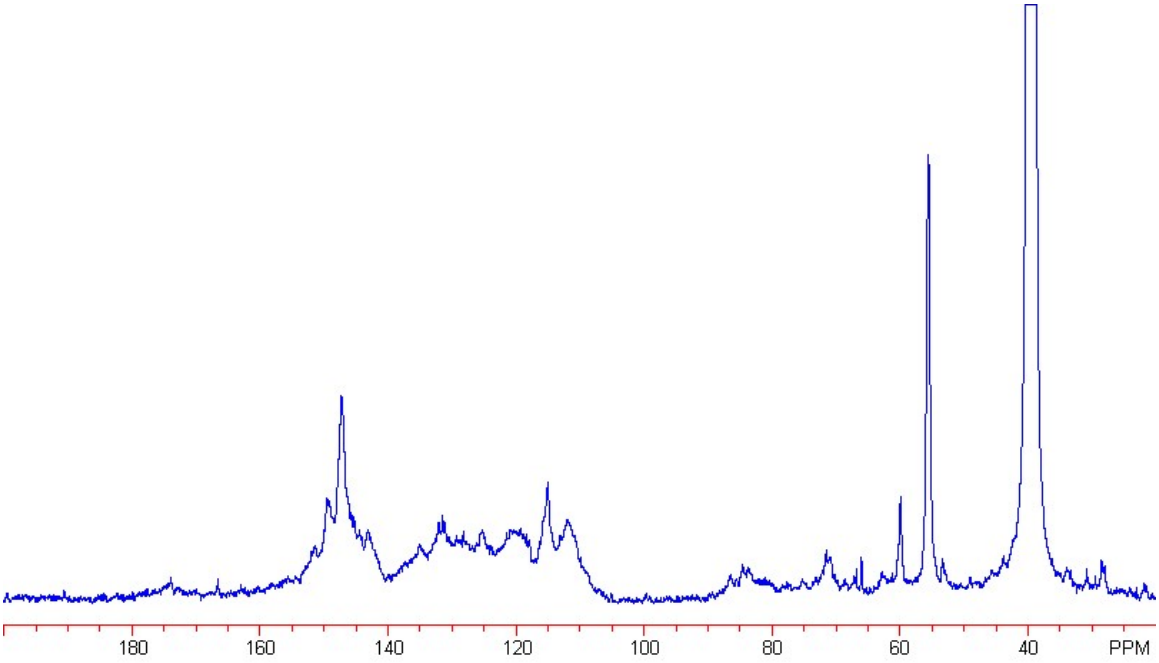

Figure A-4-126. ^{13}C NMR spectrum of residual lignin from Condition B-7 of the incremental cook series of pulps. Table A-4-2 summarizes the pulping conditions used to produce the pulp for the respective residual lignin.

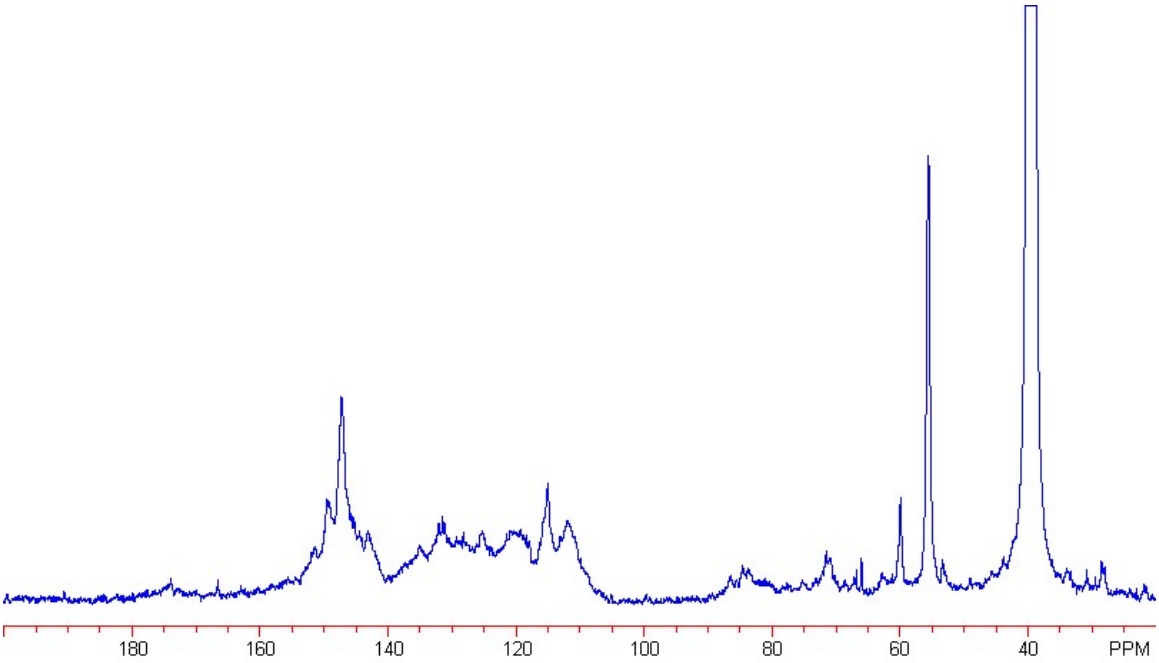

Figure A-4-127. ^{13}C NMR spectrum of residual lignin from Condition B-8 of the incremental cook series of pulps. Table A-4-2 summarizes the pulping conditions used to produce the pulp for the respective residual lignin.

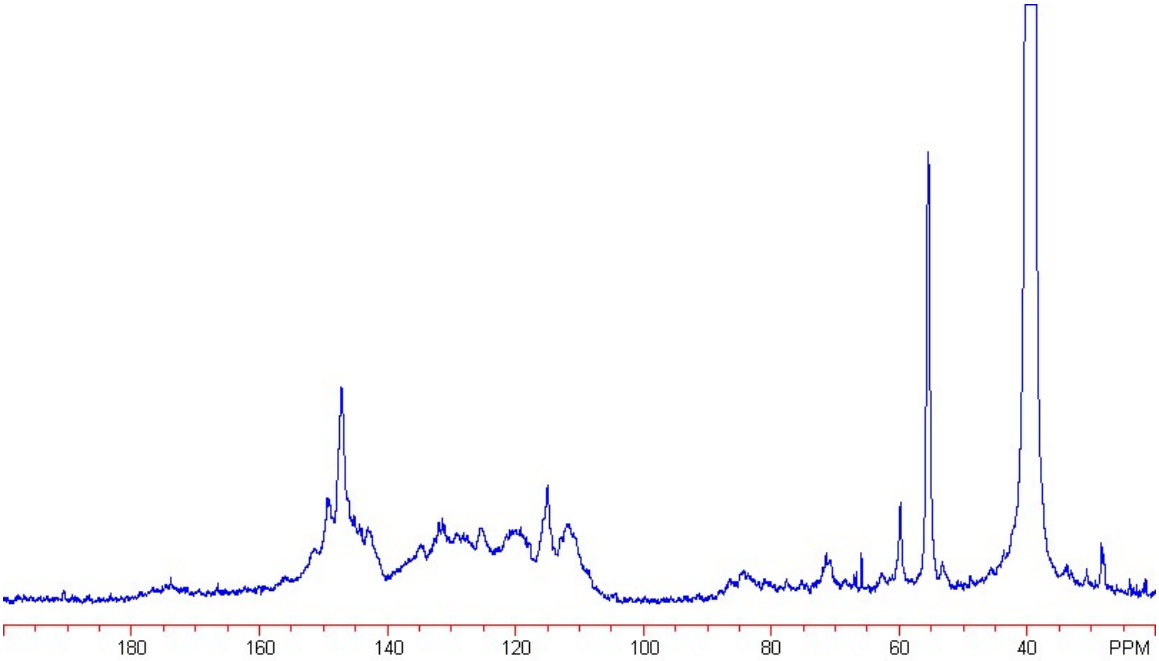

Figure A-4-128. ^{13}C NMR spectrum of residual lignin from Condition B-9 of the incremental cook series of pulps. Table A-4-2 summarizes the pulping conditions used to produce the pulp for the respective residual lignin.

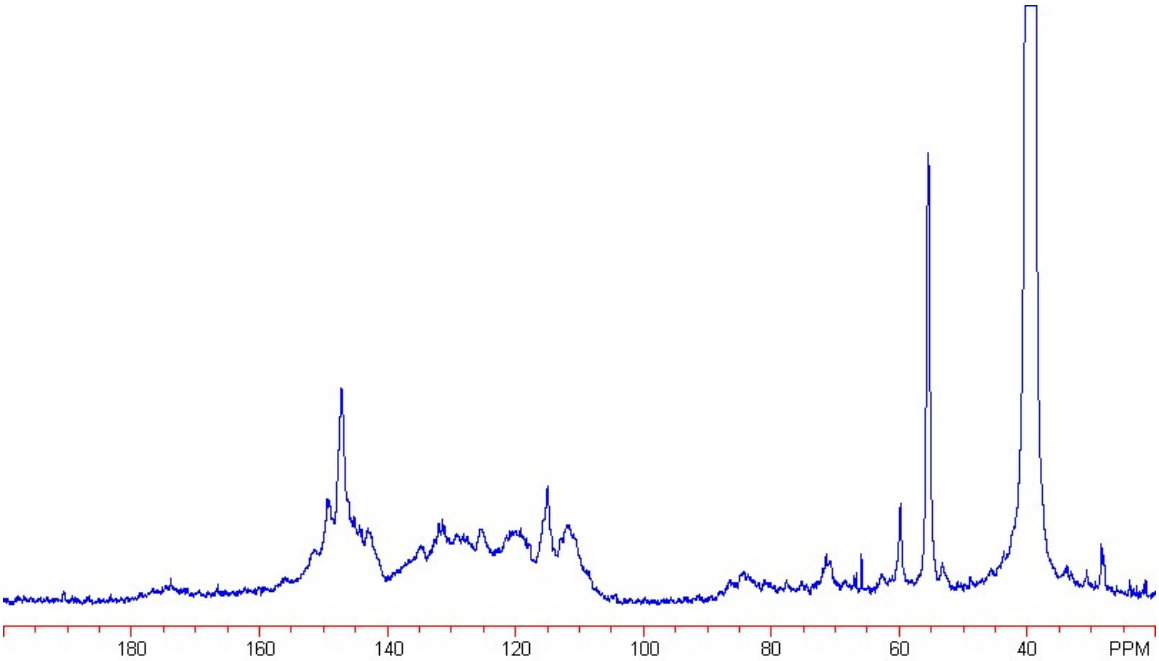

Figure A-4-129. ^{13}C NMR spectrum of residual lignin from Condition B-10 of the incremental cook series of pulps. Table A-4-2 summarizes the pulping conditions used to produce the pulp for the respective residual lignin.

18.13 Summary of ^{13}C NMR Data for Residual Lignins

Table A-4-18. ^{13}C NMR data for residual lignins isolated from the constant kappa number (approximately 30) series of pulps. Table A-4-1 summarizes the pulping conditions used to produce the pulps for the respective residual lignins.

Region	Functional group	Integral region/ppm	1 C/C_9	2 C/C_9	3 C/C_9	4 C/C_9	5 C/C_9
1	COOH	178-162.5	0.385	0.369	0.455	0.337	0.389
2	C3,C4 (-C-Ar-O)	154.0-140.0	2.058	2.108	2.070	2.096	2.071
3	C1, (-C-Ar-C)	140.0-127.0	1.463	1.410	1.439	1.407	1.442
4	C5, (-C-Ar-C)	127.0-123.0	0.500	0.491	0.504	0.495	0.503
5	C6, (-C-Ar-H)	123.0-117.0	0.778	0.775	0.779	0.791	0.769
6	C5, (-C-Ar-H)	117.0-114.0	0.480	0.488	0.470	0.507	0.482
7	C2, (-C-Ar-H)	114.0-106.0	0.722	0.728	0.738	0.702	0.733
2-4	Substituted aromatic C	154.0-123.0	4.021	4.009	4.013	3.998	4.016
5-7	Unsubstituted aromatic C	123.0-106.0	1.980	1.991	1.987	2.000	1.984
8	Aliphatic C-O (Cβ.)	90.0-78.0	0.475	0.471	0.490	0.438	0.454
9	Aliphatic C-O (Cα.)	78.0-67.0	0.533	0.547	0.553	0.495	0.510
10	Aliphatic C-OR	67.0-61.0	0.162	0.160	0.163	0.146	0.139
11	Aliphatic C-O, Cγ	61.0-57.0	0.277	0.289	0.289	0.277	0.268
12	OCH_3	57.0-54.0	0.820	0.852	0.804	0.859	0.822
13	Cβ in ββ and Cβ in β5	54.0-52.0	0.108	0.115	0.119	0.111	0.107
14	OCH_3 in MAME Structure	52.0-49.0	0.113	0.115	0.123	0.098	0.103
15	CH_2 in Diaryl methane	29.5-27.0	0.148	0.117	0.128	0.106	0.135

Table A-4-19. ^{13}C NMR data for residual lignins isolated from the constant kappa number (approximately 30) series of pulps. Table A-4-1 summarizes the pulping conditions used to produce the pulps for the respective residual lignins.

Region	Functional group	Integral region/ppm	6 C/C_9	7 C/C_9	8 C/C_9	9 C/C_9	10 C/C_9
1	COOH	178-162.5	0.403	0.410	0.396	0.439	0.380
2	C3,C4 (-C-Ar-O)	154.0-140.0	2.083	2.100	2.071	2.081	2.083
3	C1, (-C-Ar-C)	140.0-127.0	1.428	1.446	1.428	1.439	1.426
4	C5, (-C-Ar-C)	127.0-123.0	0.491	0.493	0.488	0.505	0.484
5	C6, (-C-Ar-H)	123.0-117.0	0.780	0.769	0.788	0.783	0.791
6	C5, (-C-Ar-H)	117.0-114.0	0.491	0.474	0.486	0.469	0.489
7	C2, (-C-Ar-H)	114.0-106.0	0.726	0.718	0.738	0.722	0.727
2-4	Substituted aromatic C	154.0-123.0	4.002	4.039	3.987	4.025	3.993
5-7	Unsubstituted aromatic C	123.0-106.0	1.997	1.961	2.012	1.974	2.007
8	Aliphatic C-O (Cβ.)	90.0-78.0	0.469	0.459	0.504	0.446	0.514
9	Aliphatic C-O (Cα.)	78.0-67.0	0.525	0.518	0.539	0.496	0.543
10	Aliphatic C-OR	67.0-61.0	0.158	0.151	0.154	0.148	0.160
11	Aliphatic C-O, Cγ	61.0-57.0	0.270	0.276	0.292	0.258	0.291
12	OCH_3	57.0-54.0	0.841	0.820	0.826	0.794	0.836
13	Cβ in ββ and Cβ in β5	54.0-52.0	0.114	0.104	0.115	0.105	0.116
14	OCH_3 in MAME Structure	52.0-49.0	0.099	0.100	0.106	0.103	0.110
15	CH_2 in Diaryl methane	29.5-27.0	0.112	0.128	0.122	0.120	0.113

Table A-4-20. ^{13}C NMR data for residual lignins isolated from the constant kappa number (approximately 30) series of pulps. Table A-4-1 summarizes the pulping conditions used to produce the pulps for the respective residual lignins.

Region	Functional group	Integral region/ppm	11 C/C_9	12 C/C_9	13 C/C_9	14 C/C_9	15 C/C_9
1	COOH	178-162.5	0.420	0.370	0.423	0.464	0.483
2	C3,C4 (-C-Ar-O)	154.0-140.0	2.903	2.069	2.071	2.104	2.114
3	C1, (-C-Ar-C)	140.0-127.0	1.424	1.441	1.445	1.432	1.444
4	C5, (-C-Ar-C)	127.0-123.0	0.509	0.499	0.493	0.488	0.497
5	C6, (-C-Ar-H)	123.0-117.0	0.779	0.779	0.767	0.771	0.770
6	C5, (-C-Ar-H)	117.0-114.0	0.484	0.490	0.489	0.483	0.473
7	C2, (-C-Ar-H)	114.0-106.0	0.711	0.723	0.735	0.723	0.701
2-4	Substituted aromatic C	154.0-123.0	4.836	4.009	4.009	4.024	4.055
5-7	Unsubstituted aromatic C	123.0-106.0	1.974	1.992	1.991	1.977	1.944
8	Aliphatic C-O (Cβ.)	90.0-78.0	0.466	0.513	0.504	0.464	0.457
9	Aliphatic C-O (Cα.)	78.0-67.0	0.518	0.554	0.538	0.494	0.493
10	Aliphatic C-OR	67.0-61.0	0.152	0.163	0.157	0.138	0.152
11	Aliphatic C-O, Cγ	61.0-57.0	0.265	0.295	0.283	0.260	0.273
12	OCH_3	57.0-54.0	0.854	0.816	0.802	0.805	0.819
13	Cβ in ββ and Cβ in β5	54.0-52.0	0.116	0.116	0.113	0.104	0.102
14	OCH_3 in MAME Structure	52.0-49.0	0.112	0.120	0.105	0.084	0.106
15	CH_2 in Diaryl methane	29.5-27.0	0.119	0.127	0.127	0.117	0.096

Table A-4-21. ^{13}C NMR data for residual lignins isolated from the constant kappa number (approximately 30) series of pulps. Table A-4-1 summarizes the pulping conditions used to produce the pulps for the respective residual lignins.

Region	Functional group	Integral region/ppm	16 C/C_9	17 C/C_9	18 C/C_9	19 C/C_9	20 C/C_9
1	COOH	178-162.5	0.436	0.306	0.358	0.404	0.433
2	C3,C4 (-C-Ar-O)	154.0-140.0	2.092	2.100	2.103	2.084	2.094
3	C1, (-C-Ar-C)	140.0-127.0	1.424	1.415	1.414	1.430	1.425
4	C5, (-C-Ar-C)	127.0-123.0	0.501	0.497	0.504	0.494	0.492
5	C6, (-C-Ar-H)	123.0-117.0	0.787	0.779	0.781	0.787	0.775
6	C5, (-C-Ar-H)	117.0-114.0	0.481	0.481	0.480	0.478	0.479
7	C2, (-C-Ar-H)	114.0-106.0	0.716	0.728	0.718	0.726	0.736
2-4	Substituted aromatic C	154.0-123.0	4.017	4.012	4.021	4.008	4.011
5-7	Unsubstituted aromatic C	123.0-106.0	1.984	1.988	1.979	1.991	1.990
8	Aliphatic C-O (Cβ.)	90.0-78.0	0.467	0.456	0.424	0.454	0.434
9	Aliphatic C-O (Cα.)	78.0-67.0	0.492	0.544	0.483	0.490	0.479
10	Aliphatic C-OR	67.0-61.0	0.144	0.154	0.142	0.138	0.132
11	Aliphatic C-O, Cγ	61.0-57.0	0.273	0.298	0.268	0.262	0.255
12	OCH_3	57.0-54.0	0.815	0.877	0.846	0.820	0.801
13	Cβ in ββ and Cβ in β5	54.0-52.0	0.106	0.123	0.102	0.104	0.103
14	OCH_3 in MAME Structure	52.0-49.0	0.095	0.125	0.095	0.089	0.083
15	CH_2 in Diaryl methane	29.5-27.0	0.124	0.131	0.125	0.116	0.121

Table A-4-22. ^{13}C NMR data for residual lignins isolated from the incremental cook series of pulps. Table A-4-2 summarizes the pulping conditions used to produce the pulps for the respective residual lignins.

Region	Functional group	Integral region/ppm	A-1 C/C_9	A-2 C/C_9	A-3 C/C_9	A-4 C/C_9
1	COOH	178-162.5	0.360	0.408	0.441	0.303
2	C3,C4 (-C-Ar-O)	154.0-140.0	2.073	2.043	2.035	1.864
3	C1, (-C-Ar-C)	140.0-127.0	1.371	1.436	1.582	1.504
4	C5, (-C-Ar-C)	127.0-123.0	0.407	0.432	0.415	0.466
5	C6, (-C-Ar-H)	123.0-117.0	0.819	0.800	0.752	0.785
6	C5, (-C-Ar-H)	117.0-114.0	0.548	0.514	0.484	0.488
7	C2, (-C-Ar-H)	114.0-106.0	0.781	0.775	0.733	0.893
2-4	Substituted aromatic C	154.0-123.0	3.851	3.911	4.032	3.834
5-7	Unsubstituted aromatic C	123.0-106.0	2.148	2.089	1.969	2.166
8	Aliphatic C-O (Cβ.)	90.0-78.0	0.612	0.587	0.521	0.384
9	Aliphatic C-O (Cα.)	78.0-67.0	0.587	0.582	0.590	0.397
10	Aliphatic C-OR	67.0-61.0	0.176	0.167	0.157	0.093
11	Aliphatic C-O, Cγ	61.0-57.0	0.355	0.322	0.304	0.232
12	OCH_3	57.0-54.0	0.908	0.873	0.842	0.782
13	Cβ in ββ and Cβ in β5	54.0-52.0	0.129	0.131	0.122	0.106
14	OCH_3 in MAME Structure	52.0-49.0	0.109	0.111	0.102	0.077
15	CH_2 in Diaryl methane	29.5-27.0	0.097	0.137	0.248	0.189

Table A-4-23. ^{13}C NMR data for residual lignins isolated from the incremental cook series of pulps. Table A-4-2 summarizes the pulping conditions used to produce the pulps for the respective residual lignins.

Region	Functional group	Integral region/ppm	A-5 C/C_9	A-6 C/C_9	A-7 C/C_9	A-8 C/C_9
1	COOH	178-162.5	0.398	0.306	0.400	0.263
2	C3,C4 (-C-Ar-O)	154.0-140.0	2.060	1.860	2.071	1.799
3	C1, (-C-Ar-C)	140.0-127.0	1.414	1.476	1.449	1.502
4	C5, (-C-Ar-C)	127.0-123.0	0.476	0.495	0.484	0.510
5	C6, (-C-Ar-H)	123.0-117.0	0.791	0.795	0.787	0.789
6	C5, (-C-Ar-H)	117.0-114.0	0.500	0.484	0.486	0.485
7	C2, (-C-Ar-H)	114.0-106.0	0.759	0.889	0.723	0.915
2-4	Substituted aromatic C	154.0-123.0	3.950	3.831	4.004	4.811
5-7	Unsubstituted aromatic C	123.0-106.0	2.050	2.168	1.996	2.189
8	Aliphatic C-O (Cβ.)	90.0-78.0	0.545	0.350	0.459	0.376
9	Aliphatic C-O (Cα.)	78.0-67.0	0.579	0.417	0.497	0.435
10	Aliphatic C-OR	67.0-61.0	0.167	0.105	0.147	0.108
11	Aliphatic C-O, Cγ	61.0-57.0	0.315	0.220	0.274	0.217
12	OCH_3	57.0-54.0	0.865	0.798	0.851	0.794
13	Cβ in ββ and Cβ in β5	54.0-52.0	0.138	0.101	0.114	0.107
14	OCH_3 in MAME Structure	52.0-49.0	0.127	0.085	0.121	0.089
15	CH_2 in Diaryl methane	29.5-27.0	0.128	0.228	0.148	0.257

Table A-4-24. ^{13}C NMR data for residual lignins isolated from the incremental cook series of pulps. Table A-4-2 summarizes the pulping conditions used to produce the pulps for the respective residual lignins.

Region	Functional group	Integral region/ppm	B-1 C/C_9	B-2 C/C_9	B-3 C/C_9	B-4 C/C_9	B-5 C/C_9
1	COOH	178-162.5	0.328	0.209	0.394	0.249	0.210
2	C3,C4 (-C-Ar-O)	154.0-140.0	2.066	1.950	2.085	1.950	1.905
3	C1, (-C-Ar-C)	140.0-127.0	1.385	1.383	1.402	1.429	1.415
4	C5, (-C-Ar-C)	127.0-123.0	0.414	0.431	0.445	0.462	0.489
5	C6, (-C-Ar-H)	123.0-117.0	0.814	0.816	0.809	0.805	0.802
6	C5, (-C-Ar-H)	117.0-114.0	0.536	0.525	0.504	0.507	0.513
7	C2, (-C-Ar-H)	114.0-106.0	0.785	0.895	0.755	0.847	0.875
2-4	Substituted aromatic C	154.0-123.0	3.865	3.764	3.932	3.841	3.809
5-7	Unsubstituted aromatic C	123.0-106.0	2.135	2.236	2.068	2.159	2.190
8	Aliphatic C-O (Cβ.)	90.0-78.0	0.640	0.569	0.578	0.483	0.460
9	Aliphatic C-O (Cα.)	78.0-67.0	0.603	0.563	0.574	0.507	0.478
10	Aliphatic C-OR	67.0-61.0	0.178	0.150	0.171	0.136	0.129
11	Aliphatic C-O, Cγ	61.0-57.0	0.374	0.323	0.342	0.296	0.284
12	OCH_3	57.0-54.0	0.898	0.876	0.875	0.844	0.838
13	Cβ in ββ and Cβ in β5	54.0-52.0	0.130	0.136	0.127	0.120	0.114
14	OCH_3 in MAME Structure	52.0-49.0	0.099	0.097	0.105	0.100	0.101
15	CH_2 in Diaryl methane	29.5-27.0	0.116	0.131	0.111	0.159	0.111

Table A-4-25. ^{13}C NMR data for residual lignins isolated from the incremental cook series of pulps. Table A-4-2 summarizes the pulping conditions used to produce the pulps for the respective residual lignins.

Region	Functional group	Integral region/ppm	B-6 C/C_9	B-7 C/C_9	B-8 C/C_9	B-9 C/C_9	B-10 C/C_9
1	COOH	178-162.5	0.374	0.358	0.317	0.377	0.355
2	C3,C4 (-C-Ar-O)	154.0-140.0	1.924	2.084	1.962	2.102	1.842
3	C1, (-C-Ar-C)	140.0-127.0	1.550	1.436	1.522	1.440	1.619
4	C5, (-C-Ar-C)	127.0-123.0	0.478	0.493	0.487	0.504	0.490
5	C6, (-C-Ar-H)	123.0-117.0	0.773	0.788	0.778	0.778	0.766
6	C5, (-C-Ar-H)	117.0-114.0	0.476	0.471	0.453	0.454	0.464
7	C2, (-C-Ar-H)	114.0-106.0	0.800	0.728	0.799	0.722	0.819
2-4	Substituted aromatic C	154.0-123.0	3.952	4.013	3.971	4.046	3.951
5-7	Unsubstituted aromatic C	123.0-106.0	2.049	1.987	2.030	1.954	2.049
8	Aliphatic C-O (Cβ.)	90.0-78.0	0.471	0.480	0.423	0.431	0.403
9	Aliphatic C-O (Cα.)	78.0-67.0	0.568	0.513	0.500	0.490	0.527
10	Aliphatic C-OR	67.0-61.0	0.141	0.141	0.123	0.144	0.124
11	Aliphatic C-O, Cγ	61.0-57.0	0.274	0.287	0.288	0.285	0.253
12	OCH_3	57.0-54.0	0.794	0.843	0.826	0.830	0.760
13	Cβ in ββ and Cβ in β5	54.0-52.0	0.117	0.117	0.131	0.118	0.110
14	OCH_3 in MAME Structure	52.0-49.0	0.107	0.107	0.128	0.108	0.113
15	CH_2 in Diaryl methane	29.5-27.0	0.240	0.131	0.252	0.149	0.316

18.14 ^{31}P NMR for Quinones Spectra of Residual Lignins

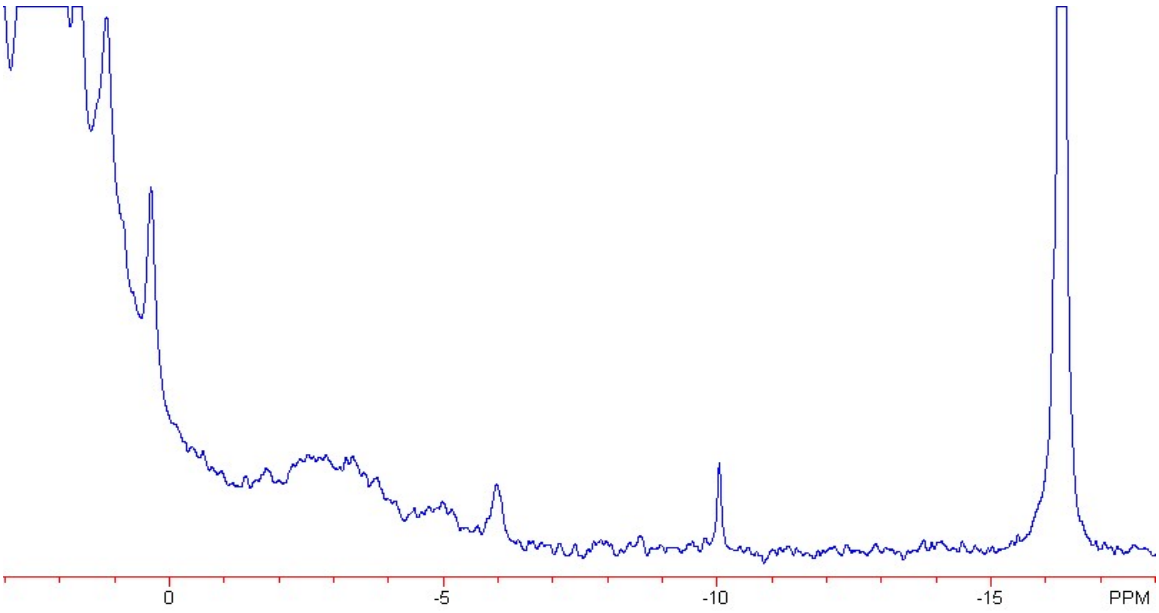

Figure A-4-130. ^{31}P NMR for quinones spectrum of residual lignin from Condition 1 of the constant kappa number (approximately 30) series of pulps. Table A-4-1 summarizes the pulping conditions used to produce the pulp for the respective residual lignin.

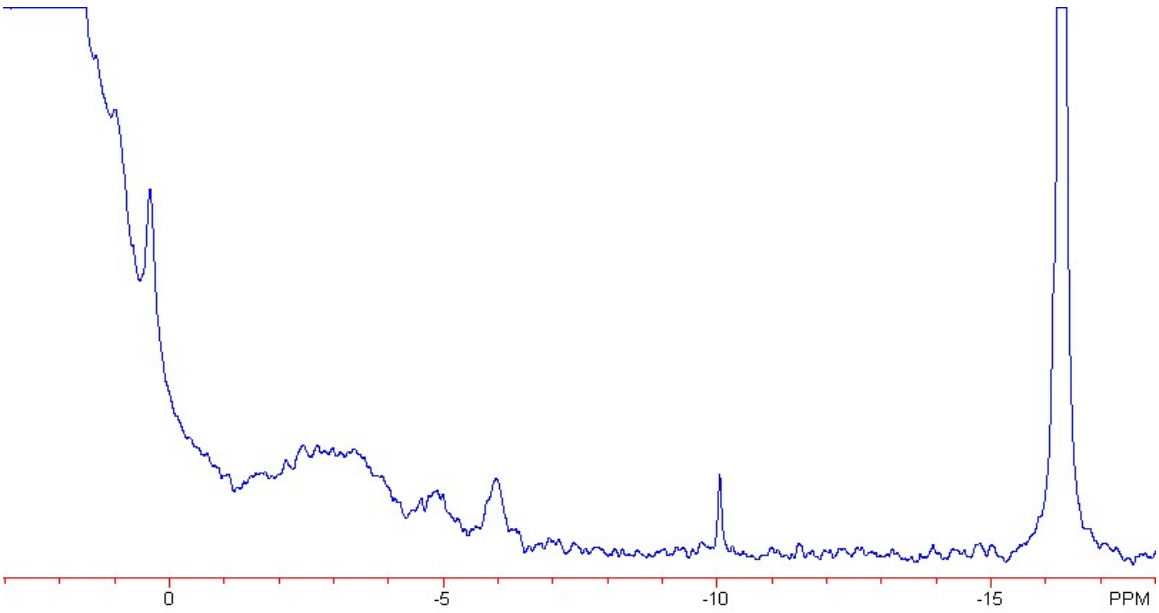

Figure A-4-131. ^{31}P NMR for quinones spectrum of residual lignin from Condition 2 of the constant kappa number (approximately 30) series of pulps. Table A-4-1 summarizes the pulping conditions used to produce the pulp for the respective residual lignin.

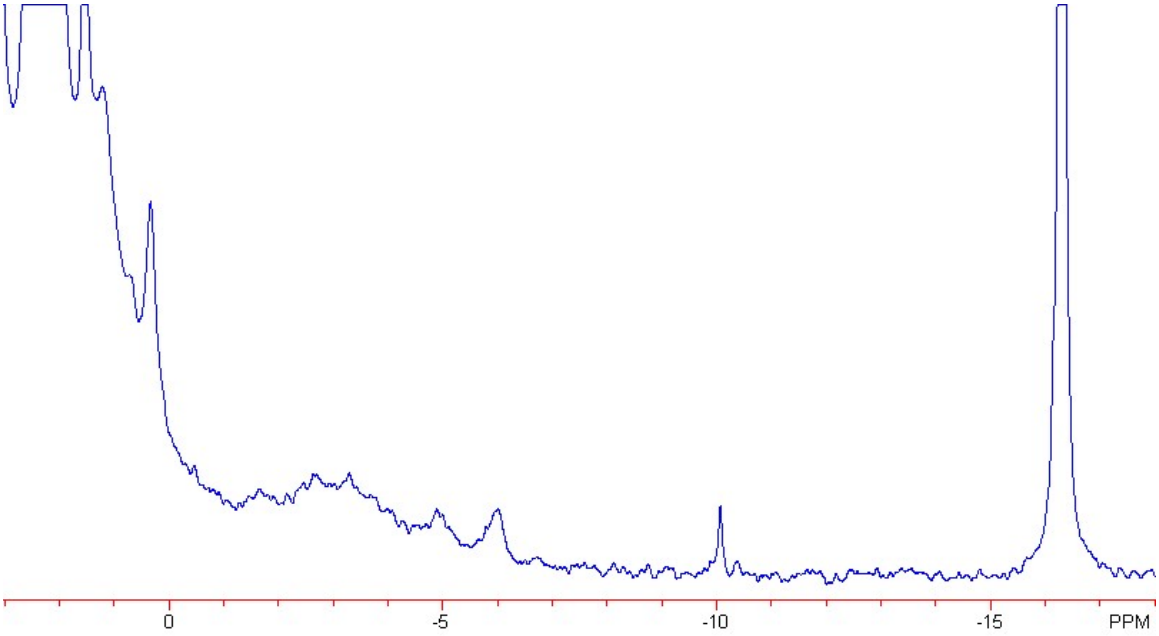

Figure A-4-132. ^{31}P NMR for quinones spectrum of residual lignin from Condition 3 of the constant kappa number (approximately 30) series of pulps. Table A-4-1 summarizes the pulping conditions used to produce the pulp for the respective residual lignin.

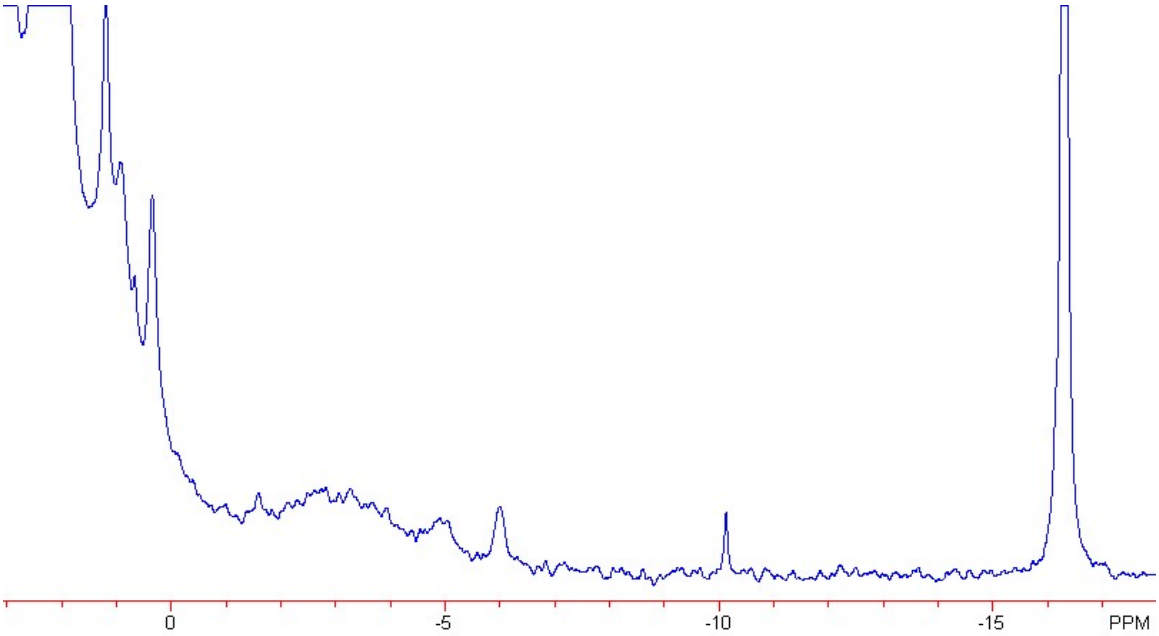

Figure A-4-133. ^{31}P NMR for quinones spectrum of residual lignin from Condition 4 of the constant kappa number (approximately 30) series of pulps. Table A-4-1 summarizes the pulping conditions used to produce the pulp for the respective residual lignin.

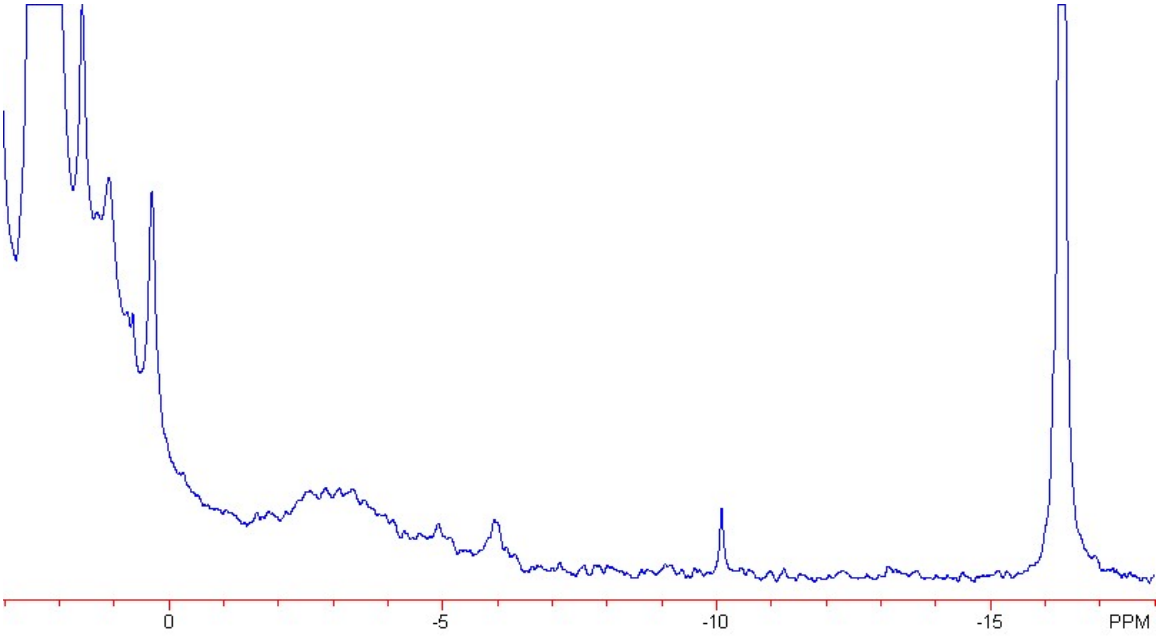

Figure A-4-134. ^{31}P NMR for quinones spectrum of residual lignin from Condition 5 of the constant kappa number (approximately 30) series of pulps. Table A-4-1 summarizes the pulping conditions used to produce the pulp for the respective residual lignin.

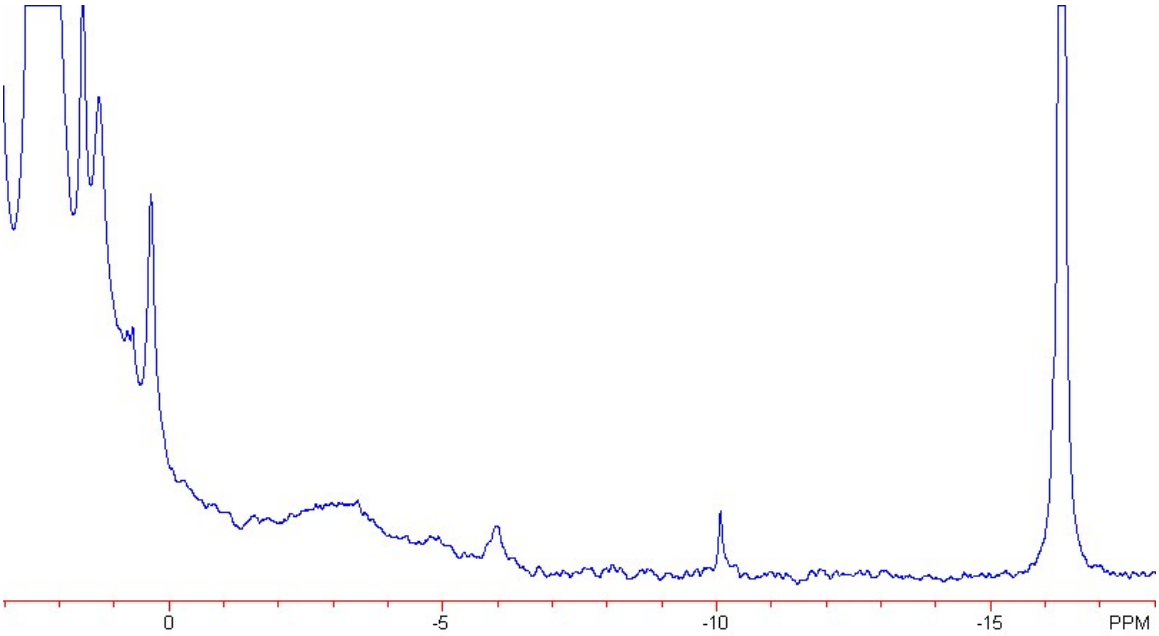

Figure A-4-135. ^{31}P NMR for quinones spectrum of residual lignin from Condition 6 of the constant kappa number (approximately 30) series of pulps. Table A-4-1 summarizes the pulping conditions used to produce the pulp for the respective residual lignin.

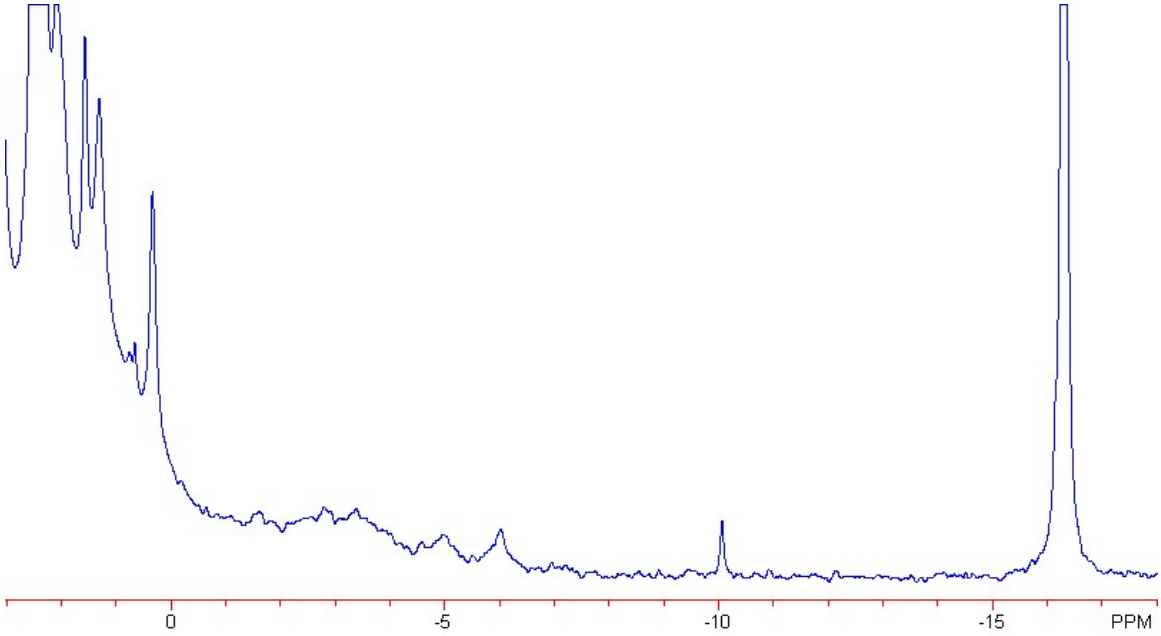

Figure A-4-136. ^{31}P NMR for quinones spectrum of residual lignin from Condition 7 of the constant kappa number (approximately 30) series of pulps. Table A-4-1 summarizes the pulping conditions used to produce the pulp for the respective residual lignin.

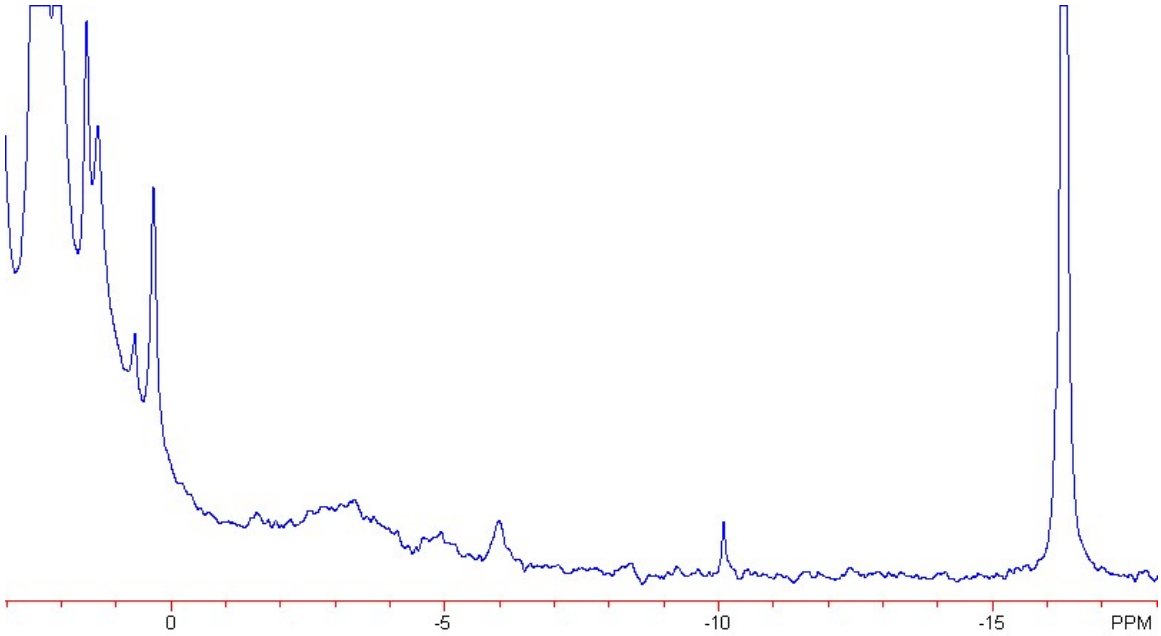

Figure A-4-137. ^{31}P NMR for quinones spectrum of residual lignin from Condition 8 of the constant kappa number (approximately 30) series of pulps. Table A-4-1 summarizes the pulping conditions used to produce the pulp for the respective residual lignin.

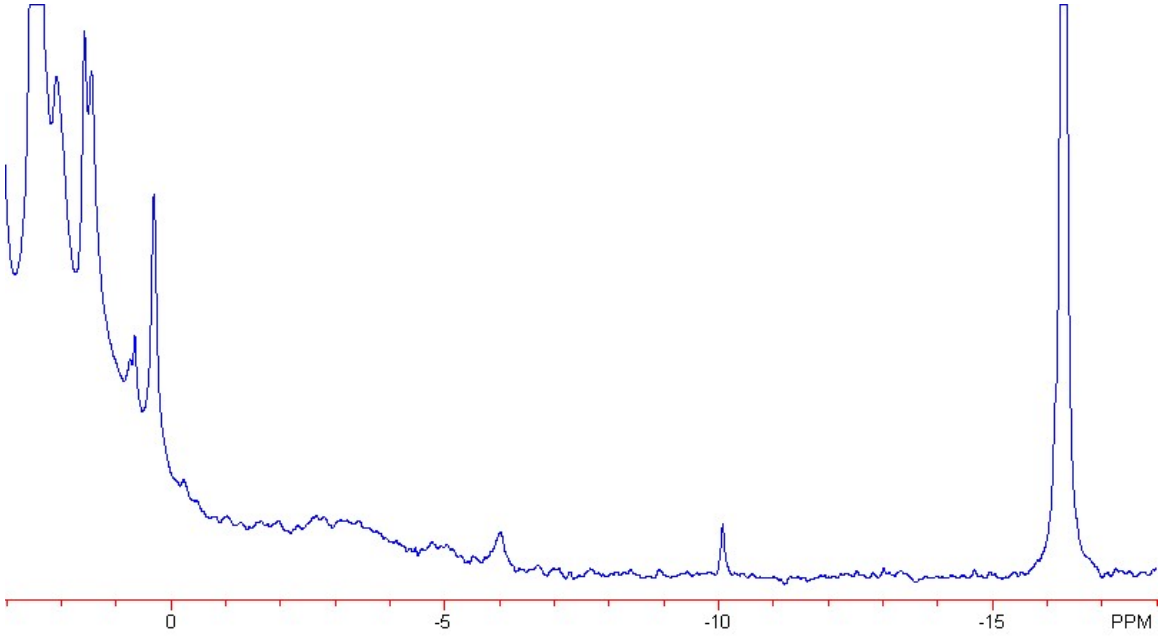

Figure A-4-138. ^{31}P NMR for quinones spectrum of residual lignin from Condition 9 of the constant kappa number (approximately 30) series of pulps. Table A-4-1 summarizes the pulping conditions used to produce the pulp for the respective residual lignin.

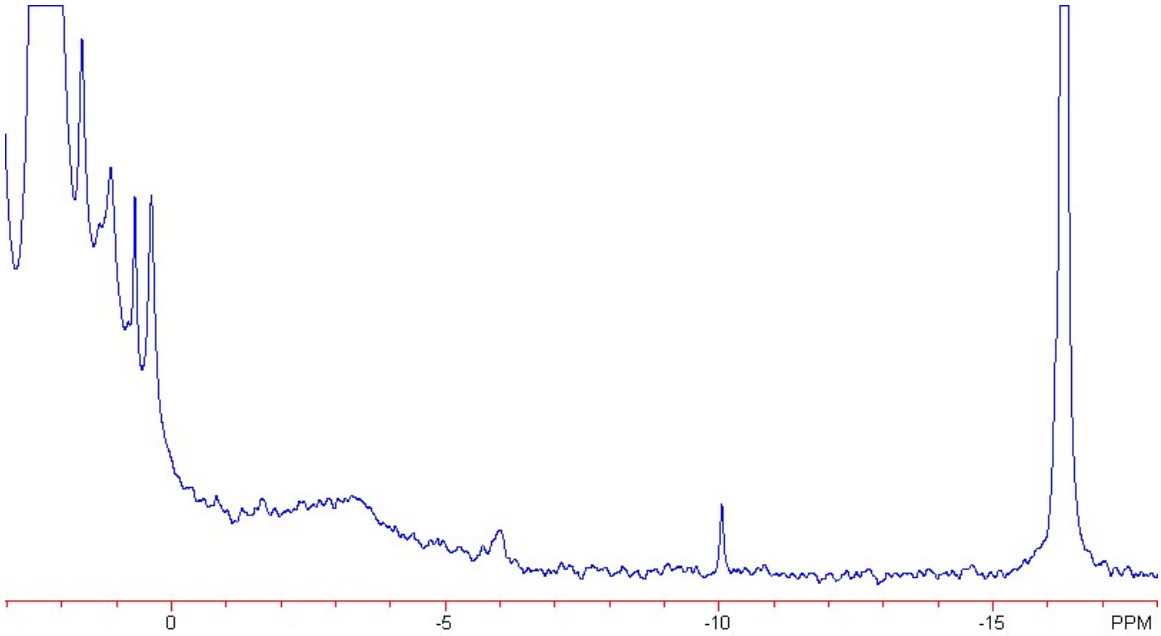

Figure A-4-139. ^{31}P NMR for quinones spectrum of residual lignin from Condition 10 of the constant kappa number (approximately 30) series of pulps. Table A-4-1 summarizes the pulping conditions used to produce the pulp for the respective residual lignin.

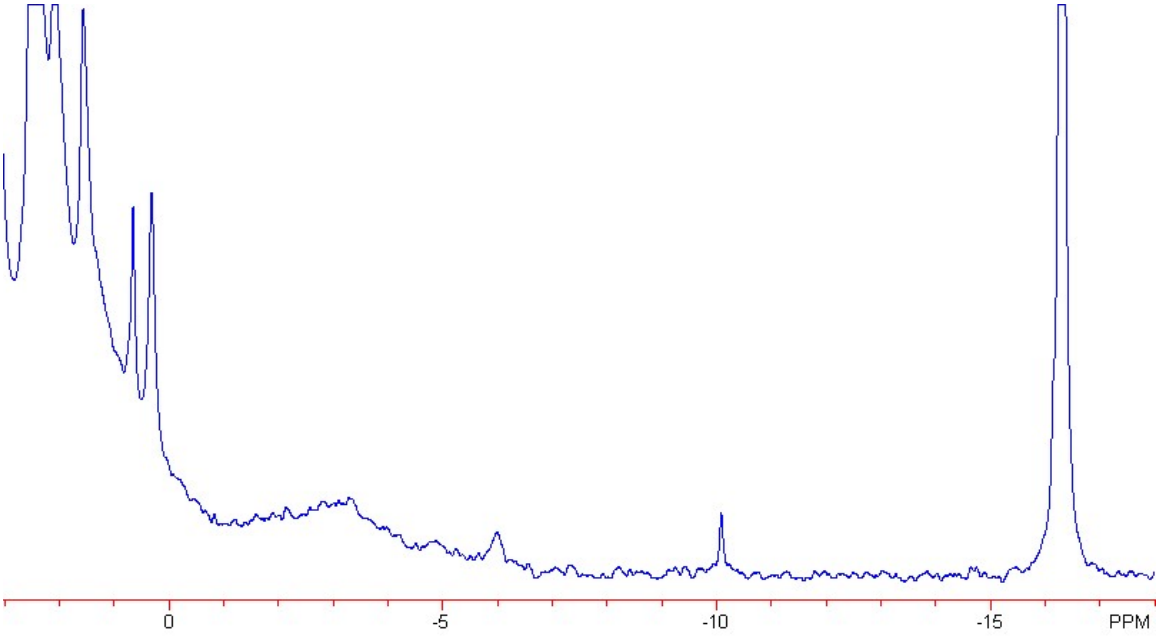

Figure A-4-140. ^{31}P NMR for quinones spectrum of residual lignin from Condition 11 of the constant kappa number (approximately 30) series of pulps. Table A-4-1 summarizes the pulping conditions used to produce the pulp for the respective residual lignin.

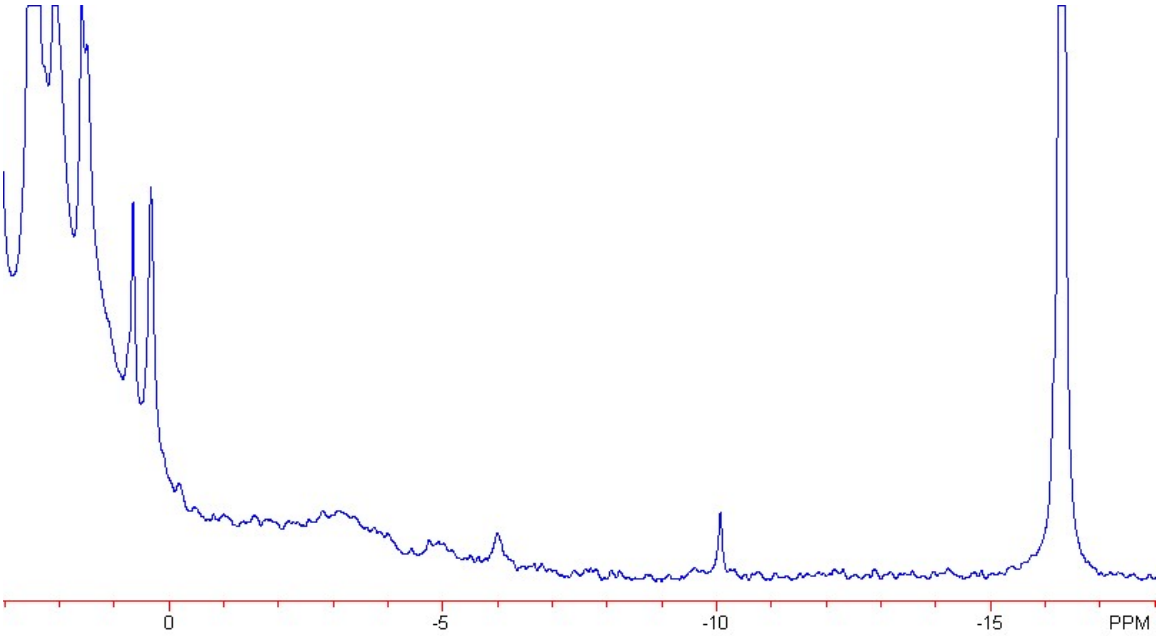

Figure A-4-141. ^{31}P NMR for quinones spectrum of residual lignin from Condition 12 of the constant kappa number (approximately 30) series of pulps. Table A-4-1 summarizes the pulping conditions used to produce the pulp for the respective residual lignin.

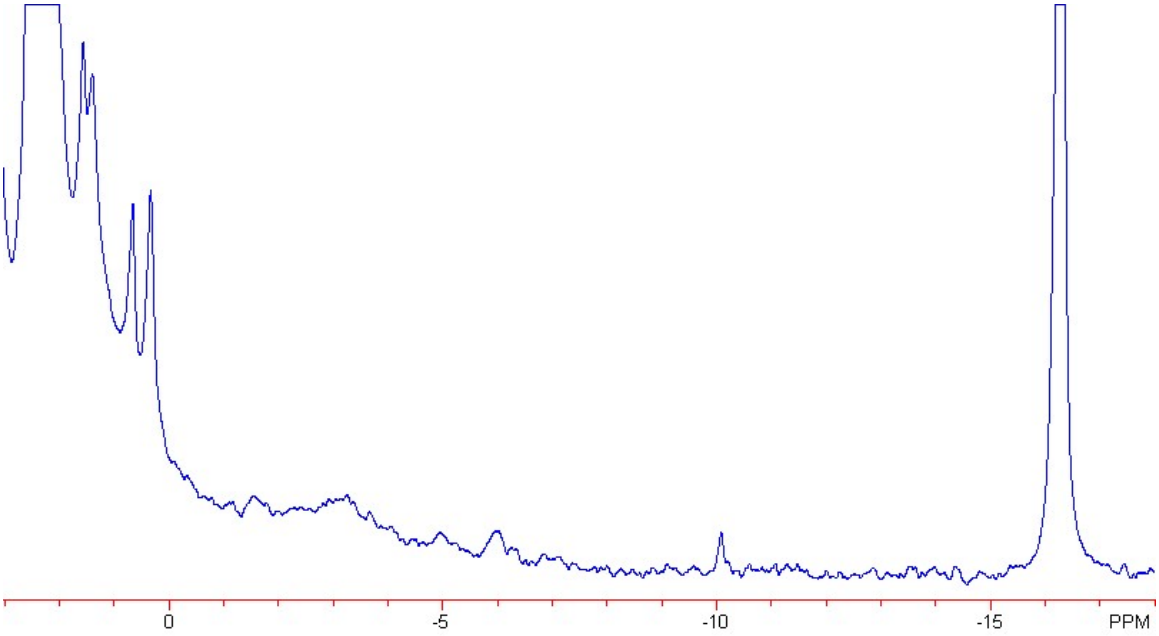

Figure A-4-142. ^{31}P NMR for quinones spectrum of residual lignin from Condition 13 of the constant kappa number (approximately 30) series of pulps. Table A-4-1 summarizes the pulping conditions used to produce the pulp for the respective residual lignin.

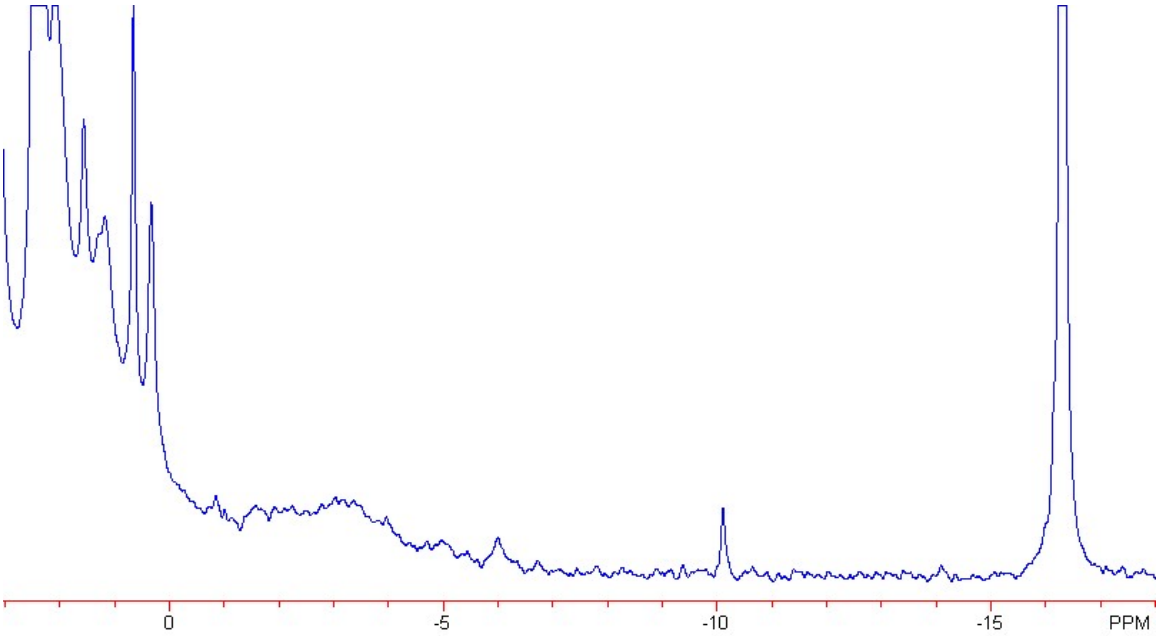

Figure A-4-143. ^{31}P NMR for quinones spectrum of residual lignin from Condition 14 of the constant kappa number (approximately 30) series of pulps. Table A-4-1 summarizes the pulping conditions used to produce the pulp for the respective residual lignin.

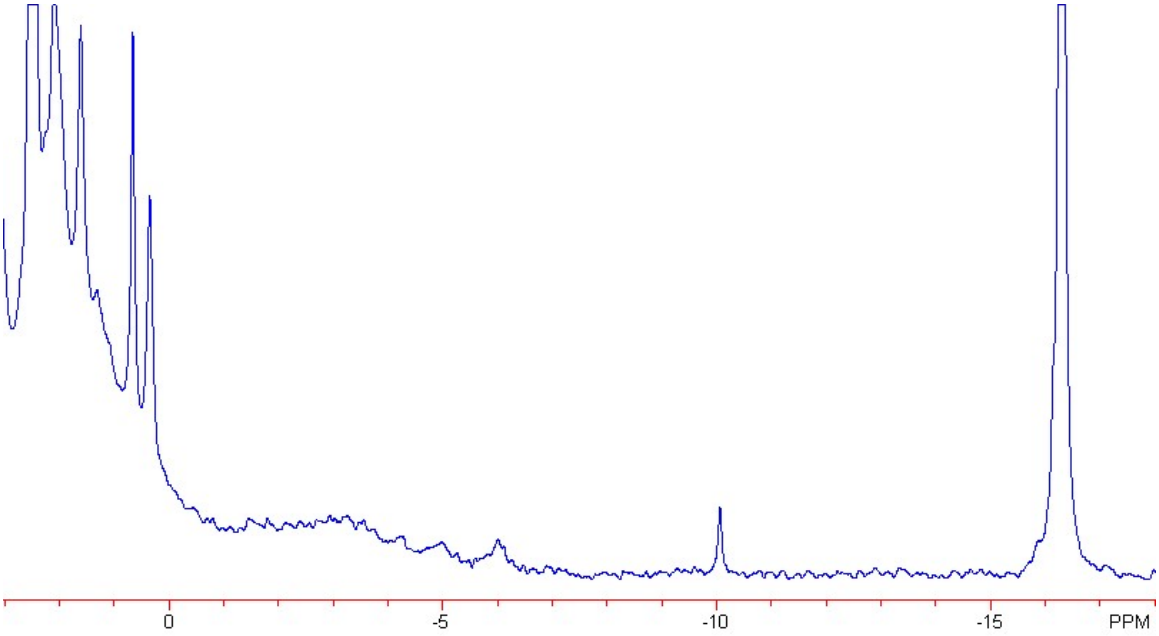

Figure A-4-144. ^{31}P NMR for quinones spectrum of residual lignin from Condition 15 of the constant kappa number (approximately 30) series of pulps. Table A-4-1 summarizes the pulping conditions used to produce the pulp for the respective residual lignin.

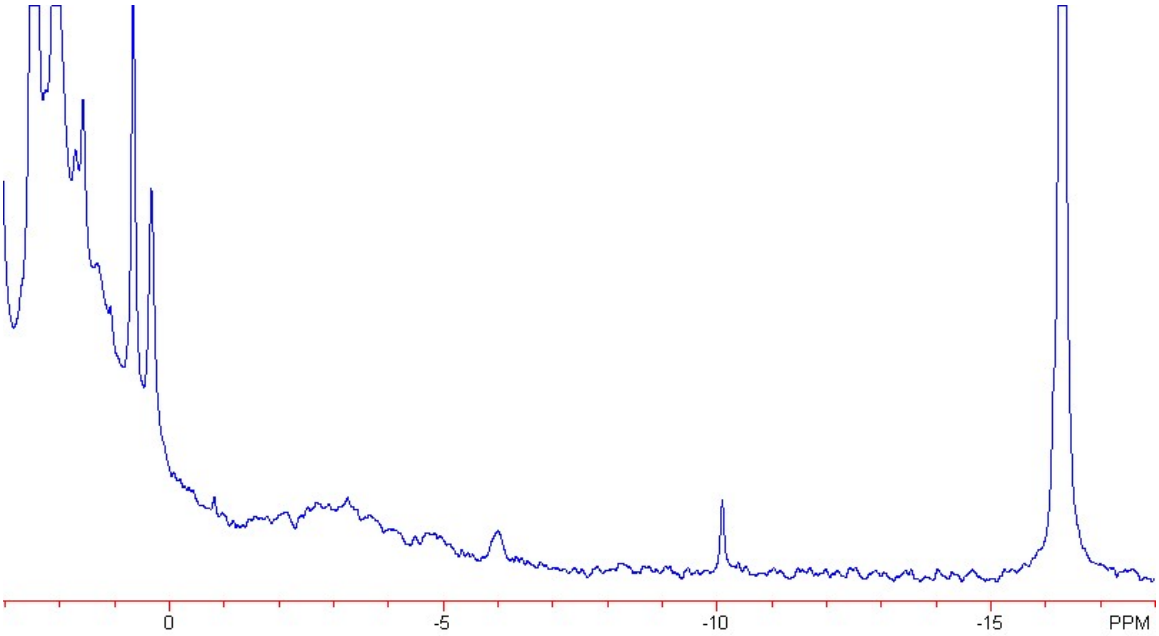

Figure A-4-145. ^{31}P NMR for quinones spectrum of residual lignin from Condition 16 of the constant kappa number (approximately 30) series of pulps. Table A-4-1 summarizes the pulping conditions used to produce the pulp for the respective residual lignin.

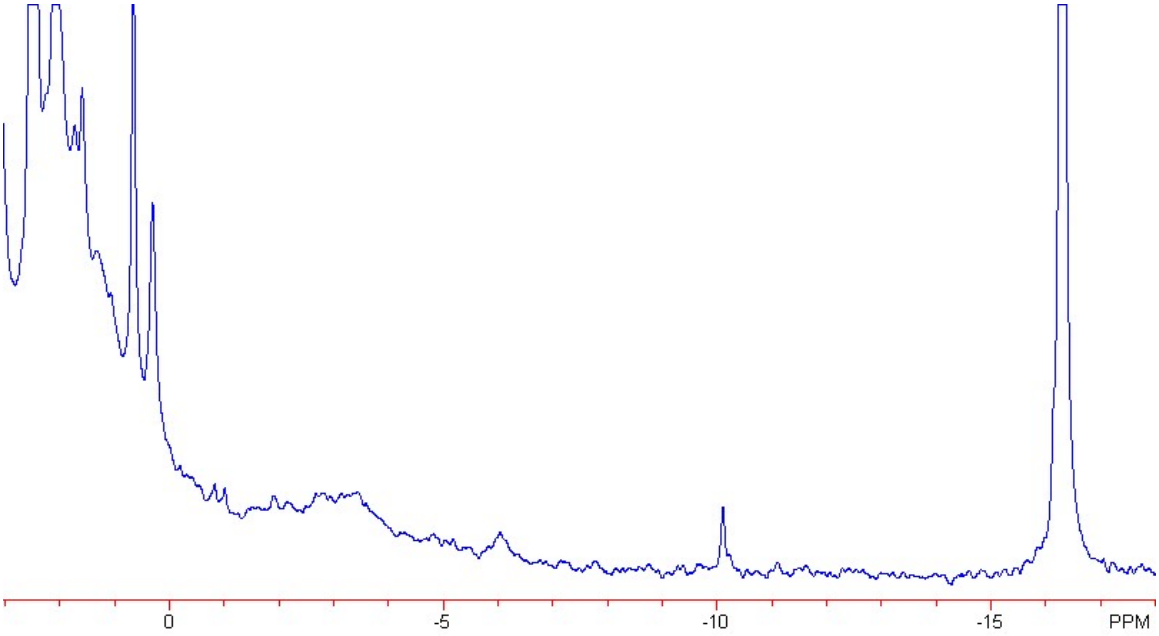

Figure A-4-146. ^{31}P NMR for quinones spectrum of residual lignin from Condition 17 of the constant kappa number (approximately 30) series of pulps. Table A-4-1 summarizes the pulping conditions used to produce the pulp for the respective residual lignin.

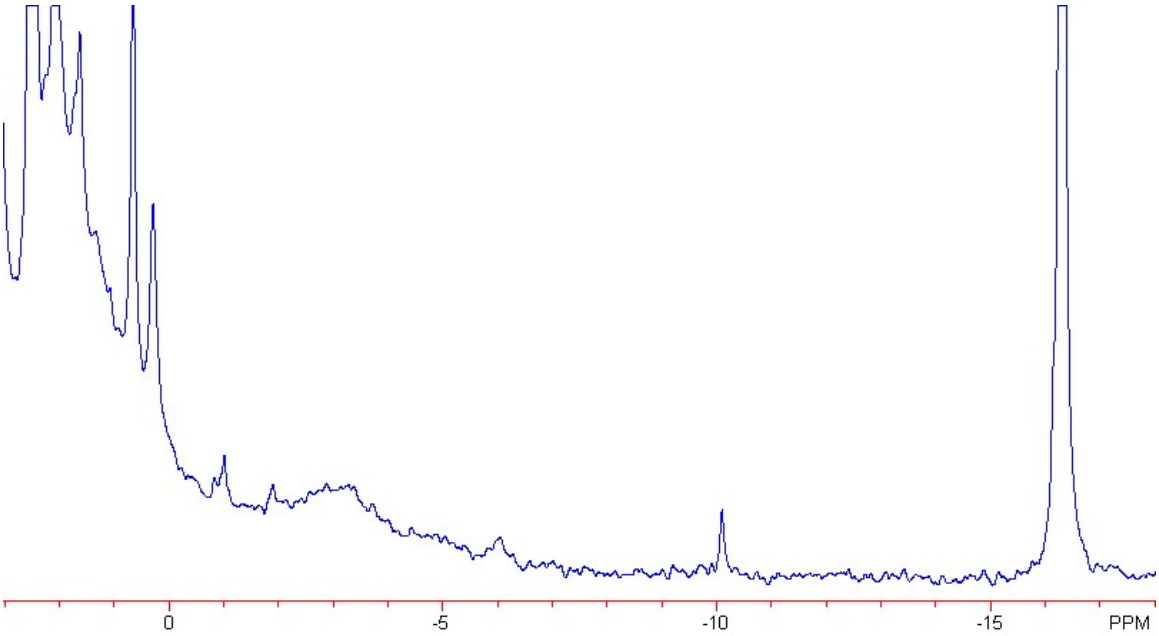

Figure A-4-147. ^{31}P NMR for quinones spectrum of residual lignin from Condition 18 of the constant kappa number (approximately 30) series of pulps. Table A-4-1 summarizes the pulping conditions used to produce the pulp for the respective residual lignin.

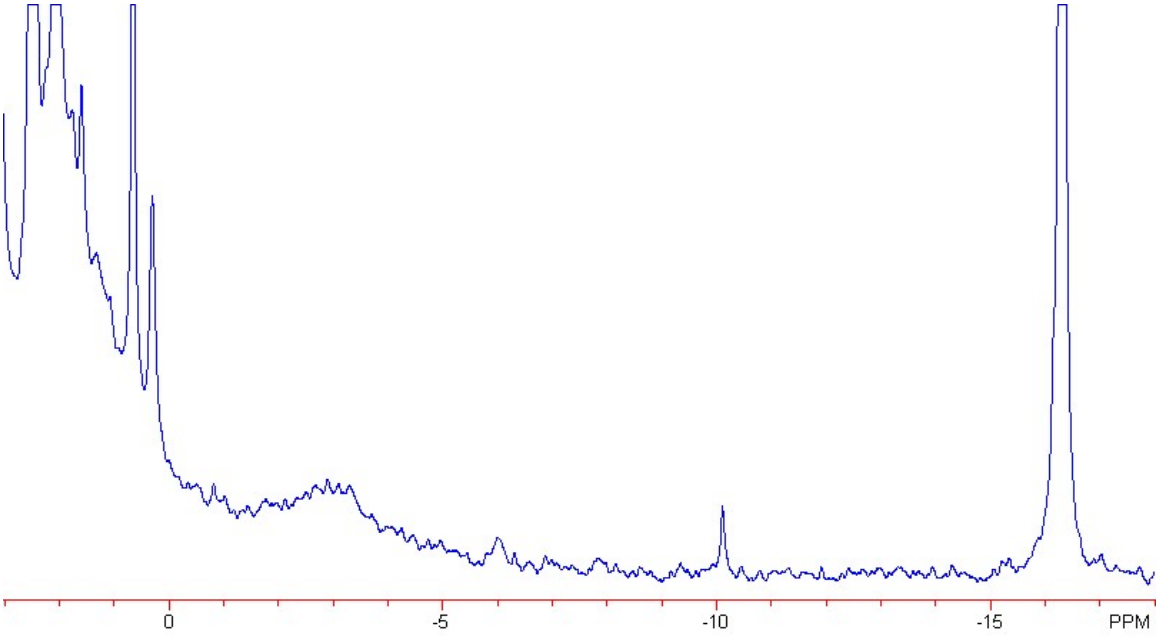

Figure A-4-148. ^{31}P NMR for quinones spectrum of residual lignin from Condition 19 of the constant kappa number (approximately 30) series of pulps. Table A-4-1 summarizes the pulping conditions used to produce the pulp for the respective residual lignin.

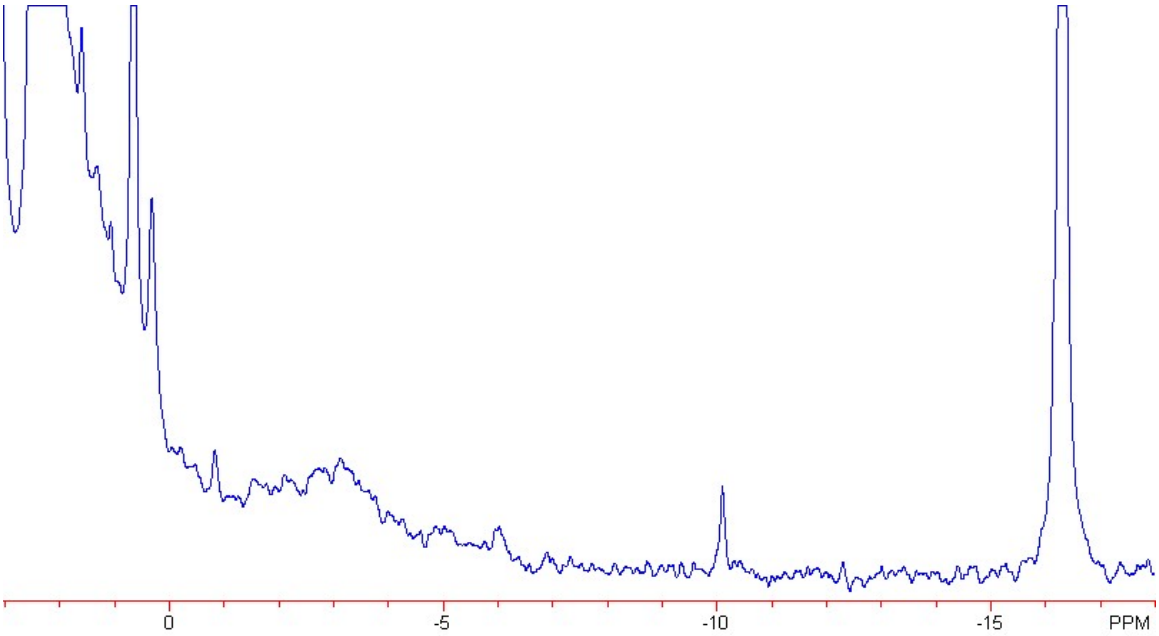

Figure A-4-149. ^{31}P NMR for quinones spectrum of residual lignin from Condition 20 of the constant kappa number (approximately 30) series of pulps. Table A-4-1 summarizes the pulping conditions used to produce the pulp for the respective residual lignin.

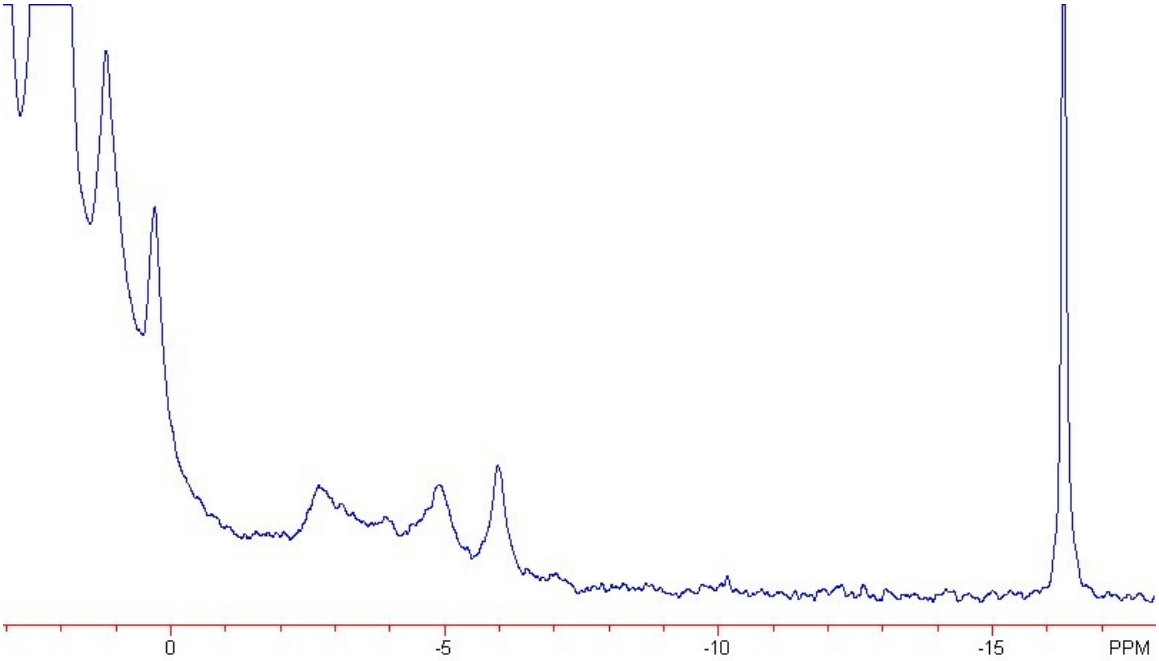

Figure A-4-150. ^{31}P NMR for quinones spectrum of residual lignin from Condition A-1 of the incremental cook series of pulps. Table A-4-2 summarizes the pulping conditions used to produce the pulp for the respective residual lignin.

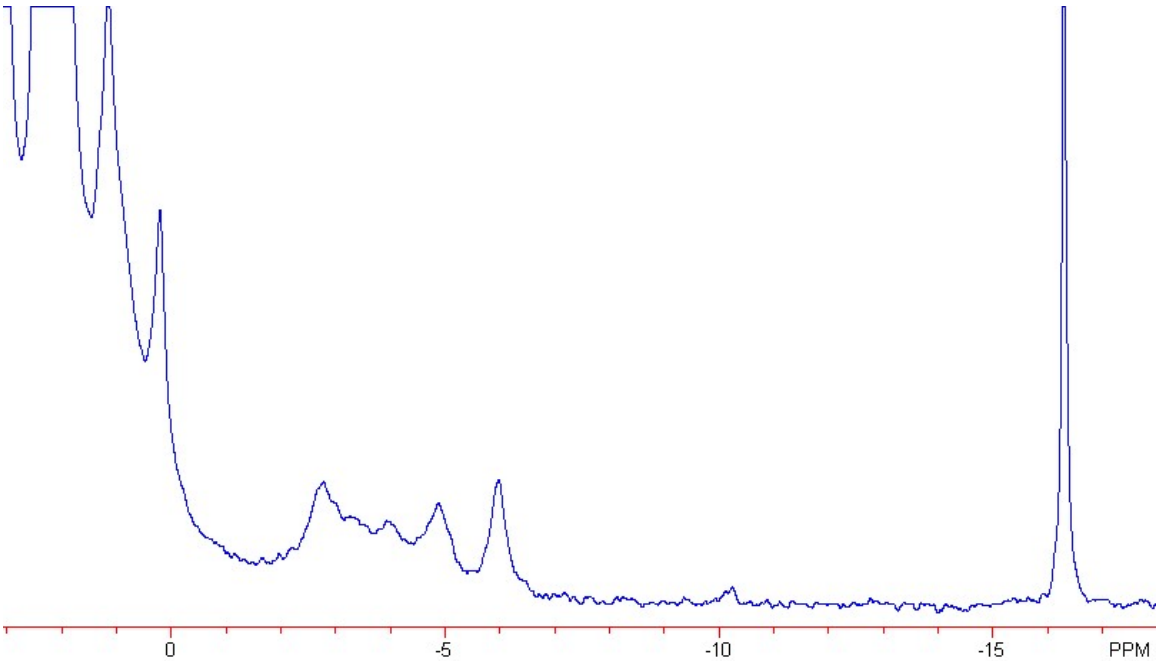

Figure A-4-151. ^{31}P NMR for quinones spectrum of residual lignin from Condition A-2 of the incremental cook series of pulps. Table A-4-2 summarizes the pulping conditions used to produce the pulp for the respective residual lignin.

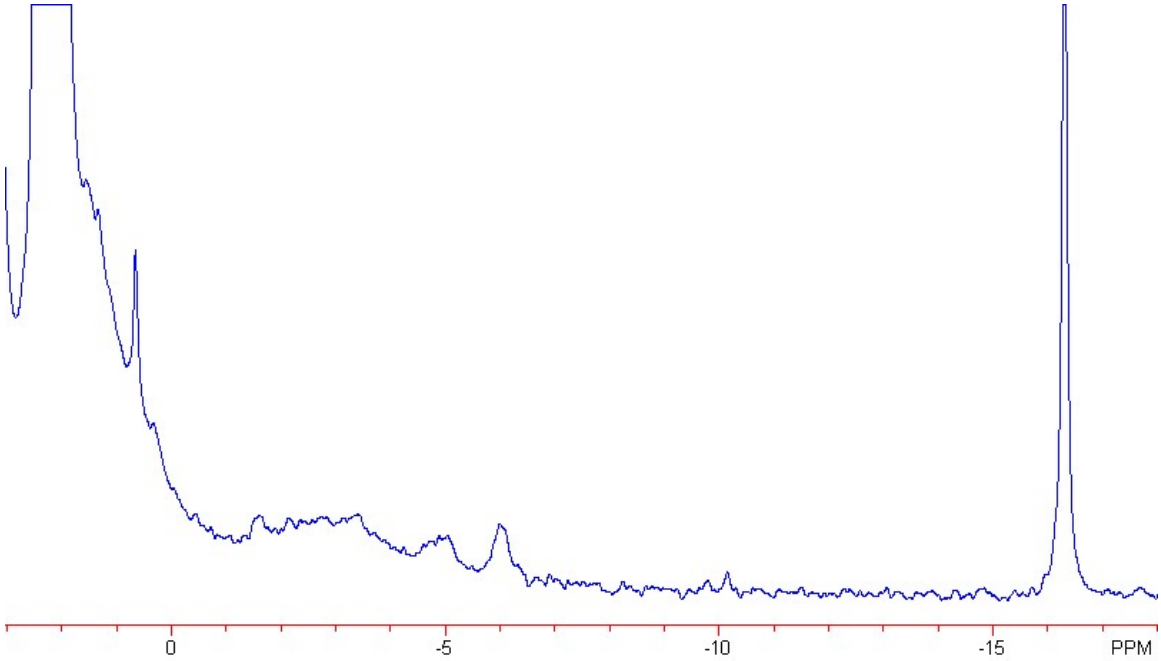

Figure A-4-152. ^{31}P NMR for quinones spectrum of residual lignin from Condition A-3 of the incremental cook series of pulps. Table A-4-2 summarizes the pulping conditions used to produce the pulp for the respective residual lignin.

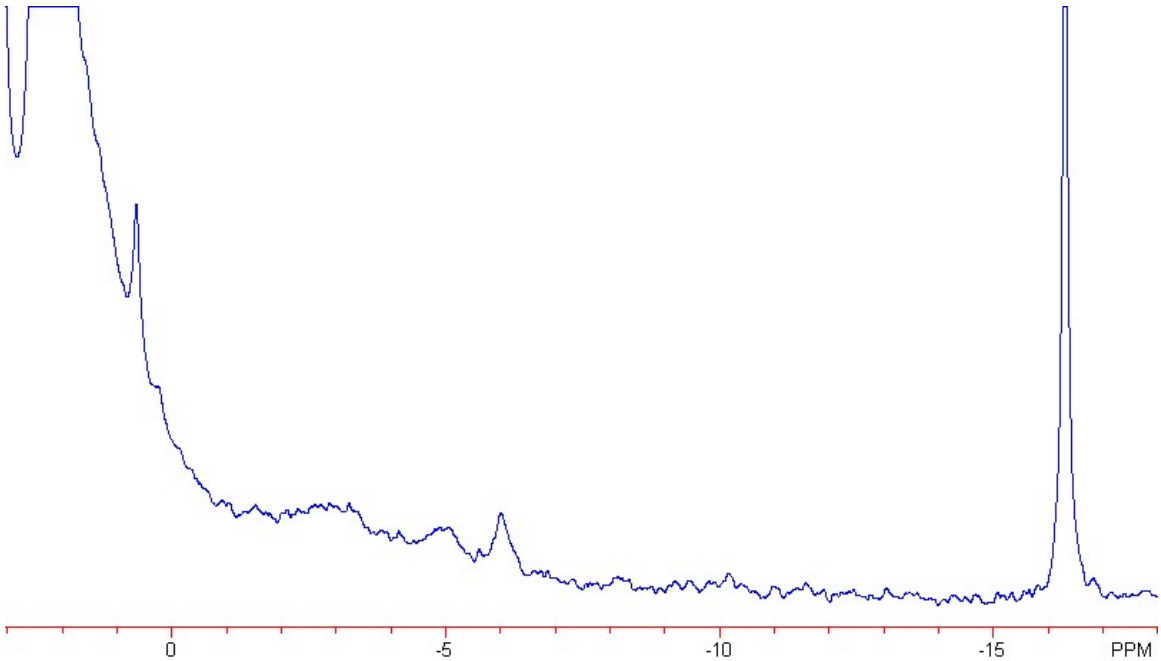

Figure A-4-153. ^{31}P NMR for quinones spectrum of residual lignin from Condition A-4 of the incremental cook series of pulps. Table A-4-2 summarizes the pulping conditions used to produce the pulp for the respective residual lignin.

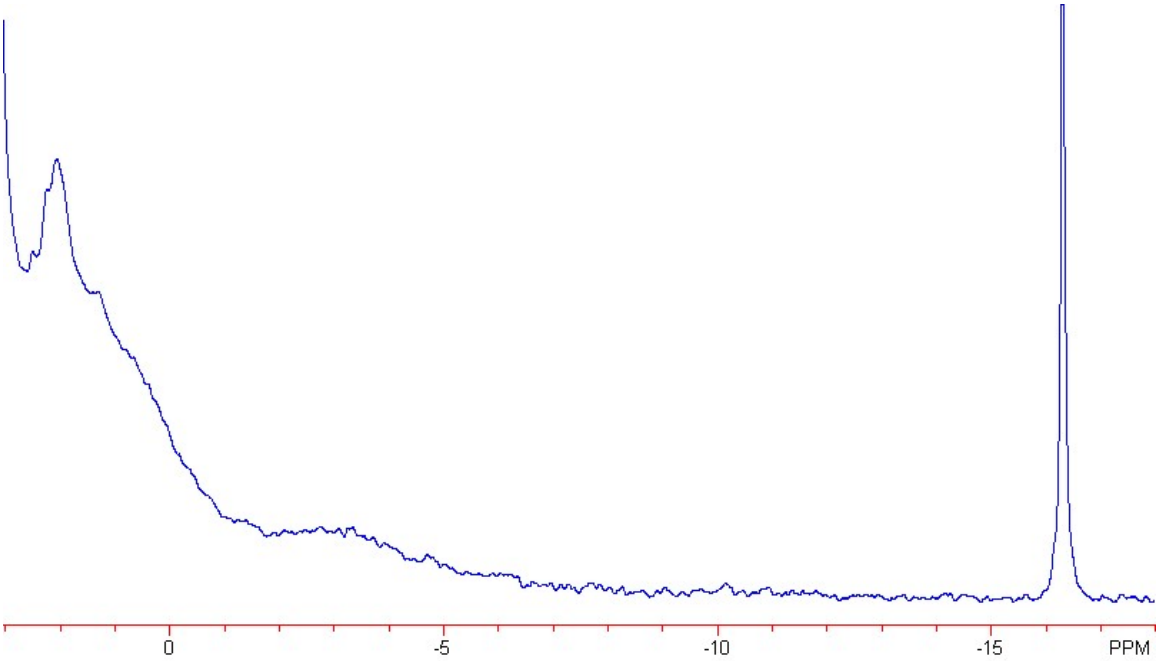

Figure A-4-154. ^{31}P NMR for quinones spectrum of residual lignin from Condition A-5 of the incremental cook series of pulps. Table A-4-2 summarizes the pulping conditions used to produce the pulp for the respective residual lignin.

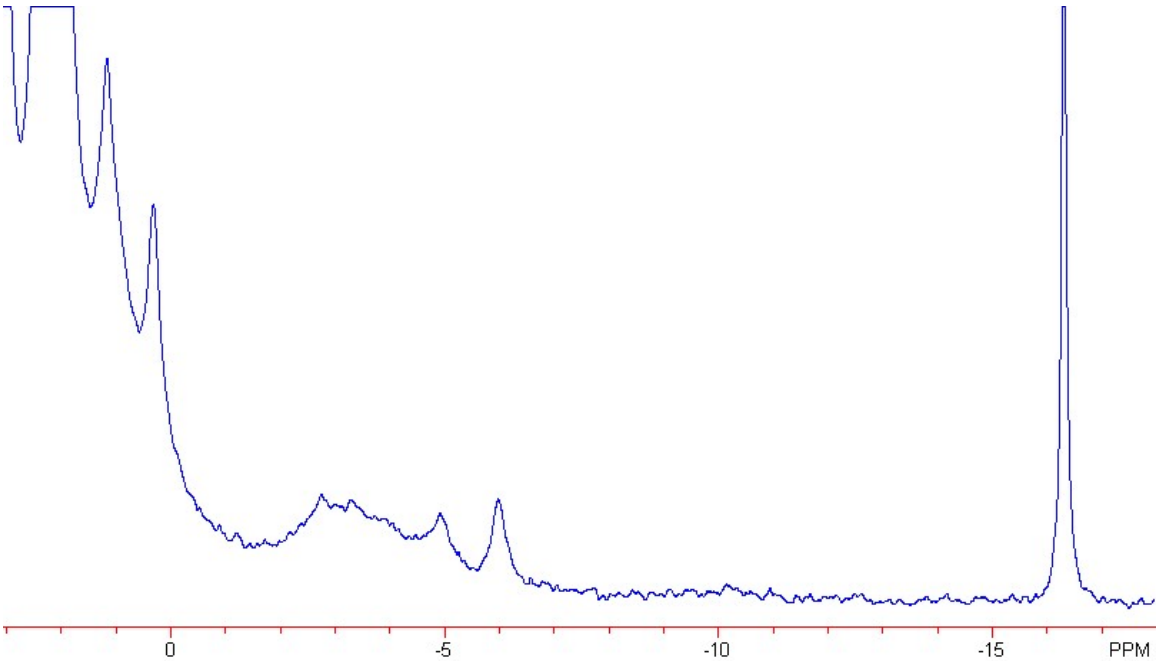

Figure A-4-155. ^{31}P NMR for quinones spectrum of residual lignin from Condition A-6 of the incremental cook series of pulps. Table A-4-2 summarizes the pulping conditions used to produce the pulp for the respective residual lignin.

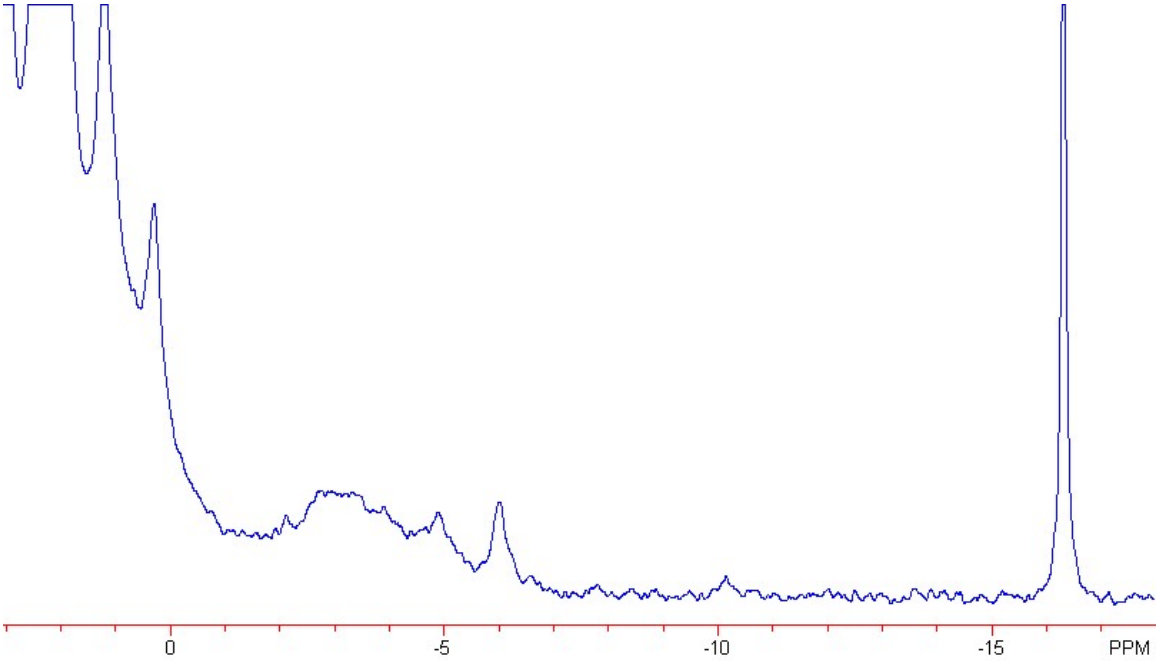

Figure A-4-156. ^{31}P NMR for quinones spectrum of residual lignin from Condition A-7 of the incremental cook series of pulps. Table A-4-2 summarizes the pulping conditions used to produce the pulp for the respective residual lignin.

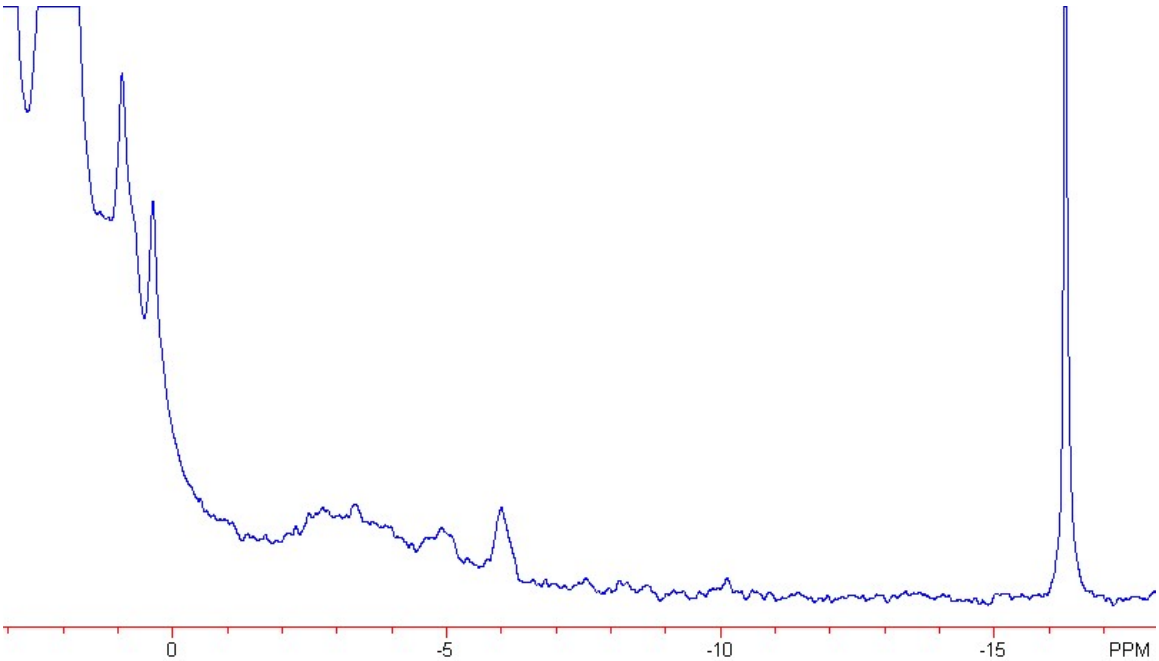

Figure A-4-157. ^{31}P NMR for quinones spectrum of residual lignin from Condition A-8 of the incremental cook series of pulps. Table A-4-2 summarizes the pulping conditions used to produce the pulp for the respective residual lignin.

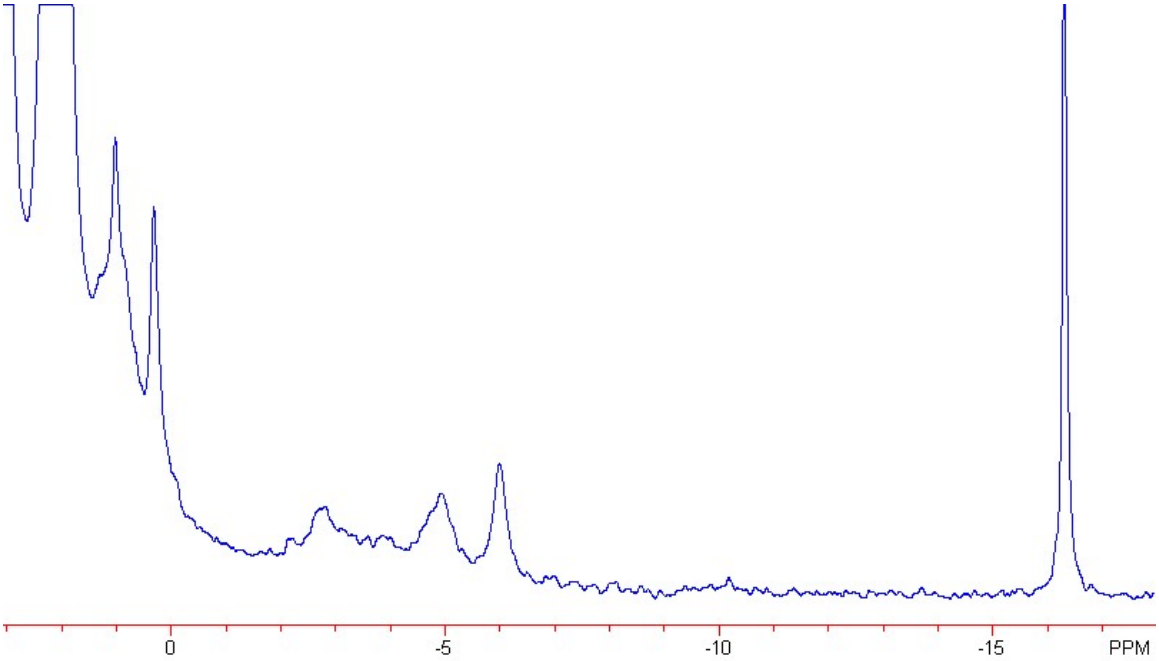

Figure A-4-158. ^{31}P NMR for quinones spectrum of residual lignin from Condition B-1 of the incremental cook series of pulps. Table A-4-2 summarizes the pulping conditions used to produce the pulp for the respective residual lignin.

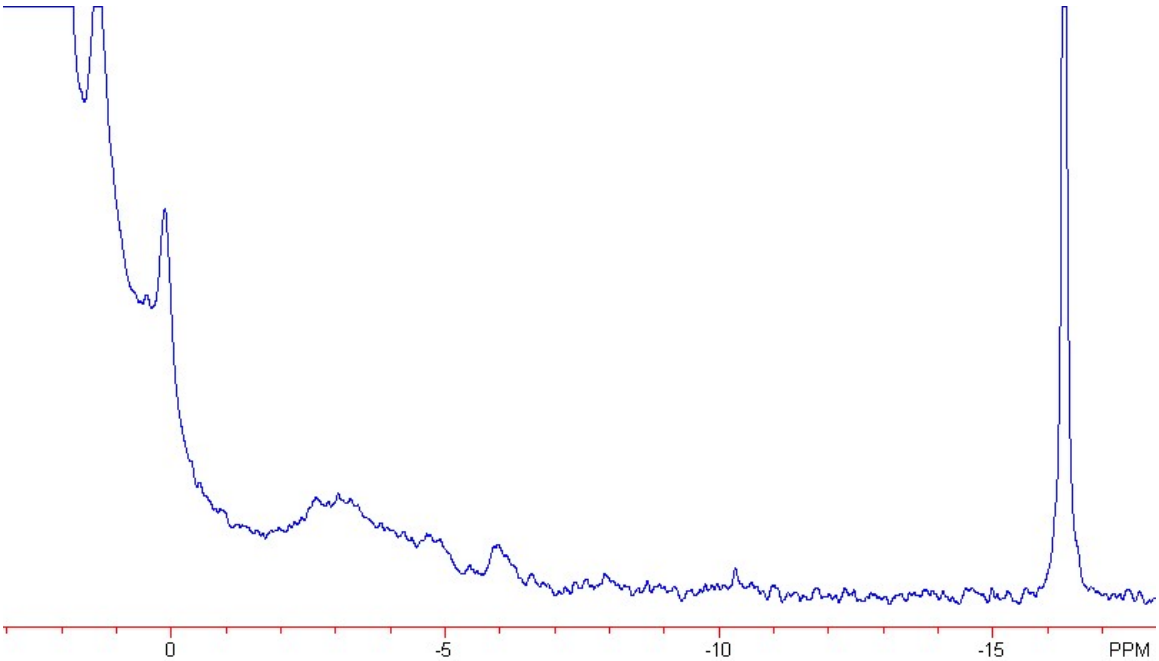

Figure A-4-159. ^{31}P NMR for quinones spectrum of residual lignin from Condition B-2 of the incremental cook series of pulps. Table A-4-2 summarizes the pulping conditions used to produce the pulp for the respective residual lignin.

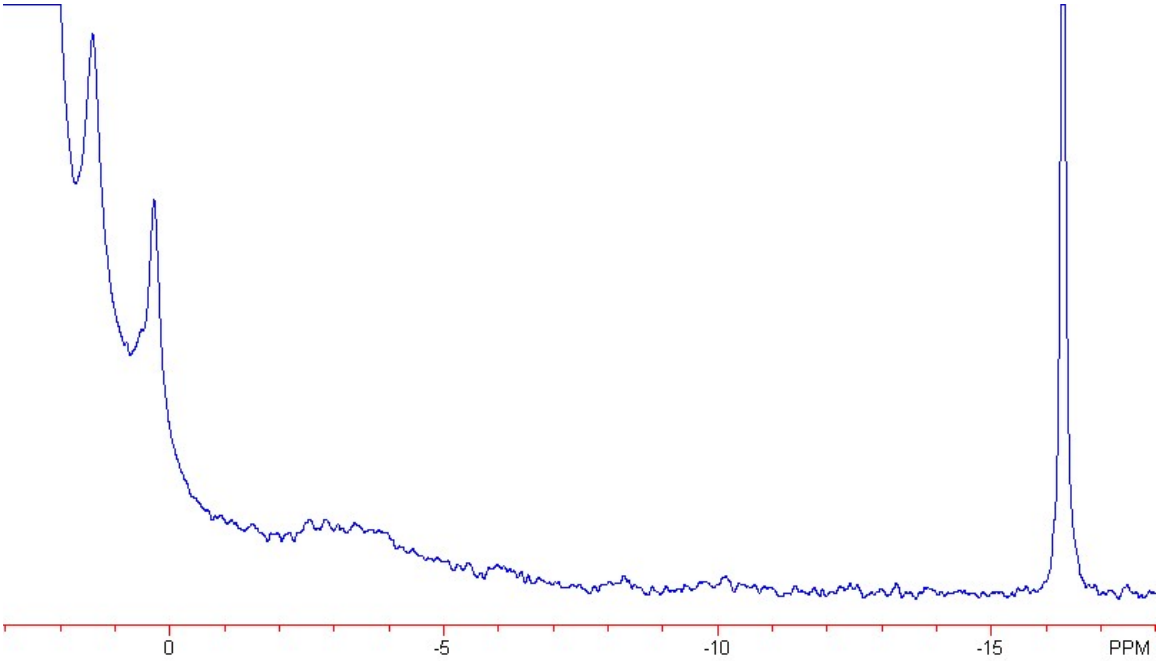

Figure A-4-160. ^{31}P NMR for quinones spectrum of residual lignin from Condition B-3 of the incremental cook series of pulps. Table A-4-2 summarizes the pulping conditions used to produce the pulp for the respective residual lignin.

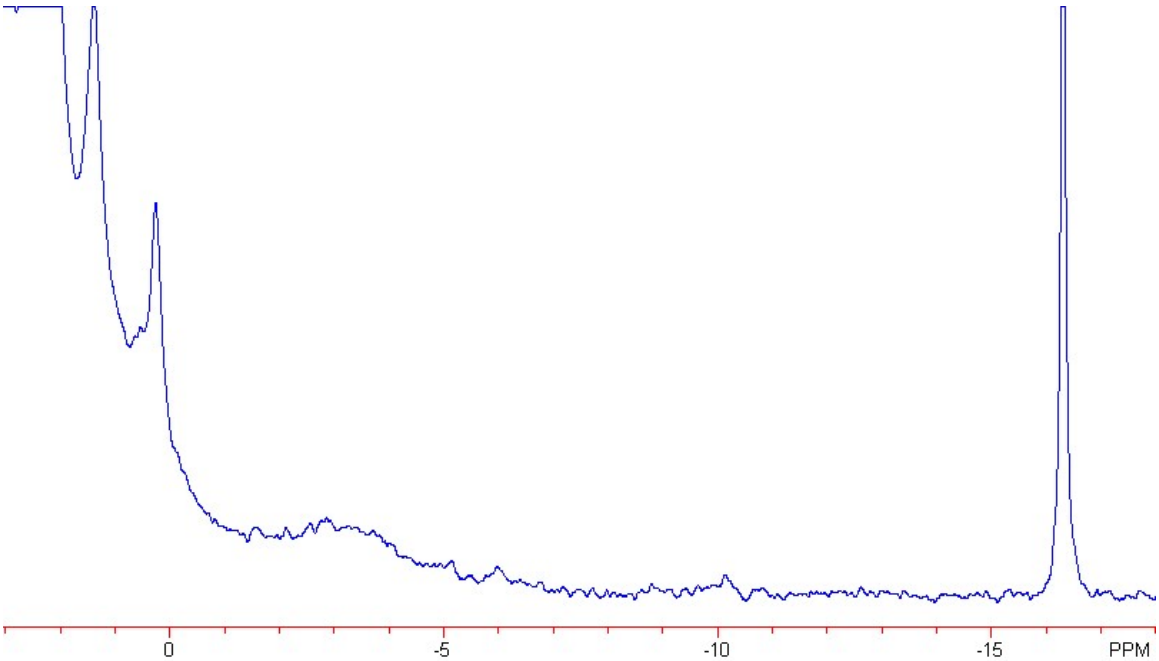

Figure A-4-161. ^{31}P NMR for quinones spectrum of residual lignin from Condition B-4 of the incremental cook series of pulps. Table A-4-2 summarizes the pulping conditions used to produce the pulp for the respective residual lignin.

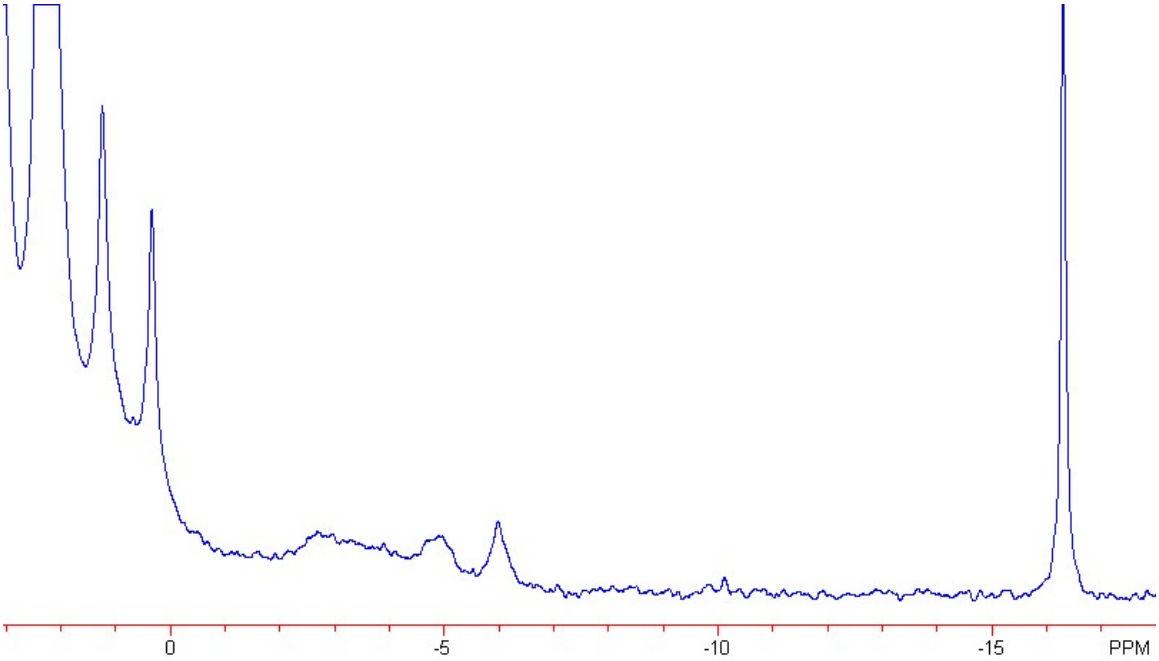

Figure A-4-162. ^{31}P NMR for quinones spectrum of residual lignin from Condition B-5 of the incremental cook series of pulps. Table A-4-2 summarizes the pulping conditions used to produce the pulp for the respective residual lignin.

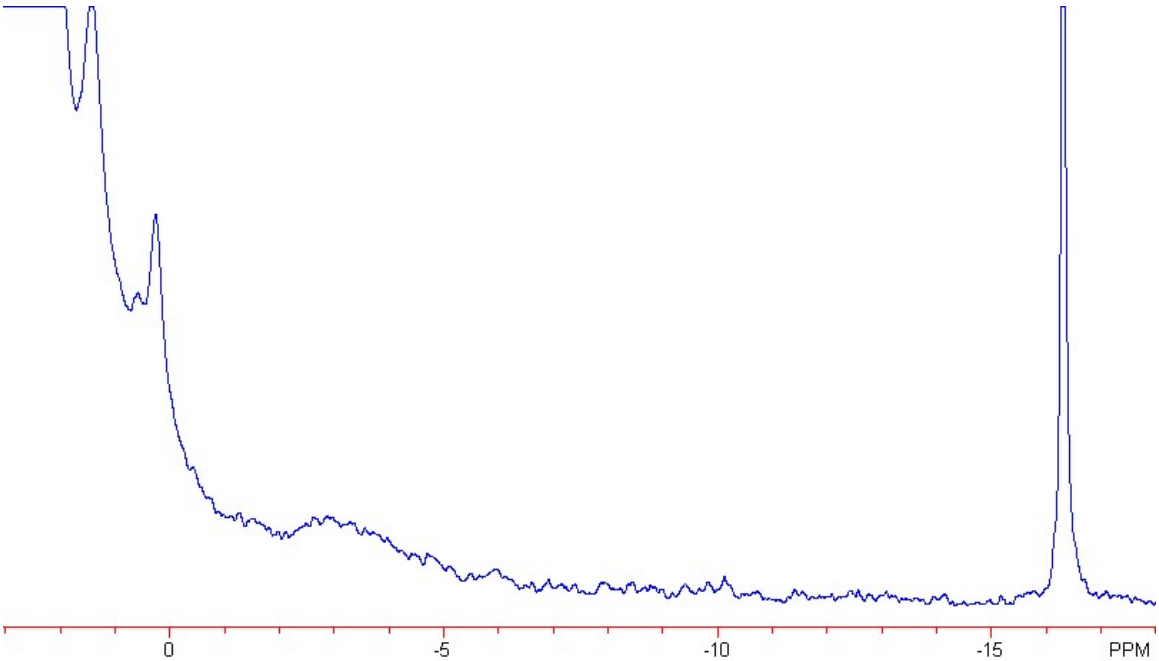

Figure A-4-163. ^{31}P NMR for quinones spectrum of residual lignin from Condition B-6 of the incremental cook series of pulps. Table A-4-2 summarizes the pulping conditions used to produce the pulp for the respective residual lignin.

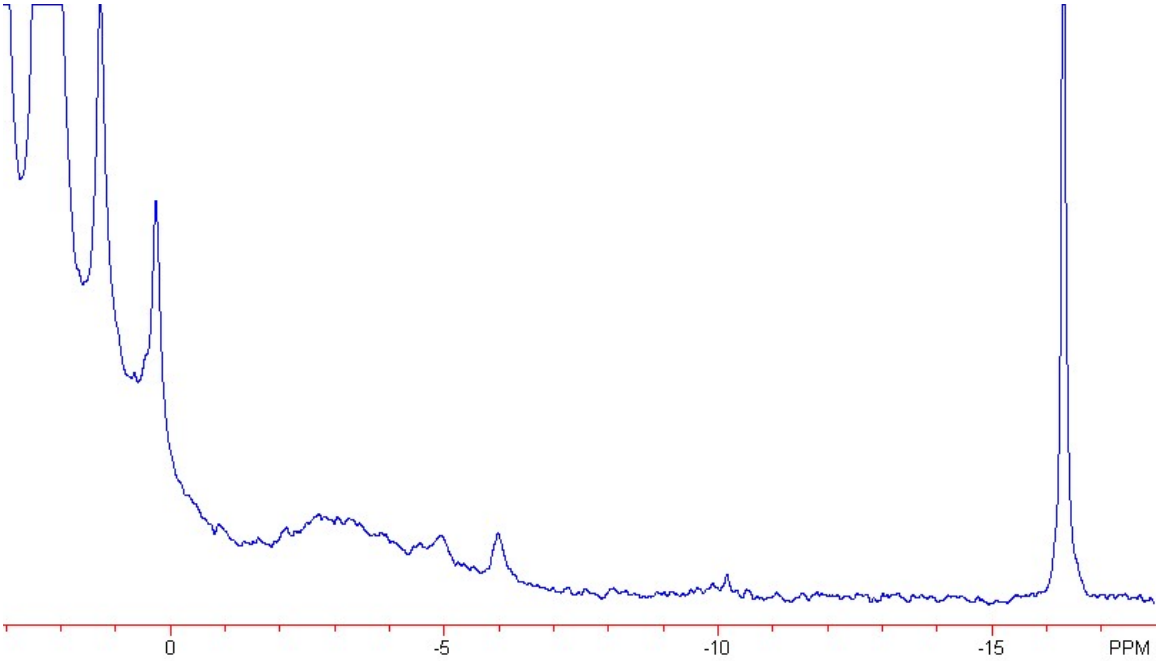

Figure A-4-164. ^{31}P NMR for quinones spectrum of residual lignin from Condition B-7 of the incremental cook series of pulps. Table A-4-2 summarizes the pulping conditions used to produce the pulp for the respective residual lignin.

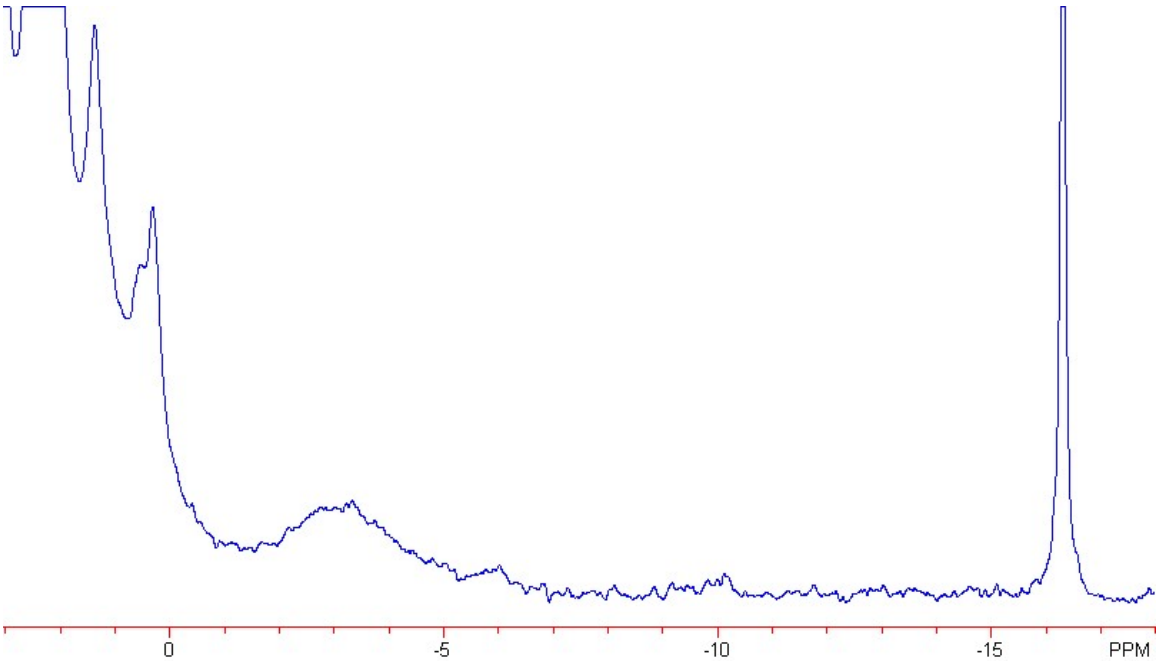

Figure A-4-165. ^{31}P NMR for quinones spectrum of residual lignin from Condition B-8 of the incremental cook series of pulps. Table A-4-2 summarizes the pulping conditions used to produce the pulp for the respective residual lignin.

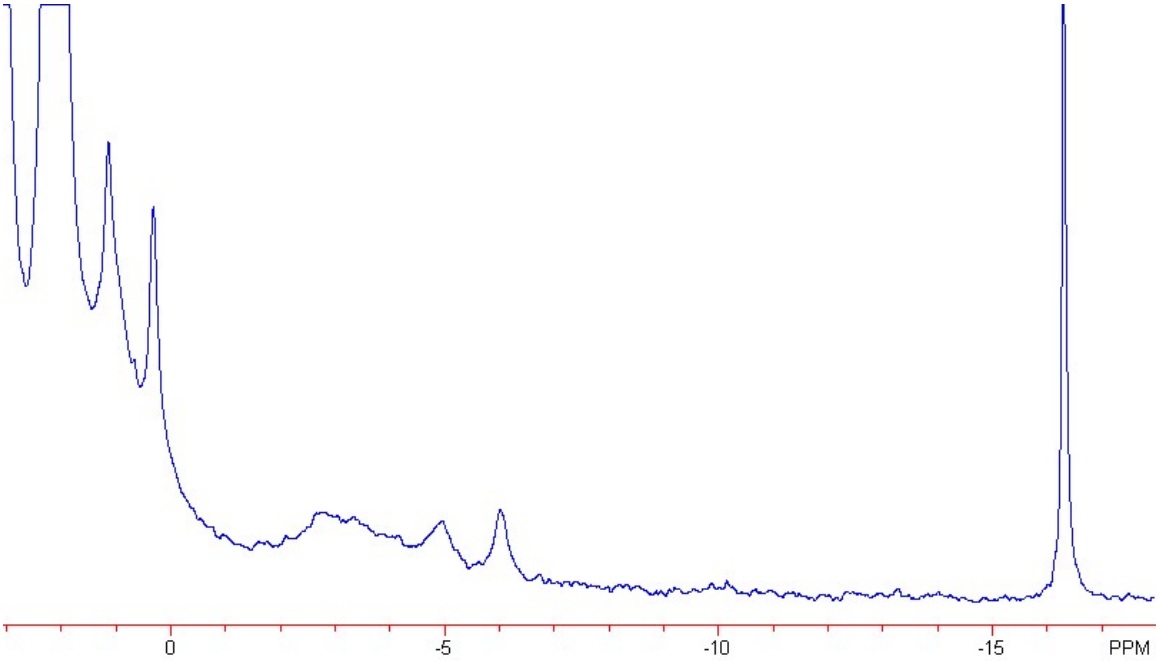

Figure A-4-166. ^{31}P NMR for quinones spectrum of residual lignin from Condition B-9 of the incremental cook series of pulps. Table A-4-2 summarizes the pulping conditions used to produce the pulp for the respective residual lignin.

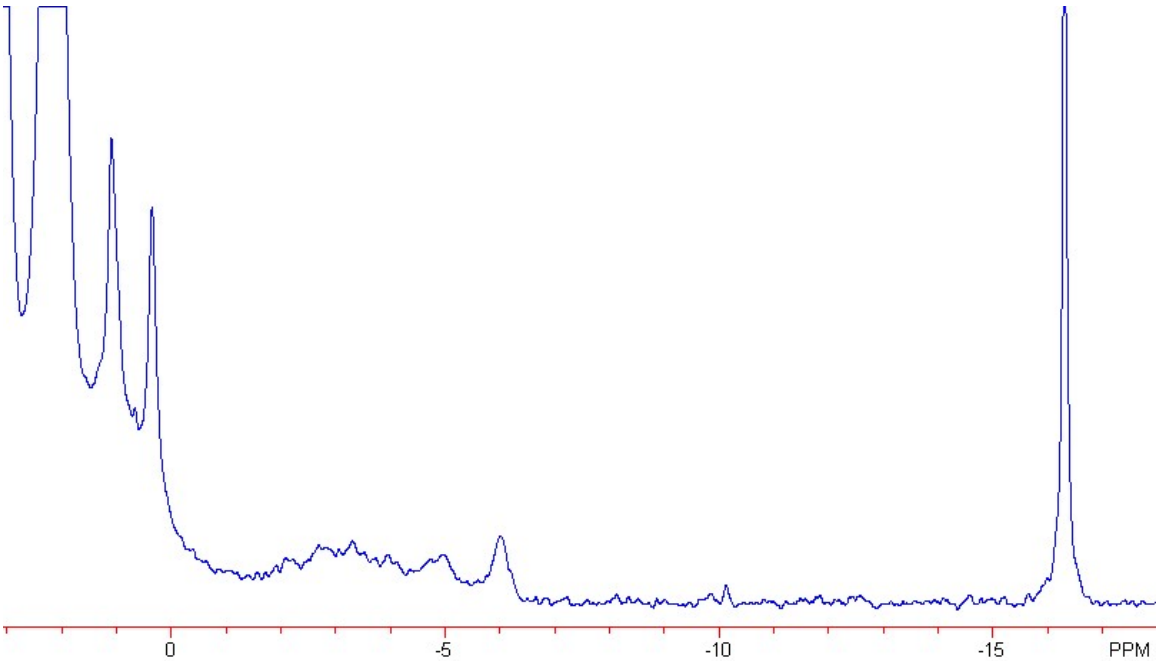

Figure A-4-167. ^{31}P NMR for quinones spectrum of residual lignin from Condition B-10 of the incremental cook series of pulps. Table A-4-2 summarizes the pulping conditions used to produce the pulp for the respective residual lignin.

18.15 Summary of ^{31}P NMR for Quinones Data for Residual Lignins

Table A-4-26. ^{31}P NMR quinone data for residual lignins from the constant kappa number (approximately 30) series of pulps. Table A-4-1 summarizes the pulping conditions used to produce the pulps for the respective residual lignins.

Sample	Combined *o*- and *p*-quinones δ -0.3 - -7.0 ppm (mmol/g)
1	0.085
2	0.095
3	0.094
4	0.101
5	0.106
6	0.102
7	0.094
8	0.095
9	0.088
10	0.089
11	0.085
12	0.090
13	0.087
14	0.082
15	0.097
16	0.094
17	0.091
18	0.081
19	0.096
20	0.092

Table A-4-27. ^{31}P NMR quinone data for residual lignins from the incremental cook series of pulps. Table A-4-2 summarizes the pulping conditions used to produce the pulps for the respective residual lignins.

Sample	Combined *o*- and *p*-quinones δ -0.3 - -7.0 ppm (mmol/g)
A-1	0.218
A-2	0.212
A-3	0.240
A-4	0.232
A-5	0.241
A-6	0.208
A-7	0.164
A-8	0.247
B-1	0.198
B-2	0.175
B-3	0.133
B-4	0.136
B-5	0.166
B-6	0.155
B-7	0.170
B-8	0.124
B-9	0.244
B-10	0.126

18.16 ^{19}F NMR Spectra of Residual Lignins

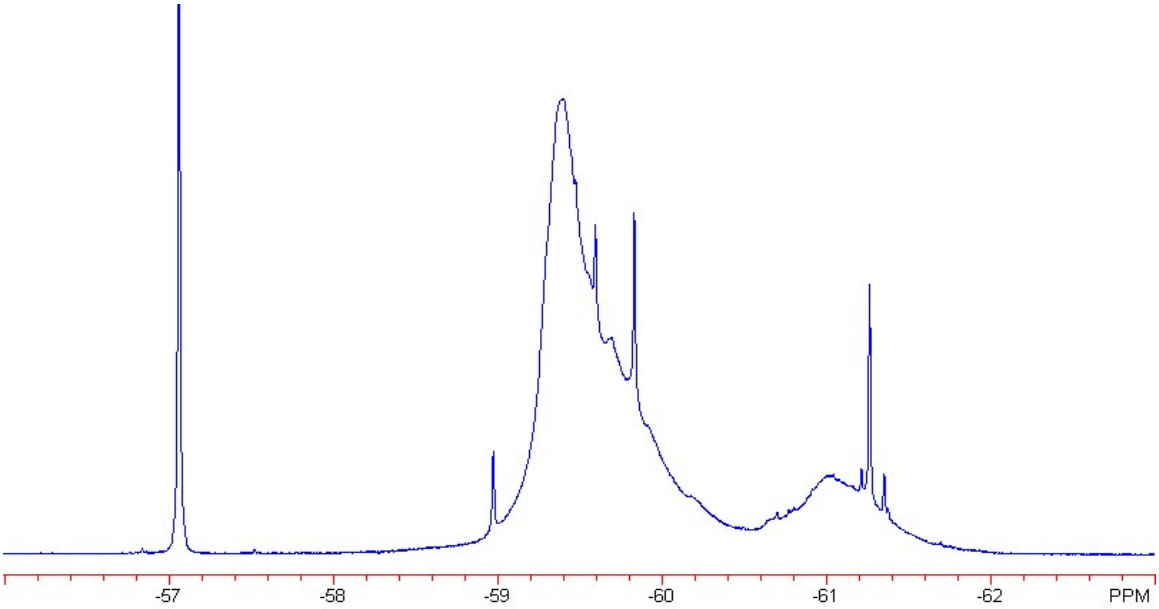

Figure A-4-168. ^{19}F NMR spectrum of residual lignin from Condition 1 of the constant kappa number (approximately 30) series of pulps. Table A-4-1 summarizes the pulping conditions used to produce the pulp for the respective residual lignin.

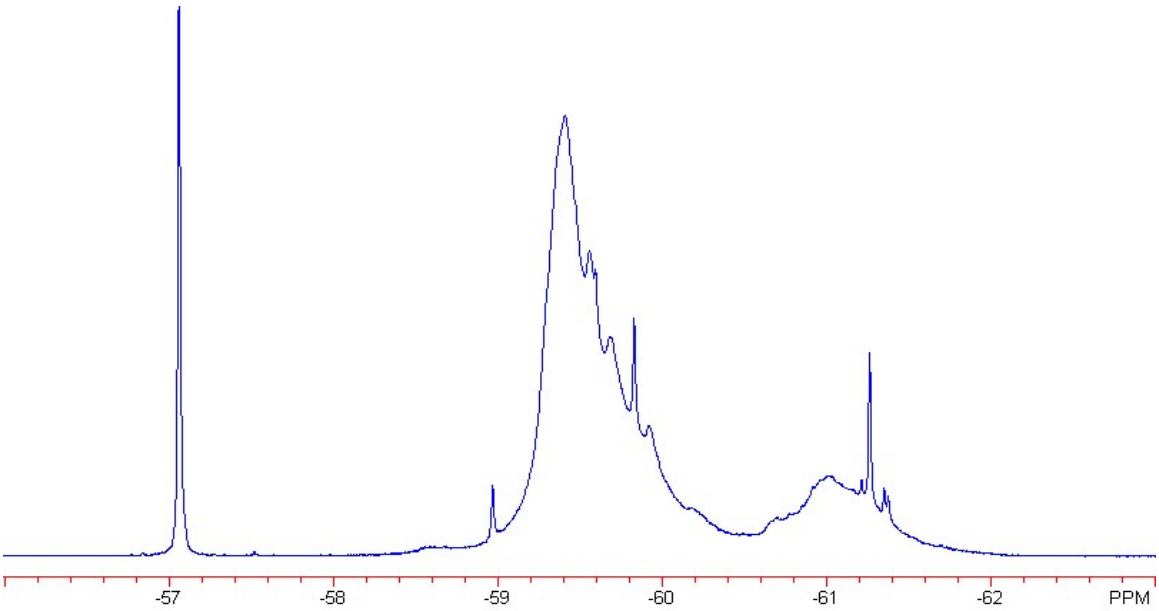

Figure A-4-169. ^{19}F NMR spectrum of residual lignin from Condition 2 of the constant kappa number (approximately 30) series of pulps. Table A-4-1 summarizes the pulping conditions used to produce the pulp for the respective residual lignin.

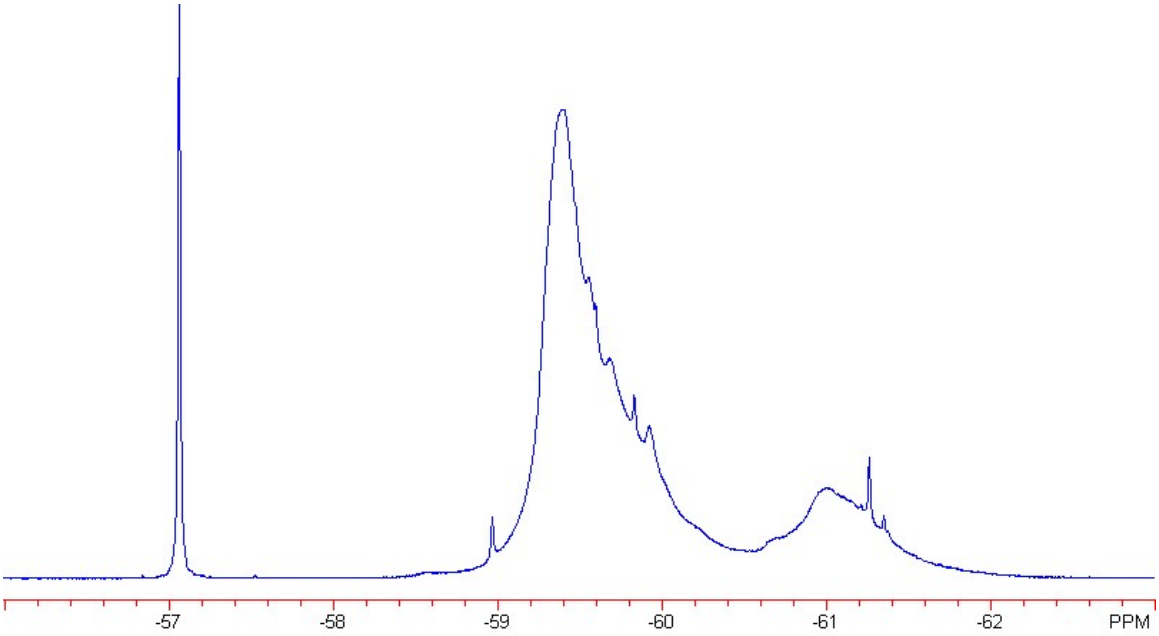

Figure A-4-170. ^{19}F NMR spectrum of residual lignin from Condition 3 of the constant kappa number (approximately 30) series of pulps. Table A-4-1 summarizes the pulping conditions used to produce the pulp for the respective residual lignin.

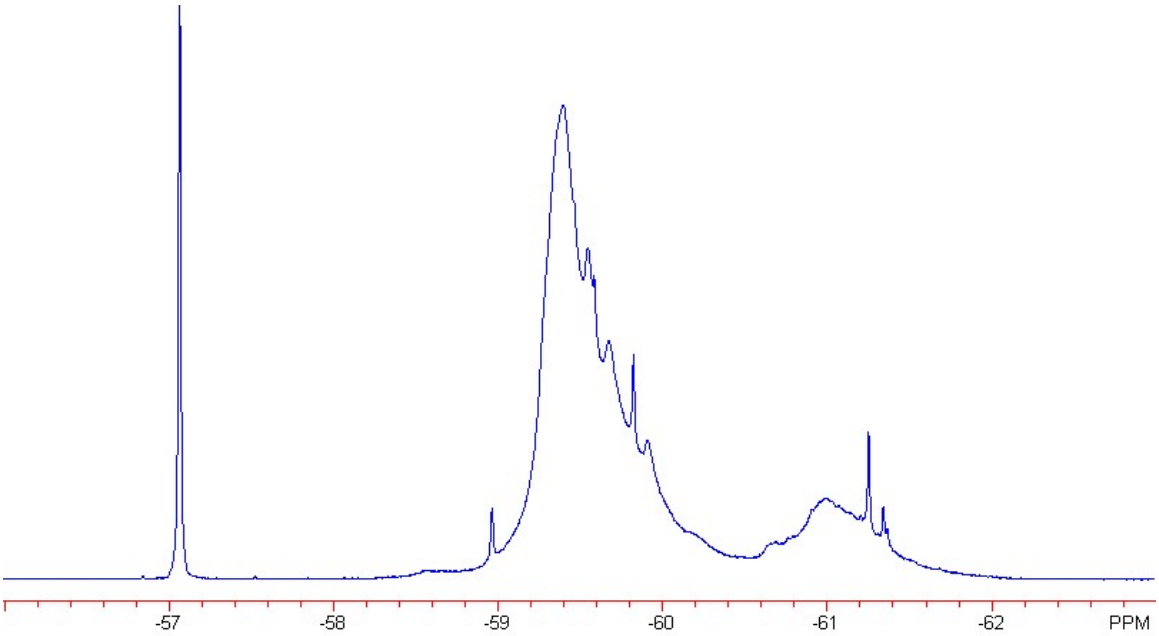

Figure A-4-171. ^{19}F NMR spectrum of residual lignin from Condition 4 of the constant kappa number (approximately 30) series of pulps. Table A-4-1 summarizes the pulping conditions used to produce the pulp for the respective residual lignin.

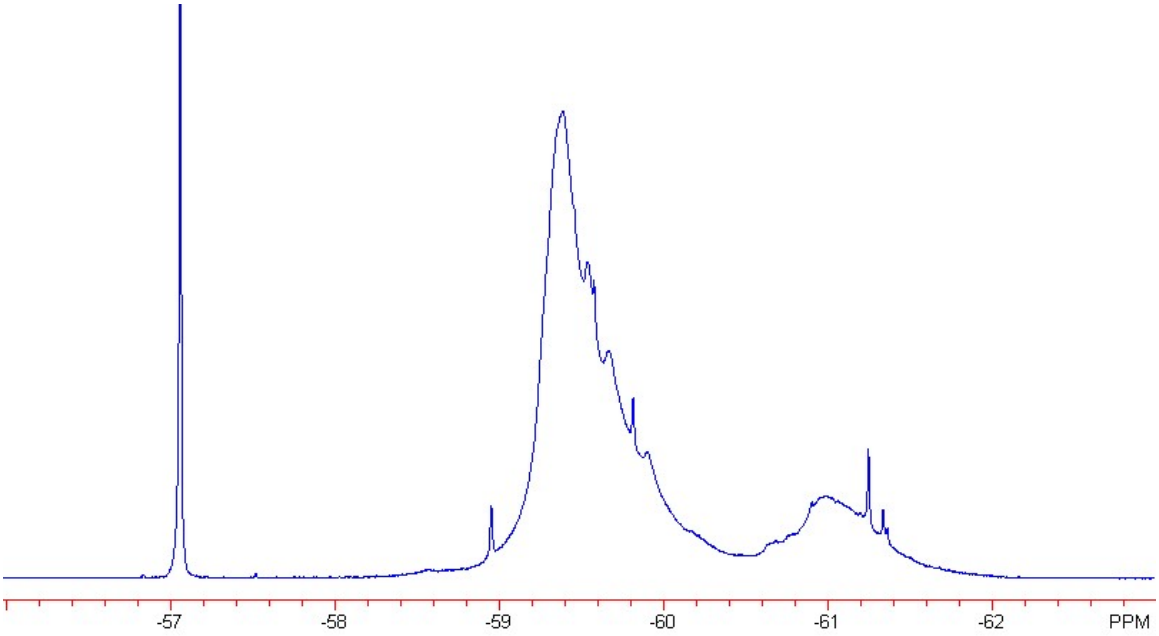

Figure A-4-172. ^{19}F NMR spectrum of residual lignin from Condition 5 of the constant kappa number (approximately 30) series of pulps. Table A-4-1 summarizes the pulping conditions used to produce the pulp for the respective residual lignin.

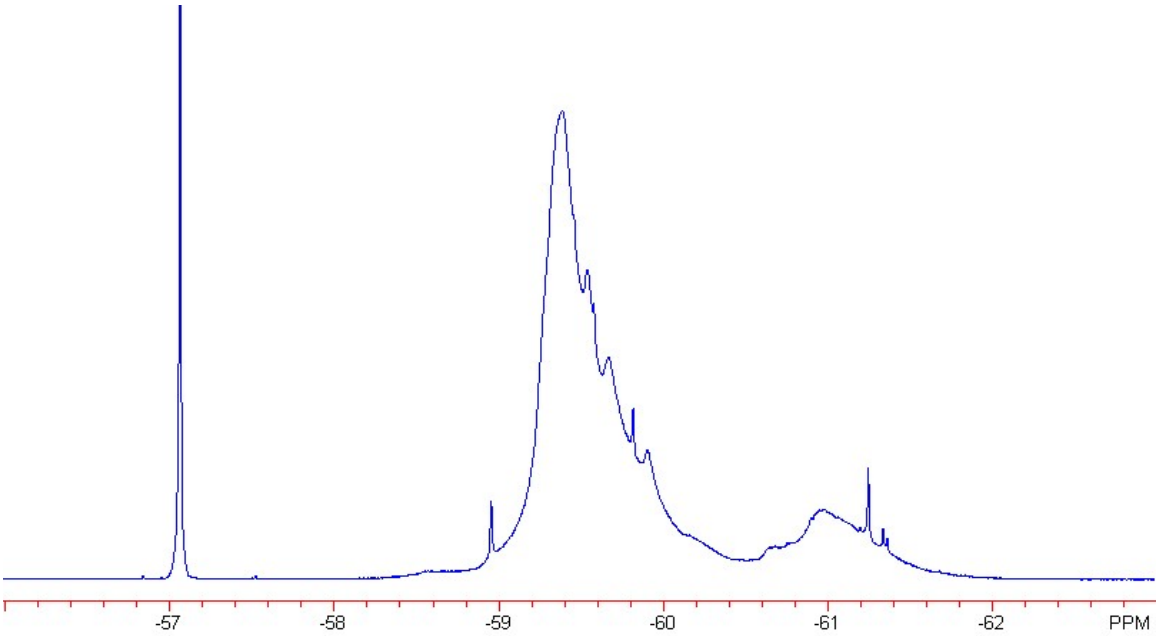

Figure A-4-173. ^{19}F NMR spectrum of residual lignin from Condition 6 of the constant kappa number (approximately 30) series of pulps. Table A-4-1 summarizes the pulping conditions used to produce the pulp for the respective residual lignin.

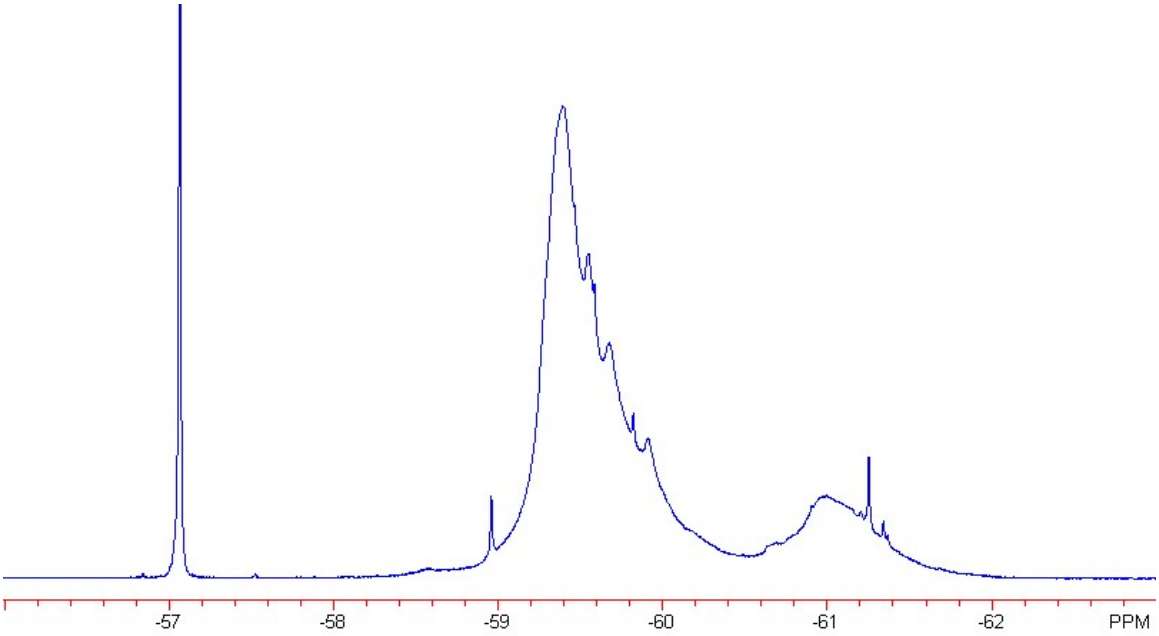

Figure A-4-174. ^{19}F NMR spectrum of residual lignin from Condition 7 of the constant kappa number (approximately 30) series of pulps. Table A-4-1 summarizes the pulping conditions used to produce the pulp for the respective residual lignin.

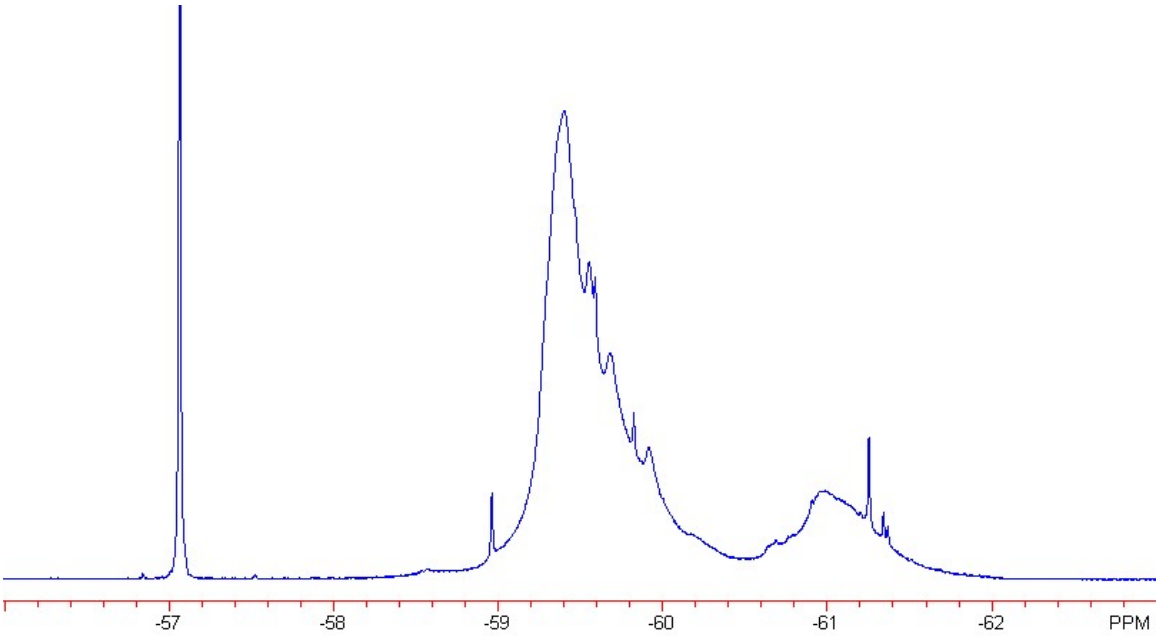

Figure A-4-175. ^{19}F NMR spectrum of residual lignin from Condition 8 of the constant kappa number (approximately 30) series of pulps. Table A-4-1 summarizes the pulping conditions used to produce the pulp for the respective residual lignin.

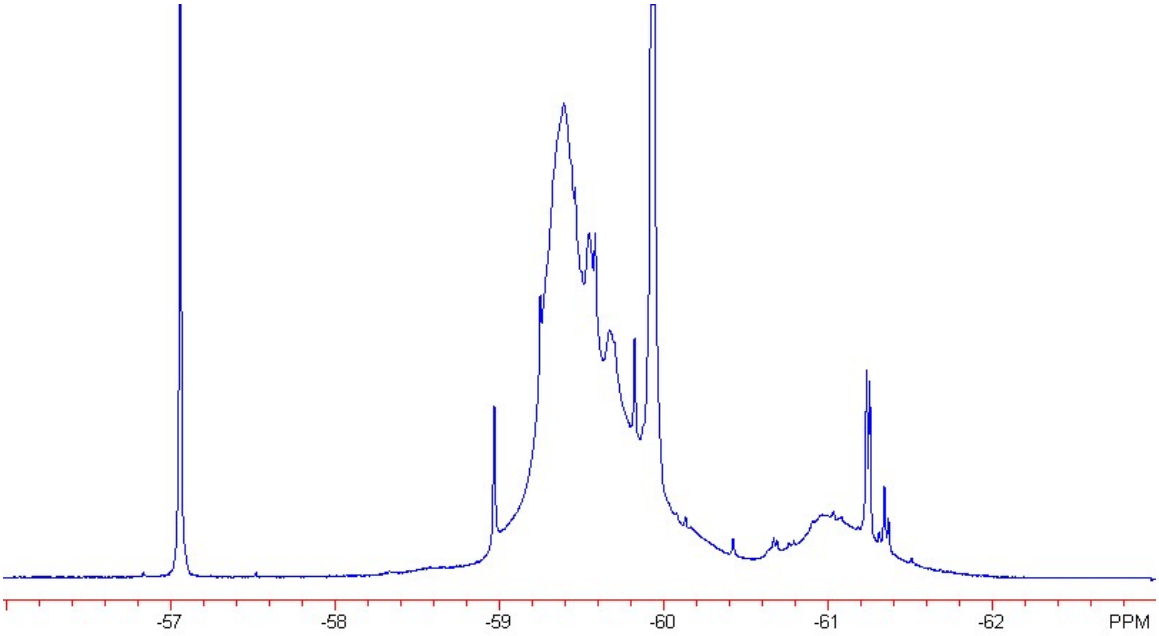

Figure A-4-176. ^{19}F NMR spectrum of residual lignin from Condition 9 of the constant kappa number (approximately 30) series of pulps. Table A-4-1 summarizes the pulping conditions used to produce the pulp for the respective residual lignin.

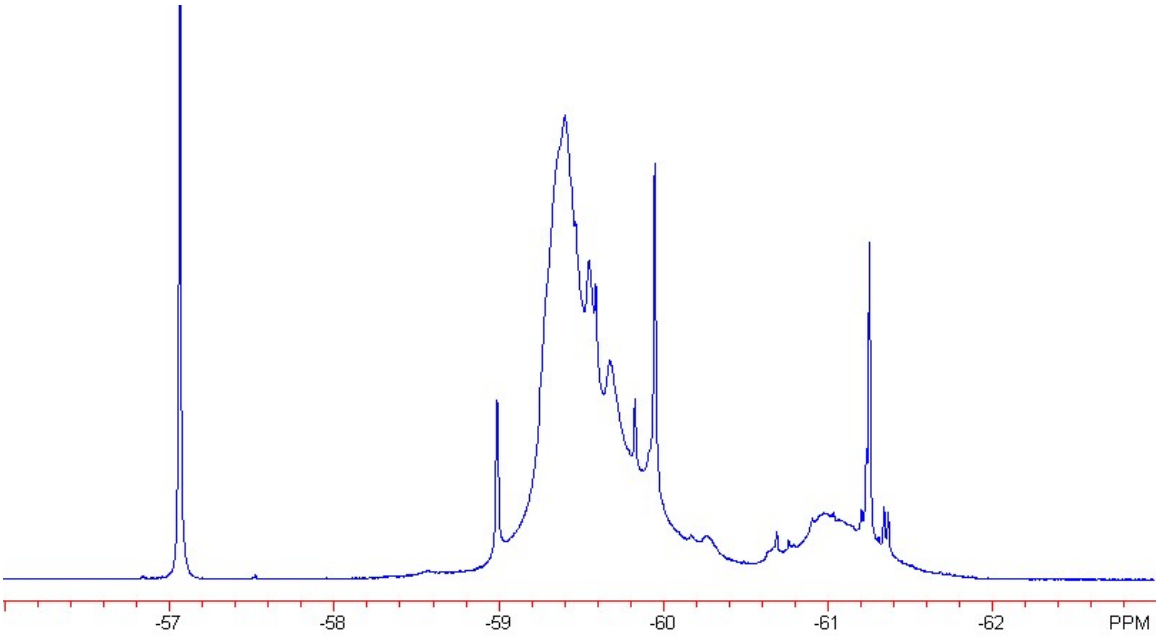

Figure A-4-177. ^{19}F NMR spectrum of residual lignin from Condition 10 of the constant kappa number (approximately 30) series of pulps. Table A-4-1 summarizes the pulping conditions used to produce the pulp for the respective residual lignin.

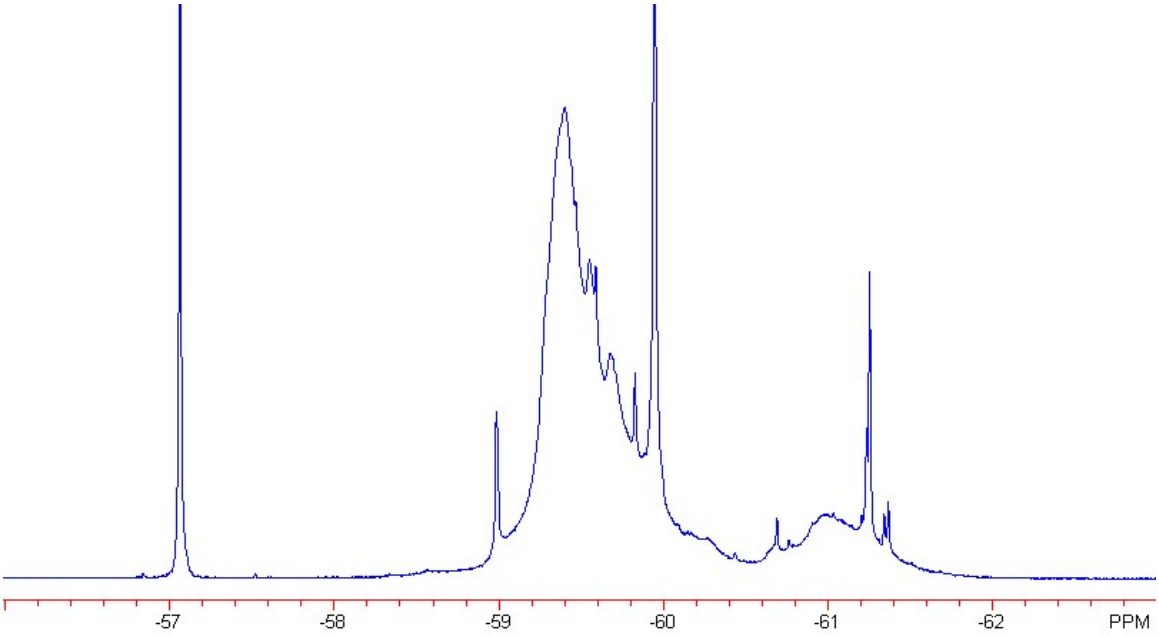

Figure A-4-178. ^{19}F NMR spectrum of residual lignin from Condition 11 of the constant kappa number (approximately 30) series of pulps. Table A-4-1 summarizes the pulping conditions used to produce the pulp for the respective residual lignin.

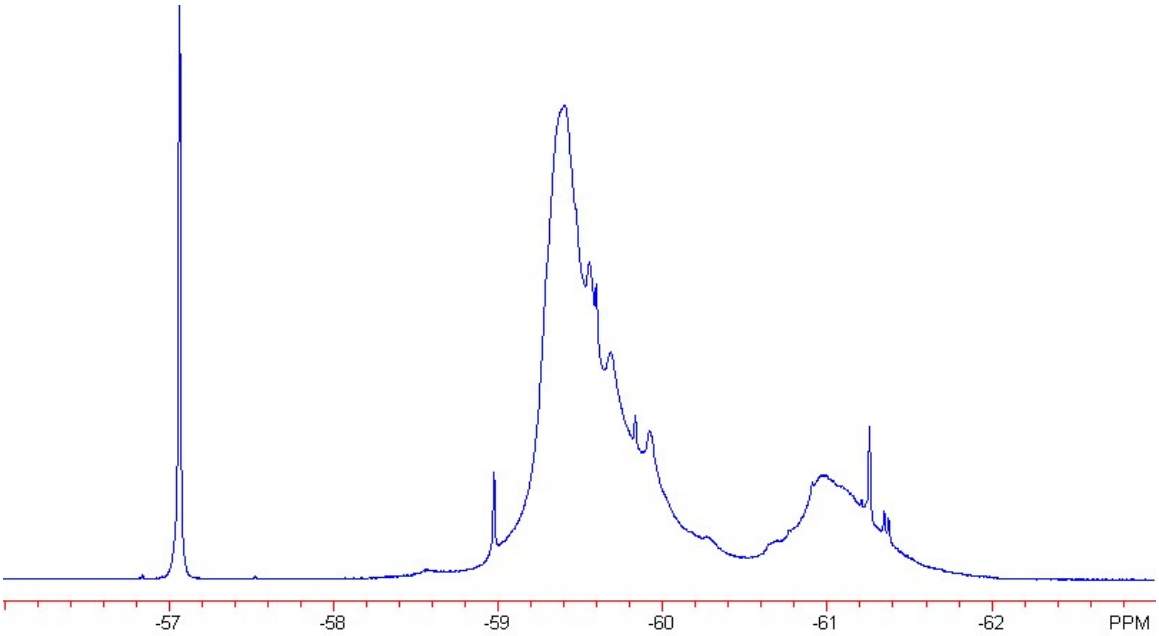

Figure A-4-179. ^{19}F NMR spectrum of residual lignin from Condition 12 of the constant kappa number (approximately 30) series of pulps. Table A-4-1 summarizes the pulping conditions used to produce the pulp for the respective residual lignin.

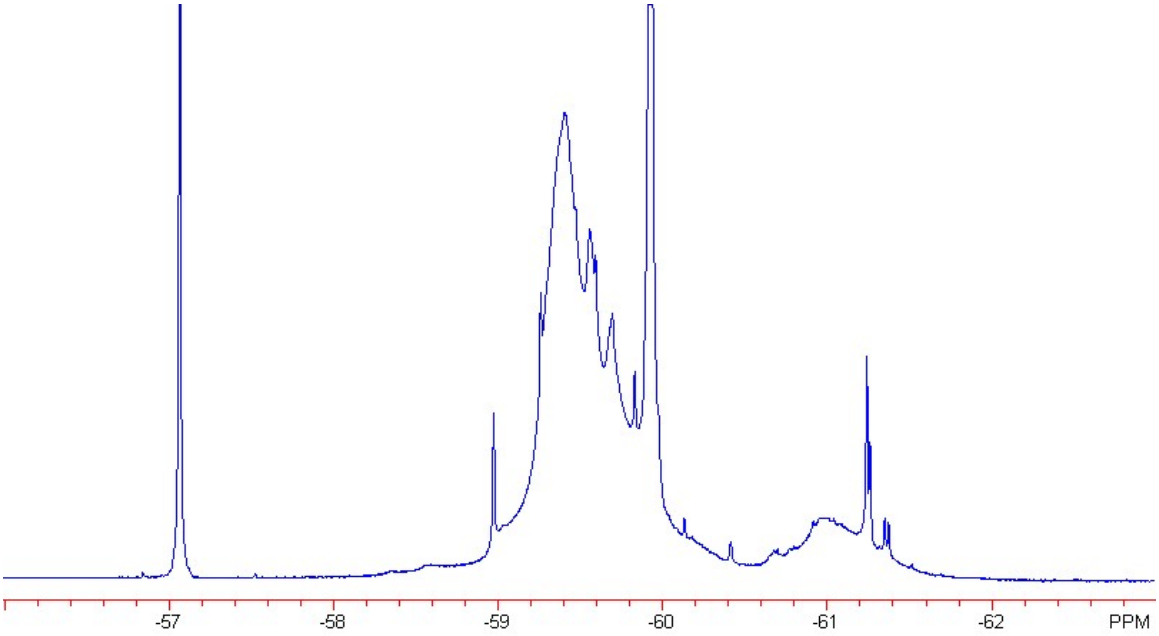

Figure A-4-180. ^{19}F NMR spectrum of residual lignin from Condition 13 of the constant kappa number (approximately 30) series of pulps. Table A-4-1 summarizes the pulping conditions used to produce the pulp for the respective residual lignin.

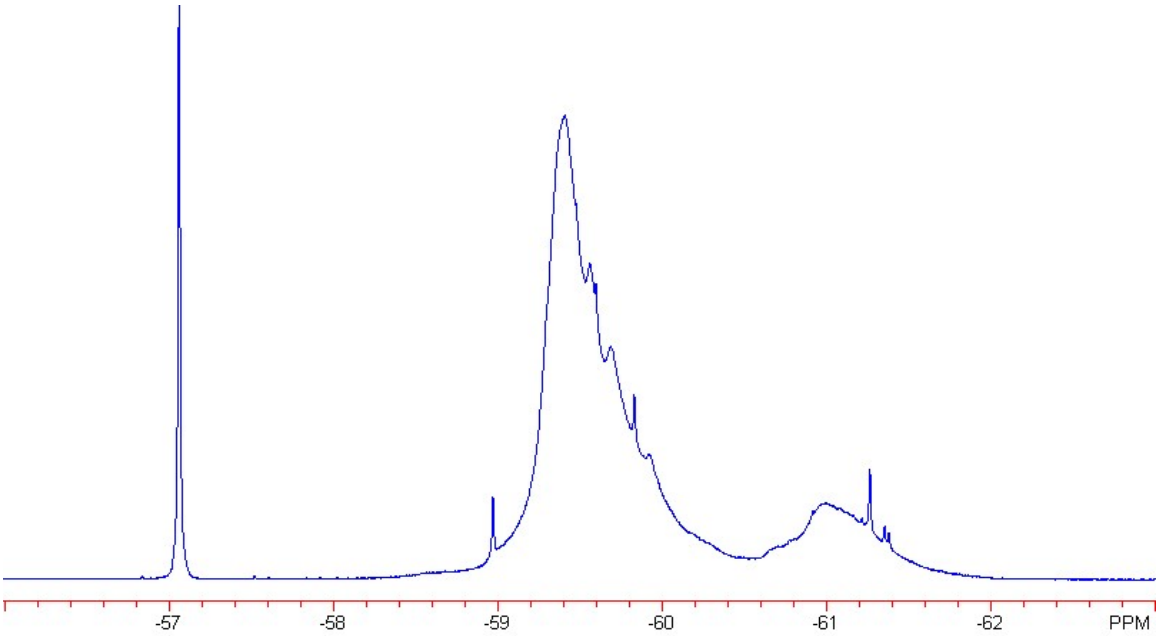

Figure A-4-181. ^{19}F NMR spectrum of residual lignin from Condition 14 of the constant kappa number (approximately 30) series of pulps. Table A-4-1 summarizes the pulping conditions used to produce the pulp for the respective residual lignin.

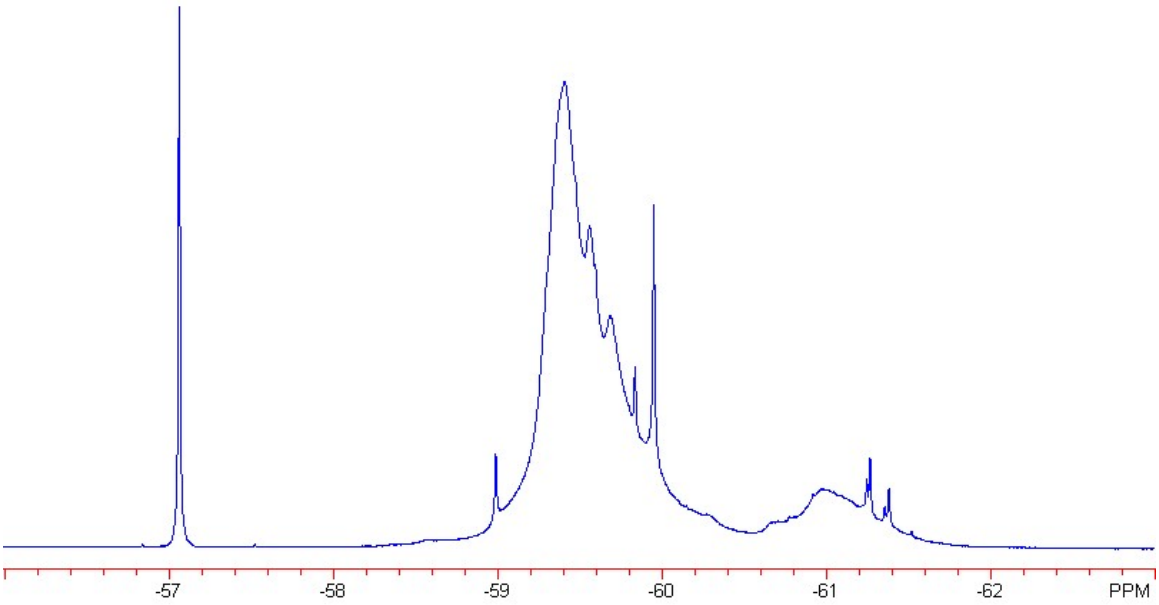

Figure A-4-182. ^{19}F NMR spectrum of residual lignin from Condition 15 of the constant kappa number (approximately 30) series of pulps. Table A-4-1 summarizes the pulping conditions used to produce the pulp for the respective residual lignin.

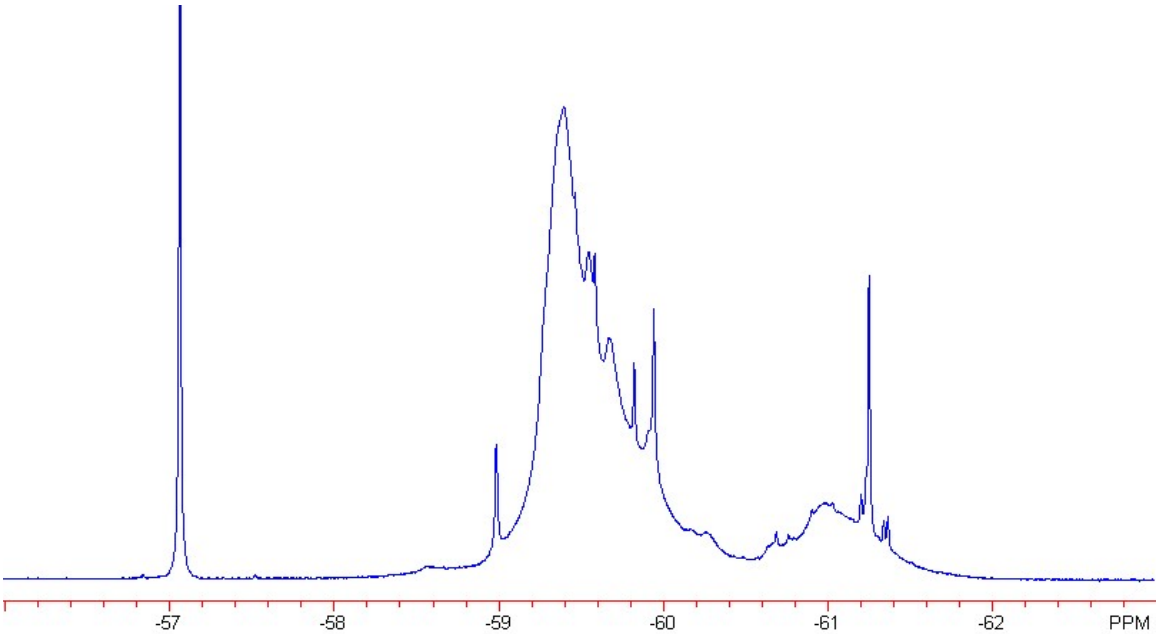

Figure A-4-183. ^{19}F NMR spectrum of residual lignin from Condition 16 of the constant kappa number (approximately 30) series of pulps. Table A-4-1 summarizes the pulping conditions used to produce the pulp for the respective residual lignin.

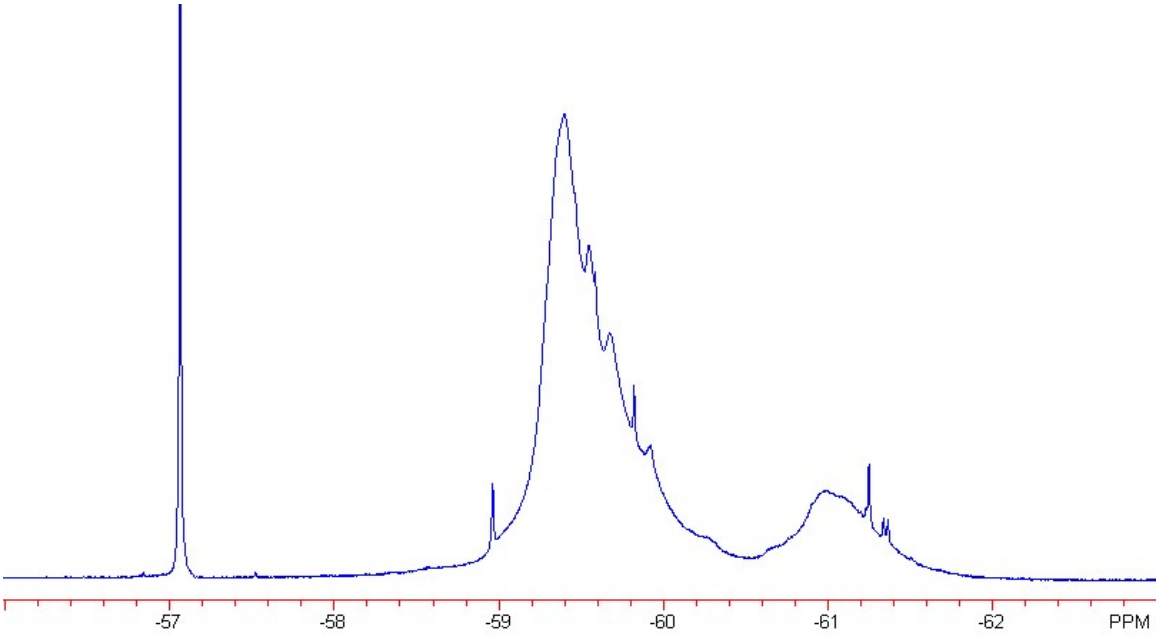

Figure A-4-184. ^{19}F NMR spectrum of residual lignin from Condition 17 of the constant kappa number (approximately 30) series of pulps. Table A-4-1 summarizes the pulping conditions used to produce the pulp for the respective residual lignin.

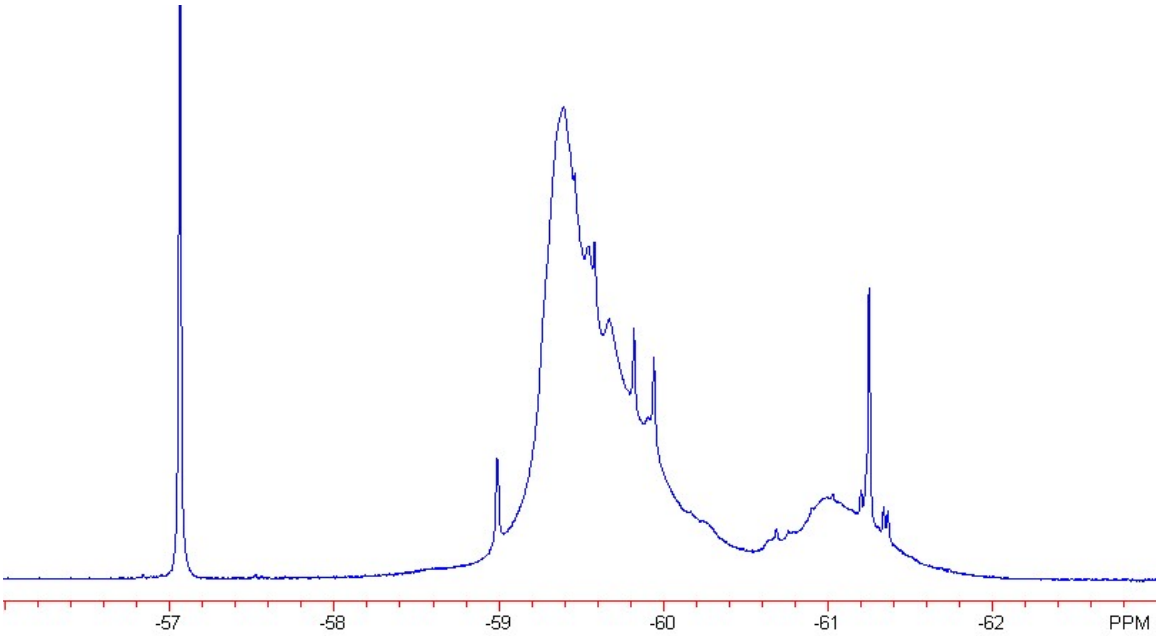

Figure A-4-185. ^{19}F NMR spectrum of residual lignin from Condition 18 of the constant kappa number (approximately 30) series of pulps. Table A-4-1 summarizes the pulping conditions used to produce the pulp for the respective residual lignin.

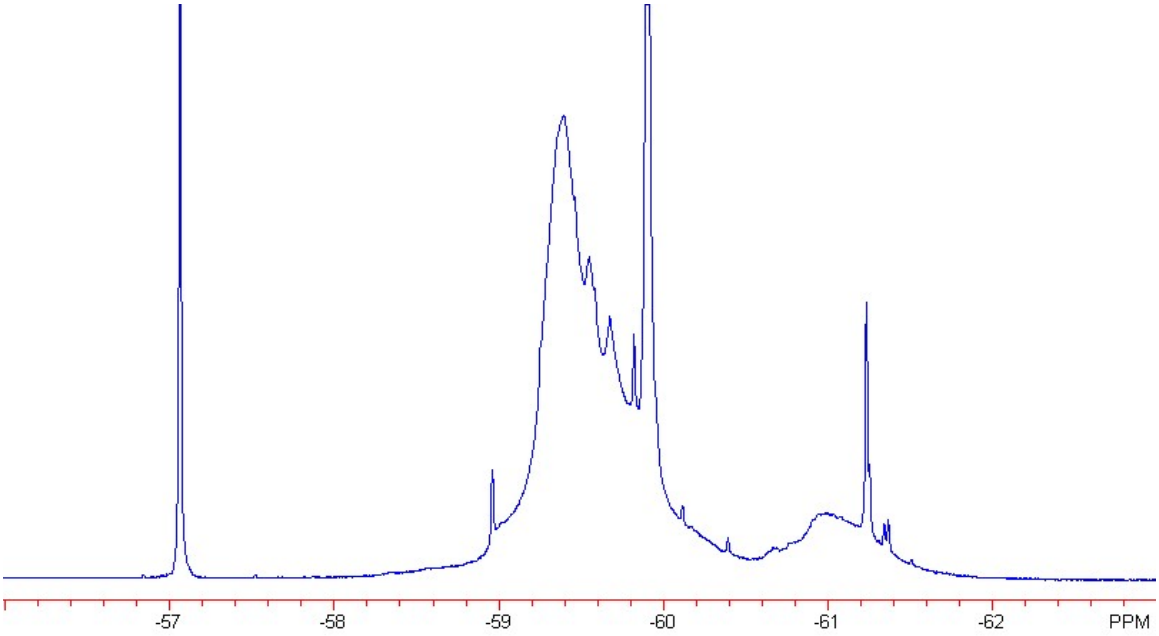

Figure A-4-186. ^{19}F NMR spectrum of residual lignin from Condition 19 of the constant kappa number (approximately 30) series of pulps. Table A-4-1 summarizes the pulping conditions used to produce the pulp for the respective residual lignin.

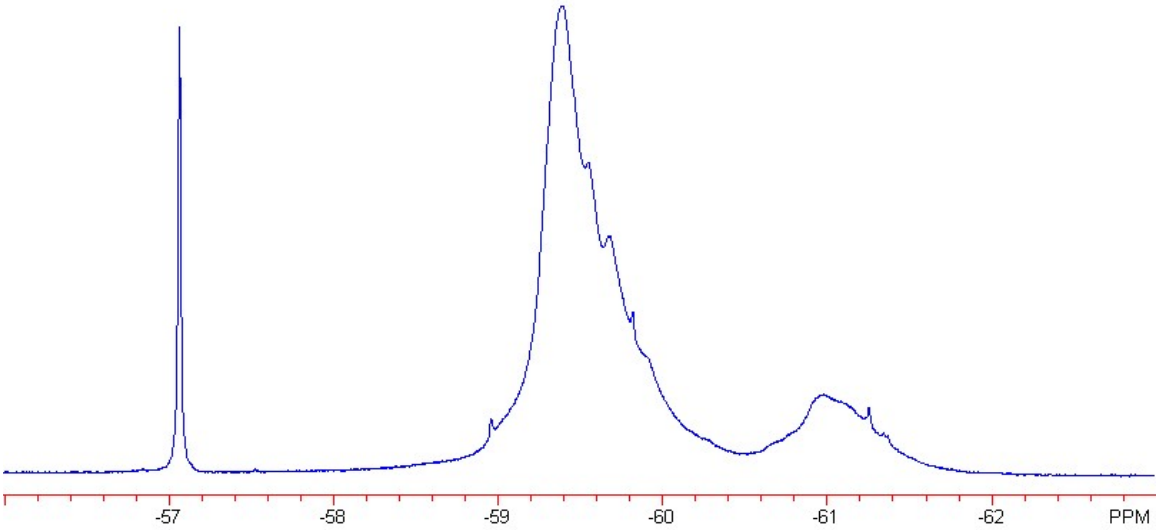

Figure A-4-187. ^{19}F NMR spectrum of residual lignin from Condition 20 of the constant kappa number (approximately 30) series of pulps. Table A-4-1 summarizes the pulping conditions used to produce the pulp for the respective residual lignin.

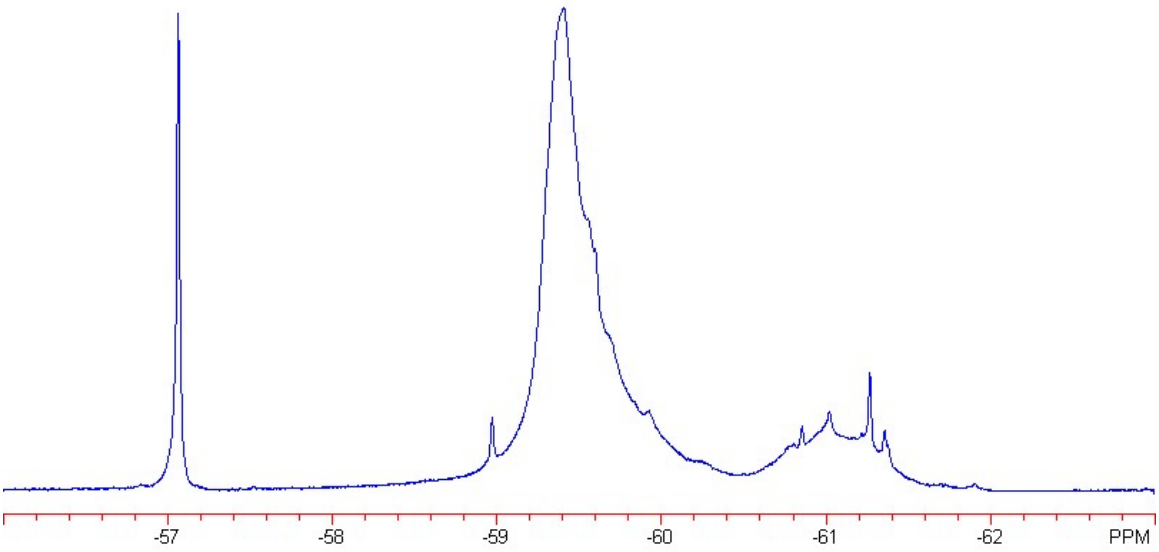

Figure A-4-188. ^{19}F NMR spectrum of residual lignin from Condition A-1 of the incremental cook series of pulps. Table A-4-2 summarizes the pulping conditions used to produce the pulp for the respective residual lignin.

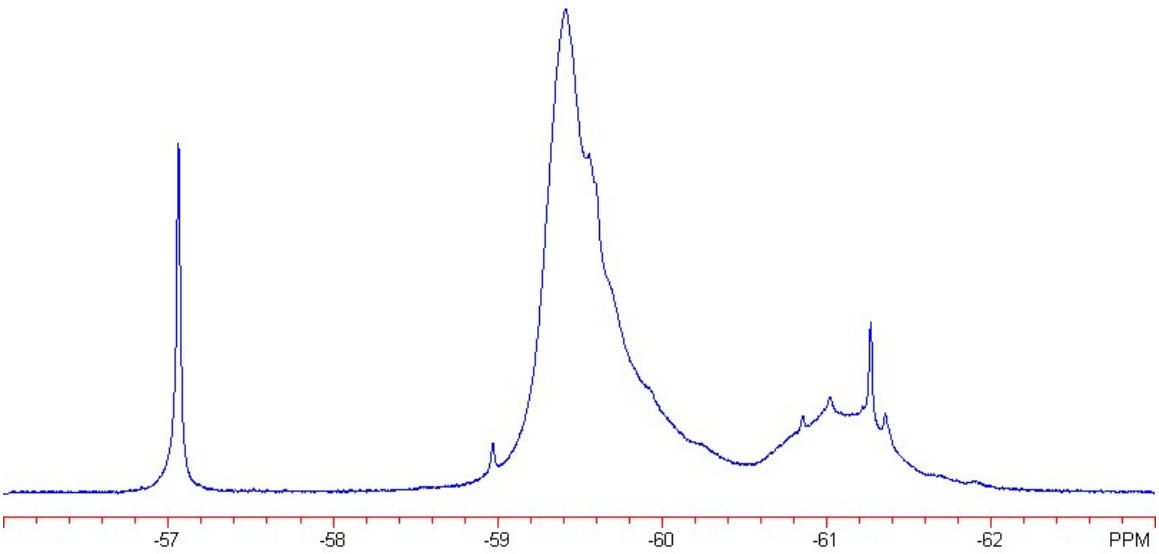

Figure A-4-189. ^{19}F NMR spectrum of residual lignin from Condition A-2 of the incremental cook series of pulps. Table A-4-2 summarizes the pulping conditions used to produce the pulp for the respective residual lignin.

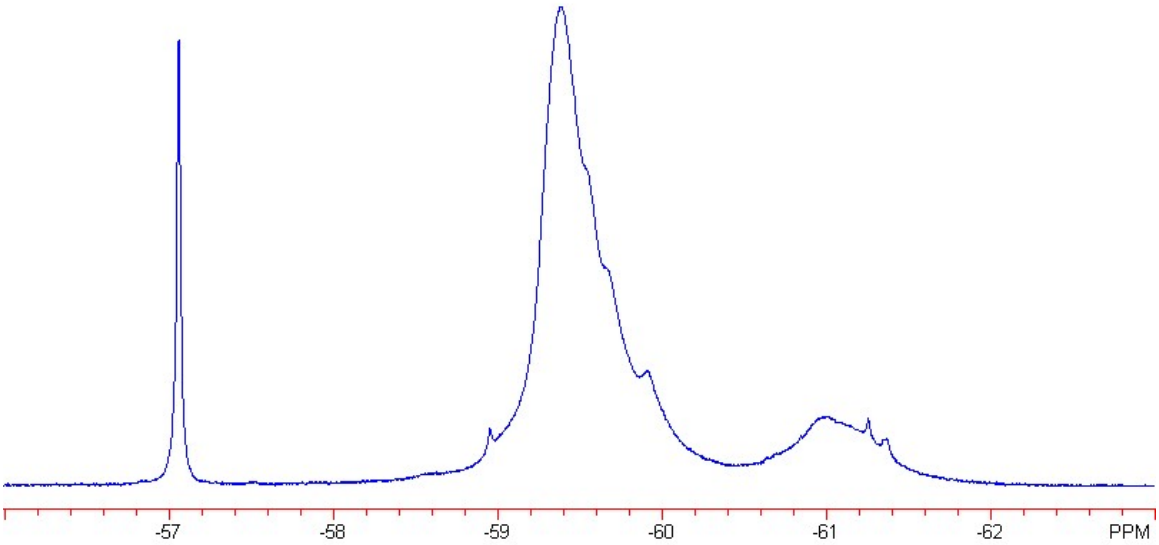

Figure A-4-190. ^{19}F NMR spectrum of residual lignin from Condition A-3 of the incremental cook series of pulps. Table A-4-2 summarizes the pulping conditions used to produce the pulp for the respective residual lignin.

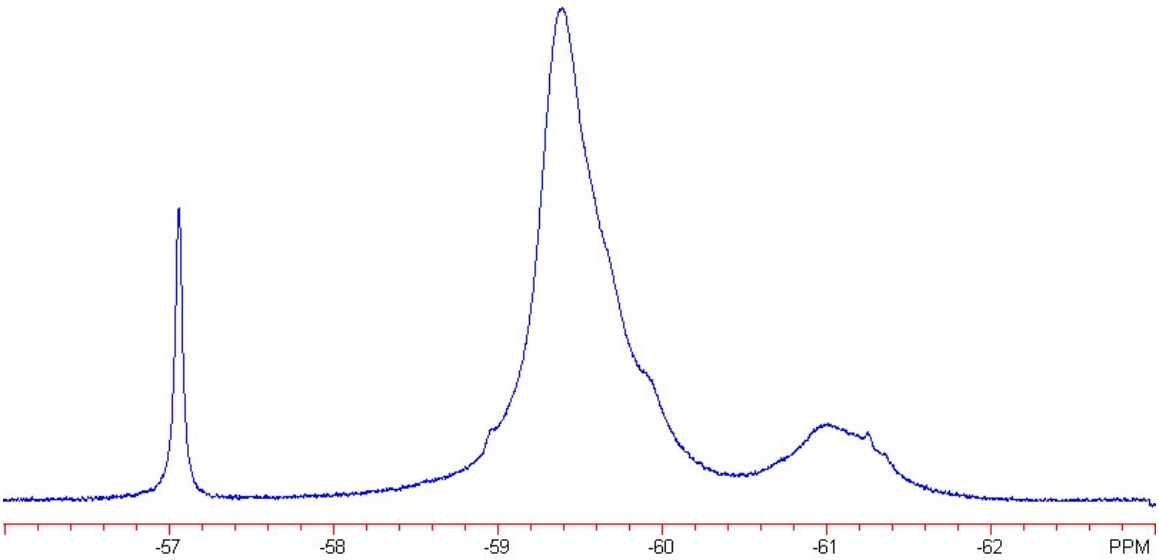

Figure A-4-191. ^{19}F NMR spectrum of residual lignin from Condition A-4 of the incremental cook series of pulps. Table A-4-2 summarizes the pulping conditions used to produce the pulp for the respective residual lignin.

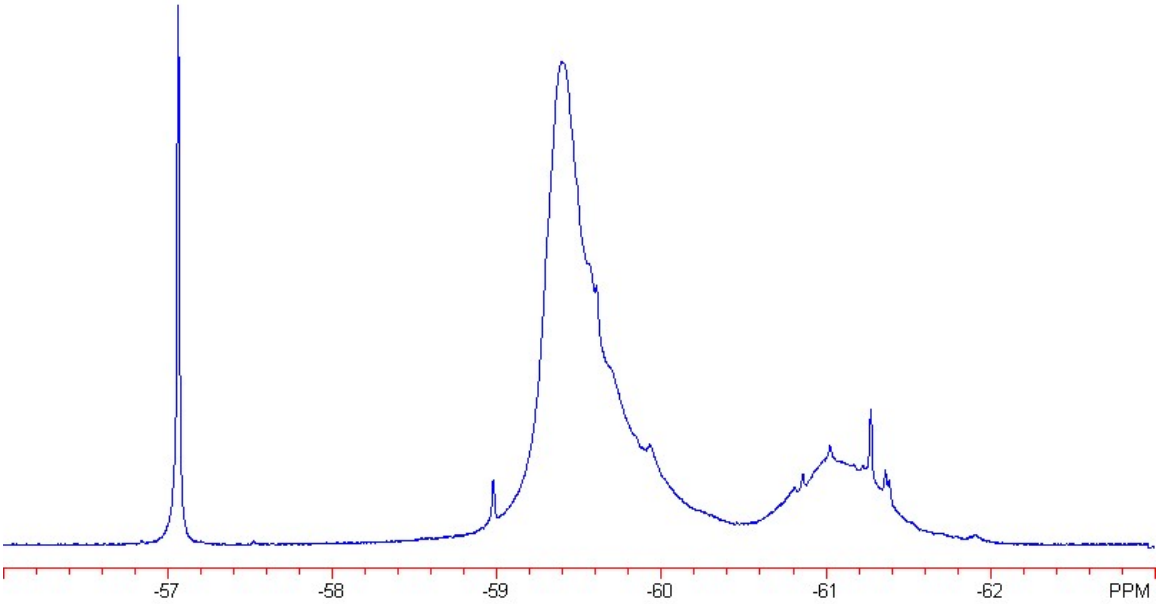

Figure A-4-192. ^{19}F NMR spectrum of residual lignin from Condition A-5 of the incremental cook series of pulps. Table A-4-2 summarizes the pulping conditions used to produce the pulp for the respective residual lignin.

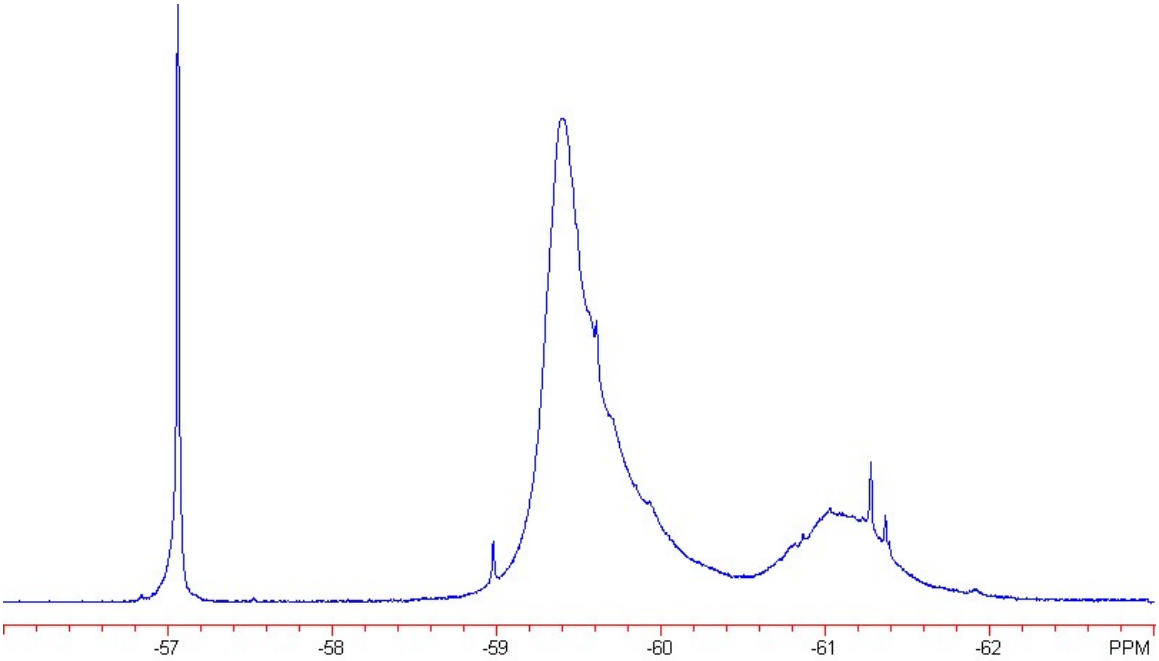

Figure A-4-193. ^{19}F NMR spectrum of residual lignin from Condition A-6 of the incremental cook series of pulps. Table A-4-2 summarizes the pulping conditions used to produce the pulp for the respective residual lignin.

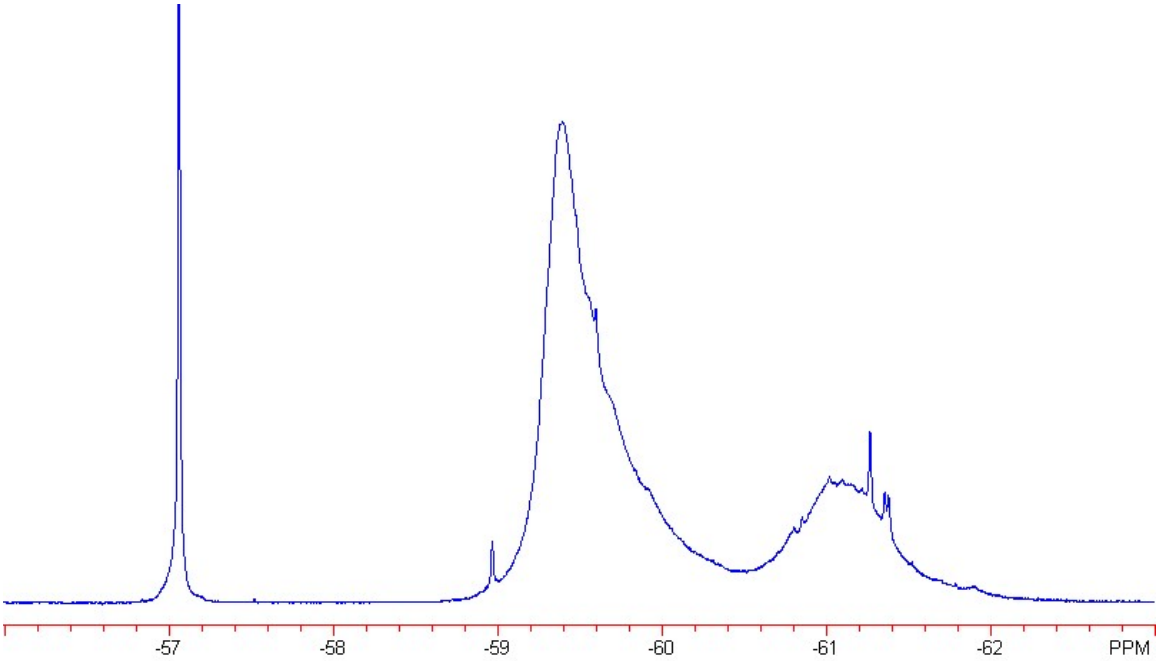

Figure A-4-194. ^{19}F NMR spectrum of residual lignin from Condition A-7 of the incremental cook series of pulps. Table A-4-2 summarizes the pulping conditions used to produce the pulp for the respective residual lignin.

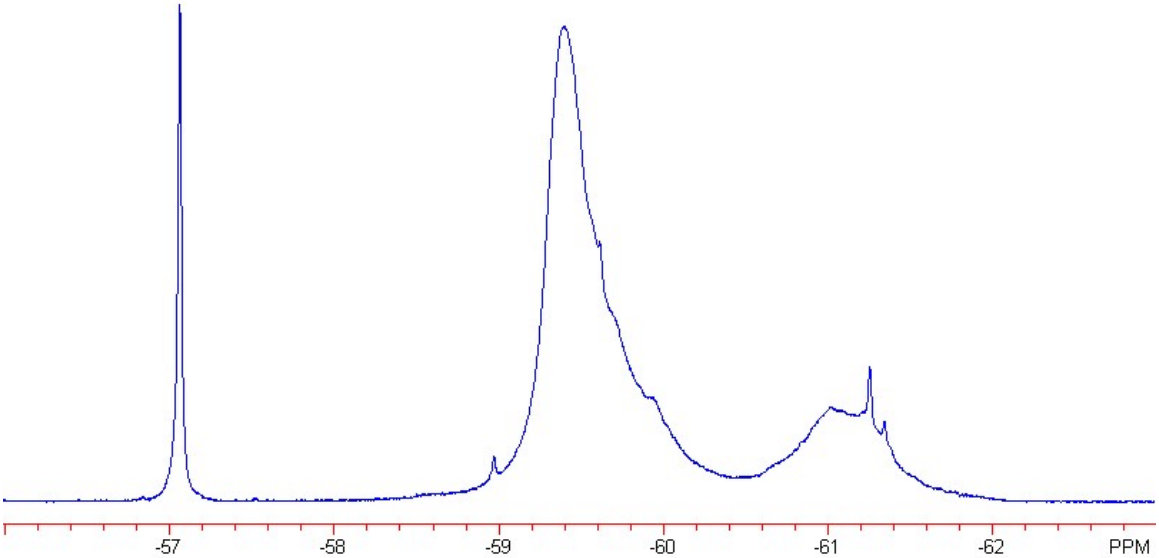

Figure A-4-195. ^{19}F NMR spectrum of residual lignin from Condition A-8 of the incremental cook series of pulps. Table A-4-2 summarizes the pulping conditions used to produce the pulp for the respective residual lignin.

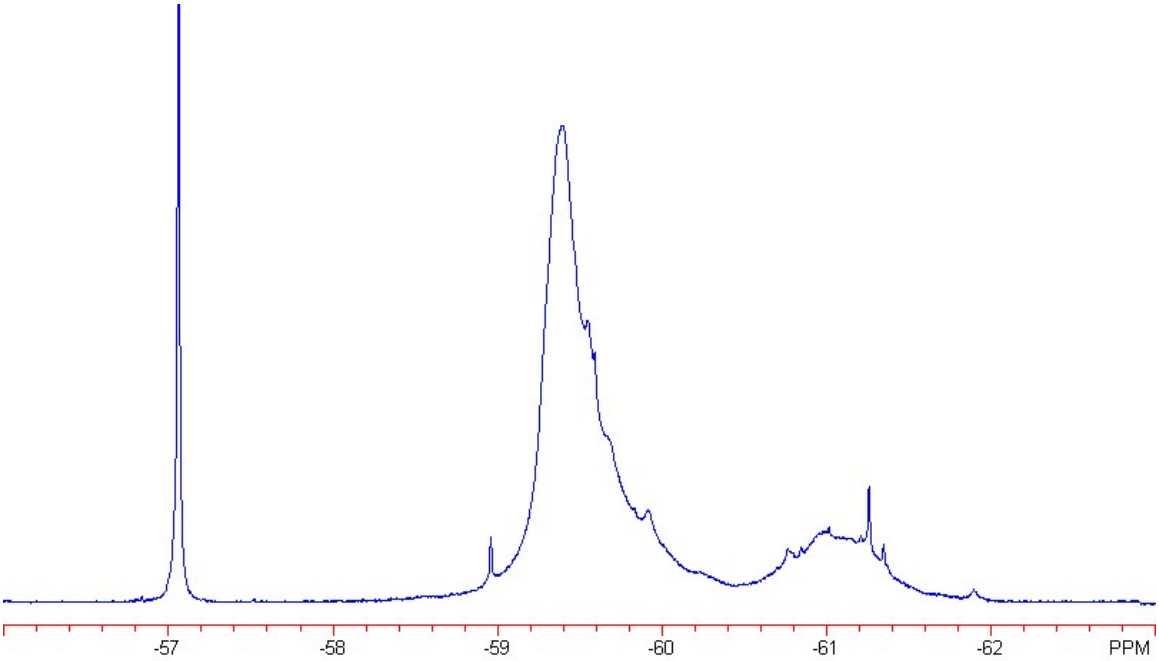

Figure A-4-196. ^{19}F NMR spectrum of residual lignin from Condition B-1 of the incremental cook series of pulps. Table A-4-2 summarizes the pulping conditions used to produce the pulp for the respective residual lignin.

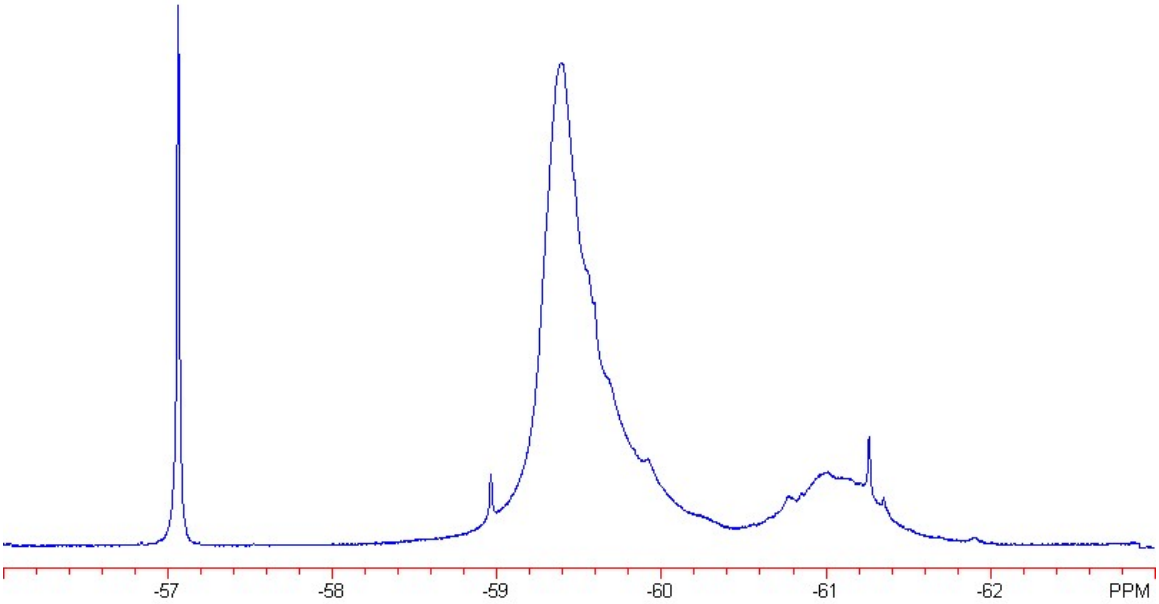

Figure A-4-197. ^{19}F NMR spectrum of residual lignin from Condition B-2 of the incremental cook series of pulps. Table A-4-2 summarizes the pulping conditions used to produce the pulp for the respective residual lignin.

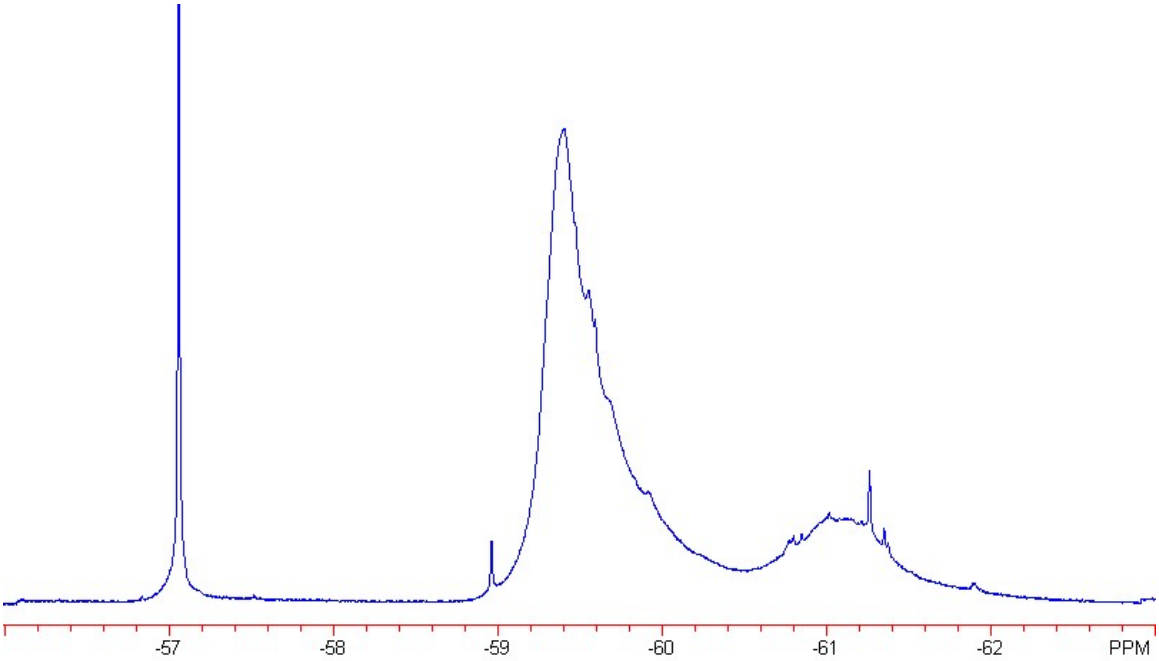

Figure A-4-198. ^{19}F NMR spectrum of residual lignin from Condition B-3 of the incremental cook series of pulps. Table A-4-2 summarizes the pulping conditions used to produce the pulp for the respective residual lignin.

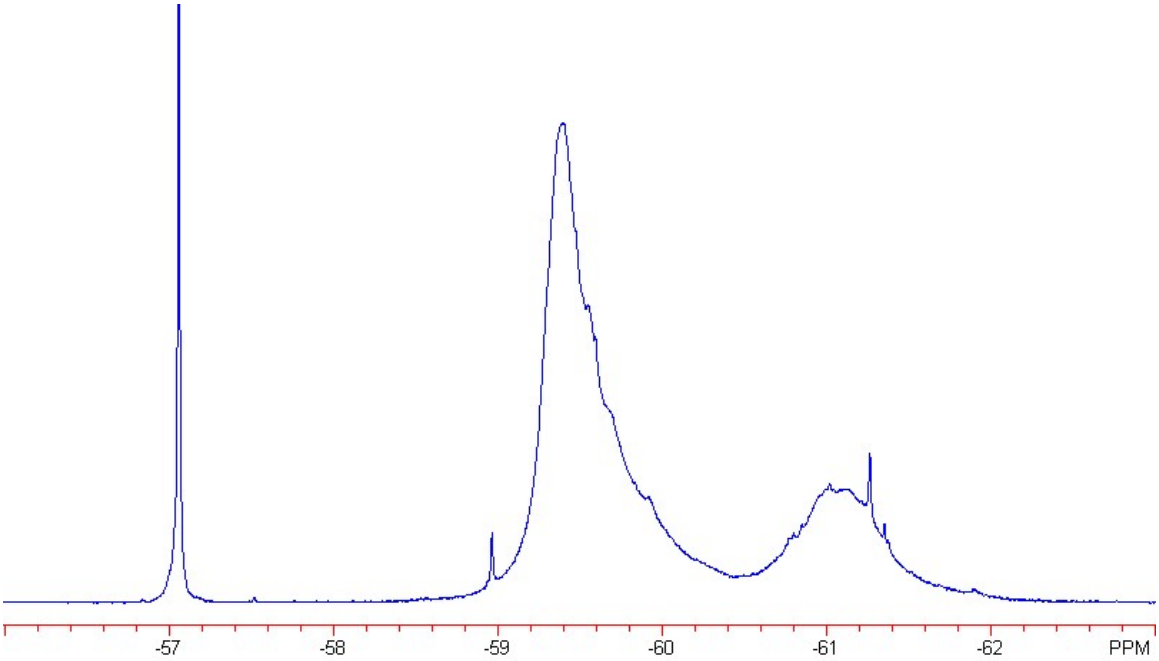

Figure A-4-199. ^{19}F NMR spectrum of residual lignin from Condition B-4 of the incremental cook series of pulps. Table A-4-2 summarizes the pulping conditions used to produce the pulp for the respective residual lignin.

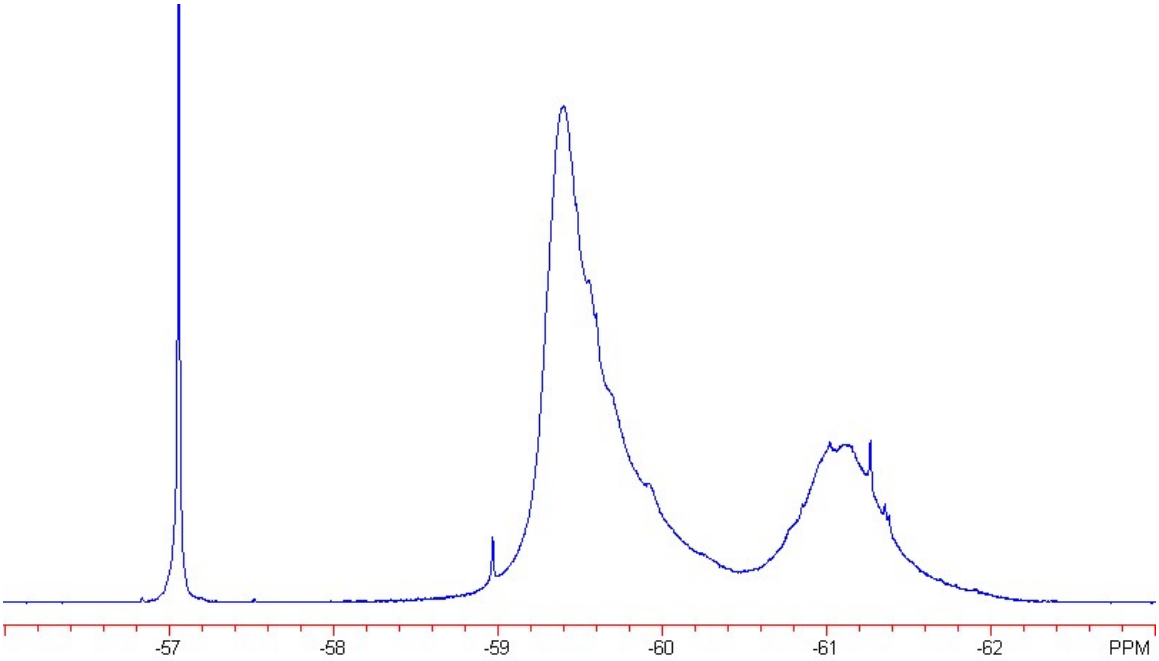

Figure A-4-200. ^{19}F NMR spectrum of residual lignin from Condition B-5 of the incremental cook series of pulps. Table A-4-2 summarizes the pulping conditions used to produce the pulp for the respective residual lignin.

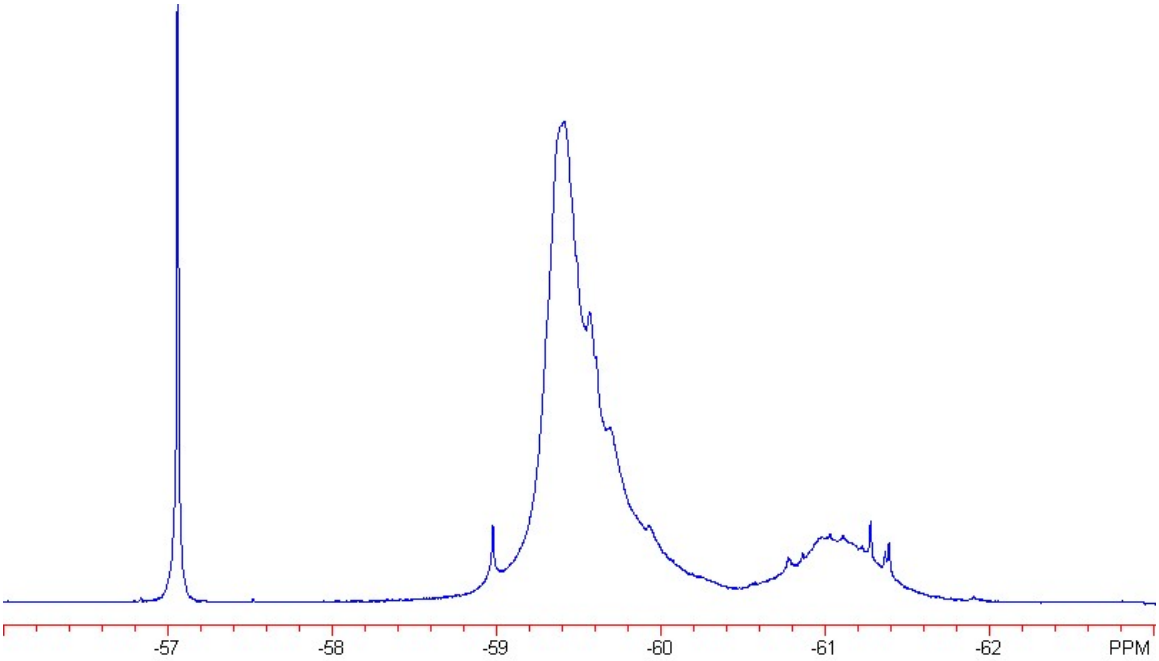

Figure A-4-201. ^{19}F NMR spectrum of residual lignin from Condition B-6 of the incremental cook series of pulps. Table A-4-2 summarizes the pulping conditions used to produce the pulp for the respective residual lignin.

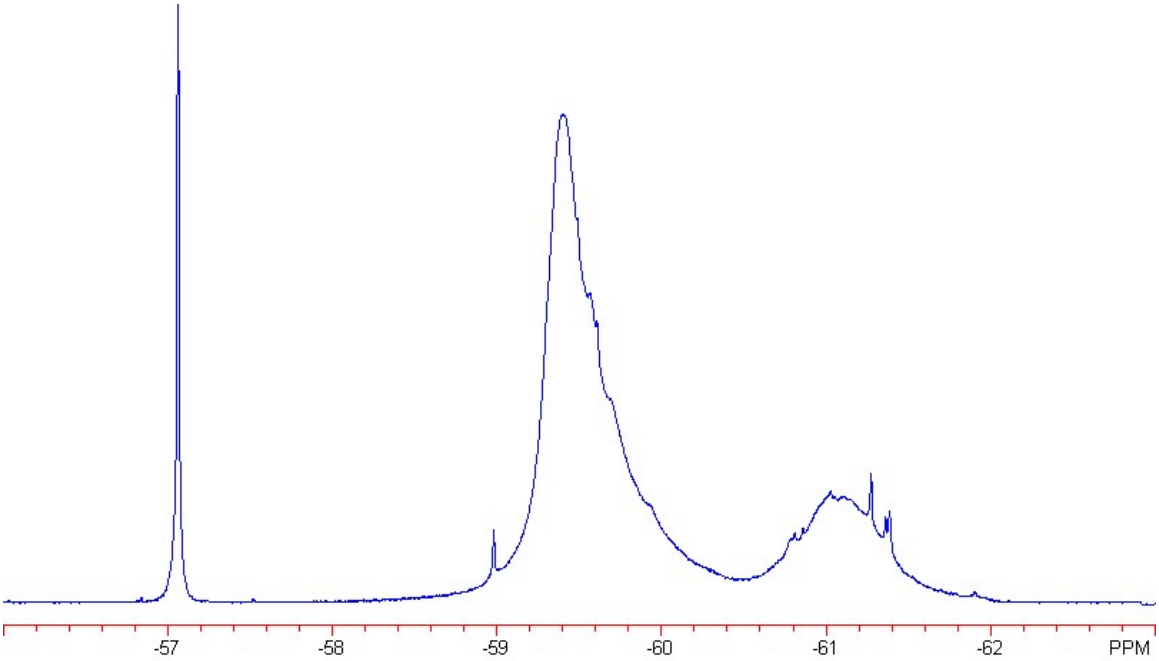

Figure A-4-202. ^{19}F NMR spectrum of residual lignin from Condition B-7 of the incremental cook series of pulps. Table A-4-2 summarizes the pulping conditions used to produce the pulp for the respective residual lignin.

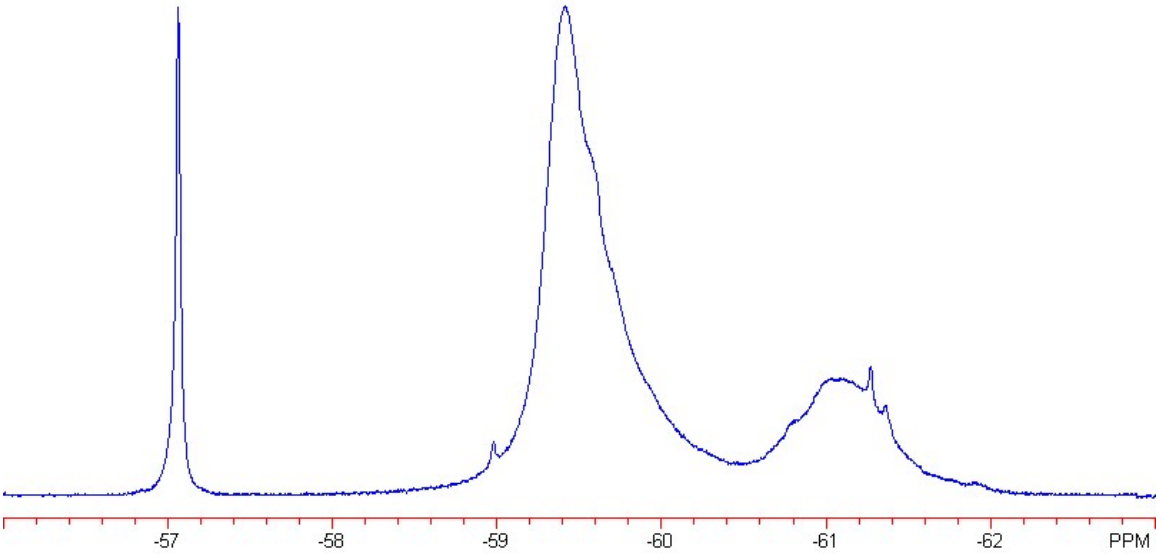

Figure A-4-203. ^{19}F NMR spectrum of residual lignin from Condition B-8 of the incremental cook series of pulps. Table A-4-2 summarizes the pulping conditions used to produce the pulp for the respective residual lignin.

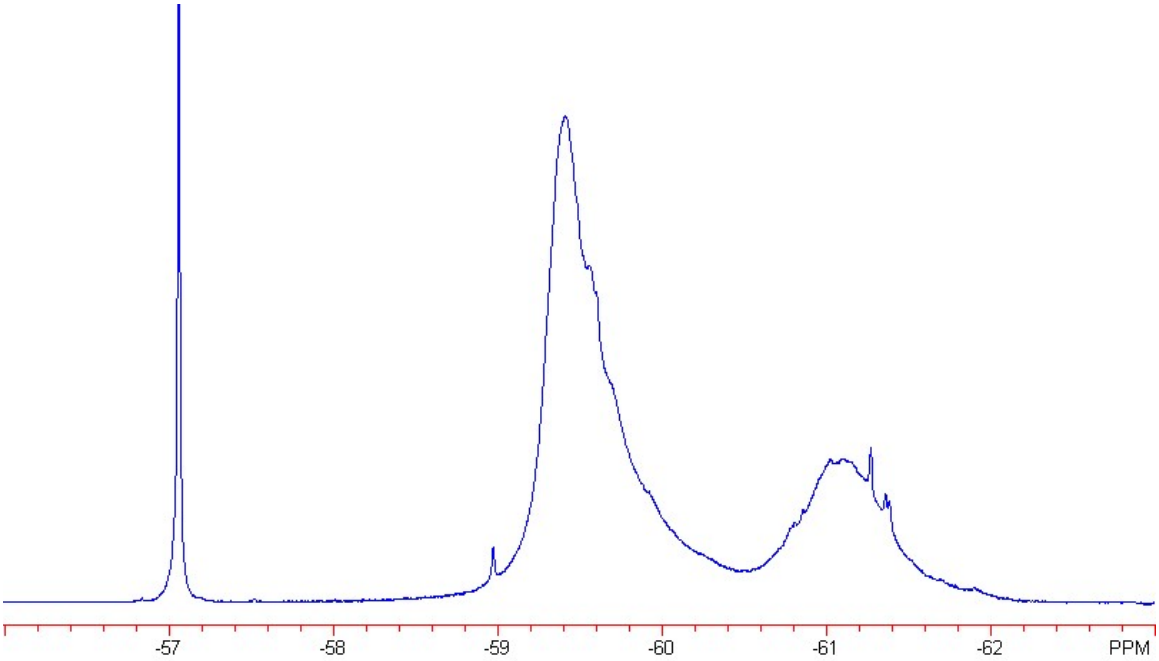

Figure A-4-204. ^{19}F NMR spectrum of residual lignin from Condition B-9 of the incremental cook series of pulps. Table A-4-2 summarizes the pulping conditions used to produce the pulp for the respective residual lignin.

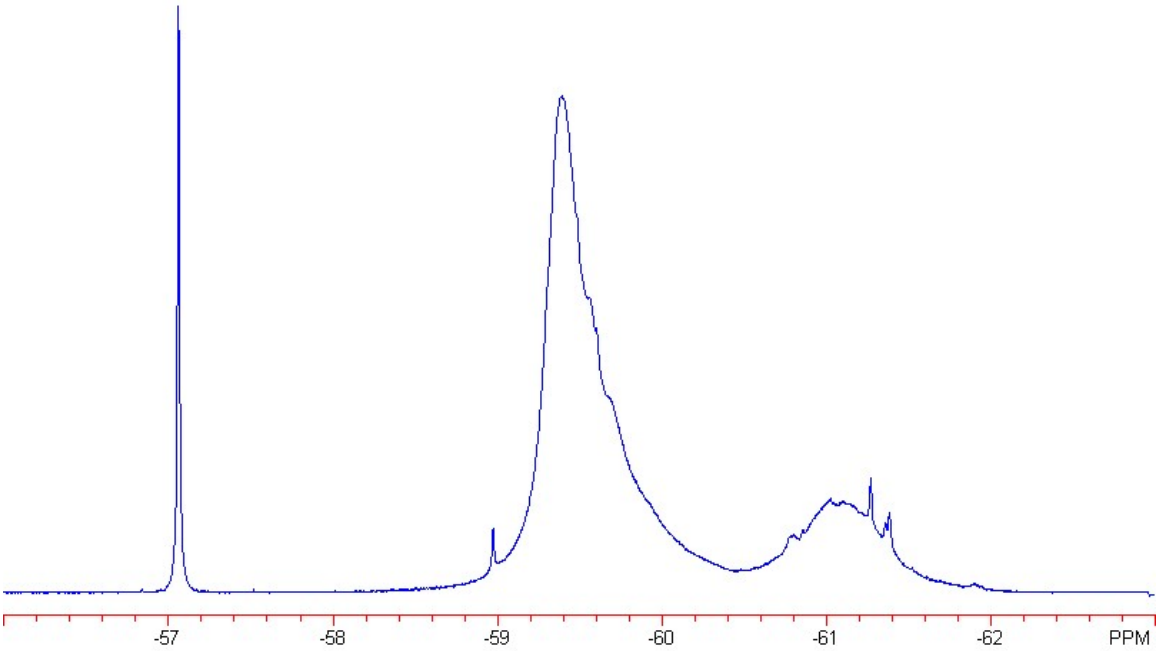

Figure A-4-205. ^{19}F NMR spectrum of residual lignin from Condition B-10 of the incremental cook series of pulps. Table A-4-2 summarizes the pulping conditions used to produce the pulp for the respective residual lignin.

18.17 Summary of ^{19}F NMR Data for Residual Lignins

Table A-4-28. ^{19}F NMR quinone data for residual lignins from the constant kappa number (approximately 30) series of pulps. Table A-4-1 summarizes the pulping conditions used to produce the pulps for the respective residual lignins.

Sample	Aliphatic Carbonyl (mmol/g)	Aromatic Carbonyl (mmol/g)
1	0.666	0.157
2	0.710	0.181
3	0.710	0.185
4	0.703	0.162
5	0.722	0.172
6	0.721	0.142
7	0.702	0.159
8	0.706	0.174
9	0.749	0.117
10	0.804	0.169
11	0.896	0.166
12	0.723	0.194
13	0.818	0.099
14	0.780	0.168
15	0.874	0.141
16	0.747	0.161
17	0.780	0.173
18	0.751	0.175
19	0.793	0.119
20	0.759	0.148

Table A-4-29. ^{19}F NMR quinone data for residual lignins from the incremental cook series of pulps. Table A-4-2 summarizes the pulping conditions used to produce the pulps for the respective residual lignins.

Sample	Aliphatic Carbonyl (mmol/g)	Aromatic Carbonyl (mmol/g)
A-1	0.544	0.122
A-2	0.561	0.177
A-3	0.565	0.116
A-4	0.569	0.112
A-5	0.588	0.174
A-6	0.556	0.176
A-7	0.635	0.252
A-8	0.655	0.192
B-1	0.522	0.131
B-2	0.548	0.132
B-3	0.595	0.193
B-4	0.581	0.213
B-5	0.621	0.273
B-6	0.574	0.149
B-7	0.598	0.192
B-8	0.506	0.176
B-9	0.642	0.269
B-10	0.700	0.204

19. APPENDIX 5. SUPPORTING DATA FOR CHAPTER #5

19.1 Summary of Experimental Conditions

Table A-5-1. Constant kappa number (approximately 30) conditions for pulps produced from unextracted softwood chips.

Condition	Alias	EA % as Na_2O	Sulfidity % as Na_2O	Maximum Temperature	H-Factor
1	31	16.0	30.0	165.0	1294
2	32	20.0	30.0	165.0	790
3	33	16.0	50.0	165.0	929
4	34	20.0	50.0	165.0	570
5	35	16.0	30.0	175.0	1294
6	36	20.0	30.0	175.0	790
7	37	16.0	50.0	175.0	929
8	38	20.0	50.0	175.0	522
9	39	14.6	40.0	170.0	1352
10	40	21.4	40.0	170.0	565
11	41	18.0	23.2	170.0	1217
12	42	18.0	56.8	170.0	646
13	43	18.0	40.0	161.6	806
14	44	18.0	40.0	178.4	806
15	45	18.0	40.0	170.0	806
16	46	18.0	40.0	170.0	806
17	47	18.0	40.0	170.0	806
18	48	18.0	40.0	170.0	806
19	49	18.0	40.0	170.0	806
20	50	18.0	40.0	170.0	806

Table A-5-2. Incremental cook conditions. Condition A pulps were produced under high effective alkali, low sulfidity while Condition B pulps were produced under low effective alkali, high sulfidity conditions.

Condition	Alias	EA % as Na_2O	Sulfidity % as Na_2O	Maximum Temperature	H-factor
A-1	71-1	21.4	23.2	170.0	120
A-2	71-2	21.4	23.2	170.0	240
A-3	71-3	21.4	23.2	170.0	360
A-4	71-4	21.4	23.2	170.0	480
A-5	71-5	21.4	23.2	170.0	600
A-6	71-6	21.4	23.2	170.0	720
A-7	71-7	21.4	23.2	170.0	840
A-8	71-8	21.4	23.2	170.0	863
B-1	72-1	14.6	56.8	170.0	120
B-2	72-2	14.6	56.8	170.0	240
B-3	72-3	14.6	56.8	170.0	360
B-4	72-4	14.6	56.8	170.0	480
B-5	72-5	14.6	56.8	170.0	600
B-6	72-6	14.6	56.8	170.0	720
B-7	72-7	14.6	56.8	170.0	840
B-8	72-8	14.6	56.8	170.0	960
B-9	72-9	14.6	56.8	170.0	1080
B-10	72-10	14.6	56.8	170.0	1151

19.2 Summary of Properties for Different Types of Water

Table A-5-3. Properties of tap water, deionized water, and Nanopure water utilized in these studies.

Property	Tap	Tap	Deionized	Deionized	Nanopure	Nanopure
pH	7.44	7.23	6.67	6.68	6.49	6.38
Conductivity (mS/m)	7.67	7.68	0.09	0.11	0.28	0.18
Chloride (ppm)	7.7		< 1		< 1	
Sulfate (ppm)	11.8		< 1		< 1	
Nitrate (ppm)	2.3		< 1		< 1	
Phosphate (ppm)	2.0		< 1		< 1	
Fe (mg/L)	0.02		< 0.003		< 0.003	
Cr (mg/L)	< 0.006		< 0.006		< 0.006	
Mn (mg/L)	0.001		< 0.001		< 0.001	
Na (mg/L)	7.16		0.199		0.493	
Ca (mg/L)	7.41		0.319		0.13	
Mg (mg/L)	1.47		< 0.031		< 0.031	
Cu (mg/L)	0.157		0.006		<0.002	

19.3 Summary of ICP Metals Content for Wood and Kraft Pulps

Table A-5-4. Metals content of constant kappa number (approximately 30) pulps employed in this study. Metals contents are in units of mg/kg. Table A-5-1 summarizes the pulping conditions utilized in this study.

Metals	1	2	3	4	5
Cr	0.4	0.4	0.3	0.3	1.6
Mn	35.2	50.3	36.3	41.6	39.4
Fe	8.6	6.5	6.8	5.2	11.6
Co	0.2	0.2	0.2	0.2	0.3
Ni	0.3	0.3	0.3	0.3	0.7
Cu	13.3	6.2	7.3	6.4	5.3
Zn	9.3	6.0	5.2	4.1	5.6
Al	1.5	0.7	2.1	1.4	4.2
B	1.4	0.2	0.4	0.1	0.1
Si	6.3	8.5	7.3	4.9	4.8
P	21.7	22.5	22.9	22.1	23.1
S	632.0	618.0	626.0	633.0	534.0
Se	4.0	4.1	4.2	4.1	4.3
As	3.0	3.1	3.2	3.1	3.2
Mo	0.6	0.6	0.6	0.6	0.6
Sn	1.6	1.6	1.6	1.6	1.6
Sb	1.8	1.9	1.9	1.8	1.9
Pb	1.9	2.0	2.0	2.0	2.1
Tl	4.1	4.2	4.3	4.1	4.3
Sr	6.0	3.2	5.8	3.6	5.2
Ba	4.6	2.2	6.5	2.4	4.2
Na	0.7	6.4	2.4	9.9	0.8
Mg	239.0	248.0	286.0	260.0	245.0
K	1.5	2.1	1.3	4.0	1.7
Ca	1760.0	1080.0	1790.0	1190	1590.0

Table A-5-5. Metals content of constant kappa number (approximately 30) pulps employed in this study. Metals contents are in units of mg/kg. Table A-5-1 summarizes the pulping conditions utilized in this study.

Metals	6	7	8	9	10
Cr	0.7	0.3	0.5	0.3	0.6
Mn	55.2	57.6	61.1	38.0	63.6
Fe	8.0	5.6	8.5	5.3	7.8
Co	0.2	0.2	0.2	0.2	0.2
Ni	0.3	0.3	0.3	0.3	0.3
Cu	4.0	4.8	5.1	3.6	4.7
Zn	5.8	7.4	5.9	6.8	6.6
Al	1.0	4.9	3.0	2.7	1.6
B	0.1	0.1	0.1	0.1	0.1
Si	6.5	6.8	5.6	8.8	8.3
P	22.1	22.0	21.8	22.3	22.0
S	531.1	574.0	725.0	612.0	706.0
Se	4.1	4.1	4.0	4.1	4.1
As	3.1	3.1	3.1	3.1	3.1
Mo	0.6	0.6	0.6	0.6	0.6
Sn	1.6	1.6	1.6	1.6	1.6
Sb	1.8	1.8	1.8	1.9	1.8
Pb	2.0	2.0	1.9	2.0	2.0
Tl	4.1	4.1	4.1	4.2	4.1
Sr	2.8	4.8	3.7	6.2	3.4
Ba	2.5	4.5	2.7	5.5	2.6
Na	1.5	0.7	9.6	0.7	10.3
Mg	252.0	272.0	286.0	244.0	284.0
K	1.3	2.2	1.3	2.6	1.8
Ca	980.0	1430.0	1220.0	1840.0	1110.0

Table A-5-6. Metals content of constant kappa number (approximately 30) pulps employed in this study. Metals contents are in units of mg/kg. Table A-5-1 summarizes the pulping conditions utilized in this study.

Metals	11	12	13	14	15
Cr	0.7	0.4	0.6	0.5	0.3
Mn	54.7	59.2	60.4	53.2	49.8
Fe	7.9	8.1	7.9	6.4	8.3
Co	0.2	0.2	0.2	0.2	0.2
Ni	0.3	0.3	0.3	0.3	0.3
Cu	4.6	4.3	5.1	4.6	5.6
Zn	5.6	6.2	8.0	6.9	5.6
Al	1.7	4.1	1.5	1.1	3.1
B	0.1	0.1	0.1	0.1	0.1
Si	5.9	5.2	7.9	5.3	5.3
P	22.3	22.7	22.4	21.2	21.8
S	564.0	653.0	723.0	576.0	593.0
Se	4.1	4.2	4.3	3.9	4.0
As	3.1	3.2	3.1	3.0	3.1
Mo	0.6	0.6	0.6	0.5	0.6
Sn	1.6	1.6	1.6	1.5	1.6
Sb	1.9	1.9	1.9	1.8	1.8
Pb	2.0	2.0	2.0	1.9	1.9
Tl	4.2	4.2	4.2	4.0	4.1
Sr	3.8	4.0	4.4	3.5	3.8
Ba	4.0	7.0	3.3	4.7	4.4
Na	0.7	0.7	3.1	0.7	1.6
Mg	267.0	265.0	304.0	251.0	260.0
K	2.8	1.9	3.1	1.8	4.0
Ca	1230.0	1230.0	1430.0	1120.0	1160.0

Table A-5-7. Metals content of constant kappa number (approximately 30) pulps employed in this study. Metals contents are in units of mg/kg. Table A-5-1 summarizes the pulping conditions utilized in this study.

Metals	16	17	18	19	20
Cr	1.4	0.6	0.4	0.3	0.4
Mn	48.1	52.4	49.5	53.3	65.8
Fe	10.5	7.3	7.4	6.7	5.3
Co	0.2	0.2	0.2	0.2	0.2
Ni	0.6	0.3	0.3	0.3	0.3
Cu	7.6	4.4	5.1	5.0	6.3
Zn	7.5	5.9	6.3	5.5	6.3
Al	2.5	1.9	1.6	2.5	6.5
B	0.1	0.1	0.1	0.1	2.9
Si	6.5	6.6	6.2	6.8	5.1
P	21.6	21.8	21.7	21.4	23.0
S	628	640.0	588.0	635.0	698.5
Se	4.0	4.0	4.0	3.9	4.2
As	3.0	3.1	3.0	3.0	3.2
Mo	0.6	0.6	0.6	0.6	0.6
Sn	1.5	1.6	1.6	1.5	1.6
Sb	1.8	1.8	1.8	1.8	1.9
Pb	1.9	1.9	1.9	1.9	2.0
Tl	4.0	4.1	4.1	4.0	4.3
Sr	4.2	4.0	3.6	4.0	4.8
Ba	3.5	2.9	7.2	3.4	4.0
Na	3.3	5.3	1.1	5.2	27.7
Mg	272.0	272.0	240.0	273.0	319.8
K	2.0	2.5	3.4	2.4	4.1
Ca	1200.0	1270.0	1120.0	1230.0	1380.0

Table A-5-8. Metals content of constant kappa number (approximately 30) pulps employed in this study. Metals contents are in units of mg/kg. Table A-5-1 summarizes the pulping conditions utilized in this study.

Metals	1	2	3	4	5
Cr	0.3	0.4	0.3	0.3	0.4
Mn	7.3	8.4	5.3	7.1	8.4
Fe	10.4	7.1	4.9	6.2	6.7
Co	0.5	0.5	0.5	0.5	0.5
Ni	0.6	0.6	0.5	0.6	0.5
Cu	7.5	2.9	2.7	2.8	3.2
Zn	5.3	2.5	2.8	3.2	4.1
Al	1.3	1.3	1.3	1.3	2.2
B	2.3	1.9	1.9	0.8	0.5
Si	9.5	14.3	27.4	12.9	30.3
P	42.8	42.7	42.4	42.7	41.9
S	778.8	746.0	598.0	768.0	641.0
Se	8.7	8.8	9.4	13.0	7.7
As	6.0	6.0	5.9	6.0	5.9
Mo	1.1	1.1	1.3	1.1	1.1
Sn	3.0	3.0	3.0	3.0	3.0
Sb	3.5	3.6	3.5	3.5	3.5
Pb	3.8	3.8	3.8	3.8	3.7
Tl	7.8	8.0	7.9	8.0	7.8
Sr	1.1	0.5	0.8	0.6	1.0
Ba	2.3	1.8	1.2	1.4	1.7
Na	13.3	19.4	26.6	22.6	12.3
Mg	45.1	39.4	38.8	43.4	47.5
K	9.1	5.9	9.4	15.9	10.2
Ca	368.6	193.0	282.0	226.0	340.0

Table A-5-9. Metals content of constant kappa number (approximately 30) pulps employed in this study. Metals contents are in units of mg/kg. Table A-5-1 summarizes the pulping conditions utilized in this study.

Metals	6	7	8	9	10
Cr	0.5	0.3	0.3	0.3	0.3
Mn	7.2	10.6	9.3	7.5	9.8
Fe	7.4	6.3	6.0	5.2	7.1
Co	0.5	0.5	0.5	0.5	0.5
Ni	2.3	0.5	0.5	0.6	0.6
Cu	5.1	3.9	2.5	2.5	2.9
Zn	4.1	3.8	2.7	3.9	18.6
Al	1.3	2.1	1.3	2.2	1.3
B	0.7	1.6	1.0	0.5	0.8
Si	7.1	5.4	13.6	6.0	18.5
P	42.6	42.1	42.2	43.1	43.1
S	636.0	700.0	778.0	702.0	824.0
Se	7.8	11.0	15.5	8.0	12.2
As	6.0	5.9	5.9	6.0	6.0
Mo	1.1	1.1	1.1	1.1	1.1
Sn	3.0	3.0	3.0	3.1	3.1
Sb	3.5	3.5	3.5	3.6	3.6
Pb	3.8	3.7	3.7	3.8	3.8
Tl	7.9	7.8	7.9	8.0	7.0
Sr	0.4	0.9	0.6	1.1	0.5
Ba	1.2	1.5	2.3	2.2	1.1
Na	15.1	10.5	20.9	18.7	17.1
Mg	31.5	47.1	42.8	44.7	42.3
K	6.8	6.9	8.6	8.5	7.2
Ca	141.0	279.0	206.0	382.0	190.0

Table A-5-10. Metals content of constant kappa number (approximately 30) pulps employed in this study. Metals contents are in units of mg/kg. Table A-5-1 summarizes the pulping conditions utilized in this study.

Metals	11	12	13	14	15
Cr	0.4	0.3	0.3	0.7	0.3
Mn	6.0	10.8	12.2	9.5	8.8
Fe	8.5	5.0	7.4	8.7	9.1
Co	0.4	0.5	0.5	0.5	0.5
Ni	0.5	0.6	0.6	0.5	0.5
Cu	2.1	2.4	2.7	2.4	3.5
Zn	3.3	3.0	3.3	3.4	3.6
Al	1.2	1.3	1.3	1.2	2.5
B	0.8	0.2	1.1	0.7	0.6
Si	19.9	16.2	11.2	17.9	30.1
P	41.3	43.1	43.2	41.9	41.8
S	585.0	673.0	730.0	621.0	640.0
Se	9.6	13.3	9.8	15.9	13.4
As	5.8	6.0	6.0	5.9	5.8
Mo	1.1	1.1	1.1	1.1	1.1
Sn	2.9	3.1	3.1	3.0	3.0
Sb	3.4	3.6	3.6	3.5	3.5
Pb	3.7	3.8	3.8	3.7	3.7
Tl	7.7	8.0	8.1	7.8	7.8
Sr	0.4	0.8	0.8	0.6	0.7
Ba	1.5	1.0	2.0	1.5	1.3
Na	25.4	28.0	17.1	18.1	28.8
Mg	28.0	47.3	55.8	43.4	43.8
K	8.9	9.0	7.7	10.5	11.8
Ca	158.0	259.0	300.0	224.0	228.0

Table A-5-11. Metals content of constant kappa number (approximately 30) pulps employed in this study. Metals contents are in units of mg/kg. Table A-5-1 summarizes the pulping conditions utilized in this study.

Metals	16	17	18	19	20
Cr	0.3	0.4	0.3	0.3	0.3
Mn	12.2	10.8	7.9	10.1	11.0
Fe	6.7	6.1	5.3	5.6	4.7
Co	0.5	0.5	0.5	0.5	0.5
Ni	0.5	0.5	0.6	0.5	0.5
Cu	3.3	2.4	2.2	2.4	2.8
Zn	4.4	4.3	2.7	2.8	5.5
Al	1.2	1.3	1.3	1.3	1.2
B	0.7	0.3	0.8	0.5	0.6
Si	12.0	29.7	17.2	14.9	21.3
P	41.9	42.3	43.7	41.9	42.2
S	634.0	672.0	621.0	672.0	677.9
Se	12.2	7.8	8.0	8.2	10.7
As	5.9	59	6.1	5.9	5.9
Mo	1.1	1.1	1.1	1.1	1.1
Sn	3.0	3.0	3.1	3.0	3.0
Sb	3.5	3.5	3.6	3.5	3.5
Pb	3.7	3.7	4.1	3.7	3.7
Tl	7.8	7.9	8.1	7.8	7.9
Sr	0.9	0.8	0.5	0.7	0.8
Ba	1.1	1.7	0.8	1.3	1.5
Na	28.2	18.2	29.6	25.1	27.5
Mg	58.2	52.1	36.8	49.6	50.4
K	12.6	7.8	18.5	8.3	8.9
Ca	290.0	280.0	208.0	252.0	266.8

Table A-5-12. Metals content of incremental cook pulps employed in this study. Metals contents are in units of mg/kg. Table A-5-2 summarizes the pulping conditions utilized in this study.

Metals	A-1	A-2	A-3	A-4
Cr	0.3	0.4	0.3	0.7
Mn	79.5	81.8	71.9	73.0
Fe	12.6	11.7	10.5	12.6
Co	0.5	0.5	0.5	0.5
Ni	0.6	1.0	0.7	2.8
Cu	17.5	12.0	8.9	7.4
Zn	27.6	25.1	13.5	14.6
Al	11.4	11.5	11.9	12.5
B	11.2	20.4	14.9	21.6
Si	12.7	14.4	15.9	15.1
P	43.8	43.4	41.9	42.0
S	2590.0	2335.0	1850.0	1560.0
Se	8.1	8.0	7.7	7.7
As	6.1	6.1	5.9	5.9
Mo	1.1	1.1	1.1	1.1
Sn	3.1	3.1	3.0	3.0
Sb	3.6	3.6	3.5	3.5
Pb	3.9	3.8	3.7	3.7
Tl	8.2	8.1	7.8	7.8
Sr	10.0	7.5	5.6	4.3
Ba	9.1	7.2	4.5	3.8
Na	72.7	83.0	68.0	99.3
Mg	553.0	463.7	381.0	379.0
K	12.3	13.0	10.6	15.5
Ca	4020.0	3240.0	2400.0	1960.0

Table A-5-13. Metals content of incremental cook pulps employed in this study. Metals contents are in units of mg/kg. Table A-5-2 summarizes the pulping conditions utilized in this study.

Metals	A-5	A-6	A-7	A-8
Cr	0.4	0.3	1.4	0.7
Mn	64.4	0.3	52.5	54.2
Fe	9.1	0.2	11.1	19.4
Co	0.5	0.5	0.5	0.5
Ni	1.0	0.6	1.8	1.1
Cu	10.2	0.1	9.4	8.3
Zn	14.0	0.2	12.6	12.8
Al	6.6	1.3	5.6	8.9
B	2.1	1.3	4.1	33.3
Si	10.9	0.5	22.2	12.7
P	42.6	42.9	43.0	42.2
S	1230.0	26.5	822.0	843.0
Se	7.8	7.9	7.9	7.8
As	6.0	6.0	6.0	5.9
Mo	1.1	1.1	1.1	1.1
Sn	3.0	3.1	3.1	3.0
Sb	3.5	3.6	3.6	3.5
Pb	3.8	5.6	3.9	3.7
Tl	7.9	8.0	8.0	7.9
Sr	3.2	0.0	2.4	2.1
Ba	2.8	0.2	3.0	3.7
Na	61.3	1.4	44.7	120.0
Mg	340.0	1.6	229.0	267.0
K	14.2	4.1	9.6	13.4
Ca	1480.0	396.0	1040.0	1010.0

Table A-5-14. Metals content of incremental cook pulps employed in this study. Metals contents are in units of mg/kg. Table A-5-2 summarizes the pulping conditions utilized in this study.

Metals	B-1	B-2	B-3	B-4	B-5
Cr	0.3	0.3	0.3	0.3	0.5
Mn	46.9	49.9	50.7	44.4	33.5
Fe	6.0	11.3	10.0	4.6	11.5
Co	0.5	0.5	0.5	0.5	0.5
Ni	1.9	2.5	2.6	2.2	2.1
Cu	11.9	11.7	9.1	3.3	6.3
Zn	11.9	19.0	16.4	5.9	7.3
Al	10.0	7.7	7.5	4.2	5.2
B	3.9	2.2	2.1	1.5	1.3
Si	9.7	8.4	9.6	7.5	8.1
P	44.5	42.5	43.7	43.7	43.1
S	1910.0	1610.0	1525.0	1100.0	893.0
Se	8.2	8.6	8.0	8.0	8.8
As	6.2	6.0	6.1	6.1	6.0
Mo	1.2	1.1	1.1	1.1	1.1
Sn	3.2	3.0	3.1	3.1	3.1
Sb	3.7	3.5	4.1	3.6	3.6
Pb	3.9	3.8	3.9	3.9	3.8
Tl	8.3	7.9	8.1	8.1	8.0
Sr	8.0	6.7	6.4	5.3	4.9
Ba	6.6	6.3	5.5	5.0	4.7
Na	74.8	53.1	52.9	43.4	54.6
Mg	390.0	354.0	353.5	282.0	289.0
K	12.1	11.7	11.7	8.0	11.3
Ca	3150.0	2740.0	2644.8	2110.0	1820.0

Table A-5-15. Metals content of incremental cook pulps employed in this study. Metals contents are in units of mg/kg. Table A-5-2 summarizes the pulping conditions utilized in this study.

Metals	B-6	B-7	B-8	B-9	B-10
Cr	0.3	0.3	0.3	0.3	0.3
Mn	32.5	31.0	29.6	30.0	30.5
Fe	5.0	4.7	9.2	7.1	5.5
Co	0.5	0.5	0.5	0.5	0.5
Ni	9.9	2.2	1.9	3.8	3.1
Cu	5.1	6.2	4.4	3.0	6.5
Zn	7.3	13.5	6.0	7.1	9.2
Al	6.0	6.4	4.4	3.9	3.9
B	3.4	4.0	1.6	1.3	1.1
Si	10.5	19.4	8.0	8.0	10.3
P	42.5	42.8	44.1	43.6	42.5
S	838.0	804.0	688.0	688.0	626.0
Se	11.2	7.9	9.5	10.2	11.5
As	6.0	6.0	6.2	6.1	5.9
Mo	1.1	1.1	1.2	1.1	1.1
Sn	3.0	3.0	3.1	3.1	3.0
Sb	3.5	3.6	3.7	3.6	3.5
Pb	3.8	3.8	3.9	3.9	3.8
Tl	7.9	8.0	8.2	8.1	7.9
Sr	5.2	5.1	4.6	4.8	4.6
Ba	4.9	4.9	4.6	4.9	5.4
Na	52.6	56.7	44.2	43.3	39.9
Mg	262.0	262.0	234.0	242.0	224.0
K	9.9	10.2	7.4	9.8	9.7
Ca	1900.0	1850.0	1650.0	1700.0	1610.0

Table A-5-16. Metals content of a pulp washed completely in deionized water and another pulp completely washed in deionized water and rinsed in tap water. Metals contents are in units of mg/kg.

Metals	Deionized Water	Tap Water Rinse
Cr	1.5	7.0
Mn	28.8	11.0
Fe	10.0	36.2
Co	0.5	0.6
Ni	2.8	6.4
Cu	8.5	32.9
Zn	18.8	48.6
Al	3.3	10.2
B	0.2	0.3
Si	9.0	10.7
P	43.1	56.3
S	612.0	580.5
Se	7.9	10.4
As	6.0	7.9
Mo	1.1	1.5
Sn	3.1	4.0
Sb	3.6	4.7
Pb	3.8	5.0
Tl	8.0	10.5
Sr	3.3	4.9
Ba	9.5	5.3
Na	242.0	51.2
Mg	278.0	263.1
K	27.6	7.5
Ca	893.0	1196.3

Table A-5-17. Metals content of untreated, acid treated, and chelated wood chips. Metals contents are in units of mg/kg.

Metals	Untreated	Acid Treated	Chelated
Cr	0.1	0.3	0.3
Mn	88.0	62.0	25.9
Fe	7.1	17.5	9.3
Co	0.1	0.5	0.7
Ni	0.2	0.5	0.6
Cu	0.9	1.0	0.3
Zn	6.8	6.2	1.2
Al	8.9	7.4	5.5
B	2.2	13.5	4.8
P	40.8	48.4	42.8
S	81.9	98.5	73.4
Se	2.0	7.9	7.9
As	1.5	6.0	6.0
Mo	0.3	1.1	1.1
Sn	0.8	3.0	3.0
Sb	0.9	3.5	3.6
Pb	0.9	3.8	3.8
Tl	2.0	8.0	8.0
Sr	2.6	1.8	2.1
Ba	4.9	3.9	4.7
Na	4.0	148.0	271.0
Mg	151.4	97.7	69.0
K	487.9	116.0	98.7
Ca	572.4	424.0	320.0

Table A-5-18. Metals content of pulps obtained from untreated, acid treated, and chelated wood chips. Metals contents are in units of mg/kg.

Metals	Untreated	Acid Treated	Chelated
Cr	0.3	1.6	0.9
Mn	30.0	25.7	15.4
Fe	7.1	14.1	9.0
Co	0.5	0.5	0.5
Ni	3.8	2.2	1.9
Cu	3.0	3.5	2.9
Zn	7.1	7.4	4.8
Al	3.9	2.5	2.4
B	1.3	2.6	0.8
P	43.6	43.7	43.9
S	688.0	590.2	567.5
Se	10.2	8.0	8.1
As	6.1	6.1	6.1
Mo	1.1	1.1	1.1
Sn	3.1	3.1	3.1
Sb	3.6	3.6	3.6
Pb	3.9	3.9	3.9
Tl	8.1	8.1	8.2
Sr	4.8	2.7	2.6
Ba	4.9	4.0	4.4
Na	43.3	787.9	884.0
Mg	242.0	196.3	189.2
K	9.8	21.6	23.7
Ca	1700.0	692.5	678.8

19.4 Summary of Pulp Properties

Table A-5-19. Brightness and chromophore index of the constant kappa number (approximately 30) series of pulps prior to the cold acid treatment. Table A-5-1 summarizes the pulping conditions utilized in this study.

Condition	Brightness (%)	Chromophore Index
1	29.2 ± 0.19	119.7 ± 2.5
2	32.1 ± 0.19	102.8 ± 0.9
3	28.2 ± 0.43	131.2 ± 3.1
4	30.3 ± 0.32	115.3 ± 3.9
5	29.2 ± 0.51	121.7 ± 2.0
6	30.8 ± 0.32	108.8 ± 0.7
7	27.7 ± 0.55	136.7 ± 2.2
8	31.2 ± 0.41	110.7 ± 2.7
9	27.5 ± 0.15	141.1 ± 2.0
10	31.6 ± 0.19	107.7 ± 1.6
11	30.2 ± 0.28	115.0 ± 1.3
12	30.6 ± 0.23	115.0 ± 1.7
13	29.9 ± 0.34	117.9 ± 0.9
14	30.6 ± 0.17	112.3 ± 0.8
15	30.5 ± 0.43	111.6 ± 0.8
16	30.1 ± 0.43	112.5 ± 0.7
17	29.9 ± 0.43	112.9 ± 1.9
18	31.1 ± 0.43	103.5 ± 1.2
19	30.0 ± 0.43	109.8 ± 3.6
20	30.6 ± 0.43	106.6 ± 4.0

Table A-5-20. Brightness and chromophore index of the constant kappa number (approximately 30) series of pulps after the cold acid treatment. Table A-5-1 summarizes the pulping conditions utilized in this study.

Condition	Brightness (%)	Chromophore Index
1	33.1 ± 0.15	66.9 ± 2.5
2	34.9 ± 0.87	58.0 ± 0.9
3	32.9 ± 0.66	64.3 ± 3.1
4	35.2 ± 0.21	58.8 ± 3.9
5	32.4 ± 0.30	69.2 ± 2.0
6	35.7 ± 0.53	57.0 ± 0.7
7	34.1 ± 0.30	61.2 ± 2.2
8	34.3 ± 0.30	60.0 ± 2.7
9	32.4 ± 0.32	68.8 ± 2.0
10	35.5 ± 0.11	57.8 ± 1.6
11	34.5 ± 0.17	59.7 ± 1.3
12	34.8 ± 0.21	58.1 ± 1.7
13	34.4 ± 0.21	61.4 ± 0.9
14	35.1 ± 0.45	58.4 ± 0.8
15	34.0 ± 0.53	61.6 ± 0.8
16	34.5 ± 0.19	60.1 ± 0.7
17	34.0 ± 0.30	61.3 ± 1.9
18	35.4 ± 0.38	56.5 ± 1.2
19	34.4 ± 0.23	58.9 ± 3.6
20	34.4 ± 0.77	57.3 ± 4.0

Table A-5-21. Brightness and chromophore index of the pulps washed completely in deionized water and another later rinsed in tap water.

Condition	Brightness (%)	Chromophore Index
Deionized Water	28.6 ± 0.23	143.5 ± 5.6
Tap Water	27.8 ± 0.23	156.9 ± 5.3

Table A-5-22. Brightness and chromophore index of pulps obtained from untreated, acid treated, and chelated wood chips.

Condition	Brightness (%)	Chromophore Index
Untreated	25.3 ± 0.28	153.2 ± 3.3
Acid Treated	28.7 ± 0.36	140.4 ± 3.3
Chelated	28.4 ± 0.19	145.1 ± 3.0

20. APPENDIX 6. SUPPORTING DATA FOR CHAPTER #6

20.1 Summary of ICP Metals Content for Kraft Pulps

Table A-6-1. Metals content obtained from normal kraft, PS, AQ, and PS/AQ pulps. Metals contents are in units of mg/kg.

Metals	Normal Kraft	PS	AQ	PS/AQ
Cr	0.7	1.0	0.5	0.6
Mn	35.7	43.2	35.9	38.1
Fe	10.2	8.2	8.1	5.5
Co	0.4	0.4	0.4	0.4
Ni	0.7	0.5	07	0.5
Cu	24.2	19.7	13.8	8.7
Zn	29.9	24.8	16.5	12.5
Al	1.7	1.3	2.5	2.0
B	1.4	2.3	0.5	1.2
P	38.8	38.4	38.3	40.2
S	544.4	583.0	574.7	567.6
Se	7.1	7.1	7.1	7.4
As	5.4	5.4	5.4	5.6
Mo	1.0	1.0	1.0	1.0
Sn	2.8	2.7	2.7	2.9
Sb	3.2	3.7	3.2	3.3
Pb	3.4	3.4	3.4	3.6
Tl	7.2	7.2	7.1	7.5
Sr	7.0	6.8	6.3	6.1
Ba	15.0	16.4	13.4	13.4
Na	52.7	51.4	42.9	34.4
Mg	137.9	129.3	99.4	101.8
K	12.8	12.4	10.9	9.4
Ca	2230.0	2330.0	1920.0	2030.0

20.2 ^{31}P NMR for Hydroxyl Group Spectra of Residual and Dissolved Lignins

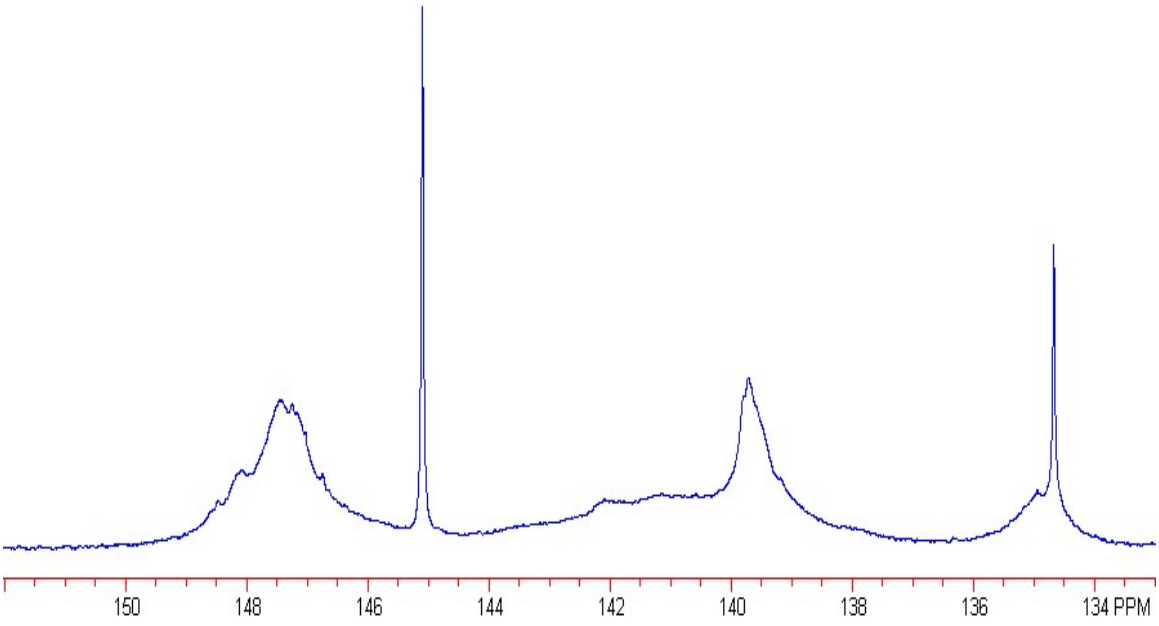

Figure A-6-1. ^{31}P NMR spectrum of residual lignin isolated from conventional kraft pulp.

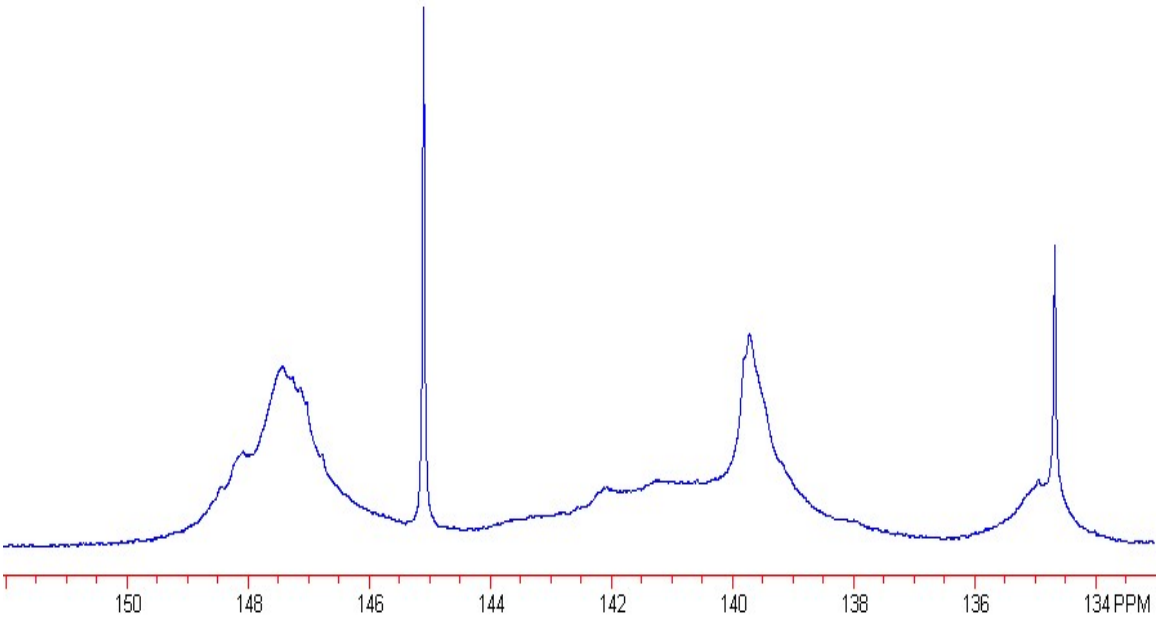

Figure A-6-2. ^{31}P NMR spectrum of residual lignin isolated from polysulfide (PS) kraft pulp.

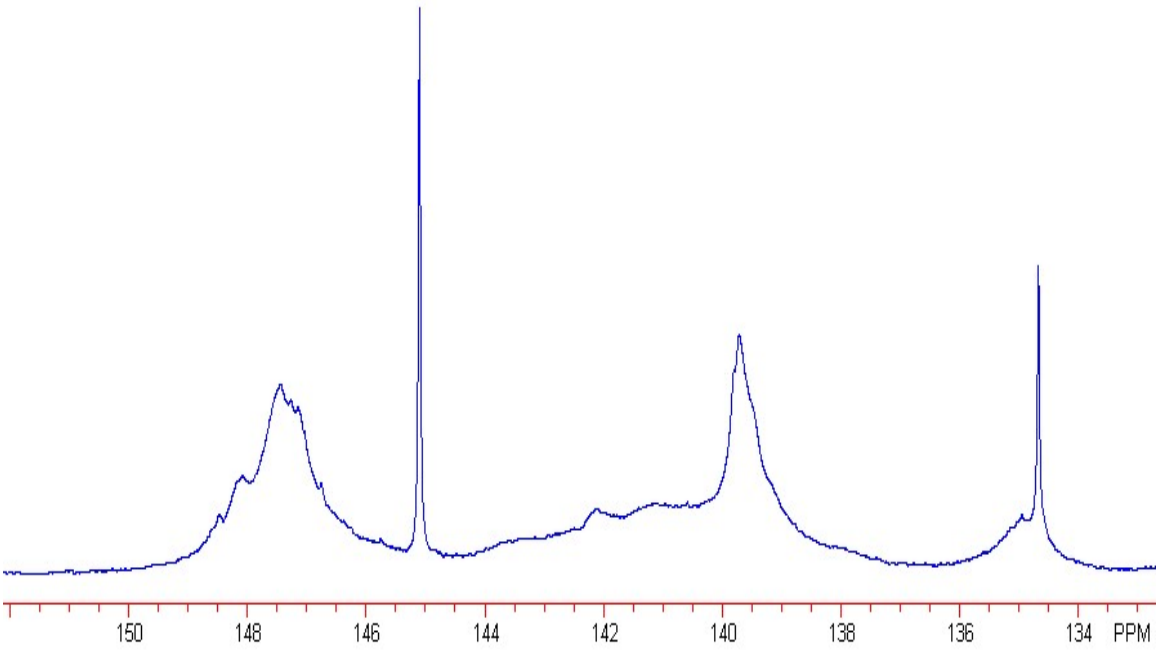

Figure A-6-3. ^{31}P NMR spectrum of residual lignin isolated from anthraquinone (AQ) kraft pulp.

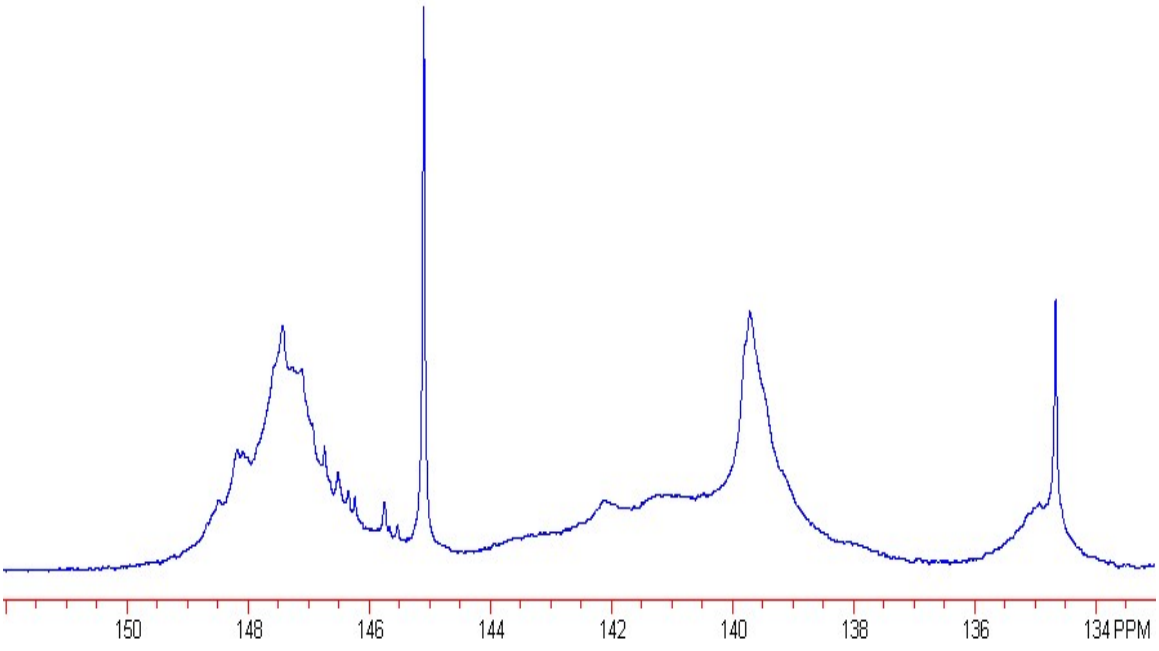

Figure A-6-4. ^{31}P NMR spectrum of residual lignin isolated from polysulfide/anthraquinone (PS/AQ) kraft pulp.

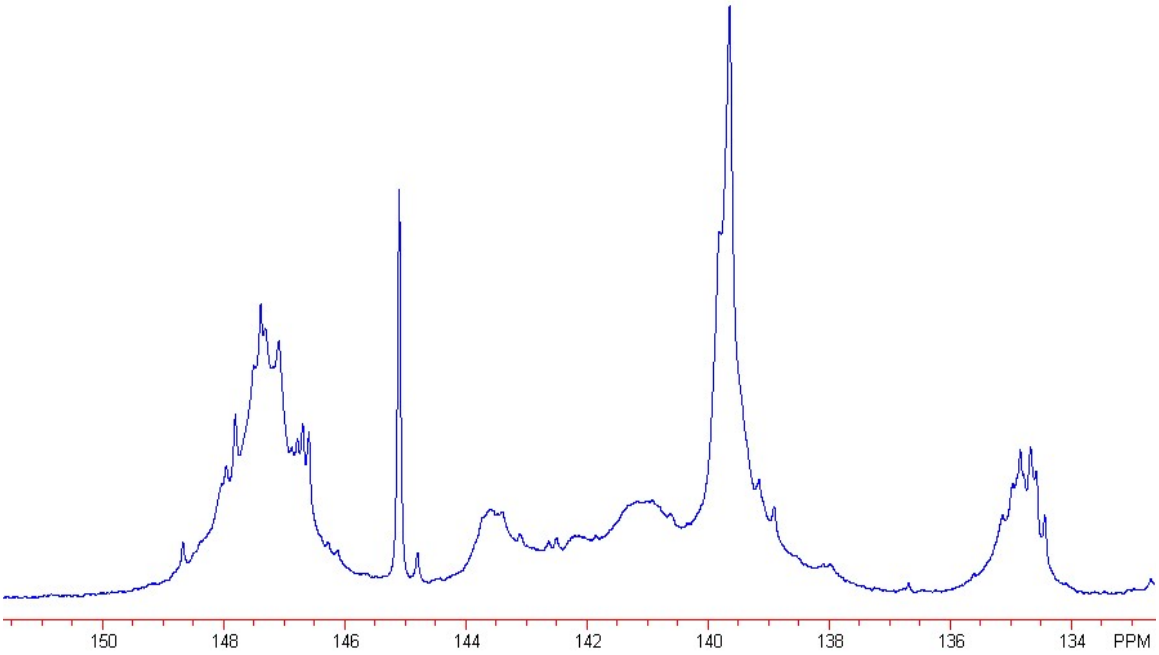

Figure A-6-5. ^{31}P NMR spectrum of residual lignin isolated from normal reference kraft black liquor #1.

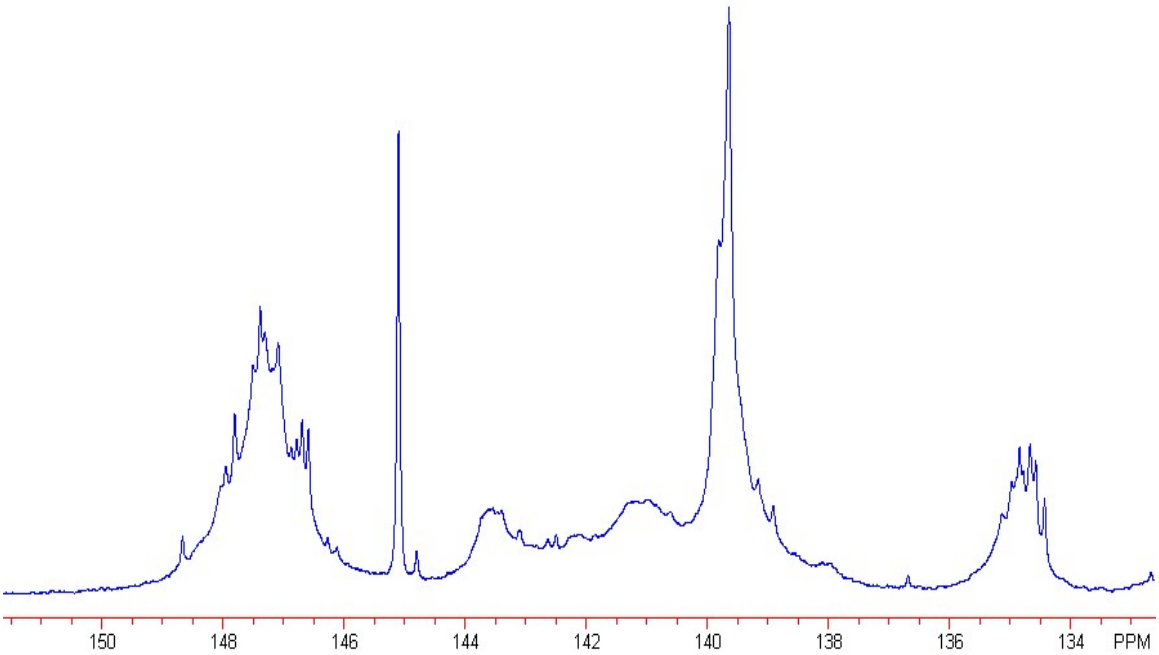

Figure A-6-6. ^{31}P NMR spectrum of dissolved kraft lignin isolated from normal reference kraft black liquor #2.

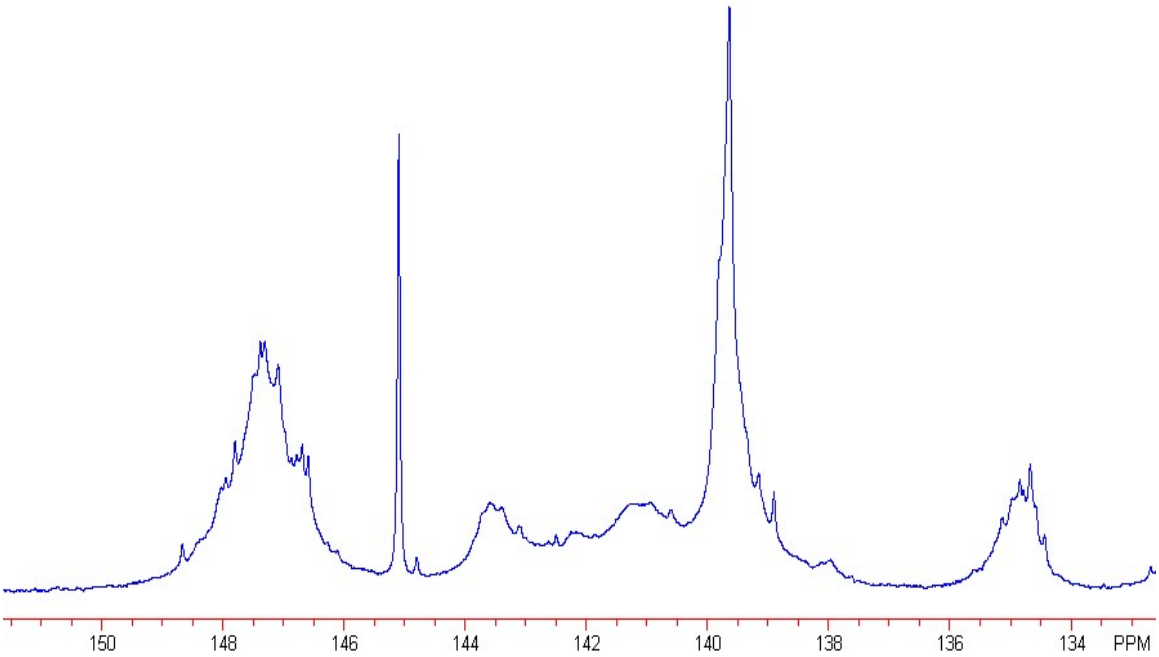

Figure A-6-7. ^{31}P NMR spectrum of dissolved kraft lignin isolated from normal reference kraft black liquor #3.

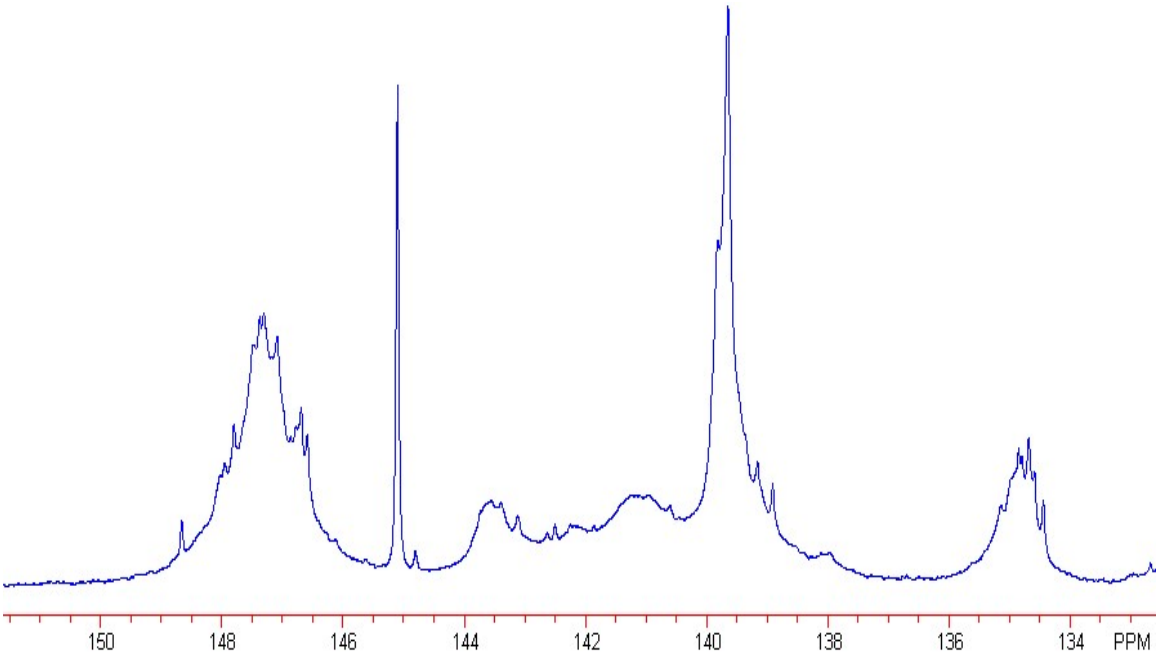

Figure A-6-8. ^{31}P NMR spectrum of dissolved kraft lignin isolated from polysulfide (PS) kraft black liquor.

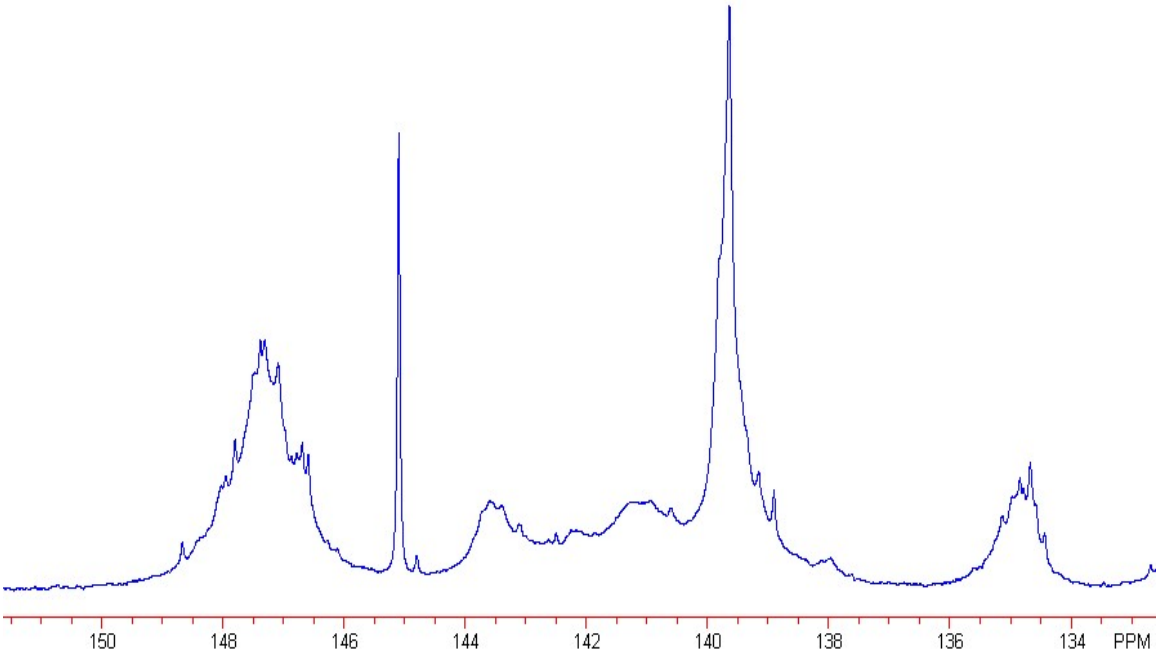

Figure A-6-9. ^{31}P NMR spectrum of dissolved kraft lignin isolated from anthraquinone (AQ) kraft black liquor.

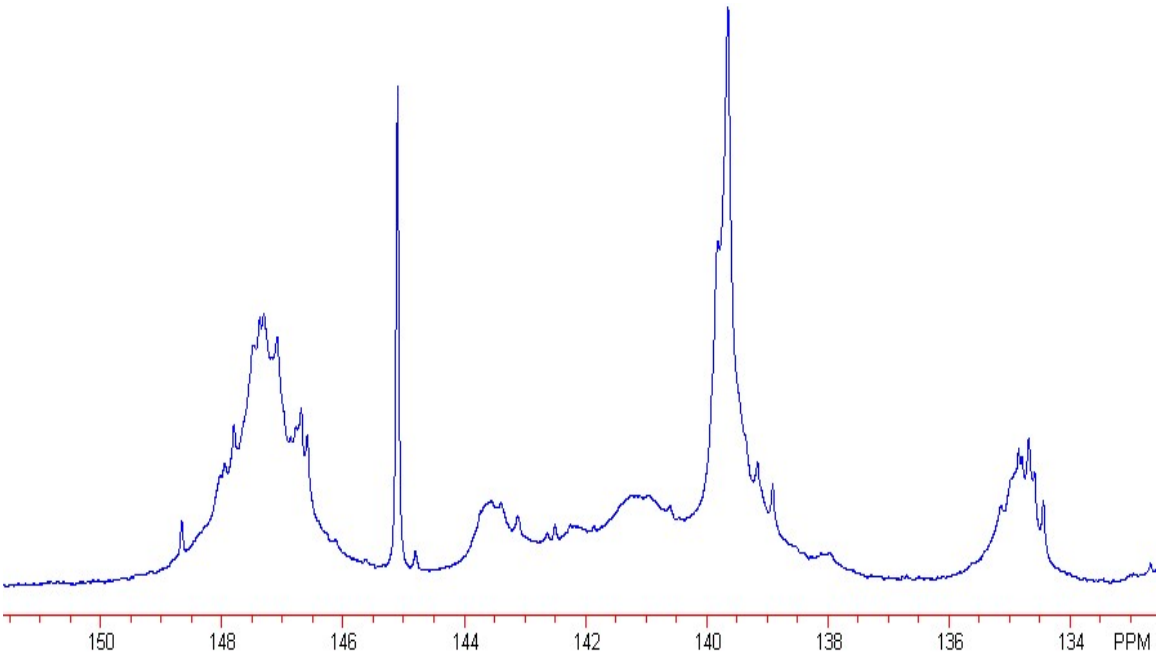

Figure A-6-10. ^{31}P NMR spectrum of dissolved kraft lignin isolated from polysulfide/anthraquinone (PS/AQ) kraft black liquor.

20.3 Summary of ^{31}P NMR for Hydroxyl Group Data for Residual and Dissolved Lignins

Table A-6-2. ^{31}P NMR data for residual lignins from the normal kraft, PS, AQ, and PS/AQ pulps.

Functional group	Integration Region/ppm	Normal Kraft (mmol/g)	PS (mmol/g)	AQ (mmol/g)	PS/AQ (mmol/g)
Aliphatic OH	149.0-145.6	1.090	1.178	1.165	1.284
C5 condensed phenolic OH	144.4-140.4	0.710	0.754	0.813	0.757
5-5'-Biphenyl OH	141.7-140.4	0.378	0.408	0.423	0.407
C5 noncondensed phenolic OH	140.4-137.6	0.806	0.872	0.924	0.891
Catechol OH	139.0-138.2	0.124	0.132	0.135	0.127
p-hydroxyphenyl OH	138.2-137.3	0.078	0.079	0.081	0.072
Carboxyl OH	136.0-133.8	0.384	0.378	0.336	0.326

Table A-6-3. ^{31}P NMR data for dissolved kraft lignins from the normal kraft, PS, AQ, and PS/AQ pulps.

Functional group	Integration Region/ppm	Normal Kraft (mmol/g)	PS (mmol/g)	AQ (mmol/g)	PS/AQ (mmol/g)
Aliphatic OH	149.0-145.6	1.450	1.576	1.484	1.616
C5 condensed phenolic OH	144.4-140.4	1.050	1.110	1.154	1.098
5-5'-Biphenyl OH	141.7-140.4	0.506	0.524	0.534	0.510
C5 noncondensed phenolic OH	140.4-137.6	1.301	1.356	1.397	1.374
Catechol OH	139.0-138.2	0.156	0.173	0.165	0.171
p-hydroxyphenyl OH	138.2-137.3	0.076	0.093	0.088	0.082
Carboxyl OH	136.0-133.8	0.452	0.498	0.441	0.447

21. APPENDIX 7: SUPPORTING DATA FOR CHAPTER #7

21.1 Photographs of Pretreated Wood Chips

Figure A-7-1. Photograph of normal, untreated wood chips.

Figure A-7-2. Photograph of laccase + 2,2´-azino-*bis*(3-ethylbenzthiazoline-6-sulfonate) (ABTS) treated wood chips.

Figure A-7-3. Photograph of laccase + 1-hydroxybenzotriazole (HBT) treated wood chips.

Figure A-7-4. Photograph of laccase + violuric acid (VA) treated wood chips.

21.2 ^{13}C NMR Spectra of Pretreatment Effluents and Dissolved Lignins

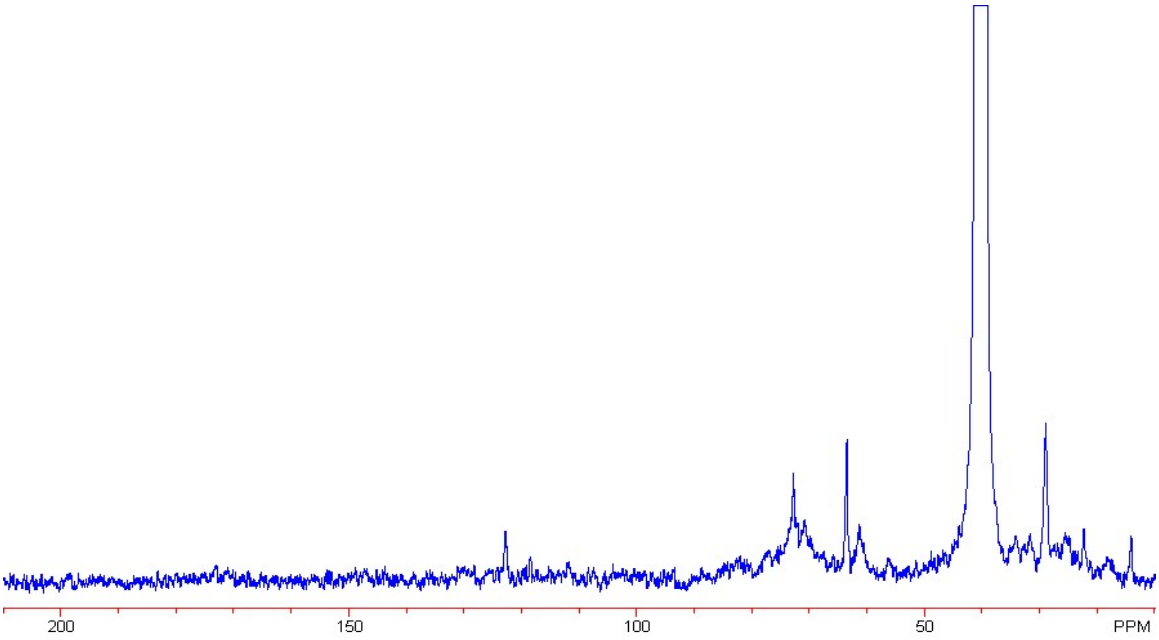

Figure A-7-5. Effluent from control pretreatment adjusted to pH 4.5 and containing no laccase or mediator.

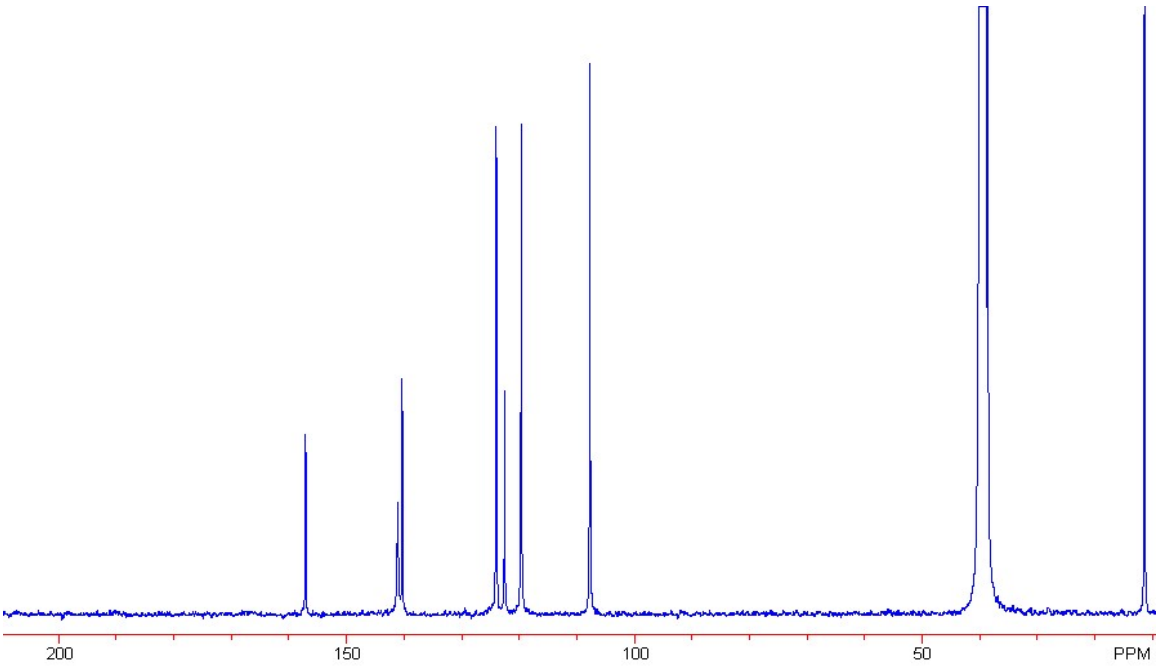

Figure A-7-6. Effluent from ABTS pretreatment adjusted to pH 4.5 and containing 44 mmol/100g wood chips of mediator.

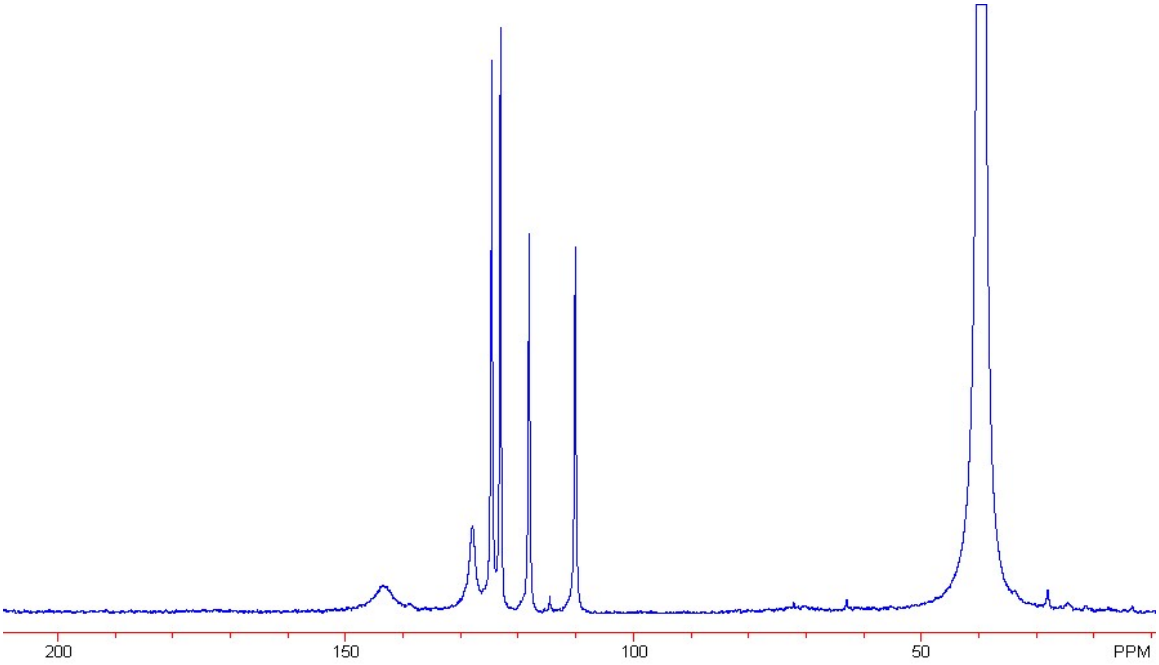

Figure A-7-7. Effluent from HBT pretreatment adjusted to pH 4.5 and containing 44 mmol/100g wood chips of mediator.

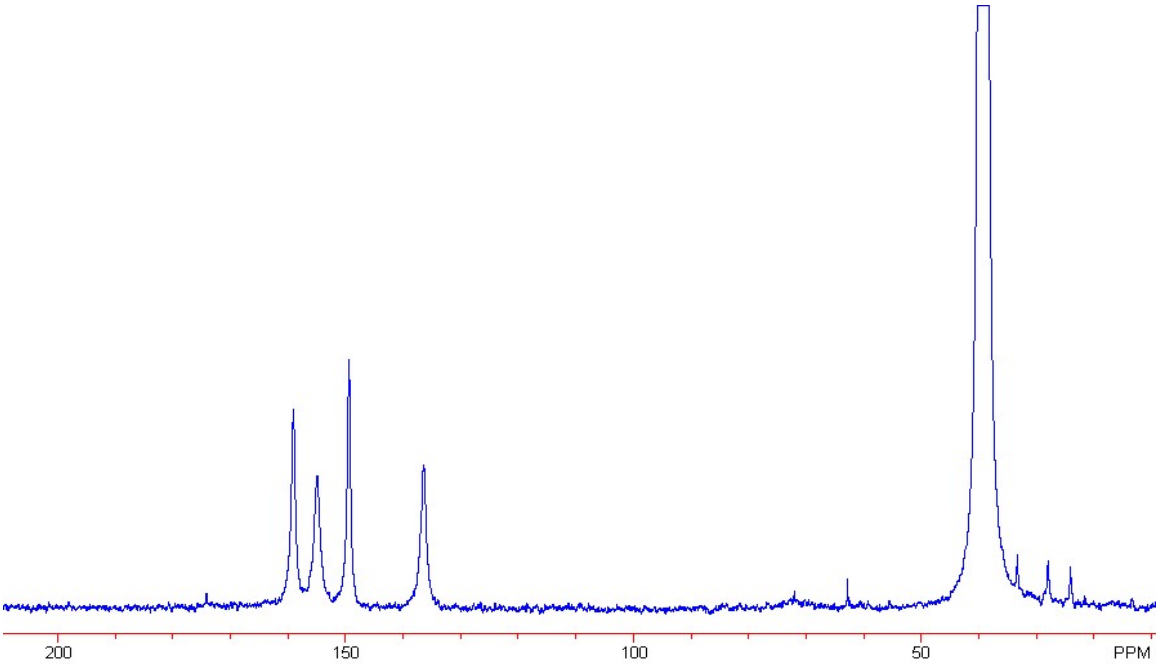

Figure A-7-8. Effluent from VA pretreatment adjusted to pH 4.5 and containing 44 mmol/100g wood chips of mediator.

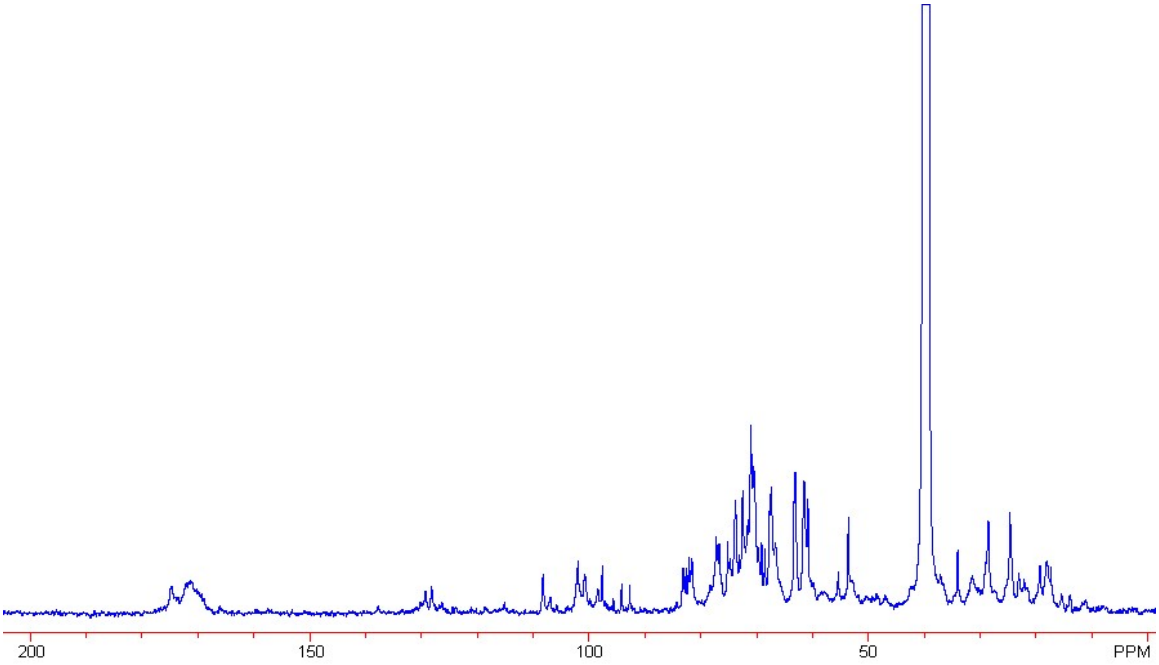

Figure A-7-9. Effluent from laccase pretreatment adjusted to pH 4.5.

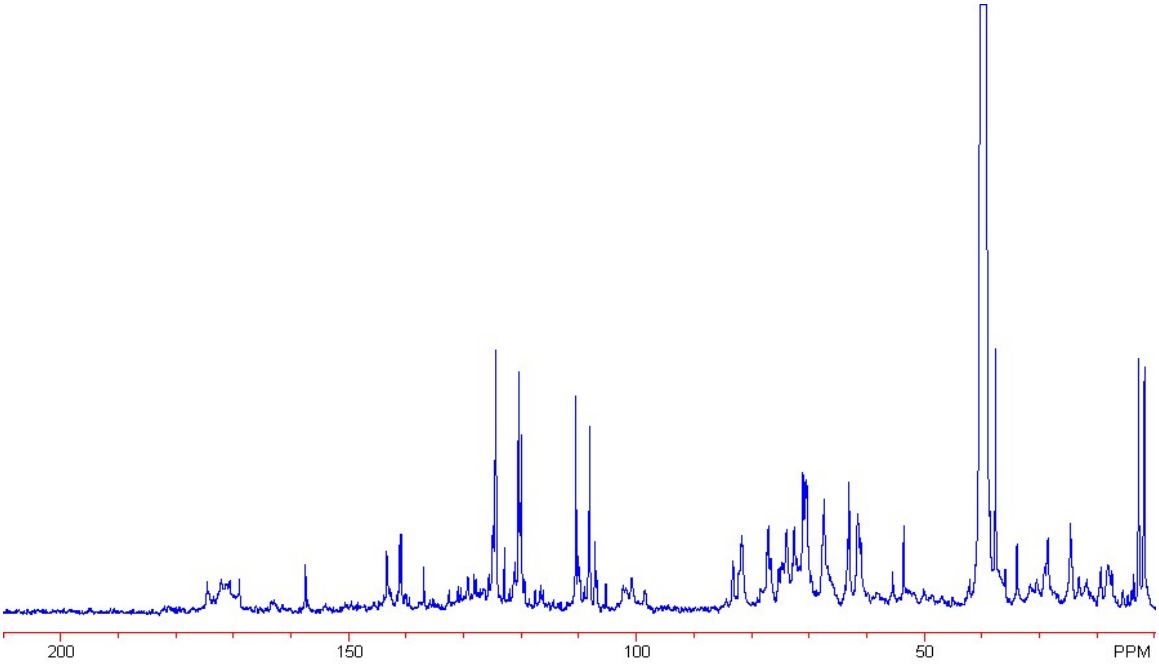

Figure A-7-10. Effluent from laccase + ABTS pretreatment adjusted to pH 4.5 and containing 11 mmol/100g wood chips of mediator.

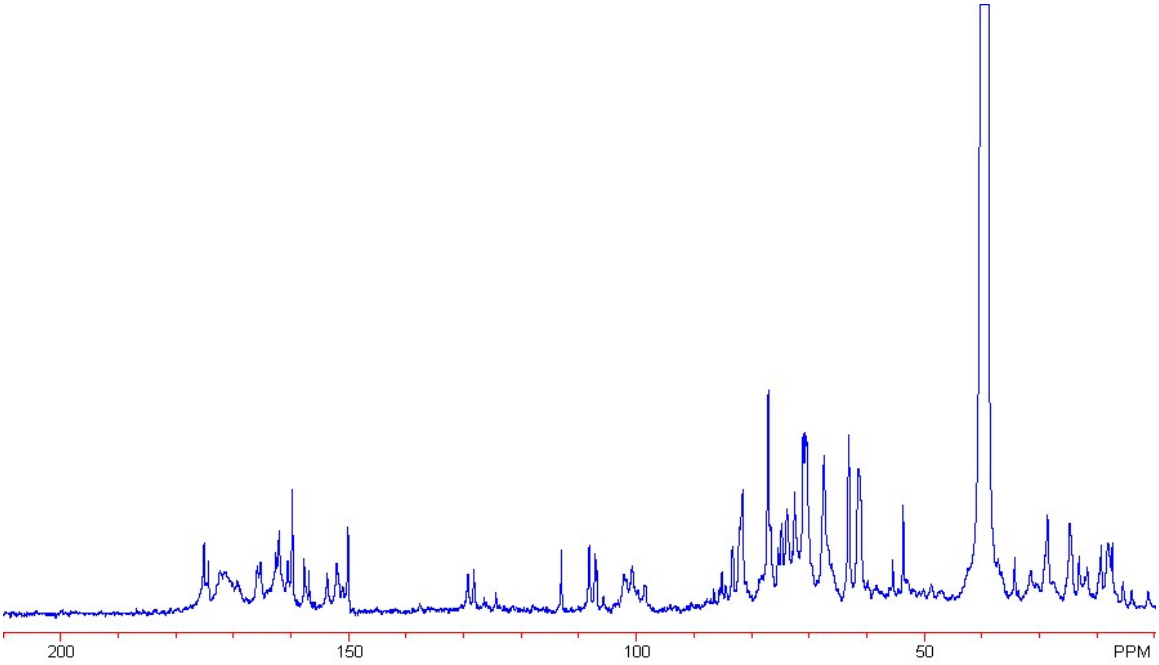

Figure A-7-11. Effluent from laccase + ABTS pretreatment adjusted to pH 4.5 and containing 22 mmol/100g wood chips of mediator.

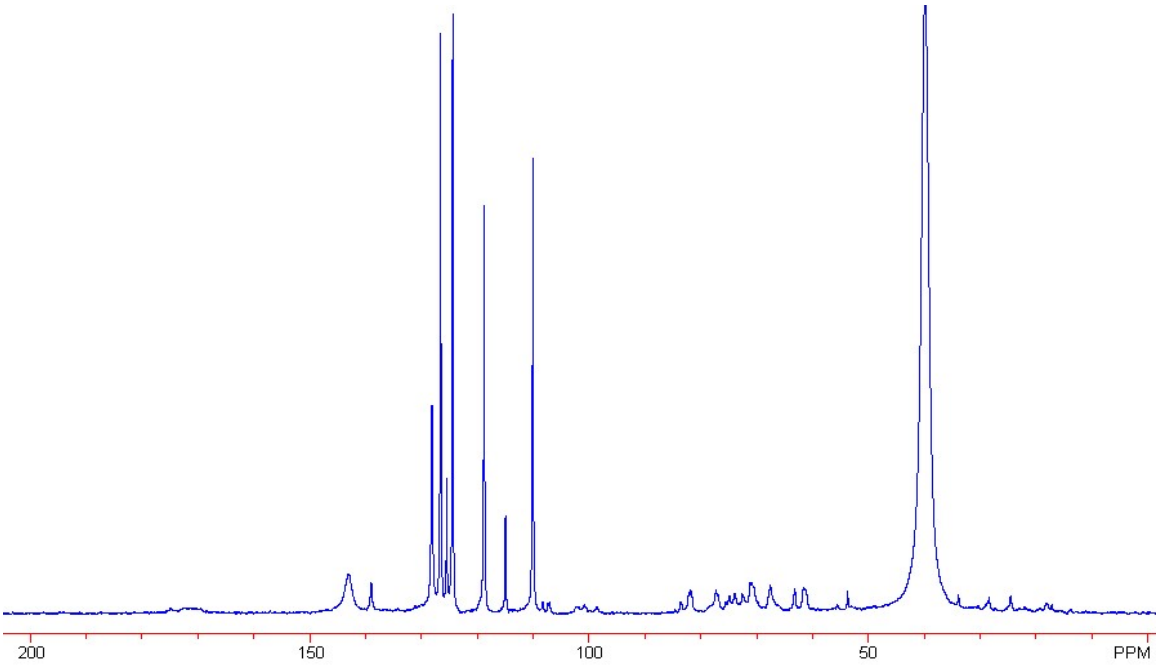

Figure A-7-12. Effluent from laccase + HBT pretreatment adjusted to pH 4.5 and containing 44 mmol/100g wood chips of mediator.

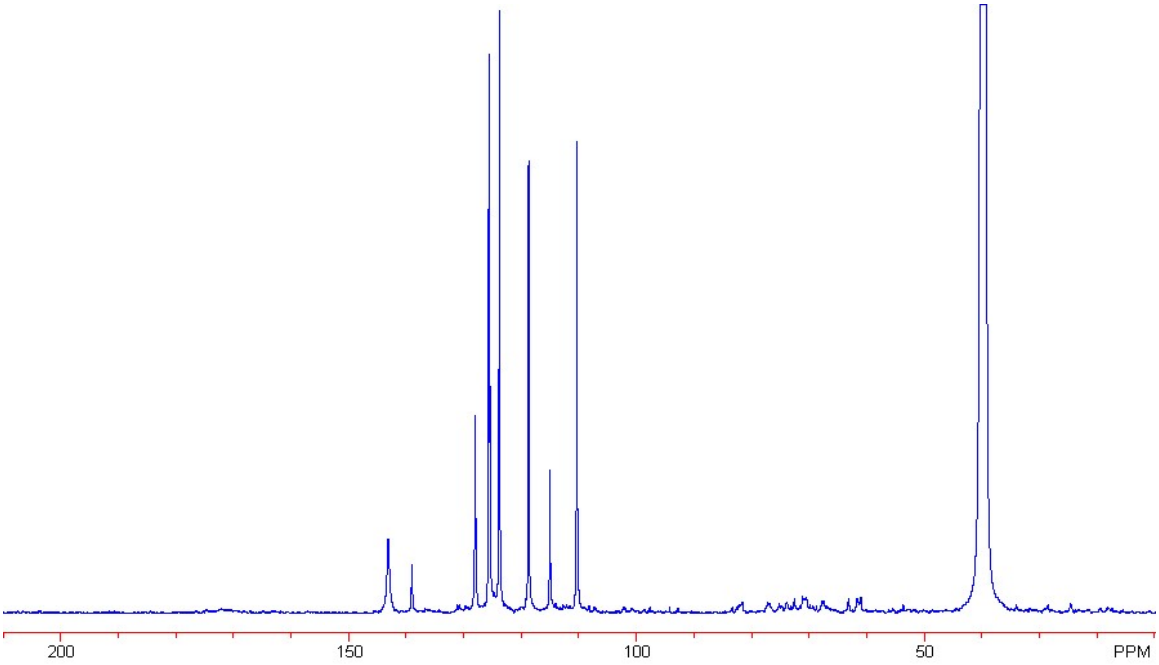

Figure A-7-13. Effluent from laccase + HBT pretreatment adjusted to pH 4.5 and containing 176 mmol/100g wood chips of mediator.

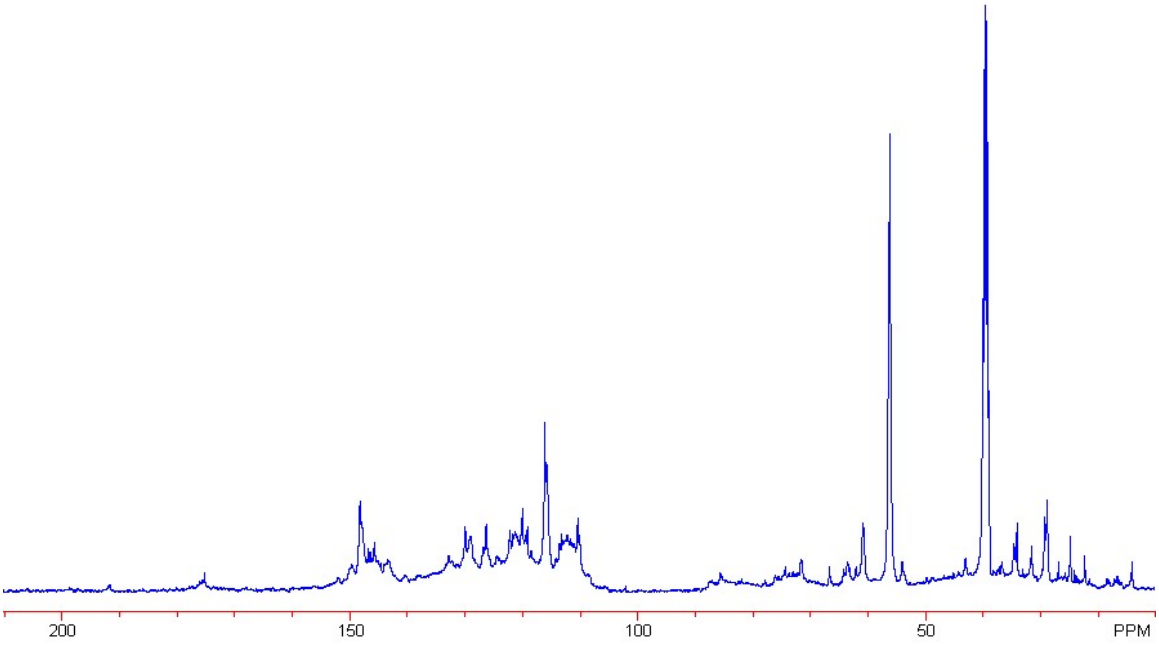

Figure A-7-14. Dissolved kraft lignin from control kraft cook. Final kappa number of resulting pulp approximately 30.

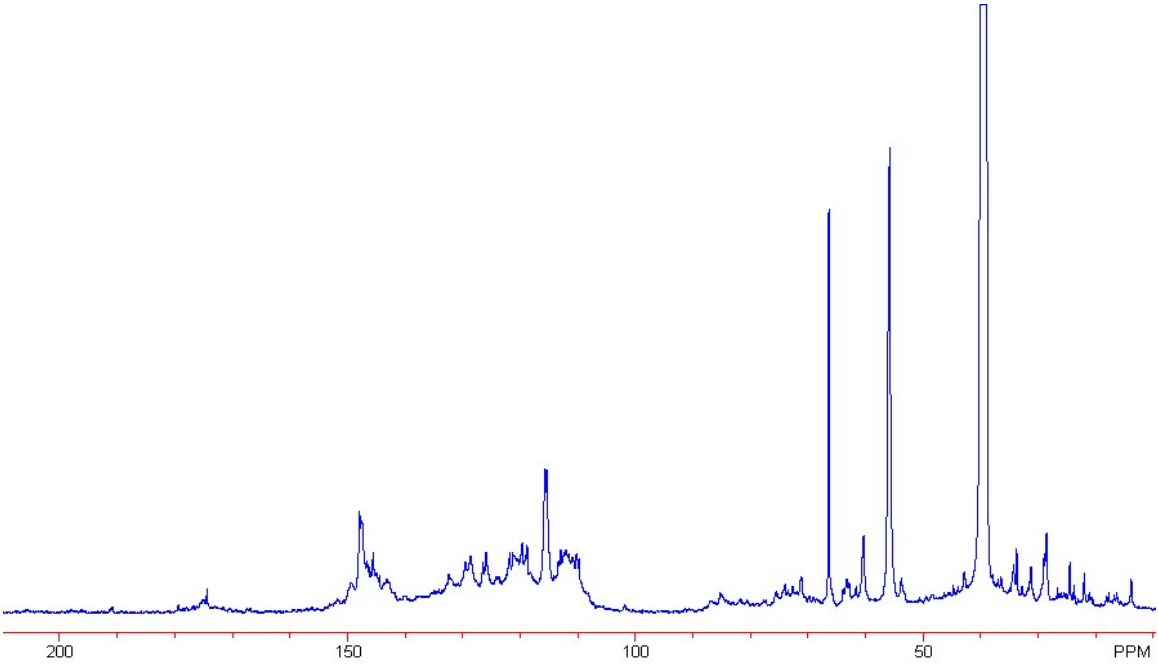

Figure A-7-15. Dissolved kraft lignin from cooked laccase pretreated wood chips. Final kappa number of resulting pulp approximately 30.

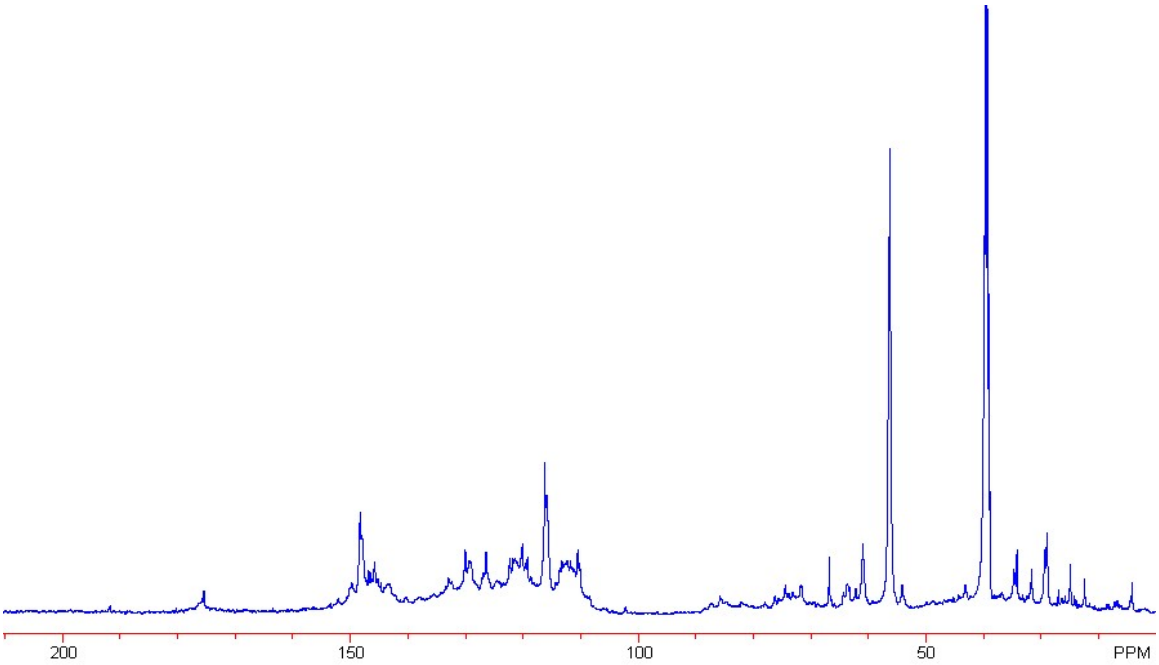

Figure A-7-16. Dissolved kraft lignin from cooked laccase + ABTS pretreated wood chips containing 11 mmol/100g wood chips ABTS. Final kappa number of resulting pulp approximately 30.

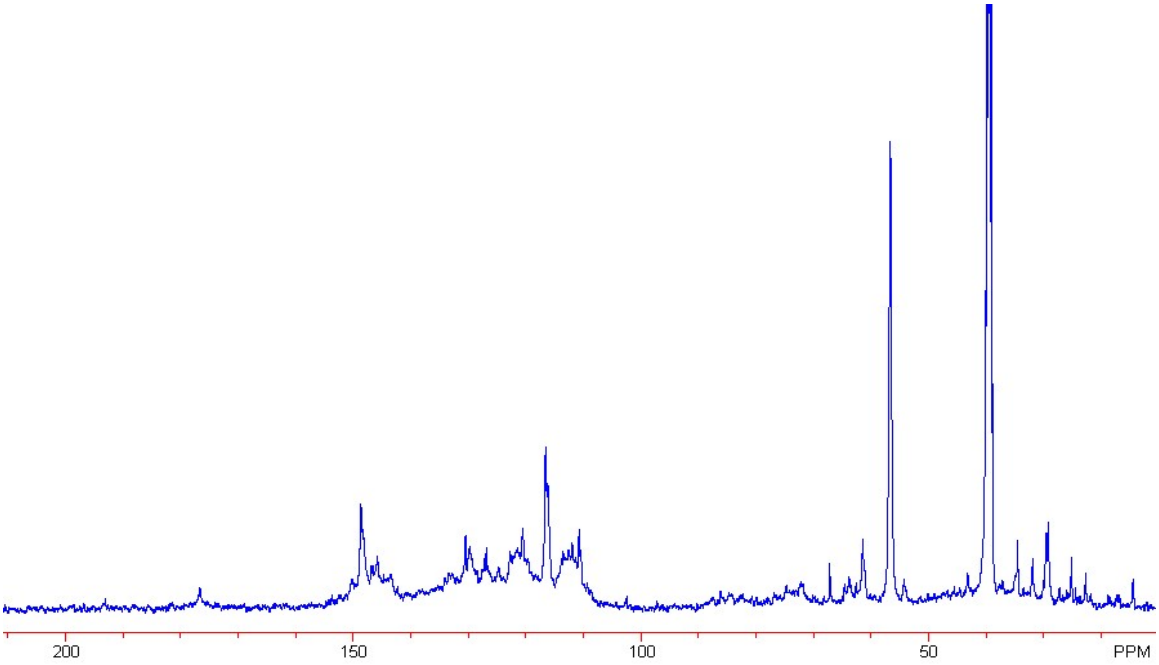

Figure A-7-17. Dissolved kraft lignin from cooked laccase + VA pretreated wood chips containing 11 mmol/100g wood chips VA. Final kappa number of resulting pulp approximately 30.

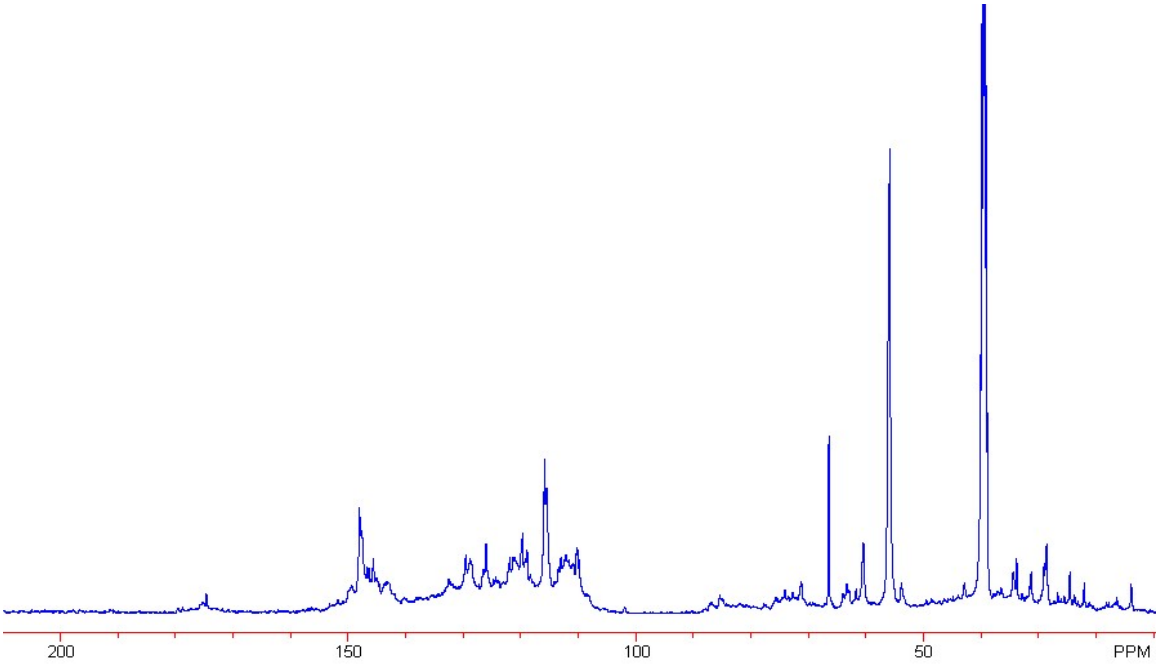

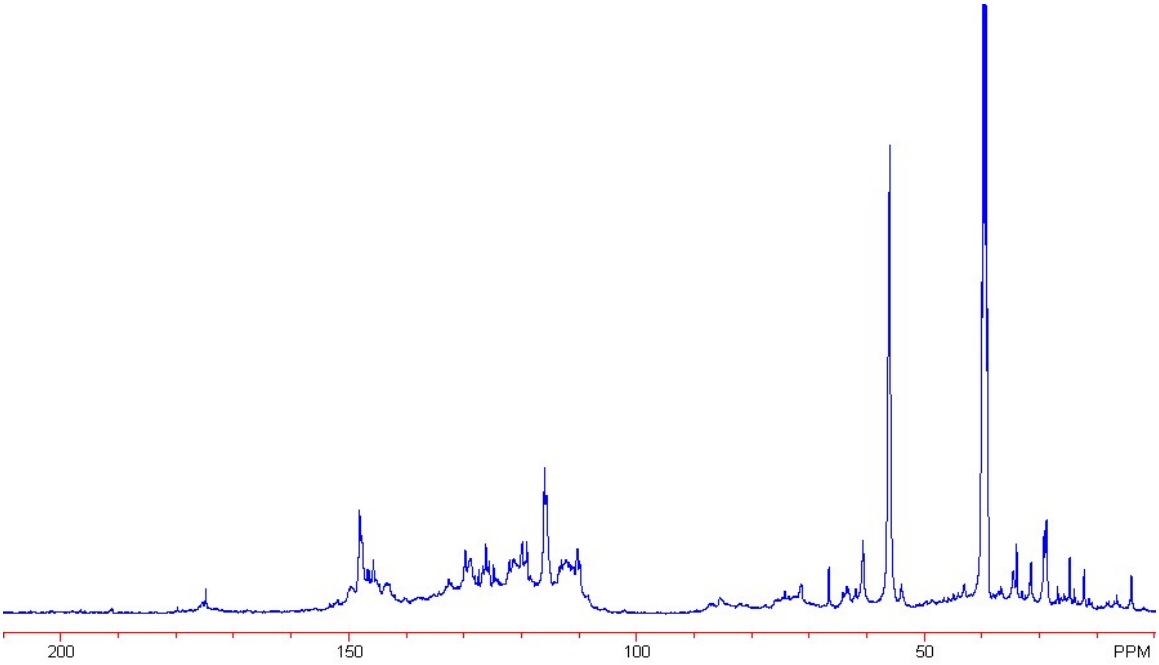

Figure A-7-19. Dissolved kraft lignin from cooked laccase + HBT pretreated wood chips containing 176 mmol/100g wood chips HBT. Final kappa number of resulting pulp approximately 30.

21.3 Summary of ^{13}C NMR Data for Dissolved Lignins

Table A-7-1. ^{13}C NMR data for dissolved kraft lignins isolated from the laccase-mediator pretreated kraft cooks.

Region	Functional group	Integral region/ppm	Normal Kraft C/C_9	Laccase C/C_9	L + HBT (44 mmol/100 g) C/C_9
1	COOH	178-162.5	0.269	0.256	0.227
2	C3,C4 (-C-Ar-O)	154.0-140.0	1.344	1.416	1.441
3	C1, (-C-Ar-C)	140.0-127.0	1.317	1.250	1.341
4	C5, (-C-Ar-C)	127.0-123.0	0.554	0.536	0.542
5	C6, (-C-Ar-H)	123.0-117.0	1.094	1.034	1.038
6	C5, (-C-Ar-H)	117.0-114.0	0.709	0.710	0.689
7	C2, (-C-Ar-H)	114.0-106.0	0.982	1.034	0.949
2-4	Substituted aromatic C	154.0-123.0	3.215	3.202	3324
5-7	Unsubstituted aromatic C	123.0-106.0	2.785	2.778	2.676
8	Aliphatic C-O (Cβ.)	90.0-78.0	0.418	0.426	0.412
9	Aliphatic C-O (Cα.)	78.0-67.0	0.594	0.675	0.614
10	Aliphatic C-OR	67.0-61.0	0.246	0.248	0.261
11	Aliphatic C-O, Cγ	61.0-57.0	0.329	0.336	0.325
12	OCH_3	57.0-54.0	1.103	1.141	1.154
13	Cβ in ββ and Cβ in β5	54.0-52.0	0.097	0.133	0.080
14	OCH_3 in MAME Structure	52.0-49.0	0.122	0.142	0.113
15	CH_2 in Diaryl methane	29.5-27.0	0.332	0.305	0.299

Table A-7-2. ^{13}C NMR data for dissolved kraft lignins isolated from the laccase-mediator pretreated kraft cooks.

Region	Functional group	Integral region/ppm	L + ABTS (11 mmol/100g) C/C_9	L + VA (22 mmol/g) C/C_9	L + HBT (176 mmol/100 g) C/C_9
1	COOH	178-162.5	0.328	0.402	0.216
2	C3,C4 (-C-Ar-O)	154.0-140.0	1.441	1.441	1.373
3	C1, (-C-Ar-C)	140.0-127.0	1.341	1.438	1.303
4	C5, (-C-Ar-C)	127.0-123.0	0.542	0.516	0.595
5	C6, (-C-Ar-H)	123.0-117.0	1.038	1.005	1.047
6	C5, (-C-Ar-H)	117.0-114.0	0.689	0.644	0.708
7	C2, (-C-Ar-H)	114.0-106.0	0.949	0.956	0.973
2-4	Substituted aromatic C	154.0-123.0	3.324	3.395	3.271
5-7	Unsubstituted aromatic C	123.0-106.0	2.676	2.605	2.728
8	Aliphatic C-O (Cβ.)	90.0-78.0	0.412	0.519	0.358
9	Aliphatic C-O (Cα.)	78.0-67.0	0.614	0.639	0.543
10	Aliphatic C-OR	67.0-61.0	0.261	0.301	0.233
11	Aliphatic C-O, Cγ	61.0-57.0	0.325	0.294	0.323
12	OCH_3	57.0-54.0	1.154	1.034	1.198
13	Cβ in ββ and Cβ in β5	54.0-52.0	0.080	0.094	0.093
14	OCH_3 in MAME Structure	52.0-49.0	0.113	0.147	0.109
15	CH_2 in Diaryl methane	29.5-27.0	0.299	0.297	0.342

22. APPENDIX 8: SUPPORTING DATA FOR CHAPTER #8

22.1 Summary of Experimental Conditions for Pretreatments

Table A-8-1. Experimental conditions for wood chip pretreatments.

Sample ID	Consistency	Temp.	Time (hrs)	pH	Dosage	$MgSO_4$	DTPA	Na_2SiO_3
Q-1	10%	50ºC	2	2.5	0	-	-	-
Q-2	10%	50ºC	2	3	0	-	-	-
Q-3	10%	50ºC	2	4	0	-	-	-
Q-4	10%	50ºC	2	5	0	-	-	-
Q-5	10%	50ºC	2	6	0	-	-	-
Q-6	10%	50ºC	2	"neutral"	0	-	-	-
Q-7	10%	50ºC	2	2.5	0.5%	-	-	-
Q-8	10%	50ºC	2	3	0.5%	-	-	-
Q-9	10%	50ºC	2	4	0.5%	-	-	-
Q-10	10%	50ºC	2	5	0.5%	-	-	-
Q-11	10%	50ºC	2	6	0.5%	-	-	-
Q-12	10%	50ºC	2	"neutral"	0.5%	-	-	-
B-1	10%	65ºC	2	"neutral"	0	-	-	-
B-2	10%	65ºC	2	"neutral"	0.5%	-	-	-
B-3	10%	65ºC	2	"neutral"	1%	-	-	-
B-4	10%	65ºC	2	"neutral"	5%	-	-	-
B-5	10%	65ºC	2	"neutral"	10%	-	-	-
B-6	10%	65ºC	2	10	0	-	-	-
B-7	10%	65ºC	2	10	0.5%	-	-	-
B-8	10%	65ºC	2	10	1%	-	-	-
B-9	10%	65ºC	2	10	5%	-	-	-
B-10	10%	65ºC	2	10	10%	-	-	-

Table A-8-2. Experimental conditions for wood chip pretreatments.

Sample ID	Consistency	Temp.	Time (hrs)	pH	Dosage	$MgSO_4$	DTPA	Na_2SiO_3
P-1	10%	70ºC	2	"neutral"	0	0.05%	0.2%	3%
P-2	10%	70ºC	2	"neutral"	1%	0.05%	0.2%	3%
P-3	10%	70ºC	2	"neutral"	2%	0.05%	0.2%	3%
P-4	10%	70ºC	2	"neutral"	4%	0.05%	0.2%	3%
P-5	10%	70ºC	2	"neutral"	8%	0.05%	0.2%	3%
P-6	10%	70ºC	2	alkaline	0	0.05%	0.2%	3%
P-7	10%	70ºC	2	alkaline	1%	0.05%	0.2%	3%
P-8	10%	70ºC	2	alkaline	2%	0.05%	0.2%	3%
P-9	10%	70ºC	2	alkaline	4%	0.05%	0.2%	3%
P-10	10%	70ºC	2	alkaline	8%	0.05%	0.2%	3%
Z-1	10%	40ºC	2	"neutral"	0.5%	-	-	-
Z-2	10%	40ºC	2	4	0.5%	-	-	-

Table A-8-3. Experimental conditions for wood chip pretreatments.

Sample ID	Consistency	Temp.	Time (hrs)	pH	Dosage	$MgSO_4$	DTPA	Na_2SiO_3
Q-13	10%	50ºC	2	3.0	0	-	-	-
Q-14	10%	50ºC	2	3.0	0.5%	-	yes	-
B-11	10%	65ºC	2	10.0	10%	-	-	-
P-11	10%	70ºC	2	alkaline	6% NaOH	0.05%	0.2%	3%
P-12	10%	70ºC	2	alkaline	4% H2O2	0.05%	0.2%	3%

Table A-8-4. Experimental conditions for wood chip multiple pretreatments.

Sample ID	Consistency	Temp.	Time (hrs)	pH	Dosage	$MgSO_4$	DTPA	Na_2SiO_3
(A)(P)	10%	50ºC	2	3.0	0	-	-	-
	10%	70ºC	2	alkaline	4%	0.05%	0.2%	3%
(A+Q)(P)	10%	50ºC	2	3.0	0.5%	-	yes	-
	10%	70ºC	2	alkaline	4%	0.05%	0.2%	3%
(B)(P)	10%	65ºC	2	10.0	10%	-	-	-
	10%	70ºC	2	alkaline	4%	0.05%	0.2%	3%
(P)(B)	10%	70ºC	2	alkaline	4%	0.05%	0.2%	3%
	10%	65ºC	2	10.0	10%	-	-	-
$(pH_{Hi})(pH_{Hi})$	10%	70ºC	2	10.0	0	-	-	-
	10%	70ºC	2	alkaline	0	-	-	-
$(pH_{Lo})(pH_{Hi})$	10%	50ºC	2	3.0	0	-	-	-
	10%	70ºC	2	alkaline	0	-	-	-

22.2 Summary of ICP Metals Contents for Pretreated Wood Chips

Table A-8-5. Metals content of pretreated wood chips. Metals contents are in units of mg/kg. Table A-8-1 summarizes the pretreatment conditions for these samples.

Metals	Q-1	Q-2	Q-3	Q-4	Q-5	Q-6
Cr	0.3	0.3	0.3	0.3	0.3	0.3
Mn	66.9	62.0	93.2	79.9	96.6	90.4
Fe	7.0	17.5	9.5	10.4	4.1	6.6
Co	0.7	0.5	0.5	0.5	0.8	0.6
Ni	0.5	0.6	0.5	0.5	0.5	0.5
Cu	0.9	1.0	0.9	0.7	0.7	0.6
Zn	7.9	6.2	7.0	6.8	6.4	6.2
Al	7.2	7.4	6.3	6.9	5.7	4.7
B	17.1	13.5	10.5	12.3	9.5	8.0
P	63.1	48.4	50.8	65.8	39.2	54.1
S	240.3	98.5	71.7	82.1	48.3	41.8
Se	7.6	7.9	7.1	7.8	7.2	7.5
As	5.8	6.0	5.1	5.9	5.5	5.7
Mo	1.1	1.1	1.0	1.1	1.0	1.1
Sn	2.9	3.0	2.8	3.0	2.8	2.9
Sb	3.4	3.5	3.2	3.5	3.3	3.4
Pb	3.7	3.8	3.4	3.8	3.5	3.6
Tl	7.7	7.9	7.2	7.9	7.3	7.6
Sr	2.0	1.8	2.4	2.5	2.0	2.2
Ba	4.1	3.9	4.7	5.1	4.4	5.4
Na	360.2	147.7	96.6	165.2	53.2	6.8
Mg	103.6	97.7	129.4	105.9	115.4	109.7
K	132.6	116.4	184.4	143.6	171.9	169.5
Ca	527.6	423.8	551.2	472.1	467.6	491.2

Table A-8-6. Metals content of pretreated wood chips. Metals contents are in units of mg/kg. Table A-8-1 summarizes the pretreatment conditions for these samples.

Metals	Q-7	Q-8	Q-9	Q-10	Q-11	Q-12
Cr	0.3	0.3	0.3	0.3	3.2	0.3
Mn	39.1	46.2	25.9	44.9	54.0	45.6
Fe	3.5	4.7	9.2	4.7	19.4	4.7
Co	0.5	0.6	0.7	0.4	0.7	0.5
Ni	0.5	0.5	0.6	0.5	1.6	0.5
Cu	0.4	0.4	0.3	0.6	0.5	0.5
Zn	2.4	2.9	1.2	3.2	2.7	3.0
Al	5.1	5.7	5.5	5.2	4.5	5.5
B	9.1	5.5	4.7	5.6	4.4	5.5
P	49.6	44.8	42.8	47.3	51.8	46.0
S	120.4	119.3	73.4	73.0	73.7	96.2
Se	7.4	7.0	7.9	6.7	6.3	6.8
As	5.6	5.3	6.0	5.1	4.8	5.2
Mo	1.0	1.0	1.1	0.9	0.9	1.0
Sn	2.8	2.7	3.0	2.6	2.4	2.6
Sb	3.3	3.2	3.6	3.0	2.8	3.1
Pb	3.5	3.4	3.8	3.2	3.0	3.3
Tl	7.4	7.1	8.0	6.8	6.4	6.9
Sr	1.7	2.3	2.1	2.1	2.2	2.2
Ba	3.1	4.9	4.7	4.2	4.5	4.6
Na	181.1	267.6	270.7	268.9	304.2	268.2
Mg	68.5	82.4	69.0	114.0	121.5	98.2
K	92.0	99.7	98.7	145.3	144.4	122.5
Ca	315.0	412.0	320.1	475.8	554.9	443.9

Table A-8-7. Metals content of pretreated wood chips. Metals contents are in units of mg/kg. Table A-8-2 summarizes the pretreatment conditions for these samples.

Metals	P-1	P-2	P-3	P-4	P-5	P-6
Cr	0.3	0.3	0.3	0.3	0.3	0.3
Mn	51.7	28.8	45.6	46.7	353.2	105.7
Fe	5.2	7.2	4.8	3.4	2.5	5.0
Co	0.4	0.7	0.5	0.4	0.5	0.9
Ni	0.5	0.5	0.5	0.5	0.5	0.5
Cu	0.4	0.4	0.6	0.5	0.3	0.7
Zn	3.1	2.1	3.6	3.6	2.2	8.0
Al	6.1	6.6	5.5	5.0	4.1	9.1
B	2.6	2.0	6.4	6.8	1.3	1.7
P	38.7	42.8	37.4	42.9	41.8	40.1
S	62.8	62.9	76.2	61.3	56.5	49.7
Se	7.1	6.8	6.9	6.8	7.7	7.4
As	5.4	5.2	5.2	5.2	5.8	5.6
Mo	1.0	1.0	1.0	1.0	1.1	1.0
Sn	2.8	2.6	2.7	2.6	3.0	2.9
Sb	3.2	3.1	3.1	3.1	3.5	3.3
Pb	3.4	3.3	3.3	3.3	3.7	3.5
Tl	7.2	6.9	7.0	6.9	7.8	7.5
Sr	2.5	2.5	3.1	3.4	2.1	2.4
Ba	5.7	4.5	6.5	7.0	4.7	5.8
Na	954.2	933.7	1150.3	879.5	710.4	11000.0
Mg	135.5	162.3	232.0	236.0	154.4	181.5
K	225.4	215.1	252.7	208.3	161.6	196.0
Ca	432.9	429.7	637.0	692.2	460.1	484.0

Table A-8-8. Metals content of pretreated wood chips. Metals contents are in units of mg/kg. Table A-8-2 summarizes the pretreatment conditions for these samples.

Metals	P-7	P-8	P-9	P-10	Z-1	Z-2
Cr	0.2	0.3	0.3	0.3	0.4	0.3
Mn	73.0	43.7	51.2	89.1	116.2	74.9
Fe	5.1	3.5	3.2	4.6	11.5	5.7
Co	0.7	0.9	0.7	0.4	0.7	0.6
Ni	0.5	0.5	0.5	0.5	0.5	0.6
Cu	0.7	0.4	0.6	0.7	0.9	0.8
Zn	5.5	2.5	3.4	7.2	10.2	7.7
Al	9.7	5.6	6.8	42.5	67	6.5
B	2.4	8.7	15.9	1.5	1.4	1.1
P	39.5	41.2	40.9	37.7	55.5	47.8
S	70.8	52.3	52.0	56.3	49.3	61.0
Se	6.5	7.6	7.5	6.9	7.5	6.7
As	5.0	5.8	5.7	5.3	5.7	5.1
Mo	0.9	1.1	1.1	1.0	1.1	1.0
Sn	2.5	2.9	2.9	2.7	2.9	2.6
Sb	2.9	3.4	3.4	3.1	3.	3.0
Pb	3.1	3.6	3.6	3.3	3.6	3.2
Tl	6.6	7.7	7.6	7.0	7.6	6.8
Sr	3.6	2.2	2.0	2.2	3.0	2.8
Ba	7.7	4.7	4.1	5.1	5.1	6.1
Na	2670.0	3040.0	4420.0	11450.0	10.5	64.9
Mg	127.8	83.6	107.3	143.0	212.4	118.8
K	228.8	184.8	160.4	207.9	154.3	133.3
Ca	638.8	392.4	336.5	440.1	755.2	559.3

Table A-8-9. Metals content of pretreated wood chips. Metals contents are in units of mg/kg. Table A-8-1 summarizes the pretreatment conditions for these samples.

Metals	B-1	B-2	B-3	B-4	B-5
Cr	0.3	0.3	0.3	0.3	0.3
Mn	91.1	121.5	105.8	79.8	70.2
Fe	5.1	6.1	5.3	6.2	4.5
Co	0.9	0.8	0.9	0.7	0.6
Ni	0.5	0.5	0.5	0.6	0.6
Cu	0.8	1.1	0.8	1.3	1.0
Zn	7.4	10.4	7.7	6.7	7.4
Al	5.8	7.4	5.2	5.8	3.3
B	1.4	220.1	343.4	1796.7	3591.9
P	50.0	42.9	42.2	45.4	54.8
S	46.6	54.7	47.7	50.3	53.7
Se	7.6	7.4	7.8	8.3	7.9
As	5.8	5.6	5.9	6.3	6.0
Mo	1.1	1.0	1.1	1.2	1.1
Sn	2.9	2.9	3.0	3.2	3.1
Sb	3.4	3.3	3.5	3.8	3.6
Pb	3.7	3.6	3.7	4.0	3.8
Tl	7.7	7.5	7.9	8.5	8.0
Sr	1.9	3.3	2.1	2.1	1.7
Ba	3.6	7.3	4.4	5.1	3.4
Na	7.6	1340.0	1650.0	6040.0	10100.0
Mg	122.5	194.1	146.2	101.9	120.3
K	156.0	296.9	188.5	142.6	160.5
Ca	537.5	784.9	569.5	462.8	425.6

Table A-8-10. Metals content of pretreated wood chips. Metals contents are in units of mg/kg. Table A-8-1 summarizes the pretreatment conditions for these samples.

Metals	B-6	B-7	B-8	B-9	B-10
Cr	0.3	0.3	0.3	0.3	0.3
Mn	79.9	112.0	97.9	90.3	97.9
Fe	7.6	5.6	6.1	4.9	6.1
Co	0.9	0.9	0.5	0.6	0.5
Ni	0.5	0.5	0.5	0.5	0.5
Cu	1.	2.2	6.0	1.5	6.0
Zn	7.2	7.6	7.7	6.7	7.7
Al	6.7	3.8	6.6	4.6	6.6
B	25.3	173.4	403.4	1895.7	403.4
P	40.3	46.0	39.7	38.0	39.7
S	88.4	39.3	62.3	45.7	62.3
Se	7.4	7.7	7.3	7.0	7.3
As	5.6	5.9	5.6	5.3	5.6
Mo	1.0	1.1	1.0	1.0	1.0
Sn	2.9	3.0	2.8	2.7	2.8
Sb	3.3	3.5	3.3	3.2	3.3
Pb	3.6	3.7	3.5	3.4	3.5
Tl	7.5	7.8	7.4	7.1	7.4
Sr	1.8	2.4	2.6	2.0	2.6
Ba	3.8	4.9	6.5	4.2	6.5
Na	295.1	1200.0	2150.0	6580.0	2150.0
Mg	120.3	156.1	133.5	108.7	133.5
K	160.5	231.9	216.8	155.3	216.8
Ca	488.6	642.3	549.4	481.1	549.4

22.3 Summary of ICP Metals Contents for Pulps Produced from Pretreated Wood Chips

Table A-8-11. Metals content of pulps from pretreated wood chips utilizing Condition B pulping conditions. Metals contents are in units of mg/kg. Table A-8-1 summarizes the pretreatment conditions for these samples.

Metals	Q-1	Q-2	Q-3	Q-4	Q-5	Q-6
Cr	2.2	1.6	0.8	2.5	1.5	1.2
Mn	27.0	25.7	36.6	37.8	35.6	35.1
Fe	19.9	14.1	16.0	16.7	10.5	11.8
Co	0.5	0.5	0.5	0.5	0.5	0.
Ni	3.1	2.2	1.4	3.5	3.7	2.0
Cu	6.0	3.5	4.1	4.4	3.1	3.6
Zn	15.1	7.4	10.5	11.8	8.0	9.0
Al	3.0	2.5	2.9	3.1	2.3	3.3
B	3.7	2.6	2.3	1.6	1.1	1.1
P	45.3	43.7	43.0	43.0	42.6	41.4
S	624.0	590.2	676.3	609.7	598.0	587.4
Se	8.3	8.0	7.9	7.9	7.8	7.6
As	6.3	6.1	6.0	6.0	6.0	5.8
Mo	1.2	1.1	1.1	1.1	1.1	1.1
Sn	3.2	3.1	3.1	3.1	3.0	2.9
Sb	3.8	3.6	3.6	3.6	3.5	3.4
Pb	4.0	3.9	3.8	3.8	3.8	3.7
Tl	8.4	8.1	8.0	8.0	7.9	7.7
Sr	2.6	2.7	3.1	3.1	3.0	3.2
Ba	4.0	4.0	5.2	5.5	5.7	5.2
Na	794.0	787.9	788.1	680.1	691.7	582.0
Mg	201.0	196.3	231.1	225.0	209.9	245.8
K	46.1	21.6	20.5	21.4	24.0	18.8
Ca	701.9	692.5	872.4	835.0	833.5	887.3

Table A-8-12. Metals content pulps from pretreated wood chips utilizing Condition B pulping conditions. Metals contents are in units of mg/kg. Table A-8-1 summarizes the pretreatment conditions for these samples.

Metals	Q-7	Q-8	Q-9	Q-10	Q-11	Q-12
Cr	2.7	0.7	0.9	1.0	1.4	1.5
Mn	16.2	20.2	15.4	19.1	20.2	21.5
Fe	14.1	5.8	9.0	7.6	29.5	11.2
Co	0.5	0.5	0.5	0.5	0.5	0.5
Ni	3.3	2.1	1.9	1.4	2.0	2.5
Cu	7.6	4.1	2.9	6.5	4.6	4.6
Zn	27.1	8.3	4.8	11.0	7.8	9.3
Al	4.3	3.3	2.4	2.6	2.3	3.4
B	1.5	2.1	0.8	0.2	0.4	0.5
P	43.1	42.8	43.9	43.5	43.1	42.8
S	606.2	568.8	567.5	607.0	622.9	580.3
Se	7.9	7.9	8.1	8.0	7.9	7.9
As	6.0	6.0	6.1	6.1	6.0	6.0
Mo	1.1	1.1	1.1	1.1	1.1	1.1
Sn	3.1	3.0	3.1	3.1	3.1	3.0
Sb	3.6	3.5	3.6	3.6	3.6	3.6
Pb	3.8	3.8	3.9	3.8	3.8	3.8
Tl	8.0	8.0	8.2	8.1	8.0	8.0
Sr	2.4	2.7	2.6	2.7	3.1	3.1
Ba	4.4	3.9	4.4	4.8	6.1	5.1
Na	956.8	819.2	884.0	878.7	847.8	751.0
Mg	185.1	211.4	189.2	203.7	212.3	215.7
K	58.3	24.0	23.7	34.3	19.0	22.9
Ca	632.6	730.4	678.8	738.9	811.7	796.6

Table A-8-13. Metals content of pulps from pretreated wood chips utilizing Condition B pulping conditions. Metals contents are in units of mg/kg. Table A-8-2 summarizes the pretreatment conditions for these samples.

Metals	P-1	P-2	P-3	P-4	P-5	P-6
Cr	2.0	1.9	0.7	0.8	4.0	0.8
Mn	33.4	28.7	30.1	30.4	29.7	17.7
Fe	11.2	10.1	6.1	7.2	31.8	7.0
Co	0.5	0.5	0.5	0.5	0.5	0.4
Ni	2.5	1.6	1.1	0.9	3.9	1.3
Cu	5.6	5.3	3.8	5.3	3.9	4.3
Zn	8.5	6.0	6.1	6.6	6.6	9.3
Al	6.2	5.8	5.1	6.5	11.0	7.2
B	0.2	0.2	0.2	0.2	0.2	0.2
P	43.2	43.4	42.4	42.5	45.4	40.8
S	568.8	540.2	564.5	556.7	557.3	364.4
Se	8.0	8.0	7.8	7.8	8.4	7.5
As	6.0	6.1	5.9	5.9	6.4	5.7
Mo	1.1	1.1	1.1	1.1	1.2	1.1
Sn	3.1	3.1	3.0	3.0	3.2	2.9
Sb	3.6	3.6	3.5	3.5	3.8	3.4
Pb	3.8	3.9	3.7	3.8	4.0	3.6
Tl	8.1	8.1	7.9	7.9	8.5	7.6
Sr	3.3	3.1	3.1	3.3	3.2	2.7
Ba	6.1	4.7	6.2	6.3	6.0	3.6
Na	911.8	819.2	858.0	915.1	973.6	511.6
Mg	307.5	314.5	316.8	308.9	305.5	128.1
K	25.0	15.5	17.7	27.6	14.2	18.8
Ca	711.1	684.1	677.9	665.3	645.6	588.6

Table A-8-14. Metals content of pulps from pretreated wood chips utilizing Condition B pulping conditions. Metals contents are in units of mg/kg. Table A-8-2 summarizes the pretreatment conditions for these samples.

Metals	P-7	P-8	P-9	P-10	Z-1	Z-2
Cr	2.5	12.6	0.8	0.8	2.4	4.7
Mn	34.1	33.1	24.6	14.3	39.5	36.2
Fe	13.1	54.8	6.3	6.3	23.0	25.3
Co	0.5	0.5	0.4	0.5	0.5	0.4
Ni	2.9	8.8	1.9	2.1	2.8	4.7
Cu	3.9	3.7	5.9	4.2	8.2	6.6
Zn	7.9	7.4	11.1	11.1	14.1	10.5
Al	7.0	4.8	6.4	6.0	4.4	6.0
B	0.2	0.2	0.2	0.2	0.2	0.2
P	42.4	41.9	41.4	42.3	42.4	41.4
S	542.1	509.6	486.8	428.5	613.7	603.6
Se	7.8	7.7	7.6	7.8	7.8	7.6
As	5.9	5.9	5.8	5.9	5.9	5.8
Mo	1.1	1.1	1.1	1.1	1.1	1.1
Sn	3.0	3.0	2.9	3.0	3.0	2.9
Sb	3.5	3.5	3.4	3.5	3.5	3.4
Pb	3.7	3.7	3.8	3.7	3.8	3.7
Tl	7.9	7.8	7.7	7.9	7.9	7.7
Sr	2.1	2.3	2.2	2.5	3.1	2.8
Ba	4.0	3.9	5.6	3.6	5.2	11.2
Na	1140.0	1070.0	1065.0	991.6	802.2	907.2
Mg	210.0	191.3	159.9	103.0	189.3	183.8
K	21.6	17.4	29.0	17.0	34.6	24.6
Ca	552.4	501.1	456.8	531.9	770.6	669.1

Table A-8-15. Metals content of pulps from pretreated wood chips utilizing Condition B pulping conditions. Metals contents are in units of mg/kg. Table A-8-1 summarizes the pretreatment conditions for these samples.

Metals	B-1	B-2	B-3	B-4	B-5
Cr	2.1	0.3	0.3	1.2	1.0
Mn	33.1	38.5	32.3	37.5	36.8
Fe	13.4	24.4	8.3	9.1	10.2
Co	0.5	0.5	0.5	0.5	0.5
Ni	2.6	2.9	2.2	2.4	2.3
Cu	3.5	4.0	3.0	5.1	3.4
Zn	8.5	8.3	5.5	9.6	8.5
Al	4.0	2.7	2.0	2.0	1.4
B	0.2	0.2	0.2	0.3	0.2
P	41.9	42.4	43.6	47.7	42.8
S	606.3	538.1	573.0	641.9	576.7
Se	7.7	7.8	8.0	8.8	7.9
As	5.9	5.9	6.1	6.7	6.0
Mo	1.1	1.1	1.1	1.2	1.1
Sn	3.0	3.0	3.1	3.4	3.0
Sb	3.5	3.5	3.6	4.0	3.6
Pb	3.7	3.7	3.9	4.2	4.3
Tl	7.8	7.9	8.1	8.9	8.0
Sr	2.8	3.0	2.6	2.1	1.8
Ba	5.1	5.0	5.9	5.0	4.9
Na	723.4	488.4	580.3	680.2	511.0
Mg	202.9	202.7	182.9	158.8	136.5
K	37.9	17.3	18.2	40.4	13.8
Ca	772.8	833.4	776.3	602.9	481.9

Table A-8-16. Metals content of pulps from pretreated wood chips utilizing Condition B pulping conditions. Metals contents are in units of mg/kg. Table A-8-1 summarizes the pretreatment conditions for these samples.

Metals	B-6	B-7	B-8	B-9	B-10
Cr	2.3	3.2	1.5	2.2	1.0
Mn	36.5	34.2	31.9	29.5	34.1
Fe	14.1	25.5	10.8	13.7	10.4
Co	0.5	0.5	0.5	0.5	0.5
Ni	2.7	2.9	2.1	4.4	1.7
Cu	5.4	4.6	3.6	5.2	7.3
Zn	25.5	13.8	6.9	22.8	11.6
Al	4.9	1.9	2.3	1.5	1.8
B	0.2	0.2	0.2	0.2	0.2
P	43.2	43.3	42.7	43.0	42.5
S	574.0	614.7	587.4	569.9	601.7
Se	7.9	8.0	7.9	7.9	7.8
As	6.0	6.1	6.0	6.0	5.9
Mo	1.1	1.1	1.1	1.1	1.1
Sn	3.1	3.1	3.0	3.1	3.0
Sb	3.6	3.6	3.5	3.7	3.5
Pb	3.8	3.8	3.8	3.8	3.8
Tl	8.0	8.1	7.9	8.0	7.9
Sr	3.1	2.5	2.6	1.7	1.7
Ba	5.8	4.2	4.0	3.6	4.0
Na	459.6	548.3	434.9	476.1	428.7
Mg	235.4	231.4	214.9	171.6	163.1
K	66.5	27.8	23.4	24.3	17.7
Ca	930.3	791.2	837.8	554.3	528.7

Table A-8-17. Metals content of pulps from pretreated wood chips utilizing Condition A pulping conditions. Metals contents are in units of mg/kg. Table A-8-3 summarizes the pretreatment conditions for these samples.

Metals	Q-13	Q-14	B-11	P-11	P-12
Cr	1.1	0.8	0.8	9.2	0.5
Mn	31.3	15.9	36.0	19.0	22.3
Fe	9.6	6.7	8.1	51.9	7.0
Co	0.4	0.4	0.5	0.5	0.5
Ni	2.2	1.3	1.0	6.1	0.7
Cu	23.2	6.4	5.1	7.2	6.6
Zn	142.3	6.9	13.5	8.9	9.6
Al	3.3	2.1	2.2	3.0	4.3
B	0.2	0.2	0.2	0.2	0.2
P	41.5	40.4	42.7	42.9	43.6
S	630.4	512.5	651.9	522.2	520.2
Se	7.6	7.4	7.9	7.9	8.0
As	5.8	5.6	6.0	6.0	6.1
Mo	1.1	1.1	1.1	1.1	1.1
Sn	3.0	2.9	3.0	3.0	3.1
Sb	3.4	3.4	3.5	3.6	3.6
Pb	3.7	3.6	3.8	4.4	3.9
Tl	7.7	7.5	8.0	8.0	8.1
Sr	1.4	1.2	1.3	1.2	1.4
Ba	2.5	2.3	8.0	3.9	2.8
Na	326.3	314.2	257.5	283.1	353.5
Mg	229.3	199.3	189.0	167.0	220.7
K	24.4	15.8	14.7	17.0	22.2
Ca	447.1	397.7	414.7	401.6	435.6

Table A-8-18. Metals content of pulps from pretreated wood chips utilizing Condition B pulping conditions. Metals contents are in units of mg/kg. Table A-8-4 summarizes the pretreatment conditions for these samples.

Metals	(A)(P)	(A+Q)(P)	(B)(P)	(P)(B)	$(pH_{HI})(pH_{HI})$	$(pH_{LO})(pH_{HI})$
Cr	0.8	1.5	1.3	1.0	1.2	1.0
Mn	17.5	9.8	16.5	16.4	38.7	30.3
Fe	7.0	9.2	11.5	9.9	11.3	7.9
Co	0.4	0.5	0.5	0.5	0.5	0.5
Ni	1.8	1.7	1.3	1.7	1.7	1.2
Cu	5.1	7.0	5.4	9.0	5.9	8.0
Zn	14.3	10.4	69.4	11.4	8.8	12.7
Al	3.0	3.2	3.2	2.7	3.4	5.0
B	0.2	0.2	0.2	0.2	0.2	0.2
P	40.1	42.1	41.9	43.4	42.1	46.0
S	517.6	490.7	537.9	549.1	640.0	572.6
Se	7.4	7.8	7.7	8.0	7.7	8.5
As	5.6	5.9	5.9	6.1	5.9	6.4
Mo	1.0	1.1	1.1	1.1	1.1	1.2
Sn	2.9	3.0	3.0	3.1	3.0	3.3
Sb	3.3	3.5	3.5	3.6	3.5	3.8
Pb	4.8	3.7	3.7	3.8	3.7	4.1
Tl	7.5	7.8	7.8	8.1	7.8	8.6
Sr	2.0	1.7	1.4	1.4	3.0	2.7
Ba	4.3	3.0	3.2	3.3	5.6	4.9
Na	813.1	862.4	431.7	392.3	610.7	647.7
Mg	222.2	204.7	193.8	168.6	226.1	203.8
K	19.5	23.5	17.7	28.7	21.8	23.2
Ca	550.9	472.6	459.7	407.3	837.9	723.1

Table A-8-19. Metals content of pulps from pretreated wood chips utilizing Condition A pulping conditions. Metals contents are in units of mg/kg. Table A-8-4 summarizes the pretreatment conditions for these samples.

Metals	(A)(P)	(A+Q)(P)	(B)(P)	(P)(B)	$(pH_{HI})(pH_{HI})$	$(pH_{LO})(pH_{HI})$
Cr	0.7	0.4	0.9	0.4	0.9	1.0
Mn	14.3	7.5	7.6	20.6	61.0	44.9
Fe	8.4	5.9	10.5	6.4	8.3	12.6
Co	0.4	0.4	0.5	0.5	0.5	0.5
Ni	0.9	2.0	1.2	1.1	0.7	1.3
Cu	6.5	6.8	5.9	5.4	7.4	6.7
Zn	22.6	55.3	20.2	7.6	9.2	9.8
Al	3.8	2.6	3.6	2.3	1.8	1.8
B	0.2	0.2	0.2	0.2	0.2	0.2
P	41.5	41.4	42.7	43.8	41.7	43.2
S	534.6	440.2	450.4	538.8	628.7	546.9
Se	7.6	7.6	7.9	8.1	7.7	8.0
As	5.8	5.8	6.0	6.1	5.8	69.0
Mo	1.1	1.1	1.1	1.1	1.1	1.1
Sn	3.0	2.9	3.0	3.1	3.0	3.1
Sb	3.4	3.4	3.5	3.6	3.5	3.6
Pb	3.7	3.7	3.8	3.9	3.7	3.8
Tl	7.7	7.7	8.0	8.2	7.8	8.1
Sr	1.2	1.1	1.1	1.1	1.4	1.3
Ba	3.6	2.3	5.4	3.2	3.2	2.9
Na	457.3	509.3	507.0	396.6	405.9	384.2
Mg	152.6	132.2	135.5	132.9	239.9	187.7
K	35.1	19.6	19.6	13.0	17.7	13.3
Ca	330.5	277.3	280.3	308.4	371.9	323.4

22.4 Summary of Brightness and Chromophore Index Data for Pulps Produced from Pretreated Wood Chips

Table A-8-20. Brightness and chromophore index responses from the pulps produced from pretreated wood chips. Table A-8-1 summarizes the pretreatment conditions for these samples.

Condition	Brightness (%)	Chromophore Index
Q-1	28.7 ± 0.4	140.5 ± 3.0
Q-2	28.7 ± 0.4	140.4 ± 3.3
Q-3	27.0 ± 0.3	160.1 ± 1.8
Q-4	27.7 ± 0.1	148.9 ± 2.4
Q-5	28.1 ± 0.3	145.9 ± 4.3
Q-6	28.6 ± 0.3	143.1 ± 2.1
Q-7	28.1 ± 0.4	147.3 ± 4.8
Q-8	28.3 ± 0.5	145.1 ± 4.6
Q-9	28.4 ± 0.4	145.2 ± 3.0
Q-10	27.3 ± 0.2	155.2 ± 4.0
Q-11	28.5 ± 0.4	145.2 ± 1.4
Q-12	28.2 ± 0.3	148.6 ± 4.2

Table A-8-21. Brightness and chromophore index responses from the pulps produced from pretreated wood chips. Table A-8-1 and A-8-2 summarize the pretreatment conditions for these samples.

Condition	Brightness (%)	Chromophore Index
P-1	26.6 ± 0.4	165.2 ± 5.3
P-2	27.4 ± 0.4	158.5 ± 2.6
P-3	26.8 ± 0.3	163.6 ± 5.4
P-4	27.2 ± 0.4	161.0 ± 1.9
P-5	27.3 ± 0.3	158.5 ± 2.5
P-6	32.5 ± 0.4	110.8 ± 0.4
P-7	29.4 ± 0.3	137.1 ± 0.5
P-8	29.0 ± 0.3	141.0 ± 1.7
P-9	31.3 ± 0.4	120.0 ± 1.4
P-10	31.0 ± 0.3	119.5 ± 6.3
Z-1	27.5 ± 0.4	153.4 ± 3.6
Z-2	27.9 ± 0.4	149.9 ± 2.0
B-1	27.5 ± 0.3	154.0 ± 1.3
B-2	28.6 ± 0.5	141.1 ± 1.9
B-3	28.6 ± 0.3	139.4 ± 4.8
B-4	29.5 ± 0.4	133.0 ± 0.8
B-5	31.2 ± 0.4	120.4 ± 2.2
B-6	28.0 ± 0.3	147.6 ± 2.8
B-7	28.2 ± 0.3	146.0 ± 5.7
B-8	29.7 ± 0.4	133.5 ± 0.8
B-9	30.3 ± 0.4	127.6 ± 4.6
B-10	31.1 ± 0.3	120.2 ± 4.0

Table A-8-22. Brightness and chromophore index responses from the pulps produced from pretreated wood chips. Table A-8-3 summarizes the pretreatment conditions for these samples. The Condition A pulping condition involves a high effective alkali and low sulfidity while the Condition B pulping condition involves a low effective alkali and high sulfidity.

Condition	Pulping Condition	Brightness (%)	Chromophore Index
Normal Kraft	A	30.8 ± 0.3	104.5 ± 3.0
Q-13	A	32.8 ± 0.4	107.9 ± 3.1
Q-14	A	33.6 ± 0.4	102.4 ± 3.5
B-11	A	33.6 ± 0.4	103.3 ± 3.6
P-11	A	35.2 ± 0.2	91.8 ± 3.7
P-12	A	34.2 ± 0.3	98.3 ± 0.2
Normal Kraft	B	25.3 ± 0.3	141.2 ± 3.3
Q-13	B	28.7 ± 0.6	140.4 ± 3.3
Q-14	B	28.3 ± 0.5	145.1 ± 4.6
B-11	B	31.1 ± 0.3	120.2 ± 4.0
P-11	B	32.5 ± 0.4	110.8 ± 0.4
P-12	B	31.3 ± 0.4	120.0 ± 1.4

Table A-8-23. Brightness and chromophore index responses from the pulps produced from pretreated wood chips. Table A-8-3 summarizes the pretreatment conditions for these samples. The Condition A pulping condition involves a high effective alkali and low sulfidity while the Condition B pulping condition involves a low effective alkali and high sulfidity.

Condition	Pulping Condition	Brightness (%)	Chromophore Index
Normal Kraft	A	30.8 ± 0.3	104.5 ± 3.0
(A)(P)	A	36.1 ± 0.2	84.6 ± 1.2
(A+Q)(P)	A	37.0 ± 0.6	82.1 ± 3.6
(B)(P)	A	35.9 ± 0.3	88.8 ± 2.4
(P)(B)	A	35.5 ± 0.3	88.9 ± 2.9
$(pH_{HI})(pH_{HI})$	A	31.6 ± 0.3	116.2 ± 3.4
$(pH_{LO})(pH_{HI})$	A	32.3 ± 0.3	110.4 ± 2.2
Normal Kraft	B	25.3 ± 0.3	141.2 ± 3.3
(A)(P)	B	31.3 ± 0.4	119.8 ± 3.7
(A+Q)(P)	B	32.3 ± 0.4	111.2 ± 3.6
(B)(P)	B	33.2 ± 0.3	104.2 ± 0.9
(P)(B)	B	33.8 ± 0.3	101.7 ± 3.0
$(pH_{HI})(pH_{HI})$	B	28.0 ± 0.4	148.4 ± 2.7
$(pH_{LO})(pH_{HI})$	B	28.8 ± 0.4	142.1 ± 1.2

23. APPENDIX 9: FLUORESCENCE SPECTRA

23.1 Emission Spectra of Residual Lignins

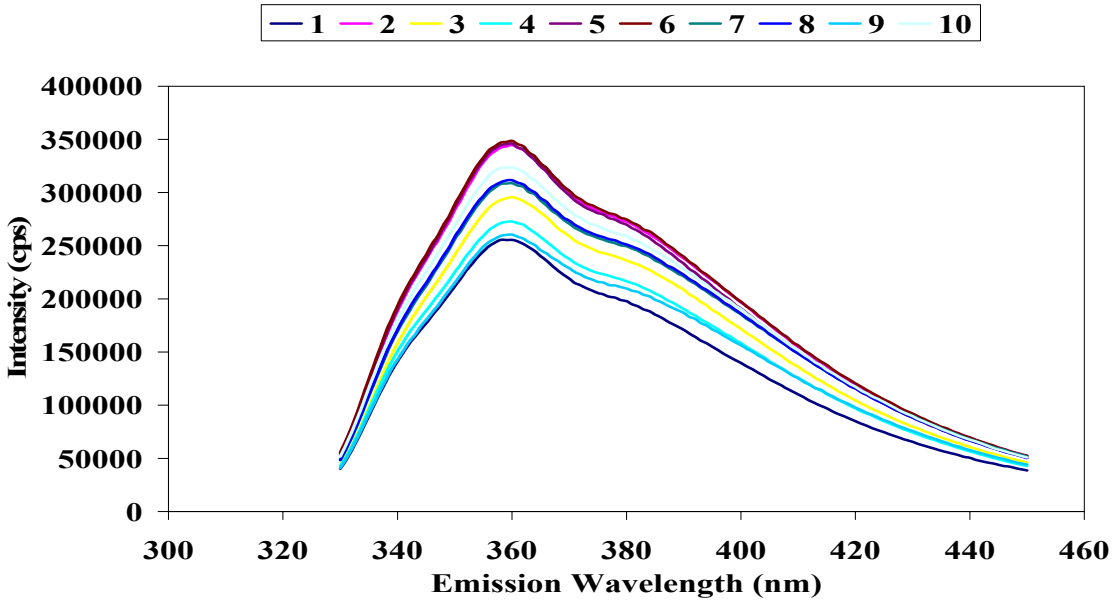

Figure A-9-1. Fluorescence emission spectra for residual lignin samples isolated from the constant kappa number series of pulps. The excitation wavelength was 310 nm.

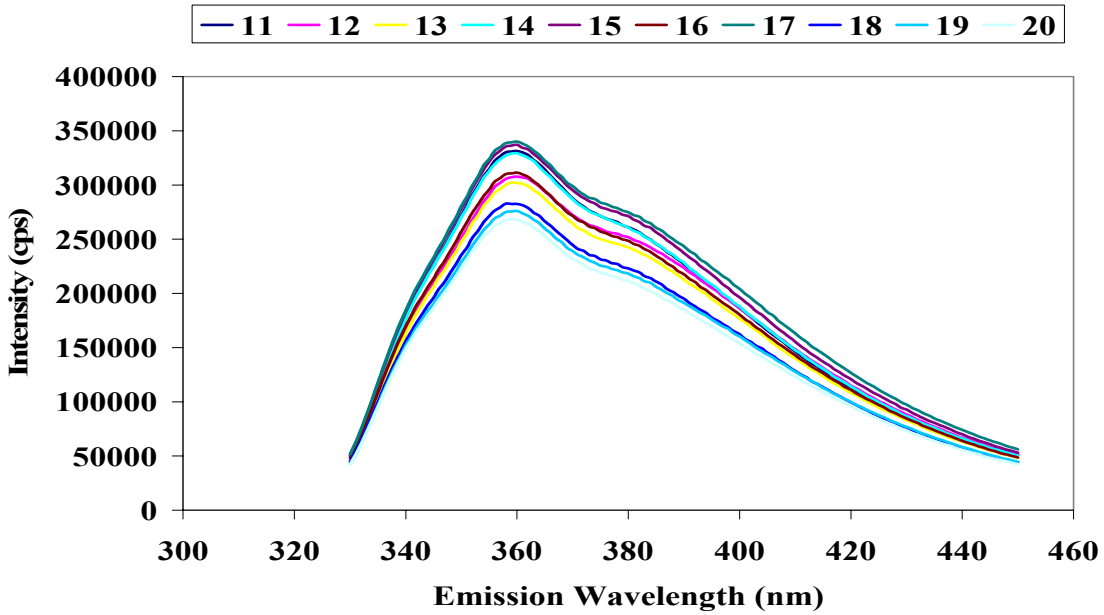

Figure A-9-2. Fluorescence emission spectra for residual lignin samples isolated from the constant kappa number series of pulps. The excitation wavelength was 310 nm.

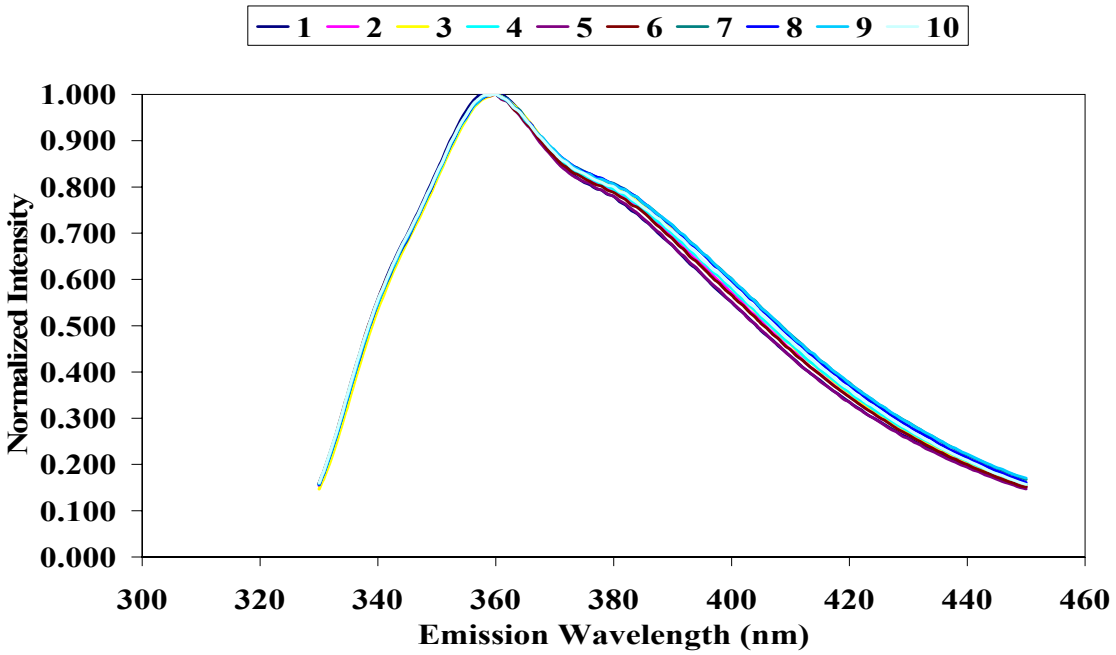

Figure A-9-3. Normalized fluorescence emission spectra for residual lignin samples isolated from the constant kappa number series of pulps. The excitation wavelength was 310 nm.

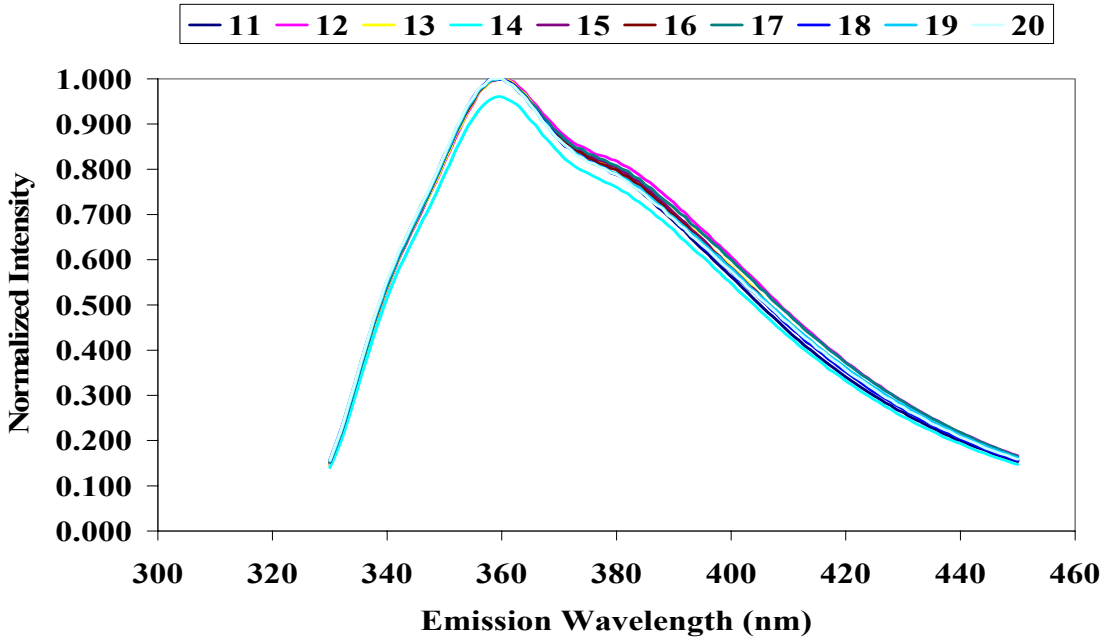

Figure A-9-4. Normalized fluorescence emission spectra for residual lignin samples isolated from the constant kappa number series of pulps. The excitation wavelength was 310 nm.

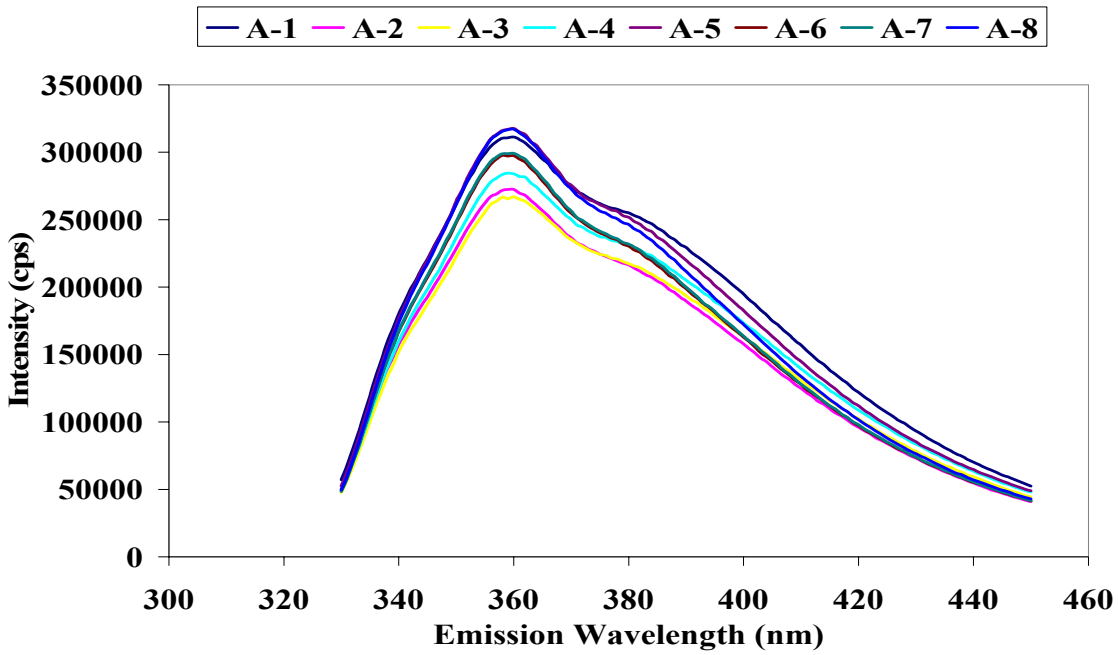

Figure A-9-5. Fluorescence emission spectra for residual lignin samples isolated from the Condition A incremental cook series of pulps. The excitation wavelength was 310 nm.

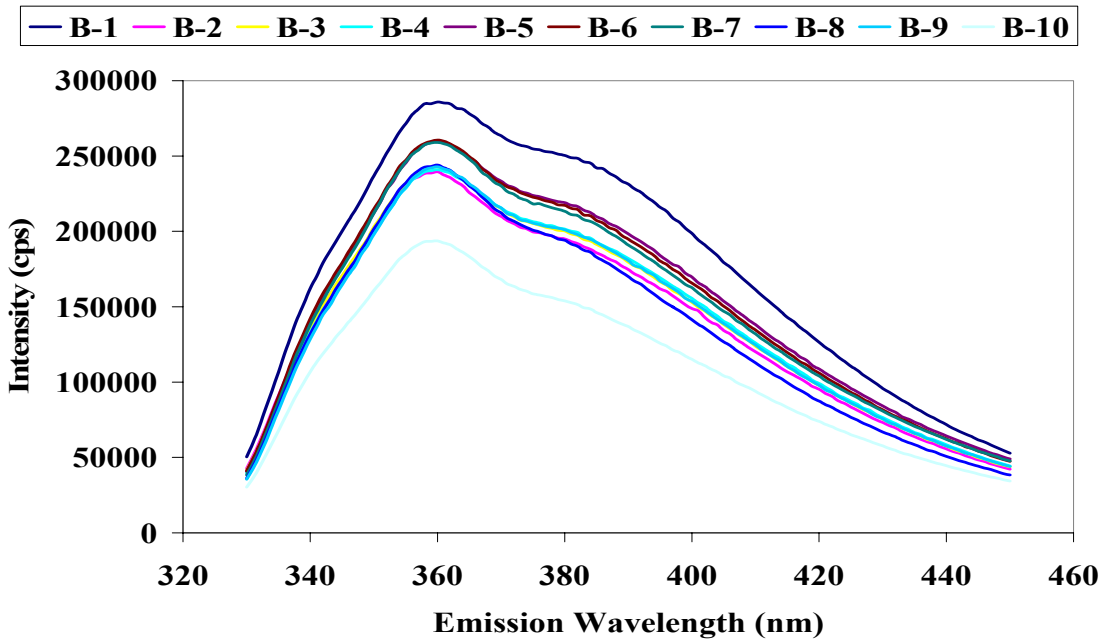

Figure A-9-6. Fluorescence emission spectra for residual lignin samples isolated from the Condition B incremental cook series of pulps. The excitation wavelength was 310 nm.

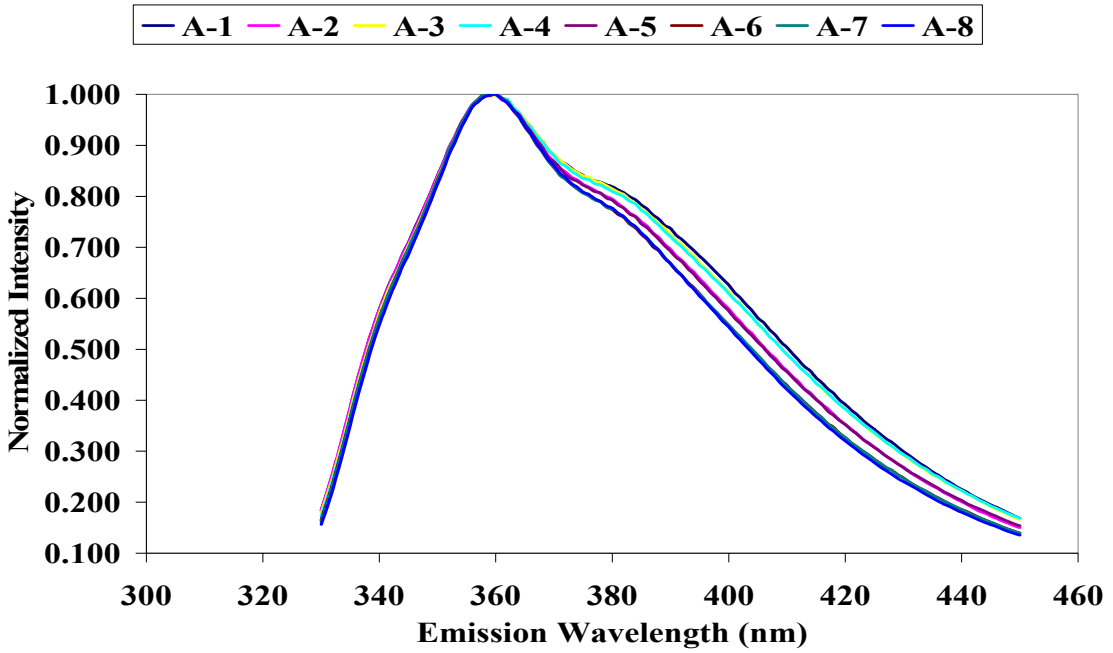

Figure A-9-7. Normalized fluorescence emission spectra for residual lignin samples isolated from the Condition A incremental cook series of pulps. The excitation wavelength was 310 nm.

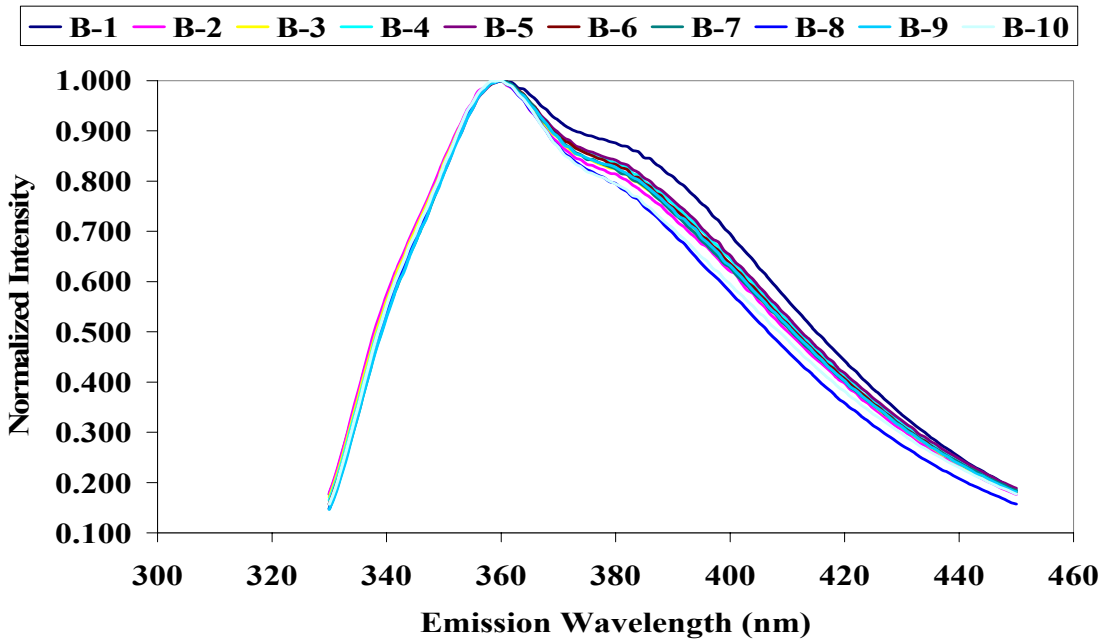

Figure A-9-8. Normalized fluorescence emission spectra for residual lignin samples isolated from the Condition B incremental cook series of pulps. The excitation wavelength was 310 nm.

23.2 Excitation Spectra of Residual Lignins

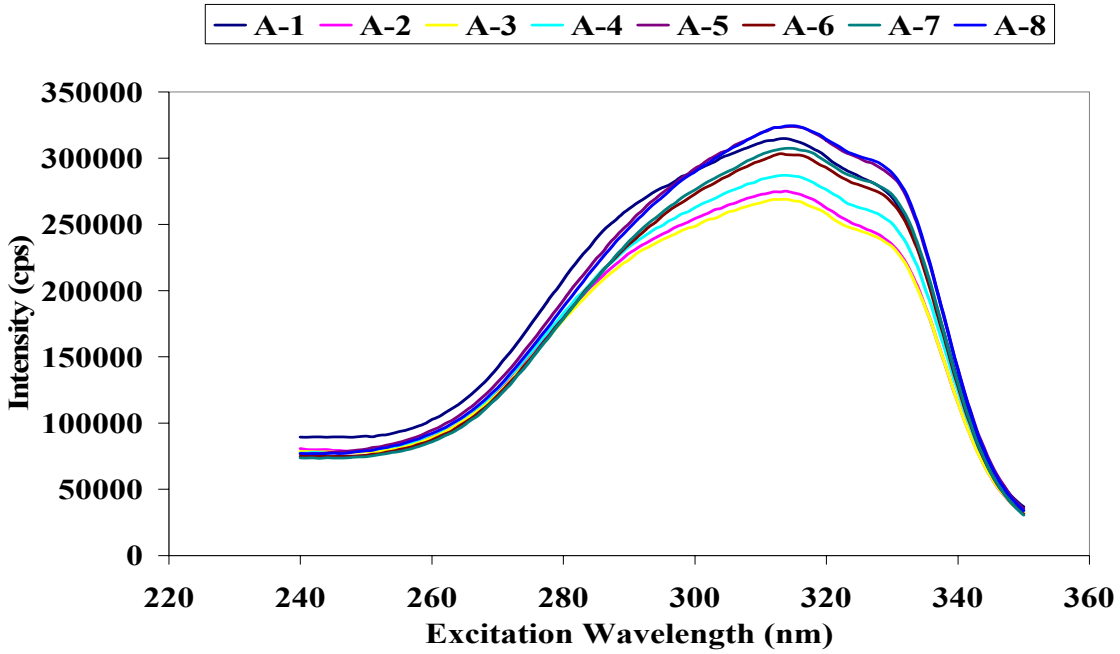

Figure A-9-9. Fluorescence excitation spectra for residual lignin samples isolated from the Condition A incremental cook series of pulps. The emission wavelength was 360 nm.

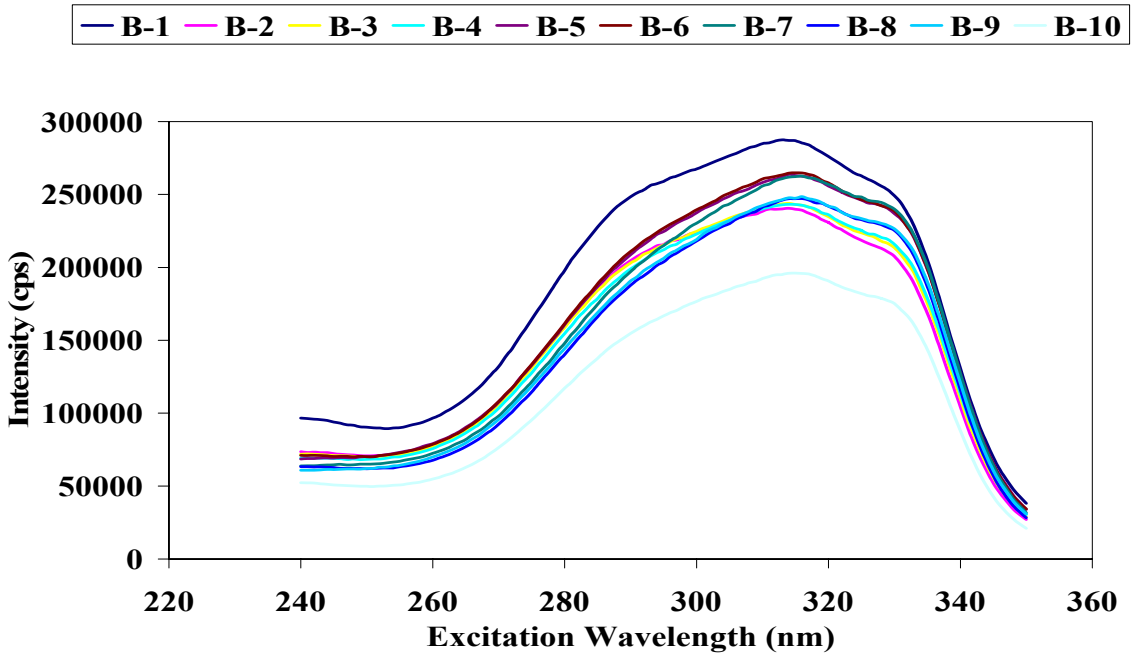

Figure A-9-10. Fluorescence excitation spectra for residual lignin samples isolated from the Condition B incremental cook series of pulps. The emission wavelength was 360 nm.

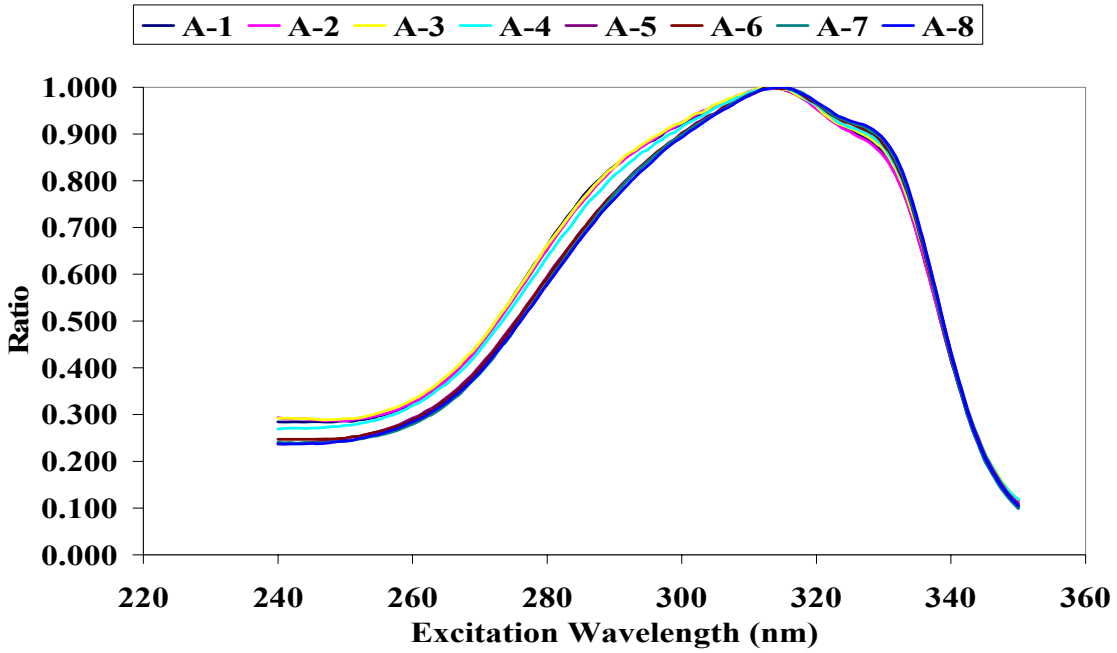

Figure A-9-11. Ratio fluorescence excitation spectra for residual lignin samples isolated from the Condition A incremental cook series of pulps. The emission wavelength was 360 nm.

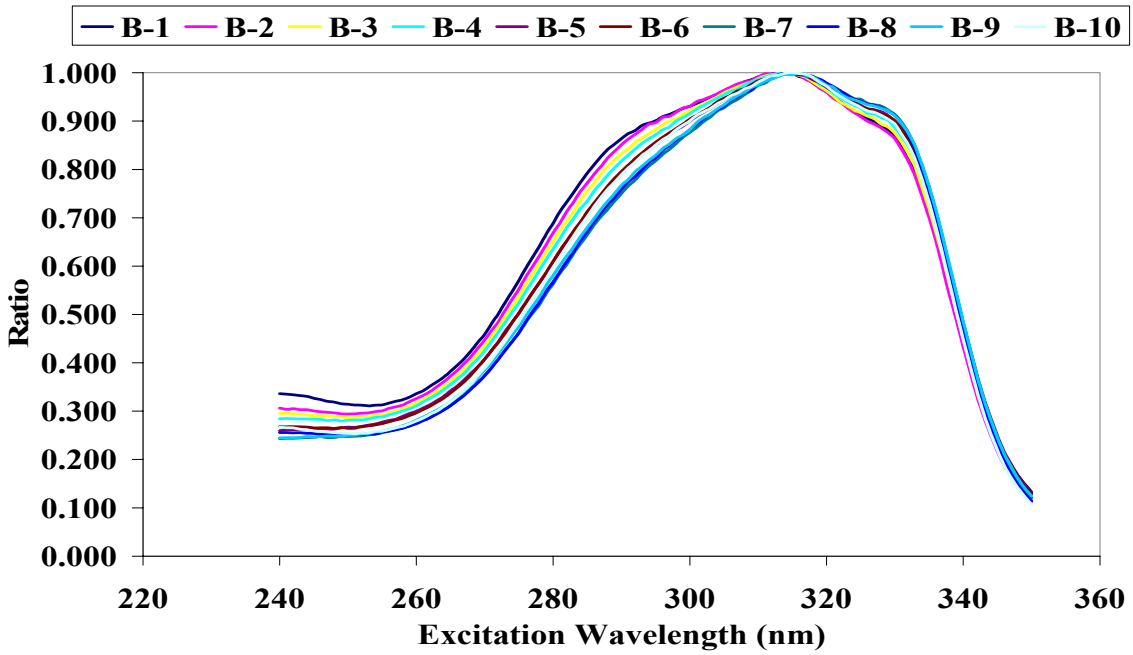

Figure A-9-12. Ratio fluorescence excitation spectra for residual lignin samples isolated from the Condition B incremental cook series of pulps. The emission wavelength was 360 nm.

24. APPENDIX 10: RELATED RESEARCH

24.1 Addendum 1. Excitation Energy Transfer in Lignin: Fluorescence of Kraft Residual Lignin

Presented at the 8th European Workshop on Lignocellulosics and Pulp
Riga, Latvia August 2004

Cameron I. Thomson, Thomas J. Dyer, and Arthur J. Ragauskas
Institute of Paper Science and Technology, Georgia Institute of Technology, Atlanta, Georgia USA

Abstract

One unique feature of the photochemical behaviour of lignin is the proposed suggestion that excitation energy can be shuttled about the macromolecule and within the fibre network. Numerous investigators have observed that lignin is capable of shuttling or dissipating absorbed light energy. The extent to which excitation energy transfer occurs in natural and residual lignin and the manner in which specific lignin functionalities participate in these processes is largely unknown, in part, due to the complexity of lignin. This paper examines the fluorescence spectra of kraft residual lignin and explores the potential implications for excitation energy transfer in lignin. The fluorescence behaviour of isolated residual lignins from *Pinus taeda* kraft pulps cooked to final Klason lignin contents of 4 - 22%. The results of this work indicate that excitation energy transfer phenomena occur in kraft residual lignin and that the emissive properties strongly correlate with the lignin carbonyl content determined by FTIR and the initial Na_2S charge during cooking.

Introduction

Although excitation energy transfer has not been directly studied in lignocellulosics, several researchers have observed indirect evidence of its occurrence. Lundquist has postulated that the fluorescence of lignin was predominantly due to a single fluorophore acting as an 'energy sink' based on the observation that solutions of spruce lignin in dioxane-water displayed emission spectra that were independent of excitation wavelength [1, 2]. Castellan did not observe the same phenomenon for milled wood lignin in 2-hydroxypropylcellulose thin films but did note that the removal of carbonyl chromophores with H_2O_2, $NaBH_4$ or H_2 (Pd/C) resulted in increased fluorescence [3, 4]. A similar observation was made by Barsberg et al who suggested that energy transfer phenomena were playing a significant role [5]. Burlakov *et al.* employed CNDO/S quantum mechanical calculations to examine the ground and excited state structures of several lignin model compounds and concluded that energy transfer from higher energy chromophores could be transferred to lower energy carbonyl containing structures[6, 7]. To the authors' knowledge, numerous studies have examined the fluorescence of milled wood lignin, lignin model compounds and pulping liquors, but not kraft residual lignin. This work discusses the fluorescence spectra of isolated lignin from different kraft pulps subjected to a variety of pulping conditions.

Experimental

Chemicals. All chemicals were purchased from Aldrich Co., Milwaukee, WI, and used as received, except for *p*-dioxane and deionized water. *p*-Dioxane was freshly distilled over $NaBH_4$ prior to its use in lignin isolation. Deionized water was prepared using the Millipore Nano-Pure system.

Kraft Pulping. The kraft pulps were prepared in an electrically-heated, rotating multi-unit digester. The liquor to wood ratio employed was constant at 4:1. Two pulping conditions were used: Condition A used high effective alkali (21.4%) and low sulfidity

(23.2%); Condition B used low effective alkali (14.6%) and high sulfidity (56.8%). The temperature for each cook was ramped from 23°C to 170°C over 90 minutes and the cooks were stopped at H-factors ranging from 120 to 1150. The cooked chips were disintegrated in an industrial blender and screened and washed in a Valley screen.

Isolation of kraft residual lignin. Residual lignin was isolated from the *Pinus taeda* kraft pulps following standard methods common in the literature [8, 9]. The pulps were thoroughly washed with water and dried prior to Soxhlet extraction with acetone for 24 hours. The pulps were then refluxed with 0.1N HCl in *p*-dioxane at 4% consistency for two hours under argon atmosphere. The solutions were then cooled and filtered through a sintered glass filter and then a second time using Celite® filter aid. The *p*-dioxane was removed under reduced pressure with a rotary evaporator. The resultant aqueous lignin solutions were acidified to pH 2.3. The samples were then frozen, thawed, centrifuged and decanted. The lignin precipitates were then washed with pH 2.3 aqueous HCl before removing water via freeze drying.

Preparation of lignin solutions. 60 mg/L solutions of kraft residual lignins were prepared using 2:1 (v/v) 2-methoxyethanol/deionized water. These solutions were further diluted to 12 mg/L with 2-methoxyethanol (14:1 (v/v) 2-methoxyethanol/deionized water) to maximize signal and reduce the optical density of the solutions below 0.1 absorbance units.

Collection of fluorescence spectra. Fluorescence spectra were collected under ambient conditions using a PC-1 steady-state fluorescence spectrophotometer (ISS) equipped with a 300W xenon arc lamp and a R928 PMT (Hamamatsu) photon-counting detector. The monochromator slits were set to achieve an 8 nm spectral bandwidth and the spectra were measured with a step size of 1 nm and a 1 second integration time. Emission spectra were collected using an excitation wavelength of 310 nm. Excitation spectra were monitored using emission at 360 nm. The spectra were corrected by blank subtraction.

Determination of lignin carbonyl group content with FTIR. Fourier Transform Infrared (FTIR) transmission spectra were collected for each of the lignin samples in the solid state using a Magna-IR System 550 (Nicolet Instrument Corporation). Pellets were formed by pressing mixtures of 2 mg of dry lignin sample and 500 mg of dry spectroscopy grade potassium bromide (KBr) at 15 psi for 3 min. under vacuum. Spectra were baseline corrected using a three-point linear approach at 4000 cm^{-1}, 1850 cm^{-1} and 400 cm^{-1}. The carbonyl content was determined using the integrated area between 1840 cm^{-1} to 1550 cm^{-1} as per Faix *et al.* [10].

Results and Discussion

The fluorescence spectra of kraft residual lignins are dominated by the unchanging emission maxima at 360 nm as illustrated in Figure 1. The three dimensional total luminescence plot shows that the emission maxima and overall shape of the spectra is virtually unchanged when the excitation wavelength is scanned from 280 nm to 330 nm. This behaviour is standard for single fluorophores; however it is unusual for mixtures of fluorophores such as those contained in the lignin macromolecule. Lundquist has suggested that phenylcoumaran structures which have an emission maximum at 360 nm are the dominant lignin fluorophores, while Castellan has suggested that biphenyl units, stilbenes, and conjugated side chain structures such as ferulic acid are significant lignin fluorophores [2, 3]. We have observed little or no relationship between fluorescence intensity and the pulp residual lignin content. Furthermore, the normalized fluorescence spectra in Figure 2 illustrate that the major characteristics of the spectra change relatively little with large changes in the pulping conditions. The λ_{ex} and λ_{em} are approximately 315 and 360 nm respectively for all of the residual lignin samples despite the dramatic differences in pulping conditions and cooking time. The Stokes shifts range from 3870-4170 cm^{-1} as the maxima vary slightly.

Table 1: Pulping conditions for selected samples along with fluorescence emission intensity measured in counts per second (cps).

Condition	% EA	% Sulfidity	H-factor	Klason Lignin	Stokes Shift	Emission Intensity (cps)
				(%)	*(cm^{-1})*	*(λ_{ex} 310 nm, λ_{em} 360 nm)*
A-1	21.4	23.2	120	21.8	4171	311391
A-8	21.4	23.2	863	3.89	3968	317126
B-1	14.6	56.8	120	20.3	4171	285914
B-8	14.6	56.8	960	4.25	3868	244040

Although the fluorescence of the residual lignins is quite similar, there are subtle differences which provide some interesting information. From the excitation spectra in Figure 2, it should be noted that as the shoulder at 290 nm decreases, a corresponding increase in relative intensity occurs at 330 nm. This is mirrored by the emission spectra where the shoulder at 380 nm changes significantly as the pulping conditions (effective alkali, sulphidity and H-factor) are altered. Table 1 indicates that the relationship between intensity of emission at 360 nm and kappa number is non-linear for both conditions. However, the Condition A samples exhibit enhanced fluorescence (10-30%) over that of the Condition B samples at the same kappa number. There are likely several contributing factors to this complicated relationship including the formation of fluorophores, the removal of fluorophores, and the generation of quenching functional groups, all of which likely occur at differing rates as the cook progresses. Fragmentation of the lignin network would also alter the potential contribution of both through-bond (Dexter type) and through-space (Förster type) energy transfer to quenching or emitting 'energy sink' structures.

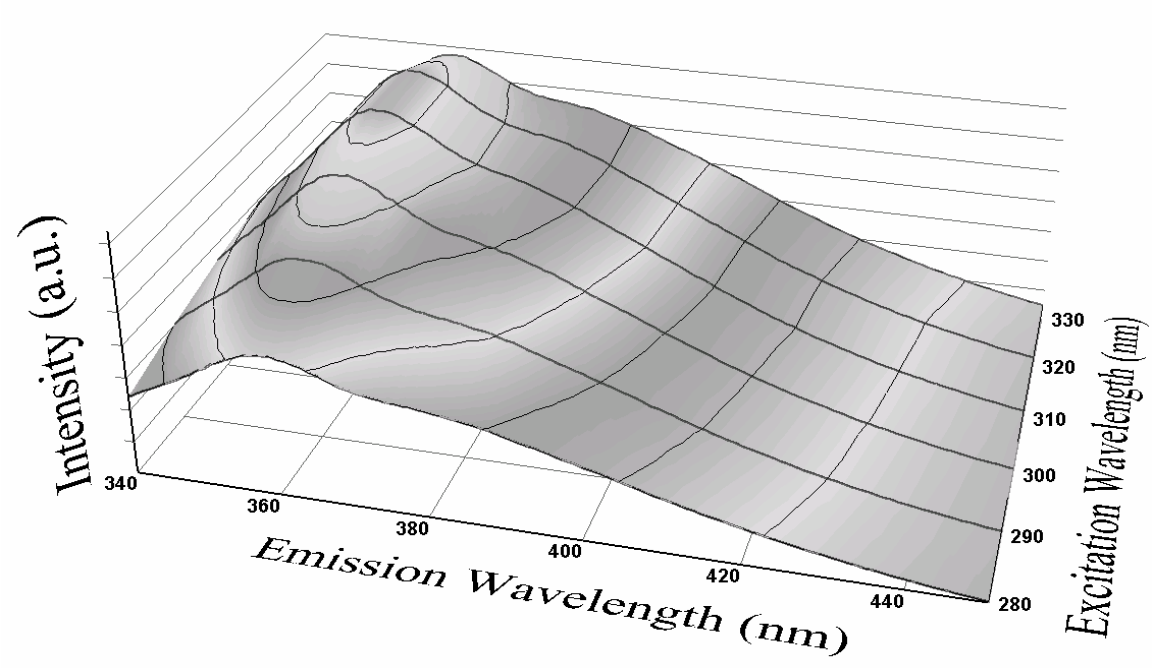

Figure 1: Total luminescence plot for a representative residual lignin sample.

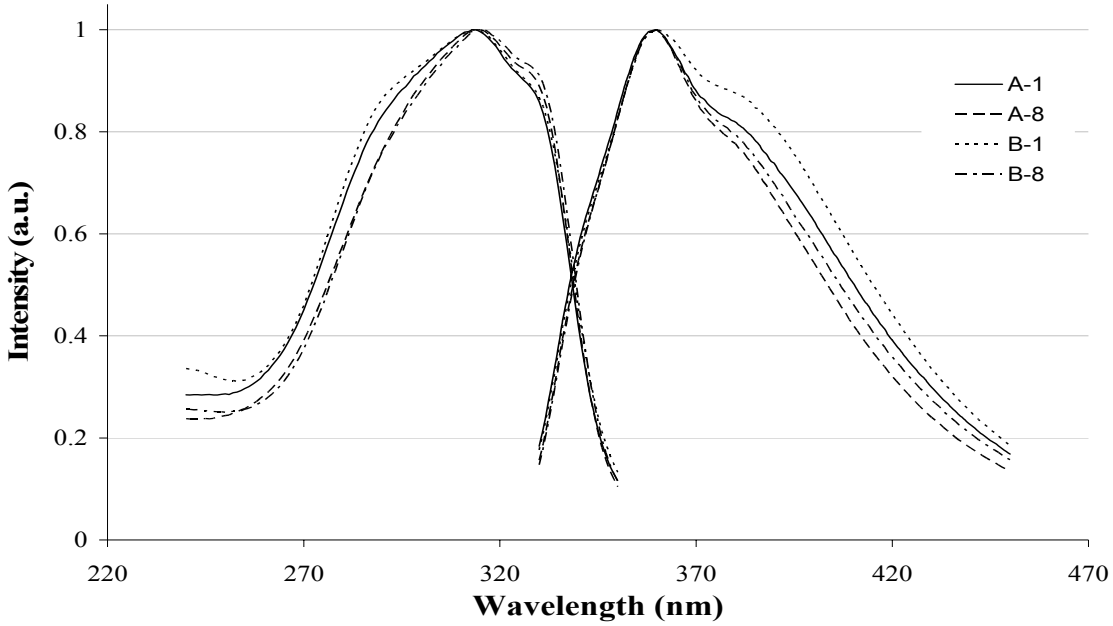

Figure 2: Normalized fluorescence spectra for Conditions A-1, A-8, B-1, and B-8.

The ratiometric response of the 330 nm and 290 nm shoulders in the excitation spectra (Figure 2) provided an interesting opportunity for the analytical chemist since such spectral signatures are typically related to quantitative chemical changes. The ratio of the emission intensities from the excitation spectra at 330 nm and 290 nm was compared to the lignin carbonyl group content as determined by FTIR. Figure 3 depicts the excellent correlation between lignin carbonyl content and this ratio from the excitation spectra. As observed earlier, there are distinct differences between the two different pulping conditions. In this case, the Condition A samples have higher levels of carbonyls at a given intensity ratio. Also the slopes for the two different conditions are different, with the Condition B samples displaying higher sensitivity to carbonyl content.

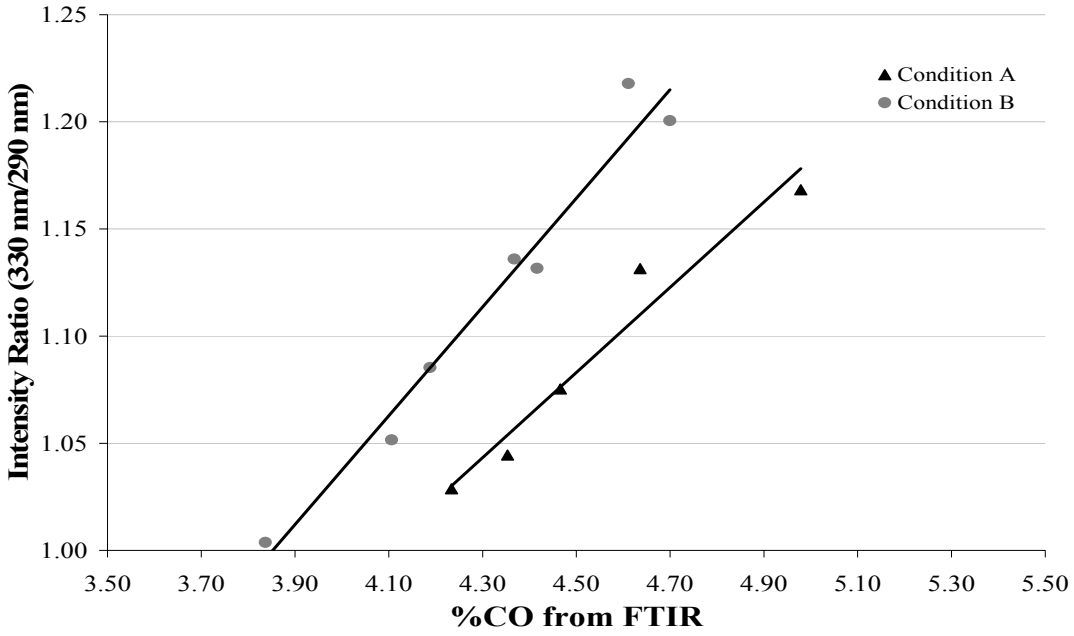

Figure 3: Ratio of fluorescence intensities (measured at 360 nm) with excitation at 330 nm and 290 nm versus percent carbonyls in lignin determined by FTIR (R^2 = 0.96 and 0.97 for Condition A and B respectively).

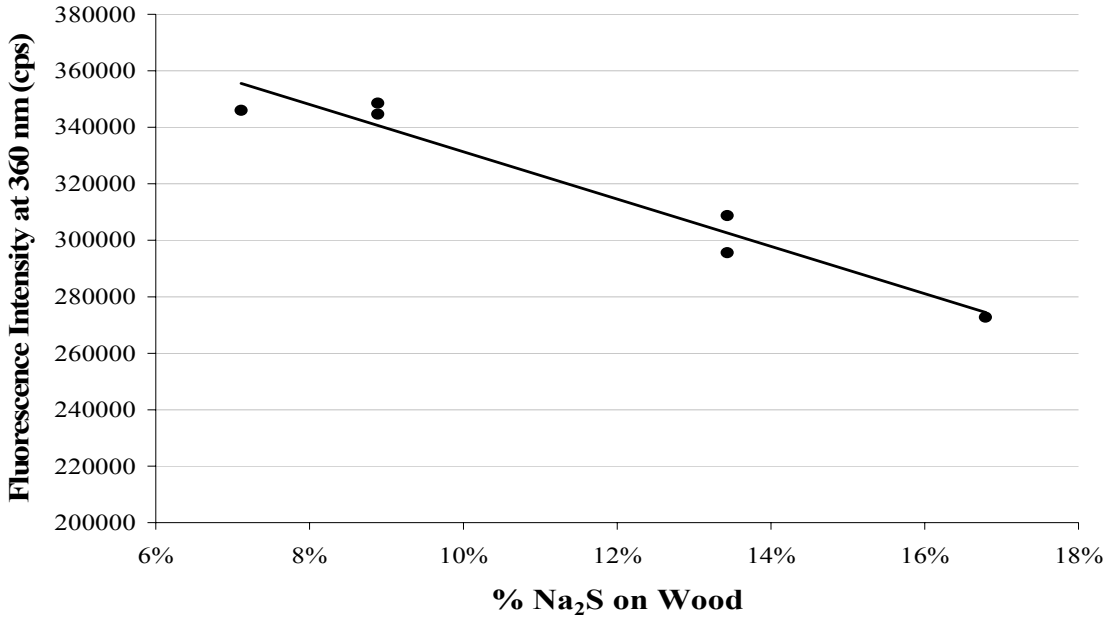

Figure 4: Fluorescence intensity at 360 nm (λ_{ex} 310 nm) versus percent Na_2S on wood during cooks to constant final residual lignin content (R^2 = 0.95).

The only pulping variable that we were able to find a significant correlation with fluorescence occurred for the amount of sodium sulfide charged to the pulping liquor. As shown in Figure 4, the fluorescence intensity for several pulps cooked under different temperatures, and chemical charges to the same final residual lignin content (3.8 – 4.0%) was reduced with increased addition of sodium sulfide. This result is likely related to the amount of sulfur incorporated into the residual lignin. Elemental analyses of the residual lignin samples yielded sulfur contents between 1.01 and 1.64%. Sulfur containing compounds have been recently been proposed to occur in kraft residual lignin [11]. Sulfur containing amino acids such as methionine and cysteine have been known to quench protein auto-fluorescence [12, 13]. Several mechanisms have been proposed including electron transfer [14] and the internal heavy atom effect, in which sulfur activates both internal conversion and non-radiative intersystem crossing relaxation pathways [15]. Further investigation of the sulfur quenching mechanism and

characterization of sulfur containing lignin structures is required to understand this observation.

Conclusions

This study indicates that the fluorescence properties of kraft residual lignin in solution are very similar to the observations made by Lundquist for solutions of spruce milled wood lignin. This suggests that the primary fluorophores in lignin are left intact during typical kraft cooking conditions. Furthermore, the shape of the excitation and emission spectra are largely independent of cooking conditions. However, the lignin carbonyl content determined by FTIR did correlate to a ratiometric response in the excitation spectra, indicating that carbonyl groups participate in the relaxation processes to a certain extent. The sodium sulfide concentration of the white liquor was found to correlate to reduced emission at 360 nm in the emission spectrum. It is interesting to note that the correlation is with the Na_2S process variable not with the final sulfur content in the residual lignin. This suggests that the non-specific presence of sulfur in lignin alone is not sufficient to result in fluorescence quenching; therefore, the chemistry of the cook dictates where the sulfur is incorporated.

Acknowledgements

The authors would like to thank Dr. Rallming Yang and the IPST analytical department for preparing the KBr pellets and collecting the FTIR spectra. Portions of this work were used by C.I.T. and T.J.D. as partial fulfillment of the requirements for the Ph.D. degree at the Georgia Institute of Technology and Institute of Paper Science and Technology.

References

1. Lundquist, K., B. Josefsson, and G. Nyquist, *Analysis of lignin products by fluorescence spectroscopy.* Holzforschung, 1978. **32**(1): p. 27-32.
2. Albinsson, B., et al., *The origin of lignin fluorescence.* Journal of Molecular Structure, 1999. **508**(1-3): p. 19-27.
3. Castellan, A., et al., *Photoyellowing of milled wood lignin and peroxide-bleached milled wood lignin in solid 2-hydroxypropyl cellulose films after sodium borohydride reduction and catalytic hydrogenation in solution: a fluorescence spectroscopic study.* Journal of Wood Chemistry and Technology, 1992. **12**(1): p. 19-33.
4. Castellan, A., P. Girard, and C. Vanucci, *A photoyellowing simulation of bleached high yield wood pulp by lignin models included in a solid carbohydrate matrix.* Journal of Wood Chemistry and Technology, 1988. **8**(1): p. 73-90.
5. Barsberg, S., T. Elder, and C. Felby, *Lignin-quinone interactions: implications for optical properties of lignin.* Chemistry of Materials, 2003. **15**(3): p. 649-655.
6. Burlakov, V.M., et al., *Characterization of electronic structure of ground and excited states of model lignin compounds. III. Quinones and quinone methides.* Cellulose Chemistry and Technology, 1992. **26**(4): p. 421-6.
7. Burlakov, V.M., et al., *Characteristics of the electronic structure of ground and excited states of lignin model compounds. I. Molecular shape.* Cellulose Chemistry and Technology, 1986. **20**(6): p. 651-62.
8. Gellerstedt, G., J. Pranda, and E.L. Lindfors, *Structural and molecular properties of residual birch kraft lignins.* Journal of Wood Chemistry and Technology, 1994. **14**(4): p. 467-82.
9. Gellerstedt, G. and E.L. Lindfors. *On the Structure and Reactivity of Residual Lignin in Kraft Pulp Fibers*. in *International Pulp Bleaching Conference*. 1991. Stockholm.

10. Faix, O., B. Andersons, and G. Zakis, *Determination of carbonyl groups of six round robin lignins by modified oximation and FTIR spectroscopy.* Holzforschung, 1998. **52**(3): p. 268-274.
11. Gellerstedt, G. *Condensation in kraft pulping. A reality?* in *12th International Symposium on Wood and Pulping Chemistry*. 2003. Madison, WI.
12. Yuan, T., A.M. Weljie, and H.J. Vogel, *Tryptophan Fluorescence Quenching by Methionine and Selenomethionine Residues of Calmodulin: Orientation of Peptide and Protein Binding.* Biochemistry, 1998. **37**(9): p. 3187-3195.
13. Chen, Y. and M.D. Barkley, *Toward understanding tryptophan fluorescence in proteins.* Biochemistry, 1998. **37**(28): p. 9976-9982.
14. Marciniak, B. and J. Rozwadowski, *Quenching of the excited singlet state of the N-(9-methylpurin-6-yl)pyridinium cation by sulfur-containing amino acids and carboxylic acids in aqueous solution.* Journal of Photochemistry and Photobiology, A: Chemistry, 1996. **101**(2-3): p. 163-169.
15. Dobrin, S., P. Kaszynski, and J. Waluk, *Stilbene-like molecules: sulfur- and selenium-heterosubstituted indolo[3,2-b]indoles.* Journal of Photochemistry and Photobiology, A: Chemistry, 1997. **105**(2-3): p. 149-152.

24.2 Addendum 2. Scattering coefficient as a measure of specific surface area in mechanical pulps

Submitted to Paperi ja Puu

Lauri K. Lehtonen and Thomas J. Dyer
Institute of Paper Science and Technology
500 10th St. NW Atlanta, GA 30332-0620 U.S.A.

Abstract

Relative bonded area (RBA) is an important paper structure-defining parameter that is reflected in the strength and optical properties of the paper. The traditional determination of RBA relies on the measurement of specific surface area either at various bonding states (Ingmansson-Thode method) or before and after rupture (Skowronski delamination method). The determination of RBA is significantly easier if the scattering coefficient can be used as a measure of specific surface area. However, in mechanical pulps, where the absorption coefficient might affect the scattering coefficient, and the pore size structure is variable, the use of scattering coefficient as a measure of specific surface area cannot be taken for granted. In this paper, the fundamental relationship between scattering coefficient and specific surface area in mechanical pulps was studied using mercury porosimetry and BET nitrogen absorption to measure specific surface area. It was shown that the scattering coefficient is a measure of specific surface area when the wavelength of light used in measuring scattering coefficient is beyond which the scattering coefficient is not limited by significant absorption, and the limit depended on the composition of the sheet and the pressing level and type used to induce bonding. However, there was no significant reduction in scattering coefficient in any of the samples when the wavelength of light used to measure scattering was beyond 600nm. The scattering efficiency, defined as the ratio of scattering coefficient and specific

surface area, was fully explained by the wavelength used to measure scattering coefficient. A plausible explanation for the wavelength dependency of the scattering efficiency was given, which relates the increase in scattering efficiency to the change in refractive index of the material when the wavelength of light to measure scattering coefficient is altered.

Suhteellinen sitoutunut pinta-ala (RBA) on tärkeä paperin rakennetta kuvaava parametri, joka vaikuttaa sekä paperin lujuuteen että optisiin ominaisuuksiin. Perinteisesti RBA:ta on mitattu käyttäen ominaispinta-alan mittausta eri sitoutumis-asteilla (Ingmansson ja Thode menetelmä), tai ennen ja jälkeen arkin palstauttamista (Skowronskin palstauttamismenetelmä). RBA:n mittaaminen on huomattavasti helpompaa, kun valonsironta kerrointa voidaan käyttää ominaispinta-alan mittauksena. Mekaanisilla massoilla ei valonsironnan käyttöä ominaispinta-alan mittaamisessa voida kuitenkaan pitää itsestään selvyytenä, koska näillä massoilla valon absorptio kerroin on suhteellisen korkea ja arkin rakenne on erittäin huokoinen. Tässä artikkelissa tutkittiin valosirontakertoimen ja ominaispinta-alan korrelaatiota eri valon aallon pituuksilla. Ominaispinta-alan mittaukseen käytettiin typpi absorptio (BET) sekä elohopea penetraatio menetelmiä. Tutkimuksessa näytettiin ensin, että valonsirontaa voidaan käyttää ominaispinta-alan mittaukseen, kunhan mittauksessa käytettävä vakio valon aallonpituus on riittävän suuri jotta absorptio ei rajoita valonsirontakerrointa. Toiseksi näytettiin, että käytettävän valonpituuden alaraja riippuu arkin rakenteesta, arkin puristustasosta ja -tavasta. Mekaanisten massojen mittaamista rajoittavaksi aallonpituuden alarajaksi määriteltiin 600 nm. Lisäksi todettiin valonsironnan tehokkuuden riippuvan valon aallonpituudesta. Tätä ei kuitenkaan pystytty selittämään arkin huokosjakaumalla, vaan valonsironnan tehokkuuden vaihtelua selitettiin valon taitekertoimen muuttumisella valon aallonpituuden funktiona.

Introduction

Kubelka-Munk theory [1] is the only readily applicable approach for estimating optical constants in paper [2]. In Kubelka-Munk theory, light flux is treated as two separate dependent parameters, and their intensity is determined by the scattering and absorption coefficients [3]. Scattering coefficient, defined using the Kubelka-Munk theory, has a special importance in understanding paper structure property-relationship due to its physical demeanor to efficiently reflect the specific surface area of the material [2, 4-19]. Thus, scattering coefficient is a very applicable parameter in estimating bonded area in paper and has been widely used for this purpose frequently in chemical pulps [4, 7, 9, 13]. However, there are a few important limiting factors that need to be addressed before scattering coefficient can be used as a measure of specific surface area in pulps which have a very porous structure with significant amount of small pores and yield high absorption coefficients, i.e., mechanical pulps.

High absorption coefficient effect

It has been shown that the K-M scattering coefficient is significantly reduced at high levels of absorption [3, 20, 21]. This effect is known as the NAM anomaly [21] or Foote effect [20]. It is not clear whether this significant decrease in scattering coefficient at higher absorption is an intrinsic error in the Kubelka-Munk theory or an actual physical material property. In the theory where the decrease in scattering coefficient at high absorption is seen as a material property, the scattering decrease has been explained to be a combination of two phenomena: the influence of the absorption on the surface reflectivity of the cell wall and the absorption of light internal to the cell wall [3]. However, it has also been shown using a discrete ordinate radiative transfer (DORT) model that there is an intrinsic error in the K-M model at high absorption levels, explaining roughly 20% of the decrease in scattering coefficient [22]. It needs to be recognized that when scattering coefficient is to be used as a measure of bonding in

paper, the wavelength of light used in the measurement should be at such a level where the scattering is not affected by the strong absorption [11].

Small pores and light scattering

Davis was the first to suggest that the K-M scattering coefficient should be proportional to the specific surface per unit mass of the material [15]. Parsons [18] was the first to obtain proof of this. They used a modified Clark [23] silvering method to measure specific surface area of pulp. Later, Haselton introduced the use of gas adsorption (nitrogen) in determining specific surface area and related it to specific scattering coefficient of paper [7]. Haselton found a linear correlation between scattering coefficient and nitrogen adsorption specific surface area of sulphite pulps refined and wet pressed to different levels of bonding. The correlation obtained by Haselton showed a linear slope of 0.045 (or 45.0 based on m^2/kg scattering and m^2/g specific surface area units). Later, Rennel [19] showed similar linear relationships between scattering coefficient and nitrogen gas adsorption specific surface area (wavelength used in scattering measurements was not mentioned) for various pulps wet pressed and refined to different levels of bonding. In his data, all pulps produced unique scattering coefficient and gas adsorption specific surface area relationships. Also, Swanson and Steber [13] showed that each type of pulp has a unique nitrogen adsorption/scattering coefficient relationship; however, the relationship approached a similar value of 0.044 (or 44.0 based on m^2/kg scattering and m^2/g specific surface area units) for the linear slope at higher wavelengths of light (650nm). Rennel also obtained similar linear slopes using cylindrical model fibers of glass, as long as the diameters of the glass fibers remained larger that 1 micrometer, or the specific surface area approximately below 1.5 m^2/g. In 1959 Van den Akker, mentioned in [13], had made an interesting observation that 0.044 is approximately the value which would be expected by application of Fresnel's law of reflection to a diffusely reflecting body of randomly oriented fibers. This has been later demonstrated theoretically, using Stoke's approach for layered paper structures, to be an accurate approximation by Scallan and Borch [12, 24].

However, there are indications that the ability to detect surface area is limited by the wavelength of light used in the scattering coefficient determination. Swanson and Steber [13] as well as Ingmansson and Thode [4] showed that by using lower wavelengths of light the measured scattering coefficient increased, depending on the pulp used. This behavior has also been observed in mechanical pulps [25].

The effect of particle shape on the scattering efficacy of various types of fibers was studied first by Arnold [6], who showed that the light scattering coefficient was greater for dog-bone shaped fibers than circular ones. Later this was confirmed by Rennel [9], who utilized model glass fibers with variable cross-sectional shapes and showed that each shape represented unique nitrogen absorption specific surface area and light scattering relationships (at 557 nm wavelength of light and a specific surface area range between 0.2 m^2/g to 0.37 m^2/g). The reason for this type of behavior was attributed to the possible variable pore size distribution in the sheet by stating "It should be borne in mind, however, that the determinations of the light-scattering coefficient and surface area (BET) are not concerned with the same thing. The former applies to surfaces down to a distance about 500-600 A, whereas the nitrogen molecule, which measures 3.6 A, record nearly all surfaces – even those not scattering light". Later, it was assumed that the specific surface area detection ability of light in a pulp sheet is approximately a half wavelength of light, based on paint and filler optical research [10, 16, 26, 27].

The microporosity approach of paper, measured with mercury intrusion, considers paper to be a continuous solid phase containing air voids that are the light scattering elements. Using this approach, Alince et al [10], Fineman et al [16], and Rundlöf et al. [14], have shown that there is a correlation between the void specific surface area and scattering coefficient in paper; however, the correlation is better when void pores smaller than 100-200nm are excluded from the data. This is believed to be due to the experimental observations that only voids with the size in the proximity of the wavelength of visible

light are optically effective. Interestingly, the relationship between the cumulative specific pore area above 200nm and scattering coefficient from the data from Alince et al. produces a linear correlation following the approximate slope of 0.045 (up to approximately 1.5 m^2/g mercury intrusion specific surface area, after which a slight curvature appears). This indicates that the minimum optically-effective pore sizes are in the range of 200nm. However, these results are not in agreement with the BET nitrogen adsorption results, wherein similar slopes between scattering coefficient and specific surface area were detected. The detection ability of the nitrogen adsorption method is related to the size of the nitrogen molecule, and thus pores down to the size of 3.6 A should be detected.

The main objective of this paper was to relate scattering coefficient and specific surface area in mechanical pulps at various wavelengths of light, but also to determine the limiting absorption coefficient beyond which the scattering coefficient is significantly reduced and cannot be used as a measure of specific surface area.

Experimental

Fiber middle and fines fractionation: The Bauer McNett apparatus was used to fractionate a hot disintegrated 110 CSF Norway spruce (Picea abies) unbleached TMP. R48 fraction (all above R48) R200 and P200 fraction was collected. P200 fraction was collected using the sedimentation method. The R48 fiber fraction was fractionated twice in order to achieve a near pure fiber fraction without any fines present.

Handsheet forming: Handsheets were formed using a standard Tappi handsheet mold with 150 mesh screen and recirculation of whitewater. Fines handsheets were formed on a dense glass fiber filter paper. Fines contents of the fiber- fines mixed sheets were measured from the formed handsheets using the DDJ method, T 261 cm-00. All

handsheets were restrain-dried if not dry after pressing. The target handsheet basis weight was 60 g/m^2 O.D.

Wet pressing: Couched handsheets were not pressed. Wet pressing was conducted at 65, 489 and 978 psi's and 23ºC using a carver press and 3 blotter papers on one side and a chrome plate on the other side of the handsheet. Wet pressed handsheets were pressed for 1 minute.

Press drying: Press drying was conducted at 6 pressing levels 0, 0.8, 8.1, 16.3, 48.9 and 163 psi's. Individual handsheets were pressed between hot plates heated to 120ºC and a sandwich that consisted of a felt, wet blotter (to increase drying time and humidity above 100ºC), handsheet, chrome plate, and a filter paper (to protect the chrome plate). All handsheets were pressed until completely dry.

Testing: BET was measured at Micromeritics, Norcross, Georgia, U.S.A., using the TriStar 3000 nitrogen absorption surface area equipment. The nitrogen gas partial pressure was changed by altering the helium/nitrogen mixture. The samples were degassed at 60ºC. Mercury intrusion porosimetry specific surface area measurements were performed also at *Micromeritics,* using the AutoPore IV equipment. The intrusion pressure and pore size was related using the Washburn equation. Since the Washburn equation is based on cylindrical capillaries with circular openings, the specific surface area based on the voidal pore structure was calculated using a cylindrical pore model assumption. The pressure range used in the mercury porosimetry was between 1.3 - 60.000 psi, corresponding to a pore size range from 150 um to 4nm.

The UV/vis spectra were recorded on a Perkin-Elmer Lambda 900 UV/vis spectrometer equipped with a diffuse reflectance and transmittance accessory (PELA-1000). The accessory is essentially an optical bench that includes double-beam transfer optics and a six-inch integrating sphere. Background corrections were recorded using a Labsphere

SRS-99-020 standard. Reflectance data were measured over a black and a white background with known reflectance values. For each sample and background, an average of five measurements was utilized to determine both the light scattering (*s*) and light absorption (*k*) coefficients. The absorption and scattering coefficients were calculated from the reflectance data by means of the Kubelka-Munk theory and the following equations:

$$k = \frac{s(1 - R_\infty)^2}{2R_\infty} \quad [1]$$

$$s = \frac{1}{w(1/R_\infty - R_\infty)} \ln \frac{(1 - R_W R_\infty)(R_\infty - R_{GW})}{(1 - R_{GW} R_\infty)(R_\infty - R_W)} \quad [2]$$

$$\frac{1}{R_\infty} + R_\infty = \frac{(R_{GW} - R_{GS})(1 + R_W R_S) - (R_W - R_S)(1 + R_{GW} R_{GS})}{R_S R_{GW} - R_W R_{GW}} \quad [3]$$

where R_∞ is the reflectance of an optically thick sample, k is the absorption coefficient (m^2/kg), s is the scattering coefficient (m^2/kg), w is the grammage (kg/m^2), R_{GW} is the reflectance for the white background, R_{GS} is the reflectance for the black background, R_W is the reflectance for the sample over a white background, and R_S is the reflectance for the sample over a black background. Data were collected from 300 to 800 nm.

Results

Limiting absorption. The method used in the analysis was similar to that of Rundlof et al. [25], where the scattering and absorption coefficients were measured at a broad range of wavelengths, as shown in Figures 1 and 2.

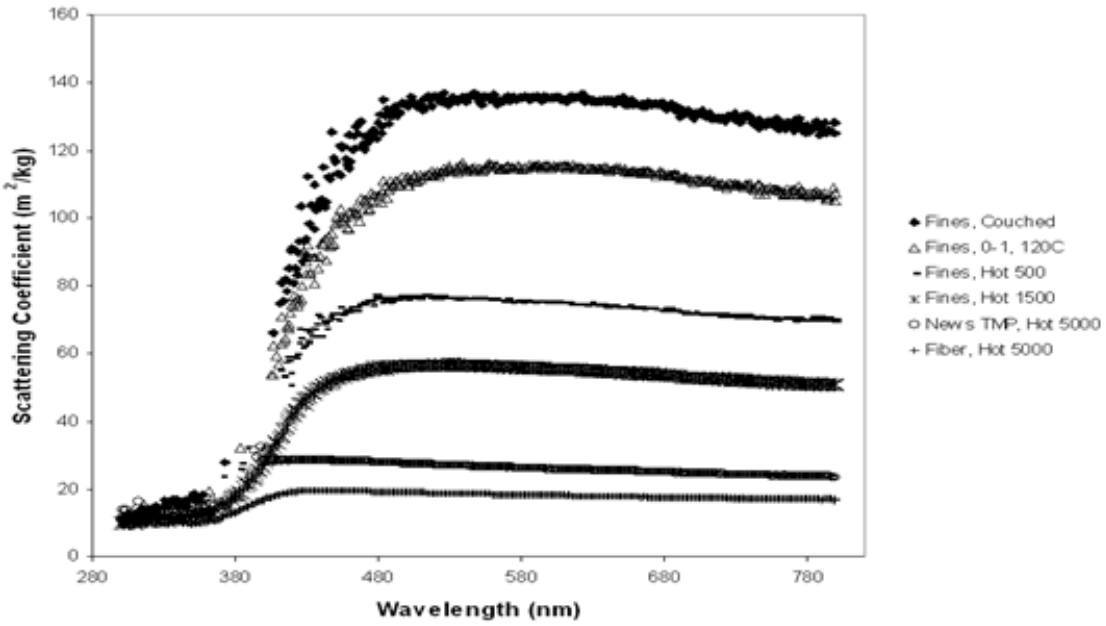

Figure 1. Scattering coefficient at various wavelengths of fines (P200), whole pulp (TMP) and fiber (R48) sheets wet pressed and press-dried to various levels of bonding.

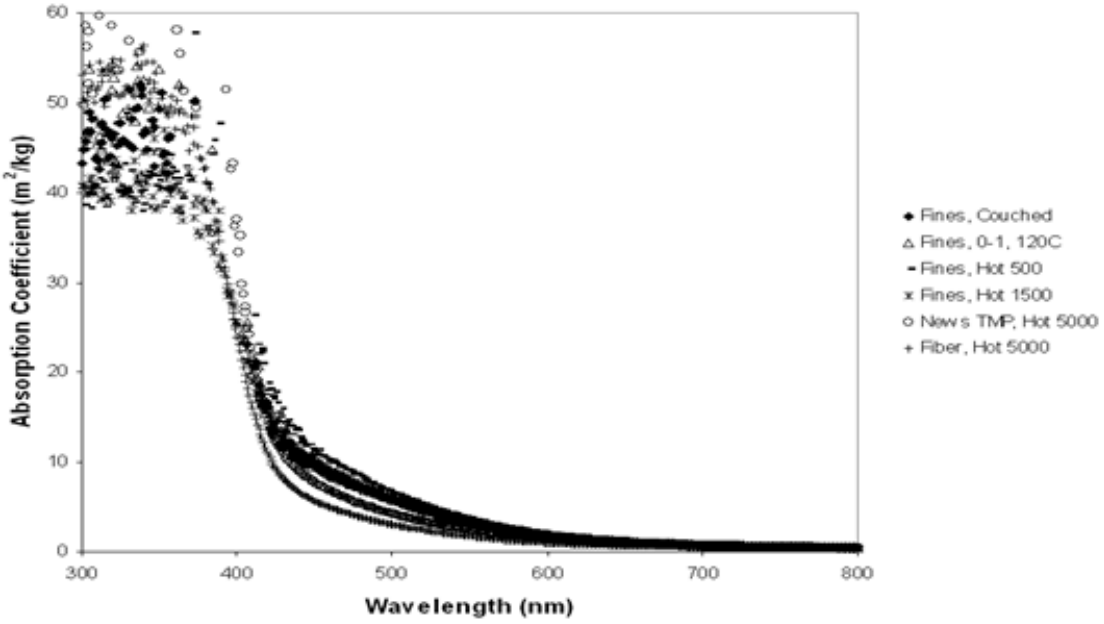

Figure 2. Absorption coefficient at various wavelengths of fines (P200), whole pulp (TMP) and fiber (R48) sheets wet pressed and press dried to various levels of bonding.

The range between the scattering coefficient at the highest wavelength 800 nm and the maximum scattering coefficient was considered as the range where scattering coefficient was not affected by the strong absorption. For this range, a linear least significant squared correlation line was calculated. This methodology is depicted in Figure 3.

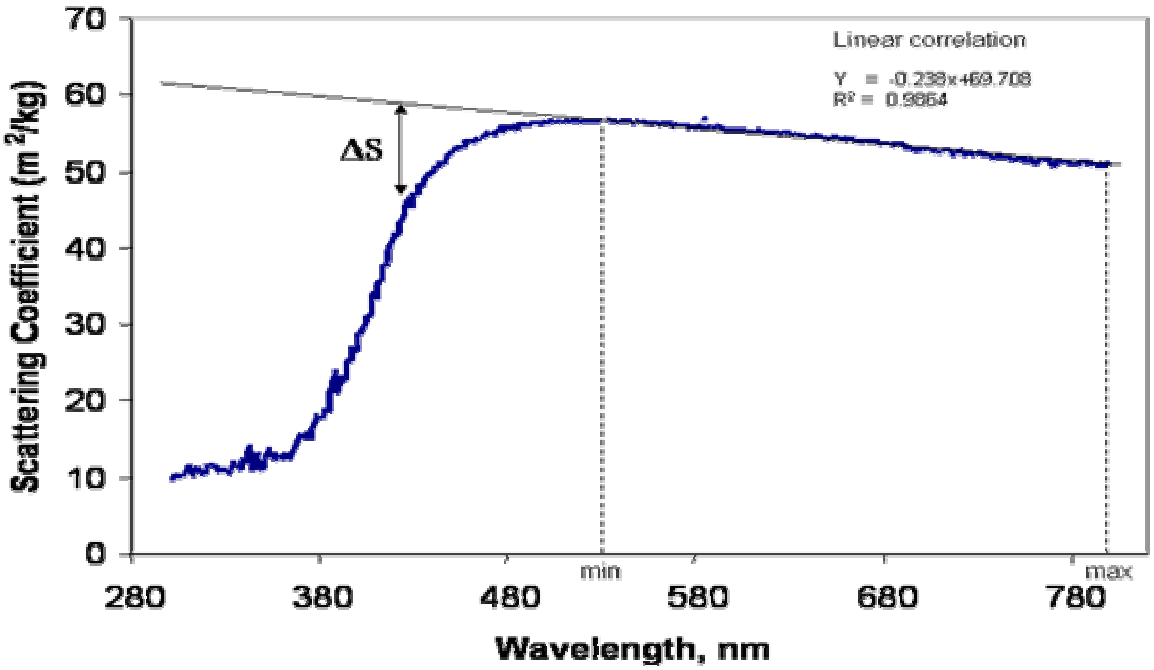

Figure 3. Scattering coefficient wavelength dependency of fines sheet press dried at 120ºC and 48.9 psi pressure.

The linear least square correlation results for all the samples included in the study are shown in Table 1. Also the range of wavelengths where the scattering coefficient was not affected by strong absorption is shown.

Table 1. Linear correlation slopes, intercepts, applicable range and R^2 values for all samples.

Sample	Pressure	Temperature	Time	s (scattering)=xλ(wavelength)+c			Applicable λ range, nm	
	psi	°C	min	Slope	Intercept	R^2	min	max
Fines couched	0	23	0	-0.0383	157.71	0.8319	526	800
Fines wet 2000	65	23	1	-0.0438	153.57	0.9098	561	800
Fines wet 15000	489	23	1	-0.0416	134.21	0.8913	531	800
Fines wet 30000	978	23	1	-0.0381	123.96	0.933	540	800
Fines hot 0	0	120	6	-0.0409	139.76	0.908	557	800
Fines hot 30	0.8	120	6	-0.0257	102.08	0.8821	649	800
Fines hot 250	8.1	120	5	-0.0246	94.283	0.9383	608	800
Fines hot 500	16.3	120	4	-0.0269	90.866	0.9712	514	800
Fines hot 1500	48.9	120	3	-0.0238	69.708	0.9864	533	800
Fines hot 5000	163	120	3	-0.0225	57.394	0.9959	442	800
Fiber hot 5000	163	120	3	-0.0074	22.734	0.991	440	800
TMP couched	0	23	0	-0.0223	83.651	0.93	492	800
TMP wet 2000	65	23	1	-0.0304	87.25	0.9893	482	800
TMP wet 5000	163	23	1	-0.0297	84.207	0.9902	471	800
TMP wet 15000	489	23	1	-0.0289	82.036	0.9896	475	800
TMP wet 30000	978	23	1	-0.0324	80.588	0.9861	415	800
TMP wet 2000 on	65	23	1440	-0.0247	73.531	0.98	474	800
TMP hot 0	0	120	6	-0.0237	77.79	0.9754	446	800
TMP hot 30	0.8	120	6	-0.0186	61.168	0.9929	483	800
TMP hot 250	8.1	120	5	-0.0215	58.266	0.9942	440	800
TMP hot 500	16.3	120	4	-0.0199	54.502	0.9962	479	800
TMP hot 1500	48.9	120	3	-0.0177	46.718	0.9961	449	800
TMP hot 5000	163	120	3	-0.014	34.6	0.9711	398	800
TMP hot 10000	326	120	3	-0.0113	29.021	0.9978	442	800

The slope of the scattering dependency of the wavelength of light was related to the intercept of the same relationship (Figure 4), and also specific surface area obtained from the BET measurements (not shown here), clearly showing a stronger wavelength dependency of K-M scattering coefficient at higher specific surface area.

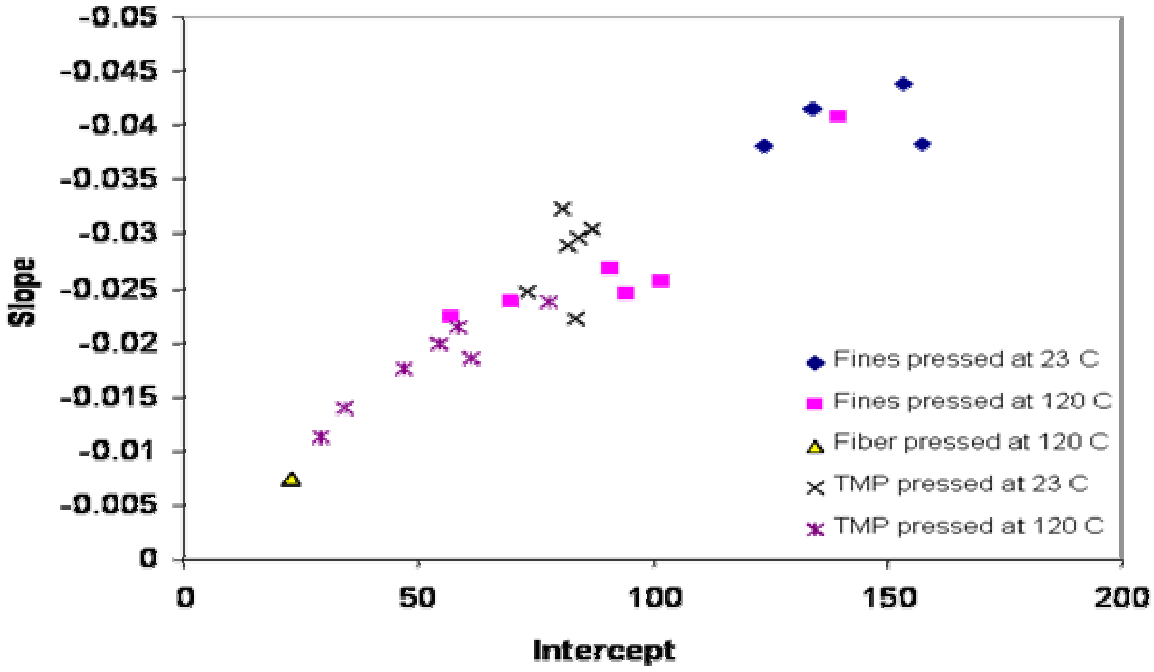

Figure 4. Scattering coefficient wavelength dependency linear slope vs. intercept.

The difference in the apparent K-M scattering coefficient and the linear model at various wavelengths of light is depicted in Figure 5, and shows that when the wavelength of light used in the scattering coefficient is beyond 600 nm, there was no significant change in the scattering coefficient regardless of pressing type, level or sheet composition. However, the limiting wavelength was different for each fraction, being mostly higher for pure fines sheets (P200) and lower for whole pulp and fiber sheets (R48).

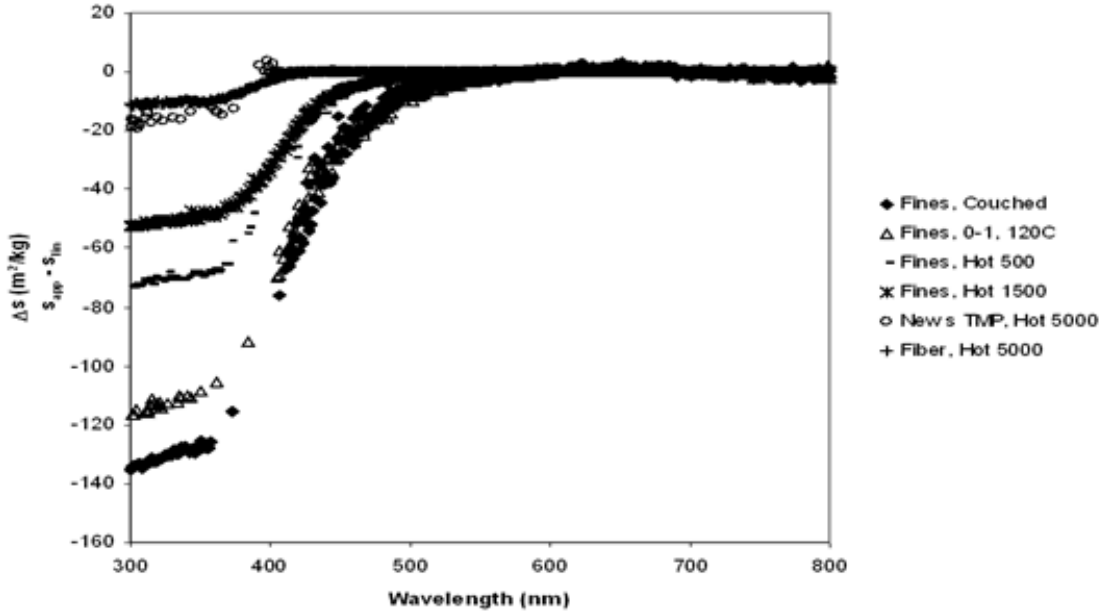

Figure 5. Reduction is scattering coefficient as a function of wavelength for various mechanical pulp whole pulp, fiber (R48) and fines (P200) sheets pressed to different levels of bonding.

This also resulted in the observation that the level of absorption at which a significant decreased in scattering coefficient occurred was dependent on the sheet composition, as shown in Figure 6. The absolute reduction in scattering coefficient at high absorption was generally related to the level of scattering coefficient at negligible absorption, being higher for the fines (P200) sheets than for the whole pulp (TMP) and fiber sheets.

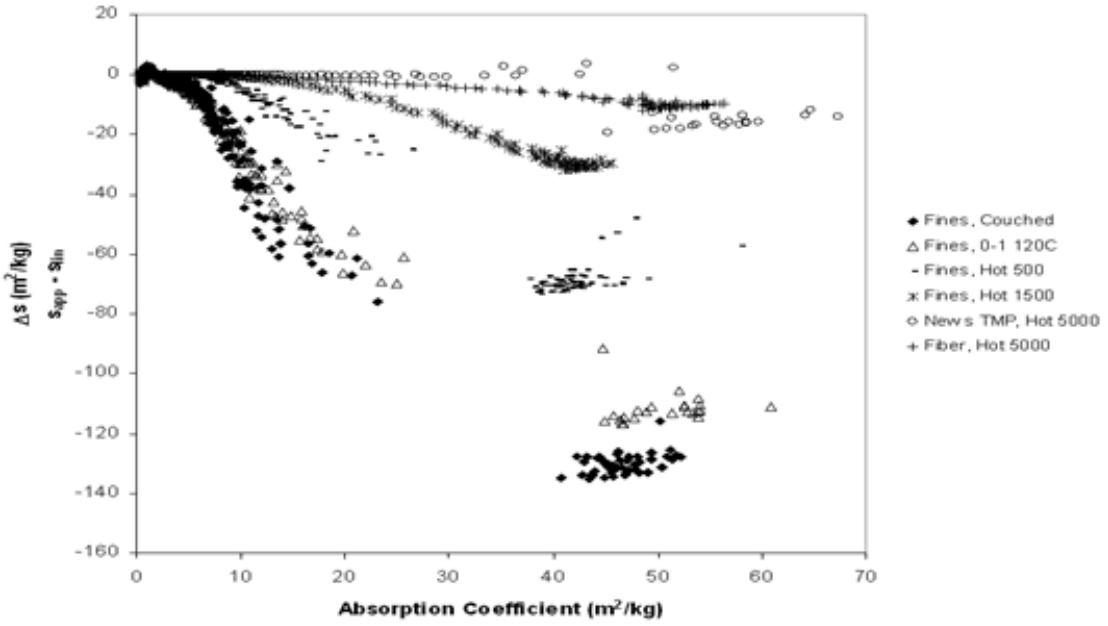

Figure 6. Reduction is scattering coefficient as a function of absorption for various mechanical pulp whole pulp, fiber (R48) and fines (P200) sheets pressed to different levels of bonding.

Scattering coefficient and Mercury porosimetry specific surface area. Earlier studies indicated that the scattering efficiency, defined as the scattering coefficient at constant specific surface area, of the sheet void structure is directly related to the wavelength of light, and that the optically effective pore size decreases as the wavelength of light is decreased. Thus, herein the K-M scattering coefficient was correlated with the cumulative specific surface area obtained from the mercury porosimetry pore size distribution measurements, using the hypothesis where the highest correlation with these two parameters at various wavelengths of light will be obtained when pore sizes close to the proximity of the wavelength of light will be excluded from the specific surface area calculation. In this section the linear wavelength dependence of scattering coefficient, shown in Table 1, was used to study the effect of pore size distribution on the scattering coefficient. The absorption limit was neglected, in order to allow the use of all samples throughout this part of the study for a wide range of wavelengths. Specific surface area was calculated from the mercury porosimetry pore volume measurements excluding

certain pores sizes systematically from the calculation. The calculated specific surface areas, where certain pore sizes were excluded, were then correlated with scattering coefficients at various wavelengths of light.

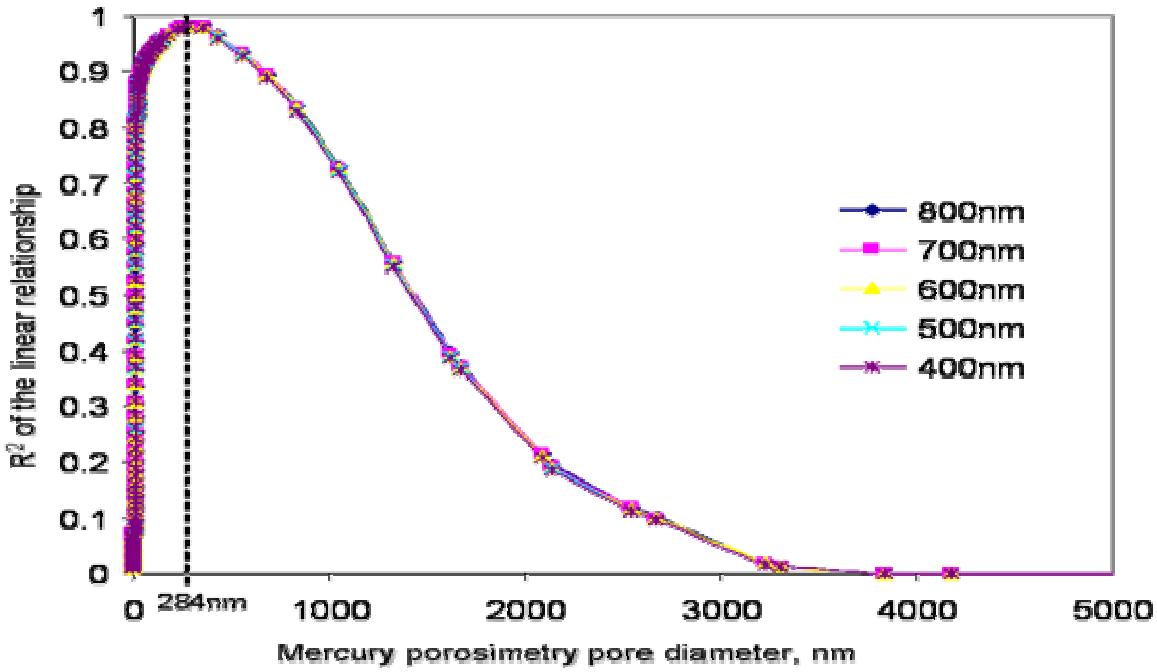

Figure 7. R^2 of the linear relationship between scattering coefficient and mercury porosimetry specific surface area as a function of the excluded pore sizes.

The hypothesis that the scattering efficiency at lower wavelength of light is due to the light's ability to detect smaller pores was not supported. The highest correlation coefficient (shown in Figure 7 as R^2) between mercury porosimetry and scattering coefficient was obtained when pores smaller than 284 nm were excluded from the calculation, independent of the wavelength of light used. The expected shift to smaller pores sizes at lower wavelengths of light did not occur.

However, the scattering efficiency of the calculated specific surface area from mercury porosimetry when pores smaller than 284 nm were excluded was yet wavelength dependent, resulting in higher scattering coefficients for lower wavelengths of light at a constant specific surface area, as seen in Figure 8. No significant differences were

observed in the scattering coefficient - specific surface area relationship between various sheet compositions and pressing conditions.

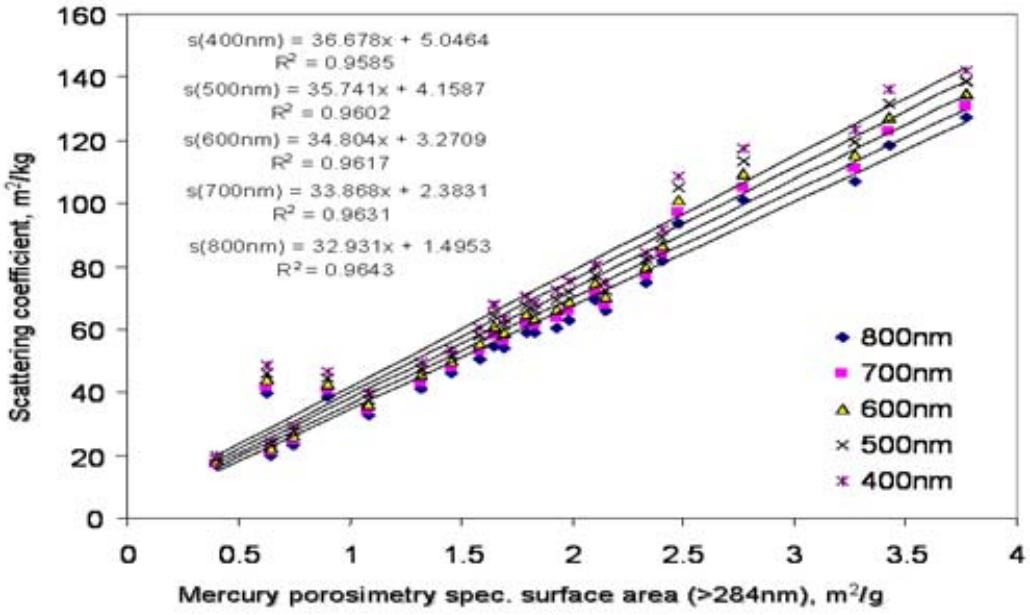

Figure 8. Mercury porosimetry specific surface area excluding surface area from pores smaller than 284 nm vs. K-M scattering coefficient at various wavelengths of light.

The slope and the intercept of the mercury porosimetry specific surface area (excluding pores smaller than 284 nm) and scattering coefficient was fully explained by the wavelength of light used in measuring scattering coefficient, depicted in Figure 9. The slope at zero intercept was 32.675, and was obtained at wavelength of 968.5 nm.

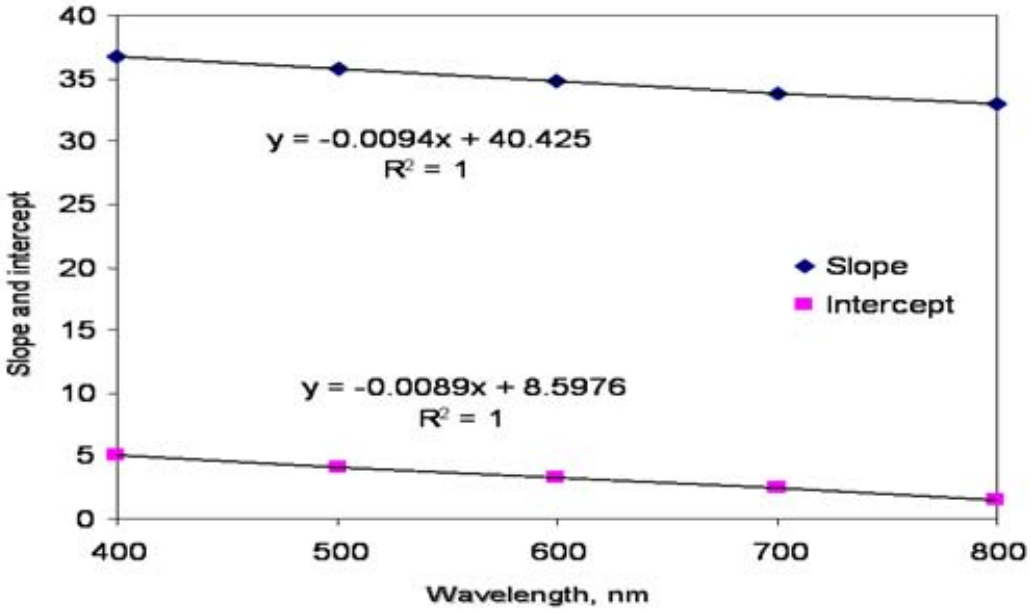

Figure 9. Wavelength dependency of the mercury porosimetry (excluding pores below 284nm) vs. scattering coefficient slope and intercept.

Scattering coefficient and BET nitrogen adsorption specific surface area. The BET nitrogen adsorption and scattering coefficient relationship was dependent on the wavelength of light used, as was observed for mercury porosimetry. An increase in scattering efficiency was observed as the wavelength of light was decreased (Figure 10).

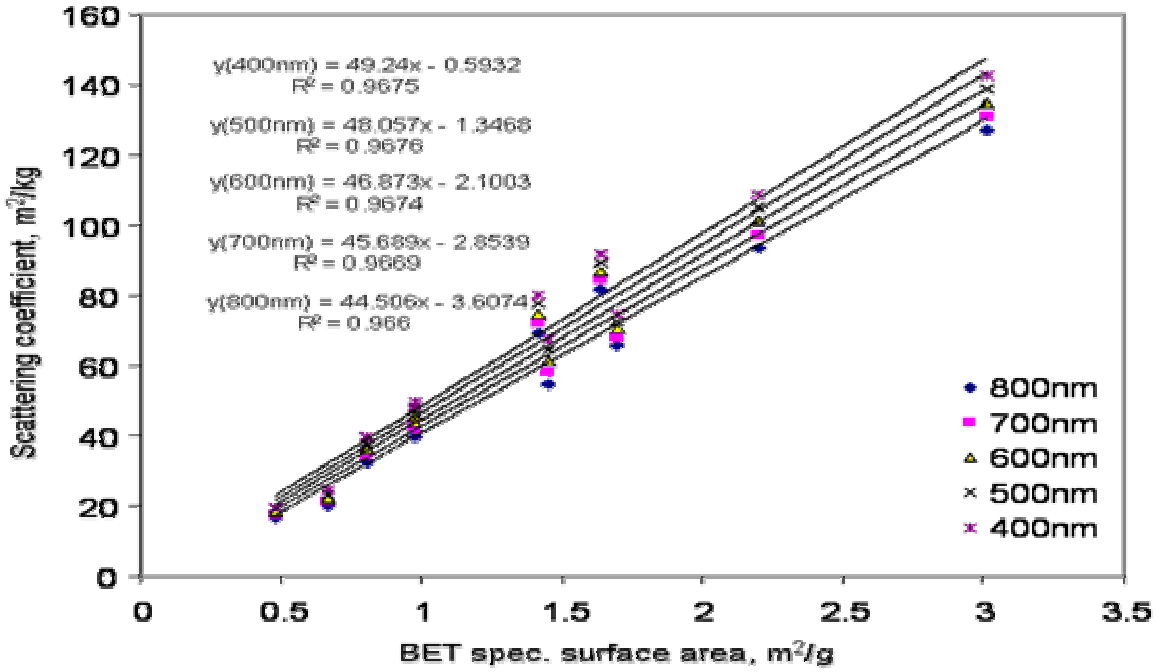

Figure 10. BET specific surface area vs scattering coefficient at various wavelengths of light.

The slope and intercept of the linear relationship was fully explained by the wavelength of light used in measuring scattering coefficient (Figure 11). The linear correlation line passed through the origin at 321 nm and the corresponding slope then was 50.2.

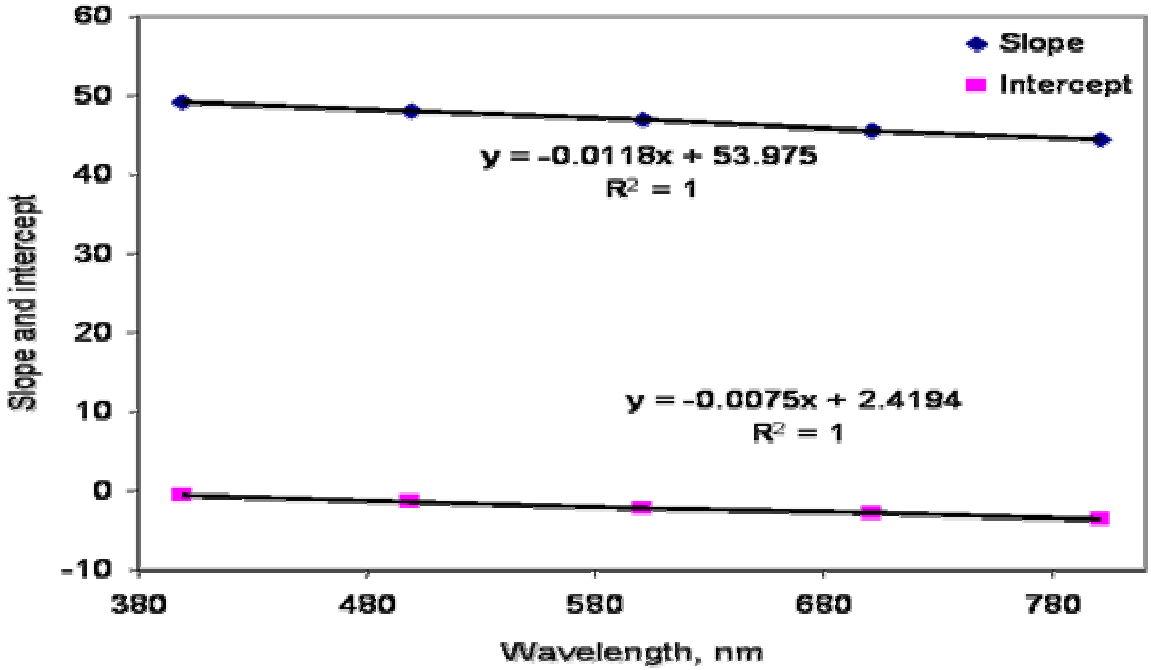

Figure 11. Wavelength dependency of the BET nitrogen adsorption – scattering relationship slope and intercept.

Discussion

In this paper we failed to show that the increase in scattering efficiency at lower wavelengths of light is due to the increased pore detection ability of the scattered light. The pore size needed to be excluded from the surface area calculation (284nm) to obtain the highest correlation (R^2=0.97) coefficient with scattering coefficient was constant regardless of wavelength of light used. However, the scattering efficiency was wavelength dependent, resulting in higher scattering coefficients for lower wavelengths of light at constant specific surface area. These findings were supported by the results obtained from the BET nitrogen absorption measurements.

The increase in the slope of the specific surface area – scattering coefficient at lower wavelengths of light regardless of specific surface area measurement method was inherent to the increase in scattering coefficient of the individual samples in the region of negligible absorption.

Scallan and Borch [12, 24], using a multilayer Stokes approach for determining scattering coefficient in paper, have shown that for pulps of negligible absorption (bleached, or measured at high wavelength) the scattering coefficient and specific surface area are related according to the following equation:

$$s = \frac{r}{(1-r)} A_0 \qquad [4]$$

where s is the specific scattering coefficient, r the reflectivity of the material (fiber) and A_0 the specific surface area of the structure.

Reflectivity on the other hand can be expressed using Fresnel equations for negligible absorption and normal incidence, with air being the medium, as a function of refractive index of the material:

$$r = \frac{(n-1)^2}{(n+1)^2} \qquad [5]$$

Earlier it has been concluded that the refractive index of the lignocellulosic fiber material is fairly constant, varying only slight depending on the chemical composition of the cell wall (cellulose 1.56, lignin 1.61), and has very little or no significant impact on the optical properties of paper [12, 17]. It is known that refractive index of material is wavelength dependent; however the variation being small in the visible wavelength region, for water for example, ranging from 1.334 to 1.35 at wavelengths from 700nm to 400nm, respectively [3, 28]. Although the increase in the refractive index appears to be minor, the impact on the scattering coefficient – specific surface area relationship is accentuated through the relationship between reflectivity and refractive index (Equation 4) as well as between reflectivity and the scattering coefficient (Equation 5).

If we then assume that the linear relationship defined (table 1) in this study between wavelength of light and scattering coefficient indeed is a true scattering coefficient, where the contribution of absorption can be neglected, the increase in scattering at lower wavelengths could be the explained by the change in refractive index. Using the variability in the refractive index of water in visible wavelength range, a decrease of 3% in refractive index results in a 10% increase in the slope of scattering coefficient-specific surface area relationship. This 10% increase is comparable with the increase in the slopes obtained in this study for scattering coefficient and specific surface area relationship (11%) for the visible wavelength range.

The calculated refractive indices based on equations 4 and 5 for the sheets studied here are depicted in Figure 12 for mercury porosimetry (excluding pores below 284 nm) and BET based linear relationships between scattering coefficient. The results obtained from the mercury porosimetry linear relationships are significantly below the values reported for pure cellulose and lignin [17]. However, the BET-based calculated refractive indices yield values in close proximity to those of the pure cell wall constitutive polymers (1.52-1.55). The wavelength explains all the variation in the calculated refractive index due to the fact that wavelength explained all the variation in scattering coefficient – specific surface area slopes. The rate of refraction index decrease is very similar to that reported by Parsons [18], where the refractive index of ramie fiber decreased from 1.6082 to 1.5969 at wavelengths 486 nm and 656 nm respectively.

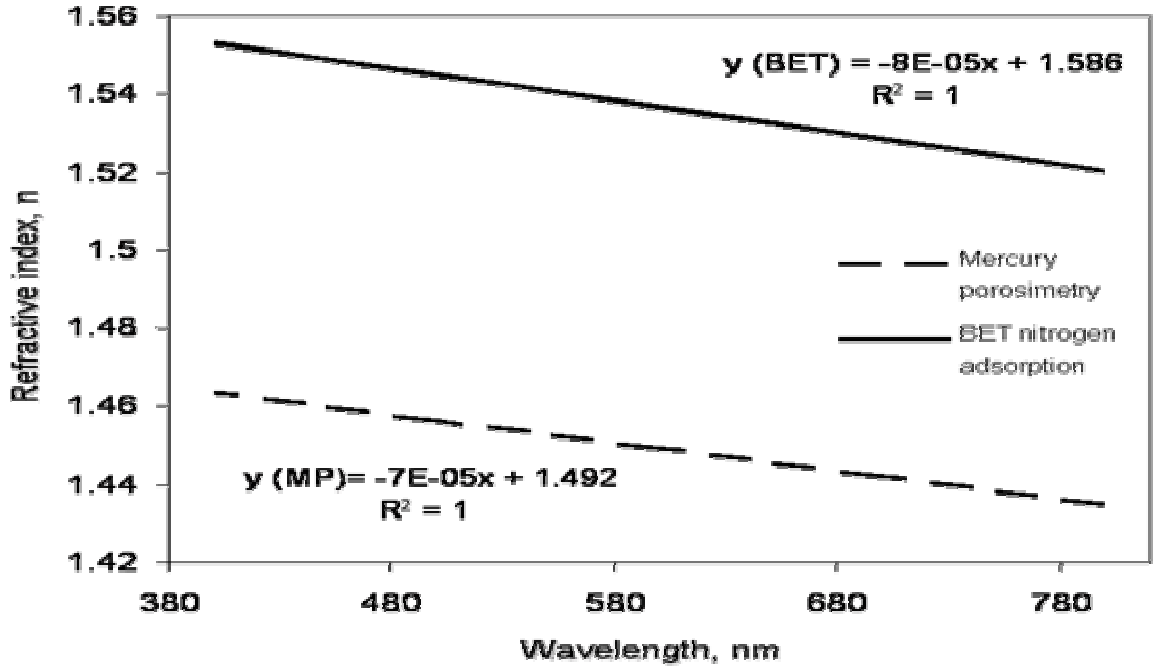

Figure 12. Wavelength dependency of refractive index for mercury porosimetry and BET nitrogen adsorption based results.

There is another plausible explanation for the discrepancy between mercury porosimetry and BET nitrogen adsorption reported here, and it leads us to believe that there is something inherently inaccurate in the mercury porosimetry specific surface area measurement. In mercury porosimetry, due to the fact that mercury doesn't wet fibers, a positive pressure is needed to penetrate the mercury into the pore structure. In order to detect nanometer-scale pores, significantly high pressures (up to 60 000 psi) are needed. It has been stated that these high pressures will possibly lead to structural changes in the material under investigation [29]. Thus, it is possible that the low correlation between specific surface area measured by mercury intrusion and light scattering coefficient beyond the 100-200 nm pore size is due to the destructive nature of the mercury intrusion method.

In Figure 13, the linear correlation coefficient (R^2 shown) of BET nitrogen absorption specific surface area and specific surface area calculated from the mercury porosimetry pore volume distribution is plotted against the excluded pore size in mercury

porosimetry. The highest correlation coefficient is obtained for exactly the same pore size as for the scattering coefficient- mercury porosimetry relationship, 284 nm. The specific surface area detection ability of nitrogen molecule is 3.6 Å, thus it is unlikely that the pore size-based highest correlation for the BET-mercury porosimetry correlation would be obtained at a pore size of 284nm. This yields support to the idea that mercury intrusion destroys the sheet beyond 284nm, which corresponds to an intrusion pressure of 637 psi.

However, due to the comparable results obtained here for BET nitrogen adsorption and scattering coefficient with the earlier findings, and the significant similarity in the calculated refractive indices with the pure lignin and cellulose we believe that scattering coefficient is indeed a measure of specific surface area in mechanical pulps.

Conclusions

In this paper, the fundamental relationship between scattering coefficient and specific surface area in mechanical pulps was studied using mercury porosimetry and BET nitrogen absorption to measure specific surface area. The pulps included in the study were sheets of TMP fines (P200), whole pulp TMP and fiber (R48) wet pressed and press dried to various levels of specific surface area. It was shown that the scattering coefficient is a measure of specific surface area when the wavelength of light used in measuring scattering coefficient is beyond which the scattering coefficient is not limited by significant absorption. For these samples the limit depended on the composition of the sheet and the pressing level and type used to induce bonding. However, there was no significant drop in scattering coefficient in any of the samples when the wavelength of light used to measure scattering was beyond 600 nm.

The scattering efficiency, defined as the ratio of scattering coefficient and specific surface area, was a factor of wavelength used to measure scattering coefficient. It was shown using mercury porosimetry pore size distribution data that the efficiency increase was not due to the ability to detect smaller pores at lower wavelengths of light. A plausible explanation was given, which relates the increase in scattering efficiency to the change in refractive index of the material when the wavelength of light to measure scattering coefficient is altered. Also the applicability of mercury intrusion porosimetry in weak structures was questioned.

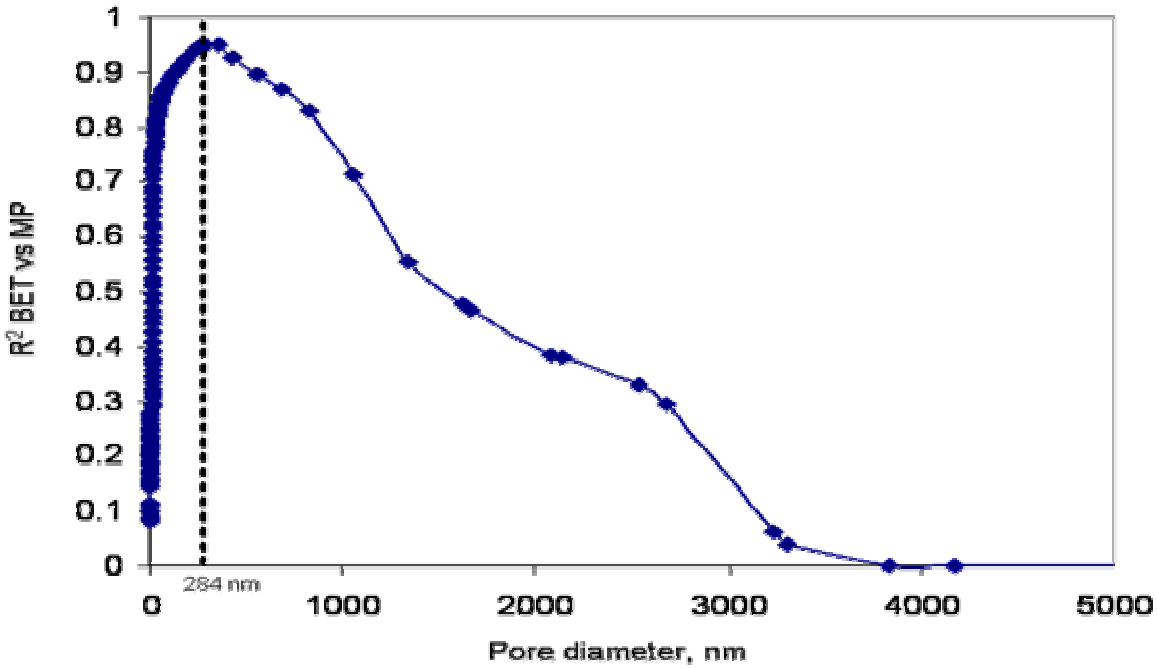

Figure 13. R^2 of the linear relationship between BET nitrogen adsorption and mercury porosimetry specific surface area as a function of the excluded pore sizes.

Acknowledgements

Portions of this work will be used as partial fulfillment of the requirements for the Ph.D. degree at the Institute of Paper Science and Technology by both authors. The authors would like to thank Mats Rundlöf and Cameron Thomson for valuable discussions. We also gratefully acknowledge the financial aid provided by the Institute of Paper Science and Technology, Finnish Cultural Foundation and Walter Ahlström Foundation.

References

1. Kubelka, P., *New Contributions to the Optical Properties of Intensely Light Scattering Materials. Part I.* J. Opt. Soc. Am., 1948. **44**(4): p. 488.
2. Leskela, M., *Optical properties*, in *Paper Physics*, N. K., Editor. 1998, Fapet Oy: Jyvaskyla. p. 117-137.
3. Koukoulas, A.A., Jordan, B.D., *Effect of Strong Absorption on the Kubelka-Munk Scattering Coefficient.* JPPS, 1997. **23**(5): p. J224-J232.
4. Ingmanson, W.L., Thode, E.F., *Factors Contributing to the Strength of a Sheet of Paper.* Tappi Journal, 1959. **42**(1): p. 83.
5. Borch, J., *Optical and Appearance Properties*, in *Handbook of Physical Testing of Paper*, L. Borch, Mark and Habeger, Editor. 2001. p. 127-138.
6. Arnold, E.A., *Light Scattering in Fibrous Sheets.* Tappi Journal, 1963. **46**(4): p. 250-256.
7. Haselton, W.R., *Gas Adsorption by Wood, Pulp and Paper II. The Application of Gas Adsorption Techniques to the Study of the Area and Structure of pulps and the Unbonded and Bonded Area of Paper.* Tappi Journal, 1955. **38**(12): p. 712-723.
8. Hartler, N., Rennel, J., *Opacity in Relation to Strength Properties of Pulps II. Light Scattering Coefficient and Surface Area of Unbonded Pulp Fibers.* Svensk Papperstidning, 1969. **72**(1): p. 9-13.

9. Rennel, J., *Opacity in Relation to Strength Properties of Pulps III, Light Scattering of Sheets of Model Fibers.* Tappi Journal, 1969. **52**(10): p. 1943-1947.
10. Alince, B., Pobuska J., Van Den Ven, T.G.M., *Light Scattering and Microporosity in Paper.* JPPS, 2002. **28**(3): p. 93-98.
11. Page, D., Appita, 1981. **35**(2): p. 173.
12. Scallan, A.M., Borch J., *An Interpretation of Paper Reflectance Based Upon Morphology, I. Initial Considerations.* Tappi Journal, 1972. **55**(4): p. 583-588.
13. Swanson, J.W., Steber, A.J., *Fiber Surface Area and Bonded Area.* Tappi Journal, 1959. **42**(12): p. 986-994.
14. Rundlof, M., Hoglund, H., Htun, M., Wagberg, L. *Effect of Fines Quality on Paper Properties*. in *Intl. Mech. Pulping Conf.* 1995. Ottawa.
15. Davis, M.N., *Use of Color Measuring Instruments in the Manufacture of Uncoated Paper,* Paper Trade Journal, 1940. **111**(14): p. 40-44.
16. Fineman, I., Bergenblad, H., Pauler, N., *Beeinflussung der Porenstruktur von Papier durch Fullstoffe.* Das Papier, 1990. **44**(10A): p. V56-V62.
17. Giertz, H.W., *Opaciteten hos pappersmassor.* Svensk Papperstidning, 1951. **54**(8): p. 267-274.
18. Parsons, S.R., *Optical characteristics of paper as a function of fiber classification.* Tech. Assoc. Pap., 1942. **1942**(25): p. 360-368.
19. Rennel, J., *Opacity in Relation to Strength Properties of Pulp; Part 4 - The Effect of Beating and Wet Pressing.* Pulp and Paper Mag. Can., 1969. **70**(10): p. T151-T158.
20. Foote, W.J., *An Investigation of the Fundamental Scattering and Absorption Coefficients in Dyed Handsheets.* Tech. Assoc. Papers (TAPPI), 1939. **22**(1): p. 397.
21. Nordman, L., Aaltonen, P., Makkonen, T. *Relationship between Mechanical and Optical Properties of Paper Affected by Web Consolidation*. In *Symposium on Consolidation of the Paper Web*. 1966: Tech. Section Brit. Paper and Board Makers' Assoc.

22. Granberg, H., Edstrom, P., *Quantification of the Intrinsic Error of the Kubelka-Munk Model Caused by Strong Light Absorption.* JPPS, 2003. **29**(11): p. J386-J390.
23. Clark, J.d.A., *A New Method for Measuring Specific Surface,* Paper Trade Journal, 1942. **115**(1): p. 32-39.
24. Borch, J., Scallan, A.M., *An Interpretation of Paper Reflectance Based Upon Morphology II. The Effect of Mass Distribution.* Tappi Journal, 1976. **59**(10): p. 102.
25. Rundlof, M., Bristow, J.A., *A Note Concerning the Interaction Between Light Scattering and Light Absorption in the Application of Kubelka-Munk Equations.* JPPS, 1997. **23**(5): p. J200-J223.
26. Alince, B., Lepoutre, P. *Plastic pigments in paper coatings: The effect of polystyrene particle size on porosity and optical properties*. In *1980 TAPPI Coating Conference*. 1980. Atlanta: TAPPI Press.
27. Lepoutre, P., Pauler, N., Alince, B., Rigdahl, M., *The Light-Scattering Efficiency of Microvoids in Paper Coatings and Filled Papers.* JPPS, 1989. **15**(5): p. J183-J185.
28. Lynch, D.K., Livingston, W., *Color and Light in Nature*. 2nd ed. 2001: Cambridge University Press.
29. Hill, C.A.S., Papadopoulos, A.N., *A Review of methods used to determine the size of the cell wall microvoids of wood,*. Journal of the Inst. of Wood Sci., 2001. **15**(6 (Issue 90)): p. 337-344.

24.3 Addendum 3. The Aptitude of Laccase to Attach to Bleached Chemical Pulps

Richard P. Chandra, Thomas J. Dyer and Arthur J. Ragauskas
Institute of Paper Science and Technology
500 10th St. NW Atlanta, GA 30332-0620 U.S.A.

Research in pulp and paper is undergoing a dramatic shift in priorities. Research programs need to improve the cost effectiveness and quality of pulp products while still addressing societal and environmental needs. Recently several researchers have begun to explore the use of chemical and enzymatic technologies to modify the surface of pulp fibers with the explicit desire to improve the physical properties of the final product. The effects of modifying the fiber chemistry of lignocellulosic pulps have been well established over the past three decades. Several literature reports and patents [1-8] have demonstrated distinct changes in fiber properties by grafting acid groups onto pulp fibers. Barzyk et al. [9] and Gatenholm et al [10] have shown that grafting of acid groups onto a fiber will affect a variety of physical properties including pulp strength and swelling properties.

In addition to these chemical processes for modifying pulp fibers, a series of enzymatic technologies are being developed. The use of cellulase and hemicellulase treatments to modify pulp properties has advanced the most rapidly, providing improvements in refining energy, freeness and fiber flexibility [11, 12]. Studies by Wong [13] and Viikari [14] have shown that the application of laccase to thermomechanical pulps results in paper strength increases. These studies build upon the prior research of Kharazipour [15, 16] and Felby [17, 18] that have shown that laccase could be used to activate mechanical pulp fibers for the formation of resin-free MDF boards with improved properties.

Previous work by Chandra and Ragauskas [19] has shown that laccase can also be employed to attach monomeric phenolic acids to high-kappa kraft pulps to increase both surface and bulk acid groups. It was postulated that laccase created phenoxy radicals by reacting with the phenolic acids that subsequently attached to the lignin on the kraft fiber surface. Later work showed that the attachment of a cationic dye (i.e., celestine blue) to the fiber could also be accomplished with laccase and the resulting biotreated fibers were found to exhibit improvements in physical strength properties, including 10-15% increases in tensile strength [20].. The current work focused on investigating the effects of laccase bio-grafting treatments on fully bleached chemical pulps. Fully bleached chemical pulp was treated with laccase in the presence of 2-hydroxyphenyl triphenylphosphonium bromide. This compound was chosen since it reacted with laccase, and possessed a cationic charged group. It was the goal of this research note to investigate the effects of bio-grafting a cationic charge on the physical properties of fully bleached kraft pulps.

Materials and Methods

Pulp. A dry-lap fully bleached ECF softwood kraft pulp was obtained from a commercial facility located in the southeastern U.S.A. The commercial pulps were exhaustively washed until the filtrate was pH neutral and colorless.

Laccase. Laccase was donated by Novo Nordisk Biotech, Raleigh, NC. The laccase was Novo NS51002 isolated from *Trametes villosa*. The activity of laccase was measured by monitoring the rate of oxidation of syringaldazine according to Sealey et al. [21]. The change in A_{530nm} of 0.001 per minute per mL of enzyme solution in a 100-mM potassium phosphate buffer (2.20 mL) and 0.216 mM syringaldazine in methanol (0.300 mL) was set to one unit (U) of activity. This test was done at 23°C and pH 4.5.

Pulp Treatments. Pulp (30.00 g) was suspended at 5.00% consistency (mass pulp/mass pulp+mass water) in a Kapak bag and combined with 5.00 mmol 2-hydroxybenzyl-

triphenylphosphonium bromide (Figure 1). The mixture was stirred and the pH was adjusted to 4.5. The pulp slurry was then immersed in a water bath set to 45°C, after which 5.00 mL of laccase (2.35 x 10^6 U/g pulp) was added, the bag was sealed, and the pulp mixture was allowed to react for 4.00 hours. A second set of analogous experiments were performed substituting 3-(carboxypropyl)-triphenylphosphonium bromide and allyl-triphenylphosponium chloride for 2-hydroxybenzyl- triphenylphosphonium bromide. The experiments performed are outlined in Table 1. After treatment, the pulp samples were filtered and washed until the filtrate was colorless and pH neutral. The pulps were then stored at -4°C and 20% consistency. The treated pulp was then soxhlet extracted for 24 h with methanol to ensure that the treated pulp was free of starting material. The soxhlet extracted pulp was water-washed and air-dried. The lignin content of the kraft pulps was determined by $KMnO_4$ titration of the pulp following TAPPI method T-236 and expressed as a "kappa number." This value is an indirect measurement of lignin content: % lignin content = 0.15 x kappa number. The permanganate number (UM 251) is the number of milliliters of 0.1*N* potassium permanganate solution that is consumed by 1 gram of oven-dry pulp under certain specified and carefully controlled conditions. This permanganate oxidation is a measure of the lignin content of the pulp and consequently a measure of the bleach demand. The permanganate number is therefore useful in determining the extent of delignification of low lignin content or fully bleached pulps.

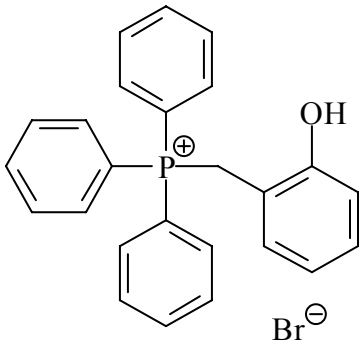

Figure 1: The Structure of 2-hydroxyphenyl triphenylphosphonium bromide.

Table 1: Treatment Regime Applied to High-Kappa Kraft Pulp Fibers and Fully Bleached Pulp.

Treatment	**Symbol**
Control	Control
Laccase + Pulp	Lac
2-hydroxy triphenylphosphonium + Pulp	Pho
2-hydroxy triphenylphosphonium + Laccase + Pulp	Lac + Pho
3-(carboxypropyl)-triphenylphosphonium bromide + Pulp	CPho
3-(carboxypropyl)-triphenylphosphonium bromide + Laccase +Pulp	Lac + CPho
Allyl-triphenylphosponium chloride + Pulp	APho
Allyl-triphenylphosponium chloride + Laccase + Pulp	Lac + APho

Results and Discussion

The goals of the present study were two-fold. The first was to evaluate the possibility that radicals created by a laccase treatment were indeed able to attach to fully bleached kraft pulp. The second goal of this study was to show the effects of laccase treatment with a cationic compound on the physical properties of the resulting pulp. It is intuitive to think that the creation of phenoxy radicals via the reaction of a phenolic compound with laccase would result in polymerization with lignin in solution [22-24], however, in previous work by Chandra and Ragauskas, it was shown that water-soluble 4-hydroxybenzoic acid could be attached to lignin on high-kappa pulp fibers with the aid of laccase [19]. In the present study, it was of interest to reveal whether the grafting ability of laccase could be expanded to fully bleached pulps which possess very small amounts of lignin. Previous work by Yamaguchi et al. [25, 26] and by Chandra and Ragauskas [19] has assumed that the bio-grafting reaction with laccase occurs on pulp lignin. In the

current literature there have not been any accounts of phenoxy radicals coupling to cellulose.

Pulps were treated with Laccase and a phenolic cationic compound 2-hydroxyphenyl (triphenylphosphonium) bromide. As shown in Figure 2, the results of phosphorous analysis after methanol extraction revealed that the samples treated with laccase and 2-hydroxyphenyl (triphenylphosphonium) bromide (Lac+Pho) possessed the highest phosphorous content. This is strong evidence in favor of laccase-facilitated grafting to cellulose. The Pho sample showed a similar phosphorous content as the control without any treatment, indicating that the methanol extraction was efficient in removing the 2-hydroxyphenyl (triphenylphosphonium) bromide that did not couple to the fiber. As supporting evidence for the laccase-facilitated coupling reaction, the samples were then tested for their total concentration of residual lignin using the p-number test.

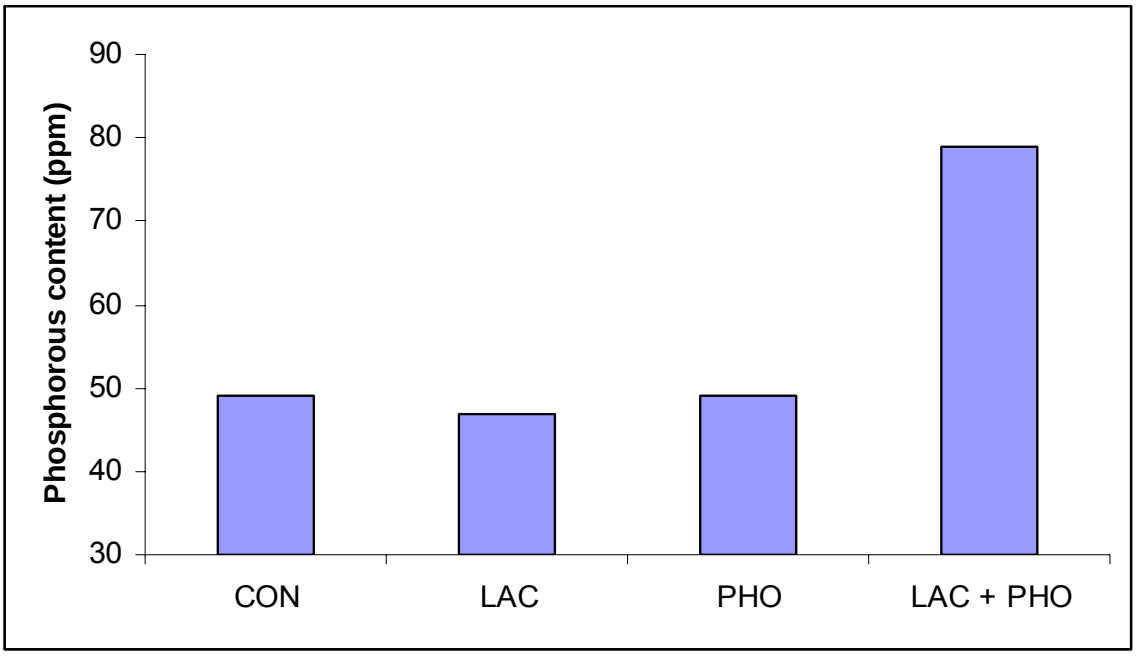

Figure 2: Phosphorous Content of Fully Bleached Pulps Treated with Laccase and 2-Phosphonium.

The coupling of 2-hydroxyphenyl (triphenylphosphonium) bromide to the fibers should result in an increase in P-number, since Pho carries four aromatic rings (Figure 1) and should react with permanganate during the P-number test [27]. The results of the P-number test showed similar trends to those observed with phosphorous content, indicating that laccase indeed facilitated the attachment of the 2-hydroxyphenyl (triphenylphosphonium) bromide to the pulp fibers. Previous work by Huttermann et al. [28] has shown that a six-hour reaction of laccase with 20% w/w solution of lignosulfonates was necessary for the irreversible attachment of the "activated" lignosulfonates to fully bleached pulp. In the present study, a four hour reaction with a 8.8 μM (0.39 % w/w) concentration of 2-hydroxyphenyl (triphenylphosphonium) bromide was required to attach the compound to the pulp. The difference in results from Huttermann et al. [28] may be due to the fact that both the pulp and laccase-generated radicals from 2-hydroxyphenyl (triphenylphosphonium) bromide were present simultaneously, allowing for instant coupling of the 2-hydroxyphenyl (triphenylphosphonium) bromide to the pulp.

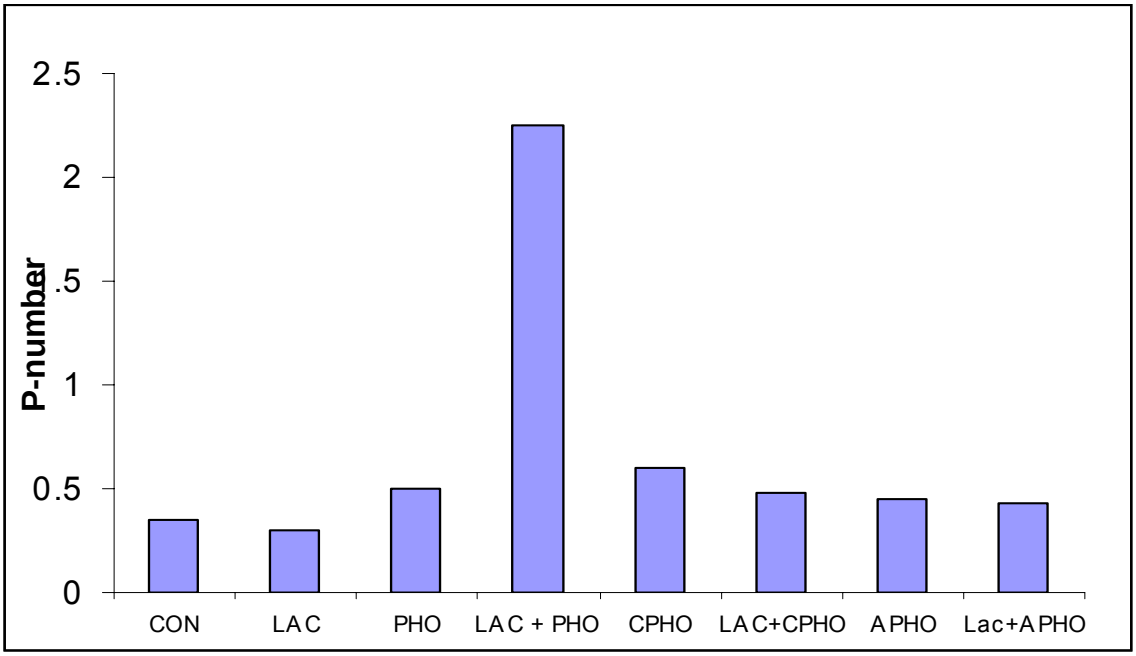

Figure 3: Phosphorous Content of Fully Bleached Pulps Treated with Laccase and 2-hydroxyphenyl-phosphonium bromide, 3-(carboxypropyl)-triphenylphosphonium bromide and allyl-triphenylphosponium chloride.

It was hypothesized that laccase reacted with the phenolic hydroxyl group on 2-hydroxyphenyl (triphenylphosphonium) bromide forming a phenoxy radical that subsequently coupled with the bleached pulp. To further explicate the effect of the laccase/2-hydroxyphenyl (triphenylphosphonium) bromide treatment on the bleached pulp, samples were reacted with two other triphenyl-phosphonium compounds: 3-(carboxypropyl)-triphenylphosphonium bromide and allyl-triphenylphosponium chloride. These compounds were not expected to react with laccase since they do not contain a phenol group on their aromatic rings. Samples were treated following the same protocol as the previous treatments. After methanol extraction, the P-number was measured on the samples indicating that laccase did not facilitate the attachment of 3-(carboxypropyl)-triphenylphosphonium bromide and allyl-triphenylphosponium chloride to the pulp. These results strongly suggest that the compound must be reacted for the laccase enzyme to couple to the pulp.

Further investigation focused on the effects of laccase-facilitated grafting of 2-hydroxyphenyl (triphenylphosphonium) bromide on paper physical properties. As shown in Table 2, the handsheets made from pulp that underwent Lac+Pho treatment suffered a decrease in pulp brightness from 85.7 to 61.9, indicative of the yellow product formed during the reaction of laccase with 2-hydroxyphenyl (triphenylphosphonium) bromide. Treatments with Laccase and 2-hydroxyphenyl (triphenylphosphonium) bromide (Lac+Pho) resulted in decreases in density, tear, and tensile strength of the treated sheets. It was apparent that the coupling of Pho to the sheet resulted in an interference in the normal consolidation of the sheets. This may be due to the large size of the Pho, since it contains four aromatic ring structures. Lignin is a polymer of aromatic ring structures. Since lignin is known to interfere with pulp fiber bonding resulting in decreases in paper strength [29-31], the coupling of a structure containing four aromatic rings such as Pho to

the bleached fibers may result in a similar effect. It is apparent from the physical data that laccase treatment with Pho results in significant decreases in all the strength properties.

Table 2: Paper Physical Properties of Samples Treated with Laccase and 2-hydroxyphenyl (triphenylphosphonium).

Treatment	Con	Pho	Lac	Lac+Pho	LSD[a]
Apparent Density (g/cm^3)	0.550	0.564	0.537	0.493	0.011
Brightness(% ISO)	85.7	86.0	83.5	61.9	2.95
Tear Index (mN m^2/g per ply)	9.06	9.27	9.44	8.53	0.230
Tensile Index (N m/g)	45.3	46.3	47.2	42.7	1.15
Wet-tensile Index (N m/g)	1.37	1.39	1.57	1.58	0.649

[a]The least significant difference value (LSD) is the standard deviation of the Lgal treatment repeated three times, multiplied by twice the student's t-value at 2 degrees of freedom and the 95% confidence level.

Conclusions

It has been shown here that laccase is capable of attaching a water-soluble exogenous compound to the surface of fully bleached pulp fibers. The changes in fibers properties did not result in increases in paper physical properties.

References

1. Stahel, E.P., Stannett, V.T., and Vitta, S.B., *Preparation and Properties of Acrylic and Methacrylic Acid Grafted Cellulose Prepared by Ceric Ion Initiation.* Journal of Applied Polymer Science, 1986. **32**(7): p. 5799-5810.

2. El-Saied, H. and Fahmy, Y., *Chemical Modification of Pulp and Physically Added Chemicals in Papermaking (2). Grafting Co-polymerization with Hydrophilic and Hydrophobic Monomers and their Binary Mixtures in Comparison to Physically Added Homopolymers and to Classical Chemical Modification.* Holzforschung, 1974. **28**(2): p. 61-66.

3. Ebhoaeye, J. and Okieimen, E.F., *Grafting Acrylonitrile and Acrylic Acid Monomers on Cellulosic Materials.* Journal of Applied Polymer Science, 1986. **31**(5): p. 1275-1280.

4. Hornof, V. and Puissant, L., *Copolymer/Homopolymer Ratio in the Grafting of Methacrylic Acid on Cellulose by the Xanthate Process.* Cellulose Chemistry and Technology, 1983. **17**(1): p. 3-10.

5. Kubota, H. and Kuwabara, S., *Water-Absorbing Characteristics of Acrylic Acid-Grafted Carboxymethyl Cellulose Synthesized by Photografting.* Journal of Applied Polymer Science, 1996. **60**(11): p. 1965-1970.

6. Sobolev, *Graft Polymerization of Acrylic Acid-Ester Mixtures to Cellulose*. 1969: United States.

7. Stannett, V.T. and Williams, J.L., *Method of Increasing the Water Absorption of Cellulose- Containing Materials*. 1977: United States.

8. Antoine, R. and Shaw, T.A., *Process for Preparing Graft Copolymers of Cellulosic Materials and Copolymers Obtained*. 1975: France.

9. Barzyk, D., Page, D.H., and Ragauskas, A.J., *Acid-Group Topochemistry and Fiber-to-Fiber Specific Bond Strength.* Journal of Pulp and Paper Science, 1997. **23**(2): p. 59-61.

10. Gatenholm, P., Gellerstedt, F., and Wagberg, L., *Swelling Behaviour of Succinylated Fibers.* Cellulose, 2000. **7**(1): p. 67-86.

11. Mansfield, S., Wong, K.K.Y., de Jong, E., and Saddler, J., *Xylanase prebleaching of fractions of Douglas-fir kraft pulp of different fibre length.* Applied and Microbial Biotechnology, 1996. **46**: p. 319-326.

12. Oksanen, T., Pere, J., Buchert, J., and Viikari, L., *The Effect of Trichoderma reesei Cellulases and Hemicellulases on the Paper Technical Properties of Never-dried Bleached Kraft Pulp.* Cellulose, 1997. **4**: p. 329-339.

13. Wong, K.K.Y., Richardson, J.D., and Mansfield, S., *Enzymatic Treatment of Mechanical Pulp Fibers for Improving Papermaking Properties.* Biotechnology Progress, 2000. **16**: p. 1025-1029.

14. Viikari, L., Harkki, T., Niku-Paavlova, M.-L., Buchert, J., and Poppius-Levlin, K. *Oxidative Enzymes for Fibre Modification*. In *7th International Conference on Biotechnology in the Pulp and Paper Industry*. 1998. Vancouver, B.C.

15. Kharazipour, A., Huttermann, A., and Luedmann, H.D., *Enzymatic activation of wood fibers as a means for the production of wood composites.* Journal of Adhesion Science and Technology, 1997. **11**(3): p. 419-427.

16. Kharazipour, A., Huttermann, A., Luedmann, H.D., and Nonninger, K., *Properties of fiber boards obtained by activation of the middle lamella lignin of wood fibers with peroxidase and H_2O_2 before conventional pressing.* Journal of Adhesion Science and Technology, 1998. **12**(10): p. 1045-1053.

17. Felby, C., Pedersen, L.S., and Nielsen, B.R., *Enhanced Auto-Adhesion of Wood Fibers Using Phenol Oxidases.* Holzforchung, 1997. **51**(3): p. 281-286.

18. Felby, C., Nielsen, B.R., Oleson, P.O., and Skibsted, L.H., *Identification and Quantification of Radical Reaction Intermediates by Electron Spin Resonance Spectrometry of Laccase Catalyzed Oxidation of Wood Fibers from Beech.* Applied Microbiology and Biotechnology, 1997. **48**: p. 459-464.

19. Chandra, R.P. and Ragauskas, A.J., *Evaluating Laccase Facilitated Coupling of Phenolic Acids to High-Kappa Kraft Pulps.* Enzyme and Microbial Technology, 2002. **30**(7): p. 855-861.

20. Chandra, R., Wolfaardt, F., and Ragauskas, A.J., *Biografting of Celestine Blue onto a High-Kappa Kraft Pulp*, in *Applications of Enzymes to Lignocellulosics*, S.D. Mansfield and Saddler, J.N., Editors. 2003, Oxford University Press: Washington, D.C. p. 66-81.

21. Sealey, J. and Ragauskas, A., *Residual lignin studies of laccase-delignified kraft pulps.* Enzyme and Microbial Technology, 1998. **23**: p. 422-426.

22. Blinkovsky, A.M. and Dordick, J.S., *Peroxidase-catalysed synthesis of lignin-phenol copolymers.* Journal of Polymer Science, Part A: Polymer Chemistry, 1993. **31**: p. 1839-1846.

23. Lund, M. and Ragauskas, A., *Enzymatic Modification of Kraft Lignin through Oxidative Coupling with Water Soluble Phenols.* Applied Microbiology and Biotechnology, 2001. **55**: p. 699-703.

24. Popp, J.L., Kirk, T.K., and Dordick, J.S., *Incorporation of p-cresol into lignins via peroxidase-catalysed copolymerization in nonaqueous media.* Enzyme and Microbial Technology, 1991. **13**: p. 964-968.

25. Yamaguchi, H., Maeda, Y., Sakata, I., *Applications of Phenol Dehydrogenative Polymerization by Laccase to Bonding among Woody-Fibers.* Mokuzai Gakkaishi, 1992. **38**(10): p. 931-937.

26. Yamaguchi, H., Maeda, Y., and Sakata, I., *Bonding among Woody Fibers by Use of Enzymatic Phenol Dehydrogenative Polymerization: Mechanism of generation of bonding strength.* Mokuzai Gakkaishi, 1994. **40**(2): p. 185-190.

27. Li, J. and Gellerstedt, G., *Kinetics and Mechanism of Kappa Number Determination.* Nordic Pulp and Paper Research Journal, 1998. **3**(2): p. 147-158.

28. Huttermann, A., Majcherczyk, A., Braun-Lullemann, A., Mai, C., Fastenrath, M., Kharazipour, A., Huttermann, J., and Huttermann, A.H., *Enzymatic Activation of Lignin Leads to an Unexpected Copolymerization with Carbohydrates.* Naturwissenshaften, 2000. **87**: p. 539-541.

29. Andersson, M., *Z-strength in pulp characterization.* Svensk Papperstidning, 1981. **84**(13): p. R6-R14.

30. Annergren, G., Rydholm, S., and Vardheim, S., *Influence of Raw Material and Pulping Process on the Chemical Composition and Physical Properties of Paper Pulps.* Svensk Papperstidning, 1963. **66**(6): p. 196-210.

31. Hartler, N. and Mohlin, U.-B., *Cellulose fibre bonding. Part 2. Influence of pulping on interfibre bond strength.* Svensk Papperstidning, 1975(8): p. 295-299.

24.4 Addendum 4. Improved Bleaching Performance with Reduced Cost: Optimizing ECF Bleaching Technologies with a Poor Man's O

Presented at the TAPPI Pulping Conference
Seattle, Washington November 2001

Thomas J. Dyer, Daniel C. Johnston, and Arthur J. Ragauskas
Institute of Paper Science and Technology
500 10th Street, NW
Atlanta, GA 30318

Abstract

ECF bleaching technologies now represent a globally accepted bleaching method that has minimal environmental impacts. The challenge that remains is how these ECF bleaching technologies can be utilized to minimize capital and operating costs. Our research has shown that the use of a D(E+O)* or (E+O)D(E+O)* sequence on pre- and post-O_2 pulps can efficiently remove lignin. Furthermore, this bleaching procedure is relatively insensitive to the presence of bleach plant effluent and black liquor carryover. This paper quantifies the impact of black liquor carryover and shows the effects of reinforcing a poor man's oxygen stage with hydrogen peroxide in an attempt to improve bleaching performance.

Introduction

Bleached chemical pulp production has undergone dramatic changes in the past several years. Environmental concern that is manifested in changing market demands and more stringent environmental regulations is one of the most important drivers of these changes in bleaching technologies. In an effort to improve the overall environmental impact of bleached chemical pulp operations, the pulp and paper industry has begun to implement a series of process changes including use of oxygen delignification technologies, fortification of extraction stages with oxygen and hydrogen peroxide, and improved brownstock washing [1-3]. In addition, the industry has had to find alternatives to elemental chlorine as a bleaching agent [4]. Hence, the demand for elemental chlorine-free (ECF) bleaching technologies, such as chlorine dioxide, hydrogen peroxide and oxygen, has been on the rise. Although these ECF bleaching technologies have been shown to address environmental concerns and produce pulps with desirable quality properties, the conversion in bleaching operations has been accompanied by increased costs [5]. Clearly, the challenge that now needs to be addressed is how ECF bleaching technologies can be utilized to minimize capital and operating costs. Several research groups have begun to address this issue and publications by Tait [6], Stapley et al. [7], Null and Cenatempo [8], Kimbrell [9], and Chakar et al. [10], are certainly indicative of this endeavor.

Several researchers have focused on extending the performance of oxygen delignification technologies, thereby providing improved costs. These researchers have noted that it is possible to improve pulp yields by halting the kraft cook at a high kappa number (i.e., 40-50 for SW kraft) before the selectivity of the kraft cook decreases in the terminal phase [10-14]. Magnotta et al. have reported improved selectivity with an extended oxygen OO system on high kappa kraft pulps. They showed that an OO system can increase yields ~4% prior to ECF bleaching [11]. Parthasarathy took a different approach by coupling modified kraft cooking conditions such as polysulfide, anthraquinone, and surfactant-based chip penetrants to gain bleached pulp yields (as much as 4-6%) when pulping was

ceased at a kappa number of 40-50 [14]. The observed yield benefits of extended oxygen delignification technologies could lower overall operating costs compared to conventional systems by reducing the wood requirement [11]. In addition, the yield increases are further amplified by reducing the organic load on the recovery furnace, which offers the potential for significant production increases in a recovery boiler-limited mill while increasing environmental benefits.

A mini, (E+O), or poor man's oxygen system provides an alternative approach to utilizing oxygen delignification technologies. This system usually removes less lignin but requires less capital investment than a typical oxygen delignification system and is easily retrofitted to existing pulp bleaching operations [10]. Equipment and conditions required for a mini oxygen stage are similar to those currently applied in oxygen and hydrogen peroxide-reinforced extraction stages in the bleach plant [15]. Typically, a mini oxygen delignification stage uses an upflow tube with a retention of about 30 minutes, oxygen pressure of 80-90 psig, 1% NaOH, held at 70-80°C [5]. McKenzie reported that the commercial use of a mini oxygen system has produced low AOX pulps with no loss of production due to recovery or recausticizing bottlenecks. In addition, the mini oxygen stage provided approximately 25% delignification prior to a conventional oxygen stage [16].

Recent research efforts have focused on extending the capabilities of the poor man's oxygen delignification technologies. Some modifications to the process involve the addition of other oxidative chemicals, such as hydrogen peroxide, as well as the use of multiple stages [15]. Histed has proposed using an enhanced poor man's oxygen stage to achieve higher levels of delignification. The enhanced poor man's oxygen, which is a 0.05 kappa factor D pretreatment stage followed by a higher than normal temperature in the (E+O) stage, can achieve approximately 50% delignification [17]. Chakar et al. demonstrated that (E+O) treatment of a 26.6 kappa number softwood resulted in 13-25% delignification, depending on the caustic charge. These researchers also showed that the

delignification effects of the (E+O) treatment were improved dramatically if the caustic was divided in half and the pulp was treated with a low charge of chlorine dioxide after an initial mini oxygen stage [10]. Dyer et al. further examined the benefits of an enhanced poor man's oxygen stage. They demonstrated that a (E+O)$D_{0.05}$(E+O) had 6% more delignification than a $D_{0.05}$(E+O)(E+O). The authors attributed this enhanced delignification to the initial (E+O) stage removing easily oxidized lignin prior to the low kappa factor charge of chlorine dioxide [5].

In an effort to further extend the performance of a poor man's oxygen stage, it would be useful to investigate the impact of black liquor carryover on this ECF bleaching technology. Dissolved material in an oxygen stage, unlike that from chlorination and following extraction stages, is uncontaminated by chloride ions. It can therefore be routed back to the recovery furnace, where it becomes a source of energy instead of a pollutant [18, 19].

Enz and Emmerling reported that a raw black liquor solids addition of 65 kg/o.d. ton had no impact on the delignification or pulp physical properties of a commercial oxygen delignification system. In fact, this stability allowed the mill to use a low average dilution factor to the brownstock washing system [20]. Several researchers have investigated the impact of inefficient washing systems on laboratory oxygen delignification systems. There is some evidence that small amounts of black liquor carryover might benefit an oxygen delignification system. Bokstrom and Norden [12], Miller [21], Parthasarathy [22], and Parsad et al. [23] reported increases in delignification at the addition rates used in their studies. The apparent reason for this increase in delignification is due to residual alkali left in the carryover. However, several other research groups have found that black liquor carryover impacts both alkali and oxygen consumption due to the competing reactions between pulp lignin and dissolved material in the liquor [24, 25]. This lowers the delignification rate and may even enhance the selectivity of the oxygen delignification system [18, 19, 26-29]. Although there has been

a significant contribution to the effects of black liquor carryover on an oxygen delignification system, the effects on a mini oxygen system and other ECF bleaching technologies are not yet clear. This paper further examines a poor man's oxygen stage incorporated with chlorine dioxide, hydrogen peroxide, and chelating stages in an attempt to elucidate the impact of black liquor carryover on the overall performance of these ECF bleaching technologies.

Experimental

Materials. A series of three commercial SW kraft pulps were employed for the mini oxygen delignification studies in this paper. Two preoxygen stage pulps had kappa numbers of 26.3 and 24.2, respectively, while a postoxygen pulp had a kappa number of 8.9. The preoxygen pulps had respective viscosity values of 27.4 and 26.5 cP while the postoxygen pulp had a viscosity value of 21.0 cP. Prior to the mini oxygen delignification studies, the pulps were extensively washed until the wash water was pH neutral and colorless. All chemicals employed for these studies, with the exception of chlorine dioxide, were purchased commercially and used as received.

Metals Analysis of Pre- and Post-O_2 Pulps. Nonprocess elements of the kappa 24.2 and 8.9 SW kraft pulp were determined using standard ICP methods [30, 31]. Table I summarizes the results of the ICP analysis.

Table I. Metals analysis of pre- and post-O_2 pulps.

Metal	24.2 Kappa Pre-O_2 SW Kraft Pulp (ppm)	8.9 Kappa Post-O_2 SW Kraft Pulp (ppm)
Fe	12	10
Co	<1	<1
Mn	36	32
Mg	510	482
Ni	2	<1
Cu	<1	13
Cr	<1	<1
Na	1310	280
Ca	1315	1555
K	86	94

Mini Oxygen Delignification. A 1000-mL capacity Parr reactor equipped with a stirrer, a pressure gauge, a heating mantle, and connected to a Parr 4842 temperature controller was charged with 20.0 grams of never-dried fibers (solids basis). The pulp consistency was adjusted to 10% by adding distilled water. Table II summarizes the delignification conditions.

Table II. Mini oxygen bleaching conditions.

Stage	O_2 Pressure/ psi	NaOH/ %	H_2O_2/ %	$MgSO_4$/ %	Temp./ °C	Time/ Min.
(E+O)	90	1.25	-	0.1	80.0	20.0
(E+P+O)	90	1.25	0.5	0.1	80.0	20.0
O	90	2.50	-	0.1	105.0	60.0

Chlorine Dioxide Stages. The chlorine dioxide (D) stages were performed on 20.0 grams of never-dried fibers (solid basis) at 10% consistency in sealed plastic bags immersed in a constant temperature water bath. Table III summarizes the experimental conditions for these stages.

Table III. Chlorine dioxide stage conditions.

Stage	Kappa Factor	Exiting pH	Temp./ °C	Time/ min.
D	0.05	2.2	70.0	30.0
D	0.20	2.2	70.0	30.0

Pulp Characterization. Delignified pulps were analyzed for kappa number following TAPPI Method T 236 cm-85 [32]. Typical experimental standard deviations for the preoxygen pulps were determined to be 0.09 and 0.08 for the postoxygen pulps. Pulp viscosity values were determined in accordance with TAPPI Method T 230 om-89 [33] and standard deviations for the preoxygen pulps were 0.6 and 0.2 for the pre- and postoxygen pulps, respectively. Pulp brightness measurements were reported as ISO brightness and were performed in accordance with TAPPI Method T 525 om-92 [34]. Typical brightness standard deviations for the preoxygen pulps were determined to be 0.1 and 0.08 for the postoxygen pulps. The handsheets for these measurements were made using TAPPI Method T 218 sp-97 [35]. Nonprocess elements of the pre- and postoxygen pulps were determined using standard ICP methods [30, 31].

Results and Discussion

Mini O_2 and Black Liquor Carryover. Previous studies reported by Chakar et al. [10] and others [17, 36, 37] have shown that the delignification effects of a mini oxygen treatment are improved if the caustic charge is split into two and the pulp is oxidized with a low charge of chlorine dioxide. Furthermore, Dyer et al. [5] have shown that there are no significant detrimental impacts on a (E+O)$D_{0.05}$(E+O) sequence when not employing interstage washing. These studies are beneficial to understanding the advantages of an enhanced poor man's oxygen stage although the conditions employed for these studies may not mimic an actual bleach plant setting. As a result, the impact of black liquor carryover on mini oxygen delignification as well as other ECF bleaching technologies is not fully understood [12, 18-29]. In addition, the advantages of an enhanced poor man's oxygen sequence have not been explored on postoxygen delignified kraft pulps.

This study explores the impact of black liquor carryover on mini oxygen delignification as part of a sequence using chlorine dioxide. The experimental conditions were selected from previous literature reports [5, 10, 38]. The consistency of all the stages was maintained at 10% while a constant charge of magnesium sulfate in the mini oxygen stages was employed to minimize the number of experimental variables. The mini oxygen delignification studies were maintained at an oxygen pressure of 90 psi and were stirred at a constant rate throughout the experiment. Black liquor was added to the pulp at two different charges, 2 and 10 kg solids per o.d. ton of pulp. There was no interstage washing employed in any of the studies employing black liquor carryover. These results were then compared to control studies that did not employ any black liquor or bleach plant effluent.

The delignification response for the 26.3 kappa SW kraft pulp under varying mini oxygen delignification conditions is summarized in Figure 1. It is interesting to observe that the black liquor carryover seemed to enhance delignification under most cases except where

the chemical charge was high, i.e., $D_{0.20}$(E+O)(E+O) and (E+O)$D_{0.20}$(E+O). The mild conditions of the (E+O)(E+O) sequence yielded 43% delignification for both 2 and 10 kg/ton of black liquor carryover and 35% delignification with no carryover. The increase in delignification with the addition of black liquor is presumably due to residual alkali left in the carryover [12, 21-23]. The use of a low charge of ClO_2 and splitting the caustic charge between two (E+O) stages significantly improved the response of the pulp toward delignification in the second (E+O) stage, as was also reported by Chakar et al. [10]. However, the increase in delignification compared to the (E+O)(E+O) sequence was 6% and 10% for the 2 and 10 kg/ton carryover levels, respectively, while an 18% increase in delignification is apparent for pulp having interstage washing and no carryover. This effect is presumably due to partial consumption of ClO_2 by the black liquor carryover, thereby decreasing the overall efficiency of this bleaching agent. The delignification response using 10 kg/ton carryover was often lower than that of a 2 kg/ton black liquor carryover charge. It would seem reasonable that this decreased delignification can be attributed to an increase in the total number of competing reactions between pulp lignin and dissolved material in the black liquor, as was reported by earlier researchers [24, 25].

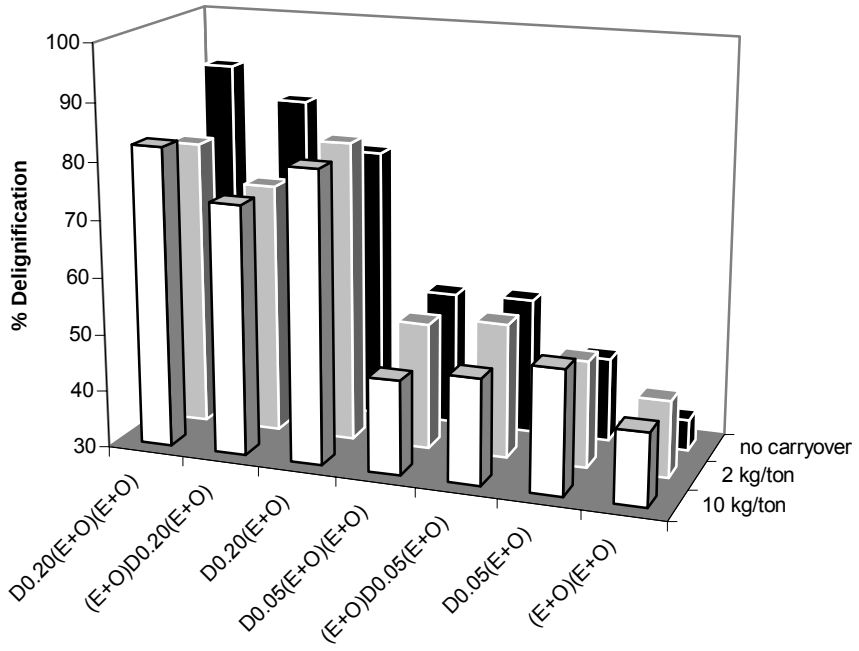

Figure 5. Mini oxygen delignification responses for a 26.3 kappa SW kraft pulp with no carryover, 2 kg/ton carryover, and 10 kg/ton carryover. The pulps having no carryover involved interstage washing while the pulps having added carryover involved no interstage washing.

The viscosity losses for the no carryover, 2 kg/ton, and 10 kg/ton carryover SW kraft pulps are summarized in Figure 2. The initial viscosity of this pulp was 33.2 cP. As expected, the viscosity loss for the $D_{0.05}$(E+O)(E+O) sequence is smaller than that for the (E+O)$D_{0.05}$(E+O) sequence due to the placement of the first (E+O) stage in the sequence. Interestingly, the viscosity losses increased as a function of the amount of carryover in the pulp. It is anticipated that black liquor carryover introduces transition metal ions to the pulp. These transition metal ions can then form radicals, leading to degradation of the carbohydrates. The (E+O)$D_{0.05}$(E+O) sequence yielded a greater viscosity loss than the (E+O)(E+O) sequence, although it provided improved delignification. This could be attributed to the selectivity of the intermediate chlorine dioxide stage.

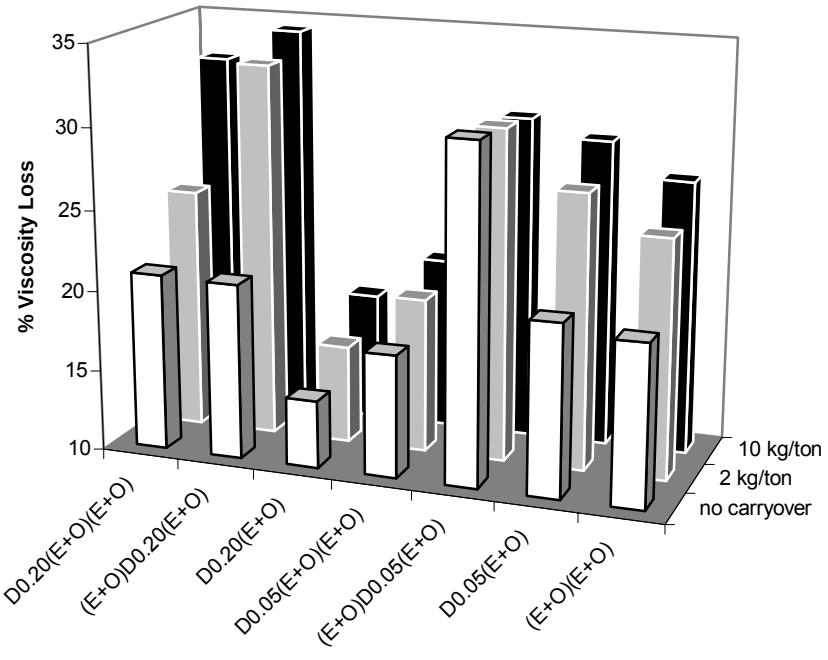

Figure 6. Mini oxygen delignification pulp viscosity losses (%) for a 26.3 kappa SW pulp with no carryover, 2 kg/ton, and 10 kg/ton black liquor carryover. The pulps having no carryover involved interstage washing while the pulps having added carryover involved no interstage washing.

Figure 3 presents the selectivity (defined as Δkappa/Δviscosity) data for the no carryover, 2 kg/ton, and 10 kg/ton carryover SW kraft pulps. In general, the selectivity decreases as a function of black liquor carryover load. This observation is contrary to results reported by others [18, 19, 26-29]. However, the conditions used in those studies indicate that much higher levels of carryover were used. In addition, the carryover used in those studies may have been model compounds or black liquor with low metals content. The selectivity of the (E+O)$D_{0.05}$(E+O) sequence is much lower than that for the $D_{0.05}$(E+O)(E+O) sequence, due primarily to the large change in viscosity that was brought about by the placement of the (E+O) sequence. As a result, the selectivity of the (E+O)$D_{0.05}$(E+O) sequence is comparable to that of a (E+O)(E+O) sequence. Meanwhile, the sequences involving high kappa factor D stages were the most selective

of this study, due to their high delignification compared to the other sequences employed in this study.

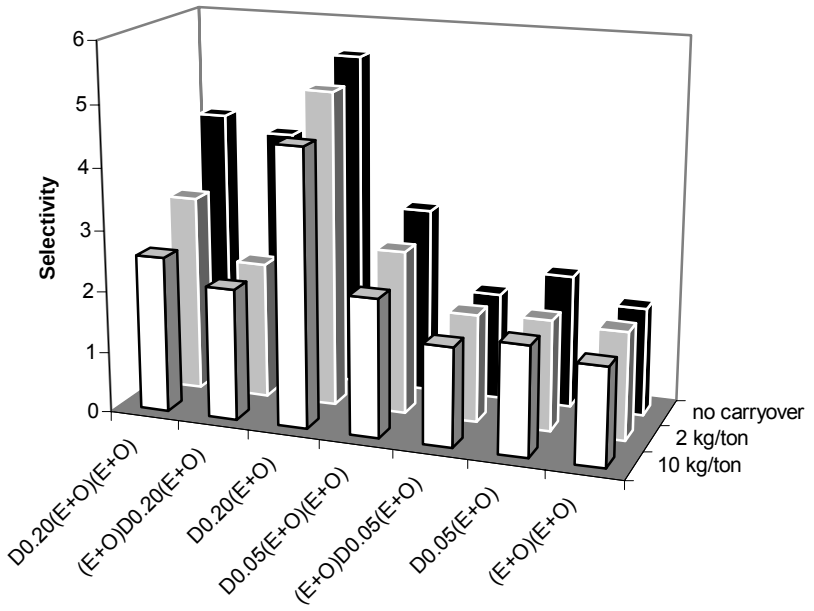

Figure 7. Mini oxygen delignification selectivity (Δkappa/Δviscosity) of SW kraft pulp with no carryover, 2 kg/ton, and 10 kg/ton black liquor carryover. The pulps having no carryover involved interstage washing while the pulps having added carryover involved no interstage washing.

Mini O_2 Reinforced with H_2O_2. In an effort to further enhance a poor man's oxygen stage, this study was extended to investigate the impact of black liquor carryover on a mini oxygen delignification system reinforced with hydrogen peroxide for both pre- and postoxygen delignified SW kraft pulps. The consistency of all the stages was maintained at 10% while a constant charge of magnesium sulfate in the mini oxygen stages was employed to minimize the number of experimental variables. The mini oxygen delignification studies were maintained at an oxygen pressure of 90 psi and were stirred at a constant rate throughout the experiment. Black liquor was added to the pulp at only one level, 10 kg solids per o.d. ton of pulp. There was no interstage washing employed in

any of the studies employing black liquor carryover. These results were then compared to control studies that did not employ any black liquor or bleach plant effluent.

The delignification response for the preoxygen with no carryover as well as the pre- and postoxygen delignified SW kraft pulps with 10 kg/ton of black liquor carryover is summarized in Figure 4. The kappa 26.3 pre-O_2 pulps with no black liquor carryover exhibited a greater extent of delignification than the kappa 24.2 pre-O_2 pulps with carryover, as was also observed in our earlier study. In addition, the 24.2 kappa pre-O_2 pulp exhibited a greater extent of delignification than that of the 8.9 kappa post-O_2 pulp except in the case of the O_2 treatment. This effect is presumably due to the nature of the residual lignin in the post-O_2 pulp. This lignin is further oxidized than the lignin in the pre-O_2 pulps and is thus more resistant to additional oxidation. The extent of delignification was proportional to the amount of hydrogen peroxide in the bleaching sequence. As the hydrogen peroxide was decreased, the extent of delignification also decreased. It is interesting to observe the differences in delignification for the (E+O+P)$D_{0.05}$(E+O) and (E+O)$D_{0.05}$(E+O+P) sequences. Although there was a difference observed in delignification for these two sequences for the pre-O_2 pulps with no carryover, there was no apparent difference for either the pre- or post-O_2 pulps having added black liquor carryover. This further suggests that there are competing reactions occurring between the pulp lignin and dissolved material in the black liquor, thereby leading to a lower bleaching effectiveness [24, 25].

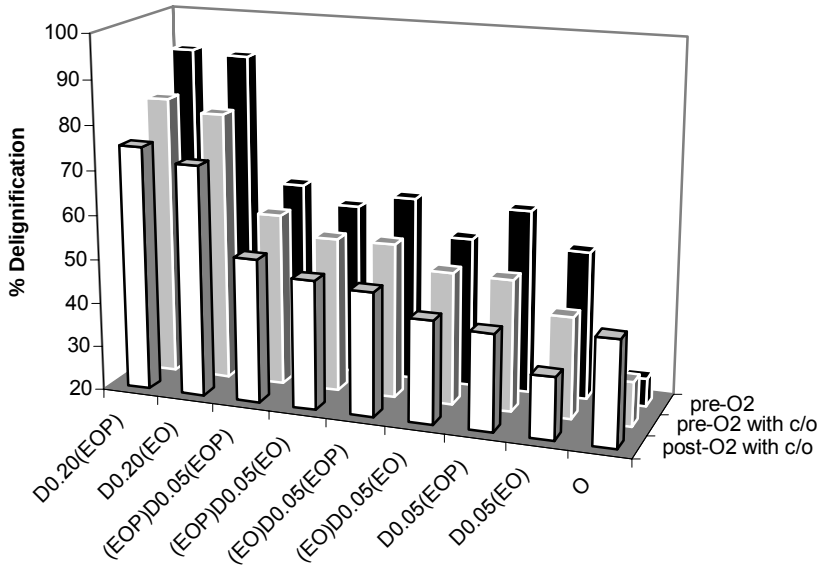

Figure 4. Delignification responses (%) for a pre-O_2 pulp with no black liquor carryover and a pre-O_2 and post-O_2 SW kraft pulp with 10 kg/ton of black liquor carryover. The pulps having no carryover involved interstage washing while those having added carryover employed no interstage washing.

The changes in pulp viscosity for the 27.4 cP pre-O_2 pulps with no carryover as well as the 26.5 cP pre-O_2 and 21.0 cP post-O_2 SW kraft pulps with 10 kg/ton of black liquor carryover are summarized in Figure 5. Although the extent of delignification increased with greater amounts of hydrogen peroxide, the loss in viscosity is also greater for increasing amounts of hydrogen peroxide. This effect is presumably due to the decreased selectivity of hydrogen peroxide under increased oxygen pressure. In general, a greater viscosity loss was observed for both pre-O_2 pulps when compared to that for the post-O_2 pulps. It is interesting to observe that the viscosity loss was often greater for the pre-O_2 pulps with no carryover than for the pre- and post-O_2 pulps with added carryover. This effect further reinforces the theory that there are competing reactions between pulp lignin and the dissolved material in the black liquor [24, 25]. The black liquor may indirectly protect the carbohydrates from degradation by providing these competing reaction

pathways. However, this effect was not observed for the post-O_2 SW kraft pulp treated with another oxygen stage.

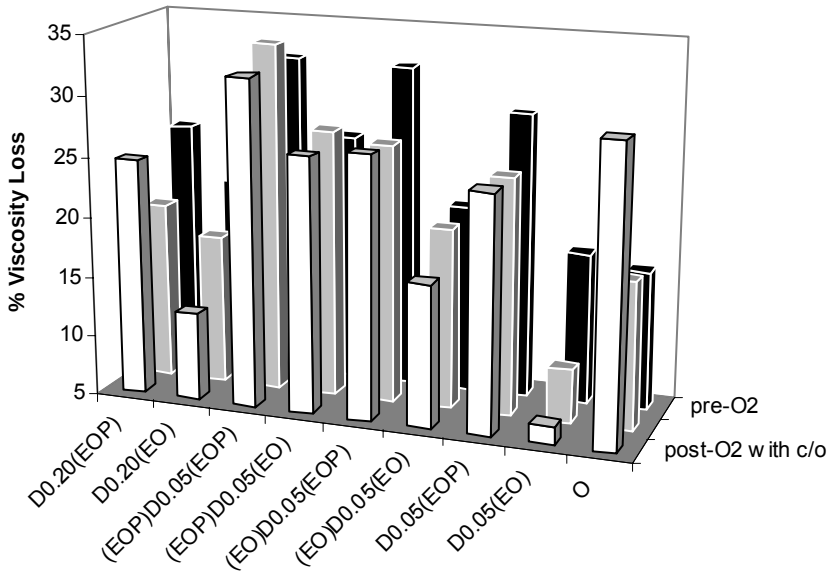

Figure 5. Viscosity losses (%) for a 27.4 cP pre-O_2 pulp with no black liquor carryover and a 26.5 cP pre-O_2 and 21.0 cP post-O_2 SW kraft pulp with 10 kg/ton of black liquor carryover. The pulps having no carryover involved interstage washing while those having added carryover employed no interstage washing.

Figure 6 presents the selectivity (defined as Δkappa/Δviscosity) data for the pre-O_2 pulps with no carryover and the pre- and post-O_2 SW kraft pulps with black liquor carryover. In general, the selectivity decreased when comparing the pre-O_2 pulps with no carryover to the pre-O_2 pulps with 10 kg/ton carryover. This effect is presumably due to the extent of delignification outweighing the viscosity loss for the pulps with no black liquor carryover. In addition, the selectivity decreased when comparing the pre-O_2 pulps with carryover to that of the post-O_2 pulps with carryover. The reason for this is presumably due to the nature of the residual lignin. The residual lignin remaining in the post-O_2 pulps may be more difficult to oxidize than the residual lignin in the pre-O_2 pulps,

thereby reducing the overall selectivity. An exception to this is observed in both the $D_{0.20}$(E+O) and $D_{0.05}$(E+O) sequences. These short sequences actually improved the selectivity of the post-O_2 over the pre-O_2 pulps with carryover and without carryover.

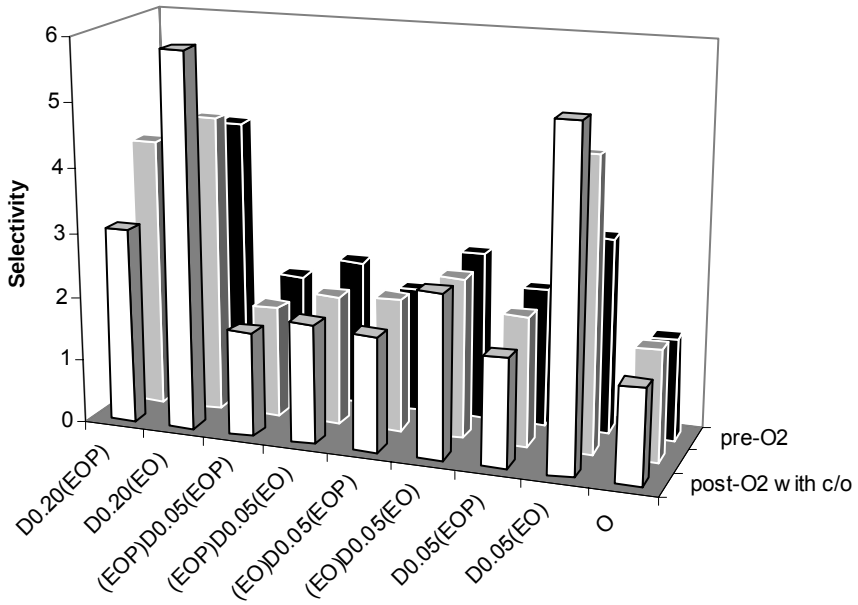

Figure 6. Selectivity responses for a pre-O_2 pulp with no black liquor carryover and a pre-O_2 and post-O_2 SW kraft pulp with 10 kg/ton of black liquor carryover. The pulps having no carryover involved interstage washing while those having added carryover employed no interstage washing.

The changes in brightness for the pre-O_2 pulps with no carryover as well as the pre-O_2 and post-O_2 SW kraft pulps with 10 kg/ton of black liquor carryover are summarized in Figure 7. The changes in brightness follow trends similar to the delignification responses illustrated earlier. The kappa 26.3 pre-O_2 pulp with no black liquor carryover exhibited a greater brightness change for all treatments than the kappa 24.2 pre-O_2 pulp with carryover. In addition, the 24.2 kappa pre-O_2 pulp exhibited a greater brightness change than the 8.9 kappa post-O_2 with the exception of the O_2 treatment. It is interesting to

observe that the brightness change was based on the exiting bleaching stage. This observation is most notable in the sequences involving three stages. Those sequences ending with an (E+O+P) stage often increased the brightness compared to those ending in an (E+O) stage, presumably due to the ability of the hydrogen peroxide to react with and destroy chromophores remaining in the pulp.

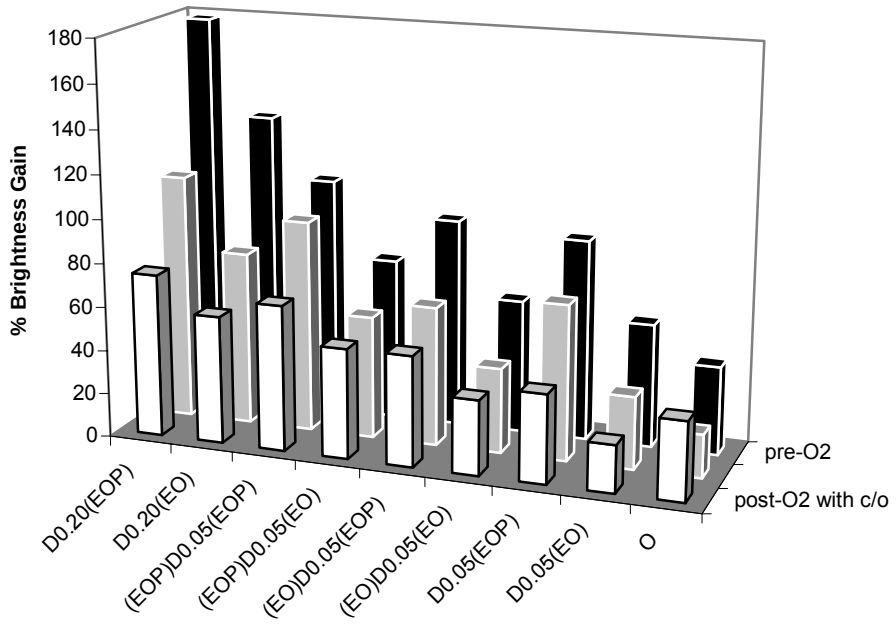

Figure 7. Changes in brightness(%) for a pre-O_2 pulp with no black liquor carryover and a pre-O_2 and post-O_2 SW kraft pulp with 10 kg/ton of black liquor carryover. The pulps having no carryover involved interstage washing while those having added carryover employed no interstage washing.

Summary

The mini oxygen delignification studies with black liquor carryover confirmed that using a poor man's O to remove lignin from kraft pulps continues to be a promising technology. Analysis of the mini O_2 systems indicated that these technologies had superior performance with pre-O_2 pulps when compared to post-O_2 SW kraft pulps.

Furthermore, these studies confirmed the proposed benefits of splitting the charge of the mini O in two and further oxidizing the pulp with a low kappa factor chlorine dioxide stage. Analysis of the mini oxygen systems reinforced with hydrogen peroxide revealed that the addition of hydrogen peroxide in the last stage of a (E+O)*D(E+O)* sequence had a greater impact on bleaching performance than if placed in the front of the sequence. These studies also confirmed that black liquor carryover has little or no effect on the final pulp physical properties. However, the modest levels of black liquor carryover employed in this study may not be entirely indicative of an actual bleach plant. Hence, future studies within our research group will address this issue and will be reported in the near future.

Acknowledgements

The authors would like to thank the U.S. Department of Energy (DOE) and the member companies of the Institute of Paper Science and Technology for their support of this research. This manuscript was prepared, in part, with the support of DOE Cooperative Agreement No. DE-FC07-00ID13870. However, any opinions, findings, conclusions, or recommendations expressed herein are those of the author(s) and do not necessarily reflect the views of DOE. Portions of this work were used by T.J.D. and D.C.J. as partial fulfillment of the requirements for the Ph.D. and M.Sc. degrees, respectively, at the Institute of Paper Science and Technology.

References

1 "What's in the Pipeline?" *Pulp and Paper Europe* 5(3): p. 4 (2000).

2 Jensen, K.P.; "US Bleached Pulp Mills Move Towards Compliance of Phase I of Cluster Rule." *Pulp & Paper* 73(9): p. 71 (1999).

3 Oblak-Rainer, M.; "Kraft Process Today and Tomorrow, Part 2, Alternative Cooking Processes." *Papir* 28(3-4): p. 75 (2000).

4 Chakar, F.S., Ragauskas, A.J., and Nilvebrant, N.-O.; "Biobleaching of High Lignin Content Kraft Pulps via Laccase-Mediator Systems." *TAPPI Pulping Conference Proceedings*. Montreal, Canada. 10 p. (1998).

5 Dyer, T.J., Lucia, L.A., and Ragauskas, A.J.; "Mini-Oxygen Stages: More Delignification with Less Capital." *TAPPI Pulping Conference Proceedings*. Boston, MA. TAPPI Press. (2000).

6 Tait, D.H.; "Advances in Bleach Plant Design Lower Capital and Operating Costs." *Pulp & Paper* 60(1): p. 70-72 (1986).

7 Stapley, C.E., Butner, R.E., and Kangas, M.Y.; "Strategic Investment in [the US] Pulp and Paper Industry." *27º Congresso Anuale de Celulose e Papel*. São Paulo, Brazil. p. 797-811 (1994).

8 Null, D. and Cenatempo, D.; "Paper Company Strategies Should Focus on Building Economic Value." *Pulp & Paper* 71(9): p. 59-62 (1997).

9 Kimbrell, S.; "Low-Capital Washer Improvements at Boise Cascade's DeRidder Mill." *Pulp Washing Conference Proceedings*. Vancouver, BC. p. 81-84 (1996).

10 Chakar, F.S., Lucia, L.A., and Ragauskas, A.J.; "Extending the Limits of Oxygen Delignification." *International Pulp Bleaching Conference Proceedings*. Halifax, Nova Scotia. p. 123-130 (2000).

11 Magnotta, V., Kirkman, A., Jameel, H., and Gratzl, J.; "High-Kappa-[No.] Pulping and Extended Oxygen Delignification to Increase Yield." *Breaking the Pulp Yield Barrier Symposium Proceedings*. Atlanta, GA. TAPPI Press. p. 165-182 (1998).

12 Bokstrom, M. and Norden, S.; "Extended Oxygen Delignification." *International Pulp Bleaching Conference*. Helsinki, Finland. p. 327-334 (1998).

13 Chirat, C. and Lachenal, D.; "Limits of Oxygen Delignification." *TAPPI Pulping Conference Proceedings*. Quebec. p. 619-624 (1998).

14 Parthasarathy, V.; "Use of Digester Additives and Oxygen Delignification to Gain Bleached Pulp Yield and Achieve Environmental Objectives." *Breaking the Pulp Yield Barrier Symposium*. Atlanta, GA. p. 219-227 (1998).

15 Johnson, S.E., Epiney, M., and Hornsey, D.; "EO Prebleaching as an Effective Means to Delignify Pulp Prior to the Bleach Plant." *TAPPI Pulping Conference Proceedings*. Chicago, IL. p. 5-9 (1995).

16 McKenzie, D.J.; "Evolution of Pulp Bleaching Practices at Harmac Pacific." *Pulp & Paper Canada* 96(6): p. 55-58 (1995).

17 Histed, J.A.; "Simplified Bleaching; Environmental Advantages for Existing Bleach Plants." *Pulp & Paper Canada* 98(10): p. 77-80 (1997).

18 McDonough, T.J.; "Recent Advances in Bleached Chemical Pulp Manufacturing Technology; Extended Delignification, Oxygen Delignification, Enzyme Applications and ECF and TCF Bleaching." *Tappi Journal* 78(3): p. 55-62 (1995).

19 Iijima, J.F. and Taneda, H.; "Effects of Several Factors on Medium-Consistency Oxygen Delignification." *International Pulp Bleaching Conference Proceedings*. Washington, D.C. p. 403-410 (1996).

20 Enz, S.M. and Emmerling, F.A.; "North America's First Fully Integrated, Medium Consistency Oxygen Delignification Stage." *Tappi Journal* 70(6): p. 105-112 (1987).

21 Miller, W., Kwon, H., Liukkonen, A., and Genco, J.M.; "Medium-Consistency Oxygen Delignification Design Utilizing a Two-Phase Concept." *TAPPI Pulping Conference Proceedings*. Chicago, IL. 393-404 (1995).

22 Parthasarathy, V.; "Entrained Black Liquor Solids and Viscosity Selectivity in Oxygen Delignification Reinforced Hydrogen Peroxide." *Tappi Journal* 73(9): p. 243-247 (1990).

23 Parsad, B., Kirkman, A., Jameel, H., Gratzl, J., and Magnotta, V.; "Mill Closure with High-Kappa Pulping and Extended Oxygen Delignification." *Tappi Journal* 79(9): p. 144-152 (1996).

24 Lindstrom, L.A. and Norden, S.; "Efficient Postoxygen Washing - Crucial for Low Bleach-Plant Emissions." *Appita Journal* 43(5): p. 373-376 (1990).

25 Lindstrom, L.A.; "Oxygen-Stage Design and Performance." *TAPPI Bleach Plant Operations Short Course Proceedings*. Hilton Head, SC p. 89-95 (1990).

26 Sixta, H., Schuster, J., Mayrhofer, C., Krotscheck, A.W., and Rückl, W.; "Towards Effluent-Free TCF Bleaching of Eucalyptus Prehydrolysis Kraft Pulp." *Das Papier* 48(8): p. 526-537 (1994).

27 Allison, R.W. and McGrouther, K.G.; "Improved Oxygen Delignification with Interstage Peroxymonosulfuric Acid Treatment." *International Pulp Bleaching Conference Proceedings*. Vancouver, BC. p. 121-128 (1994).

28 Miller, W.J., Shackford, L.D., Jiang, H., and Genco, J.M.; "Effect of Entrained Black Liquor Carryover on Medium-Consistency Oxygen Delignification." *TAPPI Oxygen Delignification Symposium*. Toronto, Canada. p. 107-113 (1990).

29 Vuorenvirta, K., Fuhrmann, A., and Gullichsen, J.; "Effect of Black Liquor Carryover on Selectivity of Oxygen Delignification." *Pulp & Paper Canada* 102(3): p. 50-52 (2001).

30 Allison, L., Ragauskas, A.J., and Hsieh, J.S.; "Metal Profiling of Southeastern U.S. Softwood and Hardwood Furnish." *Tappi Journal* 83(8): p. 97 (2000).

31 Werner, J., Jiang, J.E., Ragauskas, A.J.; "Investigations into the Intrinsic Non-Process Element Binding Capacity of Kraft Black Liquor Lignins," In *Fundamental Advances and Innovations in the Pulp and Paper Industry*, B.N. Brogdon, P.W. Hart, and C.C. Walker, Editors. AIChE Symposium Series. p. 31-36, (1999).

32 TAPPI Test Methods 1998-1999. T 236 cm-85. TAPPI Press, Atlanta.

33 TAPPI Test Methods 1998-1999. T 230 om-94. TAPPI Press, Atlanta.

34 TAPPI Test Methods 1998-1999. T 525 om-92. TAPPI Press, Atlanta.

35 TAPPI Test Methods 1998-1999. T 218 sp-97. TAPPI Press, Atlanta.

36 Homer, G., Epiney, M., Johnson, S., and Sundar, M.; "High Yield Cooking, Oxygen Delignification and Ozone for High Yield Bleached Pulp." *TAPPI Pulping Conference Proceedings*. Vancouver, BC. p. 729-738 (1997).

37 Homer, G., Johnson, S., and Epiney, M.; "State of the Art ECF: Pulping and Bleaching with Oxygen, Ozone and Chlorine Dioxide Part 2." *TAPPI Pulping Conference Proceedings*. Vancouver, BC. p. 81-91 (1996).

38 Johnston, D.C.; "Low Capital Alternatives for the Bleaching of Softwood Kraft Pulp Using Hydrogen Peroxide." *Institute of Paper Science & Technology*. Master of Science Degree. Atlanta, GA. (2001).

24.5 Addendum 5. Lignin-Extractives Complexes may Disturb Analysis of Isolated Lignins by NMR

Nils-Olof Nilvebrant[1], Art J. Ragauskas[2], Thomas Dyer[2] and Marjatta Kleen[3]

[1]STFI, P.O. Box 5604, SE-11486 Stockholm, Sweden
[2]IPST, Institute of Paper Science and Technology, 500 10th St., NW, Atlanta, GA, USA
[3]KCL Science and Consulting, P.O. Box 70, FIN-02151 Espoo, Finland

Abstract

The isolation of residual lignins (RL) from kraft pulps is one of the key techniques employed by wood chemists studying modern pulping and bleaching reactions. ^{13}C NMR analysis of these samples frequently detects a series of high-field aliphatic signals that have been attributed to reductive chemistry occurring during chemical pulping.

Wood extractives were found and identified in thoroughly solvent-extracted RL by pyrolysis-GC/MS. The long-chained saturated fatty acids were impossible to protonate and remove completely and are therefore suggested to be present as insoluble metal ion salts. The repeating CH_2 groups in saturated fatty acids may interfere with the signals from lignins in NMR.

Introduction

Fatty acids are present in wood and fatty acid derivatives account for the major part of native wood extractives, in both softwood and hardwood. In wood, fatty acids are almost exclusively present as esters. During alkaline pulping conditions, these esters are cleaved, yielding fatty acid soaps. These soaps are initially present as soluble alkali metal salts, and appear in the process liquor as such in micelles.

Most of the fatty acids and other wood extractives are removed from the pulp and recovered with the tall oil. However, some of these extractives remain with the pulp. We have recently shown that saturated fatty acids may not be completely removed from kraft pulps with the standard SCAN method (1) currently used for the extraction of pulp with acetone, not even after acidification. Traces of extractives have been identified also in enzymatically isolated RL (2,3. Non-extractable wood extractives have even been identified after acidic isolation and extraction of the RL (4).

Small residual amounts of fatty acids in pulps may significantly influence the properties of these products -e.g. the fiber bonding, surface properties (5), paper-to-paper friction (6) and odor.

Traces of extractives may be even more detrimental if they simply are assumed to be absent. Examples of this are when pulp surfaces are studied by ESCA before and after removal of all extractives by extraction (7). The difference has been attributed to wood extractives. However, a too thorough extraction may remove some lignin, but also non-extractable wood extractives may have been left. NMR interpretation of RL structures is usually performed after removal of wood extractives. For laboratory pulp samples this is frequently accomplished by Soxhlet extraction of the wood chips prior to chemical pulping (8,9). For the analysis of commercial pulps, removal of extractives is often done by Soxhlet extraction of the isolated lignin prior to lignin analysis (10,11,12). Small amounts of wood extractives may contribute to the signals from aliphatic groups and to a

lesser extent to signals from carboxylic acid groups. Thus, there is a risk for misinterpretation.

Wood extractives may, in fact, be present as lignin-extractive-complexes (LEC) in pulps. These non-extractable extractives have been ignored in previous efforts of extraction and analyses by ESCA and NMR. The aims of the present investigation were to find supporting experimental results for the presence of wood extractives in well-extracted pulps and isolated RL and study their possible interference in the interpretation of NMR spectra.

Materials and Methods

A bleaching filtrate was obtained from an oxygen prebleaching stage from a softwood kraft mill. The filtrate was acidified with acetic acid to a pH of 2 and extracted five times with a mixture of petroleum ether/acetone/methanol (PAM). The water phase was subsequently extracted five times with methyl-t-butyl ether (MTBE). The remaining filtrate was finally evaporated and analyzed by Py-GC/MS.

RL were isolated from an unbleached softwood SuperBatch pulp (A, Kappa number 19) and from an unbleached hardwood RDH kraft pulp (B, Kappa number 15.9). The amount and chemical composi tion of extractives in the original pulps used in this study were determined by GC-MS and GPC. The pulps were first extracted with acetone and then with dichloromethane. The commonly used acidic dioxane-water method was then employed (13). The dry pulp was refluxed in an 82:18 (v/v) dioxane-water solution containing 0.1 M HCl. The resulting solution was filtered and the lignin was isolated by precipitation. The isolated residual lignins (RL A and RL B) were further extracted with pentane.

RL were also isolated in large scale from a kappa 75.4 kraft pulp prepared from a sole log of *Pinus taeda.* The isolation of RL was carried out following standard literature methods

(12). The o.d. pulp was adjusted to 4% consistency by adding a 0.10 M HCl 9:1 *p*-dioxane:water solution. The slurry was then refluxed for two hours under an argon atmosphere. The pulp was filtered and the filtrate was filtered through celite, neutralized, and concentrated under reduced pressure to approximately 10% of the original volume. Water was added and the mixture was concentrated again under reduced pressure to remove the last traces of *p*-dioxane. The solution's pH was then adjusted to 2.5 with 1.00 M HCl. The precipitated lignin was collected, washed several times, and freeze-dried. Lignin yield was 46.3%. The isolated RL was Soxhlet-extracted with acetone for 24 hours.

Pyrolysis of the solid or evaporated material, in the presence of tetramethylammonium acetate (TMAAc) or tetramethylammonium hydroxide (TMAH), followed by GC-MS was used to characterize the RL. Fatty acid residues are methylated during the pyrolysis. The TMAAc reagent can methylate only free acids and fatty acid salts, whereas TMAH also cleaves ester bonds and increases the accessibility of the derivatizing reagent by increased alkali induced swelling. This technique has previously been described (14).

The inorganic content in the isolated RL, A and B, were examined by EDXA (Energy-Dispersive X-Ray Analysis).

For NMR analysis, the isolated RL were dissolved in DMSO-d6 and analyzed with a DMX 400 MHz spectrometer.

Results and Discussion

Initially, we found that wood extractives could not be removed completely by solvent extractions of the filtrate from a softwood oxygen-prebleaching stage. Most of the extractives were removed by the first PAM extraction from the acidified water, while MTBE removed more hydrophilic compounds, e.g. lignin degradation products.

However, small amounts of fatty acids were still clearly identified by Py-GC/MS in the thoroughly extracted filtrate.

In general, wood extractives in pulps are removed by extraction with different organic solvents, among which acetone is the most frequently used. Free, long-chained, fatty acids in their protonated form are soluble in organic solvents. However, the solubility in water is low - e.g. for palmitic acid (C16:0) the solubility product is 12.9 (15). Long-chained fatty acids are weak carboxylic acids with acidity constants just below 5. Thus, these acids can be practically completely protonated at a pH that is below 3 and then become extractable with an organic solvent. Alkali metal salts of the fatty acids - e.g. the Na or K salts are easily soluble in water. However, salts with alkaline earth metals like Mg and Ca are almost insoluble in water, with solubility products 15.8 and 17.4, respectively for C16:0 (16).

A more complete extraction was obtained if the pulp sample was efficiently acidified before the extraction. This is a necessity for pulps obtained from an alkaline process. The pulps used in this study originally contained about 10 g/kg acetone-soluble material. A major part of the extractives was fatty acids and most of these were unsaturated. The chemical compositions of wood extractives in the original pulps, A and B, were determined by GC-MS. Almost all fatty acids appeared as free acids, i.e. the original esters had been hydrolyzed. Only a minor part of the fatty acids were saturated, among these, palmitic acid (C16:0) was the most frequent, followed by stearic acid (C18:0). Saturated fatty acids were stable towards bleaching reagents and their relative amount increased during the bleaching sequences.

Polymeric lipophilic material was also found in e.g. the unbleached softwood kraft pulp. This high mass material could, at least partly, be extracted from acidified pulps by acetone. It was separated by GPC and constituted a major part of the total extract. After

analysis by pyrolysis, ^{1}H- and ^{13}C-NMR (Figure 1), it was concluded that this material originated from structures similar to wood extractives.

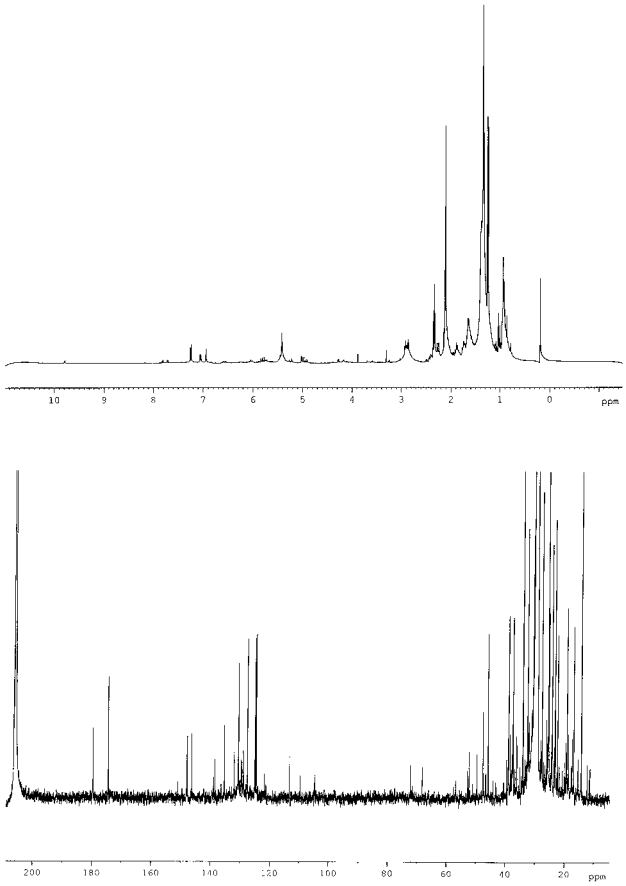

Figure 1. ^{1}H- and ^{13}C-NMR of the high molar mass fraction of an acetone extract from acidified unbleached softwood kraft pulp, A.

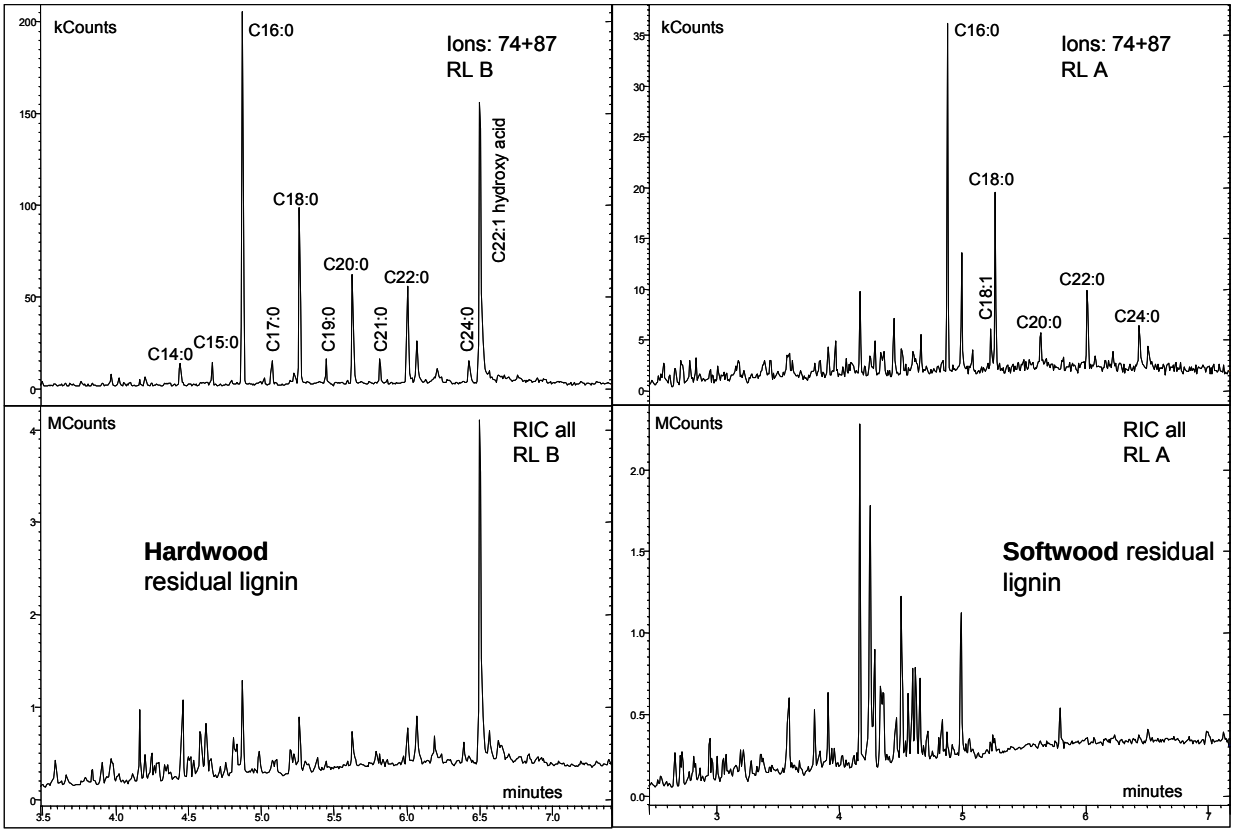

Figure 2. Py-GC/MS, in the presence of TMAH, of isolated RL obtained from thoroughly extracted pulp B and A, respectively. The pyrogram (Reconstructed Ion Chromatogram) of all fragments is shown in the lower, and that from the sum of fragments m/z 74 and 87 in the upper panel, respectively.

In addition to the filtrate and the pulps (A and B), isolated lignin samples (RL A and RL B), aimed for structural studies by NMR, were found to contain considerable amounts of fatty acids. Even though the pulps and the isolated RL samples had been extracted with different solvents. Contaminating wood extractives were detected and identified by Py-GC/MS. The pyrolysis technique is semi-quantitative; small sample amounts can be analyzed in a reproducible way and the relative composition of the sample can be calculated. The total ion current (TIC) obtained from Py-GC/MS analyses of all the pyrolysis fragments generated a lot of peaks from the RL samples in the pyrograms. The main peaks could be derived to lignin but also to fatty acids (figure 2). Dominating fragments from the fatty acids (m/z 74 and 87) were used to enhance the peaks from the saturated acids. All the RL were estimated to contain more than 1% of fatty acids.

The inorganic content in the two isolated RL were examined by EDXA and revealed the presence of calcium as the most frequent metal ion. Free fatty acids are extractable, however, here the fatty acids seem to be present as salts, since they were non-extractable and released as fatty acid methyl esters both by TMAAc and by TMAH. The C22:1 hydroxy fatty acid was only obtained when TMAH was used. This was probably not due to its presence as an ester but to the hydroxy substituent, which was only methylated by the strongly alkaline reagent. Long-chained fatty acids form insoluble salts with e.g. Ca, Mg, Cu, Mn and Fe. Iron forms the strongest complexes with fatty acids. Salts of saturated fatty acids are the most stabile among these and their solubility products increases with the chain length (15). Long-chained saturated fatty acids that form strong complexes with some metal ions become insoluble in solvents and thus non-extractable. Such salts may be difficult to protonate into the acid form, especially when water is present. Solvated protons appear hydrated by three water molecules, compare with the old denomination, hydroxonium ions $[H_3O]^+_{aq}$. The hydrophobic fatty acid tails seems to present an efficient shield against solvated protons and thereby against protonation and liberation of the free protonated fatty acid.

Theoretically, at the high pH during pulping when the phenolic groups are ionized by HO^-, a sodium ion is probably initially attached to the ionized phenolic group. However, there are several other cations present in the cooking liquor, for instance calcium. It is reasonable to believe that such ions are preferred as counter ions. But the macromolecule lignin can just offer one negative charge to the Ca^{2+} trapped at each phenolic group. The rigidity of the lignin backbone makes it usually impossible for the lignin itself to offer another phenolic group. This opens up the possibility for fatty acids to become trapped with the lignin in a LEC.

Bivalent ions, such as calcium found in the isolated RL have to be replaced by two protons. The positive charges of Ca^{2+} may repel the H^+ ions and make it more difficult,

that is, a “high pressure” of protons may be needed or a lipophilic acid. Iron is known to be the most difficult metal to remove from pulp during a closed-loop bleaching sequence.

Fatty acid soaps with iron may be the reason why the content of iron in pulps is difficult to remove in acidic stages or with DTPA in a complexing Q-stage. Iron even forms a stronger complex with long chain fatty acids than it does with commercially used complexing agents. We have previously shown that the amount of extractable wood extractives may be increased when the acetone extraction is done in the presence of EDTA. This has also been shown by the use of phosphate in a pre-extraction stage (17).

Three different ways were tested to remove the metal ions from the isolated RL, since the remaining saturated fatty acids are probably trapped as salts. The isolated RL were subjected to extensive extractions i) with EDTA, an often-used complexing agent in bleaching, ii) with 18-crown-6, which has the ability to dissolve metal ions in lipophilic solvents and iii) with NaH_2PO_4, which also form strong salts with metal ions. Different acetone extractions with and without these additives were not able to remove all saturated fatty acids present in the RL, when observed by Py-GC/MS. The attempts done, failed to remove the fatty acid impurities from RL with a solvent in the presence of different metal ion complexing additives.

Lignin structures containing a CH_2 group in the α-position have previously been observed by different techniques and attributed to reductive chemistry occurring during chemical pulping. Lignin fragments containing such a CH_2 group was found in all the studied RL by Py-GC/MS. They are easily found since they form the tropylium ions, which give very intense fragments (18). However, most of the aryl-CH_2 fragments are probably formed during pyrolysis.

Traces of saturated fatty acids in isolated lignins aimed for structural analysis by NMR may disturb the interpretation. Every long chained saturated fatty acid, with frequent CH_2

groups, trapped in the sample does contribute to the aliphatic signals. The methylene groups do appear at the same magnetic shift. Thus the interpretation of signals from reduced methylene structures and the number of carboxylic acid groups in RL may have been influenced.

Conclusions

Non-extractable wood extractives were found in bleaching filtrates, pulps and isolated RL. They may be defined as lipophilic substances originating from wood extractives that are extremely difficult to completely remove from pulps. Some saturated fatty acid metal salts can be examples of such lignin-extractive complexes (LEC). Polymerized wood extractives may be another explanation, however it is less probable, even though such material was identified in the pulps.

It is reasonable to believe that the saturated fatty acids trapped in RL may disturb the interpretation of NMR spectra of isolated lignins. Since ESCA and NMR analysis may rely on complete extractions, the non-extractable extractives may disturb the analyses.

Acknowledgement

Hanne-Lise Hardell is acknowledged for the essential analysis by Py-GC/MS.

References

1. SCAN-CM 49:93, Determination of acetone-soluble matter (1993).
2 Hortling, B., Tamminen, T., Ranua, M., IPBC, June 1-5, 1998, Helsinki, Finland, Book 2, 295-300 (1998).
3 Laine C; Tamminen T; Nilvebrant N-O, EWLP, Bordeaux, France, 3-6 Sept., 425-428 (2000).
4 Kleen, M., Int. Symp. on Cellulose and Lignocellulosics Chemistry, Kunming, China, 290-4 (2000).
5 Korpela, A., Holz- und Zellstoff., Das Papier, 10, 604-10 (1999).

6 Garoff, N., Jernberg, S., Nilvebrant, N.-O., Fellers, C. and Bäckström, M., Nord. Pulp Paper Res. J., 14 (4) 320-9 (1999)

7 Laine, J., Stenius, P., Carlsson, G. and Ström, G., Nord. Pulp Pap. Res. J., 11(3) 201-210 (1996).

8 Pepper, J.M., Baylis, P.E.T. Baylis, and E. Adler. Can. J. Chem., 37, 1241-1248 (1969).

9 Kringstad, K.P. and R. Mörck, Holzforschung, 37, 237-244 (1983).

10 Akim, L.G., J.L. Colodette, and D.S. Argyropoulos. Proceed. Int. Pulp Bleach. Conf., Halifax, 103-113 (2000).

11 Froass, P.M., A.J. Ragauskas, and J.E. Jiang. Holzsforschung, 52(4), 385-390 (1998).

12 Froass, P.M., A.J. Ragauskas, and J.E, Jian, J. Wood Chem. Technol., 16(4), 347-365 (1996).

13 Gellerstedt, G., J. Pranda, and E.-L. Lindfors. J. Wood Chem. Technol., 14(4) 467-482 (1994).

14 Hardell, H.-L., Nilvebrant, N.-O., J. Anal. Appl. Pyrolysis 52,1-14 (1999).

15 Hunter, K.A. and Liss, P.S. J. Electroanal. Chem. 73, 347-358 (1976).

16 Attar al, A.A.A. and Beck, W.-H., J. Electroanal. Chem. 27, 59-67 (1970).

17 Schultz v., S. and Holmbom, B., Master thesis (2000) in Swedish.

18 Kleen, M. and Gellerstedt, G., J. Anal. Appl. Pyrolysis, 19, 139-152 (1991).

24.6 Addendum 6. On the Improved Selectivity of Oxygen Delignification. 1. Fiber curl, crystallinity, and length

Poster presentation at the 11th International Symposium on Wood and Pulping Chemistry
Nice, France June 2001

Juha P. T. Fiskari, Thomas J. McDonough, Thomas J. Dyer, Arthur J. Ragauskas, John F. Waterhouse

Institute of Paper Science and Technology
500 10th Street, N.W.
Atlanta, GA 30318, USA

Abstract

The purpose of this research was to gain a better understanding of the phenomena affecting fiber quality in oxygen delignification. Softwood kraft pulps were oxygen delignified to six different extents using different temperatures and alkali charges as variables in a factorial experiment. Each of the oxygen-delignified pulp samples, as well as two brownstock samples, was subjected to conventional DEDED bleaching at a constant first-stage kappa factor. The fully bleached samples were then characterized in terms of fiber length and curl by image analysis and amorphous/crystalline cellulose ratio by CP/MAS ^{13}C-NMR.

Introduction

Pulps that have been oxygen delignified to an extent of 50% or less generally exhibit a tear factor at a given tensile strength that is similar to that of conventionally bleached pulps, despite having a lower viscosity [1]. However, it is well established that intensive oxygen delignification, e.g., two-stage oxygen treatment prior to non-chlorine chemical bleaching, tends to be nonselective. Under these conditions, there may be significant effects on fiber properties. For example, cellulose crystallinity may be affected, fiber curl may be introduced, or the ability of the fibers to form bonds with other fibers may be compromised. Furthermore, fiber strength may be affected. The resulting reductions in pulp quality become evident when the pulps are compared to pulps prepared by conventional chlorine dioxide bleaching, which is known to be very selective.

The purpose of this research was to gain a better understanding of the phenomena affecting fiber quality in oxygen delignification.

Experimental

The pulp sample (softwood kraft) was obtained from a Finnish mill. The properties of the pulp sample were as follows: kappa number 25.6, viscosity 1244 mL/g, and brightness 27.3% ISO.

The softwood pulps were oxygen delignified to six different extents of delignification by using temperature and alkali charge as variables. All combinations of the following temperatures and alkali charges were included in the experiments: 80ºC and 95ºC; 1%, 2%, and 4% NaOH. Oxygen delignification was performed in a Quantum mixer at 10% consistency and 90 psi pressure. No magnesium salt was used.

Each of these oxygen-delignified pulp samples as well as two reference brownstock samples underwent a conventional chlorine dioxide (ECF) bleaching in the DEDED sequence. Chemical charges in the bleaching stages varied and depended on the post-

oxygen kappa number (constant kappa factor 0.2 in D_0). Otherwise, the conditions were the same for all pulps. All D and E bleaching stages were carried out in a water bath except the D_0 stage for the Reference 2 pulp sample, which was performed in a Quantum mixer. A Hobart mixer was used for pulp homogenizations between the bleaching stages. The target brightness after bleaching was 88+. The brownstock and fully bleached samples as well as a fully bleached mill pulp sample (10 samples in all) were then characterized.

Analysis

Brightness, kappa number, and viscosity were determined according to ISO 2469:1994(E), TAPPI T236 cm-85, and SCAN-CM 15:88, respectively.

The pulp samples were analyzed with an Optest Fiber Quality Analyzer (FQA) for fiber length and curl, both length-weighted averages.

The pulp samples were Wiley milled using a screen with 0.050" diameter holes. The samples were then analyzed with Cross Polarization Magic Angle Spinning Carbon-13 Nuclear Magnetic Resonance Spectroscopy (CP/MAS ^{13}C-NMR) for amorphous and crystalline cellulose. The measurements were carried out with a Bruker 400 MHz DMX Spectrometer. Similar methods have been described elsewhere [2-4].

Results and Discussion

The effect of sodium hydroxide charge and temperature on kappa number in oxygen delignification is presented in Figure 1.

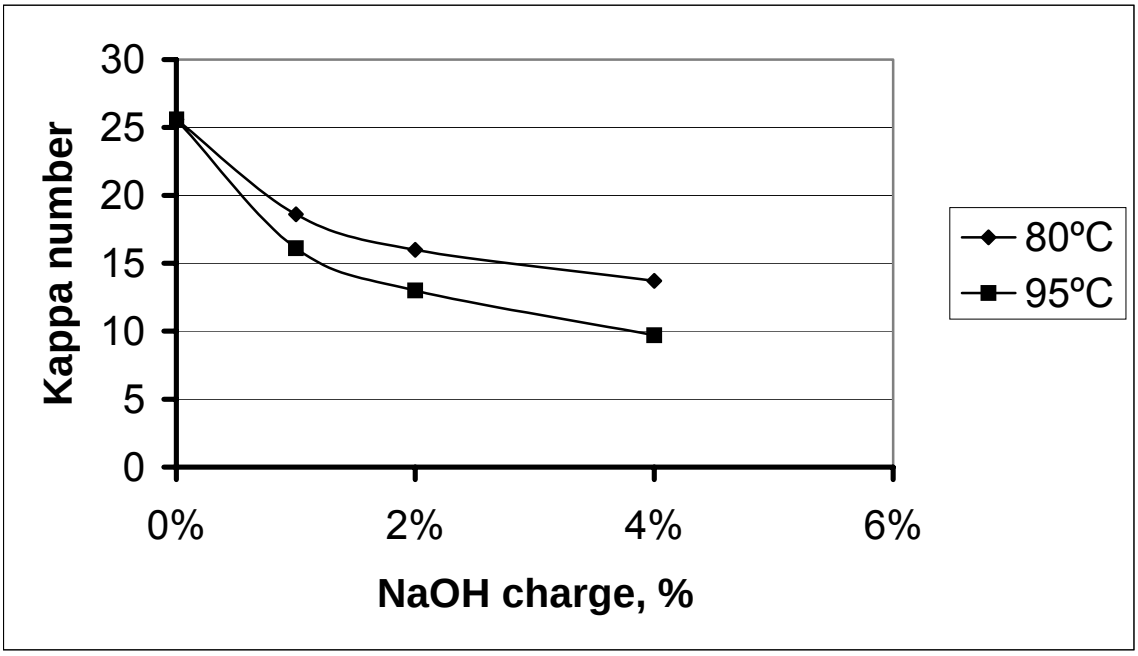

Figure 1. The effect of NaOH dose and temperature on kappa number in oxygen delignification.

As can be seen in Figure 1, the highest sodium hydroxide charge (4%) and temperature (95°C) resulted in a relatively high delignification rate, about 62%. The lowest NaOH charge (1%) and 80°C temperature only decreased kappa number by some 27%. The effect of sodium hydroxide charge and temperature on selectivity (viscosity as a function of kappa number) in oxygen delignification is presented in Figure 2.

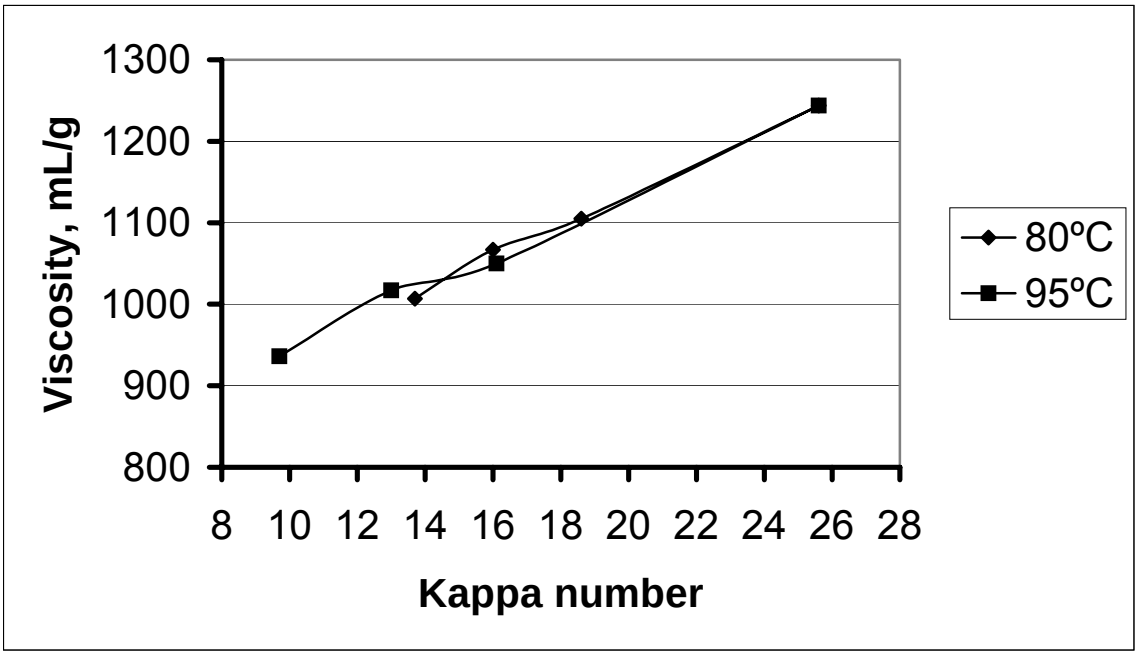

Figure 2. The effect of temperature and NaOH dose on selectivity in oxygen delignification.

As Figure 2 illustrates, the change in viscosity as a function of kappa number decrease was quite linear. In fact, the specific viscosity drop was between 18 and 20 mL/g for all pulp samples.

After oxygen delignification, all eight oxygen-delignified pulp samples as well as two reference brownstock samples were bleached in a DEDED sequence. The most important findings of the bleaching experiments are presented in Table 1.

Table 1. DEDED or ODEDED bleaching results.

DEDED or ODEDED bleaching treatment	Total ClO_2 %	Bright, % ISO	Visco, mL/g
No O_2, D_0 in water bath	4.35	89.0	908
No O_2, D_0 in Quantum	3.45	88.5	1040
95°C & 4% NaOH in O_2	1.70	89.4	863
95°C & 2% NaOH in O_2	2.20	89.0	939
95°C & 1% NaOH in O_2	2.60	89.1	943
80°C & 4% NaOH in O_2	2.25	89.9	920
80°C & 2% NaOH in O_2	2.60	88.9	957
80°C & 1% NaOH in O_2	3.20	89.6	879
Oxygen-ECF mill pulp	n/a	86.5	975

As can be seen in Table 1, the use of a Quantum mixer in the D_0 stage greatly increased the efficiency of chlorine dioxide delignification and therefore decreased the need for chlorine dioxide in the following D stages. As a result of this, the final viscosity also remained on a substantially higher level. The large beneficial effect of good mixing in the D_0 stage resulted, in part, from the fact that this particular pulp had not been subjected to oxygen delignification in the Quantum mixer. Prior treatment in the Quantum mixer facilitated mixing in subsequent stages.

The final brightnesses demonstrate that the use of oxygen delignification is an efficient means of reducing the kappa number and therefore decreasing the use of chlorine dioxide. The pulps that had been treated with an O_2 stage did not, on average, suffer a viscosity drop any greater than the DEDED reference pulp bleached in a water bath. The reference ECF mill pulp also had relatively high viscosity. The brightness of the mill pulp sample had ebbed a couple of ISO brightness units after being shipped from the mill,

apparently due to ordinary brightness reversion. Other bleaching results are presented in the Appendix.

The FQA results are presented in Table 2.

Table 2. FQA results after bleaching.

DEDED or ODEDED bleaching treatment	Fiber length (l/w), mm	Curl (l/w)
No O_2, D_0 in water bath	2.23	0.276
No O_2, D_0 in Quantum	2.18	0.318
95°C & 4% NaOH in O_2	2.09	0.335
95°C & 2% NaOH in O_2	2.12	0.345
95°C & 1% NaOH in O_2	2.09	0.344
80°C & 4% NaOH in O_2	2.14	0.338
80°C & 2% NaOH in O_2	2.11	0.337
80°C & 1% NaOH in O_2	2.19	0.321
Oxygen-ECF mill pulp	2.17	0.250

As Table 2 shows, fiber length apparently underwent a slight decrease as a result of oxygen delignification, while curl increased. The fiber length of the reference mill pulp equaled those of the mildly treated oxygen-delignified laboratory pulps. The more severe the oxygen treatment, the greater was the introduction of curl and the greater the apparent decrease in fiber length. It is likely that the apparent fiber length decrease is an artifact of the measurement method, inasmuch as curled fibers that are not aligned within the plane of measurement will project an apparent length that is less than their true length. The laboratory mixers, both Quantum and Hobart, probably introduced most of this fiber curl.

The CP/MAS ^{13}C-NMR spectrum of an extensively oxygen-delignified (95°C and 2% NaOH) and bleached kraft pulp sample is shown in Figure 3.

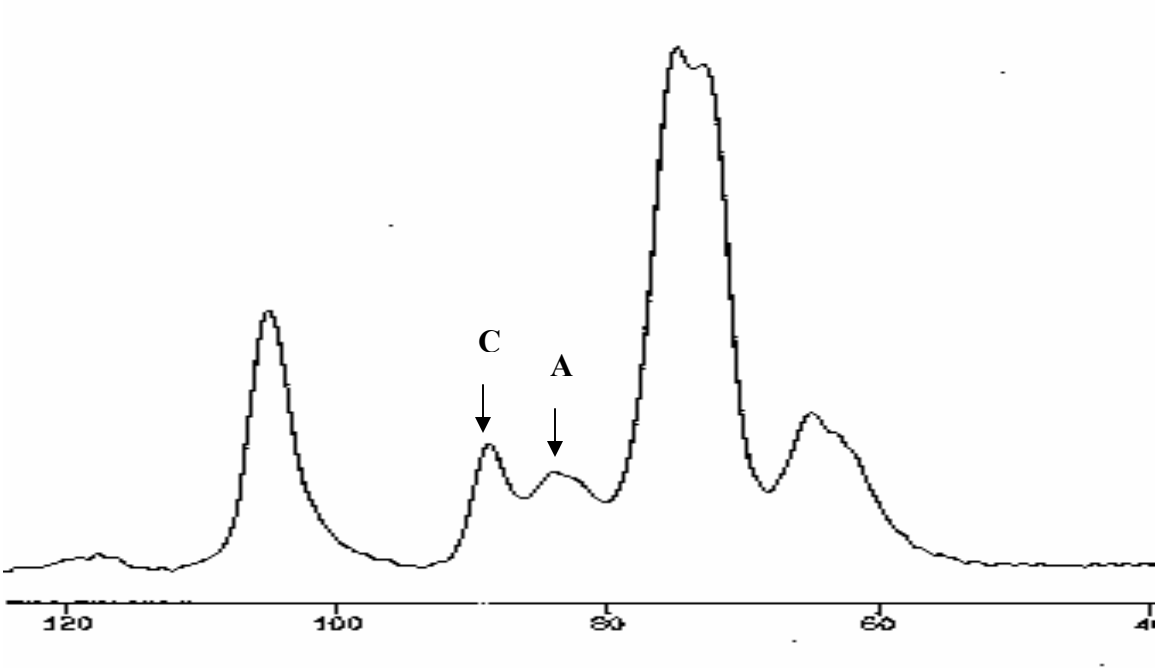

Figure 3. CP/MAS ^{13}C-NMR spectrum of fully bleached kraft pulp. A and C denote amorphous and crystalline cellulose, respectively.

As can be seen in Figure 3, the spectrum shows signals of crystalline and amorphous celluloses and can therefore be used to determine the ratios of the contents of these celluloses [2-4]. When the spectra of this study were observed visually, little or no difference could be seen. The calculated results obtained from CP/MAS ^{13}C-NMR spectra of the fully bleached samples are presented in Table 3.

Table 3. Solid-state ^{13}C-NMR spectroscopy results.

O_2 treatment of the fully bleached sample	Amorphous cellulose/ crystalline cellulose ratio
No O_2, D_0 in water bath	1.05
No O_2, D_0 in Quantum	1.04
95°C & 4% NaOH in O_2	1.03
95°C & 2% NaOH in O_2	1.03
95°C & 1% NaOH in O_2	1.04
80°C & 4% NaOH in O_2	1.03
80°C & 2% NaOH in O_2	1.06
80°C & 1% NaOH in O_2	1.04
Oxygen-ECF mill pulp	1.00

As can be seen in Table 3, the amorphous/crystalline cellulose ratios are virtually the same for all laboratory pulp samples. The amorphous/crystalline cellulose ratio of the brownstock was 1.04. Therefore, the ratio did not change as a result of laboratory bleaching. The mill reference pulp, however, shows a slightly lower amorphous/crystalline cellulose ratio, which is probably due to the more severe treatment in mill conditions.

Conclusions

According to the results, the Scandinavian softwood used in these experiments was resistant to viscosity loss during oxygen delignification. The use of extensive oxygen delignification did, however, introduce a considerable fiber curl, which was accompanied by an apparent slight decrease in fiber length. The mixing devices used in the laboratory were probably responsible for the introduction of curl.

Results obtained from CP/MAS ^{13}C-NMR spectra showed no differences among the laboratory pulps in terms of the amorphous/crystalline cellulose ratio. Even the pulp

samples that had experienced extensive oxygen delignification had virtually the same amorphous/crystalline cellulose ratio as that of the brownstock pulp. The amorphous/crystalline cellulose ratio of the mill reference pulp was slightly lower than those of the laboratory pulps, which is obviously due to the more severe treatments in the mill.

Acknowledgements

The authors thank UPM-Kymmene Corporation for partially financing this research project. The expert advice of Chuck Courchene is gratefully acknowledged. Thanks also go to Donna Jernigan and Ruth Zehfuss for linguistic revisions.

REFERENCES

1. McDonough, T.J. Oxygen delignification. In: Pulp Bleaching – Principles and Practice, Editors Carlton W. Dence & Douglas W. Reeve, pp. 213–239.

2. Newman, R.H. & Hemmingson, J.A. Determination of the degree of cellulose crystallinity in wood by carbon-13 nuclear magnetic resonance spectroscopy. Holzforschung, 44(5), 351–355, 1990.

3. Kunze, J. & Fink, H.-P. Charakterisierung von Cellulose und Cellulosederivaten mittels hochauflösender Festkörper-^{13}C-NMR-Spektroskopie 53(12), 753–764, 1999.

4. Hult, E.-L., Larsson, P.T. & Iversen, T. A comparative study of cellulose structure in spruce wood and kraft pulp. Cellulose, 7(1), 35–55, 2000.

APPENDIX

Table 4. Oxygen delignification results.

DEDED or ODEDED bleaching treatment	Kappa number	Brightness, % ISO	Viscosity, mL/g	Specific viscosity drop, mL/g
95°C & 4% NaOH in O_2	9.7	42.3	936	19
95°C & 2% NaOH in O_2	13.0	35.3	1017	18
95°C & 1% NaOH in O_2	16.1	31.3	1050	20
80°C & 4% NaOH in O_2	13.7	34.9	1007	20
80°C & 2% NaOH in O_2	16.0	31.8	1067	18
80°C & 1% NaOH in O_2	18.6	29.3	1105	20

Table 5. Bleaching results after the initial bleaching stages, ODED

DEDED or ODEDED bleaching treatment	ClO_2 in D_0, %	NaOH in E_1, %	ClO_2 in D_1, %	Brightness, % ISO	Viscosity, mL/g
No O_2, D_0 in water bath	1.95	2.6	1.2	69.0	1102
No O_2, D_0 in Quantum	1.95	2.6	1.2	80.4	1083
95°C & 4% NaOH in O_2	0.75	1.1	0.75	81.9	871
95°C & 2% NaOH in O_2	1.0	1.4	0.9	79.9	963
95°C & 1% NaOH in O_2	1.2	1.7	1.0	78.6	1001
80°C & 4% NaOH in O_2	1.05	1.4	0.9	80.4	955
80°C & 2% NaOH in O_2	1.2	1.7	1.0	79.4	1008
80°C & 1% NaOH in O_2	1.4	2.0	1.1	75.9	1034

Table 6. Chemical charges in the E_2 and D_2 stages.

DEDED or ODEDED bleaching treatment	NaOH in E_2, %	ClO_2 in D_2, %
No O_2, D_0 in water bath	0.7	1.2
No O_2, D_0 in Quantum	0.7	0.3
95°C & 4% NaOH in O_2	0.7	0.2
95°C & 2% NaOH in O_2	0.7	0.3
95°C & 1% NaOH in O_2	0.7	0.4
80°C & 4% NaOH in O_2	0.7	0.3
80°C & 2% NaOH in O_2	0.7	0.4
80°C & 1% NaOH in O_2	0.7	0.7

24.7 Addendum 7. Mini-Oxygen Stages: More Delignification with Less Capital

Presented at the TAPPI Pulping Conference
Boston, Massachusetts November 2000

Thomas J. Dyer, Lucian A. Lucia, and Arthur J. Ragauskas*
Institute of Paper Science and Technology
500 10th Street
Atlanta, GA 30318

Hasan Jameel
North Carolina State University
Department of Wood and Paper Science
Raleigh, NC

Abstract

The delignification properties of a conventional O-stage and a mini-O treatment were studied with a SW kraft pulp. Delignification studies indicated that a (E+O) or (E+O)(E+O) treatment could remove only 36% of the lignin that a conventional oxygen stage can accomplish. The application of a 0.05 kappa factor charge of chlorine dioxide prior to (E+O)(E+O) or between the two mini-O stages (i.e., (E+O)$D_{kf:0.05}$(E+O)) can improve the overall delignification properties, yielding approximately 77% of the performance of a conventional O-stage. The milder conditions of the mini-O treatments were also shown to yield pulps with higher viscosities. Additional investigations into the effects of interstage washing suggest that not washing between stages of (E+O)$D_{kf:0.05}$(E+O) or $D_{kf:0.05}$(E+O)(E+O) did not significantly impact the overall pulp delignification properties or pulp viscosities.

Introduction

Chemical pulp bleaching operations have been dramatically altered over the past decade, largely in response to environmental concerns. In North America, these concerns have resulted in a dramatic reduction in elemental chlorine usage and an increase in chlorine dioxide and oxygen delignification. Although these new bleaching technologies have been shown to address environmental concerns and provide pulps with desirable quality properties this conversion in bleaching technologies has been accompanied by increased capital costs. As discussed by several industry leaders, the production of wood pulp is not providing sufficient return on equity for the amounts of capital required to produce bleached kraft pulp. (i, ii) This poses a new challenge for researchers in the field of kraft pulping and bleaching operations. Certainly, several research groups have begun to address this issue, and publications by Stapley *et al*. (iii), Null and Cenatempo (iv), Kimbrel (v), Tait (vi), McDonough *et al*. (vii), Chakar *et al*. (viii), and Histed (ix) are reflective of this effort.

Although the capital costs of an oxygen stage are substantial, it is generally believed that the overall performance of an O-stage can be significantly improved, thereby improving the overall return on capital. Extended oxygen delignification studies by Magnotta *et al*. (x), Bokstrom and Norden (xi), and Steffes *et al*. (xii) indicate that distinct yield benefits can be accomplished by halting the cook at a high kappa number (i.e., 40-50 for SW kraft) before the selectively of the kraft cook decreases in the terminal phase. Extended oxygen delignification of high kappa pulps followed by ECF bleaching has been shown to provide 3-4% yield benefits over conventional bleaching technologies. Minja *et al*. (xiii) and Parthasarathy (xiv) have proposed that coupling this approach with PS/AQ kraft cooking and pulping additives can provide additional 2-3% yield improvements. These observed yield benefits are then further amplified by reducing the organic load on the recovery furnace, which has potential productivity benefits for recovery boiler-limited mills. (xv)

Typically, oxygen delignification is limited to 50% of the brownstock kappa number. However a recent survey of pulp mill practices suggested that many mills do not achieve even this level of performance (xvi). Extending practical delignification past 50% typically requires the use of double-stage oxygen delignification technologies. These systems have been shown to result in 55-67% delignification for commercial operations. (xvii, xviii, xix, xx) Unfortunately, these operational benefits are accompanied by additional capital costs. An alternative approach to utilizing oxygen delignification chemistry in pulp bleaching is the application of a mini-O system. This system typically removes lesser amounts of lignin but requires less capital investment and is readily retrofitted to existing pulp bleaching operations. Histed (xxi) has reported that the use of a 0.05-kappa-factor D pretreatment stage followed by a higher than normal temperature in the (E+O) stage can achieve approximately 50% delignification of a SW kraft pulp. McKenzie *et al*. (xxii) reported that the commercial use of a mini-oxygen delignification system prior to a conventional O stage provided an additional 25% delignification of a SW kraft pulp. Typically, a mini-O stage employs an upflow tube with retention of approximately 30 minutes, oxygen pressure of 80–90 psig, 1% NaOH, held at 70–80^{o}C. A single mini-O stage has been reported to remove 25% of the lignin in a kraft brownstock. We have recently examined the fundamental bleaching and process chemistry associated with this technology.(xxiii) Treatment of a 26.6 kappa number SW kraft pulp with (E+O) was found to remove 13-25% of the lignin in the pulp depending on the charge of caustic employed (i.e., 1.5–3.5%). The delignification effects of the (E+O) treatment were shown to be dramatically improved if the caustic charge was split into two and the pulp was oxidized with a low charge of chlorine dioxide after the initial (E+O) stage (see Figure 1).

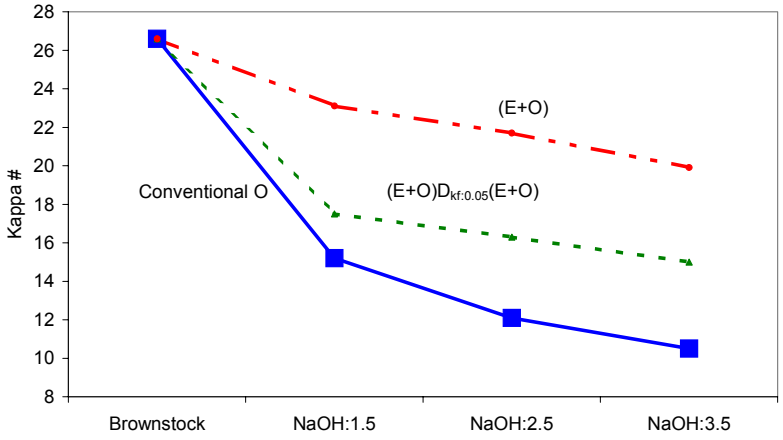

Figure 1: Delignification SW kraft pulp employing O, (E+O), and (E+O)$D_{kf:0.05}$(E+O) employing total NaOH charges of 1.5, 2.5, and 3.5%.[23]

The delignification effects observed in this process were shown to be due to the partial oxidation of phenolic lignin groups by the (E+O) and D treatments. In addition, the benefits of the mini-O system could be attributed, in part, to the extraction of leachable lignin present in kraft brownstock pulp.(xxiv, xxv) Our earlier studies did not consider the effects of carryover and/or incomplete washing. This paper further examines the benefits of a mini-O system and the effects of pulp washing. These results are then compared against a conventional oxygen stage.

Experimental

An industrial SW kraft pulp with a kappa number of 26.2 and viscosity value of 33.2 cP was employed for experiments in this study. Prior to any delignification studies, the pulp was extensively washed until the wash water was pH neutral and colorless.

Chlorine dioxide bleaching studies were accomplished in a quantum mixer following the conditions described in Table 1. The O and mini-O reactions were performed in a pressure vessel following the conditions summarized in Table 1.

Delignified pulps were analyzed for kappa number following TAPPI Standard Method T236. (xxvi) Typical experimental standard deviations for this procedure were determined to be 2.0%. Pulp viscosity values were determined in accordance with TAPPI Standard T-230 om-89 (26), and standard deviations were 0.4.

Results and Discussion

Oxygen pulp bleaching effects were performed employing a commercial SW kraft pulp with kappa number of 26.2. Oxygen bleachability of this pulp was examined employing conventional and mini-O bleaching sequences; the experimental conditions employed are summarized in Table 1.

Table 1. Oxygen and Mini-Oxygen Bleaching Conditions.

Oxygen Stage(s)	Conditions
O	10% csc, 90°C, 60 min., 2.5% NaOH
D $D_{kf:0.05}$	0.20 kf ClO_2, 10% csc, 70°C for 30 min. 0.05 kf ClO_2, 10% csc, 70°C for 30 min.
(E+O)*	10%csc, 80°C, 40 min., 2.5% NaOH
(E+O)	10%csc, 80°C, 20 min., 1.25% NaOH

Note: all O and (E+O) treatments employed 0.10% $MgSO_4$ and the O_2 pressure was held constant at 90 psig.

The delignification results achieved employing O, (EO)*, (EO)(EO), $D_{kf:0.20}$(E+O), $D_{kf:0.05}$(E+O)(E+O), and (E+O)$D_{kf:0.05}$(E+O) on a kappa 26.2 SW kraft pulp are summarized in Figure 2.

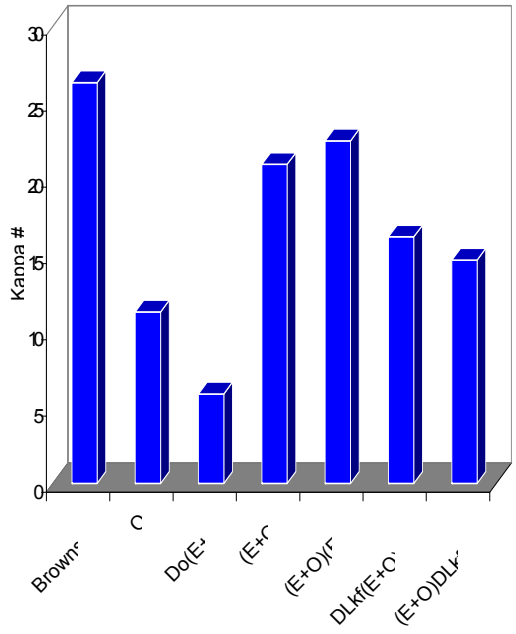

Figure 2. Delignification of SW kraft pulp (kappa 26.3) employing O, (E+O)*, D(E+O)*, (E+O)(E+O), $D_{kf:0.05}$(E+O)(E+O), and (E+O)$D_{kf:0.05}$(E+O) with washing between each bleaching stage.

The results of these initial studies yield several interesting conclusions including that a limited amount of lignin can be abstracted from the pulp employing either (E+O) or (E+O)(E+O) (i.e., 20 and 14%, respectfully). Since both of these treatments employed equal amounts of caustic, splitting the charge of NaOH between two (E+O) stages is not beneficial with respect to delignification. Of greater practical interest, is the 38% delignification of $D_{kf:0.05}$(E+O)(E+O) and 44% delignification of (E+O)$D_{kf:0.05}$(E+O). Although these treatments are not as efficient as the conventional O-stage (57% delignification) or an $D_{0.20\ kf}$(E+O) treatment (78% delignification), the application of a low charge of chlorine dioxide prior to a mini-O treatment sequence can significantly improve the performance of a mini-O system. Presumably, the improved delignification

of (E+O)$D_{kf:0.05}$(E+O) over $D_{kf:0.05}$(E+O)(E+O) can be attributed to the initial (E+O) stage removing easily oxidized lignin prior to the low kappa factor charge of chlorine dioxide. Hence, the (E+O)$D_{kf:0.05}$(E+O) sequence more efficiently utilizes the low charge of chlorine dioxide.

The viscosity values for the pulps described in Figure 2 are summarized in Figure 3. These results demonstrate that the milder bleaching conditions of the $D_{kf:0.05}$ mini-O bleaching sequences allowed for improved pulp viscosities.

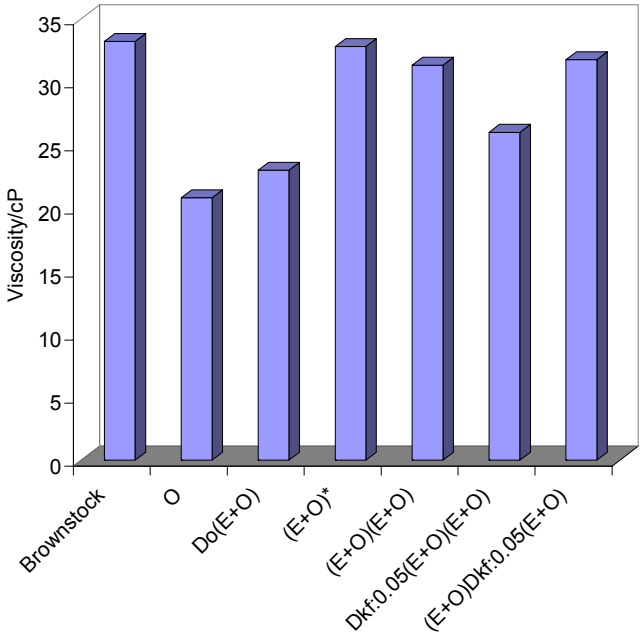

Figure 3. Pulp viscosity (cP) values of SW kraft pulp (kappa 26.3) treated with O, (EO)*, D(EO)*, (E+O)(E+O), $D_{kf:0.05}$(E+O)(E+O) and (E+O)$D_{kf0.05}$(E+O) and washed between stages.

Despite these promising results, the use of interstage washing employed in the initial studies would limit any practical applications of these sequences. To examine this issue,

we repeated the mini-O sequences without any washing between the stages, and these results are summarized in Figure 4.

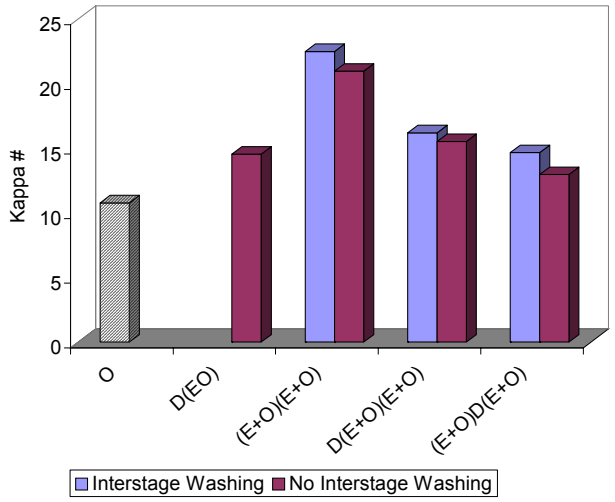

Figure 4. Effects of washing on delignification properties of (E+O)(E+O), (E+O)$D_{kf:0.05}$(E+O) and $D_{kf:0.05}$(E+O)(E+O).

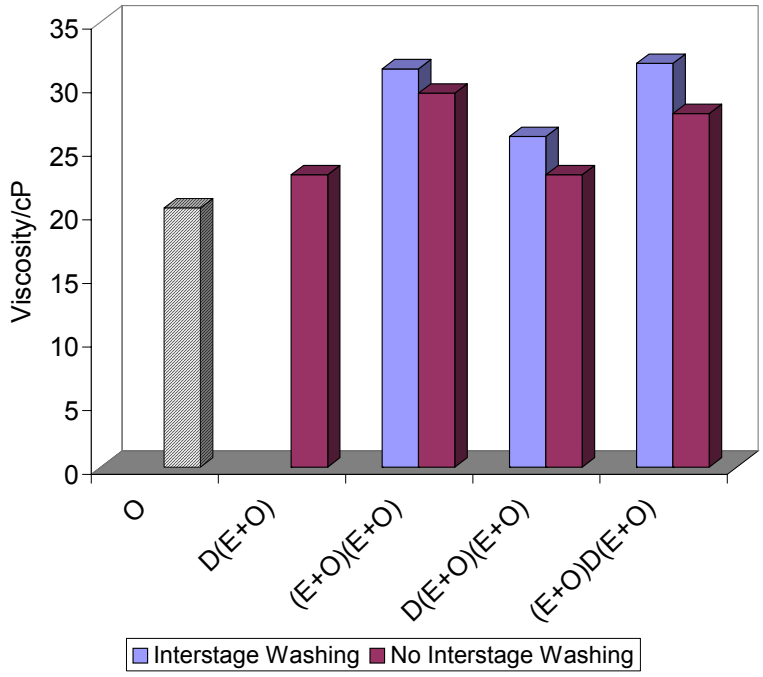

Figure 5. Effects of washing on pulp viscosity properties of (E+O)(E+O), (E+O)$D_{kf:0.05}$(E+O) and $D_{kf:0.05}$(E+O)(E+O).

The results in Figures 4 and 5 indicate that there are no significant detrimental impacts on either (E+O)$D_{kf:0.05}$(E+O) or $D_{kf:0.05}$(E+O)(E+O) caused by not employing interstage washing.

Conclusions

The mini-O treatments described in this paper serve to further highlight the potential practical applications of a mini-O system to pulp bleaching operations. The negligible effects of not washing the pulp between mini-O treatments suggest that inter-stage washing may not be required. Further, it may be possible to extend the benefits of a mini-O system by reinforcing it with low charges of hydrogen peroxide. The last remaining issue that needs to be addressed is the effect of black liquor carryover on the performance of the overall mini-O bleaching sequence. These issues are currently being examined in our group and will be reported in the near future.

Acknowledgements

The authors wish to thank the member companies of IPST and the Department of Energy for their support of this research. This manuscript was prepared, in part, with the support of the U.S. Department of Energy (DOE) Cooperative Agreement No. DE-FC07-00ID13870. However, any opinions, findings, conclusions, or recommendations expressed herein are those of the author(s) and do not necessarily reflect the views of DOE.

References

1. O'Brien, J. Paper Age's "Executive Papermaker of the Year": Pete Correll. *Paper Age,* March, 12-14(1999).

2. Phillips, R.B. Research and Development in the Pulp and Paper Industry: Year 2000 and Beyond. *TAPPI J.* 83(1), 42-46(2000).

3. Stapley, C. E.; Butner, R. E.; Kangas, M. Y. O. Strategic Investment in [the US] Pulp and Paper Industry. 27o congresso anual de celulose e papel Congresso Anuale de Papel São Paulo, BR Conference, November 7-11, 797-811(1994).

4. Null, D.; Cenatempo, D. Paper Company Strategies Should Focus on Building Economic Value, *Pulp & Paper,* 71(9), 59-62(1997).

5. Kimbrell, S. Low-Capital Washer Improvements at Boise Cascade's DeRidder Mill, Pulp Washing Conf. Proceed., Vancouver, British Columbia, CA, October, 81-84(1996).

6. Tait, D. H. Advances in Bleach Plant Design Lower Capital and Operating Costs, *Pulp Paper,* 60(1), 70-72 (1986).

7. McDonough, T.J.; Courchene, C.E.; Baromes, J.-C. Rapid D0 and Simplified Bleaching for Low Capital, Low AOX, and Low Chemical Consumption. Int. Pulp Bleaching Conf. Proceed., Halifax, NS, June, 151-158(2000).

8. Chakar, F.S.; Ragauskas, A.J.; N.-O. Nilvebrant, N.-O. Biobleaching of High Lignin Content Kraft Pulps Via Laccase-Mediator Systems, 1998 TAPPI Pulping Conference, Montreal, Canada, 1, 95(1998).

9. Histed, J. A. Simplification of the C(D)EDED and C(D)EHDED Bleach Sequences, CPPA/TAPPI Int. Pulp Bleaching Conf. Proceed., San Diego, May, 153-163(1982).

10. Magnotta, V.; Kirkman, A.; Jameel, H.; Gratzl, J. High-Kappa-[No.] Pulping and Extended Oxygen Delignification to Increase Yield. Breaking the Pulp Yield Barrier Symposium Proceed., TAPPI PRESS, Atlanta, GA, 165-182(1998).

11. Bokstrom, M.; Norden, S., "Extended Oxygen Delignification", International Pulp Bleaching Conference Proceed., Helsinki, 1, 23-31(1998).

12. Steffes, F.; Bokström, M.; Nordén, S. Pulp Yield Improvements Using Two-Stage, Extended Oxygen Delignification. Breaking the Pulp Yield Barrier Symposium Proceed., TAPPI PRESS, Atlanta, GA, 183-195(1998).

13. Minja, R.; Kleppe, P.; Moe, S. Improving the Pulp Yield by Using PS/AQ and/or Two-Stage Oxygen Delignification. Breaking the Pulp Yield Barrier Symposium Proceed., TAPPI PRESS, Atlanta, GA, 213-217(1998).

14. Parthasarathy, V. Use of Digester Additives and Oxygen Delignification to Gain Bleached Pulp Yield and Achieve Environmental Objectives. Breaking the Pulp Yield Barrier Symposium Proceed., TAPPI PRESS, Atlanta, GA, 219-227(1998).

15. Magnotta, V.; Kirkman, A.; Jameel, H.; Gratzl, J. High-Kappa-[No.] Pulping and Extended Oxygen Delignification to Increase Yield. Breaking the Pulp Yield Barrier Symposium Proceed., Atlanta, GA, 8(1), 165-182(1998).

16. Pryke, D.C.; Tam, T.W.P. ECF Bleaching Practices in Canada, II: Analysis of the PAPTAC Bleaching Committee Survey for Softwood Kraft Pulps. International Pulp Bleaching Conference Proceed., Halifax, 1, 137-151(2000).

17. Boniface, A. Lincoln Pulp & Paper Starts New Bleaching Process. *TAPPI J.*, 83(8), 47-50(2000).

18. Harrell, L. Reducing Kappa Number Variability, Controlling 2-Stage O2 Delignification, TAPPI Pulping Conference Proceed., Oct., 1, 407-417(1999).

19. Bokstrom, M. Extended Oxygen Delignification with the Oxy-Trac™ Process. TAPPI Pulping Conference Proceed., Oct., 1, 419-426(1999).

20. Sullivan D.P.; Genco, J.M.; Berndt, G. Two-Stage Oxygen Delignification Design and Operation at Weyerhaeuser Canada Ltd. In Kamloops, British Columbia. TAPPI Pulping Conference Proceed., Oct., 1, 427-432(1999).

21. Histed, J. Simplified Bleaching; Environmental Advantages for Existing Bleach Plants, *Pulp & Paper Canada,* 98(10), 77-80 (1997).

22. McKenzie, D.J., The Evolution of Pulp Bleaching Practices at Harmac Pacific, International Pulp Bleaching Conference Proceed., Helsinki, 1, 163-167(1994).

23. Chakar, F.S.; Lucia, L.; Ragauskas, A.J. Extending the Limits of Oxygen Delignification. International Pulp Bleaching Conference Proceed., Halifax, 1, 123-130(2000).

24. Li, J.; MacLeod, J. M. Alkaline Leaching of Kraft Pulps for Lignin Removal. *J. Pulp Pap. Sci.,* 19(2), J85-92(1993).

25 Ala-Kaila, K.; Reilama, I. Step-wise Delignification Response in an Industrial Two-Stage Oxygen-Alkali Delignification Process. International Pulp Bleaching Conference Proceed., Halifax, 1, 117-121(2000).

26. TAPPI Standard Methods, TAPPI PRESS, Atlanta, GA (1998).